

**PRE-CLINICAL *IN VITRO* AND *IN VIVO* TESTING OF
NOVEL ANTIMICROBIALS FOR THE TREATMENT OF
BACTERIAL INFECTIONS**



Hang Thi Nguyen

BSc, Doctor of Veterinary Medicine (Vietnam National University of Agriculture, Vietnam)

MSc, Biotechnology Studies (Flinders University, Australia)

**A thesis submitted to the University of Adelaide in fulfilment of
the requirement for the degree of Doctor of Philosophy**

**School of Animal and Veterinary Sciences
The University of Adelaide, Roseworthy Campus**

January 2022

Table of Contents

| | |
|--|-------------|
| Abstract | v |
| Declaration | viii |
| Acknowledgements | ix |
| Preamble..... | xi |
| List of Publications | xiii |
| List of Abbreviations..... | xvi |
| List of Figures | xx |
| List of Tables | xxi |
| | |
| Chapter I | 1 |
| Introduction and literature review..... | 1 |
| 1.1. Antibiotic resistance: A global health and development threat | 2 |
| 1.2. Gram-negative bacteria | 6 |
| 1.2.1. GNB infections..... | 6 |
| 1.2.2. Critical GNB KAPE pathogens | 7 |
| 1.2.3. The GNB outer membrane barrier. | 8 |
| 1.2.4. AMR mechanisms in GNB..... | 9 |
| 1.3. Current options for MDR-GNB infections..... | 13 |
| 1.3.1. Existing drug classes | 13 |
| 1.3.2. Recently approved drugs | 18 |
| 1.4. Antibiotic therapy advances to combat MDR-GNB..... | 22 |

| | |
|---|-----------|
| 1.4.1. Natural products as sources of new antibiotics..... | 22 |
| 1.4.2. Expanding antibiotic chemical diversity..... | 25 |
| 1.4.3. Efflux inhibitors | 28 |
| 1.4.4. Combination therapy | 32 |
| 1.4.4.1. Existing β -lactam antibiotics paired with new β -lactamase inhibitors | 32 |
| 1.4.4.2. Combination of existing and new antibiotics with polymyxins | 34 |
| 1.4.5. Old drug repurposing | 39 |
| 1.4.6. “Lost antibiotics” | 40 |
| 1.5. Models for testing pre-clinical efficacy of new antibiotics against bacterial infections | 40 |
| 1.5.1. <i>Galleria mellonella</i> larvae model | 40 |
| 1.5.2. Traditional mouse model. | 41 |
| 1.5.3. Bioluminescent mouse model..... | 42 |
| 1.6. Novel antibiotics assessed in the present study | 43 |
| 1.7. Conclusion | 46 |
| 1.8. Aims of the present study | 47 |
| Chapter II | 48 |
| <i>In vitro</i> activity of robenidine analog NCL195 in combination with outer membrane permeabilizers against Gram-negative bacterial pathogens and impact on systemic Gram- positive bacterial infection in mice | 48 |
| 2.1. Statement of authorship | 49 |
| 2.2. Original article | 52 |
| 2.3. Supplementary materials | 69 |

| | |
|--|------------|
| Chapter III | 70 |
| <i>In vitro</i> synergistic antimicrobial activity of NCL195 in combination with adjuvants against Gram-negative bacterial pathogens | 70 |
| 3.1. Statement of authorship | 71 |
| 3.2. Original article | 74 |
| 3.3. Supplementary materials | 87 |
| | |
| Chapter IV | 102 |
| Comparison of two transmission electron microscopy methods to visualize drug-induced alterations of Gram-negative bacterial morphology | 102 |
| 4.1. Statement of authorship | 103 |
| 4.2. Original article | 105 |
| | |
| Chapter V | 120 |
| Oral administration of a 2-aminopyrimidine robenidine analogue (NCL195) significantly reduces <i>Staphylococcus aureus</i> and <i>Escherichia coli</i> infections in the presence of sub-inhibitory colistin concentrations in a bioluminescent mouse model | 120 |
| 5.1. Statement of authorship | 121 |
| 5.2. Original manuscript | 124 |
| | |
| Chapter VI | 163 |
| Impact of a novel anticoccidial analogue on systemic <i>Staphylococcus aureus</i> infection in a bioluminescent mouse model | 163 |
| 6.1. Statement of authorship | 164 |
| 6.2. Original article | 166 |

| | |
|--|------------|
| 6.3. Supplementary materials | 182 |
| Chapter VII | 186 |
| Evaluation of benzguinols as next-generation antibiotics for the treatment of multidrug-resistant bacterial infections..... | 186 |
| 7.1. Statement of authorship | 187 |
| 7.2. Original article | 190 |
| Chapter VIII | 207 |
| General discussion and further directions | 207 |
| 8.1. General summary | 208 |
| 8.2. Major findings..... | 210 |
| 8.3. Limitations | 217 |
| 8.4. Future directions | 217 |
| 8.5. Conclusions..... | 219 |
| Appendices | 220 |
| Bibliography..... | 266 |

Abstract

New molecules are urgently required for the treatment of multidrug-resistant (MDR)-Gram-positive (GPB) and Gram-negative bacteria (GNB) infections. In the latter, these efforts are further impeded due to the presence of an outer membrane (OM) in GNB, which prevents many antibiotics from gaining entry to reach their target sites. This challenge has led to the current shortfall of new antimicrobials with novel mechanisms of action to treat MDR-GNB infections in particular. The present study aimed to identify promising lead compounds with new modes of action for pharmaceutical development to treat MDR bacterial infections, particularly GNB infections. Here, we focused on four novel antibiotic entities, the robenidine analogues NCL195 and NCL179 and benzguinol A and B, which each exhibited potent antimicrobial activity against MDR-GPB as stand-alone entities and were active against MDR-GNB when combined with adjuvants that perturb the OM.

We previously reported *in vitro* activity for the robenidine analogue NCL195 against MDR-GPB with minimum inhibitory concentrations (MIC) from 1-4 $\mu\text{g}/\text{mL}$. Here, we found partially synergistic effects of NCL195 in combination with ethylenediaminetetraacetic acid (EDTA) or polymyxin B nonapeptide (PMBN) and fully synergistic activity of NCL195 when combined with sub-inhibitory concentrations of polymyxin (PMB) or colistin against all tested GNB isolates, whereas NCL195 alone had no activity. We further used fluorescence-based membrane potential measurements to clearly show the dual mechanism of action of the NCL195 + colistin/PMB combination against *Escherichia coli*. Moreover, we used transmission electron microscopy (TEM) to demonstrate the effect of NCL195 alone and in combination with colistin on GPB (*Staphylococcus aureus*) and GNB (*E. coli* and *Pseudomonas aeruginosa*)

membrane morphology, respectively. We observed specific membrane damage and the presence of mesosome-like membrane structures in TEM images of *S. aureus* cells treated with NCL195 that were not present in untreated bacteria. No membrane morphology changes were observed in *E. coli* and *P. aeruginosa* exposure to NCL195 alone, whereas the NCL195+colistin combination treatment caused significantly more cell membrane damage compared to colistin alone. TEM images mirrored the *in vitro* antimicrobial activity of NCL195 against *S. aureus* and synergistic interaction of NCL195 + colistin against *E. coli* and *P. aeruginosa*. We also showed that NCL195 exhibited limited *in vitro* cytotoxicity (16 µg/mL) to mammalian cell lines, and low haemolytic activity (128 µg/mL) to human erythrocytes. Moreover, intraperitoneal (IP) treatment (50 mg/kg, 2 x injections, 4 h apart) of NCL195 alone, oral treatment (50 mg/kg, 4 x injections, 4 h apart) of NCL195 alone and the combination of oral NCL195 (50 mg/kg, 4 x injections, 4 h apart) with IP colistin (0.125-4 mg/kg, two-fold increasing, 4 x injections, 4 h apart) were safe to mice. Furthermore, we showed promising *in vivo* efficacy against MDR-GPB human pathogens when NCL195 was administered systemically (50 mg/kg x 2 injections, 4 h apart) and orally (50 mg/kg x 4 injections, 4 h apart) in bioluminescent mouse sepsis models, with greater potency observed via the latter route of administration. Subsequently, we found that the combination of oral NCL195 (50 mg/kg, 4 x injections, 4 h apart) with different IP doses of colistin (0.125, 0.25, 0.5, 1 or 2 mg/kg, 4 x injections, 4 h apart) resulted in a dose-dependent significant reduction in infectious load when mice were challenged with both colistin-susceptible and -resistant bioluminescent *E. coli* and prolonged survival times compared to treatment with colistin alone at similar concentrations in a GNB sepsis model.

We further investigated the potential of another analogue of robenidone (NCL179) to expand chemical diversity of this potentially new class of antimicrobial to treat MDR bacterial

infections. We showed that NCL179 exhibited potent bactericidal activity against a wide range of GPB pathogens (MICs from 1-4 $\mu\text{g}/\text{mL}$) and synergistic activity combined with sub-inhibitory concentrations of colistin against GNB (MICs return 0.5-4 $\mu\text{g}/\text{mL}$), whereas NCL179 alone had no activity. NCL179 exhibited limited *in vitro* toxicity (16 $\mu\text{g}/\text{mL}$) to mammalian cell lines, and low haemolytic activity (32 $\mu\text{g}/\text{mL}$) to human erythrocytes. Oral treatment of mice with NCL179 (50 mg/kg, 4 x injections, 4 h apart) was safe and significantly reduced *S. aureus* populations *in vivo* and prolonged survival times in a mouse sepsis model.

We also extended our research into further biological characterisation of the “lost antibiotic” unguinol and further chemical diversification of related nidulin-family fungal natural products which identified two semisynthetic derivatives, benzguinols A and B. Excellent *in vitro* activity against many clinical GPB pathogens (MICs, 0.25-1 $\mu\text{g}/\text{mL}$) and synergistic activity in combination with sub-inhibitory concentrations of colistin against GNB reference strains (MICs, 1-2 $\mu\text{g}/\text{mL}$) were observed, whereas the benzguinols alone had no activity against GNB. Moreover, benzguinol A and B showed low *in vitro* toxicity to mammalian cell lines (32 $\mu\text{g}/\text{mL}$), and low haemolytic activity (128 $\mu\text{g}/\text{mL}$) to human erythrocytes. Furthermore, IP treatment of benzguinol A or B (20 mg/kg, 4 x injections, 4 h apart) exhibited systemic safety in mice and significantly reduced bacterial loads and prolonged survival times compared to vehicle-only treated mice in a bioluminescent *S. aureus* murine sepsis challenge model.

In conclusion, NCL195, NCL179 and benzguinols A and B are viable candidates for further pre-clinical development for specific treatment of MDR-GPB and GNB infections either as stand-alone antibiotics or in combination with sub-inhibitory concentrations of colistin, respectively. They represent excellent scaffolds for further medicinal chemistry development to improve potency.

Declaration

I certify that this work contains no material which has been accepted for the award of any other degree or diploma in my name, in any university or other tertiary institution and, to the best of my knowledge and belief, contains no material previously published or written by another person, except where due reference has been made in the text. In addition, I certify that no part of this work will, in the future, be used in a submission in my name for any other degree or diploma in any university or other tertiary institution without the prior approval of the University of Adelaide and where applicable, any partner institution responsible for the joint-award of this degree.

I acknowledge that the copyright of published works contained within this thesis resides with the copyright holder(s) of those works.

I also give permission for the digital version of my thesis to be made available on the web, via the University's digital research repository, the Library Search and also through web search engines, unless permission has been granted by the University to restrict access for a period of time.

Signature of Ph.D. candidature

-
Hang Thi Nguyen

February 2022

Acknowledgements

I am really grateful to my principal Prof. Darren Trott for your expert guidance, support, encouragement, enthusiasm, for never giving me up, for always believing in me, for scholarship funding for the last year, for always giving warm smiles, full care and never being angry with my annoyance which makes me feel less pressure in the long journey of PhD in Australia. I will keep your image of a gentle and wonderful supervisor for the rest of my life.

I wish to thank my co-supervisor Dr. Abiodun David Ogunniyi for your patience, persistence, all-time dedication, for always being friendly and supportive, for treating me as your friend, not like a student to share your knowledge and life experiences, for giving me your expertise to direct me to go on the track of the PhD journey. You make my PhD life incredible learning experiences, more rewarding, smoothly, and more straightforward. Your kindness, support and care, I will treasure and appreciate forever. I would like to thank others co-supervisors, Dr. Torben Dahl Nielsen and Dr. Stephen Kidd, for your care, support, guidance, for always being friendly and for editing my thesis.

I also would like to thank an external advisor, Dr. Stephen W Page from Neoculi Pty Ltd for your financial support of the PhD project, your guidance, persistence and for editing all manuscripts and the scholarship funding for the last year of my programme.

My sincerest thanks Assoc. Prof. Henrietta Venter for your advice and expertise guidance in some of the experiments, for treating me like your student to help me overcome difficulty in research and life and for always giving me warm care. I would like to appreciate Prof. Gordon Howarth for always following up with my PhD progress, your warmly care, advices and support.

Many thanks to all my exceptional co-authors and mentors, Prof. Adam McCluskey, Dr. Kelly Young, Prof. Sanjay Garg, Dr. Manouchehr Khazandi, Assoc. Prof. Lucy Woolford, Mrs. Tania Veltman, Mrs. Ruth Williams, Dr. Lisa Anne O'Donovan, Dr. Cecilia C. Russell, Dr. Sylvia S. Sapula, Ms. Alexandra R. Boileau for providing expertise, technical guidance, drafting and editing manuscripts.

Special thanks to my lab mates Mr Alex Hongfei Pi, Dr. Wei Yee Chan and Mrs. Tamara Alhamami, Ms. Naomi Louise, Mr. Anteneh Amsalu, Mrs. Hanh Hong Nguyen, and Mrs. Hue Thi Do for your friendships and Mr. Jon Whittall at the University of South Australia for lab assisting.

My appreciations to Dr. May Song, Mrs. Krishna Sathawala, Dr. Ankitkumar Parikh, Mrs. Amanda Ruggero, Mrs. Lora Bowes, Ms. Anh Hong Nguyen and Mr. Max McClafferty at the University of South Australia for their technical assistance and formulation preparations and Mrs. Cheryl Day at the School of Animal and Veterinary Sciences for sample processing of histopathology examinations.

I really appreciate the University of Adelaide and the Vietnamese Government for a joint-funded scholarship and my university (Vietnam National University of Agriculture, Hanoi, Vietnam) for allowing me to leave for overseas study.

Last but not least, I would like thank to my beloved husband, Thien Tai Tran and my cutie girls (Chau Anh Tran and Dieu Hien Tran) for endless love, support, patience, and encouragement, and for always believing in me; to my parents and family members for your support, encouragement and infinite love, in particular to my mum for your sacrifice.

Preamble

The evolution and widespread dispersal of multidrug-resistant (MDR) bacteria urgently requires the discovery and development of new antibiotics. The situation is more critical in drug development for MDR-Gram-negative bacterial (GNB) infections due to exclusion of many molecules by the outer membrane (OM) (i.e. preventing antibiotic entry) together with efficient efflux pump systems (i.e. exporting any antibiotics that penetrate the OM). This thesis focused on four novel antibiotics as lead compound candidates to treat MDR bacterial infections. The thesis consists of six publications (five published and one is being prepared to submit) from two collaborative programmes. The robenidine research programme was initially funded by an Australian Research Council (ARC; arc.gov.au) Linkage grant (LP110200770) to Prof. Darren Trott from the University of Adelaide, Dr. Stephen W Page from Neoculi Pty Ltd as the Partner Organization, Prof. Adam McCluskey from the University of Newcastle and Assoc. Prof. Henrietta Venter from University of South Australia. The unguinol/nidulin research programme was supported by a Cooperative Research Centre Projects scheme grant (CRCPFIVE000119) awarded to Dr. Ernest Lacey from Macquarie University. Under the supervision of Prof. Darren Trott and Dr. Abiodun David Ogunniyi, I performed a series of microbiological evaluations to determine the *in vitro* and *in vivo* antibacterial profiles of four novel chemical compounds (two robenidine analogues, NCL195 and NCL179 and two nidulin analogues, benzguinols A and B).

This dissertation is presented in a publication format consisting of eight chapters. Chapter I is a literature review providing a comprehensive critical review on the development of new antibiotics with novel mechanisms of action with particular application against GNB

infections to address the shortfall in novel agents against pathogens including *Escherichia coli*, *Pseudomonas aeruginosa*, *Acinetobacter* spp. and *Klebsiella* spp. Chapter II, III, IV, and V are four articles describing *in vitro* and *in vivo* antimicrobial activity of NCL195 (4,6-bis(2-((E)-4-methylbenzylidene)hydrazinyl)pyrimidin-2-amine), a chemical analogue of the anticoccidial drug robenidine, against MDR pathogens. Chapter VI focused on further *in vitro* biological characterisation of NCL179 (2,2'-bis[(4-chlorophenyl)methylene] carbonimidic dihydrazide hydrochloride), another analogue of the anticoccidial robenidine, against Gram-positive bacteria (GPB) and GNB in the presence of a sub-inhibitory concentration of colistin as well as its efficacy against *S. aureus* in a bioluminescent infection mouse model as a proof-concept of *in vivo* activity. Chapter VII, focuses on *in vitro* activity of benzguinols against GPB and their combination with sub-inhibitory concentrations of colistin against GNB as well as their efficacy against GPB in the bioluminescent mouse infection model. The thesis concludes with chapter VIII, which provides a general discussion of the overall findings of this study in the context of the existing literature, including potential future directions. Our findings indicate all four novel antibiotic entities in this study are promising lead compounds (requiring further medicinal chemistry diversification) with potentially different mechanisms of action in bacteria compared to existing antibiotics for the future treatment of MDR infections, particularly for GNB infections when combined with sub-inhibitory concentrations of colistin.

List of Publications

Research articles on which the candidate is the first author incorporated into the thesis

1. Pi, H.; **Nguyen, H.T. (shared first author)**; Venter, H.; Boileau, A.R.; Woolford, L.; Garg, S.; Page, S.W.; Russell, C.C.; Baker, J.R.; McCluskey, A.; O'Donovan, L.A.; Trott, D.J.; Ogunniyi, A.D. *In vitro* activity of robenidine analog NCL195 in combination with outer membrane permeabilizers against Gram-negative bacterial pathogens and impact on systemic Gram-positive bacterial infection in mice. *Frontiers in Microbiology* 2020, IF 6.064, 11, doi:10.3389/fmicb.2020.01556, **Chapter II**
2. **Nguyen, H.T.**; Venter, H.; Veltman, T.; Williams, R.; O'Donovan, L.A.; Russell, C.C.; McCluskey, A.; Page, S.W.; Ogunniyi, A.D.; Trott, D.J. *In vitro* synergistic activity of NCL195 in combination with colistin against Gram-negative bacterial pathogens. *International Journal of Antimicrobial Agents* 2021, 57, 106323, IF 15.441, doi:10.1016/j.ijantimicag.2021.106323, **Chapter III**
3. **Nguyen, H.T.**; O'Donovan, L.A.; Venter, H.; Russell, C.C.; McCluskey, A.; Page, S.W.; Trott, D.J.; Ogunniyi, A.D. Comparison of two transmission electron microscopy methods to visualise drug-induced alterations of Gram-negative bacterial morphology. *Antibiotics* (Basel, Switzerland) 2021, 10, IF 5.222, doi:10.3390/antibiotics10030307, **Chapter IV**
4. **Nguyen, H.T.**; Venter, H.; Woolford, L.; Young, K.; McCluskey, A.; Garg, S.; Sapula S.S; Page, S.W.; Ogunniyi, A.D; Trott, D.J. Oral administration of a 2-aminopyrimidine robenidine analogue (NCL195) significantly reduces *Staphylococcus aureus* and *Escherichia coli* infections in the presence of sub-inhibitory colistin concentrations in a bioluminescent

mouse model. The manuscript is being prepared for submission to the Journal of Antimicrobial Chemotherapy, **Chapter V**

5. **Nguyen, H.T.**; Venter, H.; Woolford, L.; Young, K.; McCluskey, A.; Garg, S.; Page, S.W.; Trott, D.J.; Ogunniyi, A.D. Impact of a novel anticoccidial analogue on systemic *Staphylococcus aureus* infection in a bioluminescent mouse model. *Antibiotics* (Basel, Switzerland) 2022; 11, IF 5.222, doi:10.3390/antibiotics11010065, **Chapter VI**
6. **Nguyen, H.T.**; Morshed, M.T.; Vuong, D.; Crombie, A.; Lacey, E.; Garg, S.; Pi, H.; Woolford, L.; Venter, H.; Page, S.W.; Piggott, A.M.; Trott, D.J.; Ogunniyi, A.D. Evaluation of benzquinols as next-generation antibiotics for the treatment of multidrug-resistant bacterial infections. *Antibiotics* (Basel, Switzerland) 2021, 10, IF 5.222, doi:10.3390/antibiotics10060727, **Chapter VII**

Additional research articles published during the PhD period on which the candidate is a co-author but are not incorporated into the thesis.

1. Morshed, M.T.; **Nguyen, H.T.**; Vuong, D.; Crombie, A.; Lacey, E.; Ogunniyi, A.D.; Page, S.W.; Trott, D.J.; Piggott, A.M. Semisynthesis and biological evaluation of a focused library of unguinol derivatives as next-generation antibiotics. *Organic & Biomolecular Chemistry* 2021, 19, 1022-1036, doi:10.1039/d0ob02460k, **Appendix 1**
2. Pi, H.; Ogunniyi, A.D.; Savaliya, B.; **Nguyen, H.T.**; Page, S.W.; Lacey, E.; Venter, H.; Trott, D.J. Repurposing of the Fasciolicide Triclabendazole to treat infections caused by

Staphylococcus spp. and vancomycin-resistant Enterococci. *Microorganisms* 2021, 9, 1697.

doi: 10.3390/microorganisms9081697, **Appendix 2**

Conference/Symposium presentations and Awards arising from this PhD project 2020-2021

1. **Hang T. Nguyen**, Rietie Venter, Tania Veltman, Ruth Williams, Lisa A. O'Donovan, Cecilia C. Russell, Adam McCluskey, Stephen W. Page, Abiodun D. Ogunniyi, Darren J. Trott. Redesigning an anticoccidial drug for treatment of multidrug-resistant bacterial infections. E-poster presenter at Australian Society for Microbiology National Meeting 31st May-3rd June 2021, **Appendix 3**
2. Lisa A O'Donovan, **Hang T Nguyen**, Gwen Mayo, David D Ogunniyi, Darren J Trott. A Comparison of different methods for TEM analysis of Gram-negative bacterial membrane structure. Participant in a poster presentation at 26th Australian Conference on Microscopy and Microanalysis, National Convention Centre, Canberra, 16th -20th Feb 2020, **Appendix 4**
3. Australian Society for Microbiology, Students' Awards Night, Adelaide, South Australia, Australia, **Appendix 5**
4. Research Exhibition, Ingenuity 2021 event held by the University of Adelaide at Adelaide Convention Center, South Australia, Australia, **Appendix 6**
5. University of Adelaide School of Animal and Veterinary Sciences Research Committee Publication Award, 2021 for the publication, doi: 10.1016/j.ijantimicag.2021.106323, **Appendix 7**
6. Antibiotics 2021 Editor's Choice for the publication, doi: 2079-6382/10/6/727

List of Abbreviations

| | |
|------------------|--|
| ACARE | Australian Centre for Antimicrobial Resistance Ecology |
| ADME | Absorption, Metabolism, Distribution, and Excretion |
| AG | Aminoglycosides |
| AMPs | Antimicrobial peptides |
| Amp | Ampicillin |
| AMR | Antimicrobial-resistant |
| BIS | <i>In vivo</i> imaging systems |
| BLIs | β -lactamase inhibitors |
| CCCP | Proton ionophore |
| CDC | Centres for Disease Control and Prevention |
| CFU | Colony-forming units |
| CLSI | Clinical and Laboratory Standards Institute |
| CRAB | Carbapenem-resistant <i>A. baumannii</i> |
| CRE | Carbapenem-resistant Enterobacteriales |
| CRS | Clinical record sheet |
| CRPA | Carbapenem-resistant <i>P. aeruginosa</i> |
| COL | Colistin |
| COL ^R | Colistin-resistant |
| D39LUX | Bioluminescent <i>Streptococcus pneumoniae</i> |
| DiOC2(3) | 3,3-diethyloxacarbocyanine iodide |
| DRI | Dose reduction index |

| | |
|------------------|---|
| EDTA | Ethylenediaminetetraacetic acid |
| EPI | Efflux pump inhibitor |
| ESBLs | Extended spectrum β -lactamases |
| ESKAPE | <i>Enterococcus faecium</i> , <i>Staphylococcus aureus</i> , <i>Klebsiella pneumoniae</i> , <i>Acinetobacter baumannii</i> , <i>Pseudomonas aeruginosa</i> , and <i>Enterobacter</i> spp. |
| EU | European Union |
| FAO | Food and Agriculture Organization |
| FBS | Foetal bovine serum |
| FDA | Food and Drug Administration |
| FICI | Fractional inhibitory concentration index |
| FQ | Fluoroquinolones |
| GNB | Gram-negative bacteria |
| GPB | Gram-positive bacteria |
| HBA | Horse blood agar |
| HC ₅₀ | Haemolytic activity 50% |
| HEK293 | Human embryonic kidney cell line |
| Hep G2 | Human hepatocellular carcinoma cell line |
| HT | Haemolytic titer |
| KPC | <i>K. pneumoniae</i> carbapenemase |
| IC ₅₀ | 50% inhibitory concentration |
| IM | Intramuscular |
| IMP | Imipenem |

| | |
|--------|---|
| IP | Intraperitoneal |
| IV | Intravenous |
| LB | Luria–Bertani |
| LPS | Lipopolysaccharide |
| MBC | Minimum bactericidal concentration |
| MBL | Metallo- β -lactamase |
| MCR-1 | Mobilised colistin resistance |
| MDR | Multidrug-resistant |
| MIC | Minimum inhibitory concentration |
| MRSA | Methicillin-resistant <i>Staphylococcus aureus</i> |
| MRSP | Methicillin-resistant <i>Staphylococcus pseudintermedius</i> |
| MSSA | Methicillin-susceptible <i>Staphylococcus aureus</i> |
| MTD | Maximum tolerated dose |
| NCL179 | 2,2'-bis[(4-chlorophenyl)methylene] carbonimidic dihydrazide hydrochloride |
| NCL195 | 4,6-bis(2-((E)-4-methylbenzylidene)hydrazinyl)pyrimidin-2-amine |
| NDM | New delhi metallo- β -lactamase |
| NOAEL | No observed adverse effect level |
| OM | Outer membrane |
| OIE | World Organisation for Animal Health |
| PBS | Phosphate buffered saline |
| PBP | Penicillin-binding protein |
| PD | Pharmacodynamics |

| | |
|------------------------|---|
| PK | Pharmacokinetics |
| PG | Peptidoglycan |
| PM | Plasma membrane |
| PMB | Polymyxin B |
| PMBN | Polymyxin B nonapeptide |
| RND | Nodulation division superfamily |
| RBCs | Lyse red blood cells |
| RLU | Relative light units |
| SBA | Sheep blood agar |
| TEM | Transmission electron microscopy |
| VIM | Verona integron-encoded metallo- β -lactamase |
| VRE | Vancomycin-resistant enterococci |
| WHO | World Health Organization |
| WGS | Whole-genome sequencing |
| Xen14/ <i>Ec</i> Xen14 | Bioluminescent <i>Escherichia coli</i> Xen14 |
| Xen29/ <i>Sa</i> Xen29 | Bioluminescent <i>Staphylococcus aureus</i> Xen29 |
| Xen41 | Bioluminescent <i>Pseudomonas aeruginosa</i> Xen41 |

List of Figures

| | |
|--|----|
| Figure 1.1. Timeline of antibiotics approved and resistance found. | 4 |
| Figure 1.2. World Health Organization global action plan objectives | 5 |
| Figure 1.3. Structural differences of cell membrane between GNB and GPB..... | 9 |
| Figure 1.4. Mechanisms of antibiotic resistance in GNB. | 10 |
| Figure 1.5. Different mechanisms of actions of efflux inhibitors. | 28 |
| Figure 1.6. Proposed mechanism of action of polymyxins in combination with other antibiotics against GNB..... | 34 |
| Figure 1.7. Schematic representation of bioluminescent mouse model of antimicrobial efficacy testing. | 43 |
| Figure 1.8. Chemical structures of NCL812, NCL179, and NCL195..... | 45 |
| Figure 1.9. Structures of fungal metabolites nidulin and unguinol and semisynthetic unguinol derivatives, benzguinol A and benzguinol B. | 46 |

List of Tables

| | |
|--|----|
| Table 1.1. Existing options for the treatment of MDR-GNB infections | 16 |
| Table 1.2. Recently approved antibiotics for MDR-GNB infections..... | 20 |
| Table 1.3. Peptide-based antimicrobial compounds against GNB in preclinical/clinical trials. | 24 |
| Table 1.4. New antibiotics entities in different stages of development for future treatment of GNB infections | 26 |
| Table 1.5. Potential efflux inhibitors for further treatment of GNB infections..... | 30 |
| Table 1.6. New β -lactamase inhibitors couple with current cephalosporins and carbapenems | 33 |
| Table 1.7. Pre-clinical studies comparing antibiotic + colistin combination therapy vs monotherapy | 36 |
| Table 1.8. Clinical studies comparing antibiotic + colistin combination therapy vs monotherapy | 37 |

Chapter I

Introduction and literature review

Strategies to combat multidrug-resistant Gram-negative bacterial infections

1.1. Antibiotic resistance: A global health and development threat

The persistent use, misuse, and abuse of antibiotics for treating a wide range of infections in humans and animals, as well as food preservation, and agricultural applications over a sustained period have increased the prevalence MDR bacteria in clinical settings [1,2]. In Europe, AMR bacteria caused around 25,000 deaths in 2007 [3], followed by an increase to 33,000 deaths in 2015 [4]. It is estimated that more than 2.8 million AMR infections associated with 35,000 deaths occur each year in the USA (CDC, 2019) [5]. In modelling undertaken by economist Jim O'Neill, antimicrobial resistance is likely to cause 10 million deaths per year by 2050, exceeding combined deaths caused by cancers and diabetes, at a cost \$100 trillion unless the issue is adequately addressed [6].

MDR bacterial infections have become a burden for healthcare systems. It has been estimated that the treatment for a patient infected by an AMR microorganism results in an extra US\$ 10,000-40,000 in healthcare costs [7]. Antibiotic resistance also interrupts hospital activity and results in limited treatment options. In addition, increasing antibiotic resistance potentially threatens the safety and efficacy of surgical procedures and immunosuppressive chemotherapy. In the USA alone, it is estimated that 38.7% - 50.9% and 26.8% of pathogens causing surgical site and chemotherapy-associated infections, respectively are resistant to current antibiotics [8]. The situation is more dire when focusing on the six main pathogens associated with MDR, the so called ESKAPE pathogens (*Enterococcus faecium*, *Staphylococcus aureus*, *Klebsiella pneumoniae*, *Acinetobacter baumannii*, *Pseudomonas aeruginosa* and *Escherichia coli/Enterobacter spp*), which contribute to 700,000 deaths annually [9]. According to a 2019 CDC report, the national cost of treating ESKAPE infections is more than

\$4.6 billion annually [10]. In reference to the ESKAPE pathogens, drug discovery to combat MDR-Gram-negative bacteria (GNB) encounters more challenges than MDR-Gram-positive bacteria (GPB) due to the presence of an OM in GNBs, which prevents many antibiotics from gaining entry to GNB cell and exerting their effect [11]. Moreover, it was reported that while the incidence of methicillin-resistant *S. aureus* (MRSA) has slightly decreased in recent times, the incidence of MDR- GNB infections has increased [12].

Unfortunately, the rate of approval of new drugs by the FDA is not commensurate with the increasing pace of MDR pathogen evolution [13] (Figure 1.1). For example, *K. pneumoniae* immediately developed resistance to ceftaxidime-avibactam in the same year this new combination of β -lactam/ β -lactamase inhibitor was approved for clinical use (Figure 1.1). Moreover, the new drug discovery and development process can cost over US\$ 2.6 billion and may take up to 15 years from discovery to market [14-16]. Furthermore, novel drug development also carries a high risk (nearly 84%) of failure in the pre-clinical stage [17]. Some drugs have recently been approved for specific MDR infection indications such as plazomicin (aminoglycoside (AG) derivative) for complicated urinary tract infections, eravacycline (fluorocycline derivative) for complicated intra-abdominal infections, sarecycline (tetracycline derivative) for the treatment of non-nodular moderate to severe acne, omadacycline (tetracycline derivative) for skin infections and community-acquired bacterial pneumonia, rifamycin for complicated intra-abdominal infections (2018), imipenem + cilastatin + relebactam (new carbapenem + β lactamase inhibitor) combination used for complicated urinary tract infections, lefamulin (a first-in-class pleuromutilin) used in community-acquired bacterial pneumonia, and cefiderocol (cephalosporin derivative) for complicated urinary tract infections (2019) [18]. These all recently approved drugs are analogues of existing antibiotic classes. In addition, around one hundred new antibiotics are

in different stages of clinical development, with 19 current antibiotics showing potential to treat KAPE infections recorded up to December 2020 [19]. However, the suite of currently available and in development antimicrobials is not proceeding at a fast enough pace to fully combat the widespread emergence of MDR pathogens. Thus, there is a real need and urgency to develop novel antibiotic drugs and strategies to overcome MDR infections in particular those caused by GNB.

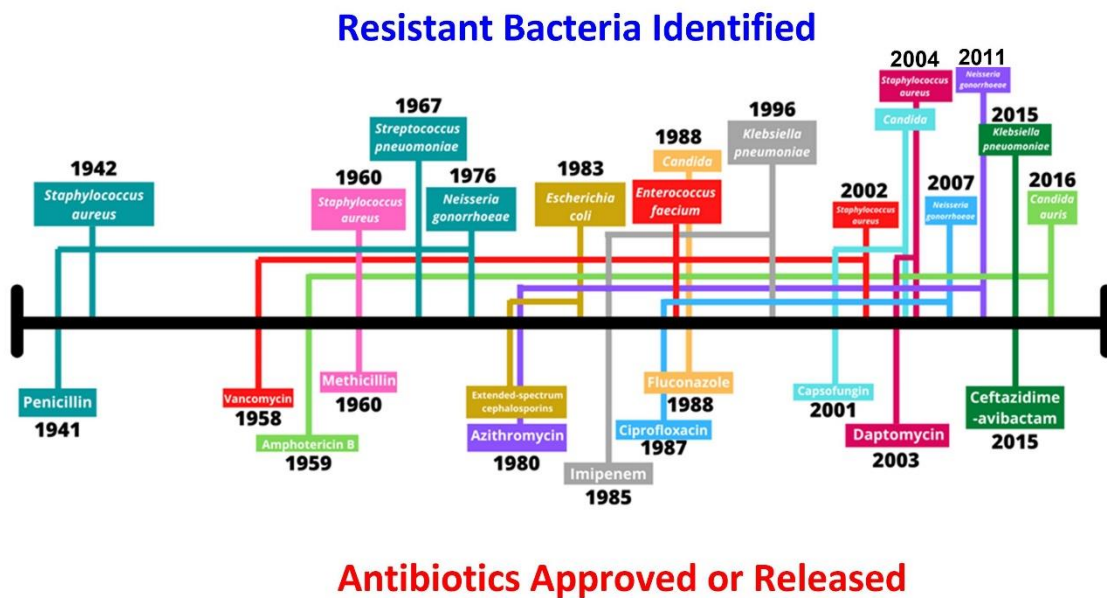


Figure 1.1. Timeline of antibiotics approved and resistance found.

Source: CDC, 2019 and modification by lgc standards [20]

To ensure the problem posed by MDR infections is strategically and urgently addressed, the WHO collaborated with FAO of the United Nations and OIE, and published a global action plan in 2015 [21]. The plan draws upon five objectives relevant to the health care, industry, and veterinary sectors (Figure 1.2). The plan aims to preserve the effectiveness of currently available antimicrobials and develop new agents to prevent, treat, and diagnose microbial infections to create a sustainable future [21]. In addition, international institutions

such as the EU, G20, UN General Assembly, World Bank, WHO, and the US and UK governments have issued documents calling for action including developing new antibiotics with novel mechanisms of action against MDR-ESKAPE pathogens [22].



Figure 1.2. World Health Organization global action plan objectives

(Geneva: World Health Organization, 2019). Adapted from Pierce *et al.*, [21]

Given the distinctive structure of GNB (i.e. presence of an OM), fewer treatment options are available for GNB infections compared to GPB infections. GNB are also more likely to acquire resistance via mobile genetic elements compared to GPB, and cause more significant morbidity and mortality worldwide. Thus, new antibiotics to treat GNB infections are urgently needed. However, pharmaceutical research has tended to focus on developing new antibiotics against the less challenging MDR-GPB while the development of new antimicrobials to MDR-GNB infections has often been neglected [14-16]. Therefore, this literature review will specifically focus on providing an overview of strategies to address the shortfall of antibiotics to combat MDR-GNB infections and will not provide in depth analysis

of approaches for GPB infections. Firstly, the review will briefly describe critical GNB pathogens listed by WHO and their different antibiotic resistance mechanisms to identify the main challenges faced in drug discovery and development to treat GNB infections. After synthesising information on existing antibiotics and indicating the limitations of current approaches, the review will provide a comprehensive critical overview of novel antibiotics and new strategies for the future treatment of MDR-GNB infections.

1.2. Gram-negative bacteria

1.2.1. GNB infections

GNB bacterial pathogens receive the highest clinical attention because infected patients often require intensive care and they are often associated with increased risk of mortality [23]. GNB pathogens including Enterobacteriales such as *E. coli*, *K. pneumoniae*, *Enterobacter* spp., *Proteus* spp. and *Serratia* spp., as well as non-fermenting opportunistic bacteria such as *P. aeruginosa* and *A. baumannii*, account for approximately half of all bacteraemias [24]. *E. coli* is the leading cause of hospital-acquired urinary tract infections and is often a component of the mixed flora found in intra-abdominal infections. *P. aeruginosa*, *K. pneumoniae* and *Enterobacter* spp. are important in nosocomial pneumonia, especially in patients with prolonged hospitalisation. *A. baumannii* notoriously causes outbreaks in the most vulnerable patients in intensive care units [22].

GNB are a major component of the ESKAPE pathogens that are a leading cause of nosocomial infections worldwide [9]. KAPE pathogens often cause severe and deadly conditions such as bloodstream infections and pneumonia and have developed resistance to a wide range of antibiotics [25,26]. Therefore, they are categorised in the most critical group of the WHO priority list of bacteria for which new antibiotic classes are urgently needed [27].

1.2.2. Critical GNB KAPE pathogens

Carbapenemase-producing *A. baumannii* (CRAB) strains carrying metallo- β -lactamases encoded by *bla*_{IMP}, and oxacillinase serine β -lactamases encoded by *bla*_{OXA} are of the most concern in health care settings due to their resistance to imipenem [28]. CRAB rates exceed 90% in Asia and Europe [29]. The mortality rate for CRAB infections (such as hospital-acquired pneumonia and bloodstream infections), is about 60% higher than for carbapenem-susceptible *A. baumannii* infections [30,31]. In addition, diseases caused by CRAB are of particular concern because they often are resistant to most traditional antibiotics as well as the last line options colistin and tigecycline [32]. Therefore, current options for CRAB infections are limited [33].

Carbapenem-resistant Enterobacteriales (CRE) represent another critical group of pathogens that produces carbapenemases such as *K. pneumoniae* carbapenemase (KPC)-type, New Delhi Metallo- β -lactamase (NDM)-type and OXA-48-type enzymes [34]. Carbapenem-resistant *K. pneumoniae* (CRKP) pathogens, which are the most clinically prominent CREs [35], are common pathogens causing severe infections such as bloodstream infections, pneumonia, complicated urinary tract infections, and complicated intra-abdominal infections [36]. CRKP was first reported in the USA in 2001 [37], then spread across several locations such as Europe, Australia, India, Sri Lanka, and China from 2005 to 2010 [38-41]. Notably, AMR hyper-virulent *K. pneumoniae* strains, cause necrotising fasciitis associated with higher mortality first emerged in Taiwan [42] and have now been detected in many developed and developing countries [41,43,44]. Extended-spectrum β -lactamase (ESBL)-containing *E. coli* also contributes significantly to the developing threat of CRE, with more than one-third of community-associated infections occurring in patients without healthcare-associated risk

factors. ESBL and KPC-producing *E. coli* isolates also confer cross-resistance to many other common antibiotics currently used to treat GNB such as quinolones and AGs [35].

P. aeruginosa is an opportunistic pathogen associated with burn wound infections, biofilm formation on medical devices and lung infection in cystic fibrosis patients [45]. Carbapenemase-producing *P. aeruginosa* (CRPA) expressing KPC, active-on-imipenem (IMP), Metallo- β -lactamase (MBL), NDM and Verona integron-encoded Metallo- β -lactamase (VIM)-producing CRPA have been identified [46]. Infections caused by *P. aeruginosa* result in higher morbidity than those caused by members of the Enterobacteriales. Moreover, infections with *P. aeruginosa* are often challenging for clinical treatments because of its intrinsic non-susceptibility to many commonly used antimicrobial drugs [47].

1.2.3. The GNB outer membrane barrier.

The OM is a distinct feature differentiating GNB from GPB (Figure 1.3) that acts as a barrier to protect GNB from the entry of many types of molecules including a number of antibiotic classes [48]. The OM is composed of a lipid bilayer divided into two leaflets. The inner leaflet of this membrane contains phospholipids and the outer leaflet is composed of glycolipids, principally lipopolysaccharide (LPS) [48]. An oligosaccharide unit, a part of the LPS, forms the *O*-antigen that is a major target for both the immune system and bacteriophages; therefore, it is one of the most variable cell membrane constituents [49]. The non-fluid continuum formed by the LPS molecules is a very effective barrier for hydrophobic molecules [50]. The OM is also characterised by the presence by various porin proteins that act as specific water-filled open channels to control the intake of hydrophilic molecules [48].

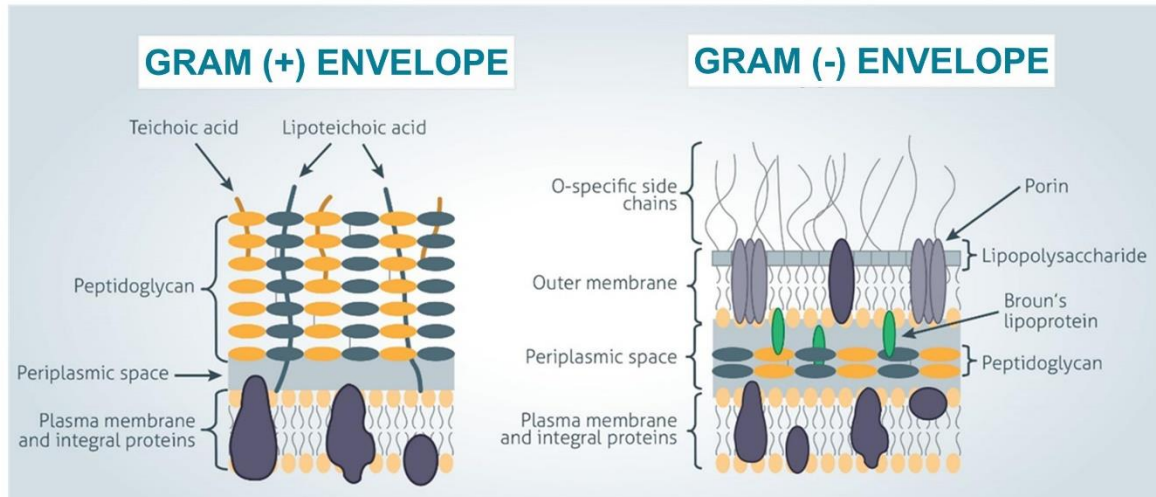


Figure 1.3. Structural differences of cell membrane between GNB and GPB.

Envelope of GPB contains a thick peptidoglycan layer interlinked with teichoic and lipoteichoic acids anchored to the plasma membrane. GNB possess inner (analogous to the GPB plasma membrane) and outer cell membrane and only a thin peptidoglycan layer located between the two. The OM, which is the unique feature of GNB, is an extra protective layer to prevent the entry of many types of molecule including some antibiotics. Adapted from Steward [48]

1.2.4. AMR mechanisms in GNB

GNB pathogens have developed resistance to a wide range of antibiotics through several different mechanisms including efflux systems, enzyme inactivation, drug modification, target modification, lipopolysaccharide modification, permeability alternation and several others (Figure 1.4).

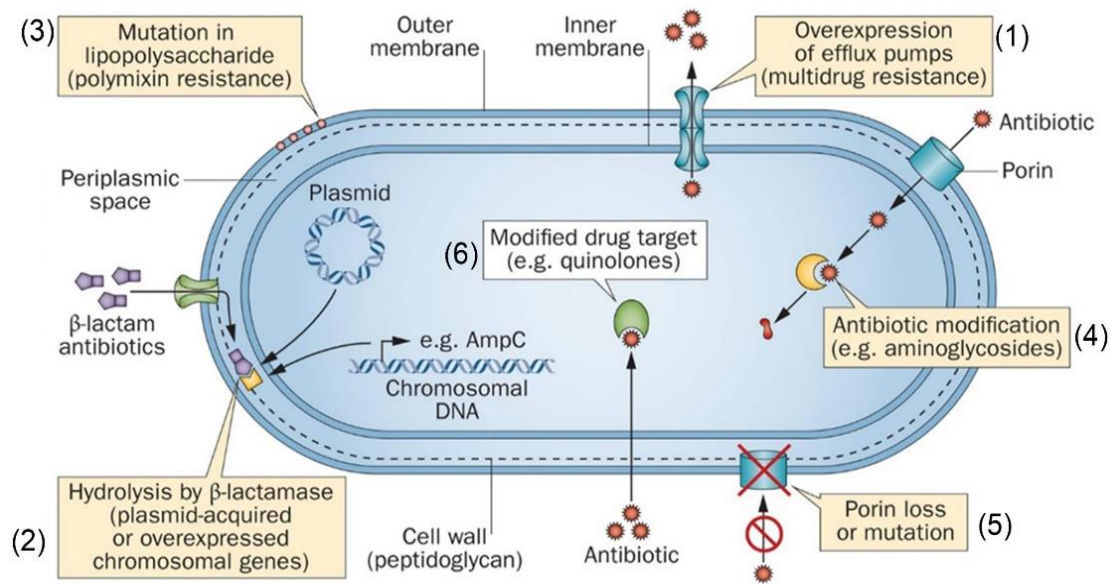


Figure 1.4. Mechanisms of antibiotic resistance in GNB.

1) Drug transporter efflux systems can export many antimicrobials out of bacteria. 2) Antibiotic inactivation by β -lactamase enzymes. 3) Inhibition of drug uptake via permeability changes to the bacterial cell wall (resistance to polymyxins). 4) Target modifications allow the bacteria to function in the presence of the antibiotic (resistance to AG). 5) Porin loss or mutation can reduce antibiotic permeability (resistance to carbapenems). 6) Alteration of the drug target to stop antibiotics (resistance to quinolones) binding to the active site. Adapted from Zowawi *et al.*, [51].

Multidrug resistance mediated by efflux pumps strongly contributes to the challenges posed in drug discovery to treat GNB infections. Efflux is initiated by active transporters localised in the cytoplasmic membrane and requires a chemical energy source to pump out unwanted compounds [52,53]. Efflux pumps are categorised into six different structural superfamilies: ATP binding cassette superfamily, major facilitator superfamily, the multidrug and toxic compound extrusion family, the small MDR superfamily, the resistance nodulation

division superfamily (RND), and the proteobacterial antimicrobial compound efflux family. Each family contains several critical efflux pumps, and each efflux pump can export more than one antibiotic [52-54]. For instance, MexAB-OprM, one of the RND family members, is responsible for resistance to meropenem, fluoroquinolones, sulfonamides, β -lactams, cephalosporins, fluoroquinolones, macrolides, novobiocin, tetracycline, chloramphenicol, and some detergents in *P. aeruginosa* [54,55].

The inactivation of β -lactam antibiotics by β -lactamases is another major MDR mechanism in GNB [26,56]. There are four classes of β -lactamases, including: (A) penicillinases, (B) ESBLs, (C) the AmpC cephalosporinases, and (D) the carbapenem-hydrolysing enzymes or OXAs β -lactamases. Class B β -lactamases have a broad range and potent carbapenemase activity imparting resistance to all β -lactam antibiotics apart from monobactams; class C are resistant to cephamycins (cefoxitin and cefotetan), penicillins and cephalosporins, and class D are specific to oxacillin and also can hydrolyse extended-spectrum cephalosporins and carbapenems [26,56]. ESBL-producing organisms are able to readily acquire resistance to other antibiotic classes such as quinolones, tetracyclines, cotrimazole, trimethoprim, and AG through plasmid-mediated and/or chromosomally encoded mechanisms [56].

Target modification mechanisms allows GNB to function in the presence of the antibiotics, which is commonly associated with AG resistance [57]. GNB produce plasmid- or transposon-encoded AG-modifying enzymes (acetyltransferases, adenylyltransferases, and phosphotransferases) [57] to modify AG class resulting in decreasing the binding affinity of the drug for its target and losing antibiotic potency [58]. AG- modifying enzymes are commonly associated with antimicrobial resistance in *A. baumannii* [57].

Lipopolysaccharide modification is a mechanism conferring resistance to antimicrobial peptides (AMPs) such as polymyxins [59]. These modifications involve the addition of positive residues to LPS structure, often to lipid A, to mitigate its negative charge. Common positively-charged additions to LPS are fatty acid, phosphoethanolamine and aminoarabinose to the lipid A components [59]. For example, *P. aeruginosa* develops resistance to AMPs by adding the amine containing sugar aminoarabinose to lipid A phosphate group [59]. .

GNB can also alter OM permeability by changing envelope structure. Porins are proteins forming channels to transport molecules across the OM; therefore, reduced or absence of expression of porins such as CarO and Omp22-33 cause carbapenem resistance in *A. baumannii* [26] or mutation in OprD increases resistance in *P. aeruginosa* mediated by AmpC β -lactamases [61].

Gram-negative bacteria modify antibiotic target sites to render the bacteria less susceptible to fluoroquinolones [62]. Fluoroquinolones form complexes with DNA gyrase and topoisomerase IV, effectively blocking bacterial DNA replication [63]. Resistance to fluoroquinolones occurs primarily via mutations that lead to amino acid substitutions within the *grlA/grlB* and *gyrA/gyrB* genes encoding subunits of DNA topoisomerase IV and DNA gyrase, respectively [64].

Capsule expression and biofilm formation are other mechanisms that contribute to the challenges posed in the treatment of GNB infections [60]. The bacterial capsule is a protective layer external to the OM that acts as an additional barrier. For example, *K. pneumoniae* capsule provides increased resistance against cationic defensins, lactoferrins and polymyxins. Furthermore, bacteria can form biofilms on diverse surfaces that both aids in adherence to surfaces and act as a barrier to unwanted chemicals [14,26].

1.3. Current options for MDR-GNB infections

1.3.1. Existing drug classes

Some currently registered antimicrobial classes including the polymyxins, AGs, tetracyclines (tigecycline only), fosfomycin, and carbapenems may still be an option in certain situations to treat complicated MDR-GNB infections, but they present limitations related to toxicity (e.g. polymyxins, AGs) and rapid development of resistance (e.g. carbapenems, tigecycline) (Table 1.1).

Polymyxins (colistin [polymyxin E] and polymyxin B [PMB]) were initially used in the 1950s for the treatment of GNB infections [65]. However, polymyxins are associated with nephrotoxicity, neurotoxicity and neuromuscular blockade [66]. Therefore, polymyxins are considered as the last line reserved treatments for GNB infections resistant to other safer antimicrobial classes [14]. Despite high toxicity levels, polymyxins have been frequently used to treat MDR-GNB infections, including CRE, CRPA, and CRAB in the past few decades when some or only one option for treatment is available. Therefore, it is necessary to optimise dosages and indications of polymyxins to maximise effectiveness, reduce toxicity and curb the emergence of further polymyxin resistance [67].

The AG class represents antibacterial agents that kill GNB pathogens by interfering with the bacterial 30S ribosomal subunit, resulting in aberrant protein production and associated cell membrane damage [68]. The most commonly used AG is gentamicin, however, amikacin is particularly potent against MDR-GNB [14]. AGs are used to treat severe urinary tract infections, bacteraemia and endocarditis. In particular, AGs have been often used to treat CR or polymyxin-resistant GNB in recent years [69]. However, their toxicity (nephrotoxicity, ototoxicity and reduced lung concentrations) and increased resistance

development have limited effective use of the classical AGs (gentamicin, amikacin) in many clinical settings [14].

Tigecycline is a bacteriostatic glycycline binding to the 30S ribosomal subunit with good tissue penetration but low serum concentrations. Tigecycline is usually used to treat CRE and CRAB infections, but not CRPA infection since *P. aeruginosa* is inherently resistant to tetracyclines. Tigecycline has also been used in combination with other agents to treat severe CRE and CRAB infections [70].

Finafloxacin is a pH-activated fluoroquinolone approved to treat severe bacterial infections associated with an acidic environment, including urinary tract infections and *Helicobacter pylori* infections [71-73]. It is highly selective for bacterial type II topoisomerases, including DNA gyrase and DNA topoisomerase IV [74]. The MIC of finafloxacin is equivalent to other class members, such as levofloxacin, ciprofloxacin, and moxifloxacin at pH 7.2–7.4 but is more potent at a pH of 5.8. This feature of finafloxacin makes it a preferred option in treating urinary infections due to the acidic environment in urinary tract [71,75,76].

Fosfomycin is an analogue of phosphoenolpyruvate that kills bacteria by inhibiting the early stages of cell wall synthesis [28]. Fosfomycin is usually used for urinary tract infections due to the high concentration of distribution this system [77]. However, the use of fosfomycin monotherapy for systemic infections may be problematic because of the potential for resistance development during treatment [78]. Therefore, it is often used with other antibiotics such as colistin and carbapenems in combination where few or no alternatives are available [14].

Carbapenems are β -lactam antibiotics commonly used to treat MDR-GNB due to their efficient broad-spectrum antibacterial effect rather than penicillin, cephalosporin, and β -lactam + β -lactamase inhibitor combinations [79]. They bind to penicillin-binding proteins (PBP) to interrupt cell synthesis resulting in bacterial lysis [80]. Carbapenems exhibit better stability against β -lactamase enzymes than other β -lactam antibiotics [79]. Clinical studies demonstrated that carbapenems do not cross the gastrointestinal tract permeability barrier; thus, they must be administered intravenously (IV) or intramuscularly (IM) [81]. The traditional carbapenem antibiotics in the market are meropenem, ertapenem, doripenem, biapenem, panipenem/betamipron in addition to newer carbapenems such as razupenem, tebipenem, tomopenem, and sanfetrinem [81]. However, the preferential use of carbapenems in clinical healthcare settings for a very long period has led to an increase in the prevalence of CR-GNB pathogens such as CRE, CRPA, and CRAB [82].

Table 1.1. Existing options for the treatment of MDR-GNB infections

| Class | Antibiotic | Mode of action | Mode of resistance | Target organism | Toxicity | References | |
|-------------|------------|---|---|---|--|--|------|
| Carbapenems | Meropenem | Binding to PBP to inhibit cell wall synthesis | Efflux pump, inactivation by β -lactamases | ESBL-producing GNB, limited activity against non-fermentative GNB | Allergy, headache, gastrointestinal symptoms, blood count changes, cramp, nephrotoxicity | [78] | |
| | Ertapenem | | | ESBL-producing GNB but limited activity against <i>P. aeruginosa</i> , <i>Acinetobacter species</i> | | [83] | |
| | Doripenem | | | The most potent <i>in vitro</i> activity against <i>P. aeruginosa</i> | | Headache, nausea, diarrhoea, rash, and phlebitis | [84] |
| | Imipenem | | | Very active against <i>P. aeruginosa</i> and <i>A. baumannii</i> | | Histopathological changes in the testis, spermatogenesis dysfunction | [85] |
| Polymyxin | Colistin | Change permeability of OM | Alteration of the lipid A negative net charge to a neutral charge | MDR-GNB including CRAB, CRE, CRPA | Nephrotoxicity, neurotoxicity and neuromuscular blockade | [66,86] | |
| | PMB | | | | | | |

Table 1.1 (continued)

| Class | Antibiotic | Mode of action | Mode of resistance | Target organism | Toxicity | Reference |
|---------------------|-------------------|--|---|---|--|------------------|
| AG | Gentamycin | Biding to 30S | Producing AG modifying | MDR-GNB | Nephrotoxicity and ototoxicity | [87] |
| | Tobramycin | ribosomal subunit to | enzymes, alteration of | | | |
| | Amikacin | inhibit protein synthesis | target site, change of uptake and efflux | | | |
| Glycycycline | Tigecycline | Biding to 30S ribosomal subunit to inhibit protein synthesis | Carry tetracycline resistance genes and efflux-mediated resistance | Highly active against the Enterobacteriales, ESBL-producing <i>E. coli</i> and <i>K. pneumoniae</i> | Nausea, vomiting and diarrhoea | [88] |
| | Fosfomycin | Inhibits the biosynthesis of peptidoglycan | Inactivation in phosphonate transport or uptake pathways, antibiotic modification using several enzymes | Common pathogenic GNB including <i>E. coli</i> , <i>P. aeruginosa</i> | Gastrointestinal symptoms, headache, vaginitis, local pain and heart failure | [89] |
| FQ | Finaxofloxacin | DNA gyrase and topoisomerase IV inhibitor | Resistant breakpoints have not yet been defined | Ciprofloxacin-resistant <i>E. coli</i> , ESBL-producing <i>E. coli</i> and <i>K. pneumoniae</i> strains | Local pruritus and nausea | [74,90] |

Note: CRAB, carbapenem-resistant *A. baumannii*; CRE, carbapenem-resistant Enterobacteriales; CRPA, carbapenem-resistant *P. aeruginosa*; ESBLs, extended spectrum β -lactamases, AG, aminoglycoside; PBP, penicillin-binding protein; GNB, Gram-negative bacteria; FQ, fluoroquinolones

1.3.2. Recently approved drugs

Some new/current expanded-spectrum cephalosporins/carbapenems and new/current β -lactamase inhibitor combinations, and few new derivatives of existing antibiotic classes have significantly improved choices for antimicrobial agents with demonstrated activity against a variety of MDR-GNB (Table 1.2). However, none of these new drugs has overcome the issues associated with OM barrier permeability and antibiotic efflux in specific GNB pathogens.

Ceftazidime-avibactam (CAZ-AVI) has been considered a promising treatment for MDR-GNB infections, particularly infections caused by CRE expressing class A, class C, and some class D carbapenemases [91]. Unfortunately, resistance has been recorded in *K. pneumoniae* isolates from several patients in the same year CAZ-AVI was approved [86]. Meropenem-vaborbactam is considered to be a first-line option to treat severe CRE infections caused by KPC-producing pathogens [92,93]. Ceftolozane-tazobactam is a novel cephalosporin + current β -lactamase combination that exhibits activity against AMR *P. aeruginosa*, ceftazidime-resistant *E. coli* and *K. pneumoniae* [94]. Imipenem + cilastatin + relebactam combination is an IV administered combination of the carbapenem (imipenem), the renal dehydropeptidase-I inhibitor (cilastatin), and a novel β -lactamase inhibitor (relebactam). Relebactam is a potent inhibitor of class A and class C β -lactamases, conferring imipenem activity against many imipenem-non-susceptible GNB [95,96]. Imipenem + cilastatin + relebactam combination has shown good antimicrobial activity against MDR-GNB including CRE and excluding MBL-producing Enterobacterales and CRAB, was approved to treat complicated urinary tract infections in the absence of alternative treatment options [97]. In particular, cefiderocol appears to be well-positioned to treat CR- and MDR-GNB including ESBL- and carbapenemase-

producing Enterobacteriales strains, KPC-producing *P. aeruginosa*, and *A. baumannii*. Cefiderocol is also more potent than ceftazidime-avibactam and meropenem against all resistance phenotypes of *P. aeruginosa*. The presence of a catechol group on the side chain at position 3 of cefiderocol is a major chemical difference compared to other β -lactams [98]

Plazomicin (new AG derivatives), eravacycline and omadacycline (new tetracycline derivatives) have recently been approved to treat MDR-GNB infections. Plazomicin, has some attractive clinical features including better pharmacokinetics and less toxicity compared to other AG class members and a broad-spectrum of activity against aerobic GNB such as ESBL-producing Enterobacteriales, CRAB, and organisms with AG-modifying enzymes [99-101]. Eravacycline has similar broad-spectrum activity compared to tigecycline but better pharmacokinetics [102-105] and good antimicrobial activity against difficult-to-treat GNB pathogens in preclinical studies such as CRE and CRAB [106,107]. Omadacycline has a similar chemical structure to tigecycline with an alkylaminomethyl group replacing the glycyclamido group at the C-9 position of the D-ring of the tetracycline core. Omadacycline exhibits broad-spectrum activity against MDR-GNB, including CRE and CRAB and remains active against GNB isolates resistant to tetracycline and other antibiotics [108].

Table 1.2. Recently approved antibiotics for MDR-GNB infections

| Class | Antibiotic | Mode of action | Mode of resistance | Target organism | Toxicity | Approval | Reference |
|--|--|---|---|---|--|----------|-----------|
| New/current cephalosporin/carbapenems + new/current β -lactamases | Ceftazidime + avibactam (novel inhibitor) | Inhibiting the activity of β -lactamases | CAZ-AVI resistance was found in <i>K. pneumoniae</i> clone ST307 harbouring <i>blaKPC-2</i> | ESBL-, AmpC-, KPC- and OXA-48-producing <i>Enterobacterales</i> and MDR- <i>P. aeruginosa</i> | Nausea, vomiting and positive Coombs test | Feb 2015 | [109] |
| | Meropenem+ vaborbactam (novel inhibitor) | Inhibiting the activity of β -lactamases | Modification of intrinsic (AmpC) and horizontally acquired β -lactamases | Serious GNB such as CRAB, CRE and CRPA | Nausea, vomiting, gastrointestinal symptoms, headache, positive comb test, fever and elevated liver values | Aug 2017 | [110] |
| | Ceftolozane + tazobactam (new β -lactam) | Binding to PBP to interrupt cell wall synthesis | Expressing ESBLs, plasmid-mediated AmpC enzymes, and carbapenem-hydrolyzing β -lactamases | ESBL-producing <i>Enterobacterales</i> , off-label for CRPA | Nephrotoxicity | Jun 2019 | [111,112] |
| | Imipenem + cilastatin + relebactam (MK-7655) | Inhibiting the activity of β -lactamases | Expressing ESBLs | MDR-GNB, CRE, CRKP | Less nephrotoxicity than colistin | Jun 2019 | [95,97] |

Table 1.2 (continued)

| Class | Antibiotic | Mode of action | Mode of resistance | Target organism | Toxicity | Approval | Reference |
|--------------|-----------------------|--|---|--|--|----------|------------------|
| β-lactams | Cefiderocol | Binding to PBP to inhibit cell wall synthesis | Producing β-lactamases | KPC-producing <i>E. coli</i> , CRAB and MDR GNB, MDR <i>P. aeruginosa</i> , <i>A. baumannii</i> . | No serious or clinically significant adverse events | Nov 2019 | [98,113,114] |
| | Plazomicin | Binding to bacterial ribosome 30S subunit to inhibit protein synthesis | Modification of the target site, alteration of AG uptake and efflux, producing AG-modifying enzymes | Aerobic GNB including ESBL-producing Enterobacteriales, CRE, and organisms with AG-modifying enzymes | Less nephrotoxicity and ototoxicity than other class members | Jun 2018 | [99-101] |
| AG | Eravacycline (TP-434) | Binding to bacterial ribosome 30S subunit to inhibit protein synthesis | Not yet reported | CRE, CRAB and GNB pathogens exhibiting TET-specific acquired resistance mechanisms | Nausea and vomiting | Aug 2018 | [18,105,115,116] |
| | Omadacycline | Binding to bacterial ribosome 30S subunit to inhibit protein synthesis | Not yet reported | <i>E. coli</i> | Nausea and vomiting | Oct 2018 | [108,117,118] |
| Tetracycline | | | | | | | |

Note: CAZ-AVI, ceftazidime + avibactam; KPC, *K. pneumoniae* carbapenemase; CRAB, carbapenem-resistant *A. baumannii*; CRE, carbapenem-resistant Enterobacteriales; CRPA, carbapenem-resistant *P. aeruginosa*; ESBLs, extended spectrum β-lactamases; AG, aminoglycoside; PBP, penicillin binding protein.

1.4. Antibiotic therapy advances to combat MDR-GNB

Obviously, currently used and newly approved antibiotics cannot completely deal with the looming AMR crisis, particularly those posed by MDR-GNB. Therefore, scientists are targeting several approaches to develop new classes of antibiotics to fight and control resistant GNB infections, including (1) discovery of natural antibiotics; (2) expanding new chemical entities; (3) finding new efflux inhibitors; (4) combination therapy; (5) drug repurposing; and (6) “lost antibiotics” strategy.

1.4.1. Natural products as sources of new antibiotics

Microbial natural products have historically been crucial in identifying and developing antibacterial agents [119]. An estimated two-thirds of antimicrobial molecules currently used in human medicine, were originally extracted from Actinobacteria and fungi [120]. In the early stage of natural antimicrobial discovery from microorganisms, new antibiotics were found using low-throughput fermentation and whole-cell screening methods. In the following stage, molecular genetics and medicinal chemistry approaches were used to modify and improve the activities of important chemical scaffolds. Later, advances in bioinformatics, proteomics, mass spectrometry, metabolomics, transcriptomics, and gene expression have driven the new field of microbial genome mining for applications in natural product discovery and development [121].

Antimicrobial peptides (AMPs), which are the most potent sources of natural products isolated and purified from bacteria, fungi, marine organisms, insects, herbs, and mammals [122], are evolutionary well-conserved amphipathic molecules with hydrophobic and cationic amino acids [123]. AMPs show high selectivity, efficiency, tolerance, and they use many modes of action to interfere with multiple biological processes in bacterial pathogens

resulting in less resistance in bacteria [124]. These properties make AMPs an attractive alternative in drug development. So far, several AMPs have been developed to treat bacterial infections [123,125]. Overall, 2,478 AMPs were already known (updated to 2016), which are mainly used for oncological and metabolic diseases [126] with only a few compounds showing potential activity against GNB pathogens presented in Table 1.3.

There are several disadvantages associated with an approach based on finding new natural products. Firstly, only a limited number of discovered natural antibiotics were actually suitable for downstream antibiotic development [127]. The significant technical challenges in the identification, purification, synthesis, and scale-up production of natural products are the second issue that requires high manufacturing costs. Peptide stability and toxicity are the third major concern that has not yet been adequately addressed [123]. Therefore, synthetic peptides mimicking natural antibiotics is considered to be the most viable future strategy to overcome these challenges [128].

Lipids, isolated from plants and marine organisms, demonstrating a broad spectrum of antimicrobial activities, are another source of natural products [129,130]. For example, fatty acids and their derivatives from n-hexane and chloroform extracts from the heartwood of *Albizia adianthifolia* exhibit antimicrobial activity against *E. coli* and *P. aeruginosa* [131-133]. These biomolecules are promising alternatives to further treat GNB infections due to demonstrating *in vitro* activity, microorganisms do not develop resistance to them, and they have high safety levels when exposed to mammalian cell lines [133]. However, natural source-derived antimicrobial lipids are complex to extract and exhibit difficulty in purification, structural characterisation, and mechanism of action investigation [129].

Table 1.3. Peptide-based antimicrobial compounds against GNB in preclinical/clinical trials.

| Name | Target organisms | Class | Mode of action | Stage of development | Reference |
|------------------------|--|-------------------------------|--|----------------------|-----------|
| Murepavadin (POL7080) | CRPA and colistin-resistant <i>P. aeruginosa</i> | Antimicrobial peptide mimetic | OM disruption via binding to protein transporter LptD | Phase II | [134-140] |
| Enterocin A-Colicin E1 | <i>E. coli</i> , <i>P. aeruginosa</i> | Bacteriocins | The permeabilisation of the cytoplasmic membrane, or inhibition of protein synthesis | Preclinical | [141] |
| SB006 | <i>P. aeruginosa</i> | Multimeric peptide | Fragmentariness and loss of solidarity of the membrane wall | Preclinical | [142] |
| Dorapactin | Colistin-resistant <i>E. coli</i> , <i>K. pneumoniae</i> , MDR- <i>E. coli</i> and | Recombinant peptide | Stabilising a closed lateral gate upon binding to BamA (an OM protein) to prevent the exit of substrates into the OM | Preclinical | [143] |

Note: CRPA, carbapenem-resistant *P. aeruginosa*; ESBLs, extended spectrum β -lactamases; MDR, multidrug-resistant; OM, outer membrane

1.4.2. Expanding antibiotic chemical diversity

Expanding the chemical diversity of antibiotics offers a path for the exploitation and improvement of natural products, including semi-synthesis, full synthesis, and synthesis biology [144]. The semi-synthesis approach is widely used to modify chemical structures of natural antimicrobial scaffolds utilising a variety of chemical reactions [127,145]. However, structures of natural products are always complex; thus, specific chemical modification is inherently challenging, resulting in the markedly slow development of this route in drug discovery [146]. Full synthesis, an alternative approach, has enabled deep-seated structural modifications that are not achievable by semi-synthesis to create many new classes of antibiotics including new derivatives of carbapenems, quinolones, chloramphenicol, oxazolidinones, metronidazole, fosfomycin, and trimethoprim [146]. Another approach is synthetic biology where gene clusters are inserted into microbes as compound-making factories to create libraries of natural products by manipulating and mutating these biosynthetic genes. This method enables the construction of chemical libraries suitable for screening and optimising any promising compounds as drug candidates [144,147].

Synthesis pathways can provide many potential compounds that medicinal chemists can readily modify in the laboratory [127]. In this approach, drug discovery foregoes the diverse bioactivity of natural products and their associated chemical complexes in favour of predictions in outcomes of totally synthetic chemistry [127]. Many examples of new antibiotic entities are summarised in Table 1.4. For instance, SPR206, a novel PMB derivative, exhibited superior potency to colistin and PMB, with 2- to 4-fold lower MIC_{50/90} values against MDR, tigecycline-resistant and non-MDR clinical isolates of GNB pathogens [148].

Table 1.4. New antibiotics entities in different stages of development for future treatment of GNB infections

| Class | Antibiotic | Target organism | Development Stage | Reference |
|------------|-------------------------|--|---|-----------|
| | QPX9003 | MDR <i>P. aeruginosa</i> , <i>A. baumannii</i> and <i>K. pneumoniae</i> | Phase 1 clinical development has commenced | [149] |
| | SPR206 | 2-4-fold lower MIC than colistin and PMB against <i>A. baumannii</i> , <i>P. aeruginosa</i> and Enterobacteriales | Phase I: generally well-tolerated after single and multiple doses without serious adverse events. | [148,150] |
| | SPR741 | MIC (16 µg/mL) against most species but in combination with azithromycin, fusidic acid, vancomycin, doxycycline, and minocycline shows activity against ESBL, carbapenemase-producing and colistin-resistant GNB | Phase I: generally well tolerated at doses up to 1,800 mg/day | [151,152] |
| Polymyxins | NAB739 and NAB815 | 2-fold higher MIC than PMB against polymyxin-susceptible <i>E. coli</i> and <i>K. pneumoniae</i> ; 4-fold higher MIC than PMB against polymyxin-susceptible <i>Acinetobacter</i> spp. and <i>P. aeruginosa</i> | Preclinical trial: better efficacy than PMB for the treatment of murine <i>E. coli</i> pyelonephritis | [153-155] |
| | CB-182, 804 | 2-fold higher MIC than PMB against MDR-GNB | Phase I: failed due to unacceptable toxicity | [156] |
| | CA824 | Similar MIC to PMB against <i>E. coli</i> , <i>K. pneumoniae</i> , and <i>P. aeruginosa</i> but 4-fold higher MIC than PMB against <i>A. baumannii</i> | Preclinical trial: similar efficacy to PMB in CRAB infected thigh mouse model but better efficacy than PMB in CRAB and CRPA mouse lung infection models | [156] |
| | MicuRx 12 and MicuRx 18 | Similar MIC to PMB against <i>E. coli</i> , <i>A. baumannii</i> , and <i>P. aeruginosa</i> | Preclinical trial: lower nephrotoxicity than PMB | [156] |

Table 1.4 (continued)

| Class | Antibiotic | Target organism | Development Stage | Reference |
|--------------|---|--|--|-----------|
| Tetracycline | KBP-7072 | CRAB, colistin-resistant <i>A. baumannii</i> , tetracycline-resistant <i>A. baumannii</i> , ESBL and MBL-producing <i>A. baumannii</i> | Preclinical trial: significant reductions in bacterial growth and a significant increase in survival rate and prolonged median in a <i>K. pneumoniae</i> , <i>S. pneumoniae</i> pneumonia model | [157-159] |
| | TP-6076 | Better activity than other tetracycline members against CRAB and colistin, amikacin, tobramycin, and levofloxacin-resistant <i>A. baumannii</i> | Preclinical trial: potent efficacy against <i>A. baumannii</i> in murine neutropenic thigh/lung infection models | [107,160] |
| β-lactam | LYS228 (a derivative of monobactam) | 32-fold lower MICs than aztreonam, ceftazidime-avibactam, ceftazidime, meropenem and cefepime against Enterobacteriales strains, including KPC-producing and CRE | Phase I: showing efficacy in a neutropenic murine thigh infection model against <i>E. coli</i> and <i>K. pneumoniae</i> strains, including strains expressing KPC and NDM carbapenemases First in human study indicated favourable safety, tolerability, and PK profile | [161,162] |
| | GSK3342830 (a derivative of cephalosporin) | MDR and CRAB isolates | Phase I: first-time-in-human study indicated its safety, tolerability, and PK profiles in healthy adults | [163] |
| | Sulopenem (a derivative of carbapenems) | ESBL-producing (MDR) Enterobacteriales | Phase III: superior activity than ciprofloxacin to treat quinolone non-susceptible pathogens causing urinary tract infections | [164,165] |

Note: MIC, minimum inhibitory concentration; MBL, metallo-β-lactamase; KPC, *K. pneumoniae* carbapenemase; CRAB, carbapenem-resistant *A. baumannii*; CRPA, carbapenem-resistant *P. aeruginosa*; ESBLs, extended spectrum β-lactamases; NDM, New Delhi Metallo-β-lactamase; PK, Pharmacokinetics

1.4.3. Efflux inhibitors

The efflux mechanism is mainly responsible for decreasing the effectiveness of almost all antibiotic classes in common use, thus there is an urgent need for research and development into compounds to circumvent or block this activity and restore/preserve antibacterial potency [166]. Several molecules are able to inhibit bacterial efflux pumps (known as efflux inhibitors) and these operate through many different mechanisms (Figure 1.5), leading to inactive drug transports or being a component of inhibitor + antibiotic combinations to treat MDR-GNB infections by potentiating antimicrobial activity [167-170].

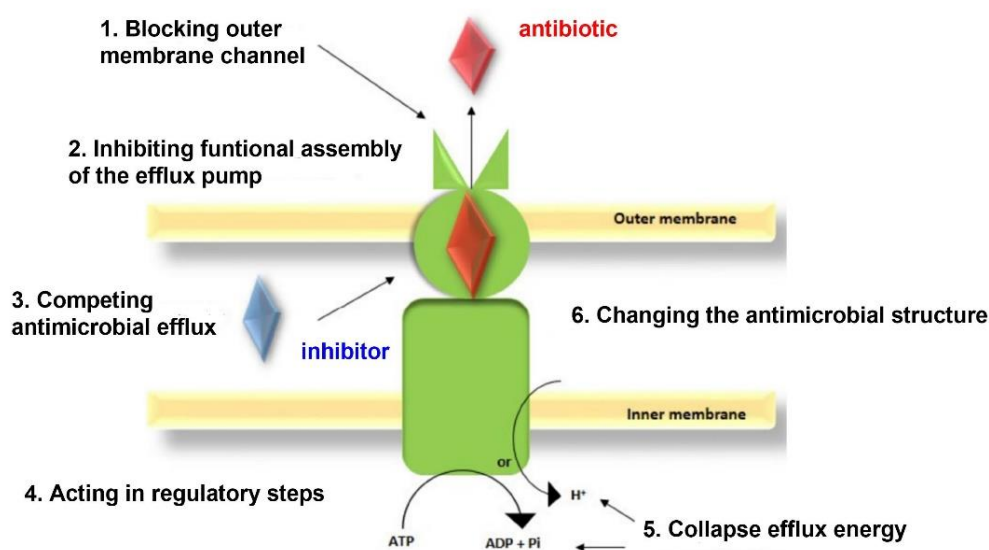


Figure 1.5. Different mechanisms of actions of efflux inhibitors.

1) Blocking the OM channels responsible for efflux systems; 2) Disrupting the assembly of the efflux systems; (3) Inhibiting antibiotic binding by using other compounds; 4) Interfering with the regulatory steps needed for the expression of the efflux transporters; (5) Interfering with the energy required for the pump activity; (6) Chemical changes in the antibiotic structure hence hindering its attachment as specific substrates. Adapted from Mottawea *et al.*, [171].

Development of efflux inhibitors is a potential approach in drug discovery to treat MDR-GNB infections for several reasons. Firstly, combining efflux inhibitors with well-known antibiotics with well-established pharmacological properties saves a lot of time, effort, and cost associated with discovering novel antibiotics [172,173]. Secondly, antibiotic + efflux inhibitor combinations can restore many current antibiotics to which bacteria have become resistant to; this would represent an excellent example of antimicrobial stewardship if such inhibitors are ultimately developed and used clinically [174]. Another significant advantage of efflux inhibitors is the low frequency of generating resistant mutants [168,171].

Unfortunately, although many efflux inhibitors have been investigated (Table 1.5), thus far none have been approved for use in human or veterinary medicine [175]. Limits to their *in vivo* application are mainly toxicity concerns to eukaryote transporters. Therefore, this gap in capacity building will take considerably more effort before efflux inhibitors are in widespread clinical use [171].

Table 1.5. Potential efflux inhibitors for further treatment of GNB infections

| Inhibitors | Target efflux pumps | Target Organisms | Antibiotics | Reference |
|---|-----------------------|---|---|-----------|
| Natural sources | | | | |
| Pheophorbide A | NorA, MexAB-OprM | <i>P. aeruginosa</i> <i>E. coli</i> | Berberine, ciprofloxacin | [176] |
| Theobromine | AcrAB-TolC | <i>K. pneumoniae</i> | Ciprofloxacin, tetracycline | [177] |
| Artesunate | AcrAB-TolC | <i>E. coli</i> | Penicillin G; ampicillin, cefazolin, cefuroxime, cefoperazone | [178] |
| Conessine | MexAB-OprM, AdeIJK | <i>P. aeruginosa</i> <i>A. baumannii</i> | Cefotaxime, levofloxacin, tetracycline, novobiocin and rifampicin | [179,180] |
| Synthetic efflux inhibitors (chemically synthesised) | | | | |
| Piperazine Arylideneimidazolones | AcrAB Tol-C and AcrEF | <i>E. coli</i> | Fluoroquinolones | [181] |
| 4-(2-(piperazin-1-ylethoxy)-2-(4-propoxyphenyl) quinolone | PQQ4R and AcrAB-TolC | <i>E. coli</i> | Ofloxacin, tetracycline | [182] |
| 13-cyclopentylthio-5-OH-TC (13-CPTC), semisynthetic tetracycline (TC) analogues | TetA or TetB | <i>E. coli</i> | Tetracycline | [183] |

Table 1.5 (continued)

| Inhibitors | Target efflux pumps | Target Organisms | Antibiotics | Reference |
|---|-------------------------------|---|---|-----------|
| PAβN (phenylalanine-arginine β-naphthylamide, also called MC207 110) | MexAB-OprM | <i>P. aeruginosa</i> <i>A. baumannii</i> <i>E. coli</i> | Levofloxacin, chloramphenicol, rifaximin, tigecycline, fluoroquinolones | [184] |
| Pyridoquinolines | AcrAB-ToIC | <i>K. pneumoniae</i> | Tetracycline, norfloxacin, chloramphenicol | [185] |
| Pyridopyrimidine analogues (D13-9001) | AcrB and MexB | <i>P. aeruginosa</i> | Fluoroquinolones | [186] |
| Pyranopyridine derivatives (MBX2319) | AcrAB | <i>E. coli</i> | Ciprofloxacin, piperacillin | [187] |
| (E)-N-(3,4-difluorophenyl)-2-(2-(3-(methylthio)phenylimino)-4-oxothiazolidin-5-yl | AbeM | <i>A. baumannii</i> | Fluoroquinolones | [188] |
| Dihydroartemisinin 27 (DHA 27) | AcrB | <i>E. coli</i> | β-lactam antibiotics | [189] |
| Sertraline | AcrAB, AcrEF, MdtEF and MexAB | <i>E. coli</i> | Tetracycline | [190] |
| Pimozide (neuroleptic drug) | AcrAB-ToIC | <i>E. coli</i> | Ethidium bromide | [181] |

1.4.4. Combination therapy

1.4.4.1. Existing β -lactam antibiotics paired with new β -lactamase inhibitors

β -lactam + β -lactamase inhibitor (BLI) combinations is an approach to bypass the resistant mechanism mediated by β -lactamases possessed by many GNB pathogens [191]. The first generation of BLIs used in the clinic include clavulanic acid, sulbactam, and tazobactam [192]. However, these BLIs have limited spectra of activity, only working against class A [193] but not class B, C, and D enzymes [194-196]. Therefore, many β -lactam + BLI combinations have lost effectiveness against carbapenemases, ESBLs or multiple β -lactamases. Some current BLIs such as avibactam, vaborbactam, relebactam, zidebactam, relebactam, and nacubactam have key chemical differences compared to old BLIs. For example, avibactam has no β -lactam core that is structurally distinct from currently used BLIs, leading to a unique mechanism that is covalent and reversible inhibition contrasting to other BLIs [197]. Some newly approved β -lactam + BLI combinations including ceftolozan + tazobactam, ceftazidime + avibactam, meropenem + vaborbactam, imipenem + relebactam, and aztreonam + avibactam are now registered for clinical treatment of GNB infections [191] and others currently in the development process include sulbactam + durlobactam, cefepime + zidebactam, meropenem + nacubactam, cefepime + nacubactam, cefepime + enmetazobactam (Table 1.6).

Table 1.6. New β -lactamase inhibitors couple with current cephalosporins and carbapenems

| β-lactamase inhibitor | Drug class | Target organism | Development stage | Reference |
|---|---|--|--------------------------|------------------|
| Cefepime/ zidebactam (WCK 5222) | β -lactam (cephalosporin) + β -lactamase inhibitor (diazabicyclooctane) | CRAB and MDR-GNB | Phase I | [198] |
| Sulbactam (SUL)/ durlobactam (SUL-DUR) | Diazabicyclooctenone β -lactamase inhibitor | <i>A. baumannii</i> | Phase II | [199] |
| Meropenem/ nacubactam , cefepime/ nacubactam | β -lactamase inhibitor | MBL-producing Enterobacteriales | Preclinical | [200,201] |
| Tebipenem (SPR859) | Carbapenem inhibitor | (ESBL)-Enterobacteriales | Preclinical | [202] |
| VNRX-5133 (taniborbactam) | β -lactamase inhibitor | β -lactamase-producing CRE and CRPA | Preclinical | [203-210] |
| Cefepime + enmetazobactam | β -lactamase inhibitor | CRE | Phase II | [211-216] |

Note: CRAB, carbapenem-resistant *A. baumannii*; CRE, carbapenem-resistant Enterobacteriales; CRPA, Carbapenem-resistant *P. aeruginosa*; ESBLs, extended spectrum β -lactamases; MBL, metallo- β -lactamase

1.4.4.2. Combination of existing and new antibiotics with polymyxins

Polymyxins are one of the last line drugs used for treating extensively drug-resistant GNB infections. However, the regrowth and the emergence of polymyxin resistance associated with polymyxin monotherapy and their inherent toxicities (associated with higher doses) have limited their use for the treatment of GNB infections [217,218]. Combining polymyxins with other antibiotics has been suggested as a potential alternative [218] associated with an increase in antimicrobial activity, and a reduction in resistant development and toxicity [219]. In combination, polymyxins are known to interact with lipopolysaccharide on the surface of GNB and then across the OM via the self-promoted uptake pathway, resulting in disruption of the normal barrier property of the OM of GNB [219,220]. Subsequently, the affected OM is hypothesised to transiently “crack”, thereby allowing passage of other antibiotics into the cell to meet the drug target sites (Figure 1.6) [221].

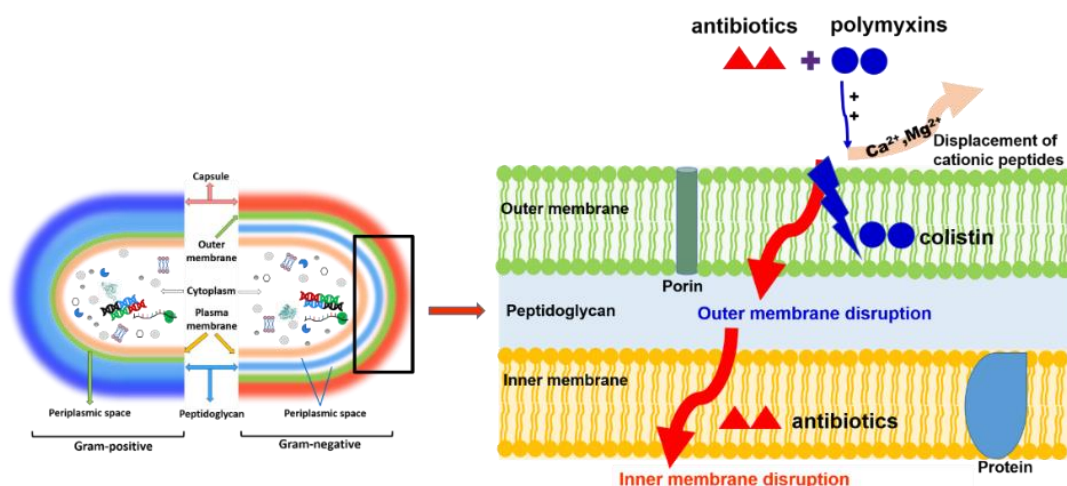


Figure 1.6. Proposed mechanism of action of polymyxins in combination with other antibiotics against GNB

The positively charged polymyxins competitively displace native divalent cations (Ca²⁺ and Mg²⁺) to interact with negatively charged divalent cation binding sites on the OM LPS of GNB.

This results in translocation of polymyxins across the OM, leading to permeability changes in the cell envelope, thereby allowing penetration of the combined antibiotics through the OM to act on the inner membrane. Adapted from Dandie *et al.* [222]

There are a variety of *in vitro* studies indicated the synergistic activities of colistin or PMB with other agents against GNB pathogens [223-239]. These include the combination of either colistin or PMB with many traditional antimicrobials such as meropenem, tigecycline, imipenem, chloramphenicol, carbapenem, doripenem, telavancin, daptomycin, minocycline, rifampicin, fosfomycin, tobramycin, imipenem, teicoplanin, vancomycin, tigecycline, imipenem, sulbactam, fosfomycin, amikacin, sitafloxacin, azidothymidine [223-234], endolysin (a peptidoglycan degrading enzyme) [235], pentamidine (a drug developed for trypanosomiasis, leishmaniasis, and *Balamuthia* infection) [236], N-acetylcysteine (lactobezoar drug) [237], pterostilbene (efflux inhibitor) [238], zidovudine (antiretroviral drug) [239] or gramicidin S (antifungal) [240]. These studies provide evidence that the approach of combining existing antibiotics with polymyxins is beneficial in broadening the range of treatment options for MDR-GNB infections.

Accordingly, many pre-clinical studies indicated the superiority of combination therapy vs monotherapy (Table 1.7) [241-246], together with *in vitro* studies supporting the potential applications of combination therapy to treat MDR- GNB infections in clinical health care settings. However, the superior efficacy of combination therapy vs monotherapy remains controversial in data from clinical studies (Table 1.8). Some clinical studies have indicated that combination therapy decreased treatment time while increasing the overall survival rate [96,247-250]. Others concluded non-inferiority of colistin monotherapy compared with combination therapy [251-253]. Therefore, there is an urgent need for appropriately designed and powered clinical trials to provide further evidence of positive vs negative effects [254]

Table 1.7. Pre-clinical studies comparing antibiotic + colistin combination therapy vs monotherapy

| Antibiotic | Study design | Target organism | Result | Reference |
|---------------------------------------|-------------------------------------|--------------------------------------|--|------------------|
| Colistin + imipenem | <i>Galleria mellonella</i> model | MDR <i>E. cloacae</i> | The combination was highly active against <i>E. cloacae</i> both <i>in vitro</i> and <i>in vivo</i> in the model | [241] |
| Colistin + rifampicin | Pneumonia mouse model | MDR- <i>P. aeruginosa</i> | The combination produced maximum survival protection against critical MDRP infections | [202] |
| Colistin+ refampicin | Murine thigh infection model | MRD- <i>A. baumannii</i> | The combination showed a 100% synergistic effect after 24 h of treatment | [242] |
| Colistin + levofloxacin | <i>Galleria mellonella</i> model | <i>A. baumannii</i> | Synergistic or additive effect of the combination was observed <i>in vitro</i> and <i>in vivo</i> against <i>A. baumannii</i> strains but not against colistin-resistant strains | [243] |
| Colistin + tigecycline | Murine thigh infection model | Colistin-resistant <i>E. coli</i> | The combination showed a significant decrease in bacterial density of colistin-resistant <i>E. coli</i> and was more active than each drug alone | [244] |
| Colistin + lysophosphatidylcholine | Murine sepsis models | <i>A. baumannii</i> | Combination enhanced bacteria clearance from spleen, lungs and blood and reduced mice mortality compared with colistin monotherapy. | [245] |
| Colistin + telavancin | <i>Galleria mellonella</i> model | <i>A. baumannii</i> | The combination was superior to colistin monotherapy in the treatment of larvae infected with <i>A. baumannii</i> | [246] |

Table 1.8. Clinical studies comparing antibiotic + colistin combination therapy vs monotherapy

| Combination | Study design | Type of infection | Result | Reference |
|-----------------------------|---|--|---|------------------|
| Colistin + meropenem | Retrospective cohort study | CRAB infections | Combination resulted in a reduction in 30-day mortality, higher clinical and microbiological responses and no increase in nephrotoxicity compared to colistin monotherapy | [96] |
| | Randomised controlled superiority trial | Hospital-acquired pneumonia and ventilator-associated pneumonia caused by MDR- <i>K. pneumoniae</i> | The combination indicated a significant decrease in mortality vs colistin alone; no significant differences in nephrotoxicity, hepatotoxicity or neurotoxicity between combination and mono drugs | [247] |
| | Randomised controlled trial | Hospital-acquired pneumonia, ventilator-associated pneumonia, bloodstream infection and urinary tract infection caused by colistin-susceptible, CRAB, CRE and CRPA | Observation of the synergistic activity of colistin and meropenem but no significant differences between combination and stand-alone drugs into clinical studies | [251] |
| | Randomised controlled superiority trial | Severe <i>A. baumannii</i> infections | Combination therapy was not superior to monotherapy. | [252] |

Table 1.8 (continued)

| Combination | Study design | Type of infection | Result | Reference |
|---|---|---|--|------------------|
| Colistin + carbapenem | Retrospectively collected data | CRAB pneumonia. | No significant differences in mortality between combination and stand-alone drug | [253] |
| Colistin+ sulbactam | Retrospective study | MDR <i>A. baumannii</i> ventilator-associated pneumonia | Clinical cure rates or bacteriological clearance rates were better in the combination than in colistin monotherapy | [248] |
| Colistin + sulbactam/ carbapenem | Randomised controlled superiority trial | MDR <i>A. baumannii</i> pneumonia | No significant differences in mortality rates between colistin + sulbactam and colistin + carbapenems combination | [255] |
| Colistin+ tobramycin | Randomised controlled superiority trial | MDR <i>P. aeruginosa</i> osteomyelitis | Combinations are more efficient than respective single antibiotics for killing <i>P. aeruginosa</i> in biofilms <i>in vitro</i> . The combination significantly reduced <i>P. aeruginosa</i> cell counts in a rat lung infection model and in patients with cystic fibrosis. | [249] |
| Colistin/PMB + tigecycline/carbapenem, respectively | Retrospectively collected data | KPC-producing <i>K. pneumoniae</i> infections | Combination therapy (colistin or PMB with tigecycline or carbapenem) showed a survival benefit in a critically ill population | [250] |

Note: MDR, multidrug-resistance; KPC, *K. pneumoniae* carbapenemase; CRAB, carbapenem-resistant *A. baumannii*; CRPA, carbapenem-resistant *P. aeruginosa*

1.4.5. Old drug repurposing

Repurposing well-known, approved medications for new indications or new commercial opportunities is a potential alternative to overcome the challenges in treating MDR-GNB infections [256-258]. Principally, many drugs have various biological activities yet to be investigated, and many different diseases share common molecular pathways or genetic factors [259]. The repurposed drugs can be developed in combination as drug adjuvants or in a new formulation that allows different biological effects to be enhanced [260]. Avoiding high costs and long development due to published pharmacokinetics, pharmacodynamics, and toxicity profiles of the drugs are the main advantages of drug repurposing [259]. The new drug discovery and development process costs over USD \$2.6 billion and can take up to 10- 17 years to be marketed, whereas drug repurposing saves 15% of the overall cost and only a 3- 12 year process to registration [261]. However, the rapidly emerging resistance in bacteria to repurposed drugs is a major concern because these antibiotics are already investigated in clinical healthcare settings for an extended period, resistant genes may be already present among the pathogenic bacterial community.

A classic example of repurposing drugs for GNB infections concerns azidothymidine (an antiretroviral drug), which shows synergistic antimicrobial activity in combination with colistin against ESBL-producing *E. coli* and *K. pneumoniae* strains, NDM-producing strains, and mobilized colistin resistance (*mcr-1*)-producing *E. coli* strains [262]. Similarly, seven non-antibacterial compounds: three antineoplastics (5-fluorouracil, 6-thioguanine and pifithrin- μ), one anti-rheumatic (auranofin), one antipsychotic (fluspirilene), one anti-inflammatory (Bay 11-7082), and one alcohol deterrent (disulfiram) inhibited the growth of an *A. baumannii* strain resistant to most antibiotics [263]. Furthermore, ciclopirox (an antifungal agent) also

showed antimicrobial activity against MDR *E. coli*, *K. pneumoniae*, and *A. baumannii* utilizing a novel mechanism of action [264]. In addition, gallium, known for more than 80 years as an anti-cancer agent [265], exhibited *in vitro* and *in vivo* antimicrobial activity against *P. aeruginosa* and *A. baumannii* [266-268].

1.4.6. “Lost antibiotics”

“Lost antibiotics” is a term to describe an approach to rediscovery of molecules with interesting antimicrobial properties investigated decades ago but which stalled in clinical development. For example, octapeptins are a family of cyclic lipopeptides, structurally similar to the polymyxins, isolated from *Bacillus circulans* and *Paenibacillus tianmuensis* in the 1970s [269] then largely ignored [270]. However, the widespread emergence of polymyxin-resistant GNB has prompted their “rediscovery”. Recently, Velko *et al.*, [271] reported octapeptin C4, a new octapeptin derivative showed antimicrobial activity against GNB by binding to and depolarizing membranes.

1.5. Models for testing pre-clinical efficacy of new antibiotics against bacterial infections

The development of novel antibiotics in pre-clinical testing requires an assessment of the infectious process and the antibiotic efficacy in different models. This process typically introduces an infectious agent, followed by treatment with the new antibiotic being investigated and quantifying the *in vivo* clearance of the infection from various sites depending on the model being studied.

1.5.1. *Galleria mellonella* larvae model

G. mellonella is an insect from the order *Lepidoptera* and the family *Pyralidae* (snout moths). Over the recent decade, the *G. mellonella* model has become increasingly popular to

study the efficacy of antibiotic treatments on various GPB and GNB [272]. This model has several advantages, including the insects having similar immune systems and innate immune responses as mammals. Therefore, the assessment of virulence of bacterial pathogens may be identical to those in mammalian models. Moreover, the larvae are not expensive to purchase, easy to use, and do not require ethical approval [273]. However, this model is still in its infancy with several disadvantages including lack of stock centres that supply reference strains, standard protocols for comparison of experiments carried out by different research groups, and limited genomic information of *G. mellonella* [272]. Furthermore, *G. mellonella* larvae are supplied by independent breeders, who sell the larvae as pet food. The difference in genotypes, breeding conditions or maintenance of *G. mellonella* may well affect their susceptibility to infections and antibiotic treatments. In addition, many factors such as housing temperature, diet and light sources, which are not easy to control, can influence the response *G. mellonella* to novel treatments [274-276]. Finally, a *G. mellonella* infection model has been held back by the lack of standardised procedures for recording morbidity and mortality and for studying antimicrobial PK/PD [277]

1.5.2. Traditional mouse model.

Traditional animal model procedures have been utilised to determine the results of *in vivo* antibiotic treatment for bacterial infections with the assistance of *in vitro* methods [278]. Mice and human genomes are 90% similar and the pathophysiology of disease in mice is similar to that of humans. The small size of the mouse facilitates large scale/high throughput studies making it a cost-effective and efficient model that resembles disease in humans [279]. However, these techniques have many limitations. Firstly, the standard *in vitro* susceptibility tests does not predict therapeutic outcomes. Secondly, conventional *in vivo* models of

antibiotic efficacy assessment lack the non-destructive, reproducible, longitudinal monitoring system that allow assessing the antibiotic efficacy in the same animal throughout the study. Finally, the major concern of the traditional method is an ethical one because mice are killed at each sampling time point, and organs are harvested for bacterial enumeration, which is labour-intensive, expensive and often involve the use of many experimental animals at each time point, including challenges associated with animal handling during experiments [280].

1.5.3. Bioluminescent mouse model

Recently, bioluminescent mouse models are considered a state of the art approach for screening antibiotic candidates *in vivo* to accelerate the development of novel antibiotics [281]. Bioluminescence imaging is a sensitive technique for rapid, non-destructive, exact and real-time monitoring of antibiotic efficacy in living animals. This method permits observation of the changes in the number of microorganisms and significantly minimises the number of animals sacrificed throughout studies [282]. A wide range of genetically modified bioluminescent bacterial strains with high virulence, pathogenesis and susceptibility similar to that of clinical isolates are commercially available, facilitating the establishment of a variety of infection models such as scald injury, thigh, lung, ear, sepsis models to test the efficacy of many antimicrobials [283,284]. However, most commercially available platforms for measuring bioluminescence such as *in vivo* imaging systems (IVIS) are designed only for imaging small animals such as mice and rats, which is a limitation of bioluminescent infection models.

The bioluminescent *in vivo* imaging system (BIS) contains a charge-coupled digital device camera cooled to -90 °C for highly sensitive photon acquisition and advanced computer software to acquire image data and analysis (Figure 1.7). BIS responds to capture photons of

light emitted by gene-modified bacteria to produce bioluminescence. Bioluminescent organisms are transformed bacteria with plasmid DNA that contain a luminescent gene cassette from *Photobacterium luminescens* or *Vibrio harveyi* containing all the machinery required for emission of light [285].

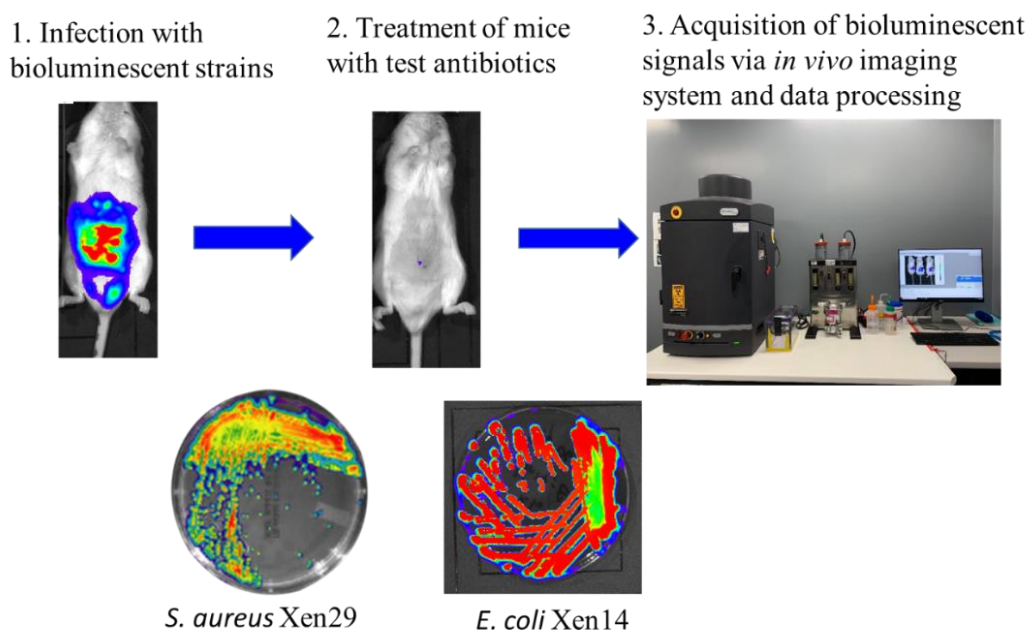


Figure 1.7. Schematic representation of bioluminescent mouse model of antimicrobial efficacy testing.

Mice are challenged with bioluminescent bacteria such as *S. aureus* Xen29 or *E. coli* Xen14 then receive treatment of tested antibiotics. Thereafter, mice are imaged on the *in vivo* imaging systems to quantify the *in vivo* clearance of the infection from the mice in real-time.

1.6. Novel antibiotics assessed in the present study

NCL195 (4,6-is(2-((E)-4-methylbenzylidene)hydrazinyl)pyrimidin-2-amine), the first new antibiotic entity, was redesigned from the anticoccidial robenidine, NCL812 (2,2'-bis[(4-chlorophenyl)methylene] carbonimidic dihydrazide hydrochloride), an oral antibiotic used since the 1970s to control coccidiosis in commercial poultry and rabbit production [286]. This

was achieved by installation of a 2,4,6-triaminopyrimidine as a guanidyl moiety bioisostere and replacement of the chloride halogen at position C4 on each phenyl ring with methyl groups (Figure 1.8) [287,288]. These changes in chemical structure resulted in NCL195 becoming less cytotoxic (at least four-fold lower IC50s in mammalian cell culture and haemolysis assays) whilst achieving similar potency against bacteria compared to the NCL812 parent compound [288]. Our previous data indicated that NCL195 exhibited *in vitro* antimicrobial activity against MRSA (MIC 1-2 µg/mL), VRE (MIC 2-4 µg/mL), and *Streptococcus pneumoniae* (MIC 2-8 µg/mL), as well as against GNB-KAPE pathogen reference isolates (*A. baumannii*, *E. coli*, *K. pneumoniae* and *P. aeruginosa*) (MICs of 0.25-8 µg/mL) in the presence of sub-inhibitory concentrations of adjuvants targeting the OM of GNB (ethylenediaminetetraacetic acid (EDTA), polymyxin nanopeptide (PMBN) and PMB) [288]. Meanwhile, NCL195 showed no activity against the GNB-KAPE pathogens in the absence of these adjuvants [288]. This promising *in vitro* antimicrobial activity of NCL195 directed our interest in testing its *in vivo* efficacy against GPB pathogens in mouse bioluminescent infection models as a proof of concept study. Additionally, we sought to further investigate the *in vitro* activity of NCL195 in combination with OM permeabilising adjuvants including colistin against a wide range of clinical GNB isolates followed by *in vivo* efficacy testing of the NCL195/colistin combination in bioluminescent mouse GNB infection models.

The second novel robenidine analogue is NCL179 (2,2'-bis[(4-chlorophenyl)methylene] carbonimidic dihydrazide hydrochloride), which is identical to NCL195, except that the halogens (Cl) characteristic of NCL812 have been retained on the phenyl rings. (Figure 1.8)

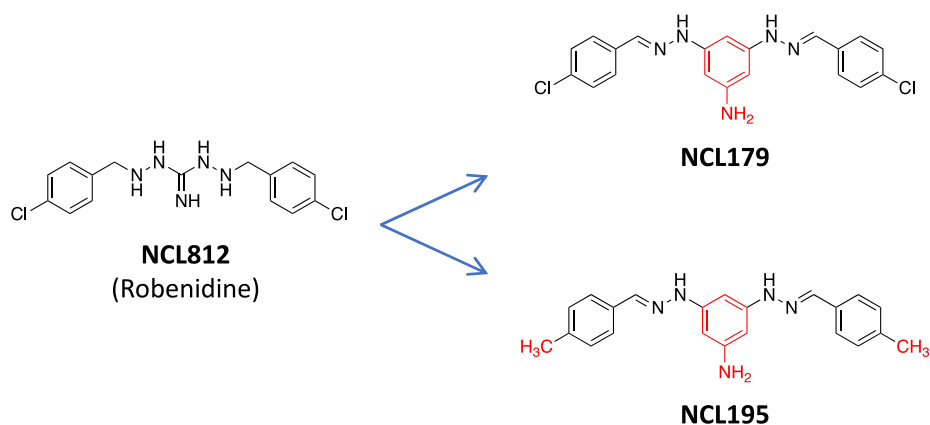


Figure 1.8. Chemical structures of NCL812, NCL179, and NCL195.

Red colouration highlights the structural changes in NCL179 and NCL195 relative to NCL812.

The guanidine to triaminopyrimidine bioisosteric modification of NCL812 yielded NCL179 (2,2'-bis[(4-chlorophenyl)methylene] carbonimidic dihydrazide hydrochloride) and NCL195 (4,6-is(2-((E)-4-methylbenzylidene)hydrazinyl)pyrimidin-2-amine). NCL195 is characterised by a methyl group in the C-4 position of the phenyl rings that distinguishes it from NCL179, where the original halogens (Cl) from NCL812 are maintained in this position.

Benzguinol A (3-O-(2,4-difluorobenzyl)unguinol) and benzguinol B (3-O-(2-fluorobenzyl) unguinol), two additional new antibiotic candidates, were also tested in this project. These were two semisynthetic analogues of the fungal depsidone antibiotics, unguinol and the related nidulin-family fungal metabolite (Figure 1.9) [289]. Our preliminary data indicated that benzguinols exhibited potent activity against MSSA and MRSA (MIC 0.25–1 µg/mL) [289], and in the present study we further investigated *in vivo* activity of benzguinols against GPB and potential against GNB in the presence of sub-inhibitory concentrations of colistin.

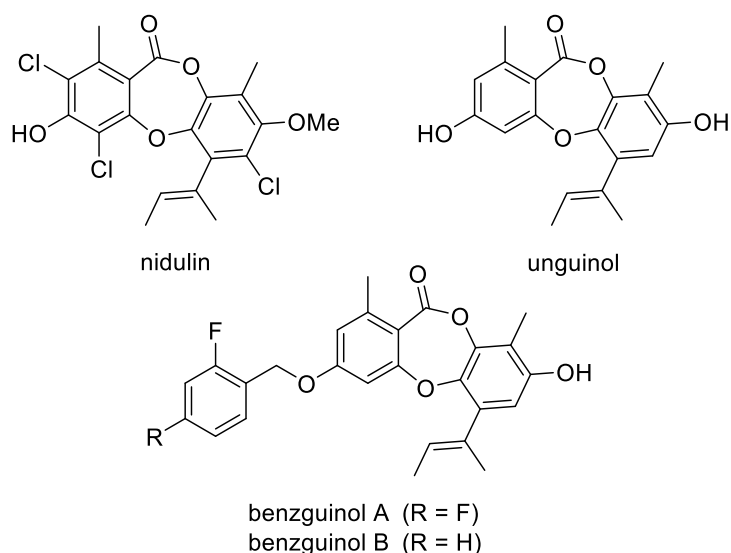


Figure 1. 9. Structures of fungal metabolites nidulin and unguinol and semisynthetic unguinol derivatives, benzguinol A and benzguinol B.

1.7. Conclusion

The reviewed literature highlights the challenges encountered in drug discovery research and focusses on finding new treatments for MDR bacterial infections, particularly GNB infections. In addition, it highlights that the novel antibiotic + low dose polymyxin combination approach is a major potential alternative route in drug discovery to overcome the outer membrane barrier inherent in GNB [24]. The combination exhibits advantages by increasing the spectrum of activity of newly discovered chemical entities, reducing resistance development via dual targeting and the potential for reducing polymyxin toxicity due to the low dose used in combination [24]. Therefore, the present study focussed on this latter strategy for confirming *in vitro* and *in vivo* efficacy of four novel chemical entities in animal models. Firstly, the *in vitro/in vivo* activity of the novel antibiotics against GPB was confirmed. Secondly, each compound was combined with low concentrations of colistin as an OM permeabilising adjuvant to confirm *in vitro/in vivo* activity against selected GNB.

1.8. Aims of the present study

The aims of this PhD project were to: (i) microbiologically evaluate the above four novel chemical entities consisting of two robenidine analogues (NCL195 and NCL179) and two 3-benzyl analogues of benzguinols (benzguinol A and benzguinol B); and (ii) develop bioluminescent mouse GNB infection models for pre-clinical *in vivo* efficacy testing of NCL195, NCL179, benzguinol A, and benzguinol B as proof-of-concept of their suitability for further preclinical development for the treatment of bacterial infections.

Chapter II describes *the in vitro* activity of robenidine analogue NCL195 combined with several adjuvants against GNB pathogens and its *in vivo* impact on systemic GPB infection in mice (via systemic route) as a proof-of-concept of *in vivo* activity. Chapter III presents *in vitro* synergistic antimicrobial activity of NCL195 in combination with colistin against GNB pathogens. Chapter IV compares different TEM methods to visualise the effect of NCL195 + colistin interaction on GNB membrane morphology. Chapter V describes the efficacy of oral NCL195 treatment against GPB infections and the impact of a combination of NCL195 and sub-inhibitory colistin concentrations in treating GNB infections, including those caused by colistin-susceptible and colistin-resistant bioluminescent *E. coli* in mouse sepsis models. Chapter VI investigates *in vitro* activity of NCL179 against GPB and NCL179 + colistin combination against GNB and its *in vivo* impact in the mouse bioluminescent *S. aureus* sepsis infection model. Chapter VII evaluates both *in vitro* and *in vivo* efficacy of benzguinol A and benzguinol B as next-generation antibiotics to treat MDR infections. Chapter VIII (General Discussion) outlines the implications of the significant findings of this thesis and proposes future directions.


Chapter II

***In vitro* activity of robenidine analog NCL195 in combination with outer membrane permeabilizers against Gram-negative bacterial pathogens and impact on systemic Gram-positive bacterial infection in mice**

Statement of Authorship

| | |
|---------------------|--|
| Title of Paper | <i>In vitro</i> activity of robenidine analogue NCL195 in combination with adjuvants against Gram-negative bacterial pathogens and impact on systemic Gram-positive bacterial infection in mice |
| Publication Status | <input checked="" type="checkbox"/> Published <input type="checkbox"/> Accepted for Publication <input type="checkbox"/> Submitted for Publication <input type="checkbox"/> Unpublished and Unsubmitted work written in manuscript style |
| Publication Details | Pi, H.; Nguyen, H.T. (shared first author) ; Venter, H.; Boileau, A.R.; Woolford, L.; Garg, S.; Page, S.W.; Russell, C.C.; Baker, J.R.; McCluskey, A., et al. <i>In vitro</i> activity of robenidine analog NCL195 in combination with outer membrane permeabilizers against Gram-negative bacterial pathogens and impact on systemic Gram-positive bacterial infection in mice. <i>Front Microbiol</i> 2020 , 11, doi:10.3389/fmicb.2020.01556. Journal Impact Factor = 6.064. |


Principal Author


| | | | |
|--------------------------------------|--|------|------------|
| Name of Principal Author (Candidate) | Hang Thi Nguyen (shared first author) | | |
| Contribution to the Paper | Contributed to study design, experiments, and participated in writing, editing, discussion | | |
| Overall percentage (%) | 40% | | |
| Certification: | This paper reports on original research I conducted during the period of my Higher Degree by Research candidature and is not subject to any obligations or contractual agreements with a third party that would constrain its inclusion in this thesis. I am the primary author of this paper. | | |
| Signature |  | Date | 01/12/2021 |

Co-Author Contributions

By signing the Statement of Authorship, each author certifies that:

- i. the candidate's stated contribution to the publication is accurate (as detailed above);
- ii. permission is granted for the candidate to include the publication in the thesis; and
- iii. the sum of all co-author contributions is equal to 100% less the candidate's stated contribution.

| | | | |
|---------------------------|--|------|------------|
| Name of Co-Author | Hongfei Pi (shared first author) | | |
| Contribution to the Paper | Contributed to study design, experiments, and participated in writing, editing, discussion | | |
| Signature |  | Date | 04/01/2022 |

| | | | |
|---------------------------|--|------|------------|
| Name of Co-Author | Henrietta Venter | | |
| Contribution to the Paper | Contributed to study design, editing, financial support, discussion, and provided expertise on the mechanism of action studies | | |
| Signature |  | Date | 15/12/2021 |

| | | | |
|---------------------------|--|------|----------|
| Name of Co-Author | Alexandra Boileau | | |
| Contribution to the Paper | Contributed to animal experiments, data analysis, editing and discussion | | |
| Signature | | Date | 22/01/22 |
| Name of Co-Author | Lucy Woolford | | |
| Contribution to the Paper | Contributed to histopathological examinations, editing and discussion | | |
| Signature | | Date | 05/01/22 |

| | | | |
|---------------------------|--|------|------------|
| Name of Co-Author | Sanjay Garg | | |
| Contribution to the Paper | Responsible for preparing formulations | | |
| Signature | | Date | 06/01/2022 |

| | | | |
|---------------------------|---|------|------------|
| Name of Co-Author | Stephen W. Page | | |
| Contribution to the Paper | Contributed to editing, discussion and provided financial support for the study | | |
| Signature | | Date | 02/02/2022 |

| | | | |
|---------------------------|---|------|------------|
| Name of Co-Author | Cecilia C. Russell | | |
| Contribution to the Paper | Responsible for synthesizing NCL195 and contributed to editing and discussion | | |
| Signature | | Date | 12/01/2022 |

| | | | |
|---------------------------|---|------|------------|
| Name of Co-Author | Jennifer R. Baker | | |
| Contribution to the Paper | Responsible for synthesizing NCL195 and contributed to editing and discussion | | |
| Signature | | Date | 18/01/2022 |

| | | | |
|---------------------------|---|------|------------|
| Name of Co-Author | Adam McCluskey | | |
| Contribution to the Paper | Responsible for synthesizing NCL195 and and contributed to editing and discussion | | |
| Signature | | Date | 06/02/2022 |

| | | | |
|---------------------------|---|------|-----------|
| Name of Co-Author | Lisa A. O'Donovan | | |
| Contribution to the Paper | Contributed to TEM technical guidance, experimentation and editing the manuscript | | |
| Signature | | Date | 5/01/2022 |

| | | | |
|---------------------------|---|------|------------|
| Name of Co-Author | Darren J. Trott | | |
| Contribution to the Paper | Contributed to study design, and participated in writing, editing, discussion, provided financial support for the study and was co-corresponding author | | |
| Signature | | Date | 07/02/2022 |

| | | | |
|---------------------------|--|------|------------|
| Name of Co-Author | Abiodun D. Ogunniyi | | |
| Contribution to the Paper | Contributed to study design, experiments, and participated in writing, editing, discussion and was co-corresponding author | | |
| Signature | | Date | 08/12/2021 |



In vitro Activity of Robenidine Analog NCL195 in Combination With Outer Membrane Permeabilizers Against Gram-Negative Bacterial Pathogens and Impact on Systemic Gram-Positive Bacterial Infection in Mice

OPEN ACCESS

Edited by:

You-Hee Cho,
CHA University, South Korea

Reviewed by:

Sun-Shin Cha,
Ewha Womans University,
South Korea
Malte Ohlmeier,
HELIOS Kliniken GmbH, Germany
Jochen Salber,
University Hospital Bochum GmbH,
Germany

*Correspondence:

Darren J. Trott
darren.trott@adelaide.edu.au
Abiodun D. Ogunniyi
david.ogunniyi@adelaide.edu.au;
david.ogunniyi@unisa.edu.au

†These authors share first authorship

Specialty section:

This article was submitted to
Antimicrobials, Resistance
and Chemotherapy,
a section of the journal
Frontiers in Microbiology

Received: 07 March 2020

Accepted: 16 June 2020

Published: 04 August 2020

Citation:

Pi H, Nguyen HT, Venter H,
Boileau AR, Woolford L, Garg S,
Page SW, Russell CC, Baker JR,
McCluskey A, O'Donovan LA,
Trott DJ and Ogunniyi AD (2020)
In vitro Activity of Robenidine Analog
NCL195 in Combination With Outer
Membrane Permeabilizers Against
Gram-Negative Bacterial Pathogens
and Impact on Systemic
Gram-Positive Bacterial Infection
in Mice. *Front. Microbiol.* 11:1556.
doi: 10.3389/fmicb.2020.01556

Hongfei Pi^{1†}, Hang Thi Nguyen^{1,2†}, Henrietta Venter³, Alexandra R. Boileau¹, Lucy Woolford⁴, Sanjay Garg⁵, Stephen W. Page⁶, Cecilia C. Russell⁷, Jennifer R. Baker⁷, Adam McCluskey⁷, Lisa A. O'Donovan⁸, Darren J. Trott^{1*} and Abiodun D. Ogunniyi^{1*}

¹ Australian Centre for Antimicrobial Resistance Ecology, School of Animal and Veterinary Sciences, The University of Adelaide, Roseworthy, SA, Australia, ² Department of Pharmacology, Toxicology, Internal Medicine and Diagnostics, Faculty of Veterinary Medicine, Vietnam National University of Agriculture, Hanoi, Vietnam, ³ Health and Biomedical Innovation, Clinical and Health Sciences, University of South Australia, Adelaide, SA, Australia, ⁴ School of Animal and Veterinary Sciences, The University of Adelaide, Roseworthy, SA, Australia, ⁵ Clinical and Health Sciences, University of South Australia, Adelaide, SA, Australia, ⁶ Neoculi Pty. Ltd., Burwood, VIC, Australia, ⁷ Chemistry, School of Environmental and Life Sciences, The University of Newcastle, Callaghan, NSW, Australia, ⁸ ARC Centre of Excellence in Plant Energy Biology, School of Agriculture, Food & Wine, The University of Adelaide, Urrbrae, SA, Australia

Multidrug-resistant (MDR) pathogens, particularly the ESKAPE group (*Enterococcus faecalis/faecium*, *Staphylococcus aureus*, *Klebsiella pneumoniae*, *Acinetobacter baumannii*, *Pseudomonas aeruginosa*, *Escherichia coli*, and *Enterobacter* spp.), have become a public health threat worldwide. Development of new antimicrobial classes and the use of drugs in combination are potential strategies to treat MDR ESKAPE pathogen infections and promote optimal antimicrobial stewardship. Here, the *in vitro* antimicrobial activity of robenidine analog NCL195 alone or in combination with different concentrations of three outer membrane permeabilizers [ethylenediaminetetraacetic acid (EDTA), polymyxin B nonapeptide (PMBN), and polymyxin B (PMB)] was further evaluated against clinical isolates and reference strains of key Gram-negative bacteria. NCL195 alone was bactericidal against *Neisseria meningitidis* and *Neisseria gonorrhoeae* (MIC/MBC = 32 µg/mL) and demonstrated synergistic activity against *P. aeruginosa*, *E. coli*, *K. pneumoniae*, and *Enterobacter* spp. strains in the presence of subinhibitory concentrations of EDTA, PMBN, or PMB. The additive and/or synergistic effects of NCL195 in combination with EDTA, PMBN, or PMB are promising developments for a new chemical class scaffold to treat Gram-negative infections. Tokuyasu cryo ultramicrotomy was used to visualize the effect of NCL195 on bioluminescent *S. aureus* membrane morphology. Additionally, NCL195's favorable pharmacokinetic and pharmacodynamic profile was further explored in *in vivo* safety

studies in mice and preliminary efficacy studies against Gram-positive bacteria. Mice administered two doses of NCL195 (50 mg/kg) by the intraperitoneal (IP) route 4 h apart showed no adverse clinical effects and no observable histological effects in major organs. In bioluminescent *Streptococcus pneumoniae* and *S. aureus* murine sepsis challenge models, mice that received two 50 mg/kg doses of NCL195 4 or 6 h apart exhibited significantly reduced bacterial loads and longer survival times than untreated mice. However, further medicinal chemistry and pharmaceutical development to improve potency, solubility, and selectivity is required before efficacy testing in Gram-negative infection models.

Keywords: bacterial sepsis, bioluminescence, cryo-ultramicrotomy, membrane potential, multidrug resistance, NCL195, polymyxin B, transmission electron microscopy

INTRODUCTION

Multidrug-resistant (MDR) pathogens, in particular the ESKAPE pathogens (*Enterococcus faecalis/faecium*, *Staphylococcus aureus*, *Klebsiella pneumoniae*, *Acinetobacter baumannii*, *Pseudomonas aeruginosa*, *Escherichia coli*, and *Enterobacter* spp.), are becoming a public health threat in both hospitals and the community. In particular, MDR Gram-negative ESKAPE pathogens significantly impact the standard care of septic patients, owing to high morbidity and mortality rates worldwide (ranging from 30 to 70%) (Giamarellou, 2010; Tamma et al., 2012; Bhattacharya, 2013; Zilberberg et al., 2014; Frieri et al., 2017). Studies have consistently identified MDR Gram-negative ESKAPE pathogens as the main cause of additional hospital-acquired infections, such as respiratory tract, urinary tract, and postsurgical infections (Cardoso et al., 2012; Pendleton et al., 2013; Santajit and Indrawattana, 2016). Moreover, therapeutic options for these infections are becoming more limited, resulting in high health care costs resulting from protracted hospital stays (Ventola, 2015; Centers for Disease Control and Prevention [CDC], 2019).

In the past, the availability of new antimicrobials kept pace with the evolution of antibiotic-resistant bacteria. However, while there is an increasing trend of multidrug resistance in both Gram-negative and Gram-positive bacteria, there has been a significant global decline of investment into new drug development (Livermore, 2012; Woolhouse and Farrar, 2014). As a result, there are only a limited number of registered alternatives for MDR Gram-negative ESKAPE pathogens and few truly novel classes of antimicrobial agents undergoing preclinical testing in the drug development pipeline (Lepore et al., 2019). Furthermore, within the new classes of antimicrobial agents being developed, most have activity only against Gram-positive pathogens, mainly due to the presence of an outer membrane in Gram-negative bacteria that deters the penetration and retention of antibiotics (Pushpakom et al., 2019; Theuretzbacher et al., 2019).

Previously, our laboratory reported that NCL 195 (4,6-bis-(2-((E)-4-methylbenzylidene)hydrazinyl)pyrimidin-2-amine), which was developed as a chemical analog of the anticoccidial drug robenidine, possessed antimicrobial activity against MRSA, vancomycin-resistant enterococci (VRE), and *Streptococcus pneumoniae*. This selectivity is likely attributable to the mode of action of NCL195, which permeabilizes the cytoplasmic

membrane of *S. pneumoniae*, VRE, and *S. aureus*, thereby hindering the establishment and maintenance of essential energy sources for cell functioning (Ogunniyi et al., 2017). In the presence of subinhibitory concentrations of outer membrane permeabilizers targeting the outer membrane of bacteria (EDTA, PMBN, and PMB), NCL195 was bactericidal against Gram-negative ESKAPE pathogens reference isolates (*A. baumannii*, *E. coli*, *K. pneumoniae*, and *P. aeruginosa*) (MICs of 0.25–8 µg/mL). Meanwhile, in the absence of these outer membrane permeabilizers, NCL195 was also bactericidal against eight *Acinetobacter calcoaceticus* isolates (MIC range from 4 to 32 µg/mL) and one *Acinetobacter anitratus* isolate (MIC = 4 µg/mL) (Abraham et al., 2016; Ogunniyi et al., 2017). Here, we further evaluated the *in vitro* antimicrobial activity of NCL195 in the presence of EDTA, PMBN, or PMB against an expanded panel of Gram-negative pathogens isolated from clinical cases. As a first proof of concept testing of the *in vivo* efficacy of NCL195 against bacterial pathogens, we assessed its *in vivo* safety and efficacy using our established/optimized bioluminescent models of Gram-positive bacterial infection.

MATERIALS AND METHODS

Antimicrobial Agents

Analytical grade NCL195 (Figure 1) was synthesized in house at the University of Newcastle as reported previously (Ogunniyi et al., 2017) and stored in a sealed sample container out of direct light at 4°C at the study site at the Infectious Diseases Laboratory, Roseworthy campus, the University of Adelaide. Polymyxin B (PMB) and its derivative, polymyxin B nonapeptide (PMBN), which is devoid of the N-terminal fatty acyl chain and the L-α-γ-diaminobutyric acid residue (and therefore lacks antibacterial activity except against *Pseudomonas* spp.) (Velkov et al., 2010), were purchased from Sigma-Aldrich (NSW, Australia). Stock solutions [containing 25.6 mg/mL of PMBN or PMB in dimethyl sulfoxide (DMSO)] were prepared and stored in 1-mL aliquots at –80°C and defrosted immediately prior to use. Ethylenediaminetetraacetic acid (EDTA, disodium salt) was purchased from Chem-Supply Pty. Ltd., South Australia and was dissolved in Milli-Q water to 200 mM.

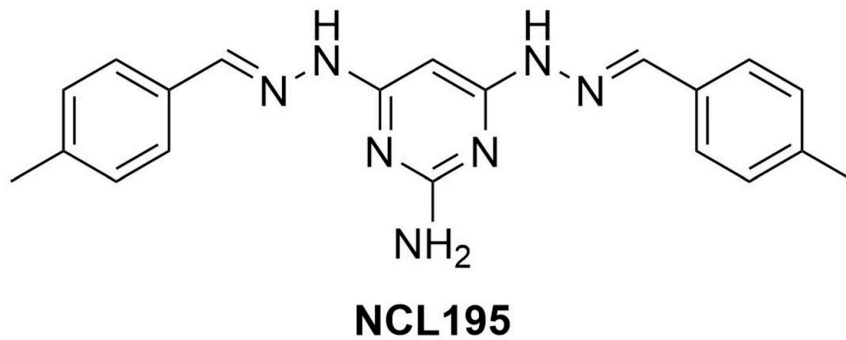


FIGURE 1 | Chemical structure of NCL195 (4,6-bis-(2-((E)-4-methylbenzylidene)hydrazinyl)pyrimidin-2-amine).

Bacterial Strains

A total of 101 Gram-negative bacteria were collected from government, private, and university diagnostic laboratories throughout Australia. These organisms were speciated using biochemical testing and matrix-assisted laser desorption/ionization–time-of-flight (MALDI-TOF) mass spectrometry (Bruker, Preston, VIC, Australia). The organisms were 18 *A. baumannii* (including two reference strains *A. baumannii* ATCC19606 and *A. baumannii* ATCC 12457), 10 *A. calcoaceticus*, 1 *A. anitratus* and 4 Neisseriae (*N. meningitidis* 423, *N. meningitidis* 424, *N. gonorrhoeae* ATCC 16599, and *N. gonorrhoeae* ATCC 49226). These organisms were kindly provided by Professor Mary Barton (University of South Australia) and the Australian Group on Antimicrobial Resistance (AGAR) for testing the antimicrobial activity of NCL195. Other antimicrobial-resistant bacteria comprising 18 *K. pneumoniae*, 18 *E. coli*, and 19 *P. aeruginosa* human clinical isolates were obtained from the Australian Centre for Antimicrobial Resistance Ecology (ACARE) collection. The following additional 11 Gram-negative reference strains were also used for combination experiments: *E. coli* ATCC 10763, *E. coli* ATCC 25922, *E. coli* ATCC 11229, *Pseudomonas putida* ATCC 17428, *P. aeruginosa* PAO1, *P. aeruginosa* ATCC 27853, *P. aeruginosa* ATCC 33347, *Proteus mirabilis* ATCC 43071, *K. pneumoniae* ATCC 13883, *K. pneumoniae* ATCC 33495, and *K. pneumoniae* ATCC 4352. Bioluminescent *E. coli* (Xen14) (PerkinElmer Inc., Waltham, MA, United States), derived from the parental strain *E. coli* WS2572, and bioluminescent *P. aeruginosa* (Xen41) (PerkinElmer Inc., Waltham, MA, United States), derived from the parental strain *P. aeruginosa* PAO1, were used for the time-dependent killing assays.

For *in vivo* efficacy evaluation of NCL195, bioluminescent *S. aureus* (Xen29), derived from the parental strain *S. aureus* ATCC 12600 (PerkinElmer Inc., Waltham, MA, United States), and bioluminescent *S. pneumoniae*, derived from the parental strain *S. pneumoniae* D39 (D39LUX) (Henken et al., 2010), were used.

Antimicrobial Susceptibility Testing

Minimum inhibitory concentrations (MICs) were determined in round-bottom 96-well microtiter trays (Sarstedt 82.1582.001),

using the modified broth microdilution method recommended by the Clinical and Laboratory Standards Institute [CLSI], 2017. Testing concentrations were as follows: NCL195: 256–0.25 $\mu\text{g/mL}$; EDTA: 3,800–45 $\mu\text{g/mL}$; PMBN: 32–0.06 $\mu\text{g/mL}$; PMB: 32–0.06 $\mu\text{g/mL}$. Luria–Bertani (LB) broth (Oxoid, VIC, Australia) was used instead of cation-adjusted Mueller–Hinton broth as it was shown previously that robenidine can chelate calcium ions resulting in loss of activity. In addition, twofold serial dilutions of NCL195 were performed in 100% DMSO, with 1 μL added to each well, as NCL compounds have very low solubility in aqueous environments (Abraham et al., 2016). The MICs for ampicillin, gentamicin, and apramycin against each isolate were determined for each test to serve as an internal quality control. The MICs of isolates were determined by visual reading and using an EnSpire Multimode Plate Reader 2300 at $A_{600\text{ nm}}$. MIC₅₀, MIC₉₀, and MIC ranges for NCL195, EDTA, PMBN, PMB, or combinations were then determined (Venter, 2019).

Minimum Bactericidal Concentration Determination

The minimum bactericidal concentration (MBC) of NCL195 alone or in combination with EDTA, PMBN, or PMB was determined against both Gram-positive and Gram-negative bacteria. Briefly, 10- μL aliquots from each duplicate well from the MIC assays (starting from the MIC for each compound) were inoculated onto a sheep blood agar (SBA) plate and incubated at 37°C. Plates were examined at 24 and 48 h and the MBC was recorded as the lowest concentration of each test compound at which a 99.95% colony count reduction was observed on the plate (Clinical and Laboratory Standards Institute [CLSI], 2017).

Synergy Testing by Checkerboard Microdilution and Dose Reduction Analysis

To assess potential synergistic activity of NCL195, MICs for a range of Gram-negative ATCC strains and clinical isolates of *K. pneumoniae*, *E. coli*, *A. baumannii*, and *P. aeruginosa* were determined in the presence or absence of 23.2–11,400 $\mu\text{g/mL}$ (0.06–30 mM) of EDTA and 0.25–128 $\mu\text{g/mL}$ of PMBN or

PMB in a modified standard checkerboard assay as described previously (Hamoud et al., 2015; Khazandi et al., 2019). Briefly, antimicrobial stock solutions were prepared at a concentration of 25.6 mg/mL in DMSO for NCL195, 12.8 mg/mL in Milli-Q water for PMBN and PMB, and 30 mM in Milli-Q water for EDTA. Then, a twofold serial dilution of each antimicrobial stock solution was prepared in its appropriate solvent from wells 12 to 3 (starting from 25.6 to 0.25 mg/mL for NCL195, 12.8 to 0.25 mg/mL for PMBN and PMB, and 30 to 0.06 mM for EDTA). One microliter of each concentration was then added to each well in the challenge plate using an electronic multichannel pipette followed by 89 μ L of the LB broth. Ten microliters of bacterial suspension of 1.5×10^6 colony forming units per milliliter (CFU/mL) was added to each well of the plate, which was subsequently incubated at 37°C for 24 h.

The fractional inhibitory concentration index (FICI) describes the results of combination, and was calculated as follows: FICI of combination = FIC A + FIC B. Where FIC A is the MIC of NCL195 in the combination/MIC of NCL195 alone, FIC B is the MIC of EDTA in the combination/MIC of EDTA alone. The results indicate synergism when the corresponding FICI ≤ 0.5 , additivity when $0.5 < \text{FICI} \leq 1$, indifference when $1 < \text{FICI} \leq 4$, and antagonism when the FICI > 4 . In this study, the FICI for NCL195 and PMBN against Gram-negative bacteria was calculated to be zero (e.g., $1 \div > 256 = 0$), where they did not show any antibacterial activity alone against Gram-negative bacteria at the highest concentration (256 μ g/mL).

The dose reduction index (DRI) shows the difference between the effective doses in combination in comparison to its individual dose. DRI was calculated as follows: DRI = MIC of drug alone/MIC of drug in combination. Given that NCL195 and PMBN did not show any antimicrobial activity against the majority of Gram-negative bacteria, the highest concentration of each compound tested against each isolate was used as its MIC alone for calculating the DRI (e.g., MIC of NCL195 alone against *E. coli* 103 was $>256 \mu\text{g/mL}$ and its MIC in combination with PMBN was 1 $\mu\text{g/mL}$; DRI = 256/1). DRI is very important clinically when the dose reduction is associated with a toxicity reduction without changing efficacy (Eid et al., 2012). Commonly, a DRI higher than 1 is considered beneficial.

Time-Dependent Killing Assays

Initial time kill assays were performed (in duplicate) for the NCL195 in the presence of PMB against a range of human ESKAPE pathogen reference strains (*E. coli* ATCC 25922, *P. aeruginosa* PAO1, *K. pneumoniae* ATCC 33495, and *A. baumannii* ATCC 19606) as described previously (Clinical and Laboratory Standards Institute [CLSI], 2017) with slight modifications. Briefly, a few colonies of each strain from overnight SBA plates were emulsified in normal saline and adjusted to $A_{600 \text{ nm}} = 0.10$ (equivalent to approx. 5×10^7 CFU/mL) and the bacterial suspensions were further diluted 1:20 in saline. NCL195 and PMB were serially diluted in 100% DMSO or Milli-Q water at 100 \times the final desired concentration and a 100- μ L aliquot of appropriate concentrations added to each 10 mL preparation. NCL195 and PMB solutions were prepared in 10-mL volumes at MIC and

2 \times MIC concentrations in LB broth. After addition of the inoculum dose to each tube, duplicate cultures were incubated at 37°C, with samples withdrawn at 0, 0.5, 1, 2, 4, 6, 8, and 24 h, serially diluted 10-fold, and plated on SBA overnight at 37°C for bacterial enumeration. The time kill assay was further refined by testing the NCL195-PMB combination on bioluminescent *E. coli* WS2572 (Xen14) and bioluminescent *P. aeruginosa* PAO1 (Xen41). According to CLSI, an antimicrobial agent is considered bactericidal if it causes a $\geq 3 \times \log_{10}$ (99.95%) reduction in CFU/mL after 18–24 h of incubation, and the combination is considered synergistic when it causes a $\geq 2 \times \log_{10}$ reduction in CFU/mL compared with either constituent alone.

Dual Mechanism of Action of NCL195-PMB Combination

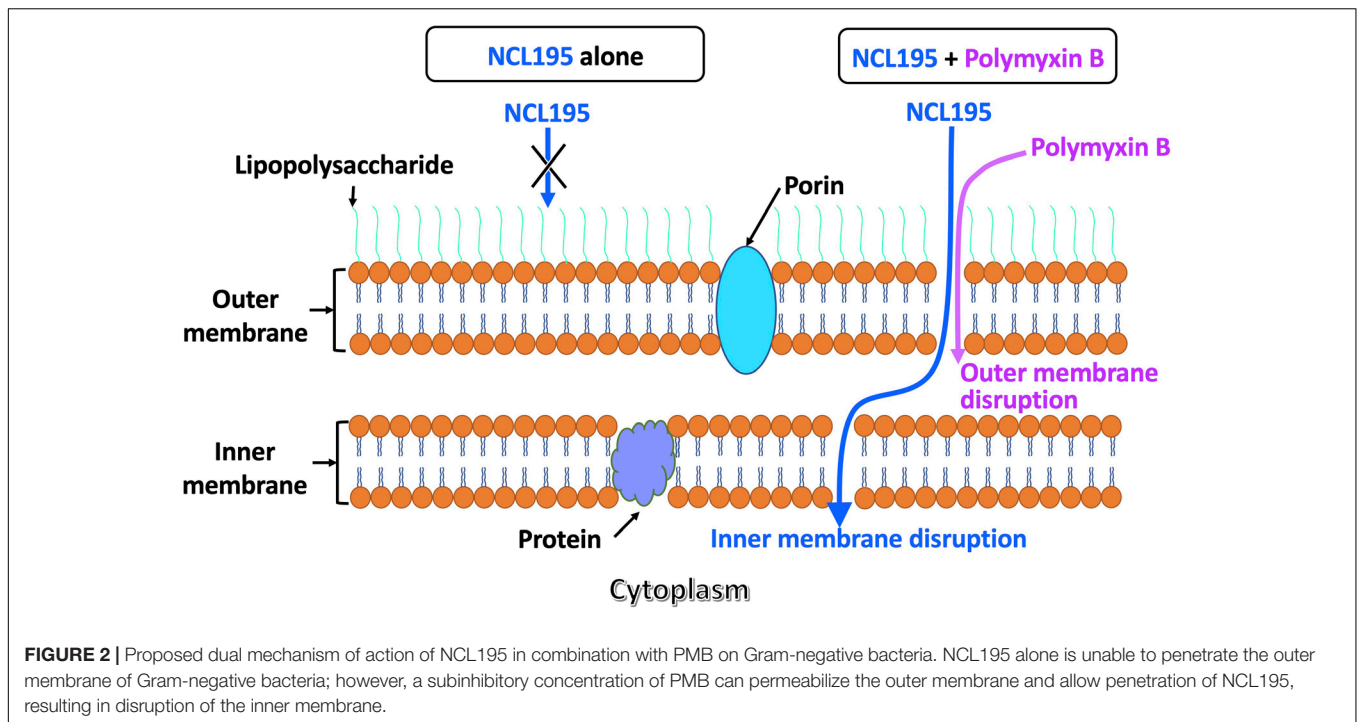
Polymyxin B has been demonstrated to disrupt the outer membrane of Gram-negative bacteria (Lin et al., 2018, 2019; Wang et al., 2020), while NCL195 has been shown to disrupt the inner membrane potential of Gram-positive bacteria (Ogunniyi et al., 2017). Thus, we hypothesized that a combination of PMB and NCL195 will disrupt the outer membrane (PMB), allowing penetration of NCL195 into the inner membrane, as shown in Figure 2.

To prove this hypothesis, the membrane potential of *E. coli* Xen14 cells was measured by fluorescence spectrometry in a LS 55 Fluorescence Spectrometer (PerkinElmer) using the fluorescent membrane potential probe 3,3-diethyloxycarbocyanine iodide [DiOC₂(3)]. A combination of Gram-negative and Gram-positive membrane potential measurement approaches was used as described previously (Venter et al., 2003; Ogunniyi et al., 2017; Wang et al., 2020). Briefly, *E. coli* Xen14 cells were prepared and resuspended in 50 mM potassium phosphate buffer (pH 7.0) to $A_{600 \text{ nm}} = 5$. PMB was used at 6.4 $\mu\text{g/mL}$, while NCL195 was used at either 12.8 or 25.6 $\mu\text{g/mL}$. The test compounds and/or their combination were incubated with the cells for either 5 or 30 min, after which DiOC₂(3) was added and the fluorescence monitored until it plateaued. The cells were then energized by the addition of glucose to establish a proton motive force (negative and basic inside the cell). This led to an increase in fluorescence associated with aggregation of the DiOC₂(3). The membrane potential was then disrupted by the addition of the proton ionophore carbonyl cyanide *m*-chlorophenyl hydrazone (CCCP).

Transmission Electron Microscopy to Visualize the Effect of NCL195 on Bioluminescent *S. aureus* ATCC12600 (Xen29) Cell Membrane

Treatment Preparation

Xen29 was grown on horse blood agar containing 200 $\mu\text{g/mL}$ of kanamycin at 37°C. A single colony was transferred to 10 mL of LB broth in 50-mL Falcon tubes and grown at 37°C under continuous agitation in a reciprocating shaker at 150 rpm. The overnight culture was then diluted 1:30 in 40 mL of LB broth and incubated at 37°C in 50-mL Falcon tubes as previously described until $A_{600 \text{ nm}} = 0.1$ was obtained. Xen29 was incubated with NCL195 (2 and 4 $\mu\text{g/mL}$) for 1 h at 37°C, with manual



mixing every 10 min. A treatment time of 1 h was chosen based on the time kill kinetic and MIC of NCL195 to ensure Xen29 cells were not killed at the time of harvest. Cells were harvested by centrifugation at $2900 \times g$ for 5 min at 4°C . Control cells were harvested at $A_{600 \text{ nm}} = 0.1$ without the addition of compound. Cells were washed twice in phosphate-buffered saline (PBS) buffer; fixed in 4.0% formaldehyde, 1.25% glutaraldehyde, 0.01 M CaCl_2 , 4% sucrose, and in the presence of 0.075% ruthenium red and 0.075% L-lysine acetate (to stabilize the peptidoglycan layer and aid in locating the bacteria during sectioning); and then stored at 4°C until processing for transmission electron microscopy (TEM). Thereafter, cells were washed twice in PBS and embedded in 12% gelatin. Small gelatin blocks containing bacteria ($<1 \text{ mm}^3$) were cut and infiltrated with 2.3 M sucrose in PBS overnight at 4°C with gentle rocking. Blocks were stored in 2.3 M sucrose at 4°C prior to sectioning.

Cryo-Ultramicrotomy and TEM

Blocks were transferred to aluminum cryo-sectioning pins (Leica) and quickly plunge-frozen in liquid nitrogen. Thin cryo-sections (80 nm) were cut at -100°C with an EM-UC6/FC7 cryo-ultramicrotome (Leica) using a cryo-diamond knife (Diatome). Cryo-sections were removed from the knife with 2.3 M sucrose using a wire loop and transferred to formvar/carbon-coated, plasma cleaned, 200-mesh copper EM grids (Proscitech). Grids were stored in an airtight container on sucrose droplets at 4°C . To stain, grids were floated face down on 2% gelatin for 30 min at 37°C before washing in PBS (3 min \times 2 min) and staining with 2% uranylacetate, pH 7 (5 min, room temperature) and methyl cellulose-uranyl acetate pH 4 on ice (10 min). Grids were looped out, drained, and allowed to dry. Samples were imaged

with a Tecnai G2 Spirit electron microscope (FEI Company) operated at 100 kV at Adelaide Microscopy, the University of Adelaide, South Australia.

Ethics Statement

For NCL195 safety and efficacy testing experiments, outbred 5- to 6-week-old male CD1 (Swiss) mice (weighing between 25 and 32 g), obtained from the Laboratory Animal Services breeding facility of the University of Adelaide, were used. Mice had access to food and water *ad libitum* throughout the experiments. The Animal Ethics Committee of the University of Adelaide (approval numbers S-2013-053 and S-2015-151) reviewed and approved all animal experiments. The study was conducted in compliance with the Australian Code of Practice for the Care and Use of Animals for Scientific Purposes (8th edition, 2013) and the South Australian Animal Welfare Act 1985.

Safety Testing of NCL195 Following Parenteral Administration

We previously determined the pharmacokinetic parameters for NCL195 after a single intraperitoneal administration of 43 mg/kg NCL195 dissolved in 20% (v/v) DMSO in PEG400 with no observed adverse reactions or compound-related side effects (Ogunniyi et al., 2017). It was then assumed that a twofold increase in dose would result in a proportional increase in NCL195 exposure. To test that a two-dose regime would be safe to administer to mice, a safety study was conducted by administering two intraperitoneal doses of NCL195 at either 10 mg/kg or 50 mg/kg 4 h apart to three mice, using two intraperitoneal doses of either PBS or 6 mg/kg daptomycin as controls. Mice were observed for clinical signs and data recorded

on a Clinical Record Sheet (CRS) approved by the Animal Ethics Committee of the University of Adelaide. At the conclusion of the experiment, mice were humanely killed and sections of liver, kidneys, spleen, heart, and brain were collected and subjected to histopathological examination.

Histopathological Examination

Mouse tissues (including liver, spleen, kidneys, heart, and brain) collected from the intraperitoneal safety challenge were fixed in 10% neutral-buffered formalin and processed routinely. The specimens were embedded in paraffin blocks and sections of 4 μm thickness were cut using a microtome. Hematoxylin and eosin staining of the sections was performed and the slides were observed and recorded under light microscopy.

Efficacy Testing of NCL195 Following Systemic Challenge of Mice With Bioluminescent Gram-Positive Bacteria

For the NCL195 efficacy testing experiments against *S. pneumoniae* challenge, luminescent strain D39 (D39LUX), which emits light constitutively at $\lambda_{\text{max}} = 490 \text{ nm}$ in metabolically active cells, was used, and has been described previously (Henken et al., 2010). Before infection, D39LUX was grown statically in serum broth (10% heat-inactivated horse serum in nutrient broth) at 37°C, 5% CO₂ to $A_{600 \text{ nm}}$ of 0.16 (equivalent to approx. 5×10^7 CFU/mL). Three groups of mice ($n = 10$ mice per group) were then challenged intraperitoneally with approx. 2.5×10^4 CFU of D39LUX in 100 μL of serum broth. At 12 h postinfection, the conditions of all mice in each group were recorded on a CRS approved by the Animal Ethics Committee of the University of Adelaide. All mice were subjected to bioluminescent imaging in a ventral position on either the Xenogen IVIS 100 system (Xenogen) or the IVIS Lumina XRMS Series III system (Caliper Life Sciences). Immediately after, group 1 mice were administered the drug vehicle only, group 2 received NCL195 at 50 mg/kg i.p., while group 3 received daptomycin at 6 mg/kg i.p. The clinical conditions of all mice were then closely monitored every 2 h, and at 18 h postinfection, all animals in each group were again subjected to bioluminescent imaging. Thereafter, group 1 mice received a second dose of drug vehicle only, while group 2 received a second dose of NCL195 at 50 mg/kg, and mice were further monitored frequently for signs of distress. The daptomycin-treated group did not receive a second dose, as their clinical conditions and bioluminescent imaging data indicated a healthy status. At 24, 30, and 60 h postinfection, mice were further subjected to bioluminescent imaging, and mice that had become moribund or showed any evidence of distress [such as loss of balance, extreme hyperactivity, severe weight loss (>20% body weight), ear temperature falling below 24°C, paralysis, or extreme reluctance or inability to move freely, and/or refusal or inability to eat or drink] were humanely killed by cervical dislocation. A second experiment ($n = 5$) was also performed essentially as described above, but with antimicrobial administration at 8 and 12 h postinfection to

assess whether earlier intervention might further prolong the survival times for mice.

For the NCL195 efficacy testing experiments against *S. aureus*, luminescent ATCC12600 strain (Xen29, PerkinElmer) was used, essentially as described previously (Ogunniyi et al., 2018). Briefly, bacteria were grown in LB broth at 37°C to $A_{600 \text{ nm}}$ of 0.5 (equivalent to approx. 1.5×10^8 CFU/mL). Three groups of mice ($n = 5$ mice per group) were challenged intraperitoneally with approx. 2.5×10^7 CFU of Xen29 in 200 μL of PBS containing 3% hog gastric mucin type III (Sigma-Aldrich). At 2 h postinfection, all mice were subjected to bioluminescent imaging in both ventral and dorsal positions on the IVIS Lumina XRMS Series III system. Immediately after, group 1 mice received the drug vehicle only, group 2 received NCL195 at 50 mg/kg i.p., while group 3 received daptomycin at 6 mg/kg i.p. The clinical conditions of all mice were closely monitored, and at 6 h postinfection, all animals in each group were subjected to bioluminescent imaging, after which a second dose of drug vehicle only, NCL195, or daptomycin was administered. Mice were further monitored frequently for signs of distress and those that had become moribund or showed any evidence of distress were humanely killed by cervical dislocation. At 10 and 16 postinfection, living mice were further subjected to bioluminescence imaging. In all experiments, signals were collected from a defined region of interest and total flux intensities (photons/s) analyzed using Living Image Software 2.5 (for IVIS 100) and 4.4 (for Lumina XRMS). Differences in median survival times (time to moribund) for mice between groups were analyzed by the log-rank (Mantel-Cox) tests. Differences in luminescence signals between groups were compared by multiple *t*-tests.

RESULTS

NCL195 Alone Shows Antimicrobial Activity Against *N. meningitidis* and *N. gonorrhoeae*

The activity of NCL195 against a range of Gram-negative bacteria (*A. baumannii* ATCC 19606, *A. baumannii* ATCC 12457, *E. coli* ATCC 10763, *E. coli* ATCC 25922, *K. pneumoniae* ATCC 33495, *K. pneumoniae* ATCC 4352, *P. aeruginosa* ATCC 27853, *P. aeruginosa* PAO1, *N. meningitidis* 423, *N. meningitidis* 424, *N. gonorrhoeae* ATCC 16599, and *N. gonorrhoeae* ATCC 49226) was investigated. The results show that NCL195 alone demonstrated antimicrobial activity against the *Neisseria* isolates and type strains tested at 32 $\mu\text{g/mL}$, but no activity was observed against the other Gram-negative bacteria tested at up to 256 $\mu\text{g/mL}$ (data not shown).

Combination of NCL195 With EDTA Demonstrates Antimicrobial Activity Against Gram-Negative Pathogen Strains

The modified checkerboard assay was used to assess the combination of NCL195 and EDTA against a range of human Gram-negative pathogen reference strains (*E. coli*

ATCC 25922, *E. coli* ATCC 11229, *P. putida* ATCC 17428, *P. aeruginosa* PAO1, *P. aeruginosa* ATCC 27853, *Proteus mirabilis* ATCC 43071, *K. pneumoniae* ATCC 13883, *A. baumannii* ATCC19606, and *A. baumannii* ATCC 12457), and one *A. calcoaceticus* clinical isolate. The results indicate a synergistic interaction of NCL195 and EDTA for *E. coli* ATCC 25922, *E. coli* ATCC 11229, *K. pneumoniae* ATCC 13883, *P. putida* ATCC 17428, *P. aeruginosa* PAO1, and *P. aeruginosa* ATCC 27853. An additive interaction was observed for *P. mirabilis* ATCC 43071, *A. baumannii* ATCC19606, *A. baumannii* ATCC 12457, and the clinical *A. calcoaceticus* isolate (Table 1).

Combination of NCL195 With Polymyxins (PMBN and PMB) Also Demonstrates Synergistic Activity Against a Range of Gram-Negative ESKAPE Pathogen Reference Strains

The antimicrobial activity of NCL195 in the presence of PMBN was investigated against a range of human ESKAPE pathogen reference strains: 3 *E. coli* strains (*E. coli* ATCC 25922, *E. coli* ATCC 11229, and *E. coli* ATCC 10763), 3 *P. aeruginosa* strains (*P. aeruginosa* ATCC 27853, *P. aeruginosa* ATCC 33347, and *P. aeruginosa* PAO1), 2 *K. pneumoniae* strains (*K. pneumoniae* ATCC 33495 and *K. pneumoniae* ATCC 4352), and 2 *A. baumannii* strains (*A. baumannii* ATCC 19606 and *A. baumannii* ATCC 12457). The combination of NCL195 and PMBN resulted in a synergistic interaction against *E. coli* ATCC 11229, *P. aeruginosa* ATCC 27853, and *K. pneumoniae* ATCC 4352. An additive interaction was recorded against *P. aeruginosa* PAO1 (Table 2). No interaction was detected against the rest of the reference strains tested.

Owing to the high cost of PMBN, we hypothesized that PMB would be a more easily acquired and cost-effective choice of outer membrane permeabilizer with similar efficacy in combination with NCL195 against Gram-negative bacteria. Therefore, the

antimicrobial activity of NCL195 and PMB in combination was tested against a larger range of human ESKAPE pathogen isolates (18 *K. pneumoniae* clinical isolates plus *K. pneumoniae* ATCC 33495 and *K. pneumoniae* ATCC 4352, 18 *E. coli* clinical isolates plus *E. coli* ATCC 10763 and *E. coli* ATCC 25922, 16 *A. baumannii* clinical isolates plus *A. baumannii* ATCC 19606 and *A. baumannii* ATCC 12457, 19 *P. aeruginosa* clinical isolates plus *P. aeruginosa* PAO1) (Table 3). The results revealed a synergistic interaction of NCL195 and PMB in combination against all Gram-negative isolates tested (reducing the MIC of NCL195 by 64- to 1,024-fold against all Gram-negative species tested).

Time Kill Kinetics of the Combination of NCL195 and PMB Shows Bactericidal Antimicrobial Activity Against *E. coli* and *P. aeruginosa* Reference Strains

Initial time kill kinetics of the NCL195-PMB combination against *E. coli* ATCC 25922, *P. aeruginosa* PAO1, *K. pneumoniae* ATCC 33495, and *A. baumannii* ATCC 19606 showed rapid, time-dependent killing of the bacteria (Supplementary Figure S1). The assay was further refined using bioluminescent *E. coli* WS2572 (Xen14) and bioluminescent *P. aeruginosa* PAO1 (Xen41). For Xen14, NCL195/PMB at 1/0.125 $\mu\text{g}/\text{mL}$ showed no antimicrobial activity; NCL195/PMB at 2/0.125 $\mu\text{g}/\text{mL}$ reduced the CFU/mL by $5 \times \log_{10}$ by 1 h post-treatment but then growth started again after 8 h; NCL195/PMB at 1/0.25 $\mu\text{g}/\text{mL}$ reduced the CFU/mL by $5 \times \log_{10}$ by 6 h post-treatment but then growth started again after 8 h; NCL195/PMB at 2/0.25 $\mu\text{g}/\text{mL}$ reduced the CFU/mL by $5 \times \log_{10}$ by 30 min post-treatment and totally cleared the bacterial growth (Figure 3A). For Xen41, NCL195/PMB at 2/1 $\mu\text{g}/\text{mL}$ reduced the CFU/mL by $5 \times \log_{10}$ within 1 h of treatment but then growth started again after 8 h; NCL195/PMB at 4/1 $\mu\text{g}/\text{mL}$ reduced the CFU/mL by $5 \times \log_{10}$ by 30 min post-treatment and totally cleared the bacterial growth; NCL195/PMB at

TABLE 1 | MIC values for NCL195 alone, EDTA alone, and in combination for Gram-negative bacteria reference strains and clinical isolates.

| Isolates | MIC ($\mu\text{g}/\text{mL}$; mM concentrations in parentheses) | | | | FICI | DRI |
|--|---|--------|-------------|--------|-------------------|-------|
| | Single drug | | Combination | | | |
| | EDTA | NCL195 | EDTA | NCL195 | | |
| <i>E. coli</i> ATCC 25922 | 3800 (10) | >256 | 950 (2.5) | 4 | 0.27 ^a | 4:64 |
| <i>E. coli</i> ATCC 11229 | 950 (2.5) | >256 | 228 (0.6) | 8 | 0.27 ^a | 4:32 |
| <i>P. putida</i> ATCC 17428 | 1900 (5) | >256 | 950 (2.5) | 1.25 | 0.50 ^a | 2:204 |
| <i>P. aeruginosa</i> PAO1 | 1900 (5) | >256 | 475 (1.25) | 1.25 | 0.25 ^a | 4:204 |
| <i>P. aeruginosa</i> ATCC 27853 | 3800 (10) | >256 | 1900 (5) | 2 | 0.50 ^a | 2:128 |
| <i>P. mirabilis</i> ATCC 43071 | 228 (0.6) | >256 | 228 (0.6) | 0.5 | 1.00 ^b | 1:512 |
| <i>K. pneumoniae</i> ATCC 13883 | 11 400 (30) | >256 | 3800 (10) | 4 | 0.35 ^a | 3:64 |
| <i>A. baumannii</i> ATCC19606 | 380 (1) | >256 | 190 (0.5) | 2 | 0.51 ^b | 2:128 |
| <i>A. baumannii</i> ATCC 12457 | 190 (0.5) | >256 | 95 (0.25) | 4 | 0.52 ^b | 2:64 |
| <i>A. calcoaceticus</i> (a clinical isolate) | 228 (0.6) | >256 | 228 (0.6) | 8 | 1.00 ^b | 1:32 |

Synergy testing by checkerboard microdilution and dose reduction analysis. DRI, dose reduction index. ^aSynergistic effect. ^bAdditive effect. The results indicate synergism when the corresponding FICI ≤ 0.5 , additivity when $0.5 < \text{FICI} \leq 1$, indifference when $1 < \text{FICI} \leq 4$, and antagonism when the FICI > 4 .

TABLE 2 | MIC values for NCL195 alone and PMBN alone and in combination for Gram-negative bacteria reference strains and clinical isolates.

| Isolates | Single drug ($\mu\text{g/mL}$) | | Combination ($\mu\text{g/mL}$) | | FICI | DRI |
|---------------------------------|----------------------------------|--------|----------------------------------|--------|-------------------|---------|
| | PMBN | NCL195 | PMBN | NCL195 | | |
| <i>P. aeruginosa</i> PAO1 | 1 | >256 | 0.5 | 4 | 0.5 ^a | 2:64 |
| <i>P. aeruginosa</i> ATCC 27853 | 2 | >256 | 0.5 | 4 | 0.27 ^a | 4:64 |
| <i>E. coli</i> ATCC 11229 | >128 | >256 | 8 | 32 | 0.19 ^a | 16:8 |
| <i>K. pneumoniae</i> ATCC 4352 | >128 | >256 | 0.125 | 4 | 0.03 ^a | 1024:64 |

DRI, dose reduction index. ^aSynergism effect. The results indicate synergism when the corresponding FICI ≤ 0.5 , additivity when $0.5 < \text{FICI} \leq 1$, indifference when $1 < \text{FICI} \leq 4$, and antagonism when the FICI > 4 .

TABLE 3 | MIC range and MIC₅₀, MIC₉₀, and DRI values for NCL195 alone, PMB alone, and in combination against 20 *K. pneumoniae*, 20 *E. coli*, 18 *A. baumannii*, and 20 *P. aeruginosa* clinical isolates.

| Isolates | Value | Antimicrobial concentration ($\mu\text{g/mL}$) | | | | Combination Effect | DRI | |
|-------------------------------|-------------------|--|--------|-------------|--------|--------------------|-----|----------|
| | | Single drug | | Combination | | | PMB | NCL195 |
| | | PMB | NCL195 | PMB | NCL195 | | | |
| <i>K. pneumoniae</i> (n = 20) | MIC range | 0.125–1 | >256 | 0.06–0.5 | 0.25–4 | Synergism | 2–4 | 64–1024 |
| | MIC ₅₀ | 0.5 | >256 | 0.125 | 2 | | 4 | 128 |
| | MIC ₉₀ | 1 | >256 | 0.25 | 4 | | 2 | 64 |
| <i>E. coli</i> (n = 20) | MIC range | 0.125–1 | >256 | 0.06–0.125 | 0.25–2 | Synergism | 2–8 | 128–1024 |
| | MIC ₅₀ | 0.5 | >256 | 0.06 | 1 | | 8 | 256 |
| | MIC ₉₀ | 0.5 | >256 | 0.125 | 2 | | 4 | 128 |
| <i>A. baumannii</i> (n = 18) | MIC range | 0.5–1 | >256 | 0.125 | 0.5–4 | Synergism | 4–8 | 64–512 |
| | MIC ₅₀ | 1 | >256 | 0.125 | 2 | | 8 | 128 |
| | MIC ₉₀ | 1 | >256 | 0.125 | 2 | | 4 | 128 |
| <i>P. aeruginosa</i> (n = 20) | MIC range | 0.25–1 | >256 | 0.06–0.25 | 1–2 | Synergism | 4–8 | 128–256 |
| | MIC ₅₀ | 0.5 | >256 | 0.125 | 1 | | 4 | 256 |
| | MIC ₉₀ | 0.5 | >256 | 0.125 | 2 | | 4 | 128 |

1/2 $\mu\text{g/mL}$ reduced the CFU/ml by $5 \times \log_{10}$ by 30 min post-treatment but then growth started again after 8 h; NCL195/PMB at 2/2 $\mu\text{g/mL}$ reduced the CFU/mL by $5 \times \log_{10}$ by 30 min post-treatment and totally cleared the bacterial growth (Figure 3B).

Combination of PMB and NCL195 Disrupts the Inner and Outer Membrane Potential of *E. coli*

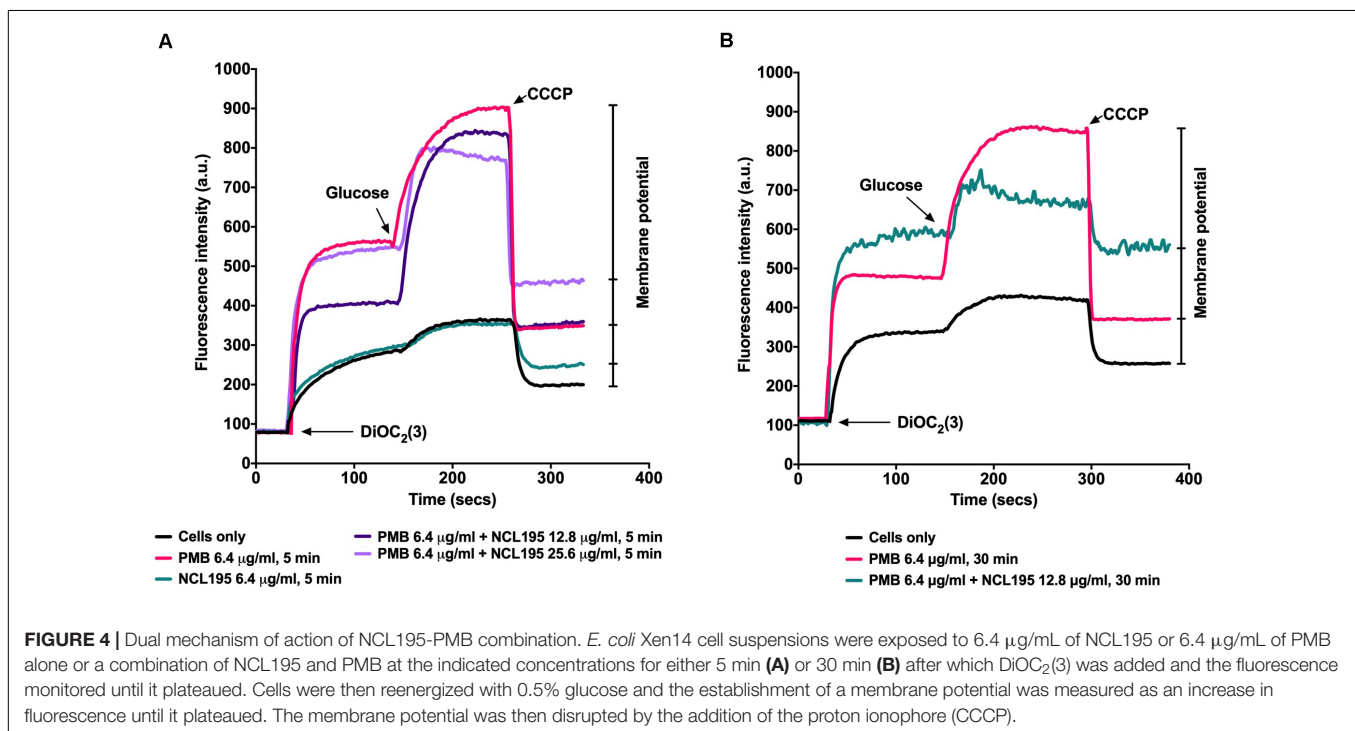
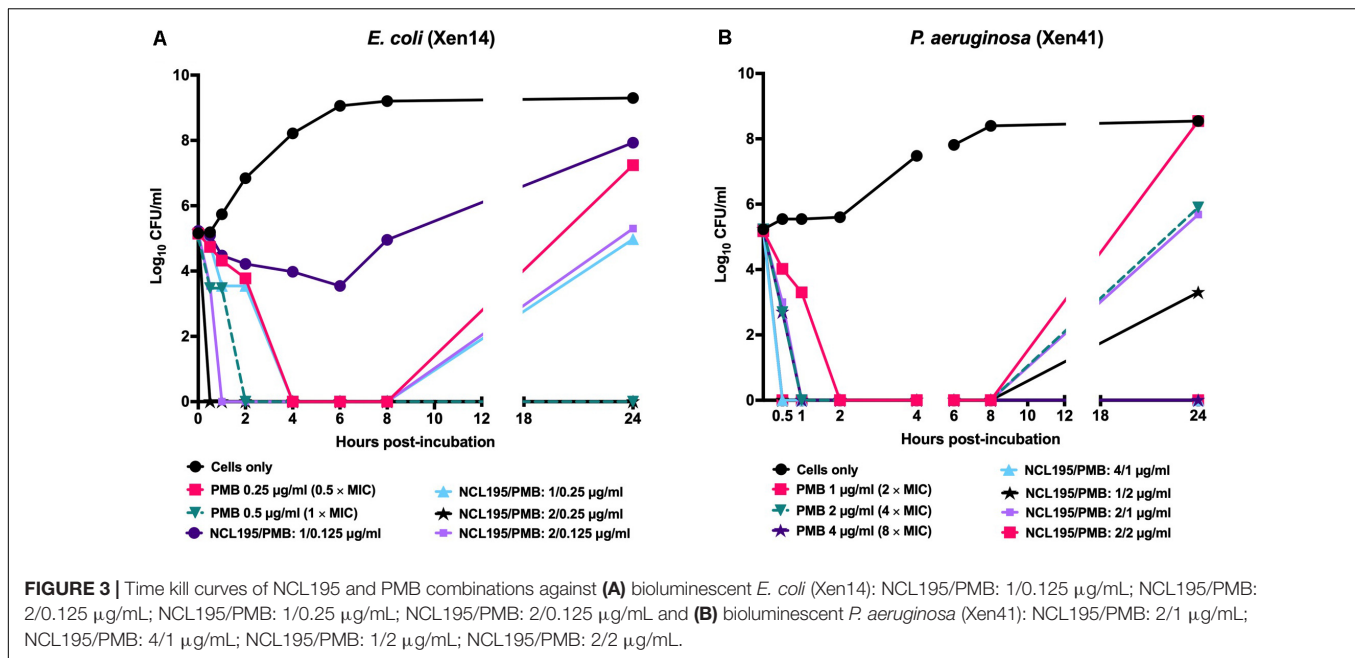
We tested the hypothesis that a combination of PMB and NCL195 will disrupt the outer membrane (PMB), allowing penetration of NCL195 into the inner membrane of Gram-negative bacteria by measuring the membrane potential of *E. coli* Xen14 cells using fluorescence spectrometry as described in Section “Materials and Methods” (see section “Dual Mechanism of Action of NCL195-PMB Combination”). We showed that preincubation of the cells with PMB at 6.4 $\mu\text{g/mL}$ permeabilized the outer membrane so that greater quantities of the DIOC₂(3) could gain entry into the cells without affecting the inner membrane (Figures 4A,B). Preincubation of the cells with the NCL195 + PMB combination resulted in a time-dependent and NCL195 concentration-dependent disruption of the inner membrane potential, clearly demonstrating the dual mechanism of action of NCL195-PMB combination.

NCL195 Exerts Its Antibacterial Action on the Cell Membrane of *S. aureus*

We previously showed that NCL195 acts on the cell membranes of *S. pneumoniae* (MIC range of 2–8 $\mu\text{g/mL}$) and *S. aureus* (MIC range of 1–2 $\mu\text{g/mL}$) via disruption of the membrane potential (Ogunniyi et al., 2017) and demonstrated changes in the appearance and thickness of the NCL195-treated cell membrane for *S. pneumoniae* by TEM, but this was not carried out for *S. aureus*. In this study, we used Tokuyasu ultrathin cryo-sections to visualize the effect of NCL195 on bioluminescent *S. aureus* Xen29 membrane morphology. TEM images showed optimal structural preservation with clear delineation of the plasma membrane and cell wall peptidoglycan layer. Samples treated with NCL195 clearly show perturbation of the membrane consistent with its membrane-acting property. In the treated sample, mesosome-like membrane structures were also observed (Figure 5).

NCL195 Shows Systemic Safety in Mice

There were no observable histopathological changes in the heart, liver, spleen, kidneys, or brain (not shown) of any of the mice in the treated groups (NCL195 10 mg/kg, NCL195 50 mg/kg, and daptomycin) compared to the control group treated with PBS (Figure 6).



Treatment of Mice With NCL195 Reduces *S. pneumoniae* and *S. aureus* Populations and Significantly Prolongs Survival Times

We evaluated the potential of NCL195 as a therapeutic drug against systemic *S. pneumoniae* infection, using a well-characterized luminescent strain (D39LUX) (Henken et al., 2010) in an intraperitoneal sepsis challenge model. We found that

at 24 h postinfection, two doses of NCL195 at 50 mg/kg i.p. (administered at 12 and 18 h postinfection) resulted in a statistically significant reduction in *S. pneumoniae* populations ($p = 0.018$, multiple t -tests; Figure 7A) and a concomitant significant increase in median survival time compared to the vehicle only control in this model ($p = 0.008$; Mantel-Cox test; Figure 7B). In a repeat experiment, intraperitoneal administration of two doses of NCL195 at 50 mg/kg at 8 and 12 h postinfection resulted in an earlier and statistically

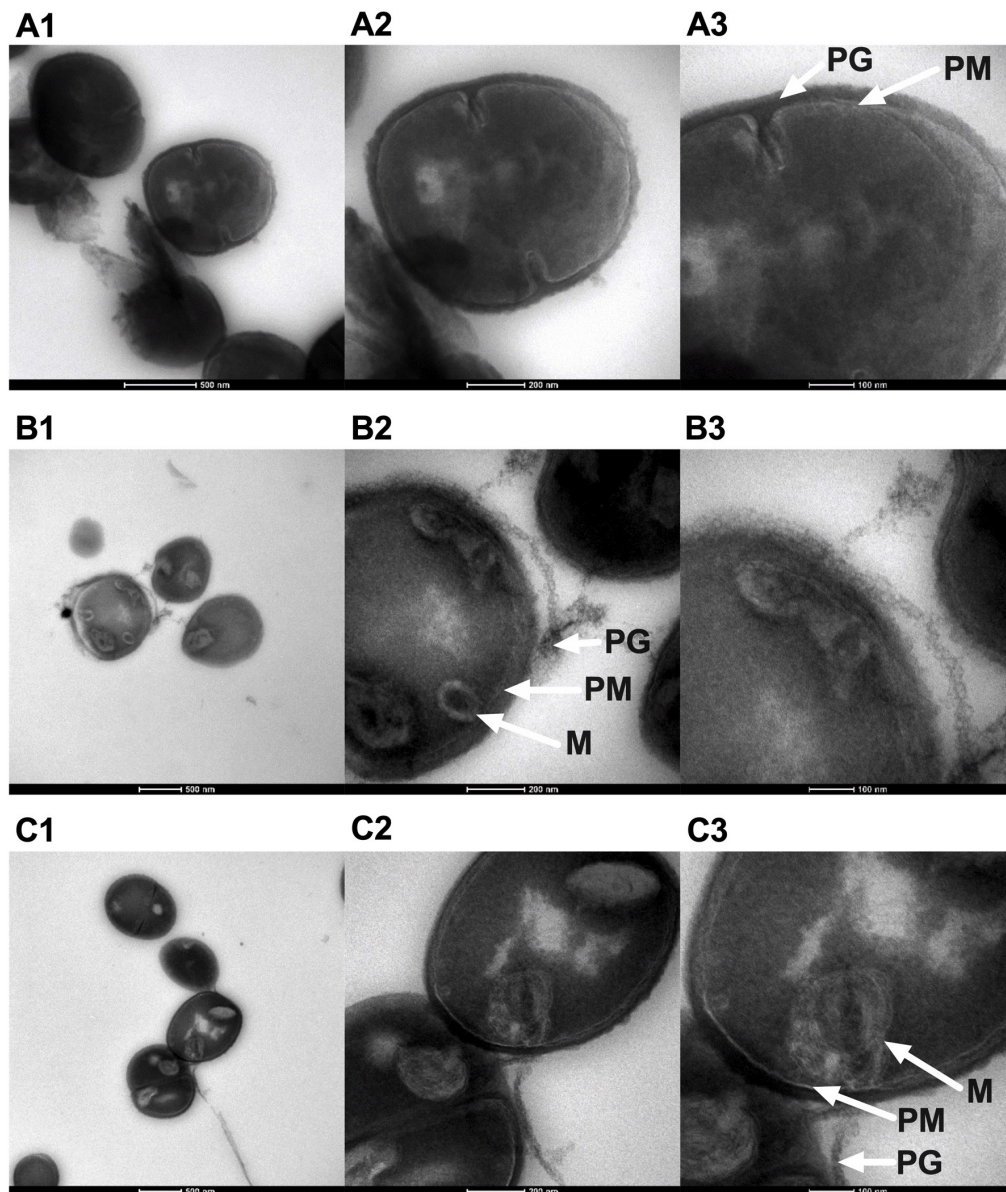


FIGURE 5 | Morphology of bioluminescent *S. aureus* Xen29 prepared using Tokuyasu cryo-ultramicrotomy and visualized by TEM. **(A1–A3)** Xen29 without treatment. **(B1–B3)** Xen29 treated with NCL195 at 2 µg/mL. **(C1–C3)** Xen 29 treated with NCL195 at 4 µg/mL. Arrows show peptidoglycan layer (PG), plasma membrane (PM) and mesosome-like structures (M). NCL195 treatment of Xen29 ($A_{600\text{ nm}} = 0.1$) at either 2 µg/mL ($1 \times \text{MIC}$) or 4 µg/mL ($2 \times \text{MIC}$) for 1 h causes detachment of the cell wall from the cell membrane. Scale bars: **(A1,B1,C1)**: 500 nm; **(A2,B2,C2)**: 200 nm; **(A3,B3,C3)**: 100 nm.

significant reduction in *S. pneumoniae* populations at 18 h postinfection ($p = 0.002$, multiple t -tests; **Figures 7C, 8**) as well as significant increase in median survival time compared to the vehicle only control ($p = 0.003$; Mantel–Cox test; **Figure 7D**). Furthermore, intraperitoneal administration of two doses of NCL195 at 50 mg/kg at 2 and 6 h postinfection resulted in a statistically significant reduction in *S. aureus* populations in the blood and mouse kidneys at 6 h postinfection ($p = 0.006$ and 0.021, respectively, multiple t -tests; **Figures 7E, 9**) as well as a significant increase in median survival time compared to the vehicle only control ($p = 0.009$; Mantel–Cox test; **Figure 7F**). No

adverse effects attributable to drug treatment were observed in the three rodent studies.

DISCUSSION

There is an urgent need to develop new broad-spectrum antimicrobials with activity against pan resistant ESKAPE pathogens, particularly Gram-negative members, with a view to overcoming the permeability barrier of the Gram-negative outer membrane (Willyard, 2017; Venter, 2019;

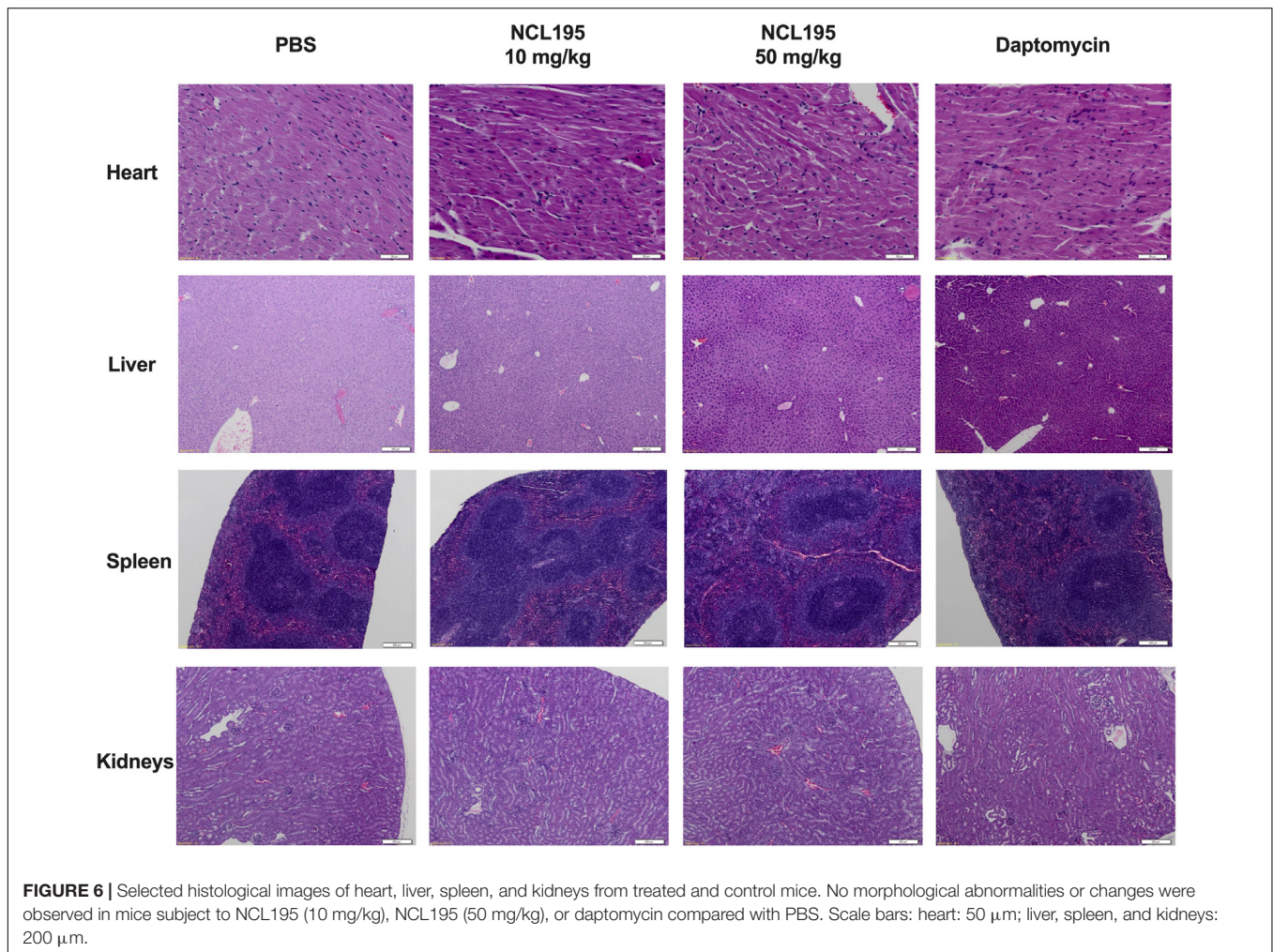


FIGURE 6 | Selected histological images of heart, liver, spleen, and kidneys from treated and control mice. No morphological abnormalities or changes were observed in mice subject to NCL195 (10 mg/kg), NCL195 (50 mg/kg), or daptomycin compared with PBS. Scale bars: heart: 50 μm ; liver, spleen, and kidneys: 200 μm .

World Health Organization [WHO], 2019). Previously, we reported that NCL195 showed potential as a new drug scaffold for the treatment of infections caused by Gram-positive bacteria on the basis of its favorable pharmacokinetic and pharmacodynamics profile compared to the parent compound robenidine (Ogunniyi et al., 2017). Here, we extended our analyses by assessing *in vitro* efficacy of NCL195 against a range of clinical human Gram-negative pathogens in the presence or absence of subinhibitory concentrations of EDTA, PMBN, or PMB and by conducting preliminary *in vivo* safety and efficacy studies against two prominent Gram-positive bacteria. This study had three major findings. First, NCL195 demonstrated antimicrobial activity against a variety of Gram-negative ESKAPE pathogens in the presence of outer membrane permeabilizers (EDTA, PMB, and PMBN). In particular, combination of NCL195 with PMB showed the best synergistic activity against all the bacteria tested. Second, NCL195 showed systemic safety in mice without any apparent morphological effects on the major organs examined. However, as this study has only examined histomorphology but not clinical chemistry and hematology, sublethal effects not resulting in morphological changes of tissues cannot be excluded. Third, systemic treatment of mice with

NCL195 reduced bioluminescent *S. pneumoniae* and *S. aureus* populations *in vivo* and significantly prolonged survival times.

We demonstrated that the combination of EDTA with NCL195 resulted in a synergistic interaction when tested against *E. coli*, *K. pneumoniae*, *P. putida*, and *P. aeruginosa* type and clinical strains. In combination, NCL195 MICs ranged from 0.5 to 8 $\mu\text{g}/\text{mL}$ in the presence of EDTA concentrations ranging from 190 to 11,400 $\mu\text{g}/\text{mL}$. However, the lowest dose of EDTA to cause a toxic effect in animals is reported to be 750 mg/kg/day (Lanigan and Yamarik, 2002). In addition, oral exposure to EDTA produced adverse reproductive and developmental effects in animals (Lanigan and Yamarik, 2002). Therefore, EDTA in synergistic combination with NCL195 is not considered to be a viable option for administration by the oral, intravenous, and intramuscular routes in humans and animals.

In combination with PMBN (which alone had no antimicrobial activity against the tested Gram-negative bacteria except for *P. aeruginosa*), NCL195 exhibited a synergistic interaction against less than half of the tested Gram-negative bacteria, with the NCL195 MICs ranging from 4 to 32 $\mu\text{g}/\text{mL}$. The lack of activity of PMBN against Gram-negative bacteria has been attributed to the absence of N-terminal fatty acyl chain

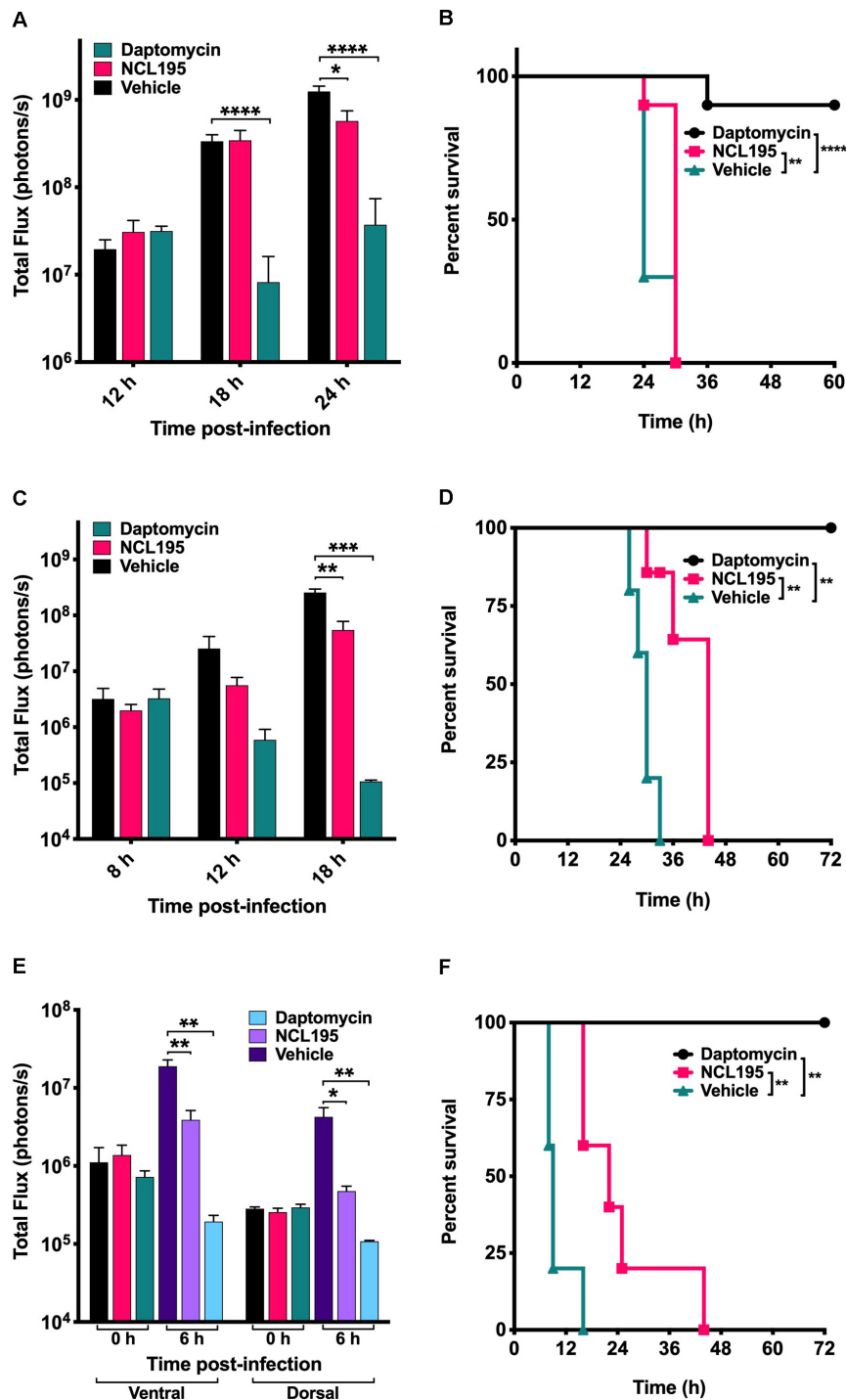


FIGURE 7 | Luminescence signal comparisons between groups of CD1 mice challenged intraperitoneally with *S. pneumoniae* (D39LUX) treated 6 h apart (A,B) or treated 4 h apart (C,D), and bioluminescent *S. aureus* ATCC 12600 (Xen29) treated 4 h apart (E,F). Mice were subjected to bioluminescent imaging on an IVIS Lumina XRMS Series III system. * $p < 0.05$; ** $p < 0.01$; *** $p < 0.001$; **** $p < 0.0001$.

present in PMB and highlights the importance of both the electrostatic and hydrophobic interactions for the mechanism of PMB action (Velkov et al., 2010). Our results demonstrated that the combination of PMBN with NCL195 is not ideal for

the treatment of human systemic Gram-negative bacterial infections. PMB, with antimicrobial activity against Gram-negative bacteria, could be a better and less expensive choice to be used in combination with NCL195 to treat Gram-negative

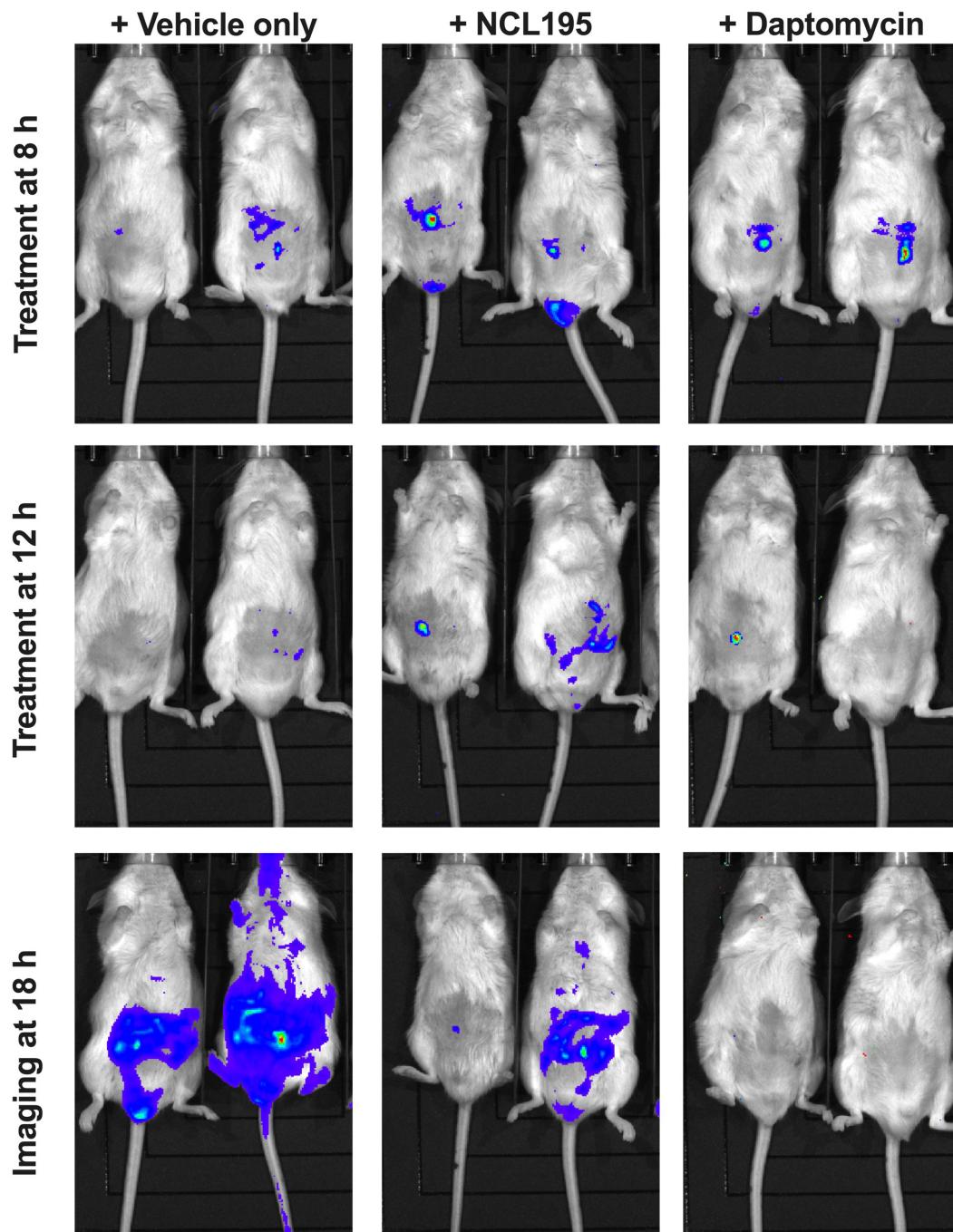
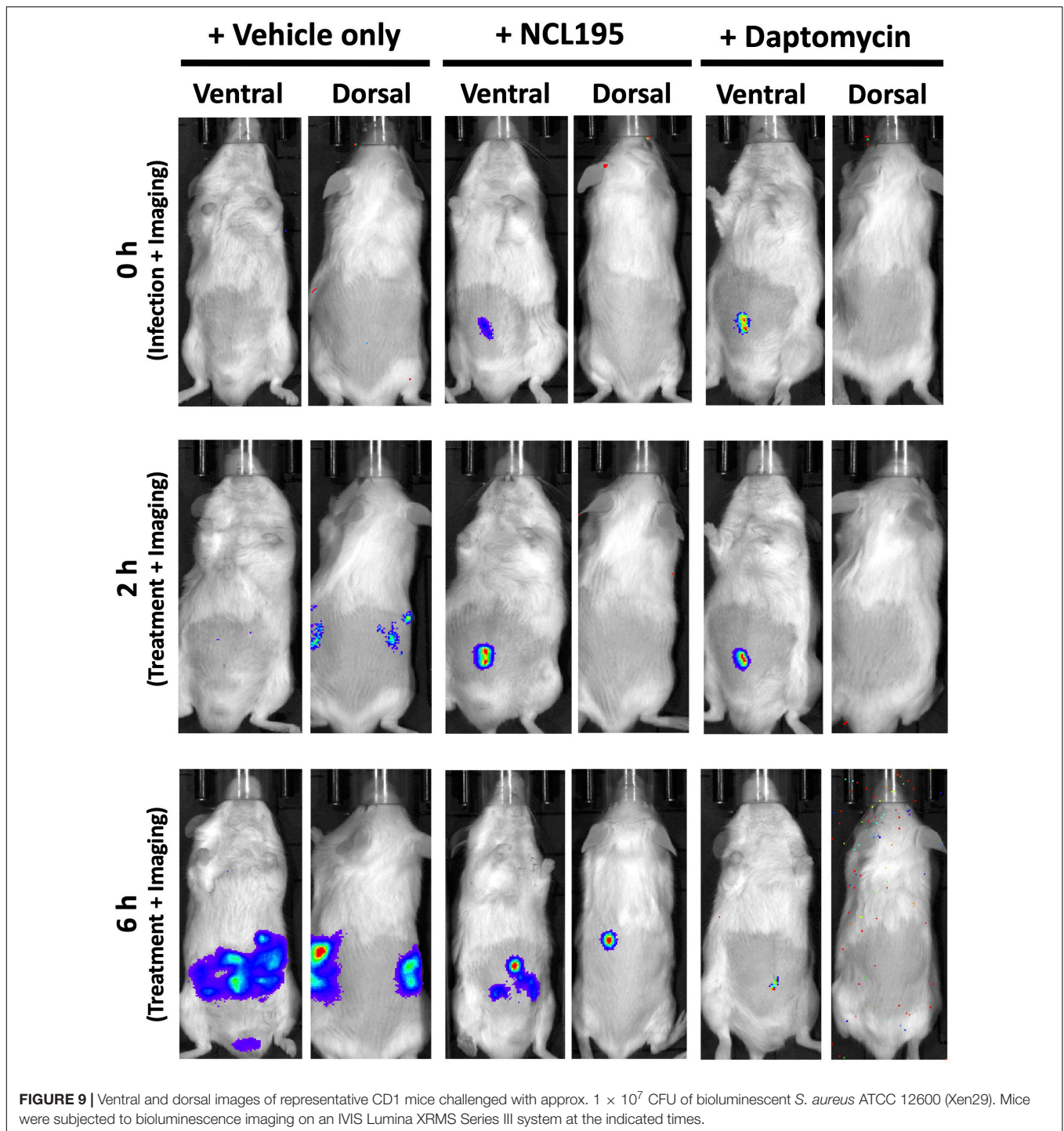


FIGURE 8 | Ventral images of representative CD1 mice challenged with approx. 1×10^7 CFU of bioluminescent *S. pneumoniae* (D39LUX). Mice were subjected to bioluminescence imaging on an IVIS Lumina XRMS Series III system at the indicated times.

bacteria, reducing the required concentrations for both drugs, and resulting in better cytotoxicity profiles (Deris et al., 2014; Brown and Dawson, 2017; Lin et al., 2018, 2019).

Previous studies investigating the metabolic pathways impacted by PMB alone or in combination with enrofloxacin was carried out to discover the mechanism of action of the combination against Gram-negative bacteria (Lin et al.,

2019). It was found that a large number of metabolites associated with fatty acid and lipid metabolism pathways were significantly perturbed following treatment of *P. aeruginosa* with subinhibitory concentration of PMB alone or in combination with enrofloxacin at 1 and 4 h, consistent with the mode of action of PMB in the disruption of the bacterial outer membrane (Lin et al., 2018, 2019). These pathways play an important role



in the DNA repair process; therefore PMB alone can disrupt these processes to prevent the self-repair mechanisms in the bacteria. On the other hand, we previously showed that NCL195 disrupts the inner membrane potential of Gram-positive bacteria and inhibits DNA and RNA synthesis, thereby hindering the establishment and maintenance of essential energy sources for cell functioning (Ogunniyi et al., 2017). Thus, we hypothesized that a combination of PMB and NCL195 will disrupt the outer

membrane (PMB), hence allowing penetration of NCL195 to the inner membrane, where it will exert its mechanism of action in preventing DNA/RNA synthesis and altering energy metabolism and cell envelope biogenesis. The combined action of PMB and NCL195 was expected to be synergistic, resulting in the antimicrobial activity of the combination against Gram-negative bacteria, as was demonstrated in the MIC results reported here. The proposed dual mechanism of action of the NCL195-PMB

combination was proven in this study by demonstrating a time-dependent and NCL195 concentration-dependent disruption of the inner membrane potential of *E. coli* cells.

Further screening of a broader range of clinical Gram-negative bacteria isolated from humans (18 *K. pneumoniae*, 18 *E. coli*, 16 *A. baumannii*, and 19 *P. aeruginosa*) proved our hypothesis that in the presence of PMB, NCL195 could inhibit the growth of the ESKAPE pathogens (MICs ranging from 0.25 to 4 $\mu\text{g}/\text{mL}$) (Ogunniyi et al., 2017). The current results show that the MIC of NCL195 was significantly reduced 32- to 512-fold, and the MIC of PMB was reduced 2- to 8-fold. Although it was previously reported that PMB is toxic for humans at a concentration of 4 $\mu\text{g}/\text{mL}$, the lowest concentration required in combination with NCL195 ranged from 0.0625 to 0.25 $\mu\text{g}/\text{mL}$, which is 64- to 16-fold lower than its cytotoxic dose (Roberts et al., 2015; Ahmed et al., 2017). Overall, PMB was the best choice among the three outer membrane permeabilizers, due to the subinhibitory activity against all Gram-negative species, as well as lower MICs and less toxicity potential.

We previously used fluorescence-based membrane potential measurements to show that NCL195 and other NCL compounds permeabilize the cytoplasmic membrane of *S. pneumoniae* and *S. aureus*, and hence hinder the establishment and maintenance of essential energy sources for cell functioning (Ogunniyi et al., 2017). In this study, we extended our investigation on the effects of NCL195 on bioluminescent *S. aureus* morphology prepared using Tokuyasu cryo-ultramicrotomy. TEM images show membrane morphology changes and the presence of mesosome-like membrane structures in NCL195-treated but not in untreated bacteria. The presence of mesosomes is possibly a consequence of cell membrane perturbation through disruption of the membrane potential, consistent with the effects of other antibiotic treatments reported by other workers (Friedrich et al., 2000; Li et al., 2008; Morita et al., 2015; Gao et al., 2019).

We also found that two intraperitoneal administrations of NCL195 at 50 mg/kg at 4 h apart was safe in mice without any demonstrable clinical signs or observable morphological effects on the main organs examined. Given these findings, there is a possibility of using PMB in combination with NCL195 for human use after appropriate testing in animal models of infection.

Based on the above, we evaluated the potential of NCL195 as a therapeutic drug against acute systemic *S. pneumoniae* or *S. aureus* infection, using luminescent derivatives of highly virulent pneumococcal strain (D39LUX) and *S. aureus* ATCC12600 (Xen29) in an intraperitoneal challenge infection model. Our results show that two 50 mg/kg i.p. doses of NCL195 resulted in a statistically significant reduction in both *S. pneumoniae* or *S. aureus* populations and prolonged survival times compared to the vehicle-only control. These results suggest that while plasma binding increases the MIC for NCL195 by fourfold against *S. aureus in vitro*, it does not appear to affect its *in vivo* activity, as judged by the statistically significant increase in the median survival times of mice that received NCL195 compared to the vehicle only group. While NCL195 did not achieve the level of potency seen with daptomycin, we have shown that no resistance developed above the MIC for *S. aureus* over 24 serial passages, whereas resistance to daptomycin

developed by day 5, and increased up to $8 \times \text{MIC}$ by day 12 of the serial passage (Ogunniyi et al., 2017). A low propensity to select resistance is a desirable characteristic for further exploration of NCL195 as a novel antimicrobial class to treat acute bacterial infections in humans. Furthermore, it is reported that daptomycin, which is active against resistant Gram-positive bacteria, does not have antimicrobial activity against most Gram-negative bacteria, even in combination with antimicrobials and outer membrane permeabilizers (Phee et al., 2013). Together, our findings demonstrate that the new antibacterial class represented by NCL195 could provide promising new scaffolds for further pharmaceutical and medicinal chemistry development. Further chemical diversification of the NCL195 scaffold is desirable to increase solubility and reduce plasma binding and potential toxicity, as well as improve potency against the antimicrobial resistant pathogens currently listed as most urgent priority for antibacterial drug discovery and development (Willyard, 2017; World Health Organization [WHO], 2019).

DATA AVAILABILITY STATEMENT

All datasets generated for this study are included in the article/Supplementary Material.

ETHICS STATEMENT

The animal study was reviewed and approved by The Animal Ethics Committee of The University of Adelaide (approval numbers S-2013-053 and S-2015-151). The study was conducted in compliance with the Australian Code of Practice for the Care and Use of Animals for Scientific Purposes (8th Edition 2013) and the South Australian Animal Welfare Act 1985.

AUTHOR CONTRIBUTIONS

HP, HN, HV, SP, AM, LO'D, DT, and AO: conceptualization. HP, HN, AB, LW, LO'D, and AO: data curation and methodology. HP, HN, HV, AB, LW, SG, SP, AM, LO'D, DT, and AO: formal analysis. HV, SG, SP, AM, DT, and AO: funding acquisition. HP, HN, AB, LW, SP, LO'D, DT, and AO: investigation. CR, JB, and AM: NCL195 synthesis. SG, SP, AM, DT, and AO: project administration. HV, LW, SG, SP, AM, and DT: resources. HV, SG, AM, DT, and AO: supervision. HV, SP, DT, and AO: validation. HP, HN, and AO: writing—original draft. HP, HN, HV, AB, LW, SG, SP, CR, AM, LO'D, DT, and AO: writing—review and editing. All authors contributed to the article and approved the submitted version.

FUNDING

This work was supported by an Australian Research Council (ARC; arc.gov.au) Linkage grant (LP110200770) to DT, AM, and SP with Neoculi Pty. Ltd. as the Partner Organization and a University of South Australia fund to HV. The funders did not

have any additional role in the study design, data collection and analysis, decision to publish, or preparation of the manuscript.

ACKNOWLEDGMENTS

The authors would like to thank Ms. Amanda Bergamin and Ms. Krishna Kathawala at the University of South Australia for kindly preparing and providing the NCL formulations. The authors would also like to thank Ms. Amanda Ruggero, Ms. Lora Bowes, and Ms. Anh Hong Nguyen at the University of South Australia for their technical

assistance. The authors acknowledge the instruments and scientific and technical assistance of Microscopy Australia at Adelaide Microscopy, The University of Adelaide, a facility that is funded by the University and state and federal governments.

SUPPLEMENTARY MATERIAL

The Supplementary Material for this article can be found online at: <https://www.frontiersin.org/articles/10.3389/fmicb.2020.01556/full#supplementary-material>

REFERENCES

- Abraham, R. J., Stevens, A. J., Young, K. A., Russell, C., Qvist, A., Khazandi, M., et al. (2016). Robenidone analogues as Gram-positive antibacterial agents. *J. Med. Chem.* 59, 2126–2138. doi: 10.1021/acs.jmedchem.5b01797
- Ahmed, M. U., Velkov, T., Lin, Y.-W., Yun, B., Nowell, C. J., Zhou, F., et al. (2017). Potential toxicity of polymyxins in human lung epithelial cells. *Antimicrob. Agents Chemother.* 61:e02690-16.
- Bhattacharya, S. (2013). Early diagnosis of resistant pathogens: how can it improve antimicrobial treatment? *Virulence* 4, 172–184. doi: 10.4161/viru.23326
- Brown, P., and Dawson, M. J. (2017). Development of new polymyxin derivatives for multi-drug resistant Gram-negative infections. *J. Antibiot.* 70, 386–394. doi: 10.1038/ja.2016.146
- Cardoso, T., Ribeiro, O., Aragão, I. C., Costa-Pereira, A., and Sarmiento, A. E. (2012). Additional risk factors for infection by multidrug-resistant pathogens in healthcare-associated infection: a large cohort study. *BMC Infect. Dis.* 12:375. doi: 10.1186/1471-2334-12-375
- Centers for Disease Control and Prevention [CDCP] (2019). *Antibiotic Resistance Threats in the United States, 2019*. Atlanta, GA: U.S. Department of Health and Human Services, CDC.
- Clinical and Laboratory Standards Institute [CLSI] (2017). *Performance Standards for Antimicrobial Susceptibility Testing, 27th ed. CLSI standard M100*. Wayne, PA: CLSI.
- Deris, Z. Z., Swarbrick, J. D., Roberts, K. D., Azad, M. A., Akter, J., Horne, A. S., et al. (2014). Probing the penetration of antimicrobial polymyxin lipopeptides into Gram-negative bacteria. *Bioconjug. Chem.* 25, 750–760. doi: 10.1021/bc500094d
- Eid, S. Y., El-Readi, M. Z., and Wink, M. (2012). Synergism of three-drug combinations of sanguinarine and other plant secondary metabolites with digitonin and doxorubicin in multi-drug resistant cancer cells. *Phytomedicine* 19, 1288–1297. doi: 10.1016/j.phymed.2012.08.010
- Friedrich, C. L., Moyles, D., Beveridge, T. J., and Hancock, R. E. (2000). Antibacterial action of structurally diverse cationic peptides on Gram-positive bacteria. *Antimicrob. Agents Chemother.* 44, 2086–2092. doi: 10.1128/aac.44.8.2086-2092.2000
- Frieri, M., Kumar, K., and Boutin, A. (2017). Antibiotic resistance. *J. Infect. Public Health* 10, 369–378.
- Gao, Z., Van Nostrand, J. D., Zhou, J., Zhong, W., Chen, K., and Guo, J. (2019). Anti-Listeria activities of linalool and its mechanism revealed by comparative transcriptome analysis. *Front. Microbiol.* 10:2947. doi: 10.3389/fmicb.2019.02947
- Giamarellou, H. (2010). Multidrug-resistant Gram-negative bacteria: how to treat and for how long. *Int. J. Antimicrob. Agents* 36(Suppl. 2), S50–S54.
- Hamoud, R., Reichling, J., and Wink, M. (2015). Synergistic antibacterial activity of the combination of the alkaloid sanguinarine with EDTA and the antibiotic streptomycin against multidrug resistant bacteria. *J. Pharm. Pharmacol.* 67, 264–273. doi: 10.1111/jphp.12326
- Henken, S., Bohling, J., Ogunniyi, A. D., Paton, J. C., Salisbury, V. C., Welte, T., et al. (2010). Evaluation of biophotonic imaging to estimate bacterial burden in mice infected with highly virulent compared to less virulent Streptococcus pneumoniae serotypes. *Antimicrob. Agents Chemother.* 54, 3155–3160. doi: 10.1128/aac.00310-10
- Khazandi, M., Pi, H., Chan, W. Y., Ogunniyi, A. D., Sim, J. X. F., Venter, H., et al. (2019). In vitro antimicrobial activity of robenidone, ethylenediaminetetraacetic acid and polymyxin B nonapeptide against important human and veterinary pathogens. *Front. Microbiol.* 10:837. doi: 10.3389/fmicb.2019.00837
- Lanigan, R. S., and Yamarik, T. A. (2002). Final report on the safety assessment of EDTA, calcium disodium EDTA, diammonium EDTA, dipotassium EDTA, disodium EDTA, TEA-EDTA, tetrasodium EDTA, tripotassium EDTA, trisodium EDTA, HEDTA, and trisodium HEDTA. *Int. J. Toxicol.* 21(Suppl. 2), 95–142. doi: 10.1080/10915810290096522
- Lepore, C., Silver, L., Theuretzbacher, U., Thomas, J., and Visi, D. (2019). The small-molecule antibiotics pipeline: 2014–2018. *Nat. Rev. Drug Discov.* 18:739. doi: 10.1038/d41573-019-00130-8
- Li, X., Feng, H. Q., Pang, X. Y., and Li, H. Y. (2008). Mesosome formation is accompanied by hydrogen peroxide accumulation in bacteria during the rifampicin effect. *Mol. Cell. Biochem.* 311, 241–247. doi: 10.1007/s11010-007-9690-4
- Lin, Y.-W., Han, M.-L., Zhao, J., Zhu, Y., Rao, G., Forrest, A., et al. (2019). Synergistic combination of polymyxin B and enrofloxacin induced metabolic perturbations in extensive drug-resistant *Pseudomonas aeruginosa*. *Front. Pharmacol.* 10:1146. doi: 10.3389/fphar.2019.01146
- Lin, Y.-W., Heidi, H. Y., Zhao, J., Han, M.-L., Zhu, Y., Akter, J., et al. (2018). Polymyxin B in combination with enrofloxacin exerts synergistic killing against extensively drug-resistant *Pseudomonas aeruginosa*. *Antimicrob. Agents Chemother.* 62:e0028-18.
- Livermore, D. M. (2012). Current epidemiology and growing resistance of Gram-negative pathogens. *Korean J. Intern. Med.* 27:128. doi: 10.3904/kjim.2012.27.2.128
- Morita, D., Sawada, H., Ogawa, W., Miyachi, H., and Kuroda, T. (2015). Riccardin C derivatives cause cell leakage in *Staphylococcus aureus*. *Biochim. Biophys. Acta* 1848, 2057–2064. doi: 10.1016/j.bbamem.2015.05.008
- Ogunniyi, A. D., Khazandi, M., Stevens, A. J., Sims, S. K., Page, S. W., Garg, S., et al. (2017). Evaluation of robenidone analog NCL195 as a novel broad-spectrum antibacterial agent. *PLoS One* 12:e0183457. doi: 10.1371/journal.pone.0183457
- Ogunniyi, A. D., Kopecki, Z., Hickey, E. E., Khazandi, M., Peel, E., Belov, K., et al. (2018). Bioluminescent murine models of bacterial sepsis and scald wound infections for antimicrobial efficacy testing. *PLoS One* 13:e0200195. doi: 10.1371/journal.pone.0200195
- Pendleton, J. N., Gorman, S. P., and Gilmore, B. F. (2013). Clinical relevance of the ESKAPE pathogens. *Expert Rev. Anti Infect. Ther.* 11, 297–308. doi: 10.1586/eri.13.12
- Phee, L., Hornsey, M., and Wareham, D. W. (2013). In vitro activity of daptomycin in combination with low-dose colistin against a diverse collection of Gram-negative bacterial pathogens. *Eur. J. Clin. Microbiol. Infect. Dis.* 32, 1291–1294. doi: 10.1007/s10096-013-1875-z
- Pushpakom, S., Iorio, F., Eyers, P. A., Escott, K. J., Hopper, S., Wells, A., et al. (2019). Drug repurposing: progress, challenges and recommendations. *Nat. Rev. Drug Discov.* 18:41. doi: 10.1038/nrd.2018.168
- Roberts, K. D., Azad, M. A., Wang, J., Horne, A. S., Thompson, P. E., Nation, R. L., et al. (2015). Antimicrobial activity and toxicity of the major lipopeptide components of polymyxin B and colistin: last-line antibiotics against multidrug-resistant Gram-negative bacteria. *ACS Infect. Dis.* 1, 568–575. doi: 10.1021/acinfecdis.5b00085

- Santajit, S., and Indrawattana, N. (2016). Mechanisms of antimicrobial resistance in ESKAPE pathogens. *BioMed Res. Int.* 2016:2475067.
- Tamma, P. D., Cosgrove, S. E., and Maragakis, L. L. (2012). Combination therapy for treatment of infections with Gram-negative bacteria. *Clin. Microbiol. Rev.* 25:450. doi: 10.1128/cmr.05041-11
- Theuretzbacher, U., Gottwalt, S., Beyer, P., Butler, M., Czaplowski, L., Lienhardt, C., et al. (2019). Analysis of the clinical antibacterial and antituberculosis pipeline. *Lancet Infect. Dis.* 19, e40–e50. doi: 10.1016/s1473-3099(18)30513-9
- Velkov, T., Thompson, P. E., Nation, R. L., and Li, J. (2010). Structure–activity relationships of polymyxin antibiotics. *J. Med. Chem.* 53, 1898–1916. doi: 10.1021/jm900999h
- Venter, H. (2019). Reversing resistance to counter antimicrobial resistance in the World Health Organisation's critical priority of most dangerous pathogens. *Biosci. Rep.* 39:BSR20180474.
- Venter, H., Shilling, R. A., Velamakanni, S., Balakrishnan, L., and Van Veen, H. W. (2003). An ABC transporter with a secondary-active multidrug translocator domain. *Nature* 426, 866–870. doi: 10.1038/nature02173
- Ventola, C. L. (2015). The antibiotic resistance crisis: part 1: causes and threats. *Pharm. Ther.* 40, 277–283.
- Wang, Y., Alenzy, R., Song, D., Liu, X., Teng, Y., Mowla, R., et al. (2020). Structural optimization of natural product nordihydroguarectic acid to discover novel analogues as AcrB inhibitors. *Eur. J. Med. Chem.* 186:111910. doi: 10.1016/j.ejmech.2019.111910
- Willyard, C. (2017). The drug-resistant bacteria that pose the greatest health threats. *Nature* 543:15. doi: 10.1038/nature.2017.21550
- Woolhouse, M., and Farrar, J. (2014). Policy: an intergovernmental panel on antimicrobial resistance. *Nat. News* 509:555. doi: 10.1038/509555a
- World Health Organization [WHO] (2019). *WHO Advisory Group on Integrated Surveillance of Antimicrobial Resistance (AGISAR): Critically Important Antimicrobials for Human Medicine 6th Revision 2018*. Geneva: WHO.
- Zilberberg, M. D., Shorr, A. F., Micek, S. T., Vazquez-Guillamet, C., and Kollef, M. H. (2014). Multi-drug resistance, inappropriate initial antibiotic therapy and mortality in Gram-negative severe sepsis and septic shock: a retrospective cohort study. *Crit. Care* 18:596.

Conflict of Interest: SP is a director of Neoculi Pty. Ltd.

The remaining authors declare that the research was conducted in the absence of any commercial or financial relationships that could be construed as a potential conflict of interest.

Copyright © 2020 Pi, Nguyen, Venter, Boileau, Woolford, Garg, Page, Russell, Baker, McCluskey, O'Donovan, Trott and Ogguniyi. This is an open-access article distributed under the terms of the Creative Commons Attribution License (CC BY). The use, distribution or reproduction in other forums is permitted, provided the original author(s) and the copyright owner(s) are credited and that the original publication in this journal is cited, in accordance with accepted academic practice. No use, distribution or reproduction is permitted which does not comply with these terms.

Supplementary Material

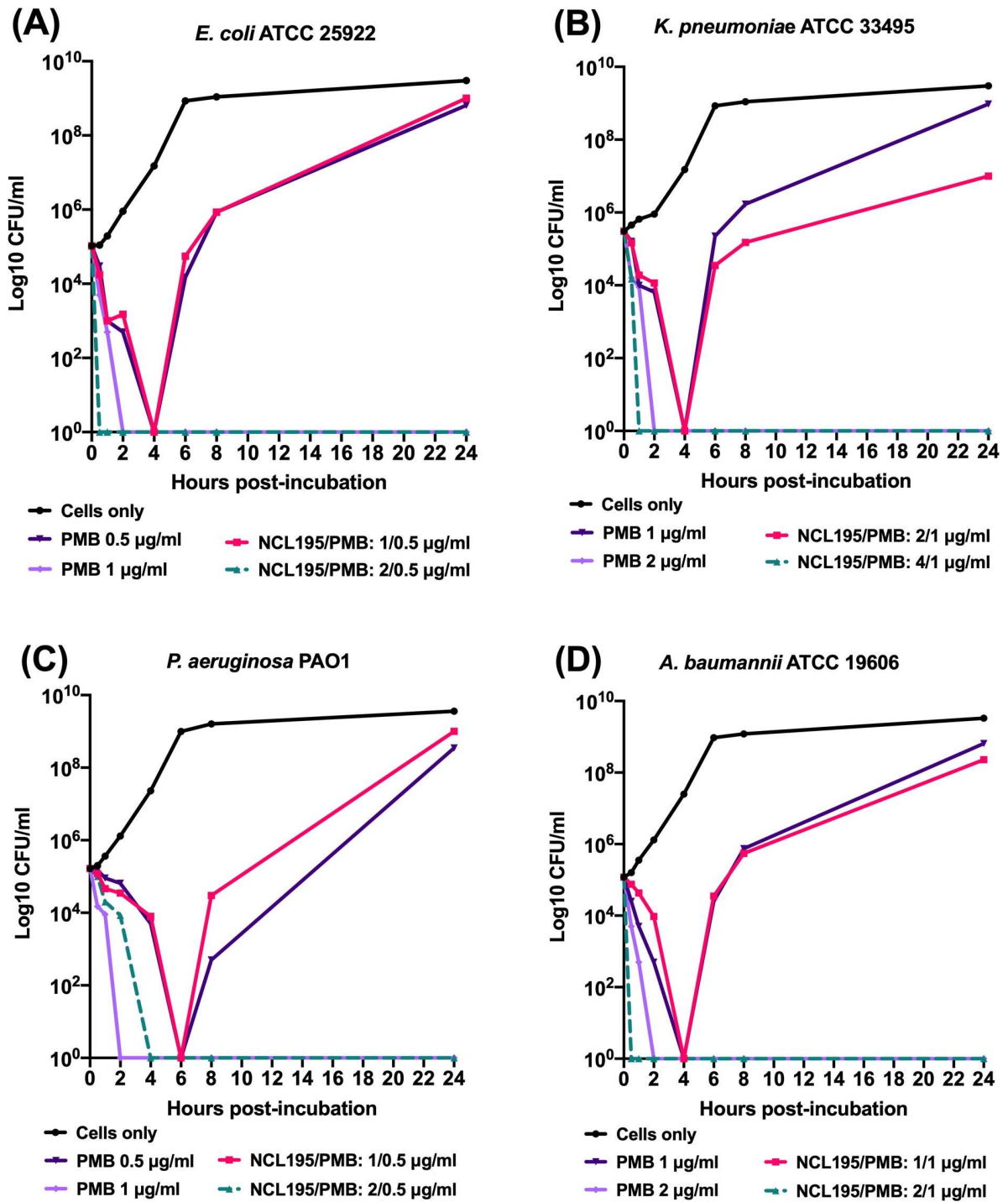


Figure S1. Time kill curves of NCL195 and PMB combinations against *E. coli* ATCC 25922 (A), *K. pneumoniae* ATCC 33495 (B), *P. aeruginosa* PAO1 (C) and *A. baumannii* ATCC 19606 (D).

Chapter III

***In vitro* synergistic antimicrobial activity of NCL195 in combination with adjuvants against Gram- negative bacterial pathogens**

Statement of Authorship

| | |
|---------------------|---|
| Title of Paper | <i>In vitro</i> synergistic activity of NCL195 in combination with colistin against Gram-negative bacterial pathogens |
| Publication Status | <input checked="" type="checkbox"/> Published <input type="checkbox"/> Accepted for Publication <input type="checkbox"/> Submitted for Publication <input type="checkbox"/> Unpublished and Unsubmitted work written in manuscript style |
| Publication Details | Nguyen, H.T. ; Venter, H.; Veltman, T.; Williams, R.; O'Donovan, L.A.; Russell, C.C.; McCluskey, A.; Page, S.W.; Ogunniyi, A.D.; Trott, D.J. <i>In vitro</i> synergistic activity of NCL195 in combination with colistin against Gram-negative bacterial pathogens. <i>Int J Antimicrob Agents</i> 2021 , 57, 106323, doi: https://doi.org/10.1016/j.ijantimicag.2021.106323 . Journal Impact Factor = 15.441. |

Principal Author

| | | | |
|--------------------------------------|--|------|-------------|
| Name of Principal Author (Candidate) | Hang Thi Nguyen | | |
| Contribution to the Paper | Contributed to the study design, performed all experiments and wrote the preliminary manuscript | | |
| Overall percentage (%) | 70% | | |
| Certification: | This paper reports on original research I conducted during the period of my Higher Degree by Research candidature and is not subject to any obligations or contractual agreements with a third party that would constrain its inclusion in this thesis. I am the primary author of this paper. | | |
| Signature | | Date | 01/12/20221 |

Co-Author Contributions

By signing the Statement of Authorship, each author certifies that:

- i. the candidate's stated contribution to the publication is accurate (as detailed above);
- ii. permission is granted for the candidate to include the publication in the thesis; and
- iii. the sum of all co-author contributions is equal to 100% less the candidate's stated contribution.

| | | | |
|---------------------------|--|------|------------|
| Name of Co-Author | Henrietta Venter | | |
| Contribution to the Paper | Contributed to study design, editing, financial support, discussion, and provided expertise on mechanism of action studies | | |
| Signature | | Date | 15/12/2021 |
| Name of Co-Author | Tania Veltman | | |
| Contribution to the Paper | Contributed to MALDI-TOF and Sensititre TM antimicrobial sensitivity testing | | |
| Signature | | Date | 18/01/2022 |

| | | | |
|---------------------------|---|------|------------|
| Name of Co-Author | Lucy Woolford | | |
| Contribution to the Paper | Contributed to histopathological examinations, editing and discussion | | |
| Signature | | Date | 05/01/2022 |

| | | | |
|---------------------------|---|------|------------|
| Name of Co-Author | Ruth Williams | | |
| Contribution to the Paper | Contributed to TEM technical guidance, experimentation and editing the manuscript | | |
| Signature | | Date | 12/01/2022 |

| | | | |
|---------------------------|---|------|-----------|
| Name of Co-Author | Lisa Anne O'Donovan | | |
| Contribution to the Paper | Contributed to TEM technical guidance, experimentation and editing the manuscript | | |
| Signature | | Date | 5/01/2022 |

| | | | |
|---------------------------|---|------|------------|
| Name of Co-Author | Cecilia C. Russell | | |
| Contribution to the Paper | Responsible for synthesising NCL195 and contributed to editing the manuscript | | |
| Signature | | Date | 12/01/2022 |

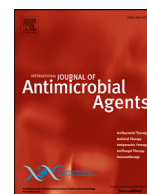
| | | | |
|---------------------------|---|------|------------|
| Name of Co-Author | Adam McCluskey | | |
| Contribution to the Paper | Responsible for synthesising NCL195 and contributed to editing the manuscript | | |
| Signature | | Date | 06/02/2022 |

| | | | |
|---------------------------|---|------|------------|
| Name of Co-Author | Stephen W. Page | | |
| Contribution to the Paper | Contributed to editing, discussion and provided financial support for the study | | |
| Signature | | Date | 02/02/2022 |

| | | | |
|---------------------------|--|------|------------|
| Name of Co-Author | Abiodun D. Ogunniyi | | |
| Contribution to the Paper | Contributed to study design, TEM technical guidance, mode of action studies, cytotoxicity assays, and participated in writing, editing, discussion and was co-corresponding author | | |
| Signature | | Date | 08/12/2021 |

| | | | |
|---------------------------|---|------|------------|
| Name of Co-Author | Darren J. Trott | | |
| Contribution to the Paper | Contributed to study design, and participated in writing, editing, and discussion, provided financial support for the study and was co-corresponding author | | |
| Signature | | Date | 07/02/2022 |

Please cut and paste additional co-author panels here as required.



In vitro synergistic activity of NCL195 in combination with colistin against Gram-negative bacterial pathogens

Hang Thi Nguyen^{a,b}, Henrietta Venter^c, Tania Veltman^a, Ruth Williams^d,
Lisa Anne O'Donovan^e, Cecilia C. Russell^f, Adam McCluskey^f, Stephen W. Page^g,
Abiodun David Ogunniyi^{a,1,**}, Darren J. Trott^{a,1,*}

^a Australian Centre for Antimicrobial Resistance Ecology, School of Animal and Veterinary Sciences, The University of Adelaide, Roseworthy, SA, Australia

^b Department of Pharmacology, Toxicology, Internal Medicine and Diagnostics, Faculty of Veterinary Medicine, Vietnam National University of Agriculture, Hanoi, Vietnam

^c Health and Biomedical Innovation, Clinical and Health Sciences, University of South Australia, Adelaide, SA, Australia

^d Adelaide Microscopy, University of Adelaide, Adelaide, SA, Australia

^e ARC Centre of Excellence in Plant Energy Biology, School of Agriculture, Food & Wine, University of Adelaide, SA, Australia

^f Chemistry, School of Environmental & Life Sciences, University of Newcastle, Callaghan, NSW, Australia

^g Neoculi Pty Ltd., Burwood, VIC, Australia

ARTICLE INFO

Article history:

Received 4 September 2020

Accepted 13 March 2021

Editor: J.-M. Rolain

Keywords:

NCL195

Colistin

Gram-negative bacteria

Multidrug resistance

Transmission electron microscopy

Synergy

ABSTRACT

In this study, the potential of using the novel antibiotic NCL195 combined with subinhibitory concentrations of colistin against infections caused by Gram-negative bacteria (GNB) was investigated. We showed synergistic activity of the combination NCL195 + colistin against clinical multidrug-resistant GNB pathogens with minimum inhibitory concentrations (MICs) for NCL195 ranging from 0.5–4 $\mu\text{g}/\text{mL}$ for *Acinetobacter baumannii*, *Escherichia coli*, *Klebsiella pneumoniae* and *Pseudomonas aeruginosa*, whereas NCL195 alone had no activity. Transmission electron microscopy of the membrane morphology of *E. coli* and *P. aeruginosa* after single colistin or combination drug treatment showed marked ultrastructural changes most frequently in the cell envelope. Exposure to NCL195 alone did not show any change compared with untreated control cells, whereas treatment with the NCL195 + colistin combination caused more damage than colistin alone. Direct evidence for this interaction was demonstrated by fluorescence-based membrane potential measurements. We conclude that the synergistic antimicrobial activity of the combination NCL195 + colistin against GNB pathogens warrants further exploration for specific treatment of acute GNB infections.

© 2021 Elsevier Ltd and International Society of Antimicrobial Chemotherapy. All rights reserved.

1. Introduction

Bacterial infections continue to pose challenges to healthcare systems in all countries. Overuse of antibiotics in the treatment of bacterial infections has resulted in the development of numerous multidrug-resistant (MDR) bacterial pathogens [1]. In particular, infections due to MDR ESKAPE (*Enterococcus faecium*, *Staphylococcus aureus*, *Klebsiella pneumoniae*, *Acinetobacter baumannii*, *Pseudomonas aeruginosa* and *Escherichia coli*/ *Enterobacter* spp.) pathogens contribute significantly to morbidity and mortality associated with antimicrobial resistance worldwide (700 000 deaths

annually) [2]. While the incidence of methicillin-resistant *S. aureus* (MRSA) has slightly decreased, the incidence of infections caused by MDR Gram-negative bacteria (GNB) (*E. coli*, *K. pneumoniae*, *P. aeruginosa*, *A. baumannii*, *Enterobacter* spp.) is reported to have increased [3]. Unfortunately, the rate of approval of new anti-GNB drugs by the US Food and Drug Administration (FDA) is not commensurate with the increasing pace of MDR-GNB infections [4].

The numerous challenges posed by MDR-GNB pathogens compared with MDR-Gram-positive bacteria (GPB) infections in new drug discovery and healthcare settings are attributable to the presence of an outer membrane in GNB that prevents antibiotics from gaining entry and exerting their effect [5]. Given that the discovery and development process of new drugs costs over US\$2.6 billion and can take up to 15 years to be marketed, pharmaceuticals have focused their research and development mostly on developing new antibiotics against MDR-GPB, while the development of

* Corresponding authors. Tel.: +61 8 8313 7989, fax: +16 8 8313 7956.

** tel.: +61 43 233 1914.

E-mail addresses: david.ogunniyi@adelaide.edu.au (A.D. Ogunniyi), darren.trott@adelaide.edu.au (D.J. Trott).

¹ These two authors should be considered as joint senior authors.

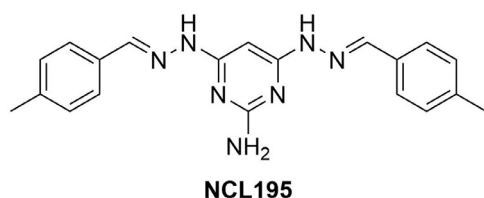


Fig. 1. Chemical structure of NCL195 [4,6-bis(2-((E)-4-methylbenzylidene)hydrazinyl)pyrimidin-2-amine].

new antimicrobials for treatment of MDR-GNB infections has been neglected [6–8]. Furthermore, novel drug development also carries a high risk (nearly 84%) of failure in the preclinical stage [9].

The majority of recently approved agents against MDR-GNB infections have been modifications of existing chemical classes, rather than new chemical classes with a novel mechanism of action [10]. Polymyxins, such as polymyxin B (PMB) and colistin, as well as other drugs such as ceftolozane/tazobactam, ceftazidime/avibactam and meropenem/vaborbactam are considered as last-resort antibiotic classes for the treatment of GNB infections [11,12]; however, resistance to polymyxins is emerging via different mechanisms [11,13]. Studies have also reported that the use of polymyxins is associated with nephrotoxicity, neurotoxicity and neuromuscular blockade [14,15]. A number of studies have provided evidence that combination of polymyxins with other antibiotics showed fully synergistic or partially synergistic activity against MDR-GNB pathogens [16–19].

Notwithstanding the current advances, it is critical that new antibiotic classes with novel mechanisms of action against GNB infections are developed to address the shortfall in novel agents against MDR ESKAPE, particularly GNB, pathogens [20]. Our team has developed a very promising robenidine pharmacophore, prototypes of which exhibit bactericidal activity [21]. Of these, the robenidine analogue NCL195 exhibits bactericidal activity against *Streptococcus pneumoniae* [minimum inhibitory concentration (MIC) range 2–8 $\mu\text{g/mL}$] and *S. aureus* (MIC range 1–2 $\mu\text{g/mL}$) via disruption of the cell membrane potential [22]. Importantly, NCL195 is less cytotoxic to a variety of mammalian cell lines than the parent compound (NCL812), is not toxic to erythrocytes at the highest concentration tested (128 $\mu\text{g/mL}$), and showed no resistance development after 24 daily sequential in vitro subcultures [22]. Our recent data also confirm that NCL195 kills the GNB pathogens *A. baumannii*, *E. coli*, *K. pneumoniae* and *P. aeruginosa* in the presence of subinhibitory concentrations of PMB (MICs of 0.25–1 $\mu\text{g/mL}$) or ethylene diamine tetra-acetic acid (EDTA) (MICs of 0.125–8 $\mu\text{g/mL}$), agents known to permeabilise the outer membrane of GNB [23] via disruption of the membrane potential [24]. We hypothesised that a combination of NCL195 with subinhibitory concentrations of colistin may result in a reduction in the toxicity of colistin and overcome colistin resistance by taking advantage of the synergistic action of the antimicrobial combination, hence this study.

2. Materials and methods

2.1. Antibiotics and chemicals

NCL195, an analogue of aminoguanidine robenidine NCL812 [21,22] (Fig. 1), was synthesised at the University of Newcastle (Callaghan, NSW, Australia). Colistin sulfate, daptomycin, kanamycin and tetracycline were purchased from Sigma-Aldrich (Australia). Stock solutions containing 25.6 mg/mL of each compound [NCL195 dissolved in dimethyl sulfoxide (DMSO); colistin, kanamycin and daptomycin dissolved in water; and tetracycline dissolved in 70% ethanol] were stored in 1 mL aliquots at -20°C away from direct light. Ruthenium red, L-lysine acetate and sucrose

were purchased from Sigma-Aldrich and were dissolved in water to the appropriate concentrations. Fixatives and cacodylate buffer were provided by Adelaide Microscopy, The University of Adelaide (Adelaide, SA, Australia).

2.2. Organisms and growth conditions

Acinetobacter baumannii (NCIMB 12457 and ATCC 19606), *E. coli* (ATCC 35218 and ATCC 25922), *K. pneumoniae* (ATCC 13883 and ATCC 33495) and *P. aeruginosa* (ATCC 27853 and PAO1) were provided by SA Pathology (Adelaide, SA, Australia). Bioluminescent *E. coli* Xen14 (derived from the parental strain *E. coli* WS2572) and bioluminescent *P. aeruginosa* Xen41 (derived from the parental strain PAO1) were purchased from PerkinElmer Inc. (Hopkinton, MA, USA); *S. aureus* ATCC 29213 and a bioluminescent derivative of *S. aureus* ATCC 12600 (Xen29; PerkinElmer) were used as internal quality controls for testing activity of NCL195 and daptomycin; 16 clinical human isolates of *A. baumannii* were provided by SA Pathology; 20 clinical human *E. coli* isolates, 18 clinical human *K. pneumoniae* isolates and 22 clinical human *P. aeruginosa* isolates were collected from Flinders Medical Centre (Bedford Park, SA, Australia). All bacteria were stored at -80°C in brain–heart infusion (BHI) broth with 15% glycerol at the Australian Centre for Antimicrobial Resistance Ecology (ACARE), School of Animal and Veterinary Sciences, The University of Adelaide.

All bacterial identities were confirmed by matrix-assisted laser desorption/ionisation time-of-flight mass spectroscopy (MALDI-TOF/MS) (microflex® LT/SH Biotyper; Bruker Daltonik, Leipzig, Germany) at ACARE prior to antimicrobial susceptibility testing. Bacteria were grown overnight on horse blood agar (HBA) and in Luria–Bertani (LB) broth. *Escherichia coli* Xen14 was grown on HBA containing 30 $\mu\text{g/mL}$ kanamycin, *P. aeruginosa* Xen41 was grown on HBA containing 60 $\mu\text{g/mL}$ tetracycline and *S. aureus* Xen29 was grown on HBA containing 200 $\mu\text{g/mL}$ kanamycin. Colistin-resistant Xen14 and Xen41 were generated by daily serial subculture in increasing concentrations of colistin from 0.25 $\mu\text{g/mL}$ to 256 $\mu\text{g/mL}$ over 12–15 days as described previously [22].

2.3. Antimicrobial susceptibility testing

2.3.1. Determination of antimicrobial resistance profiles of clinical Gram-negative bacterial isolates

The MIC of antibiotics (Table 1) was determined against 76 clinical GNB isolates (16 *A. baumannii*, 20 *E. coli*, 18 *K. pneumoniae* and 22 *P. aeruginosa*) as described previously [24]. Additionally, the resistance profiles of the 22 *P. aeruginosa* isolates were determined using Sensititre™ plates (CMV3AGNF; Thermo Fisher Scientific, Australia) using a Sensititre™ AIM platform and manually read using the Sensititre™ Vizion™ plate reader.

MIC and minimum bactericidal concentration (MBC) determinations for NCL195 (concentration range 0.5–256 $\mu\text{g/mL}$), colistin (concentration range 0.008–8 $\mu\text{g/mL}$) and the combination were performed in round-bottom 96-well microtitre trays (Sarstedt 82.1582.001) using a modified broth microdilution method recommended by the Clinical and Laboratory Standards Institute (CLSI) [25] as described previously [22]. LB broth was used in this work instead of cation-adjusted Mueller–Hinton broth because it has been shown that NCL compounds chelate cations [26]. Each MIC test against all isolates was performed in duplicate and repeated twice; the negative growth control was LB broth only and the positive growth control was bacterial suspension in LB broth. The MBC of NCL195 alone or in combination with colistin was recorded as the lowest concentration of each test compound at which a 99.9% colony count reduction was observed on the plate [27]. Time–kill assays were performed in duplicate as described previously [22,28] using clinical *A. baumannii* 248-84-D, clinical *E. coli*-14, Xen14,

Table 1
Resistance profile of clinical Gram-negative bacterial isolates used in this study

| Antibiotic | Class | <i>Acinetobacter baumannii</i> (n = 16) | | | <i>Escherichia coli</i> (n = 20) | | | <i>Klebsiella pneumoniae</i> (n = 18) | | | <i>Pseudomonas aeruginosa</i> (n = 22) | | |
|-----------------|----------------|--|-------|-------|----------------------------------|-------|-------|--|-------|-------|---|-------|-------|
| | | R (%) | I (%) | S (%) | R (%) | I (%) | S (%) | R (%) | I (%) | S (%) | R (%) | I (%) | S (%) |
| AMC | β-Lactam | – ^a | – | – | 20 | 0 | 80 | 0 | 0 | 100 | 100 | 0 | 0 |
| Ampicillin | | – | – | – | 70 | 0 | 30 | 100 | 0 | 0 | 100 | 0 | 0 |
| Cefepime | | 62.5 | 0 | 37.5 | 20 | 0 | 80 | 0 | 0 | 100 | 13.6 | 9.1 | 77.3 |
| Cefoxitin | | – | – | – | – | – | – | – | – | – | 100 | 0 | 0 |
| Ceftazidime | | 56.3 | 6.3 | 37.4 | 10 | 5 | 85 | 0 | 5.6 | 94.4 | 22.7 | 4.5 | 72.8 |
| Ceftiofur | | – | – | – | 20 | 0 | 80 | 0 | 5.6 | 94.4 | 100 | 0 | 0 |
| Ceftriaxone | | 50 | 43.7 | 6.3 | 20 | 0 | 80 | 0 | 0 | 100 | 100 | 0 | 0 |
| Cefazolin | | – | – | – | 20 | 0 | 80 | 11.1 | 0 | 88.9 | – | – | – |
| Piperacillin | | 68.8 | 31.2 | 0 | 45 | 15 | 40 | 0 | 5.6 | 94.4 | 4.5 | 13.6 | 81.9 |
| TZP | | 68.8 | 0 | 31.2 | – | – | – | – | – | – | – | – | – |
| TCC | 68.8 | 0 | 31.2 | – | – | – | – | – | – | – | – | – | |
| Amikacin | Aminoglycoside | 56.3 | 0 | 43.7 | 0 | 0 | 100 | 0 | 0 | 100 | 0 | 0 | 100 |
| Gentamicin | | 56.3 | 6.3 | 37.4 | 40 | 45 | 5 | 0 | 0 | 100 | 0 | 13.6 | 86.4 |
| Streptomycin | – | – | – | 35 | 0 | 65 | 11.1 | 0 | 88.9 | 100 | 0 | 0 | |
| Tobramycin | 56.2 | 0 | 43.8 | 15 | 75 | 10 | 0 | 11.1 | 88.9 | 0 | 0 | 100 | |
| Doripenem | Carbapenem | 62.4 | 6.3 | 31.3 | – | – | – | – | – | – | – | – | – |
| Imipenem | | 62.4 | 6.3 | 31.3 | 15 | 65 | 20 | – | – | – | 18.2 | 22.7 | 59.1 |
| Meropenem | | 62.4 | 6.3 | 31.3 | 0 | 0 | 100 | 0 | 5.6 | 94.4 | 4.5 | 9.1 | 86.4 |
| Chloramphenicol | Phenicol | – | – | – | 70 | 25 | 5 | 50 | 0 | 50 | 100 | 0 | 0 |
| Azithromycin | Macrolide | – | – | – | – | – | – | – | – | – | 100 | 0 | 0 |
| Doxycycline | Tetracycline | 31.3 | 6.3 | 62.4 | – | – | – | – | – | – | – | – | – |
| Tetracycline | 62.5 | 0 | 37.5 | 30 | 0 | 70 | 27.8 | 0 | 72.2 | 100 | 0 | 0 | |
| Minocycline | 12.5 | 12.5 | 75 | 15 | 30 | 55 | 27.8 | 16.7 | 55.5 | 100 | 0 | 0 | |
| Ciprofloxacin | Quinolone | 62.5 | 0 | 37.5 | 25 | 5 | 70 | 5.6 | 0 | 94.4 | 18.2 | 0 | 81.8 |
| Levofloxacin | | 56.3 | 6.3 | 37.4 | 0 | 5 | 95 | 5.6 | 0 | 94.4 | 9.1 | 0 | 90.9 |
| Nalidixic acid | – | – | – | – | – | – | – | – | – | 100 | 0 | 0 | |
| Nitrofurantoin | Nitrofurantoin | – | – | – | 25 | 0 | 75 | 16.7 | 0 | 83.3 | – | – | – |
| Sulfisoxazole | Sulfonamide | – | – | – | – | – | – | – | – | 100 | 0 | 0 | |
| SXT | 50 | 6.3 | 43.7 | 35 | 0 | 65 | 5.6 | 0 | 94.4 | 100 | 0 | 0 | |

R, resistant; I, intermediate; S, susceptible; AMC, amoxicillin/clavulanate; TZP, piperacillin/tazobactam; TCC, ticarcillin/clavulanate; SXT, trimethoprim/sulfamethoxazole.

^a – indicates not determined.

NOTE: *K. pneumoniae*, urine (83.2%), sputum (5.6%), wound (5.6%) and peritoneal fluid (5.6%); *E. coli*, urine (100%); *A. baumannii*, skin and soft tissue; *P. aeruginosa*: Flinders Medical Centre collection.

colistin-resistant Xen14, Xen41, clinical *P. aeruginosa*-93, colistin-resistant Xen41 and clinical *K. pneumoniae*-13.

2.3.2. Synergy testing by checkerboard assay

Synergy testing was performed by a modification of the standard checkerboard assay [24,29,30] (Supplementary material). The fractional inhibitory concentration index (FICI) for the interaction of two antibiotics was calculated as described previously (Supplementary material). Further analysis was carried out by plotting an isobologram for each isolate as described previously [30,31]. The dose reduction index (DRI) formula was used to determine the difference between the effective doses of a single compound in combination from its individual dose [30] (Supplementary material).

2.4. Transmission electron microscopy (TEM)

Escherichia coli Xen14 and *P. aeruginosa* Xen41 cells were prepared and samples were processed for TEM using a modification of protocols from previous studies [32,33] as described in the Supplementary material. Cell sections were viewed between 25 000 × and 130 000 × on a Tecnai G2 Spirit 120 kV transmission electron microscope (FEI Company). Images were obtained at 130 000 × magnification and were analysed using Olympus Soft Imaging System.

2.5. Mechanism of action studies

The membrane potential of Xen14 was measured by fluorescence spectrometry using the membrane potential probe DiOC₂(3) (3,3'-dihexyloxycarbocyanine iodide) as described previously [24,34]. For this assay, NCL195 was used at 64, 128 or 256

μg/mL, while colistin was used at either 6.4 μg/mL or 12.8 μg/mL. Cells were treated with the individual compounds or their combinations at ambient temperature for 15 min or 30 min with stirring before and during the assay.

2.6. In vitro cytotoxicity assays

We assayed NCL195 alone and in combination with colistin at 0.5 μg/mL for in vitro cytotoxicity using a panel of adherent mammalian cell lines: Hep G2 (human hepatocellular carcinoma cell line); and HEK293 (human embryonic kidney cell line) as described previously [22]. Assays were performed in duplicate in black flat-bottom 96-well tissue culture trays (Eppendorf Cat No. 0030741013) seeded with ~1.5 × 10⁴ cells per well. The viability of each cell line in the presence of NCL195 alone or NCL195 + colistin combination (using 1% DMSO only and 64 μg/mL ampicillin as controls) was assessed at 1 h intervals for 20 h at 37°C, 5% CO₂ on a Cytation 5 Cell Imaging Multi-Mode Reader (BioTek) using the RealTime-Glo™ MT Cell Viability Assay reagent (Promega).

2.7. Determination of optimal colistin concentration for mouse efficacy studies

Preliminary investigations to determine the subinhibitory concentration of colistin to be used in the colistin + NCL195 combination was carried out using three doses of colistin at 0.125, 0.25 and 0.5 mg/kg in a Xen14 mouse infection model. The protocol for preparation of the bacteria and infection is described in the Supplementary material.

Table 2
Synergistic activity of the combination NCL195 + colistin against Gram-negative bacterial pathogens (ATCC strains and clinical isolates)

| Isolate | MIC range ($\mu\text{g}/\text{mL}$) | | | | FICI ^a | DRI ^b | | MBC range ($\mu\text{g}/\text{mL}$) | | | |
|---|---------------------------------------|--------|-------------|--------|-------------------|------------------|--------|---------------------------------------|--------|-------------|--------|
| | Single antibiotic | | Combination | | | | | Single antibiotic | | Combination | |
| | Colistin | NCL195 | Colistin | NCL195 | | Colistin | NCL195 | Colistin | NCL195 | Colistin | NCL195 |
| <i>Acinetobacter baumannii</i> (n = 18) | 0.5–64 | >256 | 0.015–2 | 0.5–4 | 0.01–0.5 * | 32–128 | 64–512 | 0.5–64 | >256 | 0.015–2 | 0.5–4 |
| <i>Escherichia coli</i> (n = 23) | 0.125–0.25 | >256 | 0.008–0.125 | 0.5–4 | 0.12–0.5 * | 2–16 | 64–512 | 0.125–0.25 | >256 | 0.015–0.125 | 0.5–4 |
| <i>Klebsiella pneumoniae</i> (n = 20) | 0.125–0.25 | >256 | 0.015–0.125 | 0.5–4 | 0.12–0.5 * | 2–8 | 64–512 | 0.125–0.25 | >256 | 0.06–0.125 | 0.5–4 |
| <i>Pseudomonas aeruginosa</i> (n = 25) | 0.25–2 | >256 | 0.03–1 | 0.5–4 | 0.12–0.5 * | 2–8 | 64–512 | 0.25–4 | >256 | 0.06–2 | 1–8 |

MIC, minimum inhibitory concentration; MBC, minimum bactericidal concentration.

^a FICI, fractional inhibitory concentration index: * synergistic, $\text{FICI} \leq 0.5$; additive or partially synergistic, $0.5 < \text{FICI} \leq 1$; indifferent, $1 < \text{FICI} \leq 4$; and antagonistic, $\text{FICI} > 4$.

^b DRI, dose reduction index. Bioluminescent *Staphylococcus aureus* Xen29 was used as control each time the MIC and checkerboard assays were performed; the MIC of NCL195 against *S. aureus* Xen29 in each of these assays was always 2 $\mu\text{g}/\text{mL}$.

3. Results

3.1. Clinical Gram-negative bacteria exhibit multidrug resistance profiles

The drug resistance profiles of the 76 clinical GNB isolates used in this study against multiple classes of antimicrobials were evaluated. Unsurprisingly, a very high proportion of the clinical GNB isolates (particularly *A. baumannii* and *P. aeruginosa*) exhibit resistance to multiple drug classes (Table 1).

3.2. NCL195 is potent against Gram-negative bacterial pathogens in the presence of subinhibitory concentrations of colistin

The activity of NCL195 alone, colistin alone and NCL195 + colistin combination was tested on the 76 clinical isolates listed in Table 1 as well as 10 reference strains (2 *A. baumannii*, 3 *E. coli*, 2 *K. pneumoniae* and 3 *P. aeruginosa*). NCL195 had no activity against any of the GNB; therefore, the MIC of NCL195 was considered as 256 $\mu\text{g}/\text{mL}$ for calculation of the FICI and DRI. The MIC of colistin alone ranged from 0.125–0.25 $\mu\text{g}/\text{mL}$ against *K. pneumoniae* and *E. coli*, 0.5–64 $\mu\text{g}/\text{mL}$ against *A. baumannii* and 0.25–2 $\mu\text{g}/\text{mL}$ against *P. aeruginosa*. In combination with colistin, the MIC range for NCL195 was 0.5–4 $\mu\text{g}/\text{mL}$ against all of the GNB, while the MIC range for colistin was 0.015–2 $\mu\text{g}/\text{mL}$ against *A. baumannii*, 0.008–0.125 $\mu\text{g}/\text{mL}$ against *E. coli*, 0.015–0.125 $\mu\text{g}/\text{mL}$ against *K. pneumoniae* and 0.03–1 $\mu\text{g}/\text{mL}$ against *P. aeruginosa* (Table 2). The FICIs of all combinations for all GNB ranged from 0.01–0.5 indicating a synergistic effect of the NCL195 + colistin combination. In addition, the dose of NCL195 and colistin reduced by 64–512-fold and 2–128-fold, respectively, if combined, compared with either drug alone. MBC values were similar to MIC results except for *P. aeruginosa* where the MBC was generally two-fold higher than the MIC, further confirming that NCL195 is bactericidal against GNB in the presence of subinhibitory concentrations of colistin. We also investigated whether the combination of NCL195 + colistin remains effective against colistin-resistant *A. baumannii*, *E. coli* and *P. aeruginosa*. We found that the FICI of the combination was still synergistic for all strains (Table 3).

It was shown previously that the MIC of NCL195 against *S. aureus* isolates ranged from 1–2 $\mu\text{g}/\text{mL}$ [22], while the MIC of daptomycin (a well-known inner membrane active GPB drug) against *S. aureus* isolates ranged from 0.06–2 $\mu\text{g}/\text{mL}$ [35]. However, it was reported that a combination of daptomycin and PMB nonapeptide or colistin is not effective against *E. coli* or other GNB pathogens (except against *A. baumannii*) [36,37]. Therefore, checkerboard assays were performed using a combination of NCL195 + colistin

or daptomycin + colistin against the 10 GNB reference strains. *Staphylococcus aureus* Xen29 and *S. aureus* ATCC 29213 were used as controls. As expected, no synergy was observed for the daptomycin + colistin combination (except for *A. baumannii*), whereas synergistic activity was observed for the NCL195 + colistin combination for all strains (Supplementary Fig. S2; Table 3), strongly indicating that the NCL195 target in the inner membrane differs from that of daptomycin.

3.3. NCL195 + colistin combination exhibits time- and concentration-dependent killing of Gram-negative bacteria

In a time–kill kinetic assay for Xen14 (Fig. 2a), the combination NCL195 + colistin resulted in more rapid killing than colistin alone. The combination of NCL195 at 2 $\mu\text{g}/\text{mL}$ and colistin at 0.06 $\mu\text{g}/\text{mL}$ ($0.25 \times \text{MIC}$) killed all of the cells at 2 h post-treatment, similar to the kill time by colistin alone at 0.5 $\mu\text{g}/\text{mL}$ ($2 \times \text{MIC}$). The combination of NCL195 at 4 $\mu\text{g}/\text{mL}$ and colistin at 0.06 $\mu\text{g}/\text{mL}$ killed all of the bacteria at 0.5 h, while a combination of NCL195 at 1 $\mu\text{g}/\text{mL}$ and colistin at 0.25 $\mu\text{g}/\text{mL}$ killed cells slightly faster than colistin alone at 0.25 $\mu\text{g}/\text{mL}$. Finally, the time to kill for colistin alone at 0.25 $\mu\text{g}/\text{mL}$ was 4 h, while the combination of NCL195 at 2 $\mu\text{g}/\text{mL}$ + colistin at 0.25 $\mu\text{g}/\text{mL}$ ($1 \times \text{MIC}$) killed all Xen14 cells at 0.5 h.

In a time–kill kinetic assay using *P. aeruginosa* Xen41 (Fig. 2b), the NCL195 + colistin combination killed *P. aeruginosa* Xen41 more rapidly than colistin alone. NCL195 at 2 $\mu\text{g}/\text{mL}$ in combination with colistin at 2 $\mu\text{g}/\text{mL}$ killed cells at 0.5 h, similar to the kill time for colistin alone at 4 $\mu\text{g}/\text{mL}$. At these concentrations, there was no re-growth of the Xen41 cells up to 24 h.

The time–kill kinetic assay using colistin-resistant Xen14 (Fig. 3a), clinical *E. coli*-14 (Fig. 3b), colistin-resistant Xen41 (Fig. 3c), clinical *P. aeruginosa*-93 (Fig. 3d), clinical *A. baumannii* 248-84-D (Fig. 3e) and clinical *K. pneumoniae*-13 (Fig. 3f) also showed that the NCL195 + colistin combination kills GNB, whereas colistin alone at the same concentration did not kill the bacteria.

3.4. *Escherichia coli* and *Pseudomonas aeruginosa* cells treated with NCL195 + colistin combination exhibit marked changes in ultrastructural morphology

3.4.1. Morphological changes in *Escherichia coli* Xen14 cells

TEM images revealed that the cell envelope in untreated of Xen14 cells (controls) was clearly visible and consisted of the plasma membrane, cell wall and outer membrane (Fig. 4a; Supplementary Fig. S3a₁–a₃). The cell envelope of Xen14 cells treated with NCL195 at 2 $\mu\text{g}/\text{mL}$ also had a similar appearance (Fig. 4b; Supple-

Table 3
Synergistic activity of NCL195 or daptomycin in combination with colistin against ATCC strains of Gram-negative bacteria.

| Strain | MIC ($\mu\text{g/mL}$) | | | | FICI ^a | DRI ^b Colistin:NCL195 | MIC ($\mu\text{g/mL}$) | | | FICI ^a |
|---|--------------------------|--------|-------------|--------|-------------------|-------------------------------------|---------------------------------|-------------|------------|-------------------|
| | Single antibiotic | | Combination | | | | Single antibiotic Daptomycin | Combination | | |
| | Colistin | NCL195 | Colistin | NCL195 | | | | Colistin | Daptomycin | |
| <i>Acinetobacter baumannii</i> NCIMB 12457 | 1 | >256 | 0.25 | 1 | 0.25 * | 8:256 | >256 | 0.5 | 16 | 0.5 * |
| <i>A. baumannii</i> ATCC 19606 | 1 | >256 | 0.25 | 1 | 0.25 * | 8:256 | >256 | 0.5 | 8 | 0.5 * |
| <i>A. baumannii</i> 248-84-D | 64 | >256 | 0.5 | 1 | <0.01 * | 128:256 | ND | ND | ND | ND |
| <i>Escherichia coli</i> ATCC 35218 | 0.25 | >256 | 0.06 | 1 | 0.24 * | 4: 256 | >256 | 0.25 | >256 | >4 # |
| <i>E. coli</i> ATCC 25922 | 0.25 | >256 | 0.06 | 1 | 0.24 * | 4:256 | >256 | 0.25 | >256 | >4 # |
| <i>E. coli</i> Xen14 | 0.25 | >256 | 0.06 | 1 | 0.24 * | 4:256 | >256 | 0.25 | >256 | >4 # |
| <i>E. coli</i> Xen14 colistin-resistant | 32 | >256 | 1 | 4 | <0.05 * | 32:64 | ND | ND | ND | ND |
| <i>Klebsiella pneumoniae</i> ATCC 33495 | 0.25 | >256 | 0.06 | 1 | 0.24 * | 4:256 | >256 | 0.25 | >256 | >4 # |
| <i>K. pneumoniae</i> ATCC 13883 | 0.25 | >256 | 0.125 | 1 | 0.50 * | 2:256 | >256 | 0.25 | >256 | >4 # |
| <i>Pseudomonas aeruginosa</i> Xen41 | 0.5 | >256 | 0.125 | 1 | 0.25 * | 4:256 | >256 | 0.5 | >256 | >4 # |
| <i>P. aeruginosa</i> Xen41 colistin-resistant | 8 | >256 | 2 | 2 | 0.25 * | 4:128 | ND | ND | ND | ND |
| <i>P. aeruginosa</i> ATCC 27853 | 0.5 | >256 | 0.125 | 1 | 0.25 * | 4:256 | >256 | 0.5 | >256 | >4 # |
| <i>P. aeruginosa</i> PAO1 | 0.5 | >256 | 0.125 | 1 | 0.25 * | 4:256 | >256 | 0.5 | >256 | >4 # |

MIC, minimum inhibitory concentration; ND, not determined.

^a FICI, fractional inhibitory concentration index: * synergistic, $\text{FICI} \leq 0.5$; additive or partially synergistic, $0.5 < \text{FICI} \leq 1$; indifferent, $1 < \text{FICI} \leq 4$; and # antagonistic, $\text{FICI} > 4$.

^b DRI = dose reduction index. The MIC of NCL195 and daptomycin against *Staphylococcus aureus* Xen29 was 2 $\mu\text{g/mL}$ and 1 $\mu\text{g/mL}$, respectively. Luria-Bertani broth supplemented with CaCl_2 at 100 $\mu\text{g/mL}$ was used for MIC and checkerboard assay testing of daptomycin alone and in combination with colistin.

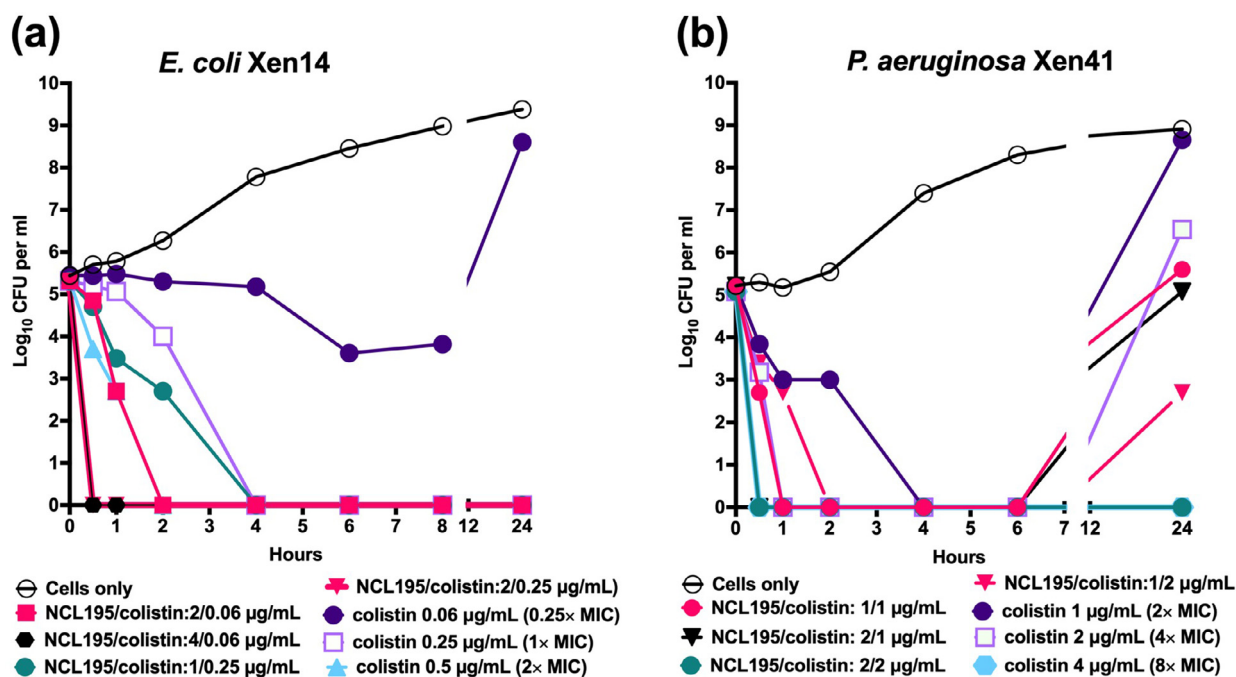


Fig. 2. Time-kill kinetics of the combination NCL195 + colistin against (a) *Escherichia coli* Xen14 and (b) *Pseudomonas aeruginosa* Xen41. (a) For Xen14, colistin alone was prepared at 0.25 ×, 1 × and 2 × MIC. Combinations were prepared as follows: NCL195 at 2 $\mu\text{g/mL}$ and colistin at 0.06 $\mu\text{g/mL}$; NCL195 at 4 $\mu\text{g/mL}$ and colistin at 0.06 $\mu\text{g/mL}$; NCL195 at 1 $\mu\text{g/mL}$ and colistin at 0.25 $\mu\text{g/mL}$; and NCL195 at 2 $\mu\text{g/mL}$ and colistin at 0.25 $\mu\text{g/mL}$. (b) For Xen41, colistin alone was prepared at 2 ×, 4 × and 8 × MIC. Combinations were prepared as follows: NCL195 at 1 $\mu\text{g/mL}$ and colistin at 1 $\mu\text{g/mL}$; NCL195 at 1 $\mu\text{g/mL}$ and colistin at 2 $\mu\text{g/mL}$; NCL195 at 2 $\mu\text{g/mL}$ and colistin at 1 $\mu\text{g/mL}$; and NCL195 2 $\mu\text{g/mL}$ and colistin 2 $\mu\text{g/mL}$. Samples were withdrawn at indicated times and plated overnight on horse blood agar at 37°C. MIC, minimum inhibitory concentration.

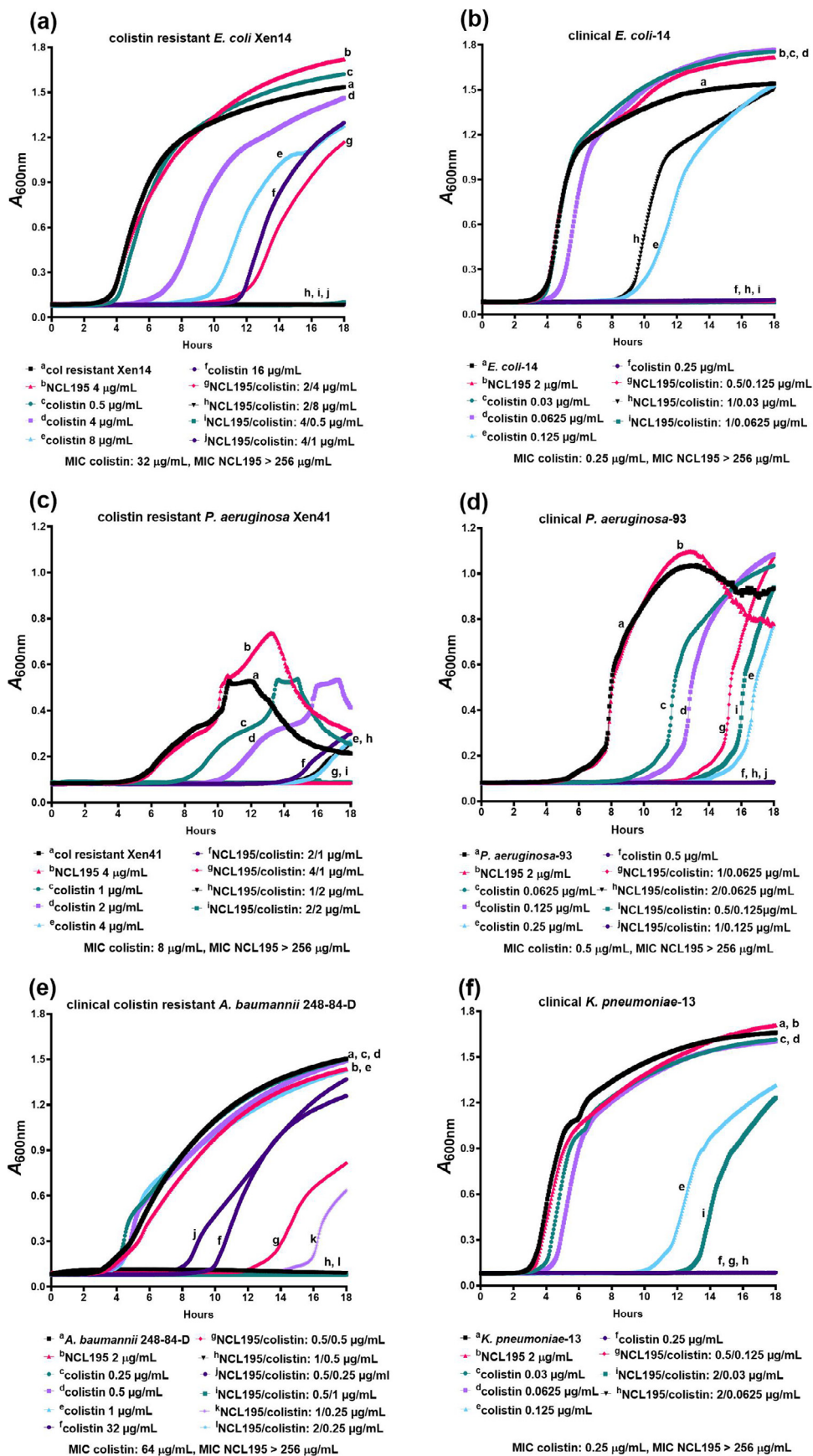


Fig. 3. Time- and concentration-dependent killing of Gram-negative bacteria (GNB) by NCL195 + colistin combination. Time-kill kinetic assay using (a) colistin-resistant Xen14, (b) clinical *E. coli*-14, (c) colistin-resistant Xen41, (d) clinical *P. aeruginosa*-93, (e) clinical *A. baumannii* 248-84-D and (f) clinical *K. pneumoniae*-13, showing that the NCL195 + colistin combination kills the GNB, whereas colistin alone at the same concentration did not kill the bacteria. MIC, minimum inhibitory concentration.

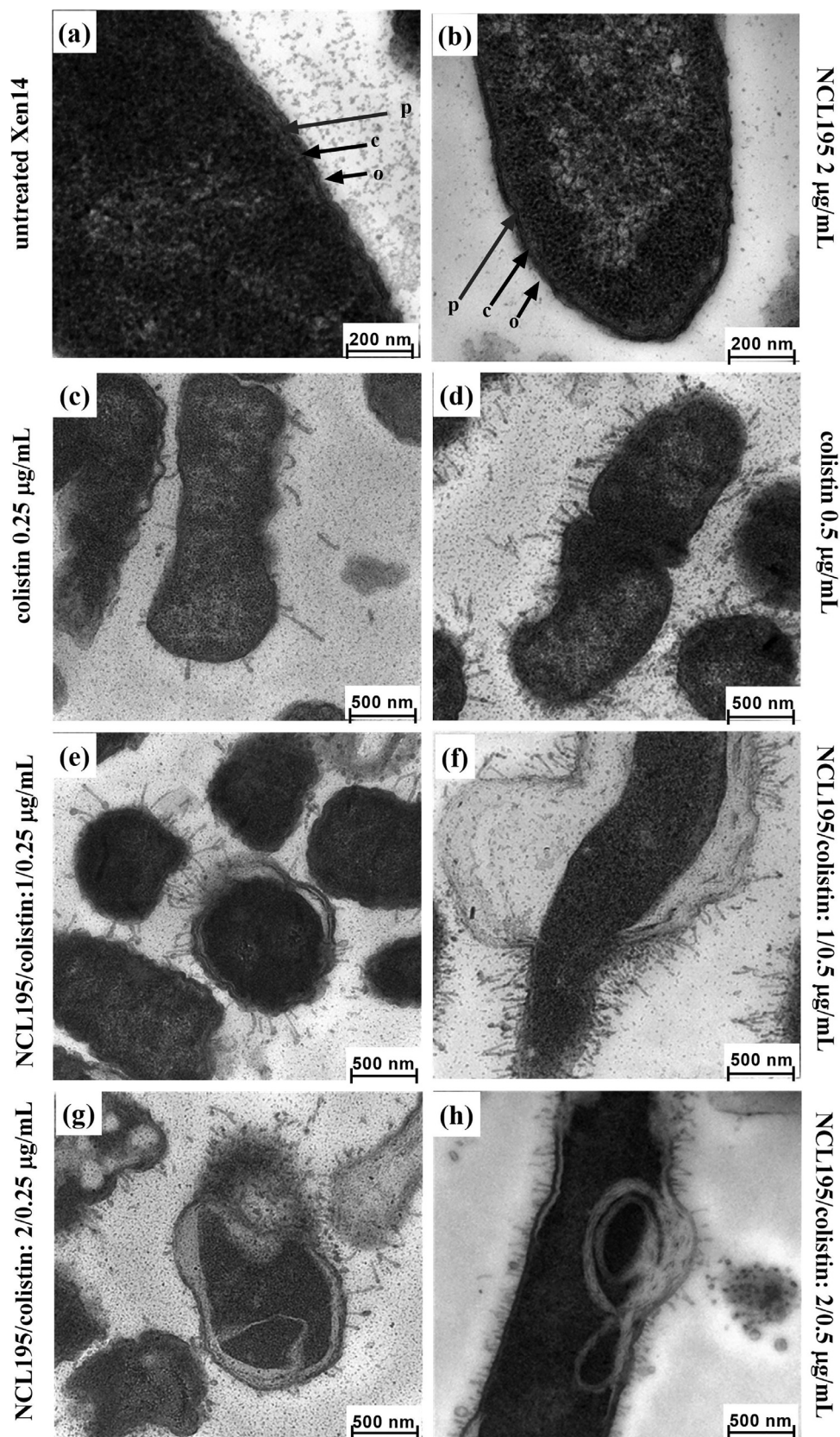


Fig. 4. Effect of NCL195 treatment on cellular morphology of *Escherichia coli* Xen14 ($\sim 5 \times 10^8$ cells) treated for 1 h: (a) cells without treatment clearly showing intact outer membrane (o), cell wall (c) and plasma membrane (p); (b) cells treated with NCL195 alone at 2 $\mu\text{g/mL}$ showing similar morphology as the untreated (control) cells; (c,d), cells treated with colistin at 0.25 $\mu\text{g/mL}$ and 0.5 $\mu\text{g/mL}$ showing a swollen envelope with tubular and fimbria-like radiant appendages; (e-h) cells treated with a combination of NCL195 at 1 $\mu\text{g/mL}$ or 2 $\mu\text{g/mL}$ and colistin at 0.25 $\mu\text{g/mL}$ or 0.5 $\mu\text{g/mL}$ showing a swollen envelope, coronate tubular and fimbria-like radiant appendages, and broken and detached plasma membrane.

mentary Fig. S3b₁-b₃). Cells exposed to colistin had a swollen envelope with tubular and fimbria-like radiant appendages (Fig. 4c,d; Supplementary Figs S4, S5 and S6a₁-a₃). The combined NCL195 and colistin treated groups exhibited coronate tubular appendages and also a swollen envelope as seen with exposure to colistin alone. In addition, the plasma membrane of cells treated with the combination was partly detached from the cell wall at low concentrations and broken or circular at increasing concentrations of the combination treatment (Fig. 4e,h; Supplementary Figs S4, S5 and S6b₁-b₃ & c₁-c₃).

3.4.2. Morphological changes in *Pseudomonas aeruginosa* Xen41 cells

TEM images of control (untreated) cells also clearly showed the cell envelope as consisting of the inner membrane, cell wall and outer membrane (Fig. 5a; Supplementary Fig. S7a₁-a₃). As expected, cells treated with NCL195 alone showed similar ultrastructural morphology to control cells, with the minor exception of a slightly wavy appearance (Fig. 5b; Supplementary Fig. S7b₁-b₃). Colistin exposure induced more ruffling around the cells and the cell membrane was wavier with a 1 µg/mL treatment (Fig. 5c; Supplementary Fig. S8a₁-a₃), while a 2 µg/mL treatment resulted in more broken fragments detached from the cells and a leaky appearance (Fig. 5d; Supplementary Fig. S9a₁-a₃). The NCL195 + colistin combination treatment caused changes similar to single colistin treatment, but with more ruffling surrounding the cells, more tubular appendages and loss of differentiation of the cell envelope layers (Fig. 5e,f; Supplementary Figs S8b₁-b₃ and S9b₁-b₃).

3.5. Combination of NCL195 and colistin cause perturbation of the inner and outer membrane potential of *Escherichia coli*

Our earlier work using a NCL195 + PMB combination showed disruption of the outer membrane of *E. coli* Xen14 cells by subinhibitory concentrations of PMB, allowing penetration of NCL195 into the inner membrane [24]. We hypothesised that a similar mechanism would be operational with a combination of NCL195 + colistin (Supplementary Fig. S10). We tested this hypothesis by measuring the membrane potential of Xen14 after treatment with NCL195 and/or colistin using fluorescence spectrometry as described previously [24,34] and in Section 2.5. We showed that pre-incubation of the cells with colistin at 6.4 µg/mL or 12.8 µg/mL permeabilised the outer membrane of Xen14 so that greater quantities of the membrane potential probe DiOC₂(3) could gain entry into the cells without affecting the inner membrane (Fig. 6). As expected, pre-incubation of the cells with the NCL195 + colistin combination resulted in a time-dependent and NCL195 concentration-dependent disruption of the inner membrane potential, clearly showing the dual mechanism of action of the NCL195 + colistin combination.

3.6. Combination of NCL195 and colistin show limited cytotoxicity to mammalian cell lines

We have previously shown that NCL195 demonstrates limited cytotoxicity to a variety of mammalian cell lines and no acute toxicity to mice [22,24]. In this work, we investigated any potential toxic effects of the combination of NCL195 + colistin to Hep G2 (liver) and HEK (kidney) cell lines as a prelude to in vivo efficacy testing of the combination in mouse models of GNB sepsis. We showed that at the concentrations tested, the presence of colistin in the combination did not cause any additional toxicity to the HEK293 cell line (Fig. 7a), and in the case of Hep G2 cells the addition of colistin appears to reduce the toxicity of NCL195 (Fig. 7b).

3.7. Low-dose colistin administration is unable to clear *Escherichia coli* infection in mice

Results of preliminary investigations to determine the subinhibitory concentration of colistin that would be used in the NCL195 + colistin combination show that four doses of colistin at 0.125 mg/kg was unable to clear the infection up to 10 h post-infection, whereas the effects of colistin at 0.25 mg/kg and 0.5 mg/kg were already apparent from 4 h post-infection (Fig. 8). Almost complete clearance of the bacteria was observed after four doses of colistin at 0.25 mg/kg, with complete clearance of the bacteria after four doses of colistin at 0.5 mg/kg (Fig. 8).

4. Discussion

In this work, we examined the in vitro activity of the aminoguanidine robenidine analogue NCL195 in combination with subinhibitory concentrations of colistin against a wide range of clinical human GNB to address the global need to develop new classes of antimicrobials against GNB pathogens. The NCL195 + colistin combination exhibited a time- and concentration-dependent killing of GNB, providing a useful platform for drug combination optimisation for preclinical testing. The synergistic effect of the NCL195 + colistin combination against colistin-resistant *A. baumannii*, *E. coli* and *P. aeruginosa* is encouraging, suggesting a reduced likelihood of failure of drug combination during therapy.

The dual action of colistin and NCL195 on the outer and inner membrane of GNB was clearly demonstrated by TEM of treated *E. coli* and *P. aeruginosa* cells. TEM of untreated cells and cells treated with NCL195 alone showed intact structural membrane integrity, whereas cells exposed to colistin exhibited a swollen envelope with tubular and fimbria-like radiant appendages similar to that reported by others [33]. Cells treated with NCL195 + colistin combination showed disruption of membrane integrity, including membrane detachment and appearance of dislodged cytoplasmic contents, observations that are accentuated by increasing concentrations of NCL195 in the combination.

We further ascertained the biochemical mechanism underlying the killing of GNB owing to interaction of NCL195 and colistin on the GNB membrane by membrane potential measurements. Colistin is known to interact with lipopolysaccharide on the surface of GNB and then cross the outer membrane via the self-promoted uptake pathway, resulting in disruption of the normal barrier property of the outer membrane of GNB [38,39]. Subsequently, the outer membrane is hypothesised to transiently lose its structural integrity thereby allowing the passage of NCL195 into the cell to the drug target site(s), likely to be located on the plasma membrane, as we recently described [24].

The results of this study are significant for a number of reasons. The concentration of colistin in the combination is very much lower than the toxic concentration of colistin reported by Naghmouchi et al. [40], and it has been reported that colistin is toxic to Vero cells at 1 mg/mL. Furthermore, we previously showed that no resistance developed against NCL195 above the MIC for *S. aureus* over 24 serial subcultures, whereas resistance to daptomycin developed by Day 5 and increased up to 8 × MIC by Day 12 of serial subculture [22]. A low propensity to select resistance is a desirable characteristic for further exploration of NCL195 as a novel antimicrobial class to treat acute bacterial infections. Additionally, there is potential for combination therapy using NCL195 + colistin in the face of emergence of colistin resistance among MDR-GNB pathogens, as colistin is likely to be administered as an adjuvant to permeabilise the outer membrane. As a first in vivo proof of concept for future investigation, we showed here that low-dose colistin administration was unable to clear bioluminescent *E. coli* in-

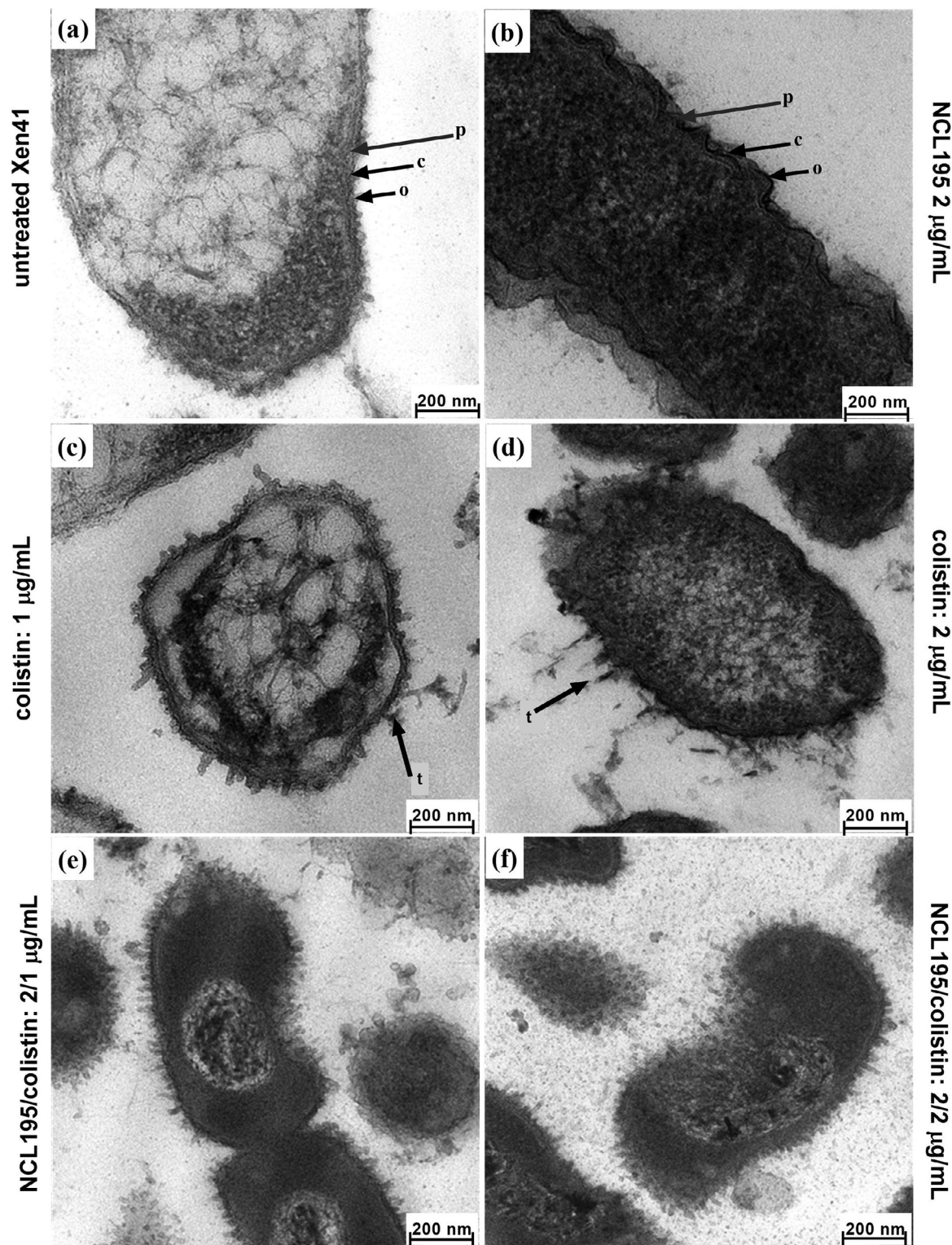


Fig. 5. Cellular morphology of *Pseudomonas aeruginosa* Xen41 ($\sim 5 \times 10^8$ cells) treated for 1 h: (a) cells without treatment clearly showing intact outer membrane (o), cell wall (c) and plasma membrane (p); (b) cells treated with NCL195 at 2 $\mu\text{g}/\text{mL}$ showing the same ultrastructural membrane morphology as the control group; (c,d) cells treated with colistin at 1 $\mu\text{g}/\text{mL}$ and 2 $\mu\text{g}/\text{mL}$ showing ruffled material surrounding the cells and tubular appendages (t); (e,f) cells exposed to a combination of NCL195 at 2 $\mu\text{g}/\text{mL}$ and colistin at 1 $\mu\text{g}/\text{mL}$ or 2 $\mu\text{g}/\text{mL}$ showing more ruffling surrounding the cells, more tubular appendages and loss of differentiation of the cell envelope layers, and broken membrane causing discharge of cellular constituents.

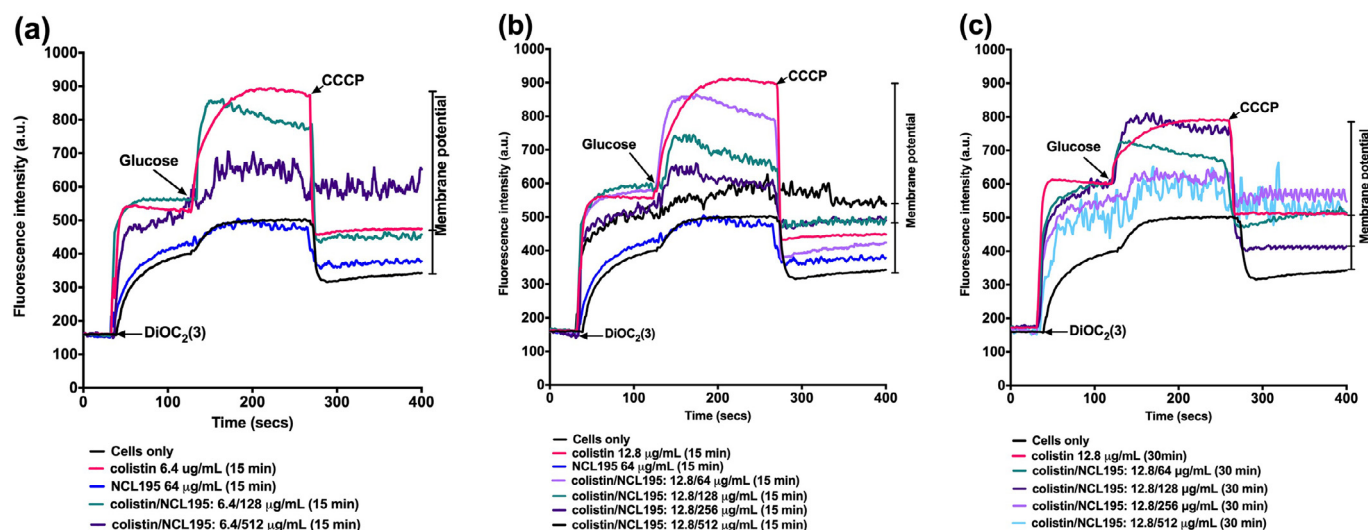


Fig. 6. Membrane potential measurement of *Escherichia coli* Xen14 after treatment with NCL195 and/or colistin. Cells were treated with NCL195 and/or colistin at the indicated concentrations for either 15 min (a,b) or 30 min (c), after which DiOC₂(3) was added and the fluorescence was monitored as described in Section 2.5. The membrane potential was disrupted by addition of the proton ionophore carbonyl cyanide *m*-chlorophenyl hydrazone (CCCP).

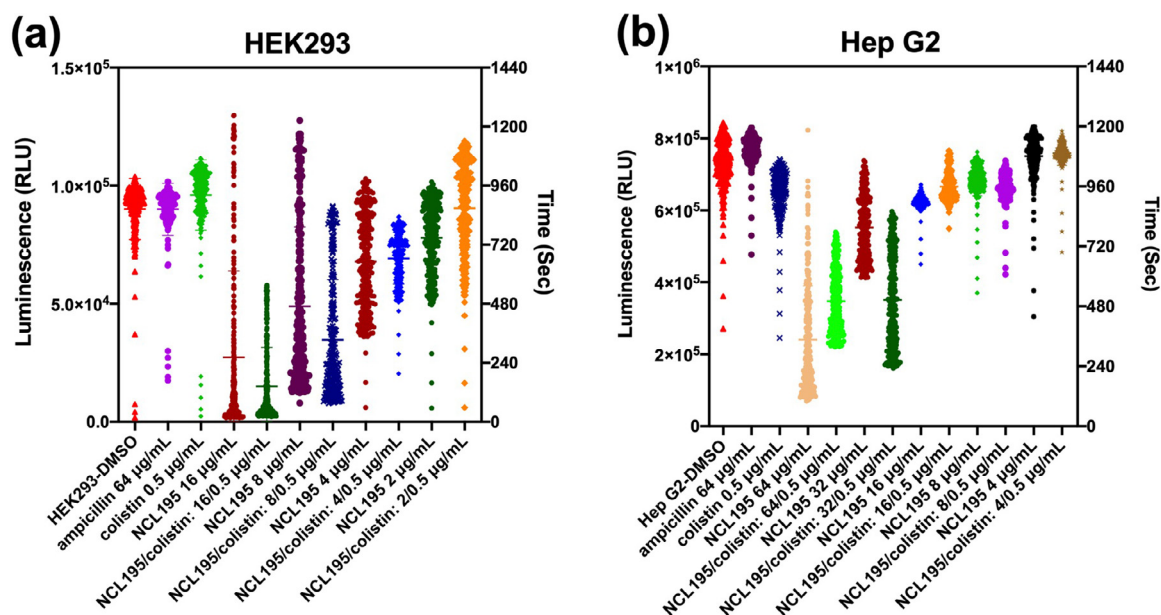


Fig. 7. Cytotoxicity assessment of the NCL195 + colistin combination. Real-time cell viability measurements for (a) HEK293 and (b) Hep G2 cells after treatment with different concentrations of NCL195 and/or colistin. Cell viability was measured every 60 min for 20 h at 37°C and 5% CO₂ on a Cytation 5 Cell Imaging Multi-Mode Reader (BioTek) using the RealTime-Glo™ MT Cell Viability Assay reagent (Promega). Data are relative light units (RLU) for each treatment per time point. DMSO, dimethyl sulfoxide.

fection in mice, providing a platform for efficacy testing of various NCL195 + colistin combinations.

The NCL195 + colistin combination showed 100% synergistic effect among all the 'KAPE' organisms in vitro and compared favourably with the synergy reported recently with a combination of colistin and an antibacterial peptide [19] and a combination of colistin and 16 conventional antibiotics [18] against MDR-GNB. The apparent better in vitro synergy of the combination against *A. baumannii* compared with the other GNB is noteworthy given the increasing incidence of MDR *A. baumannii* in clinical settings. We indicated previously that the lipid A in the outer membrane of *A. baumannii* is more hydrophobic and could render it more susceptible to amphiphilic antimicrobials such as novobiocin, tetracycline and robenidine [30]. These findings suggest that NCL195 represents a new antibacterial class that could provide promising new scaffolds for further pharmaceutical and medicinal chemistry develop-

ment, including improvements in its solubility and potency whilst retaining drug-like qualities and low cytotoxicity.

5. Conclusion

The results of this study suggest that NCL195 may be an appropriate candidate as a component of a combination with colistin for the treatment of GNB infections. Preclinical efficacy testing of this combination is therefore warranted. This would represent a good example of antimicrobial stewardship (5Rs: Responsibility, Reduction, Refinement, Replacement and Review) when the compound is ultimately developed and used clinically. NCL195 and the results of this study contribute to 'Refinement' by showing that a combination of NCL195 and low-dose colistin has the potential to overcome resistance to monotherapy with colistin, which also has toxicity concerns.

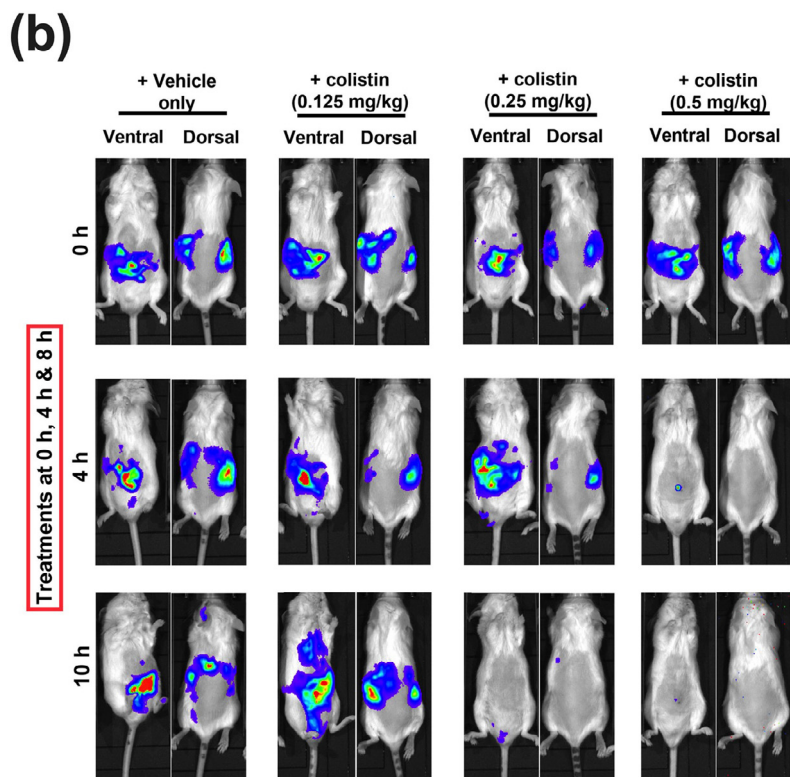
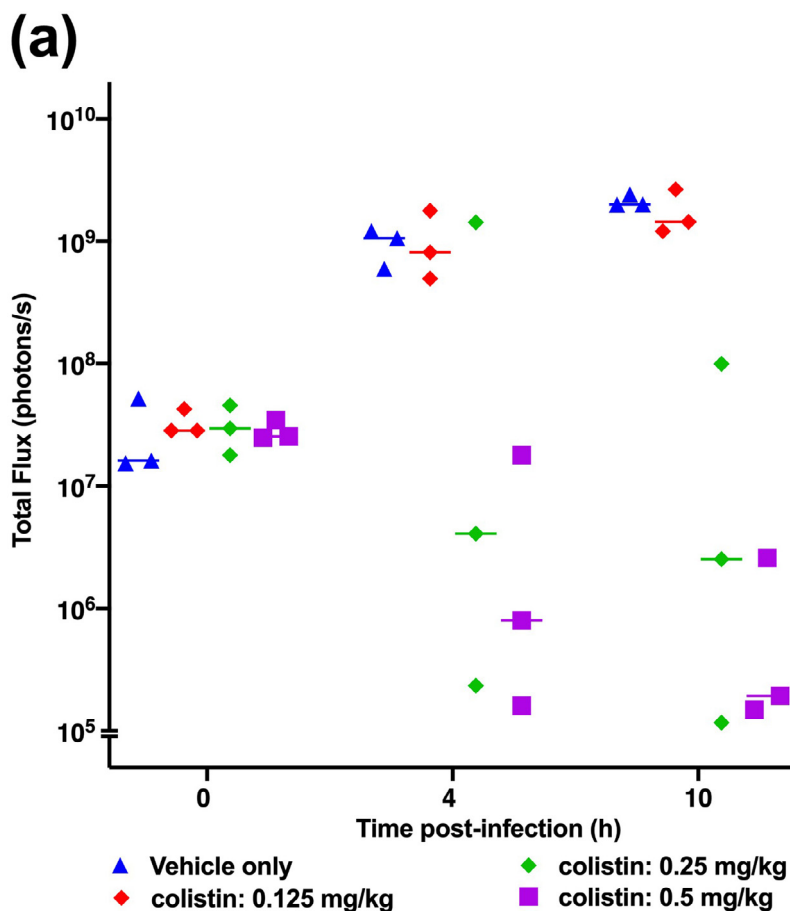


Fig. 8. Preliminary mouse infection studies to determine the appropriate colistin concentration for efficacy testing. (a) Luminescence signal comparisons between groups of CD1 mice ($n = 3$) challenged intraperitoneally with bioluminescent *Escherichia coli* Xen14 and treated at 0, 4 and 8 h apart with the indicated colistin concentrations. (b) Ventral and dorsal images of representative CD1 mice challenged with $\sim 3 \times 10^7$ CFU of Xen14. Mice were subjected to bioluminescent imaging on an IVIS Lumina XRMS Series III system at the indicated times. Broken segment on the y-axis represents the limit of detection.

Declaration of Competing Interest

SWP is a Director of Neoculi Pty. Ltd.; DJT and AM have received research funding from Neoculi Pty. Ltd. All other authors declare no competing interests.

Acknowledgments

The authors would like to thank Hongfei Pi for mentoring MIC and checkerboard assays; Amanda Ruggero, Lora Bowes, Anh Hong Nguyen and Max McClafferty at the University of South Australia for their technical assistance; Ms Jan Bell (Australian Group on Antimicrobial Resistance) for providing *A. baumannii* isolates; and Mr Chris Ossowicz at SA Pathology (Flinders Medical Centre, SA) for providing *E. coli* and *K. pneumoniae* isolates. The authors acknowledge the instruments and scientific and technical assistance of Microscopy Australia at Adelaide Microscopy, The University of Adelaide, a facility that is funded by the university and state and federal governments.

Funding

This work was supported by an Australian Research Council (ARC; arc.gov.au) Linkage grant [LP110200770] to DJT, AM and SWP, with Neoculi Pty Ltd. as the Partner Organization, and a University of South Australia fund to HV. The funders did not have any additional role in the study design, data collection and analysis, decision to publish, or preparation of the manuscript.

Ethical approval

The animal study was reviewed and approved by The Animal Ethics Committee of The University of Adelaide (approval number S-2015-151). The study was conducted in compliance with the Australian Code of Practice for the Care and Use of Animals for Scientific Purposes (8th Edition 2013) and the South Australian Animal Welfare Act 1985.

Supplementary materials

Supplementary material associated with this article can be found, in the online version, at [doi:10.1016/j.ijantimicag.2021.106323](https://doi.org/10.1016/j.ijantimicag.2021.106323).

References

- [1] Chopra I, Schofield C, Everett M, O'Neill A, Miller K, Wilcox M, et al. Treatment of health-care-associated infections caused by Gram-negative bacteria: a consensus statement. *Lancet Infect Dis* 2008;8:133–9.
- [2] Pendleton JN, Gorman SP, Gilmore BF. Clinical relevance of the ESKAPE pathogens. *Expert Rev Anti Infect Ther* 2013;11:297–308.
- [3] Diekema DJ, Hsueh PR, Mendes RE, Pfaller MA, Rolston KV, Sader HS, et al. The microbiology of bloodstream infection: 20-year trends from the SENTRY antimicrobial surveillance program. *Antimicrob Agents Chemother* 2019;63:e00355–19.
- [4] Outtersson K, Powers JH, Seoane-Vazquez E, Rodriguez-Monguio R, Kesselheim AS. Approval and withdrawal of new antibiotics and other anti-infectives in the U.S., 1980–2009. *J Law Med Ethics* 2013;41:688–96.
- [5] Arzanlou M, Chai WC, Venter H. Intrinsic, adaptive and acquired antimicrobial resistance in Gram-negative bacteria. *Essays Biochem* 2017;61:49–59.
- [6] Bassetti M, Peghin M, Vena A, Giacobbe DR. Treatment of infections due to MDR Gram-negative bacteria. *Front Med (Lausanne)* 2019;6:74.
- [7] Stewart AG, Harris PNA, Chatfield M, Evans SR, van Duin D, Paterson DL. Modern clinician-initiated clinical trials to determine optimal therapy for multidrug resistant Gram-negative infections. *Clin Infect Dis* 2019;71:433–9.
- [8] Voulgaris GL, Voulgari ML, Falagas ME. Developments on antibiotics for multidrug resistant bacterial Gram-negative infections. *Expert Rev Anti Infect Ther* 2019;17:387–401.
- [9] Zabawa TP, Pucci MJ, Parr TR, Lister T. Treatment of Gram-negative bacterial infections by potentiation of antibiotics. *Curr Opin Microbiol* 2016;33:7–12.

- [10] Talbot GH, Jezek A, Murray BE, Jones RN, Ebright RH, Nau GJ, et al. The Infectious Diseases Society of America's 10 × '20 Initiative (10 new systemic antibacterial agents US Food and Drug Administration approved by 2020): is 20 × '20 a possibility? *Clin Infect Dis* 2019;69:1–11.
- [11] Bergen PJ, Bulman ZP, Saju S, Bulitta JB, Landersdorfer C, Forrest A, et al. Polymyxin combinations: pharmacokinetics and pharmacodynamics for rationale use. *Pharmacotherapy* 2015;35:34–42.
- [12] Bush K. New antimicrobial agents in the pipeline for Gram-negative pathogens. *Int J Antimicrob Agents* 2015;45(Suppl 2):S10.
- [13] Baron S, Hadjadj L, Rolain JM, Olaitan AO. Molecular mechanisms of polymyxin resistance: knowns and unknowns. *Int J Antimicrob Agents* 2016;48:583–91.
- [14] Justo JA, Bosso JA. Adverse reactions associated with systemic polymyxin therapy. *Pharmacotherapy* 2015;35:28–33.
- [15] Nigam A, Kumari A, Jain R, Batra S. Colistin neurotoxicity: revisited. *BMJ Case Rep* 2015;2015:bcr2015210787.
- [16] Brennan-Krohn T, Pironti A, Kirby JE. Synergistic activity of colistin-containing combinations against colistin-resistant Enterobacteriaceae. *Antimicrob Agents Chemother* 2018;62:e00873–18.
- [17] Lenhard JR, Nation RL, Tsuji BT. Synergistic combinations of polymyxins. *Int J Antimicrob Agents* 2016;48:607–13.
- [18] Ontong JC, Ozioma NF, Voravuthikunchai SP, Chusri S. Synergistic antibacterial effects of colistin in combination with aminoglycoside, carbapenems, cephalosporins, fluoroquinolones, tetracyclines, fosfomicin, and piperacillin on multidrug resistant *Klebsiella pneumoniae* isolates. *PLoS One* 2021;16:e0244673.
- [19] Song M, Liu Y, Huang X, Ding S, Wang Y, Shen J, et al. A broad-spectrum antibiotic adjuvant reverses multidrug-resistant Gram-negative pathogens. *Nat Microbiol* 2020;5:1040–50.
- [20] Willyard C. The drug-resistant bacteria that pose the greatest health threats. *Nature* 2017;543:15.
- [21] Abraham RJ, Stevens AJ, Young KA, Russell C, Qvist A, Khazandi M, et al. Robenidine analogues as Gram-positive antibacterial agents. *J Med Chem* 2016;59:2126–38.
- [22] Ogunniyi AD, Khazandi M, Stevens AJ, Sims SK, Page SW, Garg S, et al. Evaluation of robenidine analog NCL195 as a novel broad-spectrum antibacterial agent. *PLoS One* 2017;12:e0183457.
- [23] Schneider EK, Reyes-Ortega F, Velkov T, Li J. Antibiotic-non-antibiotic combinations for combating extremely drug-resistant Gram-negative 'superbugs'. *Essays Biochem* 2017;61:115–25.
- [24] Pi H, Nguyen HT, Venter H, Boileau A, Woolford L, Garg S, et al. In vitro activity of robenidine analog NCL195 in combination with outer membrane permeabilizers against Gram-negative bacterial pathogens and impact on systemic Gram-positive bacterial infection in mice. *Front Microbiol* 2020;11:1556.
- [25] Clinical and Laboratory Standards Institute (CLSI) Performance standards for antimicrobial susceptibility testing. 28th ed. Wayne, PA: CLSI; 2018. CLSI supplement M100.
- [26] Rozengart EV, Saakov VS. The chelating ability of the anticoccidial drug 1,3-bis(p-chlorobenzilideneamino)guanidine: the complexes with Ca²⁺ and La³⁺. *Dokl Biochem Biophys* 2002;385:219–23.
- [27] Clinical and Laboratory Standards Institute (CLSI) Methods for determining bactericidal activity of antimicrobial agents; approved guideline, Wayne, PA: CLSI; 1999. CLSI document M26-A.
- [28] Morshed MT, Nguyen HT, Vuong D, Crombie A, Lacey E, Ogunniyi AD, et al. Semisynthesis and biological evaluation of a focused library of unguinol derivatives as next-generation antibiotics. *Org Biomol Chem* 2021;19:1022–1036.
- [29] Elemam A, Rahimian J, Doymaz M. In vitro evaluation of antibiotic synergy for polymyxin B-resistant carbapenemase-producing *Klebsiella pneumoniae*. *J Clin Microbiol* 2010;48:3558–62.
- [30] Khazandi M, Pi H, Chan WY, Ogunniyi AD, Sim JXF, Venter H, et al. In vitro antimicrobial activity of robenidine, ethylenediaminetetraacetic acid and polymyxin B nonapeptide against important human and veterinary pathogens. *Front Microbiol* 2019;10:837.
- [31] Tallarida RJ. An overview of drug combination analysis with isobolograms. *J Pharmacol Exp Ther* 2006;319:1–7.
- [32] He M, Wu T, Pan S, Xu X. Antimicrobial mechanism of flavonoids against *Escherichia coli* ATCC 25922 by model membrane study. *Appl Surf Sci* 2014;305:515–21.
- [33] Voget M, Lorenz D, Lieber-Tenorio E, Hauck R, Meyer M, Cieslicki M. Is transmission electron microscopy (TEM) a promising approach for qualitative and quantitative investigations of polymyxin B and miconazole interactions with cellular and subcellular structures of *Staphylococcus pseudintermedius*, *Escherichia coli*, *Pseudomonas aeruginosa* and *Malassezia pachydermatis*? *Vet Microbiol* 2015;181:261–70.
- [34] Venter H, Shilling RA, Velamakanni S, Balakrishnan L, Van Veen HW. An ABC transporter with a secondary-active multidrug translocator domain. *Nature* 2003;426:866–70.
- [35] Fuchs PC, Barry AL, Brown SD. Daptomycin susceptibility tests: interpretive criteria, quality control, and effect of calcium on in vitro tests. *Diagn Microbiol Infect Dis* 2000;38:51–8.
- [36] Phee L, Hornsey M, Wareham DW. In vitro activity of daptomycin in combination with low-dose colistin against a diverse collection of Gram-negative bacterial pathogens. *Eur J Clin Microbiol Infect Dis* 2013;32:1291–4.
- [37] Randall CP, Mariner KR, Chopra I, O'Neill AJ. The target of daptomycin is absent from *Escherichia coli* and other Gram-negative pathogens. *Antimicrob Agents Chemother* 2013;57:637–9.

- [38] Bergen PJ, Smith NM, Bedard TB, Bulman ZP, Cha R, Tsuji BT. Rational combinations of polymyxins with other antibiotics. In: Li J, Nation RL, Kaye K, editors. *Polymyxin antibiotics: from laboratory bench to bedside*. Springer; 2019. p. 251–88.
- [39] Zgurskaya HI, Lopez CA, Gnanakaran S. Permeability barrier of Gram-negative cell envelopes and approaches to bypass it. *ACS Infect Dis* 2015;1:512–22.
- [40] Naghmouchi K, Baah J, Hober D, Jouy E, Rubrecht C, Sané F, et al. Synergistic effect between colistin and bacteriocins in controlling Gram-negative pathogens and their potential to reduce antibiotic toxicity in mammalian epithelial cells. *Antimicrob Agents Chemother* 2013;57:2719–25.

Supplementary Material

***In vitro* synergistic activity of NCL195 in combination with colistin against Gram-negative bacterial pathogens**

Hang Thi Nguyen^{1,7}, Henrietta Venter², Tania Veltman¹, Ruth Williams³, Lisa Anne O'Donovan⁴, Cecilia C. Russell⁵, Adam McCluskey⁵, Stephen W. Page⁶, Abiodun David Ogunniyi^{1*} and Darren J. Trott^{1*}

¹Australian Centre for Antimicrobial Resistance Ecology, School of Animal and Veterinary Sciences, The University of Adelaide, Roseworthy, SA, Australia; ²Health and Biomedical Innovation, Clinical and Health Sciences, University of South Australia, Adelaide, SA, Australia; ³Adelaide Microscopy, University of Adelaide, Adelaide, SA, Australia. ⁴ARC Centre of Excellence in Plant Energy Biology, School of Agriculture, Food & Wine, University of Adelaide, SA, Australia; ⁵Chemistry, School of Environmental & Life Sciences, University of Newcastle, Callaghan NSW, Australia; ⁶Neoculi Pty Ltd., Burwood, VIC, Australia; ⁷Department of Pharmacology, Toxicology, Internal Medicine and Diagnostics, Faculty of Veterinary Medicine, Vietnam National University of Agriculture, Hanoi, Vietnam.

Synergy testing by checkerboard assay. Interaction activity between NCL195 or daptomycin with colistin was determined by a modification of the standard checkerboard assay described previously [25, 27, 28]. In all assays for daptomycin, CaCl₂ was added to the LB medium at 100 µg/mL. A typical example of checkerboard assay of combined NCL195 and colistin against *E. coli* 25922 is depicted in **Figure S1**.

Fractional inhibitory concentration index. The interaction of two antibiotics was calculated as the fractional inhibitory concentration index (FICI) using the following formula:

$$\text{FICI} = \frac{\text{MIC}_{\text{A in combination}}}{\text{MIC}_{\text{A alone}}} + \frac{\text{MIC}_{\text{B in combination}}}{\text{MIC}_{\text{B alone}}}$$

A is NCL195 or daptomycin and B is colistin. According to FICI, the interaction between two antibiotic agents were interpreted as follows: synergistic (FICI ≤ 0.5); additive or partially synergistic (0.5 < FICI ≤ 1); indifferent (1 < FICI ≤ 4); and antagonistic (FICI > 4) [29]. NCL195 or daptomycin did not show antibiotic activity against GNB; therefore 256 µg/mL (the highest concentration NCL195 or daptomycin) was used to calculate FICI.

Further analysis was carried out by plotting an isobologram for each isolate. This creates a graphical interpretation of the results and is achieved by plotting the MIC for drug A (NCL195 or daptomycin) on the *y*-axis and drug B (colistin) on the *x*-axis. A dotted line is then drawn between the intercepts of the *x*- and *y*-axis to indicate the line of indifference of activity between the two drugs, as described previously [28, 30].

Dose reduction index. The dose reduction index (DRI) was used to describe the difference between the effective doses of a single compound in combination from its individual dose. DRI was calculated using the following formula:

$$\text{DRI} = \frac{\text{MIC}_{\text{A alone}}}{\text{MIC}_{\text{A in combination}}}$$

Evaluation of DRI is important clinically because it can allow the dose of a drug to be reduced that may result in toxicity of drug in combination without changing the efficacy. DRI (>1) is considered beneficial [28].

Transmission electron microscopy (TEM)

Preparation of bacterial cells. Bioluminescent *E. coli* (Xen14) was cultured on HBA plate containing 30 $\mu\text{g/mL}$ kanamycin overnight at 37°C in normal air. A single colony was taken from the overnight growth and emulsified in 10 mL LB broth in a 50 mL flask and incubated at 37°C under continuous agitation in an orbital shaker at 150 rpm. The overnight bacterial culture was diluted 1:30 in 40 mL LB broth in 50 mL flask of LB broth and then incubated again at 37°C under continuous agitation until $A_{600\text{ nm}} = 0.1$. Untreated Xen14 cells were harvested at this time point and placed on ice as controls. The rest of the bacterial samples were then aliquoted and treated as follows: (i), NCL195 alone (2 $\mu\text{g/mL}$); (ii), colistin alone (0.125 $\mu\text{g/mL}$); (iii), colistin alone (0.25 $\mu\text{g/mL}$); (iv), colistin alone (0.5 $\mu\text{g/mL}$); (v), colistin (0.125 $\mu\text{g/mL}$) + NCL195 (2 $\mu\text{g/mL}$) combination; (vi), colistin (0.125 $\mu\text{g/mL}$) + NCL195 (4 $\mu\text{g/mL}$) combination; (vii), colistin (0.25 $\mu\text{g/mL}$) + NCL195 (1 $\mu\text{g/mL}$) combination; (viii), colistin (0.25 $\mu\text{g/mL}$) + NCL195 (2 $\mu\text{g/mL}$) combination; (ix), colistin (0.5 $\mu\text{g/mL}$) + NCL195 (1 $\mu\text{g/mL}$) combination; (x), and colistin (0.5 $\mu\text{g/mL}$) + NCL195 (2 $\mu\text{g/mL}$) combination and incubated for 1 h at 37°C under continuous agitation in a shaker at 150 rpm. During the treatment time, each sample was manually mixed every 10 min to ensure adequate antibiotic contact with the cells. A treatment time of 1 h was determined empirically to be optimal for visualisation of the effects of the single and mixed treatments of the Xen14 cells.

Bioluminescent *P. aeruginosa* (Xen41) cells were prepared for TEM essentially as described above for Xen14, but with slight modifications, as follows. Xen41 cells were cultured on HBA plates containing 60 $\mu\text{g/mL}$ tetracycline for selection. A few colonies were taken from the HBA and grown overnight in 40 mL LB broth in several 50 mL Falcon tubes at 37°C under continuous agitation in a shaker at 150 rpm for 12 h. The bacteria were then harvested by centrifugation at $2,900 \times g$ for 10 min and washed twice in PBS to reduce the polysaccharide layer of Xen41 in order to allow easier contact

between antibiotics and the cells. The pellet was then resuspended in LB broth and adjusted to $A_{600\text{ nm}} = 0.1$ and an aliquot taken as a no-treatment control. Other aliquots were treated as follows: (i), NCL195 alone (2 $\mu\text{g/mL}$); (ii), colistin alone (1 $\mu\text{g/mL}$); (iii) colistin alone (2 $\mu\text{g/mL}$); (iv) colistin (1 $\mu\text{g/mL}$) + NCL195 (2 $\mu\text{g/mL}$) combination; and (v) colistin (2 $\mu\text{g/mL}$) + NCL195 (2 $\mu\text{g/mL}$) combination and incubated for 1 h at 37°C under continuous agitation as described above for Xen14.

Sample processing for TEM. The TEM protocol was modified from previous studies [37-39]. Briefly, all cells with or without antibiotic treatment were harvested by centrifugation at $2,900 \times g$ for 5 min at 4 °C to avoid cell damage and washed twice in PBS. The cells were then fixed in 1 mL fixative containing 4.0% paraformaldehyde, 1.25% glutaraldehyde, CaCl_2 0.01M, 4% sucrose and 0.075% ruthenium red, 0.075% L-lysine acetate in 0.1M cacodylate buffer. Xen14 cells were fixed overnight while Xen41 cells were washed twice in cacodylate buffer followed by fixing in 1 mL fixative for 1.5 h on ice as overnight fixation of Xen41 cells resulted in dark TEM images.

Fixed cells were washed twice for 5 min at $2,900 \times g$ in cacodylate buffer and then post fixed in 1% osmium tetroxide in cacodylate buffer containing 0.075% ruthenium red for 1 h. Subsequently, all samples were washed twice in cacodylate buffer. Then cells were dehydrated using a graded series of 50%, 70%, 90% and 100% ethanol for 10 min (2 \times for each step but 3 \times for 15 min when using 100% ethanol). Thereafter, the cells were infiltrated using a 50:50 ratio of 100% ethanol:LR white resin for 1 h and subsequently left in 100% LR white resin overnight, which was then changed twice, 5 h apart, the following day. Subsequently, the cells were polymerized in fresh LR white resin at 50°C for 48 h.

Sections were cut to 1 μm using a glass knife, stained with 1% toluidene blue containing 1% borax and viewed under a light microscope at 400 \times magnification to identify stained bacteria. At least four ultra-thin sections were then cut to 80 nm with an ultramicrotome (Leica) using a diamond knife (Diatome) and placed on 200-mesh copper EM grids (Proscitech). Sections were sequentially stained with uranyl acetate (4% in dH_2O) and Reynolds lead citrate for 10 min each, with three washes in distilled water in-between each stain. Sections were then viewed between 25000 \times and 130000 \times on a

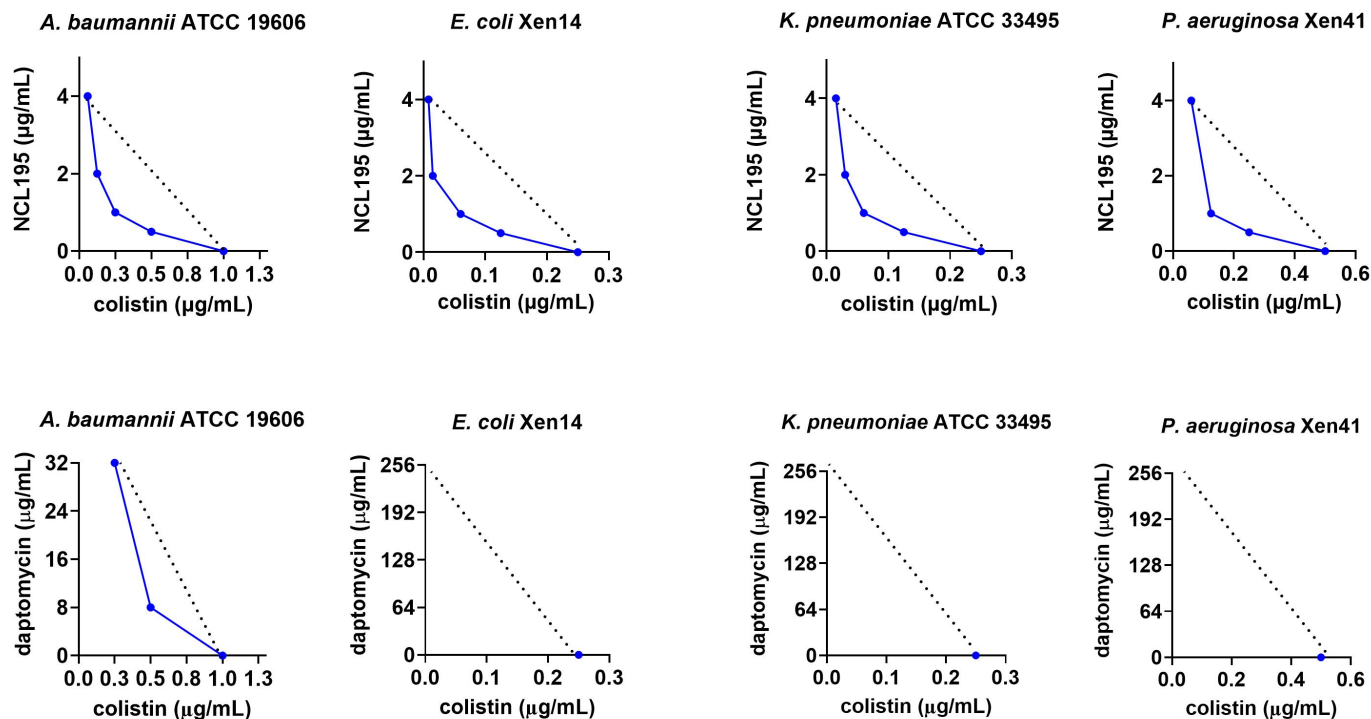
Tecnai G2 Spirit 120 kVolt Transmission Electron Microscope (FEI Company). Images were obtained at 130000× magnification and analyzed using Olympus Soft Imaging Systems.

Mouse infection and challenge studies. Outbred 5 to 6-week-old male CD1 (Swiss) mice (weighing between 25 g to 32 g) were obtained from the Laboratory Animal Services breeding facility of The University of Adelaide, and had access to food and water ad libitum throughout. The Animal Ethics Committee of The University of Adelaide (S-2015-151) reviewed and approved all animal experiments. The study was conducted in compliance with the Australian Code of Practice for the Care and Use of Animals for Scientific Purposes (8th Edition 2013) and the South Australian Animal Welfare Act 1985.

Before infection, *E. coli* Xen14 was grown in LB broth at 37°C to $A_{600\text{nm}} = 0.5$ (equivalent to approx. 1.5×10^8 CFU/mL). Four groups of mice (n= 3 mice per group) were challenged IP with approx. 3.0×10^7 CFU of Xen14 in 200 µl PBS containing 3% hog gastric mucin type III (Sigma Aldrich). All mice were then subjected to bioluminescent imaging in both ventral and dorsal positions on the IVIS Lumina XRMS Series III system. Immediately thereafter, group 1 mice received the drug vehicle only, group 2 received colistin at 0.125 mg/kg IP, group 3 received colistin at 0.25 mg/kg IP while group 4 received colistin at 0.5 mg/kg IP. At 4 h and 8 h post-infection, an identical course of treatment regimen was administered to each group. Surviving animals in each group were also subjected to bioluminescence imaging at 4 h, 6 h, 10 h, 12 h, 24 h, 48 h and 72 h post infection. Mice were monitored frequently for signs of distress and those that had become moribund or showed any evidence of distress were humanely killed by cervical dislocation. In all groups, signals were collected from a defined region of interest and total flux intensities (photons/s) analyzed using Living Image Software 2.5 (for IVIS 100) and 4.4 (for Lumina XRMS).

| | 1 | 2 | 3 | 4 | 5 | 6 | 7 | 8 | 9 | 10 | 11 | 12 | NCL195 ($\mu\text{g/mL}$) |
|---|------------|------------|-------|-------|------|------|-------|------|------|------|------|------|-----------------------------|
| A | 1.64 | 1.64 | 0.05 | 0.05 | 0.05 | 0.05 | 0.05 | 0.05 | 0.05 | 0.05 | 0.07 | 0.04 | 8 |
| B | 1.67 | 1.68 | 0.05 | 0.04 | 0.04 | 0.04 | 0.04 | 0.04 | 0.04 | 0.04 | 0.04 | 0.04 | 4 |
| C | 1.67 | 1.67 | 1.66 | 1.36 | 0.04 | 0.04 | 0.04 | 0.04 | 0.04 | 0.04 | 0.04 | 0.04 | 2 |
| D | 1.66 | 1.69 | 1.67 | 1.58 | 1.68 | 0.04 | 0.04 | 0.04 | 0.04 | 0.04 | 0.04 | 0.04 | 1 |
| E | 1.68 | 1.68 | 1.66 | 1.66 | 1.65 | 0.80 | 0.04 | 0.04 | 0.04 | 0.04 | 0.04 | 0.04 | 0.5 |
| F | 1.68 | 1.64 | 1.63 | 1.63 | 1.69 | 1.57 | 0.97 | 0.04 | 0.04 | 0.04 | 0.04 | 0.04 | 0.25 |
| G | 0.04 | 1.52 | 1.48 | 1.50 | 1.56 | 1.52 | 1.47 | 0.04 | 0.04 | 0.04 | 0.04 | 0.04 | |
| H | 0.04 | 1.58 | 1.51 | 1.56 | 1.52 | 1.54 | 1.10 | 0.04 | 0.04 | 0.04 | 0.04 | 0.04 | |
| | Growth (-) | Growth (+) | 0.008 | 0.015 | 0.03 | 0.06 | 0.125 | 0.25 | 0.5 | 1 | 2 | 4 | Colistin $\mu\text{g/mL}$ |

Figure S1. Checkerboard assay of NCL195 + colistin combination against *E. coli* ATCC 25922. Values represent $A_{600\text{ nm}}$ measurements. Colistin concentration ranged from 0.008 to 4 $\mu\text{g/mL}$ (columns 3 to 12); NCL195 concentration ranged from 0.25 to 8 $\mu\text{g/mL}$ (rows A to F); blue wells, NCL195 alone; green wells, colistin alone; red wells, bacterial growth control containing only *E. coli* and LB broth; yellow wells, LB broth only (no growth control, also representing the $A_{600\text{ nm}}$ value at the MIC of colistin alone or NCL195 + colistin combination).



3

4 **Figure S2.** Isobologram analysis showing the interaction of colistin with NCL195 or daptomycin at different combined MICs. MIC of colistin is
5 plotted on X-axis and MIC of NCL195 or daptomycin is on the Y-axis, MIC of NCL195 or daptomycin alone is higher than 256 µg/mL (not
6 shown on the graph). The blue curves below the indifference (dotted) line represent synergistic ($FICI \leq 0.5$), additive or partially synergistic (0.5
7 $< FICI \leq 1$). Therefore, no blue curve (i.e. no synergy) was observed for the daptomycin + colistin combination for *E. coli*, *K. pneumoniae* or *P.*
8 *aeruginosa*.

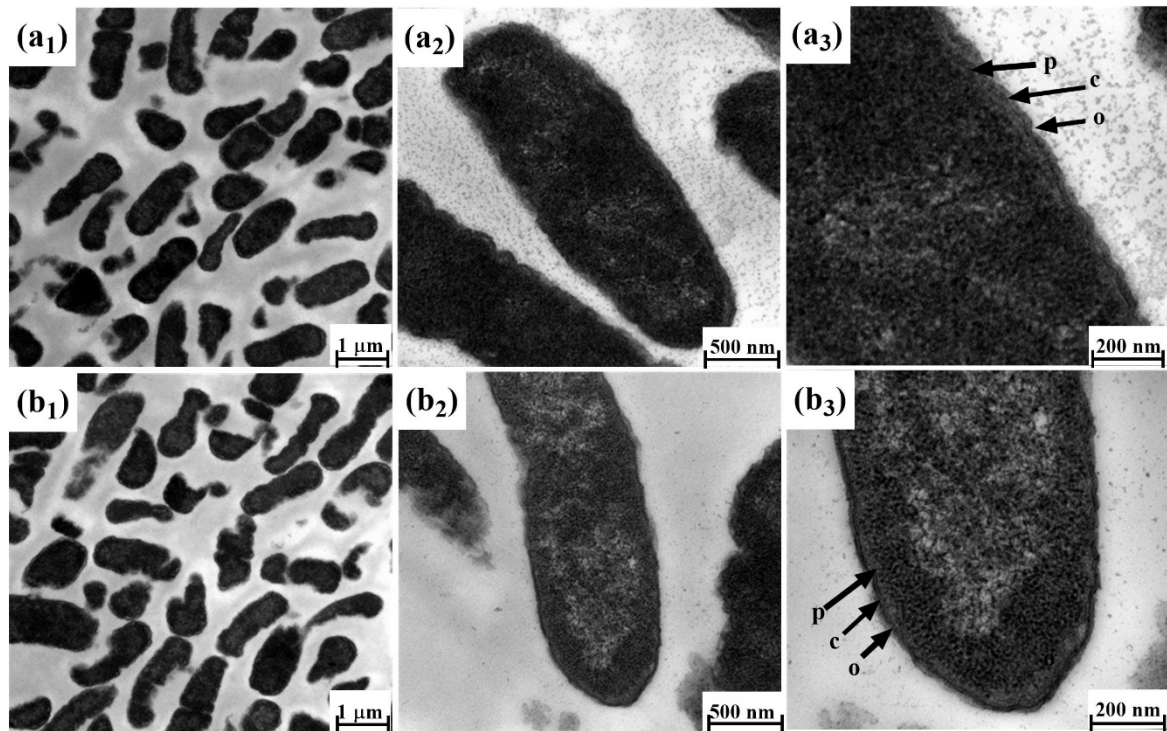


Figure S3. Morphology of *E. coli* Xen14 cells at 1 μm , 500 nm and 200 nm. Approximately 5×10^8 cells were treated for 1 h. (**a₁–a₃**), Xen14 cells without treatment clearly show intact outer membrane (o), cell wall (c) and plasma membrane (p); (**b₁–b₃**), Xen14 cells treated with NCL195 alone at 2 $\mu\text{g}/\text{mL}$ show similar morphology as the untreated (control) cells.

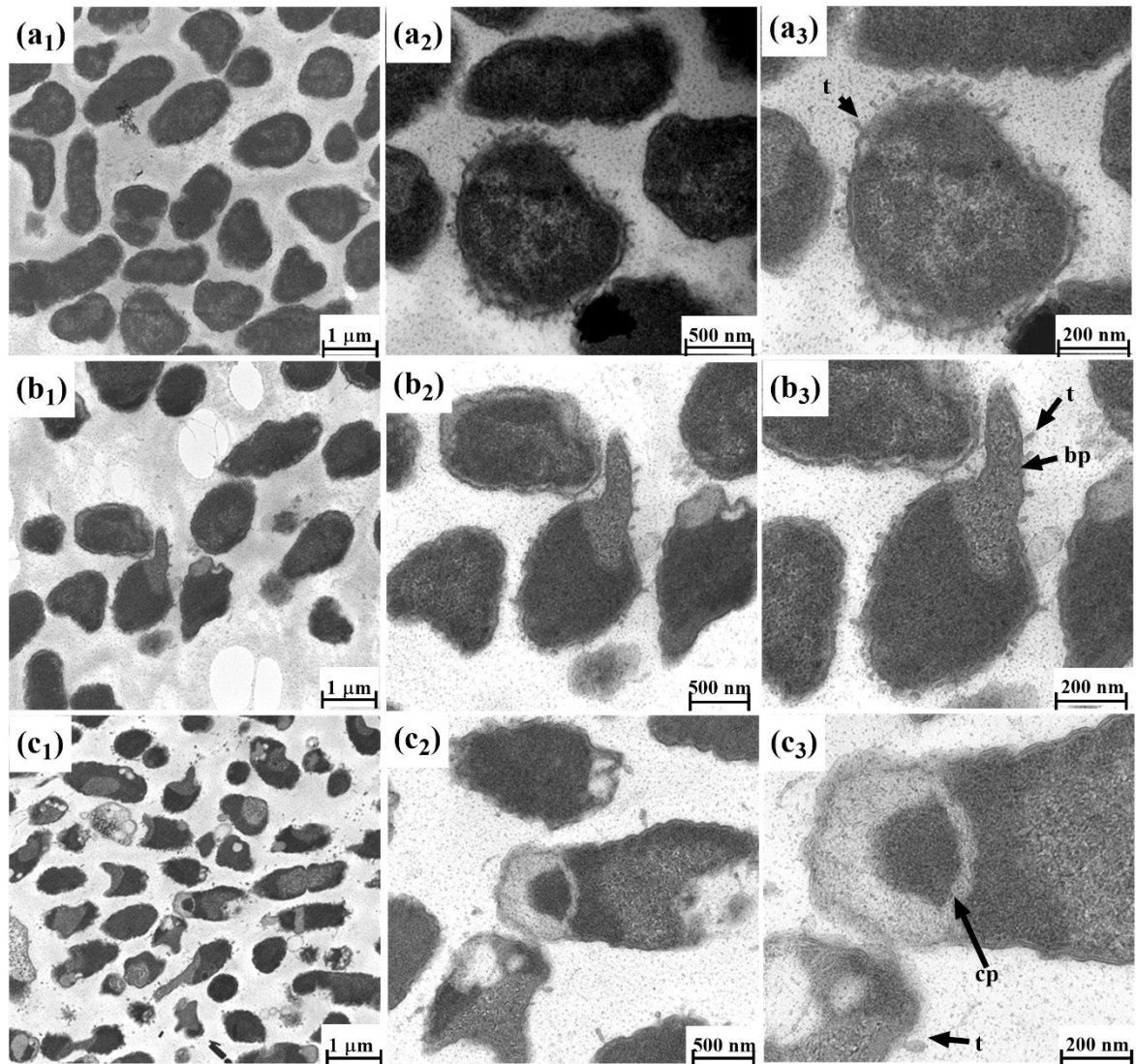


Figure S4. Morphology of *E. coli* Xen14 cells at 1 μm , 500 nm and 200 nm. Approximately 5×10^8 cells were treated for 1 h. (a₁–a₃), Xen14 cells treated with colistin at 0.125 $\mu\text{g}/\text{mL}$ show swollen envelope with tubular and fimbria like radiant appendages; (b₁–b₃), Xen14 cells treated with a combination of NCL195 at 2 $\mu\text{g}/\text{mL}$ and colistin at 0.125 $\mu\text{g}/\text{mL}$ exhibit swollen envelope with tubular (t) and fimbria-like radiant appendages and broken plasma membrane (bp); (c₁–c₃), Xen14 cells exposed to a combination of NCL195 at 4 $\mu\text{g}/\text{mL}$ and colistin at 0.125 $\mu\text{g}/\text{mL}$ showing swollen envelope with tubular and fimbria-like radiant appendages and curved plasma membrane (cp).

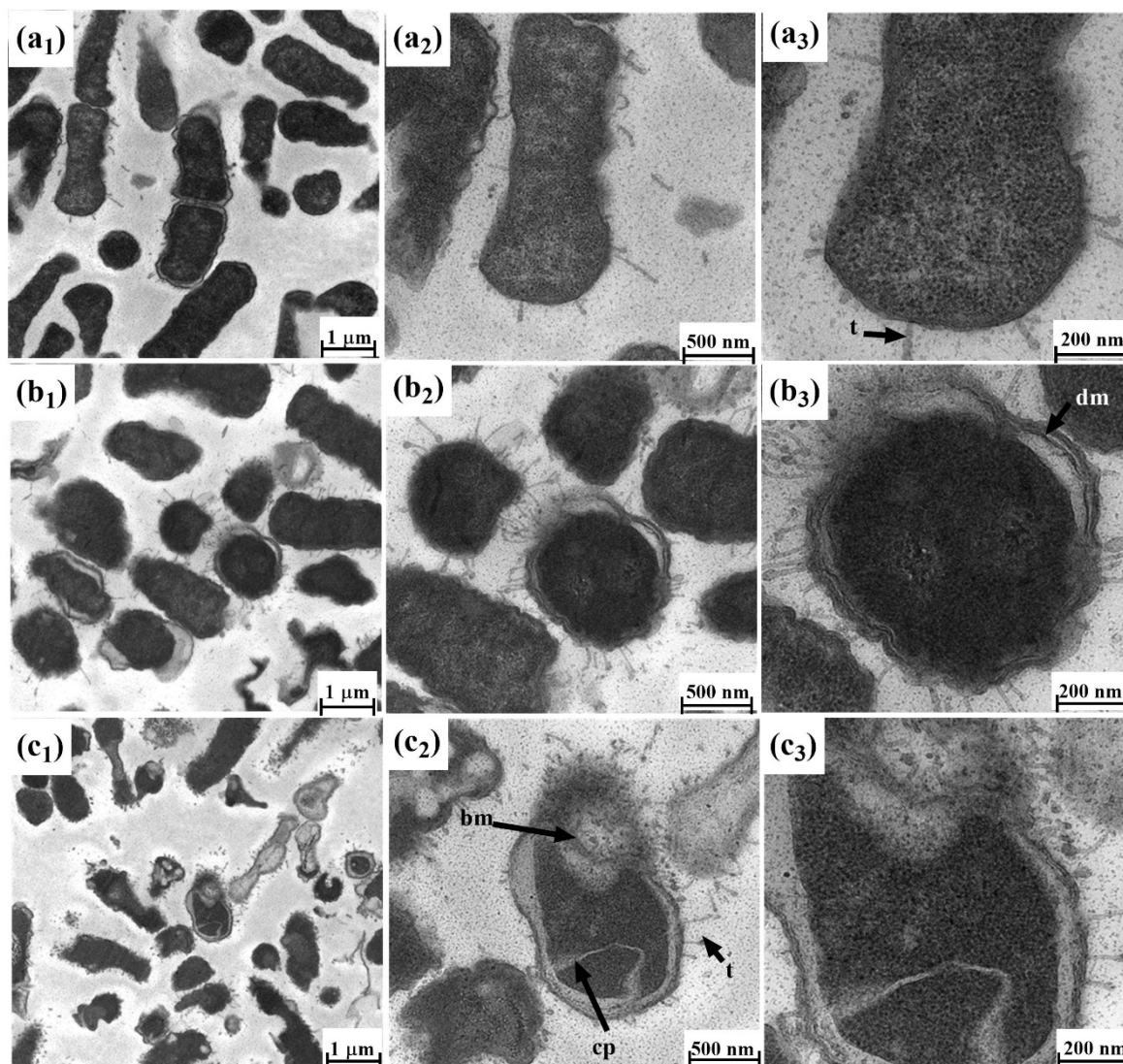


Figure S5. Morphology of *E. coli* Xen14 cells at 1 μm , 500 nm and 200 nm. Approximately 5×10^8 cells were treated for 1 h. (a₁–a₃), Xen14 cells treated with colistin at 0.25 $\mu\text{g}/\text{mL}$ show swollen envelope with tubular (t) and fimbria-like radiant appendages; (b₁–b₃), *E. coli* Xen14 cells treated with a combination of NCL195 at 1 $\mu\text{g}/\text{mL}$ and colistin at 0.25 $\mu\text{g}/\text{mL}$ exhibit a swollen envelope with tubular and fimbria-like radiant appendages and detached plasma membrane (dm); (c₁–c₃), Xen14 cells treated with a combination of NCL195 at 2 $\mu\text{g}/\text{mL}$ and colistin at 0.25 $\mu\text{g}/\text{mL}$ exhibit a swollen envelope with tubular and fimbria-like radiant appendages, detached plasma membrane (dm) and broken membrane (bm).

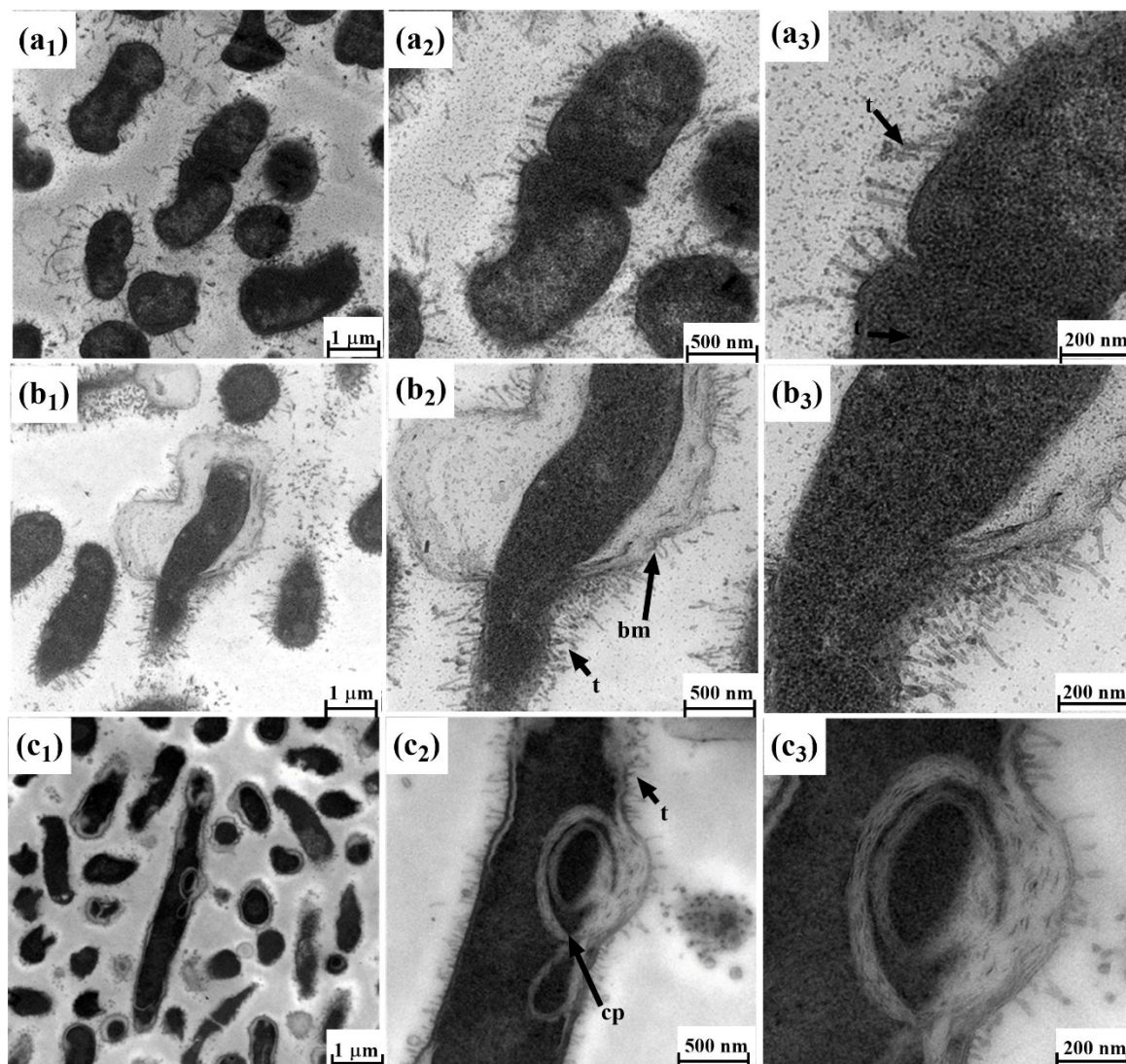


Figure S6. Morphology of *E. coli* Xen14 cells at 1 μm , 500 nm and 200 nm. Approximately 5×10^8 cells were treated for 1 h. (a₁–a₃), Xen14 cells treated with colistin at 0.5 $\mu\text{g}/\text{mL}$ showing a swollen envelope with tubular (t) and fimbria-like radiant appendages; (b₁–b₃), Xen14 cells treated with a combination of NCL195 at 1 $\mu\text{g}/\text{mL}$ and colistin at 0.5 $\mu\text{g}/\text{mL}$ showing a swollen envelope with tubular and fimbria-like radiant appendages as well as broken and detached plasma membrane (dm and bm); (c₁–c₃), Xen14 cells treated with a combination of NCL195 at 2 $\mu\text{g}/\text{mL}$ and colistin at 0.5 $\mu\text{g}/\text{mL}$ exhibiting a swollen envelope with tubular and fimbria-like radiant appendages and curved membrane (cm).

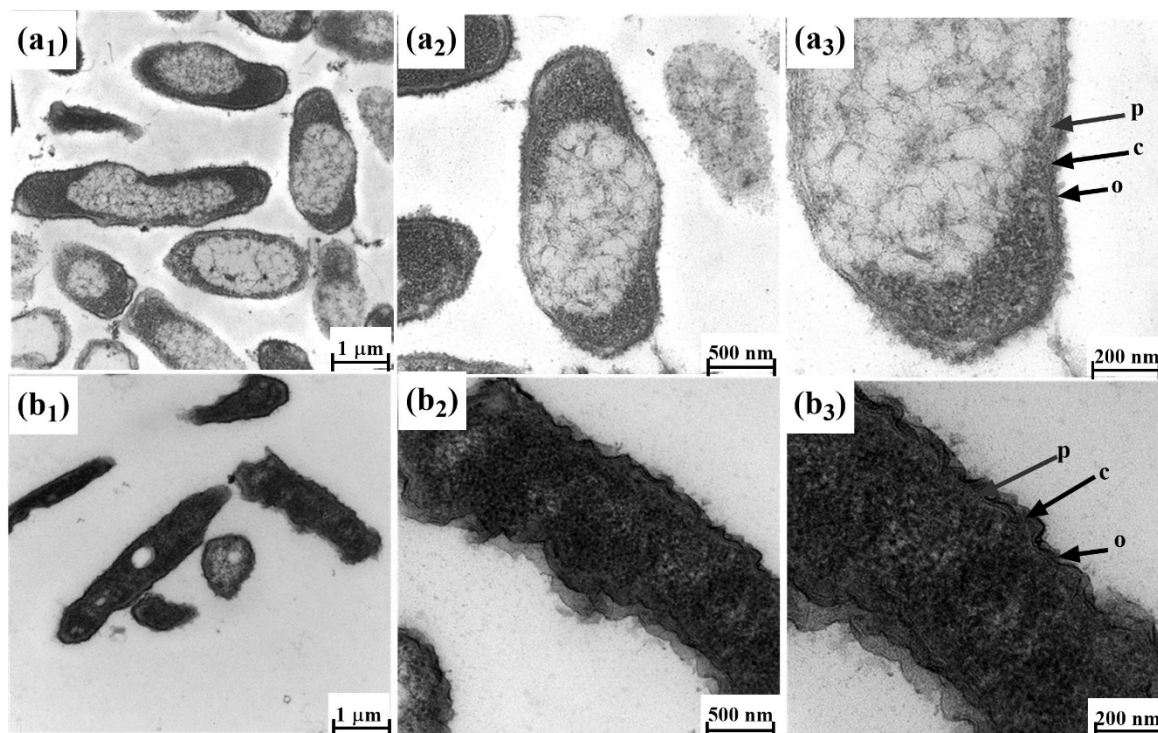


Figure S7. Morphology of *P. aeruginosa* Xen41 cells at 1 μm , 500 nm and 200 nm. Approximately 5×10^8 cells were treated for 1 h. (**a₁–a₃**), Xen41 cells without treatment clearly showing intact outer membrane (o), cell wall (c) and plasma membrane (p); (**b₁–b₃**), Xen41 cells treated with NCL195 at 2 $\mu\text{g}/\text{mL}$ maintain the same ultrastructural membrane morphology as the control group.

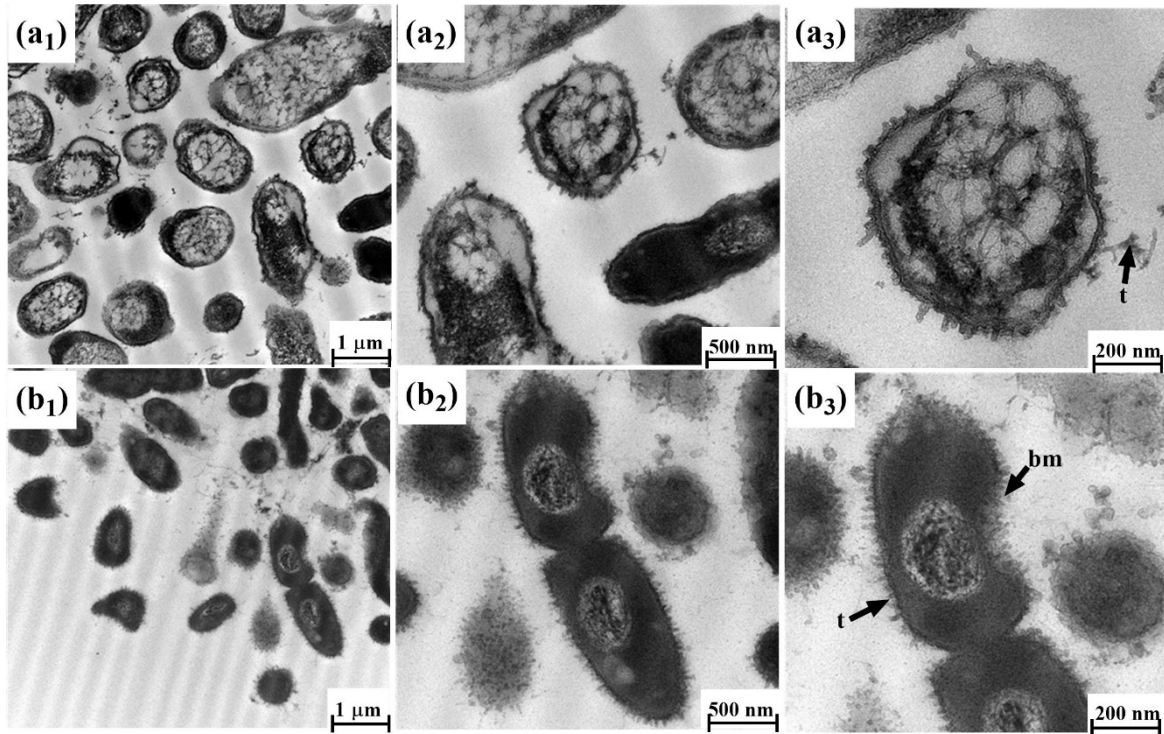


Figure S8. Morphology of *P. aeruginosa* Xen41 cells at 1 μm , 500 nm and 200 nm. Approximately 5×10^8 cells were treated for 1 h. (a₁–a₃), Xen41 cells treated with colistin at 1 $\mu\text{g}/\text{mL}$ showing fluffy materials surrounding the cells and tubular appendages (t); (b₁–b₃), Xen41 cells exposed to a combination of NCL195 at 2 $\mu\text{g}/\text{mL}$ and colistin at 1 $\mu\text{g}/\text{mL}$ show more of the fluff surrounding the cells, more tubular appendages, loss of clear delineation of the cell envelope layers and broken membrane (bm)

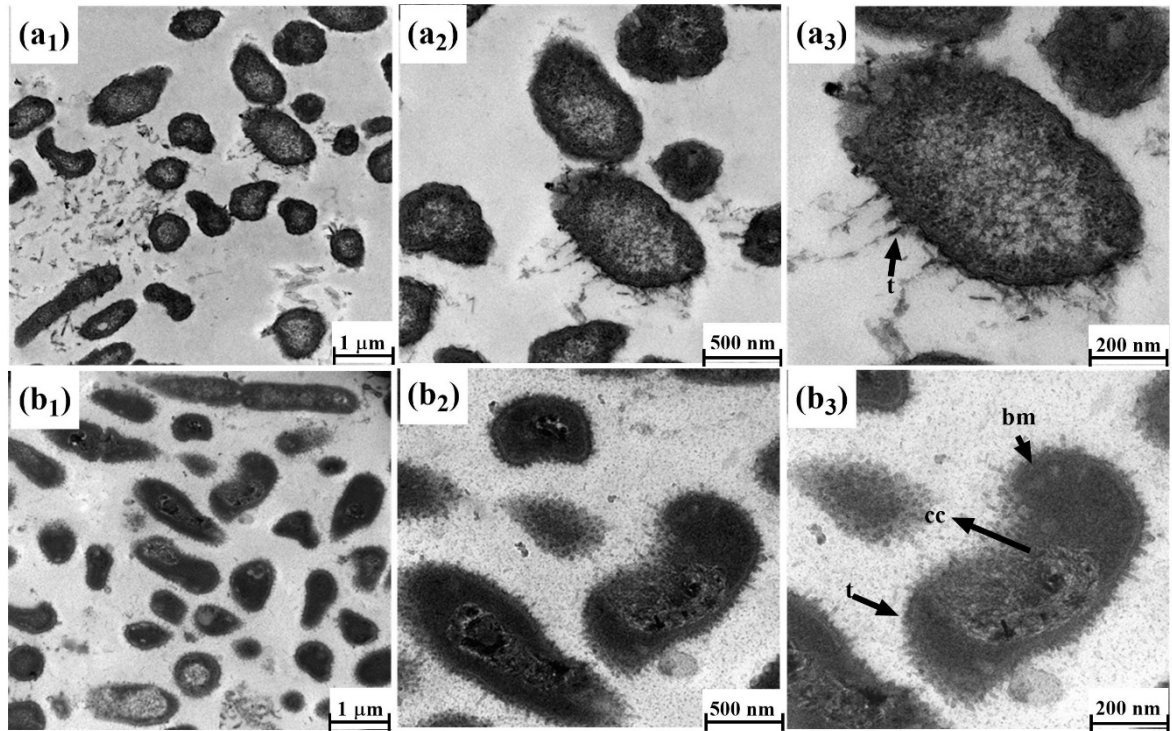


Figure S9. Morphology of *P. aeruginosa* Xen41 cells at 1 μm , 500 nm and 200 nm. Approximately 5×10^8 cells were treated for 1 h. (a₁–a₃), Xen41 cells treated with colistin at 2 $\mu\text{g}/\text{mL}$ showing fluffy materials surrounding the cells and tubular appendages (t); (b₁–b₃), Xen41 cells exposed to a combination of NCL195 at 2 $\mu\text{g}/\text{mL}$ and colistin 2 $\mu\text{g}/\text{mL}$ showing more of the fluff surrounding the cells, more tubular appendages and loss of differentiation of the cell envelope layers and broken membrane (bm) causing discharge of cellular constituents (cc).

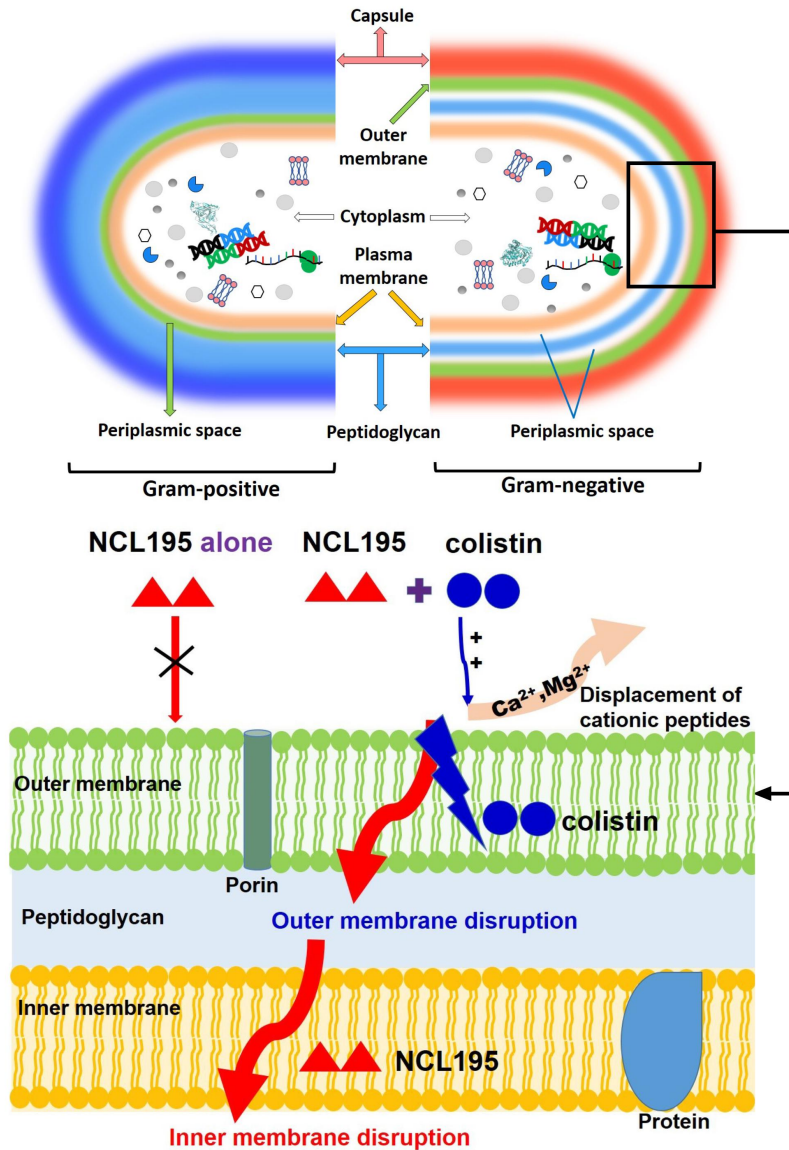


Figure S10. The hypothesized mechanism of action of NCL195 in combination with colistin on the cell membrane of GNB (modified from Dandie *et al.* [40]). The positively charged colistin competitively displaces native divalent cations (Ca^{2+} and Mg^{2+}) to interact with negatively charged divalent cation binding sites on the outer membrane LPS of GNB. This results in translocation of colistin across the outer membrane, leading to permeability changes in the cell envelope thereby resulting in penetration of NCL195 through the outer membrane to act on inner membrane.

Chapter IV

Comparison of two transmission electron microscopy methods to visualize drug-induced alterations of Gram-negative bacterial morphology

Statement of Authorship

| | |
|---------------------|--|
| Title of Paper | Comparison of two transmission electron microscopy methods to visualize drug-induced alterations of Gram-negative bacterial morphology |
| Publication Status | <input checked="" type="checkbox"/> Published <input type="checkbox"/> Accepted for Publication <input type="checkbox"/> Submitted for Publication <input type="checkbox"/> Unpublished and Unsubmitted work written in manuscript style |
| Publication Details | Nguyen, H.T.; O'Donovan, L.A.; Venter, H.; Russell, C.C.; McCluskey, A.; Page, S.W.; Trott, D.J.; Ogunniyi, A.D. Comparison of two transmission electron microscopy methods to visualize drug-induced alterations of Gram-negative bacterial morphology. <i>Antibiotics</i> (Basel). 2021 , 10, doi:10.3390/antibiotics10030307. Journal Impact Factor = 5.222. |

Principal Author

| | | | |
|--------------------------------------|--|------|------------|
| Name of Principal Author (Candidate) | Hang Thi Nguyen | | |
| Contribution to the Paper | Contributed to the study design, performed all experiments, wrote the preliminary manuscript and revised the edited manuscript | | |
| Overall percentage (%) | 70% | | |
| Certification: | This paper reports on original research I conducted during the period of my Higher Degree by Research candidature and is not subject to any obligations or contractual agreements with a third party that would constrain its inclusion in this thesis. I am the primary author of this paper. | | |
| Signature | | Date | 01/12/2021 |

Co-Author Contributions

By signing the Statement of Authorship, each author certifies that:

- i. the candidate's stated contribution to the publication is accurate (as detailed above);
- ii. permission is granted for the candidate to include the publication in the thesis; and
- iii. the sum of all co-author contributions is equal to 100% less the candidate's stated contribution.

| | | | |
|---------------------------|--|------|------------|
| Name of Co-Author | Lisa Anne O'Donovan | | |
| Contribution to the Paper | Contributed to TEM technical guidance, experimentation and edited the manuscript | | |
| Signature | | Date | 05/01/2022 |

| | | | |
|---------------------------|--|------|------------|
| Name of Co-Author | Henrietta Venter | | |
| Contribution to the Paper | Contributed to study design, editing, financial support, discussion, and provided expertise on the mechanism of action studies | | |
| Signature | | Date | 15/12/2021 |

| | | | |
|-------------------|--------------------|--|--|
| Name of Co-Author | Cecilia C. Russell | | |
|-------------------|--------------------|--|--|

| | | | |
|---------------------------|---|------|------------|
| Contribution to the Paper | Responsible for synthesizing NCL195 and contributed to editing the manuscript | | |
| Signature | | Date | 05/01/2022 |

| | | | |
|---------------------------|---|------|------------|
| Name of Co-Author | Adam McCluskey | | |
| Contribution to the Paper | Responsible for synthesizing NCL195 and edited the manuscript | | |
| Signature | | Date | 06/02/2022 |

| | | | |
|---------------------------|---|------|------------|
| Name of Co-Author | Stephen W. Page | | |
| Contribution to the Paper | Contributed to editing, discussion and provided financial support for the study | | |
| Signature | | Date | 02/02/2022 |

| | | | |
|---------------------------|--|------|------------|
| Name of Co-Author | Darren J. Trott | | |
| Contribution to the Paper | Contributed to study design, editing, and discussion, provided financial support for the study and was co-corresponding author | | |
| Signature | | Date | 07/02/2022 |

| | | | |
|---------------------------|--|------|------------|
| Name of Co-Author | Abiodun D. Ogunniyi | | |
| Contribution to the Paper | Contributed to study design, TEM technical guidance, editing, discussion and was co-corresponding author | | |
| Signature | | Date | 08/12/2021 |

Please cut and paste additional co-author panels here as required.



Article

Comparison of Two Transmission Electron Microscopy Methods to Visualize Drug-Induced Alterations of Gram-Negative Bacterial Morphology

Hang Thi Nguyen^{1,2}, Lisa A. O'Donovan³ , Henrietta Venter⁴ , Cecilia C. Russell⁵, Adam McCluskey⁵ , Stephen W. Page⁶, Darren J. Trott^{1,*} and Abiodun D. Ogunniyi^{1,*}

¹ Australia Centre for Antimicrobial Resistance Ecology, School of Animal and Veterinary Sciences, Roseworthy Campus, The University of Adelaide, Roseworthy, SA 5371, Australia; hang.t.nguyen@adelaide.edu.au

² Department of Pharmacology, Toxicology, Internal Medicine and Diagnostics, Faculty of Veterinary Medicine, Vietnam National University of Agriculture, Hanoi 100000, Vietnam

³ ARC Centre of Excellence in Plant Energy Biology, School of Agriculture Food & Wine, Waite Campus, The University of Adelaide, Urrbrae, SA 5064, Australia; lisa.odonovan@adelaide.edu.au

⁴ Health and Biomedical Innovation, Clinical and Health Sciences, University of South Australia, Adelaide, SA 5000, Australia; rietie.venter@unisa.edu.au

⁵ Chemistry School of Environmental and Life Sciences, University of Newcastle, Callaghan, NSW 2308, Australia; cecilia.russell@newcastle.edu.au (C.C.R.); adam.mccluskey@newcastle.edu.au (A.M.)

⁶ Neoculi Pty Ltd., Burwood, VIC 3125, Australia; swp@advet.com.au

* Correspondence: darren.trott@adelaide.edu.au (D.J.T.); david.ogunniyi@adelaide.edu.au (A.D.O.); Tel.: +61-8-8313-7989 (D.J.T.); +61-432-331-914 (A.D.O.)



Citation: Nguyen, H.T.; O'Donovan, L.A.; Venter, H.; Russell, C.C.; McCluskey, A.; Page, S.W.; Trott, D.J.; Ogunniyi, A.D. Comparison of Two Transmission Electron Microscopy Methods to Visualize Drug-Induced Alterations of Gram-Negative Bacterial Morphology. *Antibiotics* **2021**, *10*, 307. <https://doi.org/10.3390/antibiotics10030307>

Academic Editor: Sebastiaan Werten

Received: 9 February 2021

Accepted: 15 March 2021

Published: 17 March 2021

Publisher's Note: MDPI stays neutral with regard to jurisdictional claims in published maps and institutional affiliations.



Copyright: © 2021 by the authors. Licensee MDPI, Basel, Switzerland. This article is an open access article distributed under the terms and conditions of the Creative Commons Attribution (CC BY) license (<https://creativecommons.org/licenses/by/4.0/>).

Abstract: In this study, we optimized and compared different transmission electron microscopy (TEM) methods to visualize changes to Gram-negative bacterial morphology induced by treatment with a robenidine analogue (NCL195) and colistin combination. Aldehyde-fixed bacterial cells (untreated, treated with colistin or NCL195 + colistin) were prepared using conventional TEM methods and compared with ultrathin Tokuyasu cryo-sections. The results of this study indicate superiority of ultrathin cryo-sections in visualizing the membrane ultrastructure of *Escherichia coli* and *Pseudomonas aeruginosa*, with a clear delineation of the outer and inner membrane as well as the peptidoglycan layer. We suggest that the use of ultrathin cryo-sectioning can be used to better visualize and understand drug interaction mechanisms on the bacterial cell membrane.

Keywords: transmission electron microscopy; bacterial cell wall; bacterial membrane; Gram-negative bacteria; colistin; drug interaction; Tokuyasu cryo-ultramicrotomy

1. Introduction

Gram-negative bacterial pathogens exhibit high-level resistance to most classes of antibiotics due to the presence of an impermeable outer membrane [1,2]. Polymyxins are considered as last-line agents for the treatment of Gram-negative infections due to their unique mechanism of action targeting the outer membrane [3–6]. However, polymyxins are highly nephrotoxic and neurotoxic agents if high doses are used [7,8], resulting in a narrow therapeutic window for Gram-negative infections. The usage of polymyxins in combination with other agents is being considered as a strategy for overcoming reduced polymyxin susceptibility and toxicity without increasing polymyxin exposure [3,9]. The mechanism of beneficial combination treatment is proposed to involve complete integration of polymyxins into the outer membrane causing disorganization and neutralization of cell surface charge and consequently loss of envelope barrier function. Subsequently, the affected outer membrane is hypothesized to transiently open, allowing entry of the second antibiotic and interaction with otherwise inaccessible drug target sites [2,10–13].

Our ongoing studies have indicated potential therapeutic options using the novel pyrimidine NCL195, 4,6-bis(2-((*E*)-4-methylbenzylidene)hydrazineyl)pyrimidin-2-amine (Figure 1) combined with subinhibitory concentrations of polymyxin B (PMB) or colistin against Gram-negative infections [10,11]. We showed synergistic activity of the NCL195-PMB or NCL195-colistin combination against clinical Gram-negative bacterial pathogens, with MICs for NCL195 ranging from 0.25–4 µg/mL for *Acinetobacter baumannii*, *Escherichia coli*, *Klebsiella pneumoniae* and *Pseudomonas aeruginosa*, whereas NCL195 alone had no activity.

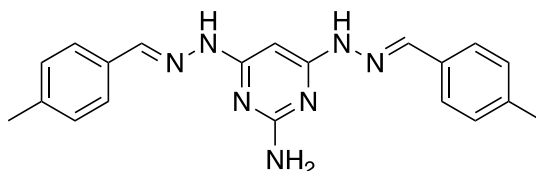


Figure 1. Chemical structure of novel pyrimidine NCL195, 4,6-bis(2-((*E*)-4-methylbenzylidene)hydrazineyl)pyrimidin-2-amine.

For decades, transmission electron microscopy (TEM) has been a valuable research tool in microbiology for high-resolution structural studies of bacteria and their components [14,15]. TEM was applied to study the effect of drug treatment on both Gram-negative and Gram-positive bacteria [16,17]. We have also used TEM to study NCL195-colistin interactions on the Gram-negative cell membrane [10]. During the investigation, the stability of Gram-negative bacterial cell morphology was affected by several factors, including buffer conditions, selected fixatives, type of resin and the embedding method. Cryo-EM and Tokuyasu cryo-ultramicrotomy have been shown to offer some advantages over conventional TEM for investigating bacterial ultrastructure, including better resolution, artifact reduction, clearer visualization of bacterial cytoskeleton and better preservation of bacterial structural integrity [18–23]. Therefore, determining the most effective technique to accurately visualize and elucidate drug interactions on bacteria is essential. The objective of the present investigation was to compare two sample preparation methods for TEM (conventional resin embedding and Tokuyasu cryo-ultramicrotomy) to visualize the morphological changes occurring on the cell membrane of *E. coli* and *P. aeruginosa* after exposure to NCL195 alone, colistin alone or NCL195-colistin combination.

2. Materials and Methods

2.1. Antibiotics and Chemicals

NCL195, a novel pyrimidine compound [24,25] (Figure 1), was synthesized at the University of Newcastle. The compound was stored in a sealed container in the dark at 4 °C at the Infectious Diseases Laboratory, Roseworthy campus, The University of Adelaide. Colistin sulphate, kanamycin and tetracycline were purchased from Sigma-Aldrich (Australia). Stock solutions containing 25.6 mg/mL of each compound (NCL195 dissolved in DMSO, colistin and kanamycin dissolved in water and tetracycline dissolved in 70% of ethanol) were stored in 1 mL aliquots at –20 °C away from direct light. Ruthenium red, L-lysine acetate and sucrose were purchased from Sigma-Aldrich, Australia, and dissolved in water to the appropriate concentrations. Fixatives and cacodylate buffer were provided by Adelaide Microscopy, The University of Adelaide, Adelaide, South Australia, Australia.

2.2. Bacterial Strains and Growth Conditions

Bioluminescent *E. coli* Xen14 (derived from the parental strain *E. coli* WS2572) and bioluminescent *P. aeruginosa* Xen41 (derived from the parental strain PAO1) were purchased from PerkinElmer Inc. (Waltham, MA, USA). *E. coli* Xen14 was grown on horse blood agar (HBA) containing 30 µg/mL kanamycin and *P. aeruginosa* Xen41 was grown in HBA containing 60 µg/mL tetracycline overnight at 37 °C in normal air for selection. A single

colony was taken from the overnight growth, suspended in 10 mL Luria-Bertani (LB) broth, Miller (Becton Dickinson, Sparks, MD, USA) in a 50 mL flask and incubated at 37 °C under continuous agitation in an orbital shaker at 150 rpm. The overnight bacterial culture was diluted 1:30 in 40 mL LB broth in 50 mL flask of LB broth and then incubated again at 37 °C under continuous agitation until $A_{600\text{nm}} = 0.1$ or 0.5.

2.3. Transmission Electron Microscopy

2.3.1. Xen14 Processing for TEM

Xen14 was prepared in five different ways (Table 1) to minimize factors that may affect the quality of TEM images. The Xen14 cells were cultured as described above, and then harvested by centrifugation at $2900 \times g$ for 5 min at 4 °C to avoid cell damage. The cells were initially resuspended in either cacodylate buffer (pH 7.0) or phosphate-buffered saline (PBS; pH 7.0) and centrifuged twice for 5 min at $2900 \times g$. Thereafter, cell pellets were fixed overnight in fixative containing 3.0% formaldehyde, 0.035% glutaraldehyde, 4% sucrose in cacodylate buffer (Procedure 1); fixative containing 4.0% formaldehyde, 1.25% glutaraldehyde, 4% sucrose in PBS buffer (Procedure 2); fixative containing 4.0% formaldehyde, 1.25% glutaraldehyde in cacodylate buffer without sucrose supplementation (Procedure 3); fixative containing 4.0% formaldehyde, 1.25% glutaraldehyde, 4% sucrose and 0.01 M CaCl_2 in cacodylate buffer (Procedures 4 and 5), as detailed in Table 1. The fixed cells were then washed in the corresponding buffer as described above, and post-fixed in 1% osmium tetroxide in cacodylate buffer or PBS containing 0.075% ruthenium red for 1 h, and subsequently washed as described above. Cells were then dehydrated in graded series of ethanol (50%, 70%, 90%, $2 \times$ each for 10 min and 100%, $3 \times$ for 15 min). Thereafter, the cells were infiltrated for 1 h each in propylene oxide: Epon-Araldite resin (50:50 ratio; Procedures 2, 3 and 5) or 100% ethanol: LR-White resin (50:50 ratio; Procedures 1 and 4). Samples were incubated in 100% Epon-Araldite resin (Procedures 2, 3 and 5) or LR-White resin (Procedures 1 and 4) overnight, followed by two resin changes 5 h apart the following day. Subsequently, the cells were polymerized in fresh Epon-Araldite resin or LR-White resin at 70 °C or 58 °C, respectively, for 48 h.

Table 1. Optimization of sample preparation for TEM and cryo-ultramicrotomy.

| Method | Buffer | Fixation | Post-fixation | Resin |
|-----------------------------------|-------------------------|--|--|---------------|
| Procedure 1 (TEM) | Cacodylate + 4% sucrose | 3.0% formaldehyde, 0.035% glutaraldehyde, 4% sucrose and 0.075% ruthenium red, 0.075% L-lysine acetate | 1% osmium tetroxide; 0.075% ruthenium red | LR-White |
| Procedure 2 (TEM) | PBS + 4% sucrose | 4.0% formaldehyde, 1.25% glutaraldehyde, 0.01 M CaCl_2 , 4% sucrose and 0.075% ruthenium red | 1% osmium tetroxide; 0.075% ruthenium red; | Epon-Araldite |
| Procedure 3 (TEM) | Cacodylate | 4.0% formaldehyde, 1.25% glutaraldehyde, 0.01 M CaCl_2 and 0.075% ruthenium red, 0.075% L-lysine acetate | 1% osmium tetroxide; 0.075% ruthenium red | Epon-Araldite |
| Procedure 4 (TEM) | Cacodylate + 4% sucrose | 4.0% formaldehyde, 1.25% glutaraldehyde, 0.01 M CaCl_2 , 4% sucrose and 0.075% ruthenium red, 0.075% L-lysine acetate | 1% osmium tetroxide; 0.075% ruthenium red | LR-White |
| Procedure 5 (TEM) | Cacodylate + 4% sucrose | 4.0% formaldehyde, 1.25% glutaraldehyde, 0.01 M CaCl_2 , 4% sucrose and 0.075% ruthenium red, 0.075% L-lysine acetate | 1% osmium tetroxide; 0.075% ruthenium red | Epon-Araldite |
| Procedure 6 (Cryo-ultramicrotomy) | Cacodylate + 4% sucrose | 4.0% formaldehyde, 1.25% glutaraldehyde, 0.01 M CaCl_2 , 4% sucrose and 0.075% ruthenium red, 0.075% L-lysine acetate | N/A | N/A |

2.3.2. Xen41 Processing for TEM

Xen41 cells were prepared essentially as described for Xen14, then processed for TEM using Procedure 4 (Table 1) with either 1 h fixation or overnight fixation followed by post fixation in 1% osmium tetroxide for 1.5 h on ice.

Sections of Xen14 and Xen41 embedded in resin were cut to 1 μm using a glass knife, stained with 1% toluidine blue containing 1% borax and viewed under a light microscope at 400 \times magnification to identify stained bacteria. Ultrathin sections were then cut to 90 nm with an ultramicrotome EM-UC6 (Leica) using a diamond knife (Diatome) and placed on 200-mesh copper EM grids (Proscitech). Sections were sequentially stained with uranyl acetate (4% in distilled H_2O) and Reynolds lead citrate for 10 min each, with three washes in distilled water in-between each stain. Sections were then viewed on a Tecnai G2 Spirit (FEI Company, Hillsboro, OR, USA) Transmission Electron Microscope operated at 100 kV at Adelaide Microscopy, The University of Adelaide.

2.3.3. Cryo-Ultramicrotomy

Xen14 and Xen41 cells were prepared as described above before being fixed in 1 mL cacodylate buffer containing 4.0% formaldehyde, 1.25% glutaraldehyde, 0.01 M CaCl_2 , 4% sucrose and 0.075% ruthenium red, 0.075% L-lysine acetate (to stabilize the peptidoglycan layer and aid in locating the bacteria during sectioning) [26,27]. Samples were then stored at 4 $^\circ\text{C}$ until processing for cryo-ultramicrotomy. Thereafter, cells were washed twice in buffer and embedded in 12% gelatin. Small gelatin blocks containing bacteria (<1 mm^3) were cut and infiltrated with 2.3 M sucrose in phosphate buffer overnight at 4 $^\circ\text{C}$ with gentle rocking. Blocks were stored in 2.3 M sucrose at 4 $^\circ\text{C}$ prior to sectioning. Blocks were transferred to aluminum sectioning pins (Leica) and quickly plunge-frozen in liquid nitrogen. Thin cryo-sections (80 nm) were cut at -100 $^\circ\text{C}$ with an EM-UC6/FC7 cryo-ultramicrotome (Leica) using a cryo-diamond knife (Diatome). Cryo-sections were removed from the knife with 2.3 M sucrose using a wire loop and transferred to formvar/carbon-coated, plasma-cleaned 200-mesh copper EM grids. Grids were stored in an airtight container on sucrose droplets at 4 $^\circ\text{C}$. To stain, grids were floated face down on 2% gelatin for 30 min at 37 $^\circ\text{C}$ before washing in PBS (3 \times 2 min) and staining with 2% uranyl acetate pH7 (5 min, 22 $^\circ\text{C}$) and methyl cellulose–uranyl acetate (pH 4) on ice (10 min). Grids were looped out, drained and allowed to dry. Samples were imaged with a Tecnai G2 Spirit electron microscope (FEI Company) operated at 100 kV at Adelaide Microscopy, The University of Adelaide.

2.4. Treated Samples Processing for TEM and Cryo-Ultramicrotomy

To determine the optimal conditions to observe NCL195–colistin interaction on Gram-negative membranes, Xen14 cells were initially grown until $A_{600\text{nm}} = 0.1$ (early logarithmic phase) and 0.5 (mid logarithmic phase) and then treated with colistin at 0.5 $\mu\text{g}/\text{mL}$ for 1 h. Subsequently, Xen14 cells grown to $A_{600\text{nm}} = 0.1$ were chosen for further analysis and were incubated with 0.5 $\mu\text{g}/\text{mL}$ colistin for 2 h and 4 h to determine optimal treatment time.

To determine NCL195–colistin interaction on the cell membrane, bacterial samples were treated as follows: For Xen14, (i) no treatment, (ii) NCL195 alone (2 $\mu\text{g}/\text{mL}$); (iii), colistin alone (0.125 $\mu\text{g}/\text{mL}$); (iv), colistin alone (0.25 $\mu\text{g}/\text{mL}$); (v), colistin (0.25 $\mu\text{g}/\text{mL}$) + NCL195 (2 $\mu\text{g}/\text{mL}$) combination. For Xen 41, cells were washed twice in cacodylate buffer and resuspended in LB broth to $A_{600\text{nm}} = 0.1$. Aliquots were then treated as follows: (i) no treatment, (ii) NCL195 alone (2 $\mu\text{g}/\text{mL}$); (iii) colistin alone (1 $\mu\text{g}/\text{mL}$); (iv) colistin (1 $\mu\text{g}/\text{mL}$) + NCL195 (2 $\mu\text{g}/\text{mL}$) combination. Aliquots of Xen14 and Xen41 were then incubated for 1 h at 37 $^\circ\text{C}$ under continuous agitation in a shaker at 150 rpm. During the treatment time, each sample was manually mixed every 10 min to ensure adequate antibiotic contact with the cells. Following treatment, Xen14 cells were washed in buffer and then fixed overnight according to Procedures 4 or 5 (Table 1), whereas treated Xen41 cells were initially fixed for 1 h then washed twice, fixed again for 1.5 h and subjected to processing as described in Procedure 4 (Table 1). For cryo-ultramicrotomy, both Xen14-

and Xen41-treated cells were fixed using Procedure 6 (Table 1) and stored at 4 °C until processing as described above.

3. Results and Discussion

3.1. Bacterial Cell Morphology Is Affected by the Fixative Used, Buffer Conditions and the Embedding Method

In this work, we sought to determine the most effective technique to accurately visualize drug interactions on the bacterial membrane as part of our on-going research aimed at gaining a better understanding of the complex interactions between membrane-active drugs and the consequent morphological changes occurring on the bacterial surface. To accomplish this, we compared two sample preparation methods for TEM (conventional resin embedding and cryo-ultramicrotomy) to visualize the cell membrane of *E. coli* and *P. aeruginosa* after exposure to NCL195 alone, colistin alone or NCL195-colistin combination. For this study, we examined the morphological changes to bacterial cells exposed to the test drugs using bioluminescent derivatives of *E. coli* and *P. aeruginosa* used routinely in our real-time in vivo assessments of drug efficacy. We initially used Xen14 cells to optimize the best TEM protocol for observing NCL195-colistin interaction on Gram-negative membranes. We found that several factors affected the morphology of the bacterial cells.

- i. Fixative: Fixative containing 3.0% formaldehyde, 0.035% glutaraldehyde, 4% sucrose and 0.075% ruthenium red, 0.075% L-lysine acetate (Procedure 1) caused shrinkage of the bacterial cell as well as detachment and perturbation of the cell membrane (Figure 2A,B). Therefore, the low concentration of formaldehyde and glutaraldehyde used in this procedure was not high enough to preserve cell membrane structure and could have affected the cell size. To circumvent this, Li, et al. [28] described a 4.0% formaldehyde solution in fixative as optimal for preservation of bacterial cell size, and our result supports this observation.
- ii. Buffer: We also found that the type of buffer used resulted in altered cell membrane morphology. PBS buffer caused detachment of the cell membrane (Figure 2C,D; Procedure 2), a similar observation as those described by others [14,29]. Furthermore, the addition of sucrose to the buffer improved preservation of cell morphology, as the cell membrane appeared brittle if sucrose was omitted from the fixative (Figure 2E,F; Procedure 3), in agreement with a previous study [30].
- iii. Embedding method: Following from the optimized fixative and buffer conditions above (Procedure 2), we observed that a TEM protocol using cacodylate buffer with fixative containing 4.0% formaldehyde, 1.25% glutaraldehyde, 0.075% ruthenium red, 0.075% L-lysine acetate, and 4% sucrose followed by embedding in LR-White resin (Procedure 4) provided the best delineation of the outer membrane, cell wall and inner membrane, with no wavy, detached or shrunk membranes (Figure 3A). This protocol is similar in some respects to that described by Voget et al. [14], but differs in the buffer and fixative composition, treatment time and embedding method. The use of Epon-Araldite resin (Procedure 5) did not appear to make a difference to the overall TEM result (Figure 3A vs. Figure 3B). However, given our findings, we suggest using LR-White resin due to its ease of use during TEM processing.

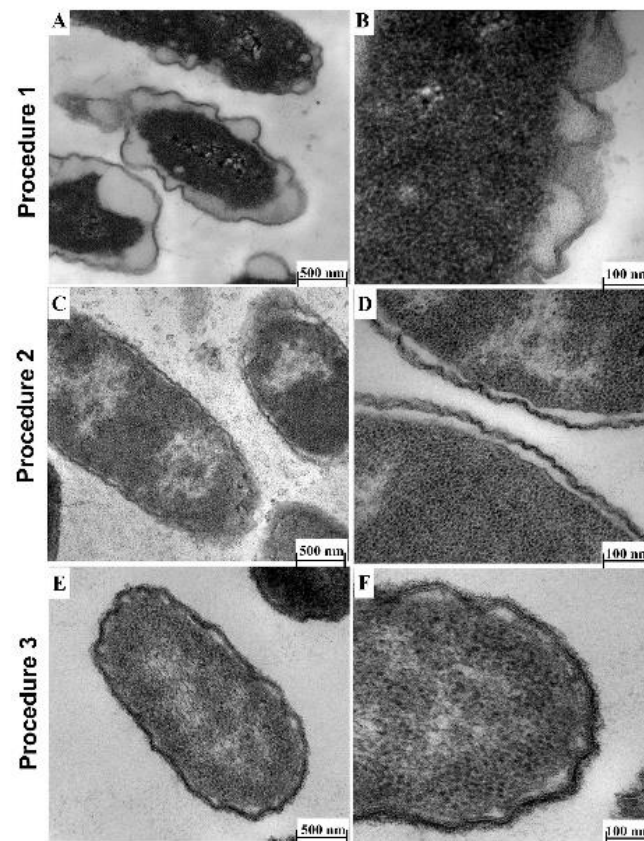


Figure 2. Effect of fixatives and buffer conditions on morphology of Xen14 cells by TEM. (A,B) TEM (Procedure 1) using fixatives containing 3.0% formaldehyde, 0.035% glutaraldehyde and 4% sucrose in LR-White resin; (C,D) TEM (Procedure 2) using PBS buffer containing 4.0% formaldehyde, 1.25% glutaraldehyde, 4% sucrose and embedded in Epon resin; (E,F) TEM (Procedure 3) using cacodylate buffer 4.0% formaldehyde, 1.25% glutaraldehyde and Epon resin embedding without sucrose supplementation.

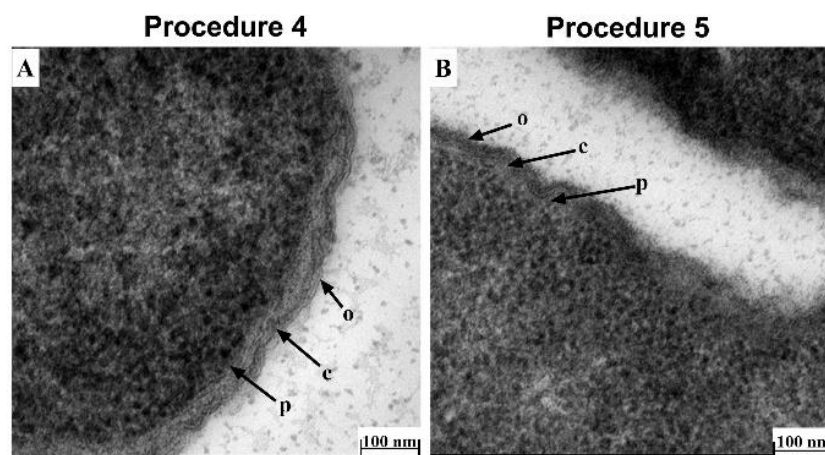


Figure 3. Effect of resin embedding on the morphology of Xen14 cells under optimized TEM conditions. TEM comparison of Xen14 morphology using cacodylate buffer and fixative containing 4.0% formaldehyde, 1.25% glutaraldehyde, 4% sucrose and 0.01 M CaCl_2 and following different embedding techniques: (A) LR-White resin embedding; and (B) Epon resin embedding. Cells clearly showed outer membrane (o), cell wall (c) and plasma membrane (p).

Having optimized the best TEM protocol for visualizing Xen14 morphology (Procedure 4), this was then applied to *P. aeruginosa* Xen41. However, due to the production of exopolysaccharide by *P. aeruginosa* [15], which may prevent access of fixatives to bacterial cell membrane, Xen41 was grown overnight on horse blood agar to reduce the amount of polysaccharide produced. Cells were washed twice in PBS buffer as described before fixation. Overnight fixation resulted in darker images which masked cell membranes/walls (Figure 4A). Therefore, the procedure was modified by first fixing cells for 1 h, followed by washing in PBS buffer and a subsequent fixation step for 1.5 h before continuing the process as described in Procedure 4. Using this method, the inner membrane, cell wall and outer membrane could clearly be observed under TEM (Figure 4B).

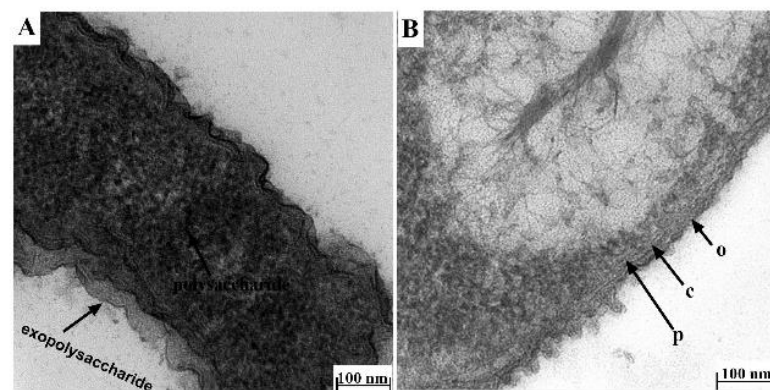


Figure 4. Effect of fixation duration and growth medium on the morphology of Xen41 cells. TEM comparison of Xen41 morphology using cacodylate buffer and fixative containing 4.0% formaldehyde, 1.25% glutaraldehyde, 4% sucrose and 0.01 M CaCl_2 and following different fixation times and growth in different media: (A) Xen41 was cultured overnight in LB broth, washed and fixed overnight and then processed according to Procedure 4; (B) Xen41 was grown overnight on horse blood agar initially, washed and fixed for 1 h, washed, and fixed again for an additional 1.5 h and then processed according to Procedure 4.

3.2. Bacterial Cell Morphology Is Affected by Cell Density and Exposure Time to Drugs

It is known that colistin interacts with the lipopolysaccharide on the surface of Gram-negative bacteria and then across the outer membrane via the self-promoted uptake pathway, resulting in disruption of the normal barrier property of the outer membrane [2,31]. Subsequently, the outer membrane is hypothesized to transiently open thereby allowing passage of NCL195 into the cell to the drug target site(s), likely to be located on the plasma membrane, as we described recently [11]. Based on this hypothesis, we initially determined the optimal time point of colistin treatment that would result in the disruption of the outer membrane using two growth stages of Xen14 ($A_{600\text{nm}} = 0.1$ or $A_{600\text{nm}} = 0.5$). For this initial analysis, the Xen14 cells were treated with colistin at $0.5 \mu\text{g}/\text{mL}$ for 1 h. Significant morphological changes were observed following 1 h incubation in colistin at $A_{600\text{nm}} = 0.1$. Compared to untreated cells (Figure 5A,B), the majority of cells showed a swollen envelope morphology with tubular and fimbria-like radiant appendages; different layers of membrane structure could also be distinguished (Figure 5C,D) under these conditions. However, treatment at $A_{600\text{nm}} = 0.5$ showed less effect (Figure 5E,F). Therefore, $A_{600\text{nm}} = 0.1$ was used for subsequent experiments as it gave better results.

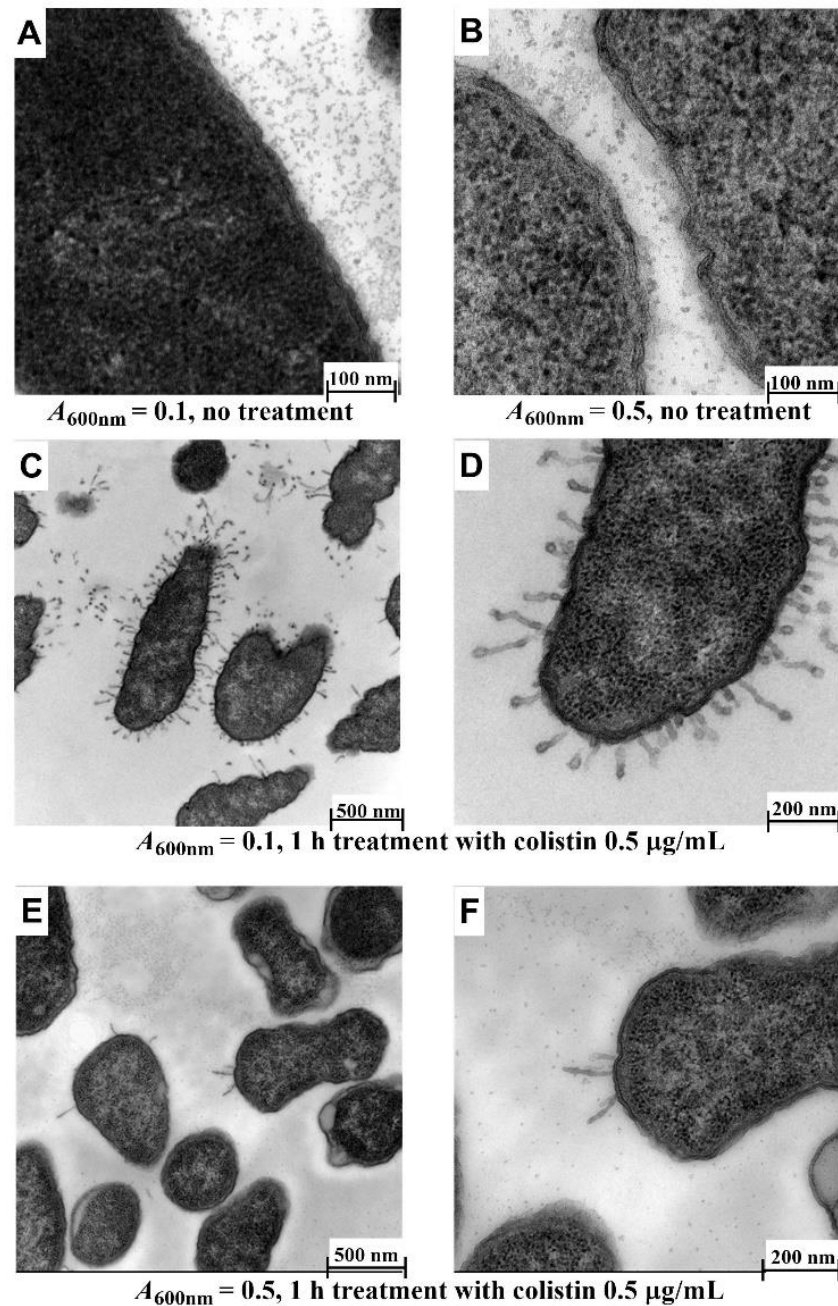


Figure 5. Effect of cell density on morphology of Xen14 cells after treatment with colistin at 0.5 µg/mL for 1 h. (A,B) Untreated cells; (C,D) cells grown to $A_{600\text{nm}} = 0.1$; (E,F) cells grown to $A_{600\text{nm}} = 0.5$. Cacodylate buffer and fixative containing 4.0% formaldehyde, 1.25% glutaraldehyde, 4% sucrose and 0.01 M CaCl_2 was used and embedded in Epon resin.

The effect of 2 h and 4 h colistin treatments on Xen14 cells grown to $A_{600\text{nm}} = 0.1$ was also investigated. Compared to untreated cells (6A,B), the majority of the tubular and fimbria-like radiant appendages were broken and had disappeared, although layered membrane structure could still be observed (Figure 6C,D) after 2 h treatment. Following 4 h treatment, all tubular and fimbria-like radiant appendages had disappeared, membrane layers could not be distinguished, and shrinkage of cell contents and detached/wavy membrane structures were observed (Figure 6E,F). These results are similar to those reported previously for polymyxin B [14], a drug with a similar mechanism of action to colistin [32].

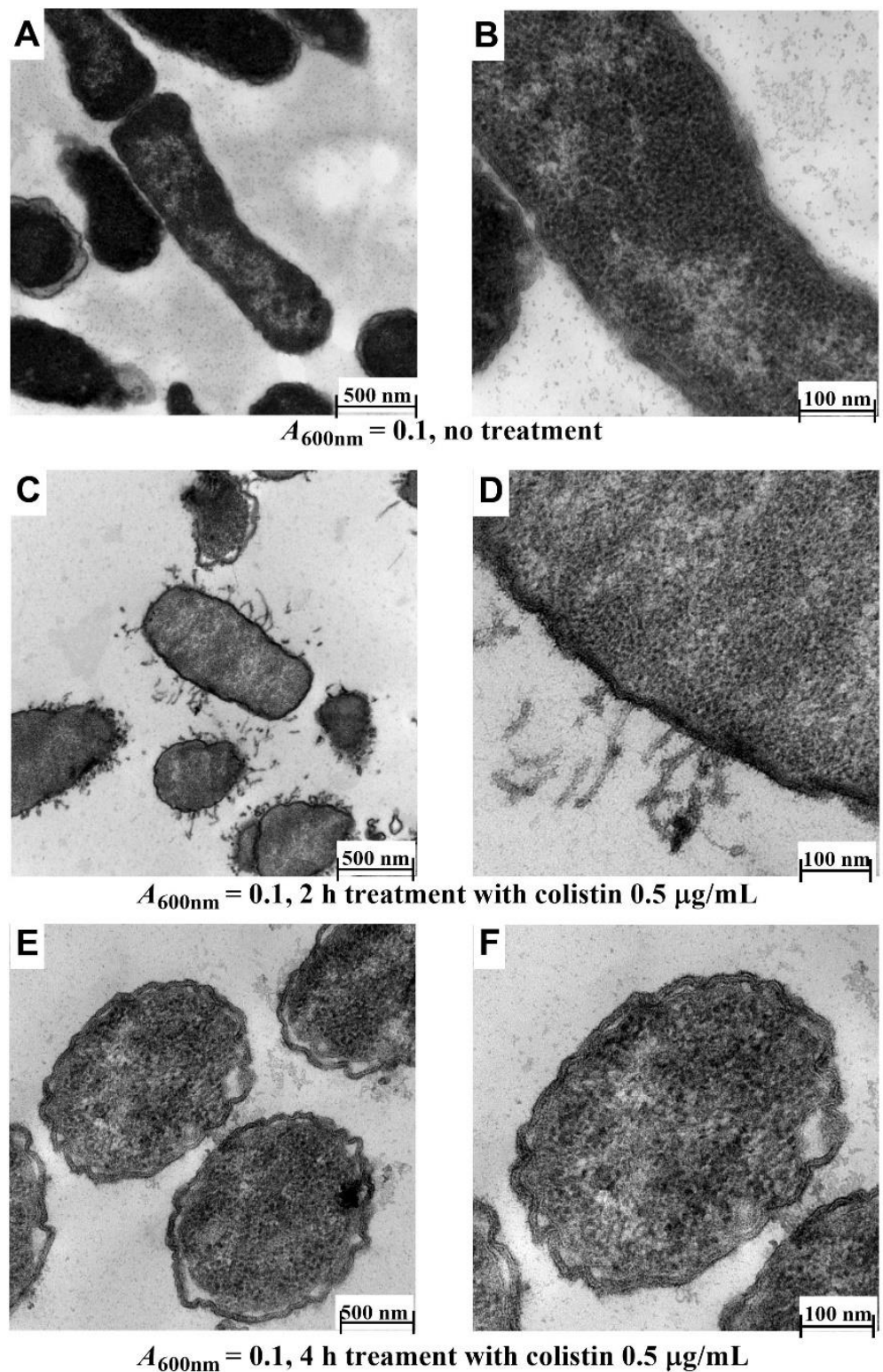


Figure 6. Effect of exposure time on morphology of Xen14. Cells were grown to $A_{600\text{nm}} = 0.1$ and then treated with colistin at 0.5 $\mu\text{g/mL}$. (A,B) untreated cells; (C,D) cells treated for 2 h; (E,F), cells treated for 4 h. Cacodylate buffer and fixative containing 4.0% formaldehyde, 1.25% glutaraldehyde, 4% sucrose and 0.01 M CaCl_2 was used and embedded in Epon resin.

3.3. Comparison of TEM and Cryo-Ultramicrotomy for Visualizing NCL195-Colistin Interaction on Cell Membrane

On the basis of the foregoing outcomes, subsequent experiments to determine the effect of NCL195 + colistin combination were conducted on Xen14 and Xen41 at $A_{600\text{nm}} = 0.1$ followed by a 1 h drug treatment. TEM of Xen14 sections cut under cryo conditions provided a clear delineation of the membrane structure, showing the outer and inner membrane and wall peptidoglycan layer, typical of Gram-negative bacteria compared with a more traditional, resin embedded TEM preparation (Figure 7A vs. Figure 7B). This result was observed in both the untreated and NCL195-treated cells (Figure 7C vs. Figure 7D).

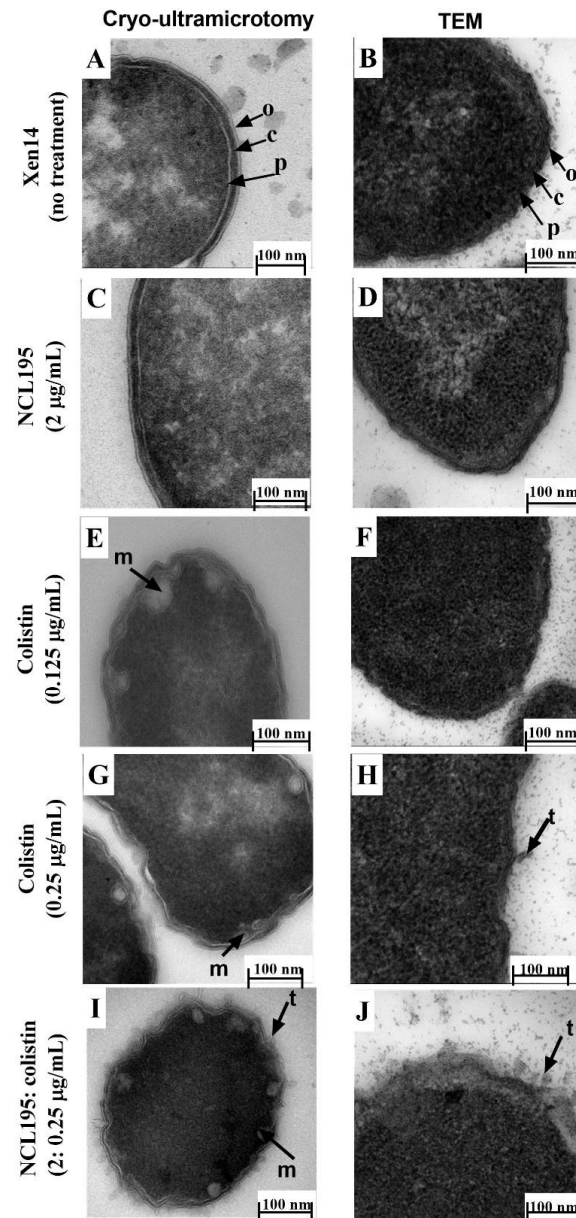


Figure 7. Comparison of Xen14 cells with and without antibiotic treatment and processed by Tokuyasu cryo-ultramicrotomy vs. conventional TEM. Approximately 5×10^8 cells were treated for 1 h; Xen14 cells. Cryo-ultramicrotomy images are indicated on the left, corresponding TEM images on the right. (A) vs. (B) cells without treatment; (C) vs. (D) treatment with NCL195 at $2 \mu\text{g}/\text{mL}$ showing no effect of NCL195 treatment on cell morphology; (E) vs. (F) cells treated with colistin at $0.125 \mu\text{g}/\text{mL}$; (G) vs. (H) cells treated colistin $0.25 \mu\text{g}/\text{mL}$; (I) vs. (J) group exposed to colistin $0.25 \mu\text{g}/\text{mL}$ + NCL195 at $2 \mu\text{g}/\text{mL}$.

For Xen14 cells exposed to colistin at 0.125 µg/mL and sectioned under cryo conditions, mesosome-like structures and swollen membranes were observed, whereas conventional TEM micrographs of cells exposed to colistin at 0.125 µg/mL showed no difference in membrane morphology compared to untreated cells (Figure 7E vs. Figure 7F). With increased colistin concentration (0.25 µg/mL), swollen envelopes and mesosome-like structures (m) were observed following cryo preparation (Figure 7G) in addition to the presence of tubular appendages (t) observed using the traditional TEM technique (Figure 7H). Cells treated with a combination of NCL195 (2 µg/mL) and colistin (0.25 µg/mL) and processed under cryo conditions exhibited increased morphological damage including coronate tubular appendages and mesosome-like structures (Figure 7I). Cells treated with the combination and visualized using conventional TEM also showed increased morphological damage, coronate tubular appendages and a swollen and detached membrane (Figure 7J) similar to that observed with cells treated with 0.25 µg/mL colistin alone. These results are summarized in Table 2.

Table 2. Comparison of cryo-ultramicrotomy preparation and traditional TEM methods for visualizing the effect of drug treatments on Xen14 cell membrane.

| Treatment | Cryo-Ultramicrotomy | Traditional TEM |
|--------------------------------|---|--|
| No treatment | clear delineation of outer and inner membrane, cell wall and peptidoglycan layer | poor delineation of membrane structure |
| NCL195 (2 µg/mL) | same as a control | same as a control |
| Colistin (0.125 µg/mL) | mesosome-like structures; swollen membranes | same as a control |
| Colistin (0.25 µg/mL) | mesosome-like structures; more swollen membranes | presence of tubular appendages |
| NCL195/colistin (2/0.25 µg/mL) | increased morphological damage; coronate tubular appendages; mesosome-like structures | increased morphological damage; coronate tubular appendages; swollen and detached membrane |

The observed morphological effects of NCL195 in the NCL195 + colistin combination are consistent with the dissipation of inner cell membrane potential demonstrated in our recent work [10], potentially resulting in leakage of vital metabolites [25].

As seen with Xen14, untreated Xen41 cells processed under cryo conditions produced a clear image of bacterial morphology with cell walls and inner and outer membranes clearly distinguishable (Figure 8A) compared to traditional TEM processing methods (Figure 8B). Cells treated with NCL195 alone under cryo conditions showed similar ultrastructural morphology as the control cells (Figure 8C), although a slightly wavy membrane morphology was observed when using traditional TEM preparations (Figure 8D).

The addition of colistin (1 µg/mL) produced clearly visualized membrane damage in cells processed under cryo conditions (Figure 8E), whereas a ruffling of the cells and wavy cell membrane structure was observed following traditional TEM embedding (Figure 8F). Increased ultrastructural damage was observed following treatment with the combined colistin and NCL195 treatment (Figure 8G vs. Figure 8H). Again, cells processed under cryo conditions showed clearer increased morphological changes with broken outer membranes and mesosome-like structures within the cell (Figure 8G vs. Figure 8H). These results are summarized in Table 3.

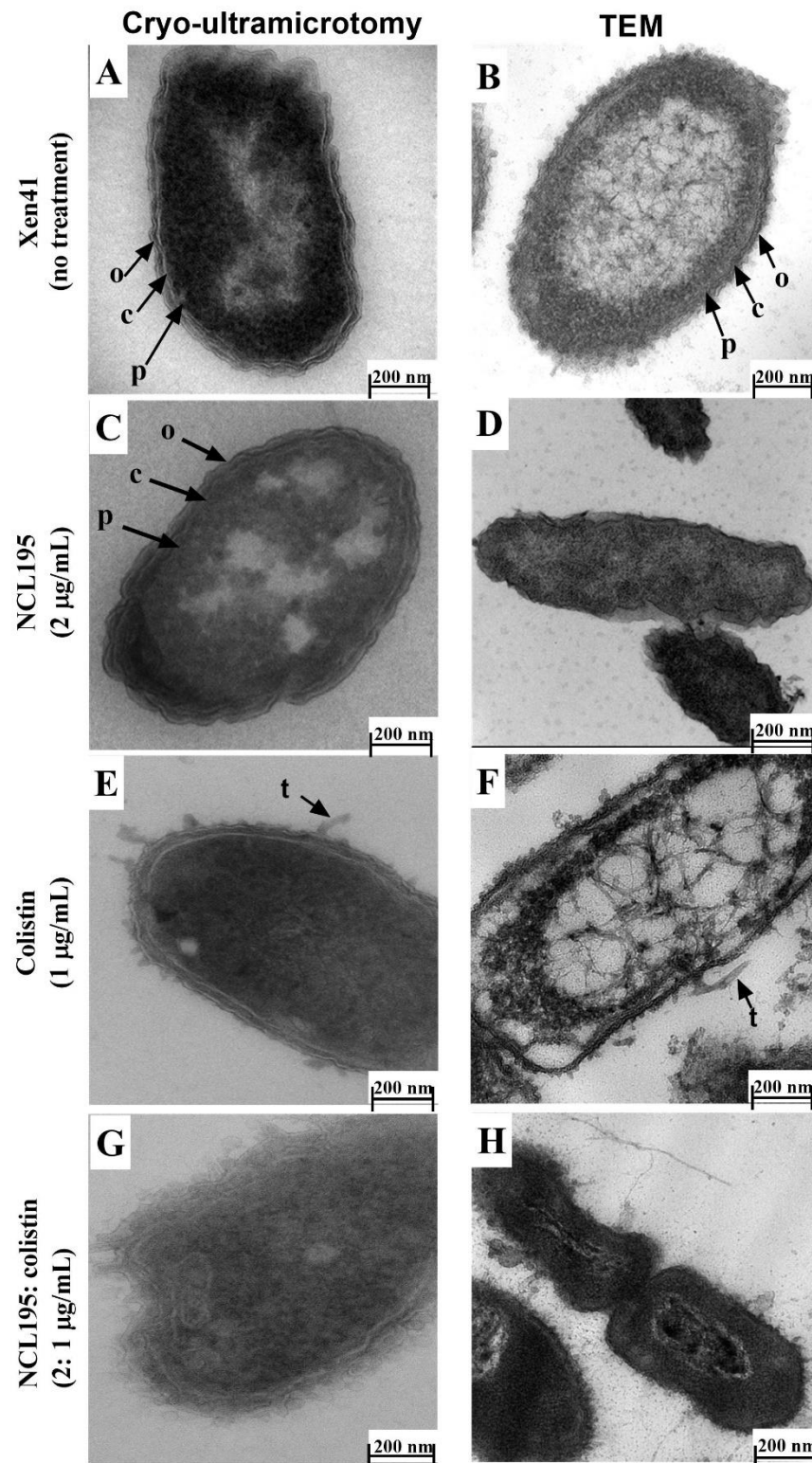


Figure 8. Comparison of Xen41 cells with or without antibiotic treatment and processed by Tokuyasu cryo-ultramicrotomy vs. conventional TEM. Approximately 5×10^8 cells were treated for 1 h. (A) vs. (B) cells without treatment; (C) vs. (D) treatment with NCL195 at $2 \mu\text{g}/\text{mL}$ showing clearer delineation of intact outer membrane, cell wall and plasma membrane than TEM images and no effect of NCL195 treatment on cell morphology; (E) vs. (F), Xen41 cells treated with colistin at $1 \mu\text{g}/\text{mL}$ and (G) vs. (H) Xen41 cells exposed to a combination of NCL195 at $2 \mu\text{g}/\text{mL}$ and colistin at $1 \mu\text{g}/\text{mL}$.

Table 3. Comparison of TEM using cryo-ultramicrotomy and traditional preparation methods to visualize the effect of drug treatments on Xen41 cell membrane.

| Treatment | Cryo-Ultramicrotomy | Traditional TEM |
|-----------------------------|--|---|
| No treatment | clear delineation of outer and inner membrane, cell wall and peptidoglycan layer | poor delineation of membrane structure |
| NCL195 (2 µg/mL) | same as control | slightly wavy membrane morphology |
| Colistin (1 µg/mL) | clearly visualized membrane damage; presence of tubular appendages | ruffling of the cells; wavy cell membrane structure; presence of tubular appendages |
| NCL195/colistin (2/1 µg/mL) | clearer increased morphological changes; broken outer and inner membrane; mesosome-like structures | increased ultrastructural damage; damaged outer and inner membrane |

4. Conclusions

In this study, we describe optimized TEM conditions for visualizing changes to Gram-negative bacterial morphology induced by treatment with a combination of NCL195, a novel pyrimidine, and colistin. We show that cacodylate buffer works better than PBS buffer, and that fixative containing 4.0% formaldehyde, 1.25% glutaraldehyde, CaCl₂ 0.01 M, 4% sucrose and 0.075% ruthenium red, 0.075% L-lysine acetate is the optimal mixture for the stability of bacterial cell membrane. We also suggest using LR-White resin due to its ease of use during TEM processing. Additionally, we show the cryo-ultramicrotomy technique provides higher resolution, artifact reduction, clearer visualization of bacterial cytoskeleton and better preservation of bacterial structural integrity compared to conventional TEM processing methods. To our knowledge, this study is the first to use Tokuyasu cryo-ultramicrotomy to examine the effects of multiple drug-interactions on the bacterial cell surface. Cryo-ultramicrotomy can also be employed in conjunction with other imaging techniques such as that described for correlative light and electron microscopy [33]. We suggest cryo-ultramicrotomy can be used for a wide range of applications including host-pathogen interaction studies and high-resolution visualization of macromolecular interactions occurring on the prokaryotic surface or other biological membranes. These should promote a better understanding of complex cellular and molecular interactions.

Author Contributions: Conceptualization, H.T.N., L.A.O., H.V., S.W.P., D.J.T. and A.D.O.; methodology, H.T.N., L.A.O., C.C.R., and A.D.O.; validation, H.T.N., L.A.O., C.C.R., A.M., D.J.T. and A.D.O.; formal analysis, H.T.N., L.A.O., H.V., C.C.R., A.M., D.J.T. and A.D.O.; investigation, H.T.N., L.A.O., D.J.T. and A.D.O.; resources, H.V., A.M., S.W.P. and D.J.T.; data curation, H.T.N., L.A.O. and A.D.O.; writing—original draft preparation, H.T.N., L.A.O. and A.D.O.; writing—review and editing, H.T.N., L.A.O., H.V., C.C.R., A.M., S.W.P., D.J.T. and A.D.O.; visualization, H.T.N. and L.A.O.; supervision, L.A.O., H.V., A.M., D.J.T. and A.D.O.; funding acquisition, H.V., A.M., S.W.P. and D.J.T. All authors have read and agreed to the published version of the manuscript.

Funding: This work was supported by an Australian Research Council (ARC; www.arc.gov.au, accessed on 17 March 2021) Linkage grant (LP110200770) to D.J.T., A.M. and S.W.P. with Neoculi Pty Ltd. as the Partner Organization and University of South Australia fund to H.V. The funders did not have any additional role in the study design, data collection and analysis, decision to publish, or preparation of the manuscript.

Institutional Review Board Statement: Not applicable.

Informed Consent Statement: Not applicable.

Data Availability Statement: The data presented in this study are available on request from the corresponding author. The data are not publicly available due to size and access restrictions.

Acknowledgments: The authors would like to thank Amanda Ruggero, Lora Bowes, Anh Hong Nguyen and Max McClafferty at the University of South Australia, South Australia 5000, Australia for their technical assistance; Gwen Mayo and Ruth Williams at Adelaide Microscopy, The University of Adelaide, Adelaide, South Australia 5005, Australia for cryo-ultramicrotomy assistance and TEM recommendations.

Conflicts of Interest: S.W.P. is a director of Neoculi Pty. Ltd. D.J.T. and A.M. have received research funding from Neoculi Pty. Ltd.

References

- Zabawa, T.P.; Pucci, M.J.; Parr, T.R., Jr.; Lister, T. Treatment of Gram-negative bacterial infections by potentiation of antibiotics. *Curr. Opin. Microbiol.* **2016**, *33*, 7–12. [[CrossRef](#)]
- Zgurskaya, H.I.; Lopez, C.A.; Gnanakaran, S. Permeability barrier of Gram-negative cell envelopes and approaches to bypass it. *ACS Infect. Dis.* **2015**, *1*, 512–522. [[CrossRef](#)] [[PubMed](#)]
- Lenhard, J.R.; Nation, R.L.; Tsuji, B.T. Synergistic combinations of polymyxins. *Int. J. Antimicrob. Agents* **2016**, *48*, 607–613. [[CrossRef](#)] [[PubMed](#)]
- Khazandi, M.; Pi, H.; Chan, W.Y.; Ogunniyi, A.D.; Sim, J.X.F.; Venter, H.; Garg, S.; Page, S.W.; Hill, P.B.; McCluskey, A. In vitro antimicrobial activity of robenidone, ethylenediaminetetraacetic acid and polymyxin B nonapeptide against important human and veterinary pathogens. *Front. Microbiol.* **2019**, *10*, 837. [[CrossRef](#)] [[PubMed](#)]
- Brennan-Krohn, T.; Pironti, A.; Kirby, J.E. Synergistic activity of colistin-containing combinations against colistin-resistant Enterobacteriaceae. *Antimicrob. Agents Chemother.* **2018**, *62*, e00873-18. [[CrossRef](#)]
- Elemam, A.; Rahimian, J.; Doymaz, M. In vitro evaluation of antibiotic synergy for polymyxin B-resistant carbapenemase-producing *Klebsiella pneumoniae*. *J. Clin. Microbiol.* **2010**, *48*, 3558–3562. [[CrossRef](#)] [[PubMed](#)]
- Garonzik, S.; Li, J.; Thamlikitkul, V.; Paterson, D.; Shoham, S.; Jacob, J.; Silveira, F.; Forrest, A.; Nation, R.L. Population pharmacokinetics of colistin methanesulfonate and formed colistin in critically ill patients from a multicenter study provide dosing suggestions for various categories of patients. *Antimicrob. Agents Chemother.* **2011**, *55*, 3284–3294. [[CrossRef](#)] [[PubMed](#)]
- Nigam, A.; Kumari, A.; Jain, R.; Batra, S. Colistin neurotoxicity: Revisited. *BMJ Case Rep.* **2015**, *2015*, bcr2015210787. [[CrossRef](#)] [[PubMed](#)]
- Otto, R.G.; van Gorp, E.; Kloezen, W.; Meletiadiis, J.; van den Berg, S.; Mouton, J.W. An alternative strategy for combination therapy: Interactions between polymyxin B and non-antibiotics. *Int. J. Antimicrob. Agents* **2019**, *53*, 34–39. [[CrossRef](#)] [[PubMed](#)]
- Nguyen, H.T.; Venter, H.; Veltman, T.; Williams, R.; O'Donovan, L.A.; Russell, C.C.; McCluskey, A.; Page, S.W.; Ogunniyi, A.D.; Trott, D.J. In vitro synergistic activity of NCL195 in combination with colistin against Gram-negative bacterial pathogens. *Int. J. Antimicrob. Agents* **2021**. under review.
- Pi, H.; Nguyen, H.T.; Venter, H.; Boileau, A.R.; Woolford, L.; Garg, S.; Page, S.W.; Russell, C.C.; Baker, J.R.; McCluskey, A.; et al. In vitro activity of robenidone analog NCL195 in combination with outer membrane permeabilizers against Gram-negative bacterial pathogens and impact on systemic Gram-positive bacterial infection in mice. *Front. Microbiol.* **2020**, *11*, 1556. [[CrossRef](#)] [[PubMed](#)]
- Song, M.; Liu, Y.; Huang, X.; Ding, S.; Wang, Y.; Shen, J.; Zhu, K. A broad-spectrum antibiotic adjuvant reverses multidrug-resistant Gram-negative pathogens. *Nat. Microbiol.* **2020**, *5*, 1040–1050. [[CrossRef](#)]
- Ontong, J.C.; Ozioma, N.F.; Voravuthikunchai, S.P.; Chusri, S. Synergistic antibacterial effects of colistin in combination with aminoglycoside, carbapenems, cephalosporins, fluoroquinolones, tetracyclines, fosfomycin, and piperacillin on multidrug resistant *Klebsiella pneumoniae* isolates. *PLoS ONE* **2021**, *16*, e0244673. [[CrossRef](#)] [[PubMed](#)]
- Voget, M.; Lorenz, D.; Lieber-Tenorio, E.; Hauck, R.; Meyer, M.; Cieslicki, M. Is transmission electron microscopy (TEM) a promising approach for qualitative and quantitative investigations of polymyxin B and miconazole interactions with cellular and subcellular structures of *Staphylococcus pseudintermedius*, *Escherichia coli*, *Pseudomonas aeruginosa* and *Malassezia pachydermatis*? *Vet. Microbiol.* **2015**, *181*, 261–270. [[CrossRef](#)] [[PubMed](#)]
- Stukalov, O.; Korenevsky, A.; Beveridge, T.J.; Dutcher, J.R. Use of atomic force microscopy and transmission electron microscopy for correlative studies of bacterial capsules. *Appl. Environ. Microbiol.* **2008**, *74*, 5457–5465. [[CrossRef](#)]
- Liao, S.; Zhang, Y.; Pan, X.; Zhu, F.; Jiang, C.; Liu, Q.; Cheng, Z.; Dai, G.; Wu, G.; Wang, L.; et al. Antibacterial activity and mechanism of silver nanoparticles against multidrug-resistant *Pseudomonas aeruginosa*. *Int. J. Nanomed.* **2019**, *14*, 1469–1487. [[CrossRef](#)] [[PubMed](#)]
- Abdel-Shafi, S.; Al-Mohammadi, A.R.; Sitohy, M.; Mosa, B.; Ismaiel, A.; Enan, G.; Osman, A. Antimicrobial activity and chemical constitution of the crude, phenolic-rich extracts of *Hibiscus sabdariffa*, *Brassica oleracea* and *Beta vulgaris*. *Molecules* **2019**, *24*, 4280. [[CrossRef](#)] [[PubMed](#)]
- Rapisarda, C.; Tassinari, M.; Gubellini, F.; Fronzes, R. Using Cryo-EM to investigate bacterial secretion systems. *Annu. Rev. Microbiol.* **2018**, *72*, 231–254. [[CrossRef](#)] [[PubMed](#)]
- Egelman, E.H. The Current Revolution in Cryo-EM. *Biophys. J.* **2016**, *110*, 1008–1012. [[CrossRef](#)] [[PubMed](#)]
- Pilhofer, M.; Ladinsky, M.S.; McDowell, A.W.; Jensen, G.J. Bacterial TEM: New insights from cryo-microscopy. *Methods Cell Biol.* **2010**, *96*, 21–45. [[CrossRef](#)]

21. Yan, R.; Venkatakrishnan, S.V.; Liu, J.; Bouman, C.A.; Jiang, W. MBIR: A cryo-ET 3D reconstruction method that effectively minimizes missing wedge artifacts and restores missing information. *J. Struct. Biol.* **2019**, *206*, 183–192. [[CrossRef](#)]
22. Griffiths, G.; Slot, J.W.; Webster, P. Kiyoteru Tokuyasu: A pioneer of cryo-ultramicrotomy. *Microscopy* **2015**, *64*, 377–379. [[CrossRef](#)]
23. Thompson, R.F.; Walker, M.; Siebert, C.A.; Muench, S.P.; Ranson, N.A. An introduction to sample preparation and imaging by cryo-electron microscopy for structural biology. *Methods* **2016**, *100*, 3–15. [[CrossRef](#)] [[PubMed](#)]
24. Abraham, R.J.; Stevens, A.J.; Young, K.A.; Russell, C.; Qvist, A.; Khazandi, M.; Wong, H.S.; Abraham, S.; Ogunniyi, A.D.; Page, S.W.; et al. Robenidine analogues as Gram-positive antibacterial agents. *J. Med. Chem.* **2016**, *59*, 2126–2138. [[CrossRef](#)]
25. Ogunniyi, A.D.; Khazandi, M.; Stevens, A.J.; Sims, S.K.; Page, S.W.; Garg, S.; Venter, H.; Powell, A.; White, K.; Petrovski, K.R. Evaluation of robenidine analog NCL195 as a novel broad-spectrum antibacterial agent. *PLoS ONE* **2017**, *12*, e0183457. [[CrossRef](#)] [[PubMed](#)]
26. Hammerschmidt, S.; Wolff, S.; Hocke, A.; Rosseau, S.; Müller, E.; Rohde, M. Illustration of pneumococcal polysaccharide capsule during adherence and invasion of epithelial cells. *Infect. Immun.* **2005**, *73*, 4653–4667. [[CrossRef](#)] [[PubMed](#)]
27. Birkhead, M.; Ganesh, K.; Ndlangisa, K.M.; Koornhof, H.J. Transmission electron microscopy protocols for capsule visualisation in pathogenic respiratory and meningeal bacteria. In *Microscopy and Imaging Science: Practical Approaches to Applied Research and Education*; Researchgate: Berlin, Germany, 2017; pp. 628–639.
28. Li, Y.; Almassalha, L.M.; Chandler, J.E.; Zhou, X.; Stypula-Cyrus, Y.E.; Hujsak, K.A.; Roth, E.W.; Bleher, R.; Subramanian, H.; Szleifer, I. The effects of chemical fixation on the cellular nanostructure. *Exp. Cell Res.* **2017**, *358*, 253–259. [[CrossRef](#)] [[PubMed](#)]
29. He, M.; Wu, T.; Pan, S.; Xu, X. Antimicrobial mechanism of flavonoids against *Escherichia coli* ATCC 25922 by model membrane study. *Appl. Surf. Sci.* **2014**, *305*, 515–521. [[CrossRef](#)]
30. Leslie, S.B.; Israeli, E.; Lighthart, B.; Crowe, J.H.; Crowe, L.M. Trehalose and sucrose protect both membranes and proteins in intact bacteria during drying. *Appl. Environ. Microbiol.* **1995**, *61*, 3592–3597. [[CrossRef](#)] [[PubMed](#)]
31. Bergen, P.J.; Smith, N.M.; Bedard, T.B.; Bulman, Z.P.; Cha, R.; Tsuji, B.T. Rational Combinations of Polymyxins with Other Antibiotics. In *Polymyxin Antibiotics: From Laboratory Bench to Bedside*; Springer: Berlin, Germany, 2019; pp. 251–288.
32. Kwa, A.; Kasiakou, S.K.; Tam, V.H.; Falagas, M.E. Polymyxin B: Similarities to and differences from colistin (polymyxin E). *Expert Rev. Anti-Infect. Ther.* **2007**, *5*, 811–821. [[CrossRef](#)] [[PubMed](#)]
33. Möbius, W.; Posthuma, G. Sugar and ice: Immunoelectron microscopy using cryosections according to the Tokuyasu method. *Tissue Cell* **2019**, *57*, 90–102. [[CrossRef](#)] [[PubMed](#)]

Chapter V

Oral administration of a 2-aminopyrimidine robenidine analogue (NCL195) significantly reduces *Staphylococcus aureus* and *Escherichia coli* infections in the presence of sub-inhibitory colistin concentrations in a bioluminescent mouse model

Statement of Authorship

| | |
|---------------------|---|
| Title of Paper | Oral administration of a 2-aminopyrimidine robenidine analogue (NCL195) significantly reduces <i>Staphylococcus aureus</i> and <i>Escherichia coli</i> infections in the presence of sub-inhibitory colistin concentrations in a bioluminescent mouse model |
| Publication Status | <input type="checkbox"/> Published <input type="checkbox"/> Accepted for Publication <input type="checkbox"/> Submitted for Publication <input checked="" type="checkbox"/> Unpublished and Unsubmitted work written in manuscript style |
| Publication Details | <p>Hang Thi Nguyen, Henrietta Venter, Lucy Woolford, Kelly A. Young, Adam McCluskey, Sanjay Garg, Sylvia Sapula, Stephen W. Page, Abiodun David Ogunniyi and Darren J. Trott. Oral administration of a 2-aminopyrimidine robenidine analogue (NCL195) significantly reduces <i>Staphylococcus aureus</i> and <i>Escherichia coli</i> infections in the presence of sub-inhibitory colistin concentrations in a bioluminescent mouse model.</p> <p>The manuscript is being prepared to submit to the Journal of Antimicrobial Chemotherapy</p> |

Principal Author

| | | | |
|--------------------------------------|--|------|------------|
| Name of Principal Author (Candidate) | Hang Thi Nguyen | | |
| Contribution to the Paper | Contributed to the study design, performed experiments, wrote the preliminary manuscript and revised the edited manuscript | | |
| Overall percentage (%) | 70% | | |
| Certification: | This paper reports on original research I conducted during the period of my Higher Degree by Research candidature and is not subject to any obligations or contractual agreements with a third party that would constrain its inclusion in this thesis. I am the primary author of this paper. | | |
| Signature | | Date | 01/12/2021 |

Co-Author Contributions

By signing the Statement of Authorship, each author certifies that:

- i. the candidate's stated contribution to the publication is accurate (as detailed above);
- ii. permission is granted for the candidate to include the publication in the thesis; and
- iii. the sum of all co-author contributions is equal to 100% less the candidate's stated contribution.

| | | | |
|---------------------------|---|------|------------|
| Name of Co-Author | Henrietta Venter | | |
| Contribution to the Paper | Contributed to study design, editing and discussion | | |
| Signature | | Date | 15/12/2021 |

| | | | |
|---------------------------|--|------|----------|
| Name of Co-Author | Lucy Woolford | | |
| Contribution to the Paper | Contributed to histopathology examinations, editing and discussion | | |
| Signature | | Date | 05/01/22 |

| | | | |
|---------------------------|--|------|------------|
| Name of Co-Author | Sylvia Sapula | | |
| Contribution to the Paper | Contributed to whole-genome sequencing, editing and discussion | | |
| Signature | | Date | 19/01/2022 |

| | | | |
|---------------------------|---|------|------------|
| Name of Co-Author | Kelly Young | | |
| Contribution to the Paper | Responsible for synthesizing NCL195 and edited the manuscript | | |
| Signature | | Date | 18/01/2022 |

| | | | |
|---------------------------|---|------|------------|
| Name of Co-Author | Adam McCluskey | | |
| Contribution to the Paper | Responsible for synthesizing NCL195 and edited the manuscript | | |
| Signature | | Date | 06/02/2022 |

| | | | |
|---------------------------|-----------------------------|------|------------|
| Name of Co-Author | Sanjay Garg | | |
| Contribution to the Paper | Contributed to formulations | | |
| Signature | | Date | 06/01/2022 |

| | | | |
|---------------------------|---|------|------------|
| Name of Co-Author | Stephen W. Page | | |
| Contribution to the Paper | Contributed to editing, discussion and provided financial support for the study | | |
| Signature | | Date | 02/02/2022 |

| | | | |
|---------------------------|---|------|------------|
| Name of Co-Author | Abiodun D. Ogunniyi | | |
| Contribution to the Paper | Contributed to study design, experiments, technical guidance, supervision, editing, discussion and is co-corresponding author | | |
| Signature | | Date | 08/12/2021 |

| | | | |
|-------------------|-----------------|--|--|
| Name of Co-Author | Darren J. Trott | | |
|-------------------|-----------------|--|--|

| | | | |
|---------------------------|--|------|------------|
| Contribution to the Paper | Contributed to study design, supervision, editing, discussion, and provided financial support for the study and is co-corresponding author | | |
| Signature | | Date | 07/02/2022 |

Please cut and paste additional co-author panels here as required.

1 **Oral administration of a 2-aminopyrimidine robenidine analogue**
2 **(NCL195) significantly reduces *Staphylococcus aureus* and *Escherichia coli***
3 **infections in the presence of sub-inhibitory colistin concentrations in a**
4 **bioluminescent mouse model**

5 **Hang Thi Nguyen^{1,2}, Henrietta Venter³, Lucy Woolford⁴, Kelly A. Young⁵, Adam**
6 **McCluskey⁵, Sanjay Garg⁶, Sylvia S. Sapula³, Stephen W. Page⁷, Abiodun David**
7 **Ogunniyi^{1†} and Darren J. Trott^{1*†}**

8 ¹*Australian Centre for Antimicrobial Resistance Ecology, School of Animal and Veterinary*
9 *Sciences, The University of Adelaide, Roseworthy, SA, Australia;* ²*Department of*
10 *Pharmacology, Toxicology, Internal Medicine and Diagnostics, Faculty of Veterinary*
11 *Medicine, Vietnam National University of Agriculture, Hanoi, Vietnam;* ³*Health and*
12 *Biomedical Innovation, Clinical and Health Sciences, University of South Australia,*
13 *Adelaide, SA, Australia;* ⁴*School of Animal and Veterinary Sciences, The University of*
14 *Adelaide, Roseworthy Campus, SA 5371 Roseworthy, Australia;* ⁵*Chemistry, School of*
15 *Environmental & Life Sciences, University of Newcastle, Callaghan NSW, Australia;*
16 ⁶*Clinical and Health Sciences, University of South Australia, Adelaide, SA, Australia;*
17 ⁷*Neoculi Pty Ltd., Burwood, VIC, Australia*

18 *Corresponding author: Australian Centre for Antimicrobial Resistance Ecology, School of
19 Animal and Veterinary Sciences, The University of Adelaide, Roseworthy, SA, Australia.

20 Tel: +61 8 8313 7989. Fax: +61 8 8313 7956; E-mail: darren.trott@adelaide.edu.au.

21 †These authors contributed equally.

22 Running title: Broad-spectrum antibacterial activity of NCL195 and colistin combination

23

24 **Synopsis**

25 **Objectives:** We have previously reported promising *in vivo* activity of the first-generation 2-
26 aminopyrimidine robenidine analogue NCL195 against Gram-positive bacteria (GPB) when
27 administered via the systemic route. In this study, we examined the efficacy of oral treatment
28 with NCL195 (-/+ low dose colistin) in comparison to oral moxifloxacin in bioluminescent
29 *Staphylococcus aureus* and *Escherichia coli* peritonitis-sepsis models.

30 **Methods:** Four oral doses of 50 mg/kg NCL195, commencing immediately post-infection,
31 were administered at 4 h intervals in the *S. aureus* peritonitis-sepsis model. We used a
32 combination of four oral doses of 50 mg/kg NCL195 and four intraperitoneal doses of colistin
33 at 0.125 mg/kg, 0.25 mg/kg or 0.5 mg/kg in the *E. coli* peritonitis-sepsis model. Subsequently,
34 the dose rates of four intraperitoneal doses of colistin were increased to 0.5 mg/kg, 1 mg/kg, or
35 2 mg/kg at 4 h intervals to treat a colistin-resistant *E. coli* infection.

36 **Results:** In the *S. aureus* infection model, oral treatment of mice with NCL195 resulted in
37 significantly reduced *S. aureus* infection loads ($p<0.01$) and longer survival times ($p<0.001$)
38 than vehicle-only treated mice. In the *E. coli* infection model, co-administration of NCL195
39 and graded doses of colistin resulted in a dose-dependent significant reduction in colistin-
40 susceptible ($p<0.01$) or colistin-resistant ($p<0.05$) *E. coli* loads compared to treatment with
41 colistin alone at similar concentrations.

42 **Conclusions:** Our results confirm that NCL195 is a potential candidate for further preclinical
43 development as a specific treatment for multidrug-resistant infections either as a stand-alone
44 antibiotic for GPB or in combination with sub-inhibitory concentrations of colistin for GNB.

45

46 **Introduction**

47 Multidrug-resistant (MDR) infections constitute a serious public health problem worldwide ¹⁻
48 ³. It is estimated that deaths caused by MDR bacteria will reach 10 million per year by 2050
49 unless urgent action is taken ^{4, 5}. The situation with MDR-Gram-negative bacterial (GNB)
50 infections is more problematic given the limited range of drug classes and ever-increasing
51 resistance. Moreover, the outer membrane of GNB, a largely asymmetric bilayer composed of
52 glycolipid lipopolysaccharides and glycerol phospholipids, serves as a barrier to protect GNB
53 from unwanted compounds and promotes antimicrobial resistance ⁶. Therefore, comparatively
54 fewer antimicrobial classes (aminoglycosides, polymyxins, tetracyclines, β -lactams and
55 fluoroquinolones) are able to penetrate the outer membrane of GNB, limiting treatment options
56 ⁷. Additionally, GNB pathogens have quickly acquired resistance to most, and in some cases,
57 to all these antibiotics via multiple mechanisms ^{2, 8}.

58 Due to the distinctive structure of GNB, no novel antibiotics with a new chemical
59 structure or a new mode of action against GNB infections has been developed and marketed
60 for several decades ⁹. To date, there are 19 potential antibiotics in clinical development for the
61 treatment of GNB pathogens but none of them has a new mode of action ¹⁰. Among currently
62 used antibiotics, polymyxins (such as polymyxin B [PMB] and colistin [polymyxin E]) are
63 highly efficacious against GNB and are considered the last line antimicrobials for the treatment
64 of GNB infections due to their specific targeting of the outer membrane ^{11, 12}; nonetheless,
65 resistance to polymyxins is emerging via different mechanisms ^{11, 13}. In addition, the use of
66 high doses of polymyxins is associated with nephrotoxicity, neurotoxicity and neuromuscular
67 blockade ^{14, 15}. To address the shortfall in effective antibiotics, to overcome the emerging
68 resistance and outer membrane protection, and to reduce toxicity of polymyxins, an antibiotic
69 combination approach provides an alternative and complementary strategy to effectively and
70 more safely control serious infections caused by MDR-GNB ¹⁶⁻¹⁸. While several studies have

71 indicated that combinations of polymyxins with other antibiotics elicit full or partially
72 synergistic activities against MDR-GNB pathogens¹⁹⁻²⁴, we report here a novel combination
73 approach.

74 In line with a combination strategy, we previously reported *in vitro* synergistic activity
75 of the anticoccidial aminoguanidine robenidine (NCL812)²⁵ analogue NCL195 with different
76 adjuvants against clinical MDR-GNB pathogens²⁶⁻²⁸. NCL195 showed 100% synergistic
77 activity when combined with sub-inhibitory concentrations of colistin and PMB against clinical
78 MDR-GNB pathogens (including colistin-resistant isolates), with MICs for NCL195 ranging
79 from 0.5–4 mg/L for *Acinetobacter baumannii*, *Escherichia coli*, *Klebsiella pneumoniae* and
80 *Pseudomonas aeruginosa*, whereas NCL195 alone had no activity^{27,28}. This strongly suggests
81 that NCL195 is a promising candidate as a component of a combination with colistin for the
82 treatment of GNB infections.

83 Our earlier investigations have shown better toxicity profiles to mammalian cell lines
84 and erythrocytes for NCL195 than NCL812 and it did not elicit observable histological effects
85 in major organs of mice^{28,29}. Furthermore, mice that received two intraperitoneal doses of 50
86 mg/kg NCL195 exhibited significantly reduced *S. aureus* loads compared to untreated mice,
87 but still succumbed to infection²⁸. Interestingly, we recently showed that mice treated with
88 four 50 mg/kg oral doses of a closely-related robenidine analogue (NCL179) had significant
89 increase in overall survival rate after *S. aureus* challenge compared to the vehicle-only control
90³⁰. This provided the opportunity to investigate the efficacy of oral NCL195 and intraperitoneal
91 colistin combination as a proof of concept of *in vivo* antimicrobial activity against GNB in a
92 bioluminescent mouse peritonitis-sepsis model.

93

94 **Materials and methods**

95 *Antibiotics and chemicals*

96 NCL195, an analogue of robenidine NCL812^{26, 29} was synthesised at the University of
97 Newcastle, NSW, Australia. Colistin sulfate, daptomycin and kanamycin were purchased from
98 Sigma-Aldrich (Australia). Stock solutions containing 25.6 g/L of each compound (NCL195
99 and daptomycin dissolved in DMSO; colistin and kanamycin dissolved in water) were stored
100 in 1 mL aliquots at -20 °C away from direct light. Moxifloxacin was used as a control drug in
101 the GPB mouse model and was prepared in almond oil (BovaVet, Australia).

102

103 *Organisms and growth conditions*

104 A bioluminescent derivative of *Staphylococcus aureus* ATCC 12600 (*SaXen29*) and
105 bioluminescent *E. coli* (*EcXen14*; derived from the parental strain *E. coli* WS2572) were
106 purchased from PerkinElmer. Colistin-resistant *EcXen14* (*col^R-EcXen14*) was generated by
107 daily serial passages in increasing concentrations of colistin from 0.06 mg/L to 256 mg/L over
108 15 days as described previously²⁹. All bacteria were stored at -80 °C in Luria Bertani (LB)
109 broth with 50% (vol/vol) glycerol at the Microbiology Laboratory, Health and Biomedical
110 Innovation, Clinical and Health Sciences, University of South Australia, Australia. Bacteria
111 were routinely grown on horse blood agar (HBA) and LB broth. *SaXen29* was grown on HBA
112 containing 200 mg/L kanamycin while *EcXen14* and *col^R-EcXen14* were grown on HBA
113 containing 30 mg/L kanamycin for selection.

114

115 *DNA extraction and Whole Genome Sequencing*

116 Genomic DNA of *EcXen14* and *col^R-EcXen14* were extracted using the PureLink® Genomic
117 DNA Kit (Invitrogen, Australia). Whole genome sequencing was performed at Public Health
118 and Epidemiology, Microbiology and Infectious Diseases, SA Pathology, Australia using the

119 Illumina NextSeq 500/550 Mid-Output kit v2.5 (300 cycles) (Illumina Inc., USA). Raw paired-
120 end reads were assembled and annotated using the TORMES pipeline v.1.3.0³¹. Amino acid
121 sequence alignments were generated using CLUSTAL OMEGA version 1.2.4³² to assess the
122 presence of mutations and visualised using ESPript v3.0³³.

123

124 ***Ethics statements***

125 Outbred 5 to 6-week-old male CD1 (Swiss) mice (25–30 g), obtained from the Laboratory
126 Animal Services breeding facility of the University of Adelaide, were used for safety and
127 efficacy assessments of NCL195, colistin and NCL195+colistin administration. Mice had
128 access to food and water *ad libitum*. The Animal Ethics Committee of The University of
129 Adelaide (approval number S-2015-151) reviewed and approved all animal experiments. The
130 study was conducted in compliance with the Australian Code of Practice for the Care and Use
131 of Animals for Scientific Purposes (8th Edition 2013) and the South Australian Animal Welfare
132 Act 1985.

133

134 ***Safety testing of NCL195 alone and in combination with colistin and histopathological*** 135 ***examination***

136 To ascertain the safety of a regimen of 4 consecutive oral doses of 10 mg/kg or 50 mg/kg
137 NCL195 at 4 h intervals of NCL195 in mice, a safety study was conducted, using the vehicle
138 (20% (v/v) DMSO in PEG400) as a control agent. Subsequently, safety of 4 oral doses (4 h
139 apart) of NCL195 (50 mg/kg) combined with 4 intraperitoneal doses (4 h apart) colistin at
140 0.125, 0.25 or 0.5 mg/kg was conducted. Later, safety of oral NCL195 (50 mg/kg) combined
141 with intraperitoneal colistin at 1, 2 or 4 mg/kg was assessed. The group that received
142 NCL195+colistin was compared with the group that received NCL195 alone or colistin alone
143 at the same concentrations or stand-alone colistin at 8 mg/kg.

144 Mice were monitored for clinical signs of adverse effects and observations recorded
145 every 4 h for the first 24 h, then at 48 h and 72 h on a Clinical Record Sheet approved by the
146 Animal Ethics Committee of The University of Adelaide. At the conclusion of the experiment
147 (72 h after the initial treatment), mice were humanely killed. Mouse organs (heart, lung, liver,
148 kidneys, spleen, stomach, small intestines and large intestines) were collected, fixed in 10%
149 neutral-buffered formalin and processed routinely. The specimens were embedded in paraffin
150 blocks and sections of 4 µm thickness were cut using a microtome. Hematoxylin staining of
151 the sections was performed and the slides were observed and recorded under light microscopy.

152

153 *Agar well diffusion method*

154 All formulations of NCL195 and colistin used for safety and efficacy assessments were tested
155 for antibacterial activity using the agar well diffusion method to ensure that the drugs were
156 released from the vehicle as a reference for the interpretation of *in vivo* activity in mice as
157 detailed in Supplementary Materials.

158

159 *Efficacy testing of NCL195 oral administration following systemic challenge with SaXen29*

160 To test the efficacy of 50 mg/kg NCL195 (four oral doses, 4 h apart) against *S. aureus*, mouse-
161 passaged SaXen29 was used. Oral 6 mg/kg moxifloxacin (four doses, 4 h apart) suspension in
162 almond oil (prepared by BovaVet, Australia, 6 mg/mL) was used as drug control. Three groups
163 of mice ($n=6$ mice per group) were challenged intraperitoneally with approx. 3×10^7 CFU of
164 SaXen29 in 200 µl saline containing 3% porcine stomach mucin type III (Sigma Aldrich), then
165 immediately subjected to bioluminescence imaging in both ventral and dorsal positions on the
166 IVIS Lumina XRMS Series III system. Subsequently, group 1 received the drug vehicle only,
167 group 2 received oral NCL195 at 50 mg/kg, while group 3 received oral moxifloxacin 6 mg/kg.
168 At 2 h post-infection, all mice were imaged as above and their clinical conditions closely

169 monitored and recorded. At 4 h post-infection, all mice were similarly imaged and received the
170 second dose. At 6 h post-infection, all mice were imaged again and the clinical conditions
171 monitored and recorded. At 8 h post-infection, all surviving mice in each group were imaged
172 and given a third identical dose. At 10 h post-infection, all surviving animals in each group
173 were imaged followed by an identical treatment regimen at 12 h as described above. Mice were
174 further monitored frequently for signs of distress at 18, 24, 28, 36, 48 and 72 h post-infection,
175 their clinical conditions recorded, imaged and those that had become moribund or showed any
176 evidence of distress were humanely killed by cervical dislocation. In all experiments, signals
177 were collected from a defined region of interest and total flux intensities (photons/s) analysed
178 using Living Image Software 4.7.2. Differences in median survival times (time to moribund)
179 for mice between groups were analysed by the Log-rank (Mantel-Cox) tests. Differences in
180 luminescence signals between groups were compared by Mann-Whitney *U*-tests, two-tailed.

181

182 ***Efficacy testing of oral NCL195+intraperitoneal colistin combination following systemic***
183 ***challenge with EcXen14 or col^R-EcXen14***

184 We have previously determined the lowest colistin dose that was unable to clear
185 *EcXen14* infection in a mouse model ²⁷. In this study, we extended our investigation to
186 determine the lowest colistin dose unable to clear col^R-*EcXen14* in an identical mouse
187 peritonitis-sepsis model, as described in Supplementary Materials. In all experiments,
188 *EcXen14* and col^R-*EcXen14* were grown in LB broth at 37 °C to *A*_{600 nm} of 0.5 (equivalent to
189 approx. 5×10^8 CFU/mL) and each mouse was challenged intraperitoneally with approx. $1 \times$
190 10^8 CFU in 200 μ L PBS containing 3% porcine stomach mucin type III (Sigma Aldrich).

191 Efficacy testing of NCL195 (4 oral doses, 4 h apart)+colistin (4 intraperitoneal doses,
192 4 h apart) in a *EcXen14* peritonitis-sepsis mouse model was performed using the following
193 treatment groups: (i) NCL195 50 mg/kg; (ii) NCL195 50 mg/kg+colistin 0.125 mg/kg; (iii)

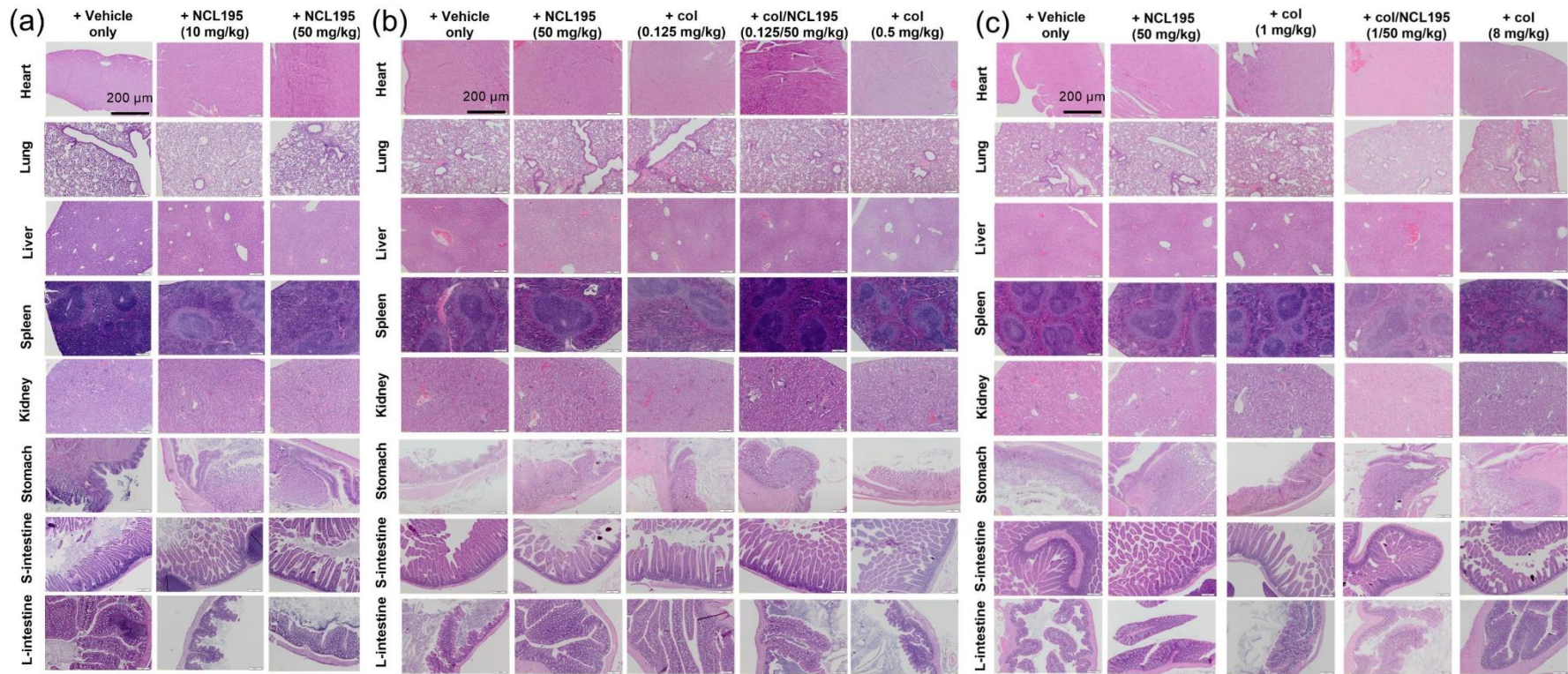
194 colistin 0.125 mg/kg; (iv) NCL195 50 mg/kg+colistin 0.25 mg/kg; (v) colistin 0.25 mg/kg; (vi)
195 NCL195 50 mg/kg+colistin 0.5 mg/kg; (vii) colistin 0.5 mg/kg. The col^R-*EcXen14* peritonitis-
196 sepsis challenge model enrolled the following treatment groups: (i) NCL195 50 mg/kg; (ii)
197 NCL195 50 mg/kg+colistin 0.5 mg/kg; (iii) colistin 1 mg/kg; (iv) NCL195 50 mg/kg+colistin
198 2 mg/kg; (v) colistin 2 mg/kg; (v) colistin 8 mg/kg (two doses at 0 and 4 h post-infection).
199 Bioluminescence imaging, treatment regimen and analysis followed the procedure described
200 above.
201

202 **Results**

203 *Oral administration of NCL195 alone or in combination with intraperitoneally-administered*
204 *colistin demonstrate systemic safety in mice*

205 As a prelude to efficacy testing of orally administered NCL195 in a GPB peritonitis-sepsis
206 model, the safety of 4 orally-administered NCL195 at 10 mg/kg or 50 mg/kg, 4 h apart) in
207 comparison with the vehicle was assessed over a 72 h period. We found there were no
208 observable histopathological changes in heart, lung, liver, spleen, stomach, kidneys, small and
209 large intestines of mice treated with either 10 mg/kg or 50 mg/kg NCL195 in comparison with
210 the vehicle at 72 h after initial treatment (Figure 1a). Subsequent administration of a
211 combination of NCL95 (4 oral doses, 50 mg/kg, 4 h apart) with colistin (4 intraperitoneal doses,
212 0.125, 0.25, 0.5, 1, 2 or 4 mg/kg, 4 h apart) showed no observed histopathological changes in
213 harvested organs from mice in comparison with vehicle, NCL195 alone or colistin alone at
214 similar concentrations (Figure 1b & c and Figure S1a & b).

215



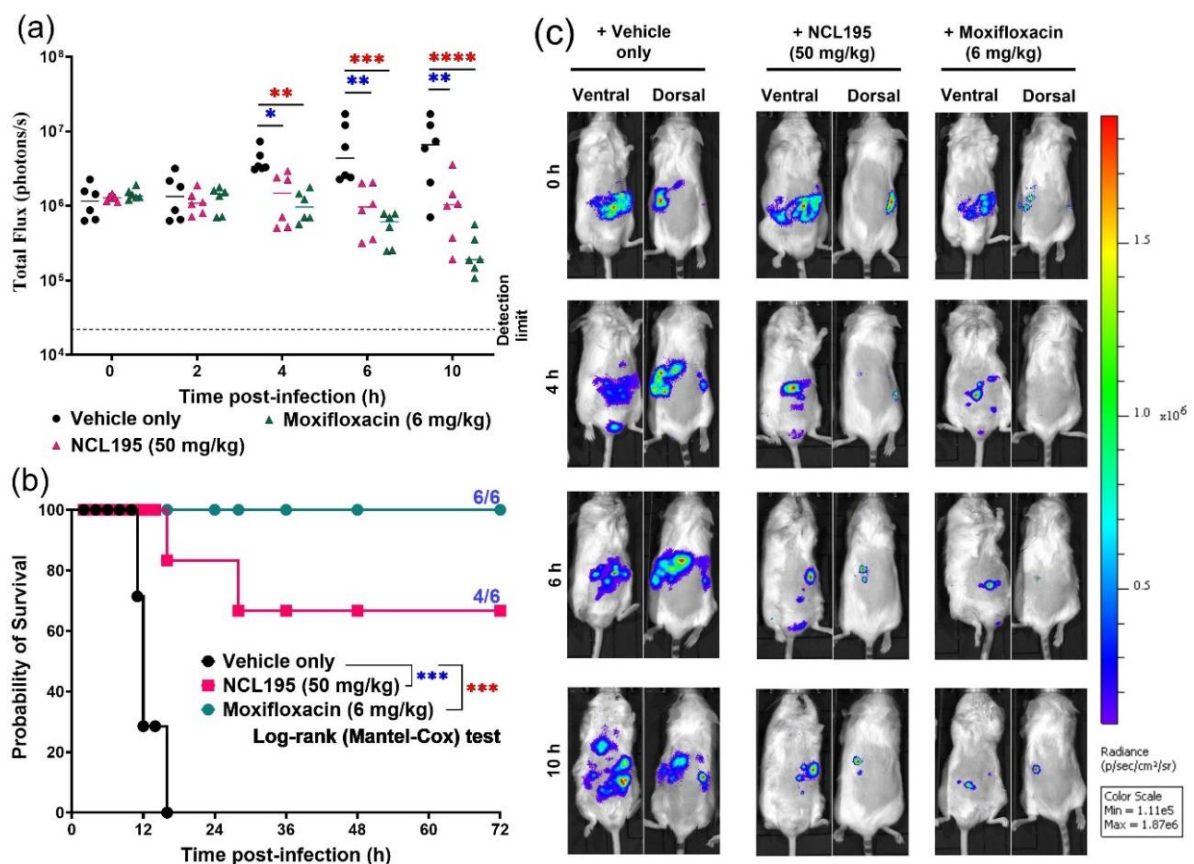
216

217 **Figure 1.** Selected histological images of organs from treated and control mice. No morphological abnormalities or no apparent changes were
 218 observed in mice orally treated NCL195 (10 or 50 mg/kg, 4 doses, 4 h apart) alone (**a**); treated with NCL195 (4 oral doses, 50 mg/kg, 4 h apart)
 219 combined with colistin (4 intraperitoneal doses, 0.125, 0.25, 0.5 or 1 mg/kg, 4 h apart) in comparison with vehicle, NCL195 (50 mg/kg) and
 220 colistin at the same concentrations after 72 h post-treatment (**b** & **c**). Scale bar: 200 µm.

221

222 *Oral treatment of mice with NCL195 reduces S. aureus populations and significantly*
 223 *prolongs survival times*

224 As a proof of concept for efficacy testing of NCL195+colistin combination in GNB peritonitis-
 225 sepsis models, the efficacy of orally-administered NCL195 at the safe dose of 50 mg/kg in a
 226 bioluminescent *SaXen29* mouse infection model was examined. We observed increasing
 227 reduction of *SaXen29* photon intensities after the first ($p<0.05$), second and third NCL195
 228 treatments ($p<0.01$) compared to the vehicle-only group (Figure 2a). Treatment of mice with
 229 four doses of NCL195 resulted in significant increase in median survival time and overall
 230 survival rate compared to the vehicle-only control ($p<0.001$; Figure 2b). As expected, treatment
 231 with moxifloxacin (control drug) showed progressively significant reduction in *SaXen29*
 232 photon intensities, increase in survival time and overall survival rate (Figure 2a-c).



233
 234 **Figure 2.** Oral efficacy of NCL195 in a bioluminescent *SaXen29* mouse peritonitis-sepsis
 235 model. (a) Comparison of luminescence signals between groups of CD1 mice ($n=6$) challenged

236 intraperitoneally with *SaXen29* and orally treated with vehicle only, 50 mg/kg NCL195 or 6
237 mg/kg moxifloxacin (4 doses 4 h apart), starting at 0 h post-infection. Mice were subjected to
238 bioluminescence imaging on IVIS Lumina XRMS Series III system at the indicated times (ns,
239 no significant; *, $p < 0.05$; **, $p < 0.01$; ***, $p < 0.001$, ****, $p < 0.0001$, Mann-Whitney *U*-test,
240 two-tailed). (b) Survival analysis for mice orally treated with NCL195, moxifloxacin and
241 vehicle (ns, no significant; *, $p < 0.05$; **, $p < 0.01$, ***, $p < 0.001$, ****, $p < 0.0001$; Log-rank
242 (Mantel-Cox) test. (c) Ventral and dorsal images of representative CD1 mice challenged with
243 approx. 3×10^7 CFU of bioluminescent *SaXen29*. Broken segment on y-axis represents limit
244 of detection.

245

246 ***Low dose colistin is unable to clear EcXen14 or col^R-EcXen14 infection in mice***

247 Preliminary investigations to determine the appropriate sub-inhibitory concentrations of
248 colistin to test the efficacy of NCL195+colistin combination in a bioluminescent *EcXen14*
249 mouse model have been reported previously²⁷. To ensure that a NCL195+colistin combination
250 will work against a colistin-resistant GNB *in vivo*, a stable col^R-*EcXen14* strain with MIC of
251 32 mg/L was generated which produced a similar bioluminescence emission profile as the
252 parent *EcXen14* (Figure S2). Whole genome sequence comparison of the col^R-*EcXen14* strain
253 with the parent revealed an amino acid substitution (Gly₅₃→Val₅₃) in PmrA (Figure S3) of the
254 PmrAB two-component system that remodels the composition and charge of lipid A and the
255 barrier properties of the outer membrane^{34,35}. Additionally, agar well diffusion results confirm
256 that NCL195 and colistin retain their antimicrobial activity when formulated (Figure S4).

257 The optimal sub-inhibitory concentration of colistin to be used for efficacy testing of
258 NCL195+colistin combinations in a col^R-*EcXen14* mouse challenge model was then explored.
259 We found 4 intraperitoneal doses of colistin 0.5 or 2 mg/kg were unable to clear the infection
260 up to 12 h post-infection, whereas almost complete bacterial clearance was observed after 4

261 intraperitoneal doses of colistin 4 mg/kg, with complete bacterial clearance after 2
262 intraperitoneal doses of colistin 8 mg/kg by 12 h post-infection (Figure S5a & b). Therefore,
263 colistin at 0.5, 1 mg/kg or 2 mg/kg were used in subsequent efficacy testing of
264 NCL195+colistin combinations against col^R-*EcXen14* intraperitoneal challenge.

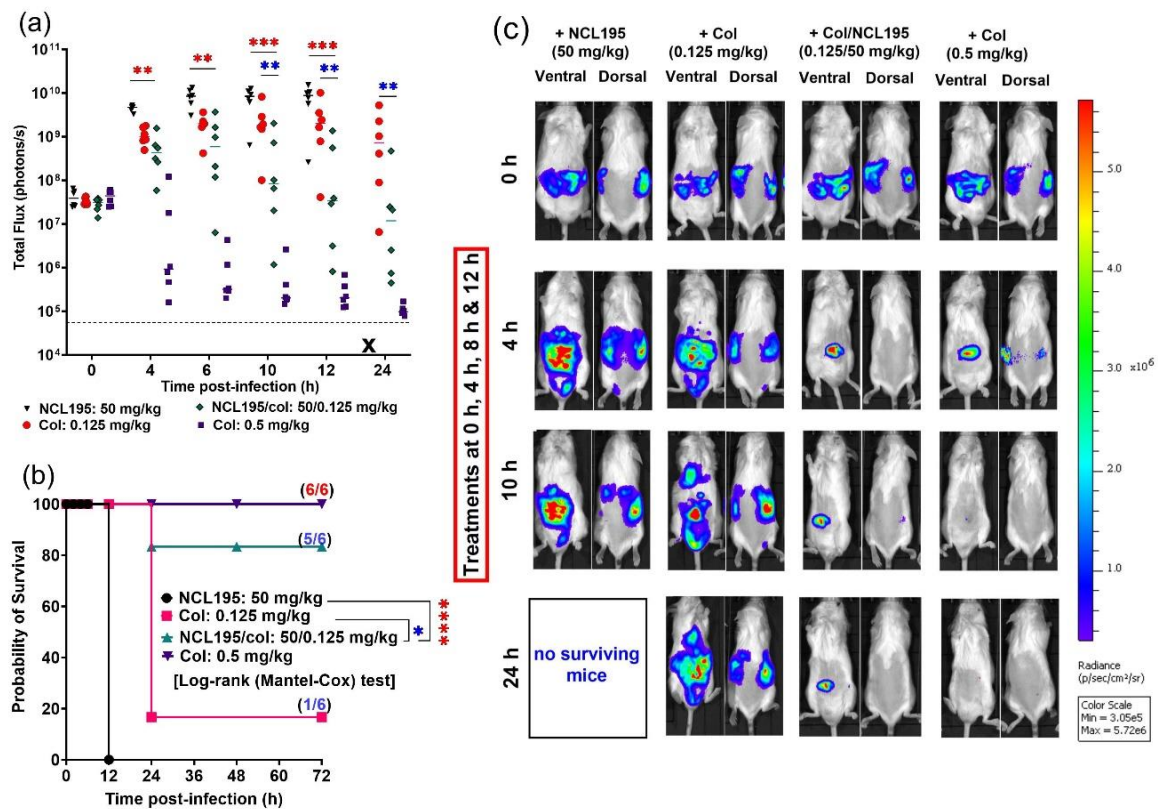
265

266 ***Treatment of mice with NCL195+colistin combination reduces EcXen14 populations and***
267 ***significantly prolongs survival times***

268 The efficacy of orally-administered NCL195 (4 doses, 50 mg/kg, 4 h apart) was tested
269 against both *EcXen14* and col^R-*EcXen14* using colistin 0.5 mg/kg and 8 mg/kg as drug controls
270 (Figure S6). We previously demonstrated that NCL195 has no *in vitro* activity against GNB
271 except for *Neisseria meningitidis* and *N. gonorrhoeae* (MIC, 32 µg/ml)^{27, 28}. Here, NCL195-
272 treated mice succumbed as rapidly as vehicle only-treated mice to *EcXen14* (Figure S6a & b)
273 or col^R-*EcXen14* (Figure S6c & d) challenge, confirming NCL195 has no activity against *E.*
274 *coli*.

275 The results of efficacy experiments with 50 mg/kg oral NCL195 (4 doses, 4 h apart) in
276 combination with colistin 0.125, 0.25 or 0.5 mg/kg (4 intraperitoneal doses, 4 h apart) in a
277 *EcXen14* peritonitis-sepsis model are shown in Figure 3 and Figure S7. Overall,
278 NCL195+colistin combinations cleared bacteria faster than colistin alone at similar
279 concentrations. All NCL195+colistin combination treatments showed statistically significant
280 reduction in *EcXen14* photon signals from 4 to 12 h in comparison with NCL195 alone ($p < 0.01$
281 to $p < 0.001$) (Figure S7a). Furthermore, all NCL195+colistin combination treatments resulted
282 in a significant increase in median survival times for mice compared to NCL195 alone
283 ($p < 0.0001$) (Figure S7b). Specifically, the NCL195 (50 mg/kg)+colistin (0.125 mg/kg)
284 combination showed statistically significant reduction in *EcXen14* photon intensities at 10, 12
285 and 24 h ($p < 0.01$) in comparison with colistin alone at the same concentration (Figure 3a).

286 Additionally, treatment with 4 doses of a combination of NCL195 (50 mg/kg)+colistin (0.125
 287 mg/kg) 4 h apart resulted in a significant increase in median survival time compared to
 288 treatment with 4 doses of NCL195 50 mg/kg ($p<0.0001$) or treatment with 4 doses of colistin
 289 0.125 mg/kg ($p<0.05$, Log-rank (Mantel-Cox) test) (Figure 3b). The bacterial reduction caused
 290 by different treatments could be clearly observed in bioluminescent images of mice (Figure 3c
 291 and Figure S7c).



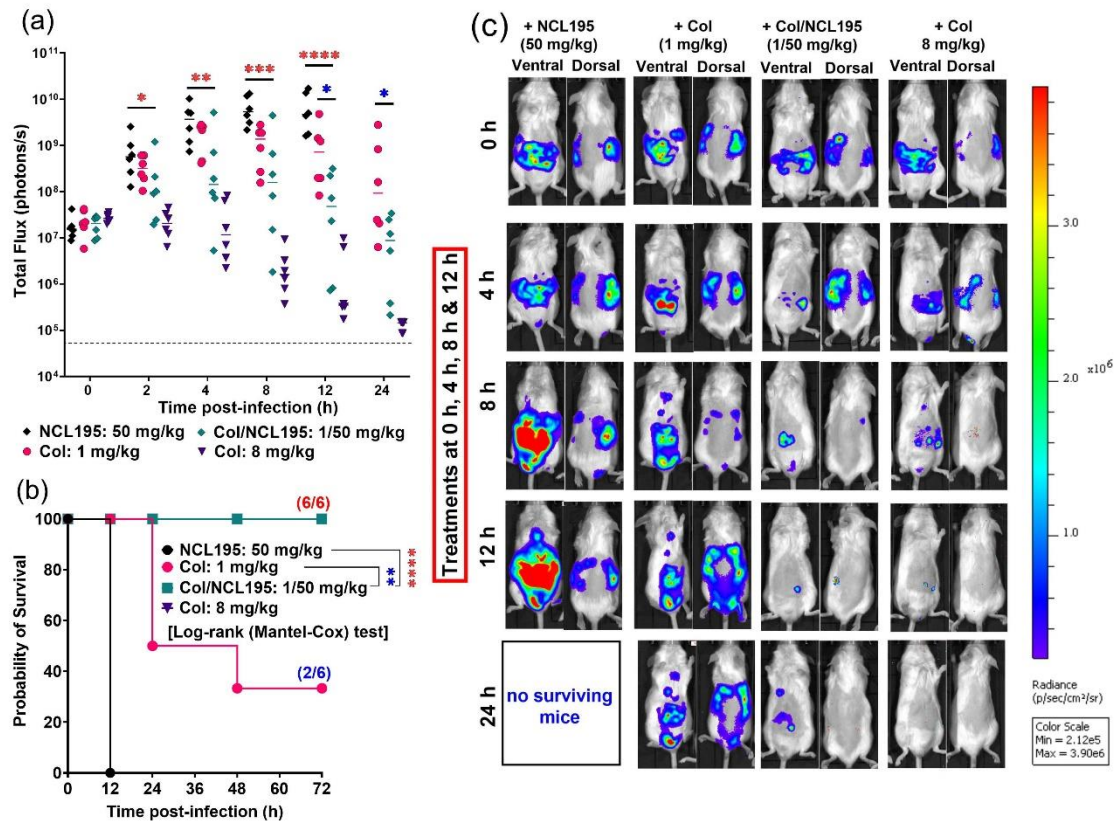
292
 293 **Figure 3.** Efficacy of NCL195+colistin combination in a bioluminescent *EcXen14* peritonitis-
 294 sepsis mouse model. (a) Luminescence signal comparisons between groups of CD1 mice ($n=6$)
 295 challenged intraperitoneally with bioluminescent *EcXen14* and treated at 0 h, 4 h, 8 h & 12 h
 296 with the indicated drug concentrations. Mice were subjected to bioluminescence imaging on
 297 IVIS Lumina XRMS Series III system at the indicated times (ns, no significant; *, $p<0.05$; **,
 298 $p<0.01$; ***, $p<0.001$, ****, $p<0.0001$, Mann-Whitney *U*-test, two-tailed). (b) Survival
 299 analysis for mice treated with the indicated drugs (ns, no significant; *, $p<0.05$; **, $p<0.01$,

300 ***, $p < 0.001$, ****, $p < 0.0001$; Log-rank (Mantel-Cox test)). (c) Ventral and dorsal images of
301 representative CD1 mice challenged with approx. 1×10^8 CFU of bioluminescent *EcXen14*.
302 Broken segment on y-axis represents limit of detection (2×10^4 photons/s). Col, colistin.

303

304 Next, we assessed the efficacy of NCL195 (4 oral doses, 50 mg/kg, 4 h apart) in
305 combination with colistin (4 intraperitoneal doses, 0.5, 1 or 2 mg/kg, 4 h apart) in a mouse
306 *col^R-EcXen14* peritonitis-sepsis challenge model. Overall, the NCL195+colistin combinations
307 cleared bacteria faster than colistin alone at the same concentrations. NCL195+colistin at 0.5
308 mg/kg combination showed statistically significant reduction in *col^R-EcXen14* photon signals
309 from 8 h and significant reduction in photon signals from 4 h when NCL195 was combined
310 with 1 or 2 mg/kg colistin in comparison with NCL195 alone ($p < 0.01$ to $p < 0.001$; Figure S8a).
311 Furthermore, all NCL195+colistin combination treatments resulted in significant increase in
312 median survival time for mice compared with NCL195 treatment alone ($p < 0.0001$; Figure
313 S8b).

314 NCL195 (50 mg/kg)+colistin (1 mg/kg) combination showed statistically significant
315 reduction in *col^R-EcXen14* photon signals at 12 and 24 h ($p < 0.05$) in comparison with a similar
316 concentration of colistin alone (Figure 4a). Treatment with NCL195 (50 mg/kg)+colistin (1
317 mg/kg) combination resulted in significant increase in median survival time compared to
318 colistin alone at 1 mg/kg ($p < 0.01$; Figure 4b). NCL195 (50 mg/kg)+colistin (2 mg/kg)
319 combination showed statistically significant reduction in *col^R-EcXen14* populations at 8, 12
320 and 24 h ($p < 0.05$) compared to treatment with 2 mg/kg colistin alone (Figure S8a). Treatment
321 with NCL195 (50 mg/kg)+colistin (2 mg/kg) combination resulted in significant increase in
322 median survival time compared to colistin alone at 2 mg/kg ($p < 0.01$; Figure S8b), clearly
323 observed in bioluminescent images of mice (Figure 4c and Figure S8c).



324

325 **Figure 4.** Efficacy of NCL195+colistin combination data in bioluminescent col^R-EcXen14

326 peritonitis-sepsis mouse model. **(a)** Luminescence signal comparisons between groups of CD1

327 mice ($n=6$) challenged intraperitoneally with bioluminescent col^R-EcXen14 and treated at 0 h,

328 4 h, 8 h & 12 h with the indicated drug concentrations. Group received two doses of colistin 8

329 mg/kg at 0 h and 4 h. Mice were subjected to bioluminescence imaging on IVIS Lumina XRMS

330 Series III system at the indicated times (ns, no significant; *, $p<0.05$; **, $p<0.01$; ***, $p<0.001$,

331 ****, $p<0.0001$, Mann-Whitney U -test, two-tailed). Broken segment on y-axis represents limit

332 of detection (2×10^4 photons/s). **(b)** Survival analysis for mice treated with the indicated drugs

333 (ns, no significant; *, $p<0.05$; **, $p<0.01$, ***, $p<0.001$, ****, $p<0.0001$; Log-rank (Mantel-

334 Cox test)). **(c)** Ventral and dorsal images of representative CD1 mice challenged with approx.

335 1×10^8 CFU of bioluminescent col^R-EcXen14. Col, colistin.

336

337 **Discussion**

338 In this study, we show that four oral doses of 50 mg/kg NCL195 and combination with four
339 intraperitoneal doses of two-fold increasing colistin concentrations (0.125–4 mg/kg) at 4 h
340 intervals could be administered to mice without any observable histopathological changes in
341 comparison to vehicle only, NCL195 alone or colistin alone at similar concentrations. We also
342 demonstrate that administration of four oral doses of NCL195 after an otherwise lethal *S.*
343 *aureus* systemic challenge significantly increased overall mouse survival. Furthermore, we
344 show that co-administration of four oral NCL195 doses with four intraperitoneal sub-inhibitory
345 colistin doses resulted in a significant dose-dependent reduction in colistin-susceptible and
346 colistin-resistant *E. coli* infection loads and significantly increased survival of mice compared
347 to treatment with colistin alone at similar concentrations. The *in vivo* efficacy was correlated
348 with previous *in vitro* time-kill kinetics showing that NCL195+colistin combinations killed
349 bacteria faster than colistin alone at similar concentrations and was associated with
350 ultrastructural damage of the outer and inner membrane of cells as assessed by transmission
351 electron microscopy^{27, 36}.

352 Robenidine is an oral antibiotic used to control coccidiosis in poultry²⁵, but chemically
353 modified to yield NCL195 to enhance potency and systemic delivery^{26, 29}. However, while
354 intraperitoneally-administered NCL195 led to significantly reduced *S. aureus* loads compared
355 to untreated mice, this did not result in increased overall survival²⁸. Our recent finding that
356 oral delivery of a closely-related robenidine analogue (NCL179) resulted in increased overall
357 survival after *S. aureus* challenge³⁰ provided the impetus for testing oral administration of
358 NCL195 in this study, which showed a significantly increased overall mouse survival. The
359 reason(s) for the superior efficacy of oral administration over the systemic route is yet
360 uncertain, but will be investigated.

361 The use of colistin therapy alone or in combination with other antibiotics for GNB
362 infections is still controversial^{16,17}. Although polymyxins (including colistin) are considered
363 last line drugs for the treatment of GNB infections, the high risk of nephrotoxicity³⁷,
364 neurotoxicity and neuromuscular blockade^{14,15} are a major reason for debate and concern about
365 use. Our results agree with other studies reporting that colistin combination therapy
366 demonstrated superiority in safety and efficacy profiles compared with monotherapy against
367 GNB infections³⁷⁻⁴². Of note, the sub-inhibitory concentration of colistin used in the
368 combination was as effective as a higher concentration of colistin alone, and the combination
369 of colistin at 1 mg/kg with NCL195 successfully treated col^R-*EcXen14* infection in mice
370 whereas colistin alone at the same concentration showed no effect. Therefore, NCL195 having
371 a proposed site of action on the bacterial inner membrane is a promising strategy to address the
372 shortfall in antibiotics for GNB infections when combined with low concentration of colistin,
373 particularly in the environment of increasing colistin-resistance among GNB.

374 We demonstrated previously that NCL195 has low propensity to select for resistance
375 in *S. aureus*²⁹, a desirable characteristic for further investigation as a novel antimicrobial class
376 to treat acute bacterial infections. Our current results add to those findings on the antibacterial
377 efficacy of NCL195 and provide further support for combination therapy with colistin in the
378 presence of colistin resistance among MDR-GNB pathogens by administering colistin as an
379 adjuvant to permeabilize the outer membrane allowing increased exposure to NCL195.
380 Together, our findings demonstrate that the new antibacterial class represented by NCL195
381 provides a promising new scaffold. Pre-clinical studies to optimise
382 pharmacokinetic/pharmacodynamic profiles and dose regimens of NCL195+colistin
383 combinations as well as cumulative toxicity testing in appropriate animal models will allow
384 refinement of dosing schedules.

385

386

387 **Supplementary Materials**

388

389 **Supplementary Methods**

390

391 ***Agar well diffusion method***

392 NCL195 was prepared as 50 mg/mL solutions in 20% (v/v) DMSO in PEG400 (vehicle).

393 Colistin was prepared as 0.037, 0.075, 0.15, 0.3, 0.6, 1.2 and 2.4 mg/mL in water corresponding

394 to 0.125, 0.25, 0.5, 1, 2, 4 and 8 mg/kg, respectively, based on consideration of later

395 administration to a 30 g mouse for the mouse safety and efficacy studies. All formulations were

396 tested for antibacterial activity using the agar well diffusion method to ensure that the drugs

397 were released from the vehicle as a reference for the interpretation of *in vivo* activity in mice.

398 For this assay, colonies from of an overnight HBA culture of *SaXen29*, *EcXen14* and col^R-

399 *EcXen14* were suspended in saline equivalent to 0.5 McFarland Standard ($A_{600\text{ nm}} = 0.1$). A

400 sterile swab was then dipped in the 0.5 McFarland Standard bacterial suspension and then

401 streaked over the entire surface of a sterile plate count agar. Duplicate holes (on each of two

402 separate occasions of safety and efficacy trials) were then punched on the agar plates using an

403 8 mm diameter biopsy punch (Livingstone International Pty Ltd, NSW, Australia). Each well

404 contained 0.03 mL of each formulation. The antimicrobial activity of each drug was then

405 determined by measuring and comparing the zone of inhibition with that of vehicle only after

406 20 h incubation at 37 °C in air.

407

408 ***Determination of the lowest colistin dose unable to clear colistin-resistant E. coli***

409 Col^R-*EcXen14* cells were grown in LB broth at 37 °C to $A_{600\text{ nm}}$ of 0.5 (equivalent to approx. 5

410 $\times 10^8$ CFU/mL) and four groups of mice ($n=3$) were challenged intraperitoneally with approx.

411 1.0×10^8 CFU of the col^R-EcXen14 in 200 μ L saline containing 3% porcine stomach mucin
412 type III (Sigma Aldrich, Australia). All mice were then subjected to bioluminescence imaging
413 in both ventral and dorsal positions on the IVIS Lumina XRMS Series III system. Immediately
414 thereafter, group 1 received the drug vehicle only, groups 2, 3 and 4 received colistin at 0.5, 2
415 and 4 mg/kg intraperitoneally, respectively, at 0, 4, 8 and 12 h while group 5 received colistin
416 at 8 mg/kg at 0 and 4 h and mice further subjected to bioluminescence imaging at 4, 6, 10, 12,
417 24, 48 and 72 h post-infection. Mice were monitored frequently for signs of distress and those
418 that had become moribund or showed any evidence of distress were humanely killed by
419 cervical dislocation. In all groups, signals were collected from a defined region of interest and
420 total flux intensities (photons/s) analysed using Living Image Software 4.7.2.

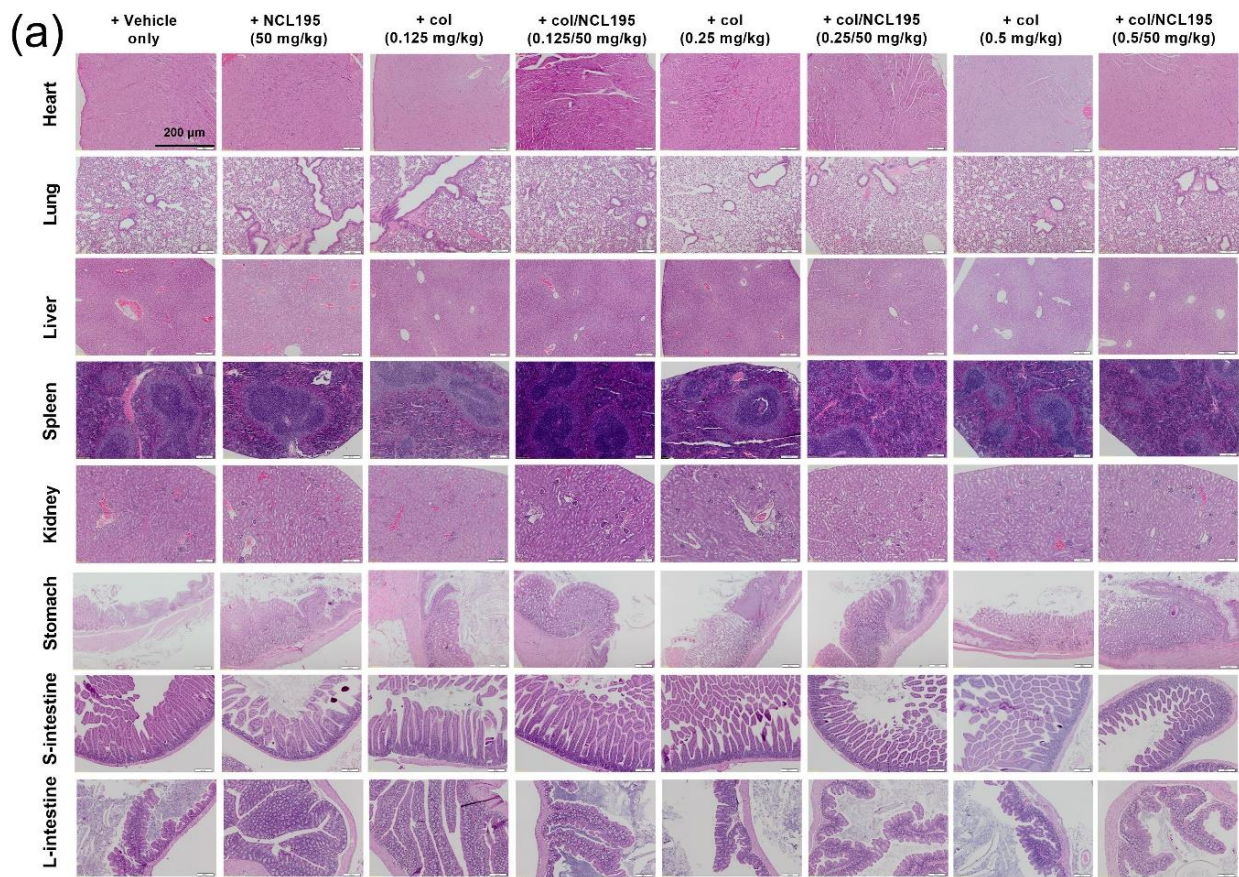
421

422

423 *Supplementary Results*

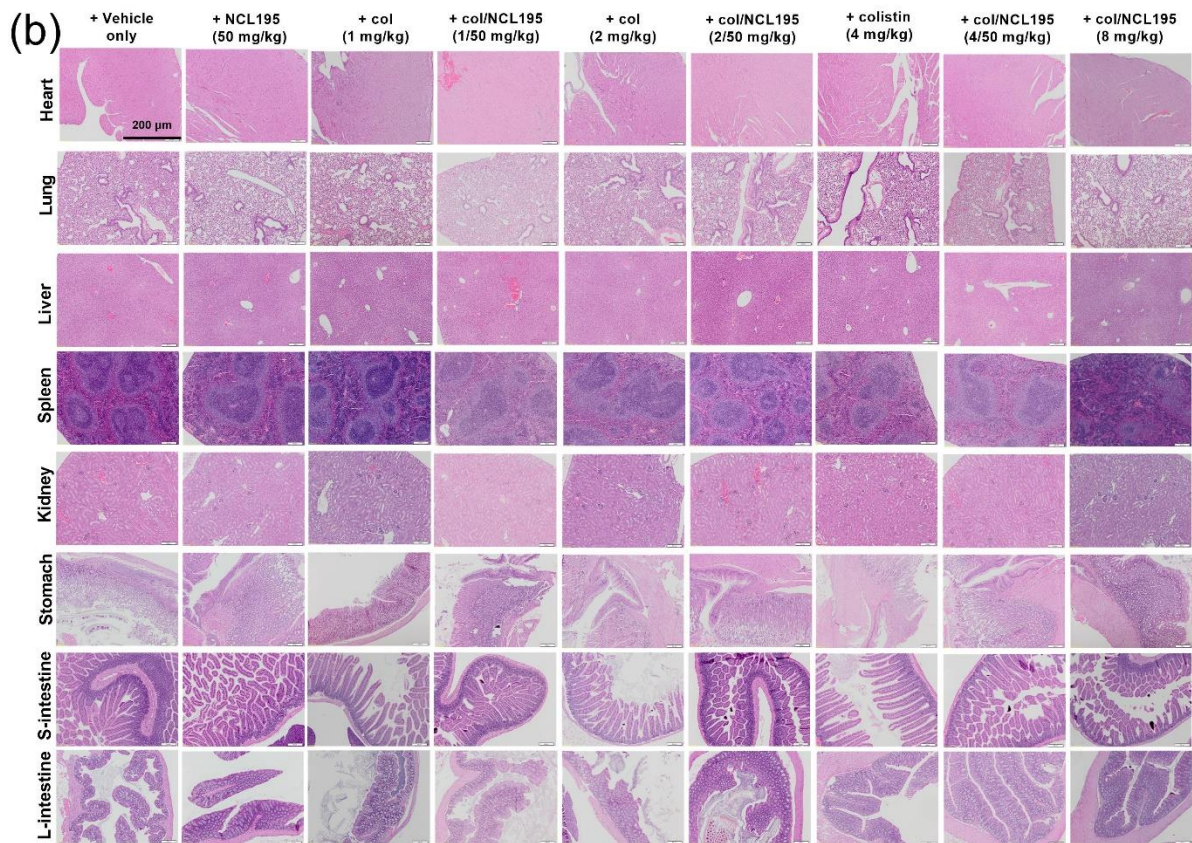
424

425 *Oral administration of NCL195 alone or in combination with intraperitoneally-*
426 *administered colistin demonstrate systemic safety in mice*



427

428



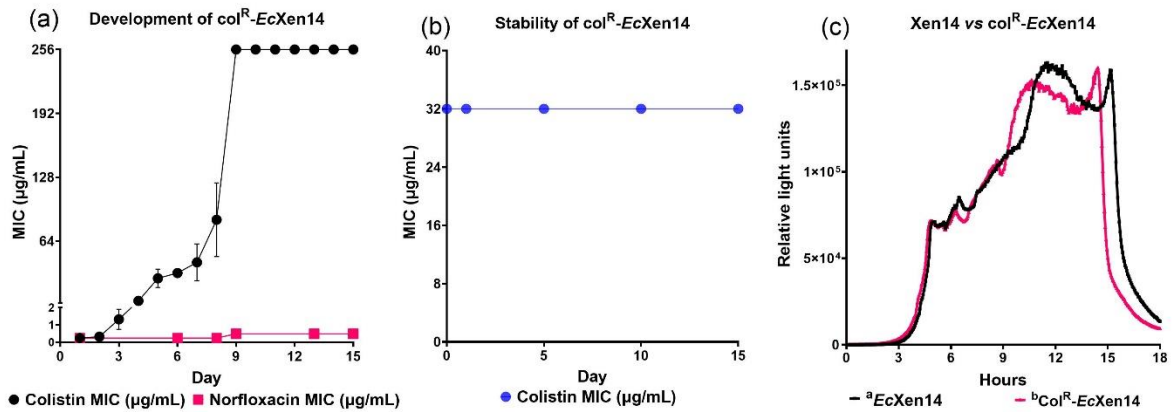
429

430 **Figure S1.** Selected histological images of organs collected from treated and control mice in
 431 the safety trial of NCL195+colistin combination. No morphological abnormalities or changes
 432 were observed in mice treated with all NCL195+colistin combination in comparison with
 433 vehicle, NCL195 alone and colistin alone at the same concentrations after 72 h post-treatment.
 434 Col, colistin. Scale bar: 200 μm.

435

436 ***Generation of colistin resistant-EcXen14***

437 Daily colistin resistance development in *EcXen14* was determined using the MIC as shown in
 438 Figure S2a. *EcXen14* started to grow in the presence of 0.06 mg/L colistin (0.25×MIC), after
 439 which it was exposed to a higher concentrations of colistin. Subsequently, col^R-*EcXen14* (MIC
 440 32 mg/L) was passaged in colistin-free LB broth for 15 days. The results indicate that the col^R-
 441 *EcXen14* was stable at 32 mg/L (Figure S2b) and it produced a similar bioluminescence
 442 emission profile as the original *EcXen14* (Figure S2c).

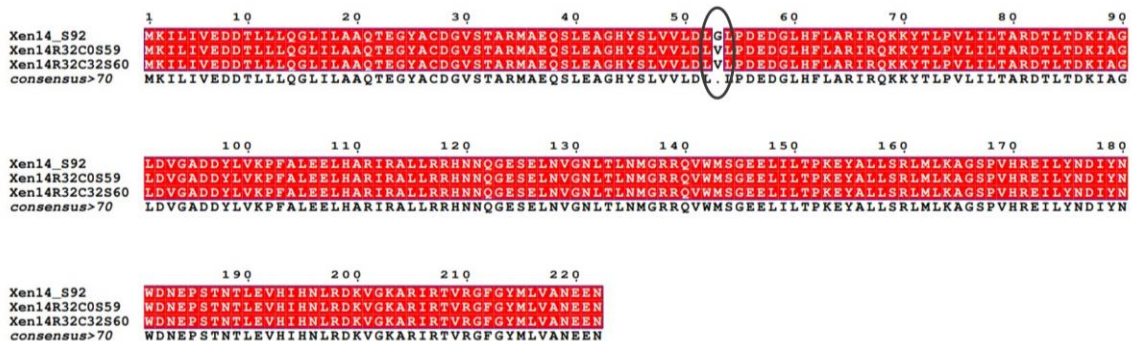


443

444 **Figure S2.** Colistin resistance development and bioluminescent emission of *col^R-EcXen14* in
 445 comparison with *EcXen14*. (a) *EcXen14* cells started to grow in LB broth in the presence of
 446 0.25×MIC, 0.5×MIC, 1×MIC, 2×MIC of colistin. On subsequent days, *EcXen14* cells that
 447 grew at the highest concentration of colistin were sub-cultured in LB containing 2-fold higher
 448 concentration of colistin. Norfloxacin (32 mg/L) was used as a control drug to ensure *col^R-*
 449 *EcXen14* was still sensitive to norfloxacin while resistant to colistin. (b). *Col^R-EcXen14* (32
 450 mg/L) passaged in colistin-free LB for 15 days; (c) bioluminescence emission intensity
 451 comparison between *EcXen14* and *col^R-EcXen14*.

452

453 Whole genome sequencing of the *col^R-EcXen14* revealed an amino acid substitution
 454 (Gly₅₃→Val₅₃) in PmrA (Figure S3).



455

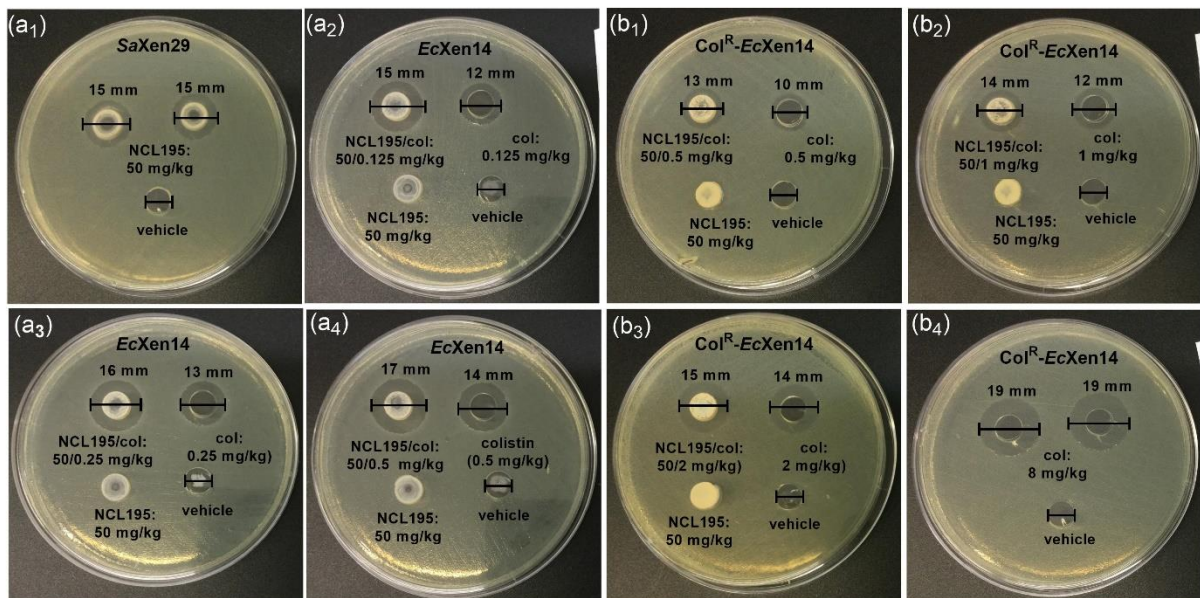
456 **Figure S3.** G53→V53 mutation in PmrA was found in *col^R-EcXen14*. *Col^R-EcXen14* cells at
 457 MIC 32 mg/L were grown overnight in LB in the absence (*EcXen14R32C0S59*) or presence

458 (*EcXen14R32C32S60*) of 32 mg/L colistin and subjected to whole genome sequencing.
459 Genome sequences of the two isolates were aligned against original *EcXen14* (MIC 0.25 mg/L)
460 (*EcXen14_S92*) for analysis.

461

462 *Agar well diffusion shows that NCL195 and colistin retain antimicrobial activity in*
463 *formulations*

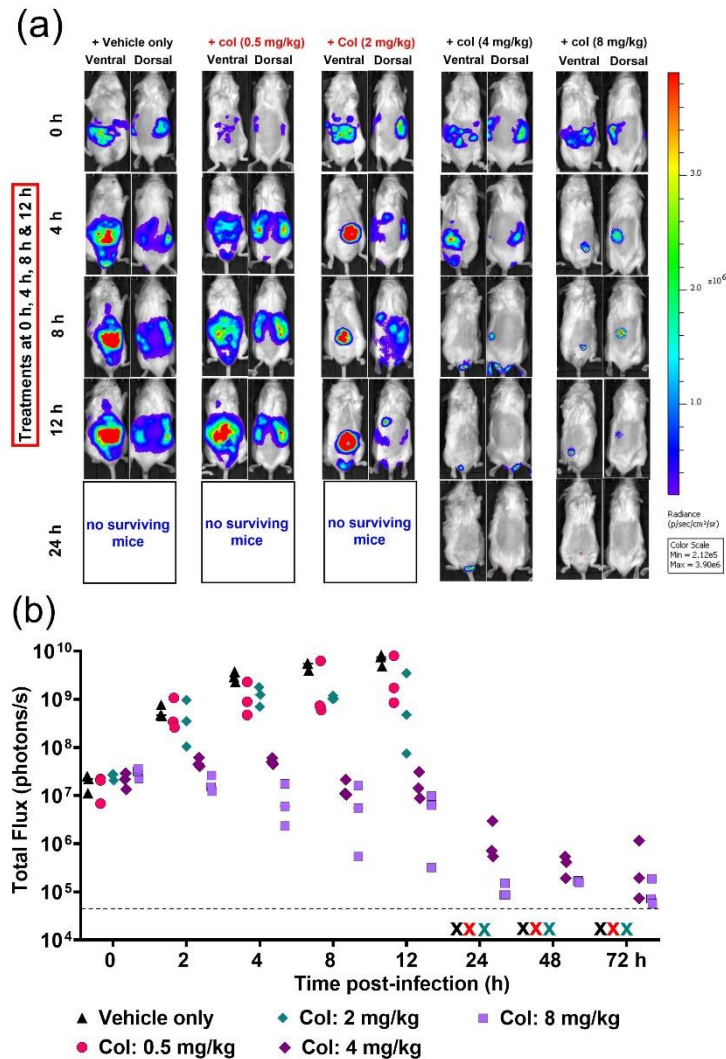
464 In order to ascertain that NCL195 and colistin remained active in the vehicle used, an agar
465 diffusion test of the formulations was carried out. NCL195 showed clear inhibitory zones of
466 15 mm against *S. aureus* Xen29 (Figure S4a₁). As expected, no inhibitory zone of NCL195
467 against *EcXen14* or col^R-*EcXen14* was observed. All NCL195+colistin combinations showed
468 a 3 mm larger inhibitory zone than for colistin alone at similar concentrations against *EcXen14*
469 (Figure S4a₂–a₄) and 1–3 mm larger inhibitory zones than for colistin alone at similar
470 concentrations against col^R-*EcXen14* (Figure S4b₁–b₄).



471

472 **Figure S4.** Selected agar well diffusion evaluation of NCL195 alone and NCL195+colistin
473 formulations used in the efficacy trial. Each well contained 0.03 mL of one formulation of
474 NCL195, colistin or vehicle only. NCL195 was prepared as a 50 mg/mL solution in vehicle

475 (20% (v/v) DMSO in PEG400). Colistin was prepared at different concentrations in water such
476 that a 0.1 mL intraperitoneal administration to a 30 g mouse would correspond to 0.125, 0.25,
477 0.5, 1, 2, 4 and 8 mg/kg, respectively. (**a1**) NCL195 formulation vs *SaXen29*; (**a2-a4**)
478 formulations vs *EcXen14*; (**b1-b4**) formulations vs col^R-*EcXen14*.
479



481

482 **Figure S5.** Dose-response testing of colistin in a bioluminescent col^R-EcXen14 mouse

483 peritonitis-sepsis model. (a) Ventral and dorsal images of representative CD1 mice challenged

484 with approx. 1×10^8 CFU of col^R-EcXen14. (b) Luminescence signal comparisons between

485 groups of CD1 mice ($n=3$) challenged intraperitoneally with bioluminescent col^R-EcXen14

486 and treated with colistin at 0.5, 2 & 4 mg/kg at 0 h, 4 h, 8 h & 12 h; colistin (8 mg/kg) at 0 h &

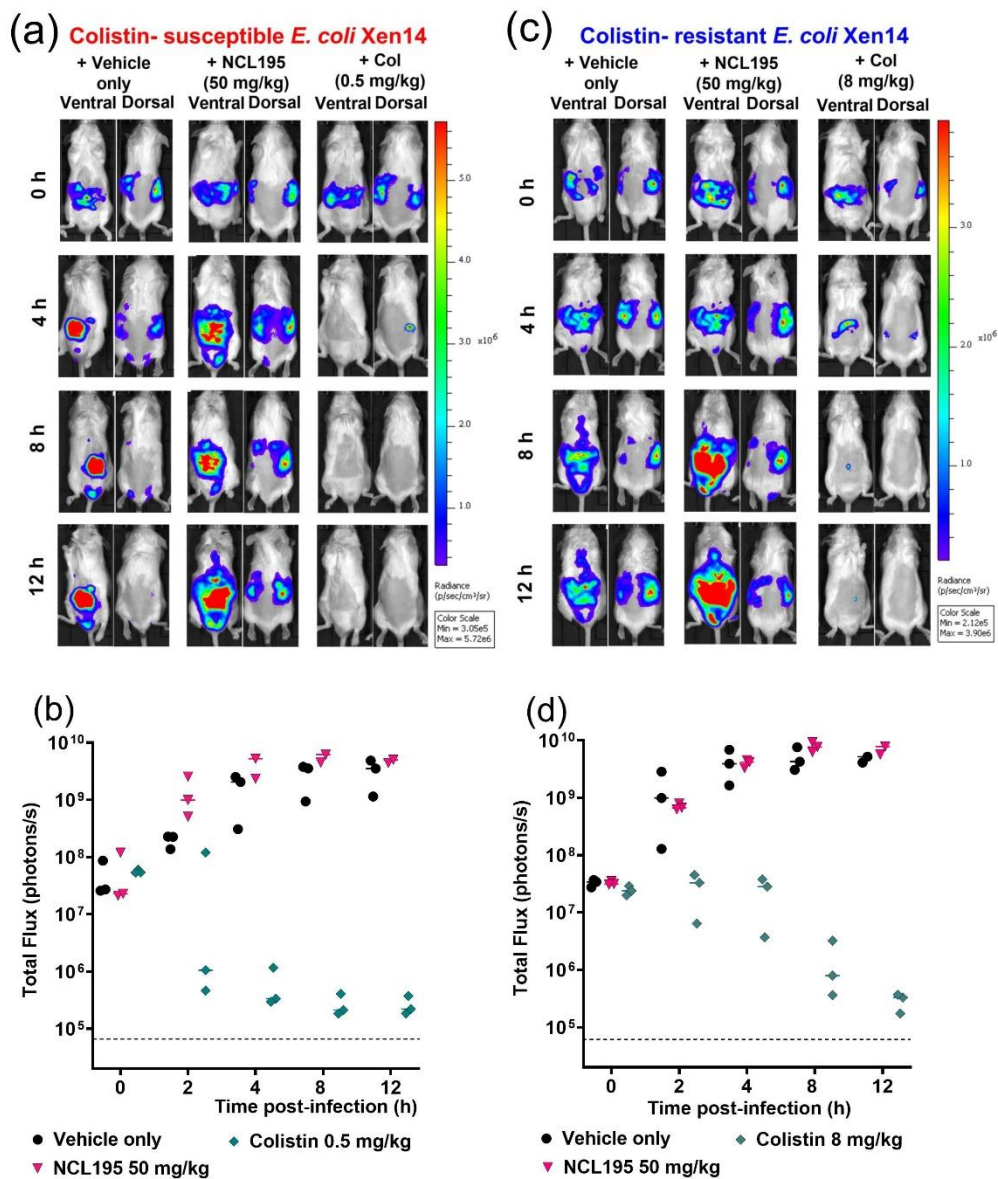
487 4 h. Mice were subjected to bioluminescence imaging on IVIS Lumina RMS Series III system

488 at the indicated times. Broken segment on y-axis represents limit of detection (2×10^4

489 photons/s). Col, colistin.

490

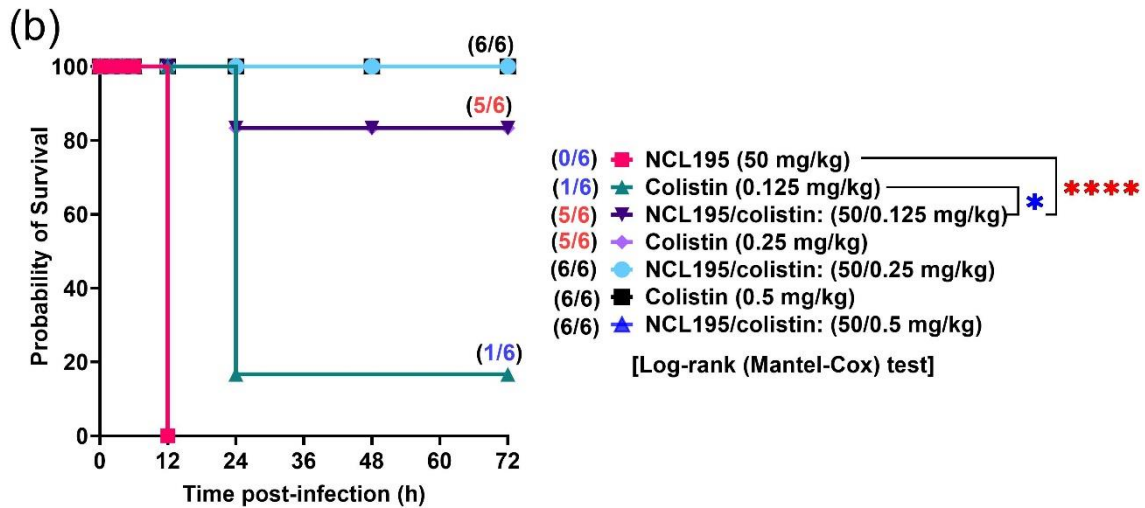
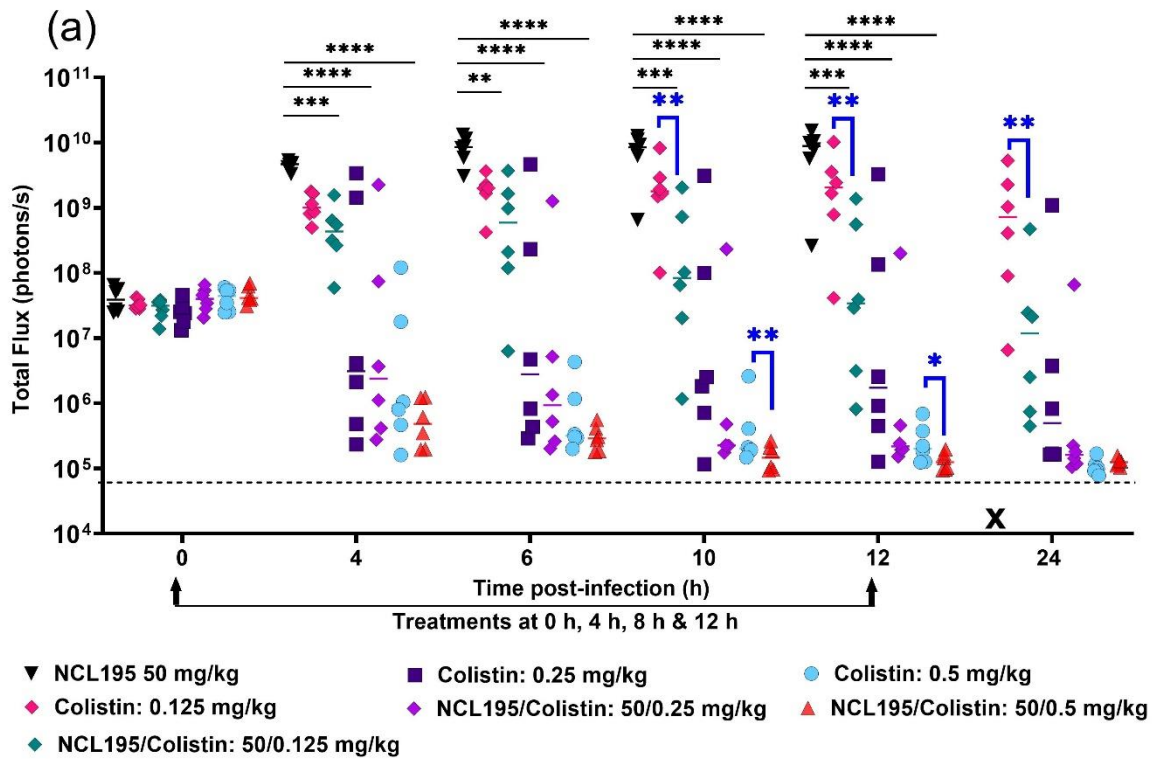
491 *Treatment of mice with NCL195+colistin combination reduces EcXen14 populations and*
 492 *significantly prolongs survival times*

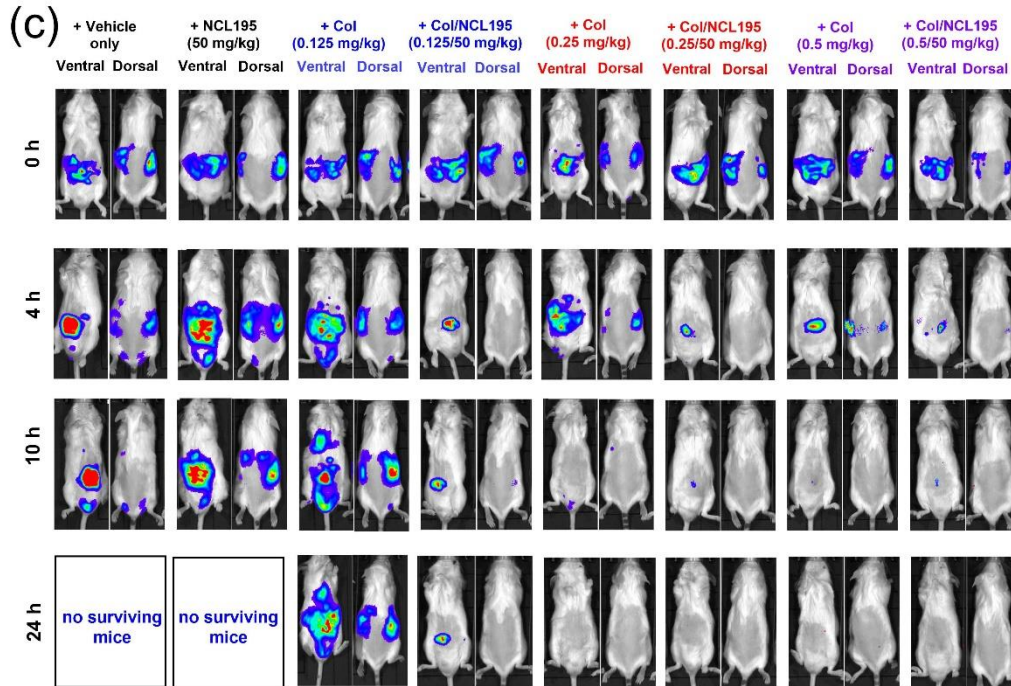


493

494 **Figure S6.** Preliminary efficacy of NCL195 in a bioluminescent Gram-negative mouse
 495 peritonitis-sepsis model. **(a & c)** Ventral and dorsal images of representative CD1 mice
 496 challenged with approx. 1×10^8 CFU of *EcXen14* or *col^R-EcXen14*. **(b & d)** luminescence
 497 signal comparisons between groups of CD1 mice ($n=3$) challenged intraperitoneally with
 498 *EcXen14* and *col^R-EcXen14* following treatments with vehicle only, NCL195 (50 mg/kg) and
 499 colistin at 0.5 mg/kg at 0 h, 4 h & 8 h apart. The group that received colistin at 8 mg/kg were

500 treated at 0 h and 4 h. Mice were subjected to bioluminescence imaging on IVIS Lumina RMS
 501 Series III system at the indicated times. Broken segment on y-axis represents limit of detection
 502 (2×10^4 photons/s).





505

506 **Figure S7.** Efficacy of NCL195+colistin combination in a bioluminescent *EcXen14* mouse

507 peritonitis-sepsis model. (a) Luminescence signal comparisons between groups of CD1 mice

508 ($n=6$) challenged intraperitoneally with bioluminescent *EcXen14* and treated at 0 h, 4 h, 8 h &

509 12 h with the indicated drug concentrations. Mice were subjected to bioluminescence imaging

510 on IVIS Lumina XRMS Series III system at the indicated times (ns, no significant; *, $p<0.05$;

511 **, $p<0.01$; ***, $p<0.001$, ****, $p<0.0001$, Mann-Whitney *U*-test, two-tailed); Broken segment

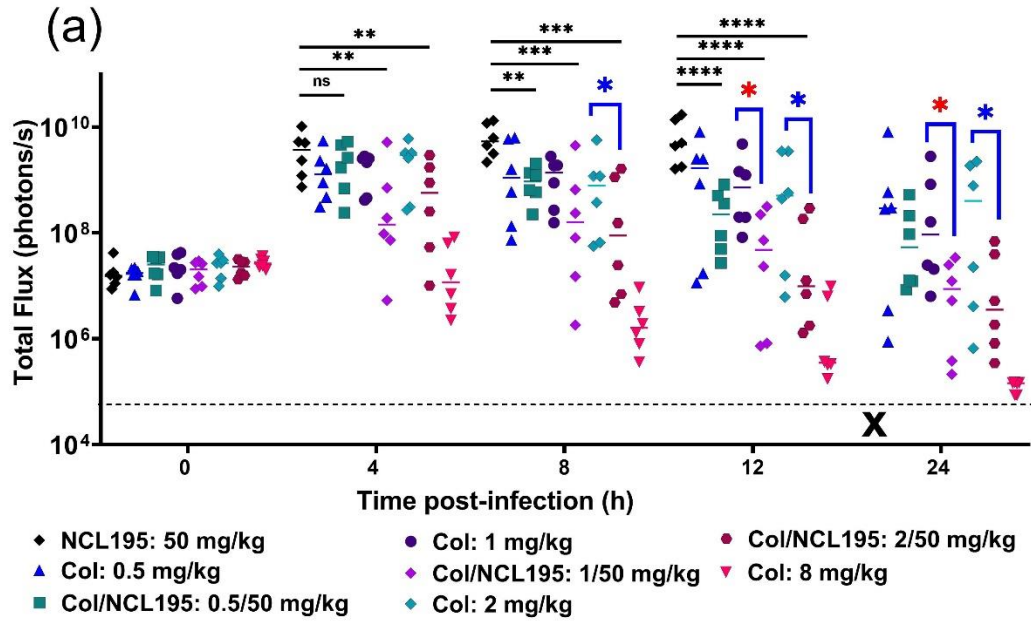
512 on y-axis represents limit of detection (2×10^4 photons/s). (b) Survival analysis for mice treated

513 with the indicated drugs (ns, no significant; *, $p<0.05$; **, $p<0.01$, ***, $p<0.001$, ****,

514 $p<0.0001$; Log-rank (Mantel-Cox test)). (c) Ventral and dorsal images of representative CD1

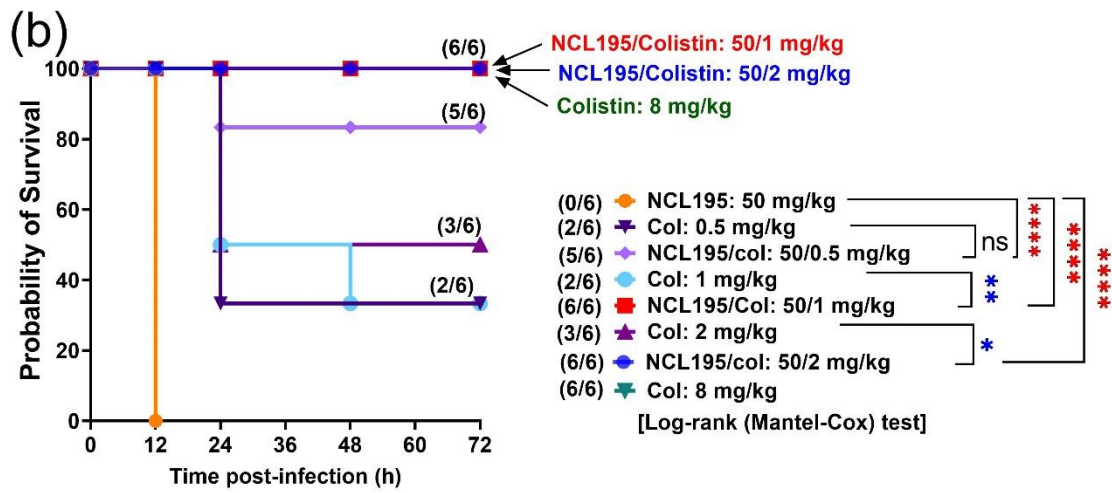
515 mice challenged with approx. 1×10^8 CFU of bioluminescent *EcXen14*. Col, colistin.

516

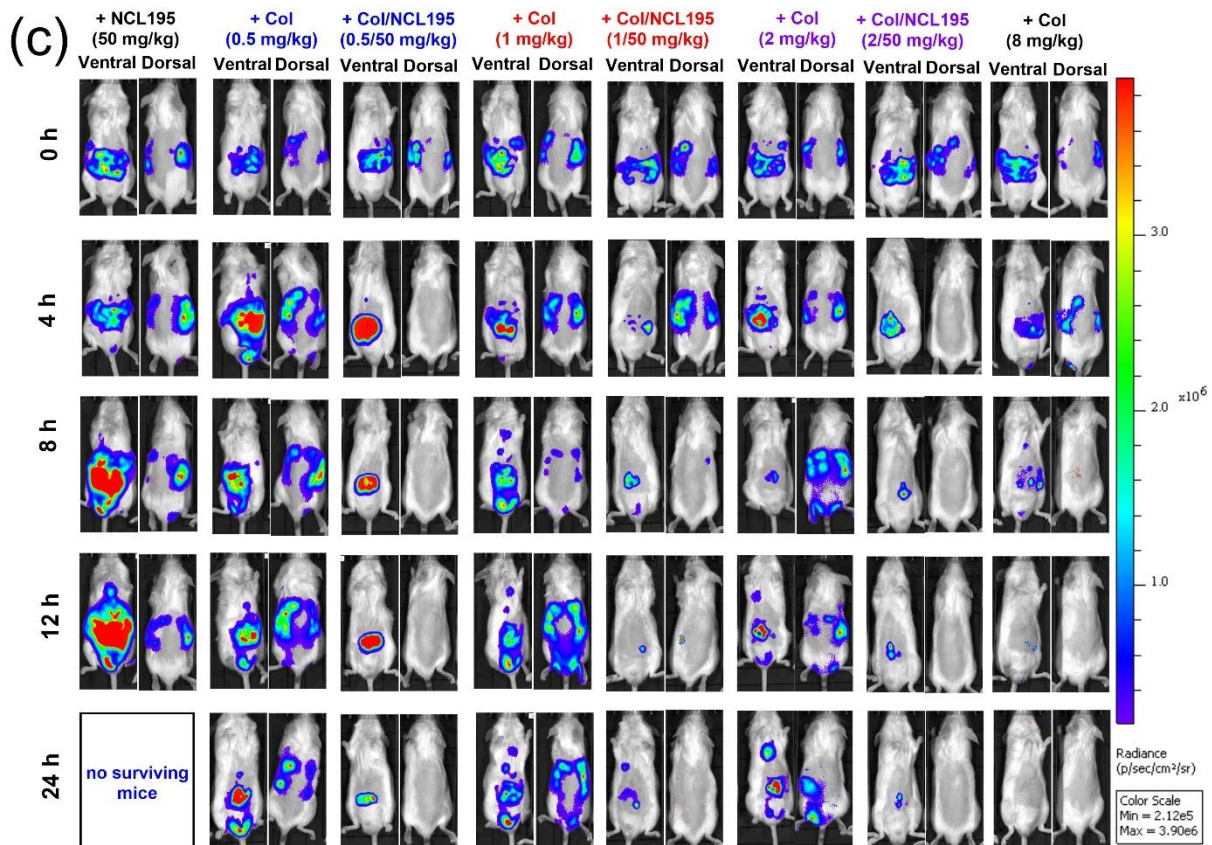


517

518



519



520

521

522 **Figure S8.** Efficacy of NCL195+colistin combination in a bioluminescent *col^R-EcXen14* mouse

523 peritonitis-sepsis model. (a) Luminescence signal comparisons between groups of CD1 mice

524 ($n=6$) challenged intraperitoneally with bioluminescent *col^R-EcXen14* and treated at 0 h, 4 h,

525 8 h & 12 h with the indicated drug concentrations. Mice were subjected to bioluminescence

526 imaging on IVIS Lumina XRMS Series III system at the indicated times (ns, no significant; *,

527 $p<0.05$; **, $p<0.01$; ***, $p<0.001$, ****, $p<0.0001$, Mann-Whitney U -test, two-tailed). Broken

528 segment on y-axis represents limit of detection (2×10^4 photons/s). (b) Survival analysis for

529 mice treated with the indicated drugs (ns, no significant; *, $p<0.05$; **, $p<0.01$, ***, $p<0.001$,

530 ****, $p<0.0001$; Log-rank (Mantel-Cox test)). (c) Ventral and dorsal images of representative

531 CD1 mice challenged with approx. 1×10^8 CFU of bioluminescent *col^R-EcXen14*. Col, colistin.

532

533

534 **Author Information**

535 Corresponding author (Darren Trott): Australian Centre for Antimicrobial Resistance Ecology,
536 School of Animal and Veterinary Sciences, The University of Adelaide, Roseworthy, SA,
537 Australia. Tel: +61 8 8313 7989. Fax: +61 8 8313 7956; E-mail: darren.trott@adelaide.edu.au.

538

539 **Author Contributions**

540 Hang Thi Nguyen contributed to the study design, performed experiments, wrote the
541 preliminary manuscript and editing. Henrietta Venter contributed to study design, editing and
542 discussion. Lucy Woolford contributed for histopathology examination, editing and discussion.
543 Sylvia Sapula contributed to whole genome sequencing, editing and discussion. Kelly Young
544 and Adam McCluskey were responsible for synthesizing NCL195 and contributed to editing
545 of the manuscript. Sanjay Garg contributed to formulations. Stephen W. Page contributed to
546 editing, discussion and provided financial support for the study. Abiodun David Ogunniyi
547 contributed to study design, experiments, technical guidance, supervision, editing, and
548 discussion. Darren Trott contributed to study design, supervision, editing, discussion, and
549 provided financial support for the study. All authors read and approved the submitted version
550 of the manuscript, in addition to contributing to manuscript revision.

551

552 **Acknowledgements**

553 The authors would like to thank Amanda Kenyon, Lora Bowes, Anh Hong Nguyen and
554 Max McClafferty at the University of South Australia for their technical assistance, Cheryl Day
555 at School of Veterinary and Animal Sciences for sample processing of histopathology
556 examination; May Song and Krishna Kathwala at the University of South Australia for
557 preparing NCL195 formulations.

558

559 **Conflicts of interest**

560 Stephen W. Page is a director of Neoculi Pty. Ltd. Darren J. Trott and Adam McCluskey have
561 received research funding from Neoculi Pty. Ltd.

562

563 **Funding statement**

564 This work was supported by an Australian Research Council (ARC; arc.gov.au) Linkage grant
565 (LP110200770) to D.J.T., A.M. and S.W.P. with Neoculi Pty Ltd as the Partner Organization
566 and University of South Australia fund to H.V. The funders did not have any additional role in
567 the study design, data collection and analysis, decision to publish, or preparation of the
568 manuscript.

569

570 **References**

- 571 1. Theriault N, Tillotson G, Sandrock CE. Global travel and Gram-negative bacterial resistance;
572 implications on clinical management. *Expert Rev Anti Infect Ther* 2021; **19**: 181-96.
- 573 2. De Oliveira DMP, Forde BM, Kidd TJ *et al*. Antimicrobial resistance in ESKAPE pathogens. *Clin*
574 *Microbiol Rev* 2020; **33**.
- 575 3. Murray CJL, Ikuta KS, Sharara F *et al*. Global burden of bacterial antimicrobial resistance in
576 2019: a systematic analysis. *The Lancet* 2022.
- 577 4. O'Neill J. Tackling drug-resistant infections globally: final report and recommendations.
578 https://amr-review.org/sites/default/files/160518_Final%20paper_with%20cover.pdf.
- 579 5. World Health Organization. New report calls for urgent action to avert antimicrobial
580 resistance crisis. [https://www.who.int/news/item/29-04-2019-new-report-calls-for-urgent-action-](https://www.who.int/news/item/29-04-2019-new-report-calls-for-urgent-action-to-avert-antimicrobial-resistance-crisis)
581 [to-avert-antimicrobial-resistance-crisis](https://www.who.int/news/item/29-04-2019-new-report-calls-for-urgent-action-to-avert-antimicrobial-resistance-crisis).
- 582 6. Giordano NP, Cian MB, Dalebroux ZD. Outer membrane lipid secretion and the innate
583 immune response to Gram-negative bacteria. *Infect Immun* 2020; **88**: e00920-19.
584 <https://doi.org/10.1128/IAI.00920-19>.
- 585 7. Tacconelli E, Carrara E, Savoldi A *et al*. Discovery, research, and development of new
586 antibiotics: the WHO priority list of antibiotic-resistant bacteria and tuberculosis. *Lancet Infect Dis*
587 2018; **18**: 318-27.
- 588 8. Doi Y, Bonomo RA, Hooper DC *et al*. Gram-negative bacterial infections: Research priorities,
589 accomplishments, and future directions of the antibacterial resistance leadership group. *Clin Infect*
590 *Dis* 2017; **64**: S30-S5.
- 591 9. Theuretzbacher U. Global antimicrobial resistance in Gram-negative pathogens and clinical
592 need. *Curr Opin Microbiol* 2017; **39**: 106-12.
- 593 10. Pewtrusts. Tracking the global pipeline of antibiotics in development, March 2021.
594 [https://www.pewtrusts.org/en/research-and-analysis/issue-briefs/2021/03/tracking-the-global-](https://www.pewtrusts.org/en/research-and-analysis/issue-briefs/2021/03/tracking-the-global-pipeline-of-antibiotics-in-development)
595 [pipeline-of-antibiotics-in-development](https://www.pewtrusts.org/en/research-and-analysis/issue-briefs/2021/03/tracking-the-global-pipeline-of-antibiotics-in-development).

- 596 11. Bergen PJ, Bulman ZP, Saju S *et al.* Polymyxin combinations: pharmacokinetics and
597 pharmacodynamics for rationale use. *J Hum Pharm Drug Ther* 2015; **35**: 34-42.
- 598 12. Falagas ME, Mavroudis AD, Vardakas KZ. The antibiotic pipeline for multi-drug resistant
599 Gram negative bacteria: what can we expect? *Expert Rev Anti Infect Ther* 2016; **14**: 747-63.
- 600 13. Baron S, Hadjadj L, Rolain JM *et al.* Molecular mechanisms of polymyxin resistance: knowns
601 and unknowns. *Int J Antimicrob Agents* 2016; **48**: 583-91.
- 602 14. Justo JA, Bosso JA. Adverse reactions associated with systemic polymyxin therapy. *J Hum*
603 *Pharm Drug Ther* 2015; **35**: 28-33.
- 604 15. Nigam A, Kumari A, Jain R *et al.* Colistin neurotoxicity: revisited. *BMJ Case Rep* 2015; **2015**:
605 bcr2015210787.
- 606 16. Petrosillo N, Ioannidou E, Falagas ME. Colistin monotherapy vs. combination therapy:
607 evidence from microbiological, animal and clinical studies. *Clin Microbiol Infect* 2008; **14**: 816-27.
- 608 17. Schmid A, Wolfensberger A, Nemeth J *et al.* Monotherapy versus combination therapy for
609 multidrug-resistant Gram-negative infections: Systematic Review and Meta-Analysis. *Sci Rep* 2019; **9**:
610 15290.
- 611 18. Venter H. Reversing resistance to counter antimicrobial resistance in the World Health
612 Organisation's critical priority of most dangerous pathogens. *Biosci Rep* 2019; **39**: BSR20180474.
- 613 19. Liu Y, Li R, Xiao X *et al.* Antibiotic adjuvants: an alternative approach to overcome multi-drug
614 resistant Gram-negative bacteria. *Crit Rev Microbiol* 2019; **45**: 301-14.
- 615 20. Brennan-Krohn T, Pironti A, Kirby JE. Synergistic activity of colistin-containing combinations
616 against colistin-resistant Enterobacteriaceae. *Antimicrob Agents Chemother* 2018; **62**: e00873-18.
- 617 21. Lenhard JR, Nation RL, Tsuji BT. Synergistic combinations of polymyxins. *Int J Antimicrob*
618 *Agents* 2016; **48**: 607-13.
- 619 22. Ontong JC, Ozioma NF, Voravuthikunchai SP *et al.* Synergistic antibacterial effects of colistin
620 in combination with aminoglycoside, carbapenems, cephalosporins, fluoroquinolones, tetracyclines,

621 fosfomycin, and piperacillin on multidrug resistant *Klebsiella pneumoniae* isolates. *PLoS One* 2021;
622 **16**: e0244673.

623 23. Song M, Liu Y, Huang X *et al.* A broad-spectrum antibiotic adjuvant reverses multidrug-
624 resistant Gram-negative pathogens. *Nat Microbiol* 2020; **5**: 1040-50.

625 24. Hagihara M, Housman ST, Nicolau DP *et al.* *In vitro* pharmacodynamics of polymyxin B and
626 tigecycline alone and in combination against carbapenem-resistant *Acinetobacter baumannii*.
627 *Antimicrob Agents Chemother* 2014; **58**: 874-9.

628 25. Kantor S, Kennett RL, Jr., Waletzky E *et al.* 1,3-Bis(p-chlorobenzylideneamino)guanidine
629 hydrochloride (robenzidene): new poultry anticoccidial agent. *Science (New York, NY)* 1970; **168**:
630 373-4.

631 26. Abraham RJ, Stevens AJ, Young KA *et al.* Robenidine analogues as Gram-positive
632 antibacterial agents. *J Med Chem* 2016; **59**: 2126-38.

633 27. Nguyen HT, Venter H, Veltman T *et al.* *In vitro* synergistic activity of NCL195 in combination
634 with colistin against Gram-negative bacterial pathogens. *Int J Antimicrob Agents* 2021; **57**: 106323.

635 28. Pi H, Nguyen HT, Venter H *et al.* *In vitro* activity of robenidine analog NCL195 in combination
636 with outer membrane permeabilizers against Gram-negative bacterial pathogens and impact on
637 systemic Gram-positive bacterial infection in mice. *Front Microbiol* 2020; **11**: 1556;
638 <https://doi.org/10.3389/fmicb.2020.01556>.

639 29. Ogunniyi AD, Khazandi M, Stevens AJ *et al.* Evaluation of robenidine analog NCL195 as a
640 novel broad-spectrum antibacterial agent. *PLoS One* 2017; **12**: e0183457.

641 30. Nguyen HT, Venter H, Woolford L *et al.* Impact of a novel anticoccidial analogue on systemic
642 *Staphylococcus aureus* infection in a bioluminescent mouse model. *Antibiotics (Basel, Switzerland)*
643 2022; **11**: 65; <https://doi.org/10.3390/antibiotics11010065>.

644 31. Quijada NM, Rodríguez-Lázaro D, Eiros JM *et al.* TORMES: an automated pipeline for whole
645 bacterial genome analysis. *Bioinformatics* 2019; **35**: 4207-12.

- 646 32. Sievers F, Higgins DG. Clustal Omega for making accurate alignments of many protein
647 sequences. *Protein Science : a publication of the Protein Society* 2018; **27**: 135-45.
- 648 33. Robert X, Gouet P. Deciphering key features in protein structures with the new ENDscript
649 server. *Nucleic Acids Res* 2014; **42**: W320-W4.
- 650 34. Froelich JM, Tran K, Wall D. A *pmrA* constitutive mutant sensitizes *Escherichia coli* to
651 deoxycholic acid. *J Bacteriol* 2006; **188**: 1180-3.
- 652 35. Sato T, Shiraishi T, Hiyama Y *et al.* Contribution of novel amino acid alterations in PmrA or
653 PmrB to colistin resistance in *mcr*-negative *Escherichia coli* clinical isolates, including major
654 multidrug-resistant lineages O25b:H4-ST131-H30Rx and Non-x. *Antimicrob Agents Chemother* 2018;
655 **62**: e00864-18.
- 656 36. Nguyen HT, O'Donovan LA, Venter H *et al.* Comparison of two transmission electron
657 microscopy methods to visualize drug-induced alterations of Gram-negative bacterial morphology.
658 *Antibiotics (Basel, Switzerland)* 2021; **10**: 307; <https://doi.org/10.3390/antibiotics10030307>.
- 659 37. Wang J, Niu H, Wang R *et al.* Safety and efficacy of colistin alone or in combination in adults
660 with *Acinetobacter baumannii* infection: A systematic review and meta-analysis. *Int J Antimicrob*
661 *Agents* 2019; **53**: 383-400.
- 662 38. Aoki N, Tateda K, Kikuchi Y *et al.* Efficacy of colistin combination therapy in a mouse model
663 of pneumonia caused by multidrug-resistant *Pseudomonas aeruginosa*. *J Antimicrob Chemother*
664 2009; **63**: 534-42.
- 665 39. Crémieux AC, Dinh A, Nordmann P *et al.* Efficacy of colistin alone and in various
666 combinations for the treatment of experimental osteomyelitis due to carbapenemase-producing
667 *Klebsiella pneumoniae*. *J Antimicrob Chemother* 2019; **74**: 2666-75.
- 668 40. Fan B, Guan J, Wang X *et al.* Activity of colistin in combination with meropenem, tigecycline,
669 fosfomicin, fusidic acid, rifampin or sulbactam against extensively drug-resistant *Acinetobacter*
670 *baumannii* in a murine thigh-infection model. *PLoS One* 2016; **11**: e0157757.

- 671 41. Ku NS, Lee SH, Lim YS *et al.* *In vivo* efficacy of combination of colistin with fosfomycin or
672 minocycline in a mouse model of multidrug-resistant *Acinetobacter baumannii* pneumonia. *Sci Rep*
673 2019; **9**: 17127.
- 674 42. Salloum NA, Kissoyan KA, Fadlallah S *et al.* Assessment of combination therapy in BALB/c
675 mice injected with carbapenem-resistant Enterobacteriaceae strains. *Front Microbiol* 2015; **6**: 999.
- 676

Chapter VI

Impact of a novel anticoccidial analogue on systemic *Staphylococcus aureus* infection in a bioluminescent mouse model

Statement of Authorship

| | |
|---------------------|---|
| Title of Paper | Impact of a novel anticoccidial analogue on systemic <i>Staphylococcus aureus</i> infection in a bioluminescent mouse model |
| Publication Status | <input checked="" type="checkbox"/> Published <input type="checkbox"/> Accepted for Publication <input type="checkbox"/> Submitted for Publication <input type="checkbox"/> Unpublished and Unsubmitted work written in manuscript style |
| Publication Details | Nguyen HT, Venter H, Woolford L et al. Impact of a novel anticoccidial analogue on systemic <i>Staphylococcus aureus</i> infection in a bioluminescent mouse model. <i>Antibiotics (Basel)</i> 2022 ; 11, doi:10.3390/antibiotics11010065. Journal Impact Factor = 5.222. |

Principal Author

| | | | |
|--------------------------------------|--|------|------------|
| Name of Principal Author (Candidate) | Hang Thi Nguyen | | |
| Contribution to the Paper | Contributed to the study design, performed experiments, wrote the preliminary manuscript and revised the edited manuscript | | |
| Overall percentage (%) | 70% | | |
| Certification: | This paper reports on original research I conducted during the period of my Higher Degree by Research candidature and is not subject to any obligations or contractual agreements with a third party that would constrain its inclusion in this thesis. I am the primary author of this paper. | | |
| Signature | | Date | 01/12/2021 |

Co-Author Contributions

By signing the Statement of Authorship, each author certifies that:

- i. the candidate's stated contribution to the publication is accurate (as detailed above);
- ii. permission is granted for the candidate to include the publication in the thesis; and
- iii. the sum of all co-author contributions is equal to 100% less the candidate's stated contribution.

| | | | |
|---------------------------|---|------|------------|
| Name of Co-Author | Henrietta Venter | | |
| Contribution to the Paper | Contributed to study design, editing and discussion | | |
| Signature | | Date | 15/12/2021 |

| | | | |
|---------------------------|--|------|----------|
| Name of Co-Author | Lucy Woolford | | |
| Contribution to the Paper | Contributed to histopathology examinations, editing and discussion | | |
| Signature | | Date | 05/01/22 |

| | | | |
|---------------------------|---|--|--|
| Name of Co-Author | Kelly Young | | |
| Contribution to the Paper | Responsible for synthesizing NCL179 and edited the manuscript | | |

| | | | |
|-----------|--|------|------------|
| Signature | | Date | 18/01/2022 |
|-----------|--|------|------------|

| | | | |
|---------------------------|---|------|------------|
| Name of Co-Author | Adam McCluskey | | |
| Contribution to the Paper | Responsible for synthesizing NCL179 and edited the manuscript | | |
| Signature | | Date | 06/02/2022 |

| | | | |
|---------------------------|-----------------------------|------|------------|
| Name of Co-Author | Sanjay Garg | | |
| Contribution to the Paper | Contributed to formulations | | |
| Signature | | Date | 06/01/2022 |

| | | | |
|---------------------------|---|------|------------|
| Name of Co-Author | Stephen W. Page | | |
| Contribution to the Paper | Contributed to editing, discussion and provided financial support for the study | | |
| Signature | | Date | 02/02/2022 |

| | | | |
|---------------------------|---|------|------------|
| Name of Co-Author | Darren J. Trott | | |
| Contribution to the Paper | Contributed to study design, supervision, editing, discussion, provided financial support for the study and was co-corresponding author | | |
| Signature | | Date | 07/02/2022 |

| | | | |
|---------------------------|--|------|------------|
| Name of Co-Author | Abiodun D. Ogunniyi | | |
| Contribution to the Paper | Contributed to study design, experiments, technical guidance, supervision, editing, discussion and was co-corresponding author | | |
| Signature | | Date | 08/12/2021 |

Article

Impact of a Novel Anticoccidial Analogue on Systemic *Staphylococcus aureus* Infection in a Bioluminescent Mouse Model

Hang Thi Nguyen ^{1,2}, Henrietta Venter ³, Lucy Woolford ⁴, Kelly Young ⁵, Adam McCluskey ⁵, Sanjay Garg ⁶, Stephen W. Page ⁷, Darren J. Trott ^{1,*} and Abiodun David Ogunniyi ^{1,*}

- ¹ Australian Centre for Antimicrobial Resistance Ecology, School of Animal and Veterinary Sciences, The University of Adelaide, Roseworthy, SA 5371, Australia; hang.t.nguyen@adelaide.edu.au
- ² Department of Pharmacology, Toxicology, Internal Medicine and Diagnostics, Faculty of Veterinary Medicine, Vietnam National University of Agriculture, Hanoi 100000, Vietnam
- ³ Health and Biomedical Innovation, Clinical and Health Sciences, University of South Australia, Adelaide, SA 5000, Australia; rietie.venter@unisa.edu.au
- ⁴ School of Animal and Veterinary Sciences, The University of Adelaide, Roseworthy Campus, Roseworthy, SA 5371, Australia; lucy.woolford@adelaide.edu.au
- ⁵ Chemistry, School of Environmental & Life Sciences, University of Newcastle, Callaghan, NSW 2308, Australia; kelly.a.young@newcastle.edu.au (K.Y.); adam.mccluskey@newcastle.edu.au (A.M.)
- ⁶ Clinical and Health Sciences, University of South Australia, Adelaide, SA 5000, Australia; sanjay.garg@unisa.edu.au
- ⁷ Neoculi Pty Ltd., Burwood, VIC 3125, Australia; swp@advet.com.au
- * Correspondence: darren.trott@adelaide.edu.au (D.J.T.); david.ogunniyi@adelaide.edu.au (A.D.O.); Tel.: +61-8-8313-7989 (D.J.T.); +61-432331914 (A.D.O.); Fax: +61-8-8313-7956 (D.J.T.)



Citation: Nguyen, H.T.; Venter, H.; Woolford, L.; Young, K.; McCluskey, A.; Garg, S.; Page, S.W.; Trott, D.J.; Ogunniyi, A.D. Impact of a Novel Anticoccidial Analogue on Systemic *Staphylococcus aureus* Infection in a Bioluminescent Mouse Model. *Antibiotics* **2022**, *11*, 65. <https://doi.org/10.3390/antibiotics11010065>

Academic Editor: Marc Maresca

Received: 30 November 2021

Accepted: 1 January 2022

Published: 6 January 2022

Publisher's Note: MDPI stays neutral with regard to jurisdictional claims in published maps and institutional affiliations.



Copyright: © 2022 by the authors. Licensee MDPI, Basel, Switzerland. This article is an open access article distributed under the terms and conditions of the Creative Commons Attribution (CC BY) license (<https://creativecommons.org/licenses/by/4.0/>).

Abstract: In this study, we investigated the potential of an analogue of robenidine (NCL179) to expand its chemical diversity for the treatment of multidrug-resistant (MDR) bacterial infections. We show that NCL179 exhibits potent bactericidal activity, returning minimum inhibitory concentration/minimum bactericidal concentrations (MICs/MBCs) of 1–2 µg/mL against methicillin-resistant *Staphylococcus aureus*, MICs/MBCs of 1–2 µg/mL against methicillin-resistant *S. pseudintermedius* and MICs/MBCs of 2–4 µg/mL against vancomycin-resistant enterococci. NCL179 showed synergistic activity against clinical isolates and reference strains of *Acinetobacter baumannii*, *Escherichia coli*, *Klebsiella pneumoniae* and *Pseudomonas aeruginosa* in the presence of sub-inhibitory concentrations of colistin, whereas NCL179 alone had no activity. Mice given oral NCL179 at 10 mg/kg and 50 mg/kg (4 × doses, 4 h apart) showed no adverse clinical effects and no observable histological effects in any of the organs examined. In a bioluminescent *S. aureus* sepsis challenge model, mice that received four oral doses of NCL179 at 50 mg/kg at 4 h intervals exhibited significantly reduced bacterial loads, longer survival times and higher overall survival rates than the vehicle-only treated mice. These results support NCL179 as a valid candidate for further development to treat MDR bacterial infections as a stand-alone antibiotic or in combination with existing antibiotic classes.

Keywords: NCL179; colistin; robenidine; Gram-positive bacteria; *Staphylococcus aureus*; Gram-negative bacteria; multidrug-resistance; bioluminescence; antibiotic combination

1. Introduction

Extensive use of antibiotics for the treatment of bacterial infections in humans and animals, for food preservation and in agricultural industries over many decades has resulted in the emergence and increase of multidrug-resistant (MDR) bacteria [1,2]. In particular, MDR ESKAPE (*Enterococcus faecium*, *Staphylococcus aureus*, *Klebsiella pneumoniae*, *Acinetobacter baumannii*, *Pseudomonas aeruginosa* and *E. coli*/*Enterobacter* spp.) pathogens are associated with high mortality rates and increased health care setting costs [3–6]. It is estimated that antimicrobial resistance may cause 10 million deaths per year worldwide,

exceeding the estimated combined deaths from cancers and diabetes and an investment of \$100 trillion US dollars annually after 2050 unless adequately addressed [7].

It is becoming increasingly evident that the golden era of antibiotics for the treatment of MDR bacterial infections has lapsed [8], and the effectiveness of single and combination therapy against MDR ESKAPE pathogens is declining [8,9]. Many recommended antibiotics against ESKAPE pathogens have been withdrawn, and few antibiotics or antibiotic combinations have been added to the Clinical and Laboratory Standards Institute (CLSI) guidelines since 2010 [10]. Alarming, there is an increasing incidence of resistance reported against critically important antibiotics, such as the carbapenems: doripenem, imipenem, meropenem and ertapenem [10,11]. The antimicrobial resistance crisis has been worsened by Gram-negative bacterial (GNB) infections, particularly KAPE infections, as the GNB outer membrane often prevents antibiotics from gaining entry to their site of action [12]. There are several recently approved antibiotics, such as ceftazidime-avibactam, cefiderocol, imipenem + cilastatin + relebactam, and plazomicin, for the treatment of GNB infections [13–17]. However, these antibiotics are far from ideal therapeutic options to fully combat the emergence of MDR GNB infection [18]. Currently, polymyxins (such as polymyxin B (PMB) and colistin) are considered last-resort antibiotics for the treatment of MDR GNB infections particularly due to their specific targeting of the outer membrane [19–21]. Nonetheless, resistance to polymyxins is emerging via multiple mechanisms [19,20,22]. Moreover, many studies have reported that the use of polymyxins is associated with nephrotoxicity, neurotoxicity and neuromuscular blockade [23]. Consequently, it is imperative to find alternative options for the treatment of MDR bacterial infections, particularly those caused by GNB KAPE pathogens [18,24]. Given the current magnitude of MDR infections, international institutions such as the European Union, G20, UN General Assembly, World Bank, World Health Organization (WHO), and the USA and UK governments have issued documents calling for urgent action and development of new antibiotics with novel mechanisms of action against MDR ESKAPE pathogens [25,26].

To address the critical need for new antimicrobials, our team has developed structure-activity data associated with the anticoccidial robenidine (NCL812), used since the 1970s to control coccidiosis in commercial poultry and rabbit production. To date, we have generated > 270 analogues with selected members showing antimicrobial activity [27]. Among these, NCL195 and NCL179 are particularly promising pyrimidine analogues differing in the presence of a methyl group (CH₃) at C4 of the terminal aromatic moieties of NCL195, while NCL179 conserved the original halogen (chlorine) of robenidine (Figure 1).

To date, we have performed several in vitro and in vivo studies that indicate NCL195 is a promising candidate for further pharmaceutical development for the treatment of MDR Gram-positive bacterial (GPB) infections and have shown its in vitro activity against MDR GNB in the presence of sub-inhibitory concentrations of different adjuvants [4,5,28,29]. In particular, the NCL195 + colistin combination has shown efficacy against both colistin-susceptible and -resistant *E. coli* in mouse models (manuscript in preparation). Given the close chemical relationship between NCL195 and NCL179, we postulated that NCL179 is likely to show in vitro and in vivo antimicrobial profiles similar to NCL195 but with potentially unique characteristics, thereby expanding the clinical utility of robenidine analogues. Thus, this study aims to evaluate the in vitro activity of NCL179 against human and animal MDR GPB pathogens, including methicillin-resistant *S. aureus* (MRSA), methicillin-resistant *S. pseudintermedius* (MRSP) and porcine vancomycin-resistant enterococci (VRE), as well as examine its activity against MDR GNB in the presence of sub-inhibitory concentrations of colistin. In addition, the efficacy of NCL179 against GPB was investigated in our validated bioluminescent mouse model of *S. aureus* sepsis.

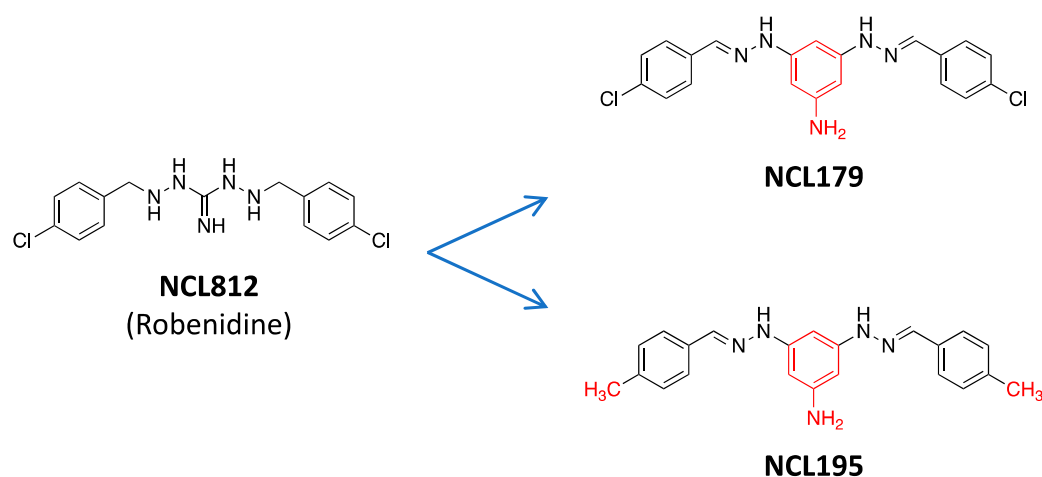


Figure 1. Chemical structures of NCL812 (Robenidine), NCL179 and NCL195. Red colouration highlights the structural changes in NCL179 and NCL195 relative to NCL812. The guanine to triaminopyrimidine novel bioisosteric modification of NCL812 yielded NCL179 (2,2'-bis[(4-chlorophenyl)methylene] carbonimidic dihydrazide) and NCL195 (4,6-bis(2-((E)-4-methylbenzylidene)hydrazinyl)pyrimidin-2-amine). NCL179 contains a halogen (chlorine) that distinguishes it from NCL195.

2. Materials and Methods

2.1. Antimicrobials and Chemicals

NCL179, an analogue of NCL812, was synthesised at the University of Newcastle (Callaghan, NSW, Australia). Amikacin, daptomycin, kanamycin, tetracycline and colistin were purchased from Sigma-Aldrich (Australia). These antibiotics were prepared as 25.6 mg/mL stock solutions as follows: NCL179, tetracycline and daptomycin were dissolved in DMSO while amikacin and kanamycin were dissolved in water. All compounds were aliquoted in 1 mL quantities and stored at $-20\text{ }^{\circ}\text{C}$ in the dark. The NCL179 formulation used in efficacy experiments was prepared as a 50 mg/mL solution in a vehicle at Clinical and Health Sciences, University of South Australia, SA 5000, Adelaide, Australia. Moxifloxacin (drug control) was obtained as Avelox IV 400, 1.6 mg/mL (Bayer, Australia) or prepared in almond oil at 6 mg/kg (BovaVet, Caringbah, NSW, Australia).

2.2. Organisms and Growth Conditions

Clinical MRSP isolates from skin wounds, ears, abscessed joints and dog urine and clinical MRSA isolates were provided by the Australian Centre for Antimicrobial Resistance Ecology (ACARE), School of Animal and Veterinary Sciences, The University of Adelaide, Roseworthy, SA. Vancomycin-resistant enterococci (VRE) were obtained from the University of South Australia collection. Bioluminescent *S. aureus* ATCC 12600 (Xen29; PerkinElmer) was used for the efficacy testing of NCL179. Reference strains *S. aureus* ATCC 29213, *A. baumannii* NCIMB 12457, *A. baumannii* ATCC 19606, *E. coli* ATCC 35218, *E. coli* ATCC 25922, *E. faecalis* ATCC 29212, *K. pneumoniae* ATCC 13883, *K. pneumoniae* ATCC 33495 and *P. aeruginosa* ATCC 27853, PAO1 were obtained from SA Pathology, Adelaide, Australia. Bioluminescent *E. coli* (Xen14, a derivative of *E. coli* WS2572) and bioluminescent *P. aeruginosa* (Xen41, a derivative of strain PAO1) were purchased from PerkinElmer Inc (Waltham, MA, USA). Clinical human *A. baumannii* isolates ($n = 16$) were provided by South Australia Pathology; clinical human *E. coli* isolates ($n = 20$), clinical human *K. pneumoniae* isolates (20) and clinical human *P. aeruginosa* isolates ($n = 22$) were collected from Flinders Medical Centre (Bedford Park, SA, Australia). All bacteria were stored at $-80\text{ }^{\circ}\text{C}$ in Luria–Bertani (LB) broth containing 50% glycerol at the Microbiology laboratory, Level 4, Basil Hetzel building, University of South Australia, SA 5000, Adelaide, Australia.

All bacterial identities were confirmed by matrix-assisted laser desorption/ionisation time-of-flight mass spectroscopy (MALDI-TOF/MS) (microflex[®]LT/SH Biotyper; Bruker Daltonik, Leipzig, Germany) at ACARE prior to antimicrobial susceptibility testing. Bacteria were grown overnight on horse blood agar (HBA) and in LB broth. *E. coli* Xen14 was grown on HBA containing 30 µg/mL kanamycin, *P. aeruginosa* Xen41 was grown on HBA containing 60 µg/mL tetracycline and *S. aureus* Xen29 was grown on HBA containing 200 µg/mL kanamycin. Colistin-resistant Xen14 were generated by daily serial subculture in increasing concentrations of colistin from 0.25 µg/mL to 256 µg/mL over 12–15 days as described previously [28].

2.3. Antimicrobial Susceptibility Testing

The minimum inhibitory concentrations (MIC) for NCL179, daptomycin and amikacin against clinical MRSP, MRSA, VRE and GNB isolates were determined in round-bottom 96-well microtitre plates (Sarstedt 82.1582.001, Nümbrecht, Germany), using the modified broth micro-dilution method recommended by the Clinical and Laboratory Standards Institute [30], as described previously [5]. Briefly, antimicrobial challenge plates were prepared by serial two-fold dilutions of 100× stock solutions (25.6 mg/mL) of NCL179 and daptomycin in DMSO, with the amikacin in water. Each dilution was then further diluted 1:100 in LB broth in 96-well plates. NCL179, daptomycin and amikacin concentrations ranged from 0.03 µg/mL to 256 µg/mL, and each MIC test was carried out in duplicate and performed on two separate occasions. Negative growth control was LB broth only; positive growth control was a bacterial suspension in LB broth. The MICs for NCL179 or daptomycin against Xen29 or *S. aureus* ATCC 29213 in the presence of 10% (vol/vol) foetal bovine serum (FBS) was also examined. The minimum bacterial concentration (MBC) was recorded as the lowest concentration of each test compound, at which a 99.9% colony count reduction was observed on the plate [31].

The interaction between NCL179 and colistin for anti-GNB activity was assessed by a modification of the standard checkerboard assay described previously [32,33]. The antibiotic challenge plates were prepared as described for the MIC testing above. One microliter of NCL179 solution from each combination was dispensed along the abscissa (from row A to F) of the 96-well microtiter plates; the second compound (colistin) was dispensed along the ordinate (from column 3 to column 12) using a 12.5 µL electronic multichannel pipette (VIAFLO Voyager II, Biotools) followed by the addition of 88 µL of LB broth. Thereafter, 10 µL of bacterial suspension was added to each well. One plate was used for each isolate, and the plates were incubated at 37 °C for 20 h and observed visually and by $A_{600\text{nm}}$ measurements. The interaction of two antibiotics was calculated as the fractional inhibitory concentration index (FICI) described previously [32–34]. The dose reduction index (DRI) was used to describe the difference between the effective dose of NCL179 in combination with colistin from the individual dose of each compound [33]. A DRI is beneficial if it is higher than 1. An example of a checkerboard assay of NCL179 + colistin combination against *E. coli* ATCC 35218 is depicted in Figure S1 (Supplementary Materials).

2.4. Time-Dependent Growth Inhibitory Assay

The time- and concentration-dependent activity of NCL179 against one clinical MRSP isolate, one clinical MRSA isolate, one clinical VRE isolate, and against one reference *E. coli* Xen14, one colistin-resistant *E. coli* Xen14, one reference *A. baumannii* strain, one colistin-resistant *A. baumannii* clinical isolate, one reference *P. aeruginosa* strain and one reference *K. pneumoniae* strain in the presence of sub-inhibitory concentrations of colistin was determined in a kinetics assay by optical density ($A_{600\text{nm}}$) measurements for 18 h on a Cytation 5 Multi-Mode Reader (BioTek, Winooski, VT, USA).

2.5. In Vitro Cytotoxicity Assays

We assayed NCL179 alone and in combination with colistin at 0.5 µg/mL for in vitro cytotoxicity using a panel of adherent mammalian cell lines: Hep G2 (human hepatocel-

lular carcinoma cell line) and HEK293 (human embryonic kidney cell line) as described previously [28]. Briefly, cell lines were maintained in Dulbecco's Modified Eagle's Medium (DMEM; Gibco Cat No: 12430, Thermo Fisher Scientific, SA, Australia) supplemented with 10% FBS and 1% PenStrep (100 U/mL Penicillin and 100 µg/mL Streptomycin) at 37 °C, 5% CO₂ and passaged every three days. Assays were performed in duplicates in black flat-bottom 96-well tissue culture trays (Eppendorf Cat No: 0030741013, Hamburg, Germany) seeded with $\sim 1.5 \times 10^4$ cells per well. After 24 h incubation, the media was removed, the cells were washed once with a medium without antibiotics, and the fresh medium supplemented with 10% (*v/v*) FBS was added. Then, either NCL179 alone or in combination with colistin was added to each well in doubling dilutions starting at the same concentrations used for MIC testing, using wells containing 1% DMSO only, colistin alone at 0.5 µg/mL and 64 µg/mL ampicillin as controls. The viability of each cell line in the presence of NCL179 alone, NCL179 + colistin combination or colistin alone (using 1% DMSO only and 64 µg/mL ampicillin as controls) was assessed at 1 h intervals for 20 h at 37 °C, 5% CO₂ on a Cytation 5 Cell Imaging Multi-Mode Reader (BioTek, Winooski, VT, USA) using the RealTime-Glo TM MT Cell Viability Assay reagent (Promega, Madison, WI, USA).

2.6. Hemolysis Assay

The potential for NCL179 to lyse red blood cells (RBCs) was examined on fresh donor human RBCs using serial 2-fold dilutions of NCL179 (starting at 128 µg/mL) in quadruplicates in a round-bottom 96-well microtiter plate (Sarstedt 82.1582.001, Nümbrecht, Germany) according to the protocol described previously [28]. Serial 2-fold dilutions of ampicillin (starting at 128 µg/mL), 1% Triton X100 or PBS only served as controls. The experiment was carried out on two separate occasions using different fresh donor human RBCs. The hemolytic titer for NCL179 was determined as the reciprocal of the dilution at which 50% of erythrocytes were lysed as determined at $A_{450\text{nm}}$.

2.7. Ethics Statements

Outbred 5 to 6-week-old male CD1 (Swiss) mice (weighing between 25 g to 30 g), obtained from the Laboratory Animal Services breeding facility of the University of Adelaide, were used to test the safety of NCL179 and assess its efficacy against *S. aureus*. The mice had access to food and water *ad libitum*. The Animal Ethics Committee of The University of Adelaide (approval number S-2015-151) reviewed and approved all animal experiments. The study was conducted in compliance with the Australian Code of Practice for the Care and Use of Animals for Scientific Purposes (8th Edition 2013) and the South Australian Animal Welfare Act 1985.

2.8. Safety Testing of NCL179 Following Oral Administration to Mice

In order to ascertain that two oral doses (8 h apart) or four oral doses (4 h apart) of either 10 mg/kg or 50 mg/kg NCL179 would be safe to administer to the mice, safety studies were conducted using oral administrations of 10 mg/kg or 50 mg/kg of NCL179 to three mice, using the vehicle (20% [*v/v*] DMSO in PEG400) as a control. The mice were observed for clinical signs (weight loss, dull/ruffled coat, poor posture, pale or sunken eyes, change in behaviour, dehydration, bleeding from the orifice, diarrhoea, breathing and reluctance to move) and the data recorded on a Clinical Record Sheet approved by the Animal Ethics Committee of The University of Adelaide. At the conclusion of the experiment, the mice were humanely killed, and sections of the heart, lung, liver, kidneys, spleen, stomach and small and large intestines were collected and subjected to histopathological examination.

2.9. Agar Well Diffusion Method

The NCL179 and moxifloxacin (drug control) formulations were tested for antibacterial activity using the agar well diffusion method to ensure that the drugs were released from the vehicle as a reference for the interpretation of in vivo activity in mice. For this assay, a few colonies of an overnight HBA culture of Xen29 were suspended in saline equivalent to 0.5 McFarland standard ($A_{600\text{nm}} = 0.1$). A sterile swab was then dipped in the 0.5 McFarland standard bacterial suspension and used to streak over the entire surface of a sterile plate count agar plate. Punch holes were then made on the agar plates using an 8 mm diameter biopsy punch (Livingstone International Pty Ltd., Sydney, NSW, Australia), and a 30 μL amount of the NCL179 formulation equivalent to a single treatment dose in mice was placed in the well. The antimicrobial activity of each drug was then determined by measuring and comparing the zone of inhibition with that of the vehicle only.

2.10. Histopathological Examination

Mouse organs (heart, lung, stomach, liver, spleen and small and large intestine) collected from the oral safety experiment were fixed in 10% neutral-buffered formalin (Chem-Supply Australia Pty Ltd., Gillman, SA, Australia) and processed routinely, embedded in paraffin blocks and sectioned to a thickness of 4 μm . The hematoxylin and eosin-stained sections were observed and recorded under light microscopy. Photomicrographs were captured using a DP25 camera and LabSens software (Olympus, Tokyo, Japan).

2.11. Oral Efficacy Testing of NCL179 Following Systemic Challenge of Mice with Bioluminescent *S. aureus*

For efficacy testing experiments of NCL179 against *S. aureus*, mouse-passaged Xen29 was used. Bacteria were grown in LB broth at 37 °C to $A_{600\text{nm}}$ of 0.5 (equivalent to approximately 1.5×10^8 CFU/mL). Three groups of mice ($n = 6$ mice per group) were challenged intraperitoneally (IP) with approximately 3×10^7 CFU of Xen29 in 200 μL PBS containing 3% hog gastric mucin-type III (Sigma Aldrich, St. Louis, MO, USA) and immediately imaged in both ventral and dorsal positions on the IVIS Lumina XRMS Series III system. Immediately thereafter, the mice in group 1 were orally administered with the vehicle, the mice in group 2 received oral NCL179 at 50 mg/kg, while the mice in group 3 received oral moxifloxacin at 6 mg/kg. The clinical conditions of all mice were closely monitored, and all mice were imaged at 2 h post-infection. In a preliminary investigation, a two-dose regime was designed for NCL179 such that the second dose was to be administered at 8 h post-infection with vehicle and moxifloxacin treatments given at 4 h, 8 h and 12 h post-infection. In a subsequent experiment, a four-dose regime was designed such that the 2nd, 3rd and 4th doses of the vehicle, NCL179 and moxifloxacin were given to the surviving mice in group 1, group 2 and group 3 at 4 h, 8 h and 12 h, respectively. At 4 h, 6h and 10 h post-infection, all surviving animals in each group were imaged. The mice were frequently monitored for signs of distress, and those that had become moribund or showed any evidence of distress were humanely killed by cervical dislocation. At 18 h, 24 h, 28 h, 36 h, 48 h and 72 h post-infection, the surviving mice were monitored and further subjected to bioluminescence imaging. At all imaging time points, signals were collected from a defined region of interest, and the total flux intensities (photons/s) were analyzed using Living Image Software 4.7.2. Differences in median survival times (time to moribund) for mice between groups were analyzed by the log-rank (Mantel-Cox) tests. Differences in luminescence signals between groups were compared by Mann-Whitney *U*-tests, two-tailed.

3. Results

3.1. NCL179 Shows In Vitro Activity against Gram-Positive Pathogens and also against Gram-Negative Pathogens in the Presence of Sub-Inhibitory Concentrations of Colistin

The antimicrobial activity of NCL179 was tested against GPB reference strains and clinical isolates, including 20 MRSA, 2 methicillin-sensitive *S. aureus* (ATCC 12600

[Xen29] and ATCC 29213), 20 MRSP, 20 VRE and 1 *E. faecalis* ATCC 29212. NCL179 showed MIC/MBCs of 1–2 µg/mL against MRSA and MRSP, MIC/MBCs 2–4 µg/mL against VRE compared to drug controls daptomycin (MIC/MBCs 0.5–2 µg/mL vs MRSA and VRE) and amikacin (MIC/MBCs 8–16 µg/mL vs MRSP) (Table 1). The MIC for NCL179 against Xen29 and *S. aureus* ATCC 29213 increased to 16 µg/mL in the presence of 10% FBS (Supplementary Materials Table S1).

Table 1. In vitro activity of NCL179 against Gram-positive ATCC strains and clinical isolates.

| Strain/Isolate | ¹ MIC and ² MBC Range (µg/mL) | | |
|------------------------------------|---|-----------------|----------|
| | NCL179 | Daptomycin | Amikacin |
| ³ MRSA (<i>n</i> = 20) | 1–2 | 0.5–2 | ND |
| ⁴ MSSA (<i>n</i> = 2) | 1 | 0.5 | ND |
| ⁵ MRSP (<i>n</i> = 20) | 1–2 | ⁷ ND | 8–16 |
| ⁶ VRE (<i>n</i> = 20) | 2–4 | 0.5–2 | ND |

¹ MIC, minimum inhibitory concentration; ² MBC, minimum bactericidal concentration; ³ MRSA, methicillin-resistant *S. aureus*; ⁴ MSSA, methicillin-sensitive *S. aureus*; ⁵ MRSP, methicillin-resistant *S. pseudintermedius*; ⁶ VRE, vancomycin-resistant enterococci; and ⁷ ND, not determined. *E. faecalis* ATCC 29212 was used as a control Gram-positive strain, and it returned MIC and MBC values of 4 µg/mL for NCL179 and MIC and MBC values of 2 µg/mL for daptomycin.

The activity of the NCL179 + colistin combination was tested against GNB reference strains and clinical isolates (18 *A. baumannii*, 24 *E. coli*, 22 *K. pneumoniae* and 25 *P. aeruginosa*), and the results are presented in Table 2. NCL179 alone had no activity against GNB; therefore, its MIC was nominally taken as 256 µg/mL (the highest concentration tested) for FICI and DRI calculations. The MIC range of colistin alone against GNB was as follows: *A. baumannii* (0.5–2 µg/mL); colistin-resistant *A. baumannii* (64–128 µg/mL); *E. coli* (0.125–0.5 µg/mL); colistin-resistant *E. coli* (32 µg/mL); *K. pneumoniae* (0.25–2 µg/mL) and *P. aeruginosa* (0.25–2 µg/mL). However, for the NCL179 + colistin combination, the MIC range of NCL179 was 0.5–4 µg/mL against all tested GNB, whereas the MIC range of colistin was 0.008–0.5 µg/mL against *A. baumannii*, 0.5–1 µg/mL against colistin-resistant *A. baumannii*, 0.008–0.125 µg/mL against *E. coli*, 0.5 µg/mL against colistin-resistant *E. coli* and 0.015–0.5 µg/mL against *K. pneumoniae* and *P. aeruginosa*. The FICI of the NCL179 + colistin combination against all GNB showed synergistic activity, and all DRIs were beneficial (Table 2).

Table 2. Synergistic activity of NCL179 in combination with colistin against reference strains and clinical isolates of Gram-negative bacteria.

| Strain/Isolate | ¹ MIC Range (µg/mL) | | | | ² FICI | ³ DRI | |
|--|--------------------------------|--------|-------------|--------|-------------------|------------------|--------|
| | Single Antibiotic | | Combination | | | Colistin | NCL179 |
| | Colistin | NCL179 | Colistin | NCL179 | | | |
| <i>A. baumannii</i> (<i>n</i> = 14) | 0.5–2 | >256 | 0.008–0.5 | 0.5–4 | 0.016–0.25 * | 4–64 | 64–512 |
| Colistin-resistant <i>A. baumannii</i> (<i>n</i> = 4) | 64–128 | >256 | 0.5–1 | 1–4 | 0.008 * | 64–128 | 64–256 |
| <i>E. coli</i> (<i>n</i> = 23) | 0.125–0.5 | >256 | 0.008–0.125 | 0.5–4 | 0.064–0.25 * | 4–16 | 64–512 |
| Colistin-resistant <i>E. coli</i> (<i>n</i> = 1) | 32 | >256 | 0.5 | 2 | 0.016 * | 64 | 128 |
| <i>K. pneumoniae</i> (<i>n</i> = 22) | 0.25–2 | >256 | 0.015–0.5 | 0.5–4 | 0.06–0.25 * | 4–16 | 64–512 |
| <i>P. aeruginosa</i> (<i>n</i> = 25) | 0.25–2 | >256 | 0.015–0.5 | 0.5–4 | 0.06–0.25 * | 4–16 | 64–512 |

¹ MIC, minimum inhibitory concentration; ² FICI, fractional inhibitory concentration index: * synergistic, FICI ≤ 0.5; additive or partially synergistic, 0.5 < FICI ≤ 1; indifferent, 1 < FICI ≤ 4; and antagonistic, FICI > 4; ³ DRI, dose reduction index. Bioluminescent *S. aureus* Xen29 was used as control each time the MIC and checkerboard assays were performed; the MIC of NCL179 against *S. aureus* Xen29 in each of these assays was 1 µg/mL.

3.2. NCL179 Exhibits Time- and Concentration-Dependent Kill Kinetics of Bacterial Growth

A time-kill kinetics assay was used to measure the time- and concentration-dependent activity of NCL179 against clinical MRSA isolate QLDpvl+, clinical MRSP isolate VDL1290

and clinical VRE isolate 49FR (Figure 2). Daptomycin was used as a drug control for the MRSA and VRE kill kinetics assay, while amikacin was used as a control drug for the MRSP kill kinetics assay. Our results show that NCL179 exhibited a time- and concentration-dependent killing of the bacteria as observed for the bactericidal control drugs.

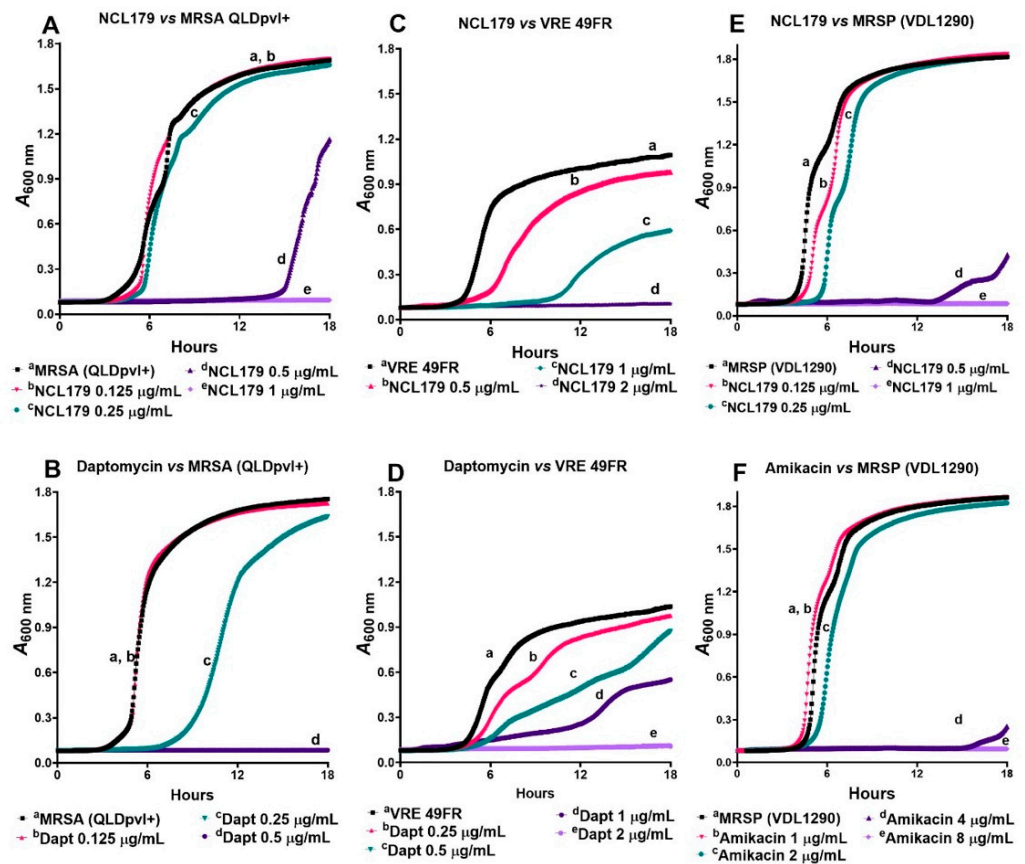


Figure 2. Time- and concentration-dependent kill kinetics of NCL179 against Gram-positive bacteria. (A), against MRSA QLDpvl+; (C), against VRE 49R; and (E), against MRSP (VDL1290) using daptomycin (B,D) and amikacin (F) as control drugs.

The time- and concentration-dependent activity of NCL179 + colistin combinations against GNB was also investigated in the kinetics assay using *A. baumannii* ATCC 19606, colistin-resistant clinical *A. baumannii* 246-53D, *E. coli* Xen14, colistin-resistant *E. coli* Xen14, *K. pneumoniae* ATCC 33495 and *P. aeruginosa* Xen41 (Figures 3 and S2). The results indicate that, in each case, the NCL179 + colistin combination worked faster than colistin alone at the corresponding concentration. In addition, the NCL179 + colistin combination killed GNB, whereas cells treated with colistin alone at the corresponding concentrations still grew. As expected, NCL179 alone was not active against any of the GNB.

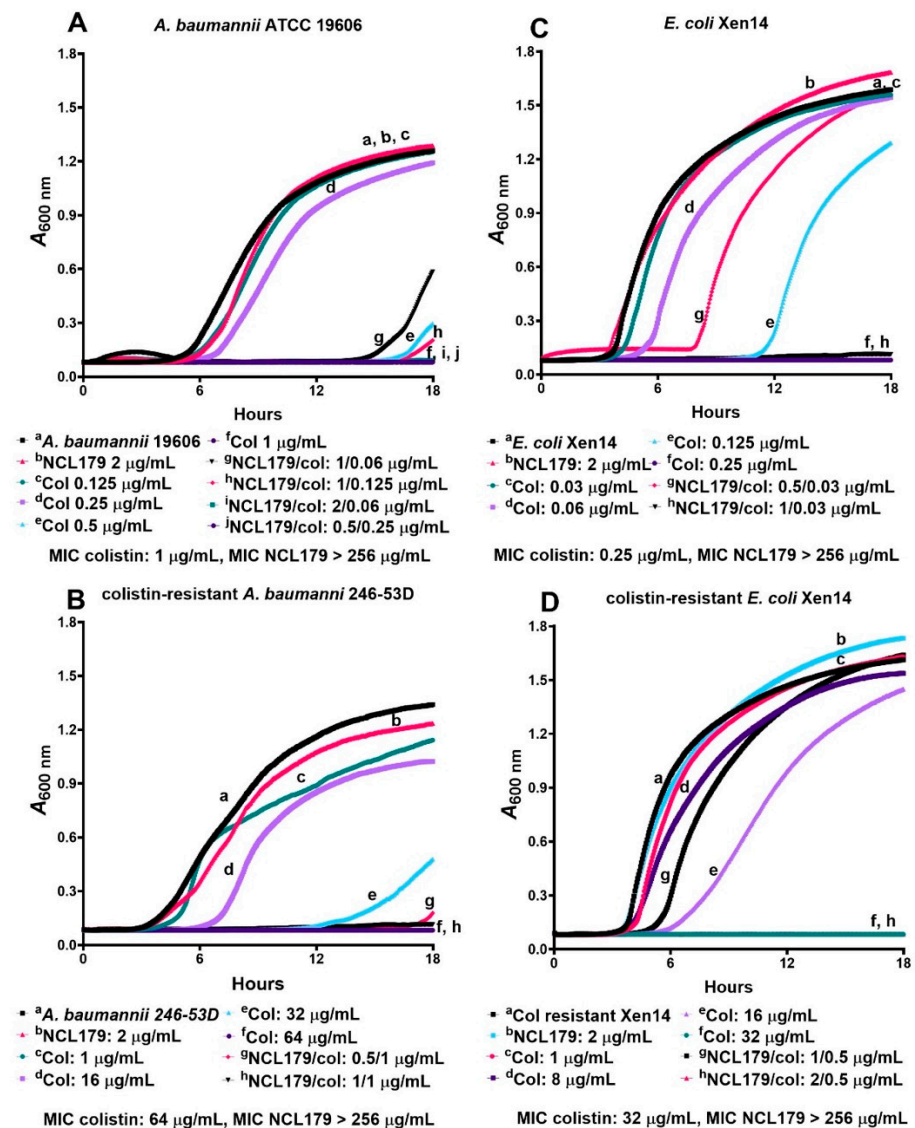


Figure 3. Time-and-concentration-dependent kill kinetics of NCL179 alone and in combination with colistin against Gram-negative bacteria. (A), NCL179 alone or in combination with colistin against *A. baumannii* ATCC 19606; (B), clinical colistin-resistant *A. baumannii* 246-53D; (C), *E. coli* Xen14; and (D), colistin-resistant *E. coli* Xen14. The concentrations of NCL179 and colistin for each combination were chosen based on data presented in Table 2. Assays were performed on a Cytation 5 Multi-Mode Reader (BioTek, Winooski, VT, USA) by optical density ($A_{600\text{nm}}$) measurements; Col, colistin.

3.3. Combination of NCL179 and Colistin Shows Limited Cytotoxicity to Mammalian Cell Lines

The effects of various concentrations of NCL179 alone or in combination with 0.5 µg/mL colistin to Hep G2 (liver) and HEK293 (kidney) cell lines were examined in an in vitro cell toxicity assay. The results indicate an IC_{50} value of 16 µg/mL for NCL179 at the concentrations tested. In addition, the presence of colistin in the combination did not alter the IC_{50} value (Figure 4).

The hemolytic titer (HC_{50}) for NCL179 was 32 µg/mL to human RBCs, whereas the HC_{50} for ampicillin was >128 µg/mL (the highest concentration used).

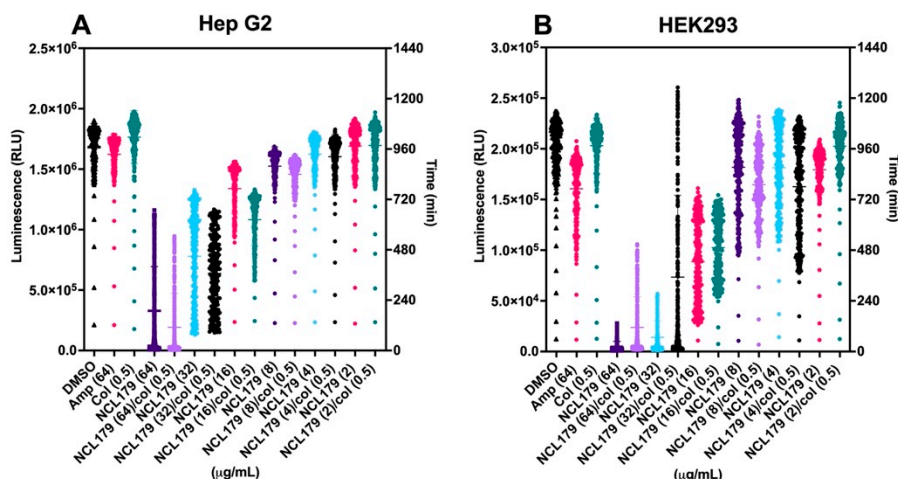


Figure 4. In vitro toxicity assessment of NCL179 alone and in combination with colistin. Real-time cell viability measurement for Hep G2 (A) and HEK293 (B) cells after treatment with different concentrations of NCL179 alone and in combination with 0.5 $\mu\text{g}/\text{mL}$ of colistin. The cell viability was determined using the RealTime-GloTM MT Cell Viability Assay reagent (Promega, Madison, WI, USA) and measured every hour for 20 h at 37 °C in 5% CO₂ on a Cytation 5 Cell Imaging Multi-Mode Reader (BioTek, BioTek, Winooski, VT, USA). Data are relative light units (RLU) for each treatment per time point; col, colistin; Amp, ampicillin.

3.4. Agar Well Diffusion Shows NCL179 Remains Active in Formulations

In order to ascertain that NCL179 retained its antimicrobial activity when formulated in the vehicle (20% [*v/v*] DMSO in PEG400), an agar diffusion test was performed. The formulations of NCL179 formed an inhibitory zone of 15 mm (Figure 5), indicating that NCL179 was released from the vehicle into the agar.

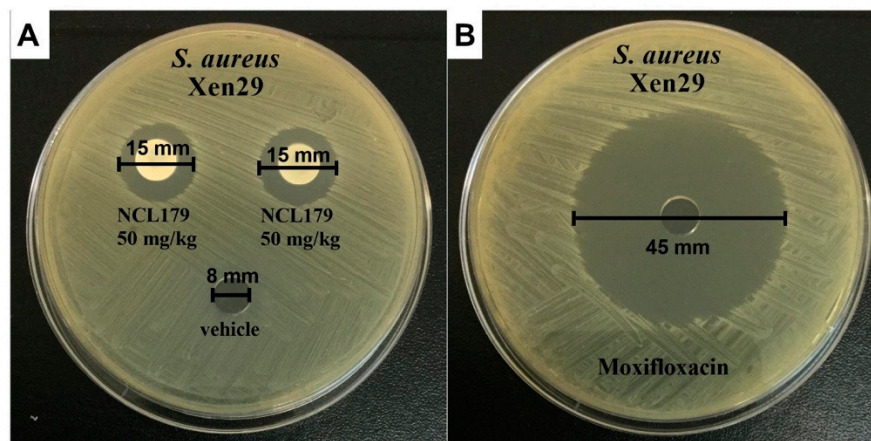


Figure 5. Selected well diffusion of NCL179 used in the efficacy trial. (A), to each well, 30 μL of either NCL179 formulation or vehicle only was added; (B), 30 μL of moxifloxacin (BovaVet, Caringbah, NSW, Australia). Concentrations of NCL179 in formulations were prepared as a 50 mg/mL solution to achieve 50 mg/kg in mice (30 g); moxifloxacin is a drug control and was prepared as a 6 mg/mL solution to achieve 6 mg/kg in mice (30 g); Xen29, *S. aureus* Xen29.

3.5. Oral Administration of NCL179 Shows Systemic Safety in Mice

There were no observable histopathological changes in the heart, lung, liver, spleen, stomach, kidneys and small and large intestines of mice orally treated with two doses of 10 mg/kg or 50 mg/kg NCL179 at 8 h apart (Figure 6A) or four doses of 10 mg/kg

or 50 mg/kg NCL179 at 4 h apart (Figure 6B) in comparison with the vehicle at 72 h post-initial treatment.

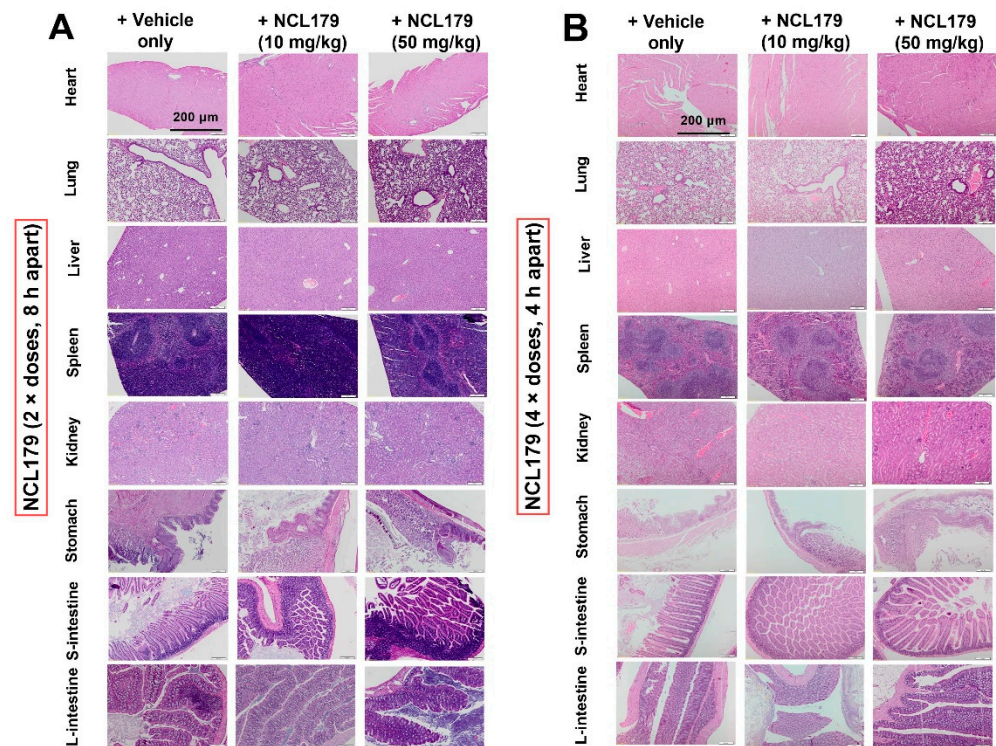


Figure 6. Representative histological images of heart, lung, liver, stomach, spleen, kidney and small and large intestines from NCL179-treated and vehicle-treated mice. No histopathological changes were observed in mice treated orally with (A), 10 mg/kg, 50 mg/kg (2 × doses, 8 h apart), or (B), with 10 mg/kg, 50 mg/kg (4 × doses, 4 h apart) of NCL179 in comparison with vehicle. S-intestine, small intestine; L-intestine, large intestine. Scale bars: 200 μm.

3.6. Oral Treatment of Mice with NCL179 Reduces *S. aureus* Populations and Significantly Prolongs Survival Times

The potential of NCL179 as an oral therapeutic drug against systemic *S. aureus* infection was examined in an IP sepsis challenge mouse model using a well-characterized bioluminescent *S. aureus* strain (Xen29). Our preliminary investigations showed that an 8 h gap between the first and second NCL179 treatment was suboptimal as all mice treated with the first dose of NCL179 had succumbed to infection by the 8 h time point, similar to the vehicle-only treated group (Figure S3).

In a subsequent experiment, four oral doses of NCL179 at 4 h apart showed good efficacy (Figure 7). After the second NCL179 dose (at 4 h post-infection), there was a statistically significant reduction in *S. aureus* photon counts when measured at 6 h (*, $p < 0.05$, Mann-Whitney *U*-test, two-tailed). After a third NCL179 dose (at 8 h post-infection), *S. aureus* photon counts continued to reduce significantly when measured at 10 h (**, $p < 0.01$, Mann-Whitney *U*-test, two-tailed) (Figure 7A). The treatment of mice with four oral doses of NCL179 at 4 h apart also resulted in a significant increase in median survival time compared to the vehicle-only control (* $p < 0.05$; Mantel-Cox test; Figure 7B). The bacterial reduction caused by the different treatments could be clearly observed on bioluminescent images of the mice (Figure 7C).

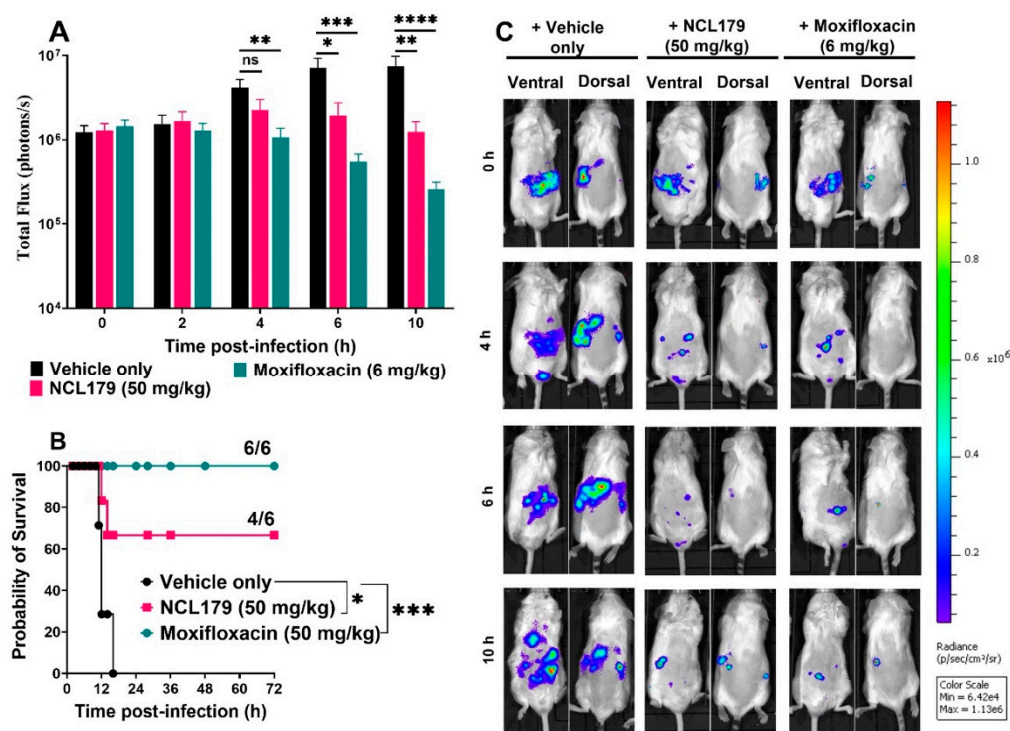


Figure 7. Oral efficacy of 4 doses of NCL179 given 4 h apart in a bioluminescent *S. aureus* Xen29 sepsis mouse model. (A), Comparison of luminescence signals between groups of CD1 mice ($n = 6$) challenged IP with Xen29 and treated with NCL179, moxifloxacin and vehicle at 0 h, 4 h, 8 h and 12 h post-infection. Mice were subjected to bioluminescence imaging on IVIS Lumina XRMS Series III system at the indicated times (ns, no significant; *, $p < 0.05$; **, $p < 0.01$; ***, $p < 0.0002$, ****, $p < 0.0001$, Mann-Whitney U -test, two-tailed). (B), Survival analysis for mice treated with NCL179, moxifloxacin and vehicle (ns, no significant; *, $p < 0.05$; ***, $p < 0.0002$; Log-rank (Mantel-Cox test)). (C), Ventral and dorsal images of representative CD1 mice challenged with approx. 3×10^7 CFU of bioluminescent *S. aureus* ATCC 12600 (Xen29). Moxifloxacin used as a control drug was prepared in almond oil at 6 mg/mL by BovaVet, Australia.

4. Discussion

The increasing resistance of ESKAPE pathogens to commonly used antimicrobials in health care settings has led to a decrease in treatment options and continues to generate a high level of global public health concern [10]. Therefore, there is an urgent need to develop new broad-spectrum antimicrobials with activity against pan-resistant ESKAPE, particularly GNB pathogens, with a novel approach to overcoming the permeability barrier of the GNB outer membrane [12,25,35–37]. In this study, we demonstrate that a second robenidine analogue, NCL179, has the potential for further development as a future treatment for bacterial infections based on three major findings. Firstly, NCL179 demonstrated potent antimicrobial activity against a variety of GPB pathogens and also against GNB pathogens in the presence of a sub-inhibitory concentration of colistin. Secondly, NCL179 showed limited in vitro toxicity to mammalian cell lines, showed low hemolytic activity to human erythrocytes and demonstrated systemic safety in mice with no observed morphological effects on the major organs examined. Thirdly, the oral treatment of mice with NCL179 reduced *S. aureus* populations in vivo and significantly prolonged survival times.

In clinical settings, bacterial co-infection and superinfections are common, reducing treatment options [38], while the use of broad-spectrum antibiotics is advantageous for wider coverage of GNB and GPB pathogens [39]. In this study, we demonstrated that NCL179 showed bacterial activity against a wide range of clinical MDR GPB pathogens, including MRSA, MRSP and VRE. Importantly, a combination of NCL179 with sub-inhibitory

concentrations of colistin resulted in a synergistic interaction against many GNB clinical isolates and reference strains, including *A. baumannii*, *E. coli*, *K. pneumoniae* and *P. aeruginosa* on the critical WHO priority list of bacteria for which new antibiotics are urgently needed [25,40].

The outer membrane is a distinctive feature of GNB that provides a barrier protecting GNB from exposure to unwanted chemical compounds, resulting in limited treatment options [12,41]. Among several proposed therapies for the further treatment of GNB infections [42,43], a combination of colistin with other antibiotics is considered a potential approach associated with overcoming the outer membrane permeability barrier, a broader antibacterial spectrum, synergistic effects and reduced risk for emerging resistance during therapy [20,44,45]. In addition, many studies have demonstrated that, in contrast to monotherapy, combination therapy may enhance antimicrobial effects and provide synergism [46–50]. In this study, the NCL179 + colistin combination showed synergistic activity against all tested GNB pathogens, including colistin-resistant *A. baumannii* and *E. coli* isolates, comparable to other synergy reports of combining colistin with other antibiotics [44,46,51]. In addition, it has been suggested that IV colistimethate sodium monotherapy may not be an optimal option if the MIC against GNB pathogens is higher than 1 µg/mL [46,52]. However, our results indicate that the MICs of colistin are from 0.008–1 µg/mL (representing a 4–128-fold dose reduction) in combination with NCL179. These results suggest that a combination of NCL179 with sub-inhibitory concentrations of colistin could potentially increase activity against colistin-resistant KAPE and other GNB. The combination could also reduce colistin toxicity levels, lower the likelihood of resistance development and decrease treatment time while increasing overall survival rate, as suggested by similar in vitro and in vivo models and analytical frameworks [53–56]. Therefore, the synergistic effect of NCL179 in combination with colistin is a promising development for a new chemical class scaffold to treat GNB infections.

The stringent criteria of a successful antibiotic require a balance between high in vivo efficacy and broad-spectrum antibacterial activity and safety to host targets (humans and animals) [57]. Here, we demonstrated the limited toxicity of NCL179 to mammalian cell lines, its low hemolytic activity, in vivo safety in mice, as well as the significant reduction in *S. aureus* populations in vivo and prolonged survival times of NCL179-treated mice. This opens the possibility of exploring NCL179 for human use after further testing in animal models of infection and chemical modification to identify more potent isosteres. Interestingly, the MIC of NCL179 against *S. aureus* increases 16-fold in the presence of 10% FBS, suggesting a high level of protein binding, which could result in a low free NCL179 concentration in plasma, thereby limiting its systemic bioavailability. Nonetheless, this does not appear to have completely limited its effectiveness. Therefore, detailed pharmacokinetic studies of NCL179 in appropriate models need to be investigated, and the chemical modification of NCL179 is desirable to reduce plasma binding and potential toxicity and improve potency against the MDR pathogens. Together, this study demonstrates that NCL179 is a potential new chemical entity for further pharmaceutical development for the treatment of ESKAPE pathogens, either alone or in combination with existing antibiotic classes.

5. Conclusions

In this study, we demonstrated the in vitro antimicrobial activity of NCL179 against GPB and GNB in the presence of a sub-inhibitory concentration of colistin. The combination of NCL179 + colistin is expected to be another promising therapeutic option for the treatment of drug-resistant bacteria that pose the greatest health threats, particularly in the era of colistin-resistant GNB infections. By showing that the NCL179 + low dose colistin combination could safely and effectively overcome resistance to monotherapy with colistin, NCL179 provides a good example of the “5R” antimicrobial stewardship element, “Refinement” (5Rs: Responsibility, Reduction, Refinement, Replacement and Review) [58].

Supplementary Materials: The following are available online at <https://www.mdpi.com/article/10.3390/antibiotics11010065/s1>, Figure S1: Representative checkerboard assay of NCL179 + colistin combination against *E. coli* ATCC 35218, Figure S2: Time- and concentration-dependent kill kinetics of NCL179 alone and in combination with colistin against Gram-negative bacteria; Figure S3: Oral efficacy of NCL179 (2 × doses, 8 h apart) in a bioluminescent *S. aureus* (Xen29) mouse sepsis model, Table S1: Effect of serum on in vitro activity of NCL179 against *S. aureus*.

Author Contributions: Conceptualization, H.T.N., A.M., S.G., S.W.P., D.J.T. and A.D.O.; Data curation, H.T.N., K.Y. and A.D.O.; Formal analysis, H.T.N., H.V., L.W., D.J.T. and A.D.O.; Funding acquisition, H.V., A.M., S.W.P. and D.J.T.; Investigation, H.T.N. and A.D.O.; Methodology, H.T.N., K.Y. and A.D.O.; Supervision, A.M., S.G. and D.J.T.; Validation, A.M., D.J.T. and A.D.O.; Visualization, H.T.N., L.W. and S.W.P.; Writing—original draft, H.T.N.; Writing—review & editing, H.T.N., H.V., L.W., K.Y., A.M., S.G., S.W.P., D.J.T. and A.D.O. All authors have read and agreed to the published version of the manuscript.

Funding: This work was supported by an Australian Research Council (ARC; arc.gov.au, accessed on 30 November 2021) Linkage grant (LP110200770) to D.J.T., A.M. and S.W.P. with Neoculi Pty Ltd. as the Partner Organization and the University of South Australia fund to H.V. The funders did not have any additional role in the study design, data collection and analysis, decision to publish or preparation of the manuscript.

Institutional Review Board Statement: The Animal Ethics Committee of The University of Adelaide (approval number S-2015-151) reviewed and approved all animal experiments. The study was conducted in compliance with the Australian Code of Practice for the Care and Use of Animals for Scientific Purposes (8th Edition 2013) and the South Australian Animal Welfare Act 1985.

Informed Consent Statement: Not applicable.

Data Availability Statement: The data presented in this study are available on request from the corresponding authors. The data are not publicly available due to privacy and access restrictions.

Acknowledgments: The authors would like to thank Amanda Kenyon, Lora Bowes, Anh Hong Nguyen and Max McClafferty at the University of South Australia for their technical assistance, Cheryl Day at the School of Veterinary and Animal Sciences for sample processing of histopathology examination and May Song and Krishna Kathwala at the University of South Australia for preparing NCL179 formulations.

Conflicts of Interest: Stephen W. Page is a director of Neoculi Pty. Ltd. Darren J. Trott and Adam McCluskey have received research funding from Neoculi Pty. Ltd.

References

1. Michael, C.A.; Dominey-Howes, D.; Labbate, M. The antimicrobial resistance crisis: Causes, consequences, and management. *Front. Public Health* **2014**, *2*, 145. [[CrossRef](#)] [[PubMed](#)]
2. Merker, M.; Tueffers, L.; Vallier, M.; Groth, E.E.; Sonnenkalb, L.; Unterweger, D.; Baines, J.F.; Niemann, S.; Schulenburg, H. Evolutionary Approaches to Combat Antibiotic Resistance: Opportunities and Challenges for Precision Medicine. *Front. Immunol.* **2020**, *11*, 1938. [[CrossRef](#)] [[PubMed](#)]
3. Pendleton, J.N.; Gorman, S.P.; Gilmore, B.F. Clinical relevance of the ESKAPE pathogens. *Expert Rev. Anti-Infect. Ther.* **2013**, *11*, 297–308. [[CrossRef](#)]
4. Nguyen, H.T.; Venter, H.; Veltman, T.; Williams, R.; O'Donovan, L.A.; Russell, C.C.; McCluskey, A.; Page, S.W.; Ogunniyi, A.D.; Trott, D.J. In vitro synergistic activity of NCL195 in combination with colistin against Gram-negative bacterial pathogens. *Int. J. Antimicrob. Agents* **2021**, *57*, 106323. [[CrossRef](#)] [[PubMed](#)]
5. Pi, H.; Nguyen, H.T.; Venter, H.; Boileau, A.R.; Woolford, L.; Garg, S.; Page, S.W.; Russell, C.C.; Baker, J.R.; McCluskey, A.; et al. In vitro Activity of Robenidine Analog NCL195 in Combination with Outer Membrane Permeabilizers against Gram-Negative Bacterial Pathogens and Impact on Systemic Gram-Positive Bacterial Infection in Mice. *Front. Microbiol.* **2020**, *11*, 1556. [[CrossRef](#)]
6. Talbot, G.H.; Jezek, A.; Murray, B.E.; Jones, R.N.; Ebright, R.H.; Nau, G.J.; Rodvold, K.A.; Newland, J.G.; Boucher, H.W. The Infectious Diseases Society of America's 10 × '20 Initiative (10 New Systemic Antibacterial Agents US Food and Drug Administration Approved by 2020): Is 20 × '20 a Possibility? *Clin. Infect. Dis.* **2019**, *69*, 1–11. [[CrossRef](#)]
7. O'Neill, J. *Tackling Drug-Resistant Infections Globally: Final Report and Recommendations*; Review on Antimicrobial Resistance: London, UK, 2016; pp. 1–84.
8. Ma, Y.X.; Wang, C.Y.; Li, Y.Y.; Li, J.; Wan, Q.Q.; Chen, J.H.; Tay, F.R.; Niu, L.N. Considerations and Caveats in Combating ESKAPE Pathogens against Nosocomial Infections. *Adv. Sci.* **2020**, *7*, 1901872. [[CrossRef](#)]

9. Bassetti, M.; Peghin, M.; Vena, A.; Giacobbe, D.R. Treatment of Infections Due to MDR Gram-Negative Bacteria. *Front. Med.* **2019**, *6*, 74. [[CrossRef](#)]
10. Mulani, M.S.; Kamble, E.E.; Kumkar, S.N.; Tawre, M.S.; Pardesi, K.R. Emerging Strategies to Combat ESKAPE Pathogens in the Era of Antimicrobial Resistance: A Review. *Front. Microbiol.* **2019**, *10*, 539. [[CrossRef](#)]
11. Sheu, C.-C.; Chang, Y.-T.; Lin, S.-Y.; Chen, Y.-H.; Hsueh, P.-R. Infections Caused by Carbapenem-Resistant Enterobacteriaceae: An Update on Therapeutic Options. *Front. Microbiol.* **2019**, *10*, 80. [[CrossRef](#)]
12. Zgurskaya, H.I.; Lopez, C.A.; Gnanakaran, S. Permeability barrier of Gram-negative cell envelopes and approaches to bypass it. *ACS Infect. Dis.* **2015**, *1*, 512–522. [[CrossRef](#)]
13. Sims, M.; Mariyanovski, V.; McLeroth, P.; Akers, W.; Lee, Y.C.; Brown, M.L.; Du, J.; Pedley, A.; Kartsonis, N.A.; Paschke, A. Prospective, randomized, double-blind, Phase 2 dose-ranging study comparing efficacy and safety of imipenem/cilastatin plus relebactam with imipenem/cilastatin alone in patients with complicated urinary tract infections. *J. Antimicrob. Chemother.* **2017**, *72*, 2616–2626. [[CrossRef](#)]
14. Powles, M.A.; Galgoci, A.; Misura, A.; Colwell, L.; Dingley, K.H.; Tang, W.; Wu, J.; Blizzard, T.; Motyl, M.; Young, K. In Vivo Efficacy of Relebactam (MK-7655) in Combination with Imipenem-Cilastatin in Murine Infection Models. *Antimicrob. Agents Chemother.* **2018**, *62*, e02577-17. [[CrossRef](#)]
15. Smith, J.R.; Rybak, J.M.; Claeyss, K.C. Imipenem-Cilastatin-Relebactam: A Novel β -Lactam- β -Lactamase Inhibitor Combination for the Treatment of Multidrug-Resistant Gram-Negative Infections. *Pharmacotherapy* **2020**, *40*, 343–356. [[CrossRef](#)] [[PubMed](#)]
16. Titov, I.; Wunderink, R.G.; Roquilly, A.; Rodríguez Gonzalez, D.; David-Wang, A.; Boucher, H.W.; Kaye, K.S.; Losada, M.C.; Du, J.; Tipping, R.; et al. A Randomized, Double-blind, Multicenter Trial Comparing Efficacy and Safety of Imipenem/Cilastatin/Relebactam Versus Piperacillin/Tazobactam in Adults with Hospital-acquired or Ventilator-associated Bacterial Pneumonia (RESTORE-IMI 2 Study). *Clin. Infect. Dis.* **2020**, *73*, e4539–e4548. [[CrossRef](#)]
17. Clark, J.A.; Burgess, D.S. Plazomicin: A new aminoglycoside in the fight against antimicrobial resistance. *Ther. Adv. Infect. Dis.* **2020**, *7*, 2049936120952604. [[CrossRef](#)] [[PubMed](#)]
18. Årdal, C.; Balasegaram, M.; Laxminarayan, R.; McAdams, D.; Outtersson, K.; Rex, J.H.; Sumpradit, N. Antibiotic development—Economic, regulatory and societal challenges. *Nat. Rev. Microbiol.* **2020**, *18*, 267–274. [[CrossRef](#)]
19. Bergen, P.J.; Bulman, Z.P.; Saju, S.; Bulitta, J.B.; Landersdorfer, C.; Forrest, A.; Li, J.; Nation, R.L.; Tsuji, B.T. Polymyxin combinations: Pharmacokinetics and pharmacodynamics for rationale use. *J. Hum. Pharmacol. Drug Ther.* **2015**, *35*, 34–42. [[CrossRef](#)]
20. Mohapatra, S.S.; Dwibedy, S.K.; Padhy, I. Polymyxins, the last-resort antibiotics: Mode of action, resistance emergence, and potential solutions. *J. Biosci.* **2021**, *46*, 85. [[CrossRef](#)] [[PubMed](#)]
21. Theuretzbacher, U. Global antimicrobial resistance in Gram-negative pathogens and clinical need. *Curr. Opin. Microbiol.* **2017**, *39*, 106–112. [[CrossRef](#)]
22. Baron, S.; Hadjadj, L.; Rolain, J.M.; Olaitan, A.O. Molecular mechanisms of polymyxin resistance: Knowns and unknowns. *Int. J. Antimicrob. Agents* **2016**, *48*, 583–591. [[CrossRef](#)]
23. Justo, J.A.; Bosso, J.A. Adverse reactions associated with systemic polymyxin therapy. *J. Hum. Pharmacol. Drug Ther.* **2015**, *35*, 28–33. [[CrossRef](#)]
24. Theriault, N.; Tillotson, G.; Sandrock, C.E. Global travel and Gram-negative bacterial resistance; implications on clinical management. *Expert Rev. Anti-Infect. Ther.* **2021**, *19*, 181–196. [[CrossRef](#)]
25. Willyard, C. The drug-resistant bacteria that pose the greatest health threats. *Nature* **2017**, *543*, 15. [[CrossRef](#)] [[PubMed](#)]
26. Tagliabue, A.; Rappuoli, R. Changing Priorities in Vaccinology: Antibiotic Resistance Moving to the Top. *Front. Immunol.* **2018**, *9*, 1068. [[CrossRef](#)]
27. Abraham, R.J.; Stevens, A.J.; Young, K.A.; Russell, C.; Qvist, A.; Khazandi, M.; Wong, H.S.; Abraham, S.; Ogunniyi, A.D.; Page, S.W.; et al. Robenidone Analogues as Gram-Positive Antibacterial Agents. *J. Med. Chem.* **2016**, *59*, 2126–2138. [[CrossRef](#)] [[PubMed](#)]
28. Ogunniyi, A.D.; Khazandi, M.; Stevens, A.J.; Sims, S.K.; Page, S.W.; Garg, S.; Venter, H.; Powell, A.; White, K.; Petrovski, K.R. Evaluation of robenidone analog NCL195 as a novel broad-spectrum antibacterial agent. *PLoS ONE* **2017**, *12*, e0183457. [[CrossRef](#)]
29. Nguyen, H.T.; O'Donovan, L.A.; Venter, H.; Russell, C.C.; McCluskey, A.; Page, S.W.; Trott, D.J.; Ogunniyi, A.D. Comparison of Two Transmission Electron Microscopy Methods to Visualize Drug-Induced Alterations of Gram-Negative Bacterial Morphology. *Antibiotics* **2021**, *10*, 307. [[CrossRef](#)] [[PubMed](#)]
30. Clinical and Laboratory Standards Institute. *Performance Standards for Antimicrobial Disk and Dilution Susceptibility Tests For Bacteria Isolated from Animals*, 4th ed.; CLSI Supplement VET08; CLSI: Wayne, PA, USA, 2018.
31. Clinical and Laboratory Standards Institute. *Methods for Determining Bactericidal Activity of Antimicrobial Agents*; Approved Guideline; CLSI: Wayne, PA, USA, 1999.
32. Elemam, A.; Rahimian, J.; Doymaz, M. In vitro evaluation of antibiotic synergy for polymyxin B-resistant carbapenemase-producing *Klebsiella pneumoniae*. *J. Clin. Microbiol.* **2010**, *48*, 3558–3562. [[CrossRef](#)]
33. Khazandi, M.; Pi, H.; Chan, W.Y.; Ogunniyi, A.D.; Sim, J.X.F.; Venter, H.; Garg, S.; Page, S.W.; Hill, P.B.; McCluskey, A. In vitro Antimicrobial Activity of Robenidone, Ethylenediaminetetraacetic Acid and Polymyxin B Nonapeptide Against Important Human and Veterinary Pathogens. *Front. Microbiol.* **2019**, *10*, 837. [[CrossRef](#)]
34. Hwang, I.S.; Hwang, J.H.; Choi, H.; Kim, K.J.; Lee, D.G. Synergistic effects between silver nanoparticles and antibiotics and the mechanisms involved. *J. Med. Microbiol.* **2012**, *61*, 1719–1726. [[CrossRef](#)]

35. Asokan, G.V.; Ramadhan, T.; Ahmed, E.; Sanad, H. WHO Global Priority Pathogens List: A Bibliometric Analysis of Medline-PubMed for Knowledge Mobilization to Infection Prevention and Control Practices in Bahrain. *Oman Med. J.* **2019**, *34*, 184–193. [[CrossRef](#)]
36. Zhen, X.; Lundborg, C.S.; Sun, X.; Hu, X.; Dong, H. Economic burden of antibiotic resistance in ESKAPE organisms: A systematic review. *Antimicrob. Resist. Infect. Control* **2019**, *8*, 137. [[CrossRef](#)] [[PubMed](#)]
37. De Oliveira, D.M.P.; Forde, B.M.; Kidd, T.J.; Harris, P.N.A.; Schembri, M.A.; Beatson, S.A.; Paterson, D.L.; Walker, M.J. Antimicrobial Resistance in ESKAPE Pathogens. *Clin. Microbiol. Rev.* **2020**, *33*, e00181-19. [[CrossRef](#)] [[PubMed](#)]
38. Langford, B.J.; So, M.; Raybardhan, S.; Leung, V.; Westwood, D.; MacFadden, D.R.; Soucy, J.R.; Daneman, N. Bacterial co-infection and secondary infection in patients with COVID-19: A living rapid review and meta-analysis. *Clin. Microbiol. Infect.* **2020**, *26*, 1622–1629. [[CrossRef](#)] [[PubMed](#)]
39. van der Eerden, M.M.; Vlaspolter, F.; de Graaff, C.S.; Groot, T.; Bronsveld, W.; Jansen, H.M.; Boersma, W.G. Comparison between pathogen directed antibiotic treatment and empirical broad spectrum antibiotic treatment in patients with community acquired pneumonia: A prospective randomised study. *Thorax* **2005**, *60*, 672–678. [[CrossRef](#)] [[PubMed](#)]
40. WHO. *New Report Calls for Urgent Action to Avert Antimicrobial Resistance Crisis*; World Health Organization: Geneva, Switzerland, 2019.
41. Petrosillo, N.; Ioannidou, E.; Falagas, M.E. Colistin monotherapy vs. combination therapy: Evidence from microbiological, animal and clinical studies. *Clin. Microbiol. Infect.* **2008**, *14*, 816–827. [[CrossRef](#)]
42. Liu, Y.; Li, R.; Xiao, X.; Wang, Z. Antibiotic adjuvants: An alternative approach to overcome multi-drug resistant Gram-negative bacteria. *Crit. Rev. Microbiol.* **2019**, *45*, 301–314. [[CrossRef](#)]
43. Doi, Y. Treatment Options for Carbapenem-resistant Gram-negative Bacterial Infections. *Clin. Infect. Dis.* **2019**, *69*, S565–S575. [[CrossRef](#)]
44. Brennan-Krohn, T.; Pironti, A.; Kirby, J.E. Synergistic activity of colistin-containing combinations against colistin-resistant Enterobacteriaceae. *Antimicrob. Agents Chemother.* **2018**, *62*, e00873-18. [[CrossRef](#)]
45. Witherell, K.S.; Price, J.; Bandaranayake, A.D.; Olson, J.; Call, D.R. Circumventing colistin resistance by combining colistin and antimicrobial peptides to kill colistin-resistant and multidrug-resistant Gram-negative bacteria. *J. Glob. Antimicrob. Resist.* **2020**, *22*, 706–712. [[CrossRef](#)]
46. Wang, Y.; Li, H.; Xie, X.; Wu, X.; Li, X.; Zhao, Z.; Luo, S.; Wan, Z.; Liu, J.; Fu, L.; et al. In vitro and in vivo assessment of the antibacterial activity of colistin alone and in combination with other antibiotics against *Acinetobacter baumannii* and *Escherichia coli*. *J. Glob. Antimicrob. Resist.* **2020**, *20*, 351–359. [[CrossRef](#)]
47. Kim, W.Y.; Moon, J.Y.; Huh, J.W.; Choi, S.H.; Lim, C.M.; Koh, Y.; Chong, Y.P.; Hong, S.B. Comparable Efficacy of Tigecycline versus Colistin Therapy for Multidrug-Resistant and Extensively Drug-Resistant *Acinetobacter baumannii* Pneumonia in Critically Ill Patients. *PLoS ONE* **2016**, *11*, e0150642. [[CrossRef](#)]
48. Katip, W.; Uitrakul, S.; Oberdorfer, P. A Comparison of Colistin versus Colistin Plus Meropenem for the Treatment of Carbapenem-Resistant *Acinetobacter baumannii* in Critically Ill Patients: A Propensity Score-Matched Analysis. *Antibiotics* **2020**, *9*, 647. [[CrossRef](#)] [[PubMed](#)]
49. Herrmann, G.; Yang, L.; Wu, H.; Song, Z.; Wang, H.; Høiby, N.; Ulrich, M.; Molin, S.; Riethmüller, J.; Döring, G. Colistin-Tobramycin Combinations Are Superior to Monotherapy Concerning the Killing of Biofilm *Pseudomonas aeruginosa*. *J. Infect. Dis.* **2010**, *202*, 1585–1592. [[CrossRef](#)]
50. Qureshi, Z.A.; Paterson, D.L.; Potoski, B.A.; Kilayko, M.C.; Sandovsky, G.; Sordillo, E.; Polsky, B.; Adams-Haduch, J.M.; Doi, Y. Treatment outcome of bacteremia due to KPC-producing *Klebsiella pneumoniae*: Superiority of combination antimicrobial regimens. *Antimicrob. Agents Chemother.* **2012**, *56*, 2108–2113. [[CrossRef](#)] [[PubMed](#)]
51. Ontong, J.C.; Ozioma, N.F.; Voravuthikunchai, S.P.; Chusri, S. Synergistic antibacterial effects of colistin in combination with aminoglycoside, carbapenems, cephalosporins, fluoroquinolones, tetracyclines, fosfomycin, and piperacillin on multidrug resistant *Klebsiella pneumoniae* isolates. *PLoS ONE* **2021**, *16*, e0244673. [[CrossRef](#)]
52. Nation, R.L.; Garonzik, S.M.; Thamlikitkul, V.; Giamarellos-Bourboulis, E.J.; Forrest, A.; Paterson, D.L.; Li, J.; Silveira, F.P. Dosing guidance for intravenous colistin in critically-ill patients. *Clin. Infect. Dis.* **2017**, *64*, 565–571. [[CrossRef](#)] [[PubMed](#)]
53. Hou, S.-Y.; Wu, D.; Feng, X.-H. Polymyxin monotherapy versus polymyxin-based combination therapy against carbapenem-resistant *Klebsiella pneumoniae*: A systematic review and meta-analysis. *J. Glob. Antimicrob. Resist.* **2020**, *23*, 197–202. [[CrossRef](#)]
54. Li, Y.Y.; Wang, J.; Wang, R.; Cai, Y. Double-carbapenem therapy in the treatment of multidrug resistant Gram-negative bacterial infections: A systematic review and meta-analysis. *BMC Infect. Dis.* **2020**, *20*, 408. [[CrossRef](#)]
55. Angst, D.C.; Tepekule, B.; Sun, L.; Bogos, B.; Bonhoeffer, S. Comparing treatment strategies to reduce antibiotic resistance in an in vitro epidemiological setting. *Proc. Natl. Acad. Sci. USA* **2021**, *118*, e2023467118. [[CrossRef](#)] [[PubMed](#)]
56. Schmid, A.; Wolfensberger, A.; Nemeth, J.; Schreiber, P.W.; Sax, H.; Kuster, S.P. Monotherapy versus combination therapy for multidrug-resistant Gram-negative infections: Systematic Review and Meta-Analysis. *Sci. Rep.* **2019**, *9*, 15290. [[CrossRef](#)] [[PubMed](#)]
57. Ross, J.S.; Dzara, K.; Downing, N.S. Efficacy and safety concerns are important reasons why the FDA requires multiple reviews before approval of new drugs. *Health Aff.* **2015**, *34*, 681–688. [[CrossRef](#)] [[PubMed](#)]
58. Lloyd, D.H.; Page, S.W. Antimicrobial stewardship in veterinary medicine. *ASM Microbiol. Spectr.* **2018**, *6*, 3–6. [[CrossRef](#)]

Supplementary materials:

Table S1. Effect of serum on *in vitro* activity of NCL179 against *S. aureus*.

| Strain | ¹ MIC (µg/mL) for: | | | |
|-----------------------------|-------------------------------|---------------------------|------------|--------------|
| | NCL179 | | Daptomycin | |
| | ² LB | LB + ³ 10% FBS | LB | LB + 10% FBS |
| <i>S. aureus</i> Xen29 | 1 | 16 | 0.5 | 0.5 |
| <i>S. aureus</i> ATCC 29213 | 1 | 16 | 0.5 | 0.5 |

¹MIC, minimum inhibitory concentration; LB, Luria–Bertani broth; FBS, foetal bovine serum

| | 1 | 2 | 3 | 4 | 5 | 6 | 7 | 8 | 9 | 10 | 11 | 12 | NCL179 ($\mu\text{g/mL}$) |
|---|------------|------------|--------|--------|--------|--------|--------|--------|--------|--------|--------|--------|-----------------------------|
| A | 1.7512 | 1.7298 | 0.0649 | 0.0564 | 0.0522 | 0.0577 | 0.0545 | 0.0602 | 0.0516 | 0.0626 | 0.0483 | 0.0508 | 8 |
| B | 1.7078 | 1.7108 | 1.6885 | 0.0524 | 0.0501 | 0.0459 | 0.0499 | 0.0523 | 0.0505 | 0.0534 | 0.0464 | 0.0468 | 4 |
| C | 1.6975 | 1.6986 | 1.6818 | 1.6416 | 0.0503 | 0.0403 | 0.0428 | 0.0429 | 0.0433 | 0.0431 | 0.0411 | 0.0405 | 2 |
| D | 1.6764 | 1.6804 | 1.6618 | 1.6124 | 1.6318 | 0.0398 | 0.0407 | 0.0415 | 0.0406 | 0.0418 | 0.0398 | 0.0403 | 2 |
| E | 1.665 | 1.6677 | 1.645 | 1.6302 | 1.6325 | 1.595 | 0.042 | 0.0424 | 0.0426 | 0.0414 | 0.0469 | 0.0429 | 0.5 |
| F | 1.6554 | 1.6418 | 1.6331 | 1.621 | 1.6303 | 1.5876 | 1.3484 | 0.0424 | 0.0418 | 0.0426 | 0.0411 | 0.0433 | 0.25 |
| G | 0.0414 | 1.5469 | 1.5311 | 1.5403 | 1.5766 | 1.5486 | 1.4634 | 0.0392 | 0.0393 | 0.0415 | 0.0404 | 0.0408 | |
| H | 0.0464 | 1.562 | 1.5558 | 1.5403 | 1.5645 | 1.5139 | 1.4283 | 0.0399 | 0.0407 | 0.043 | 0.0409 | 0.0424 | |
| | Growth (-) | Growth (+) | 0.008 | 0.015 | 0.03 | 0.06 | 0.125 | 0.25 | 0.5 | 1 | 2 | 4 | Colistin $\mu\text{g/mL}$ |

Figure S1. Representative checkerboard assay of NCL179 + colistin combination against *E. coli* ATCC 35218. Values represent $A_{600\text{ nm}}$ measurements. Colistin concentration ranged from 0.008 to 4 $\mu\text{g/mL}$ (columns 3 to 12); NCL179 concentration ranged from 0.25 to 8 $\mu\text{g/mL}$ (rows A to F); blue wells, NCL179 alone; green wells, colistin alone; red wells, bacterial growth control containing only *E. coli* and Luria–Bertani (LB) broth; orange wells, LB broth only (no growth control, also representing the $A_{600\text{ nm}}$ value at the MIC of colistin alone or NCL179 + colistin combination)

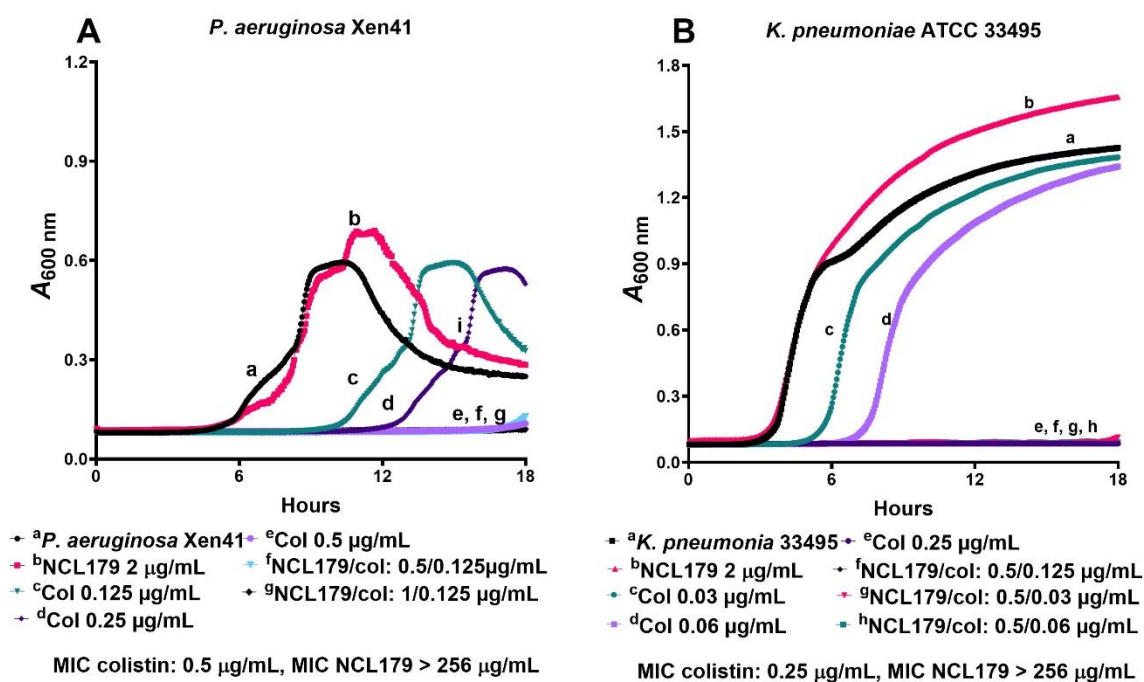


Figure S2. Time- and concentration-dependent kill kinetics of NCL179 alone and in combination with colistin against Gram-negative bacteria. (A), NCL179 alone or in combination with colistin against *P. aeruginosa* Xen41, and (B) *K. pneumoniae* ATCC 33495. Assays were performed on a Cytation 5 Multimode reader (BioTek) by optical density ($A_{600\text{ nm}}$) measurements. Col, colistin

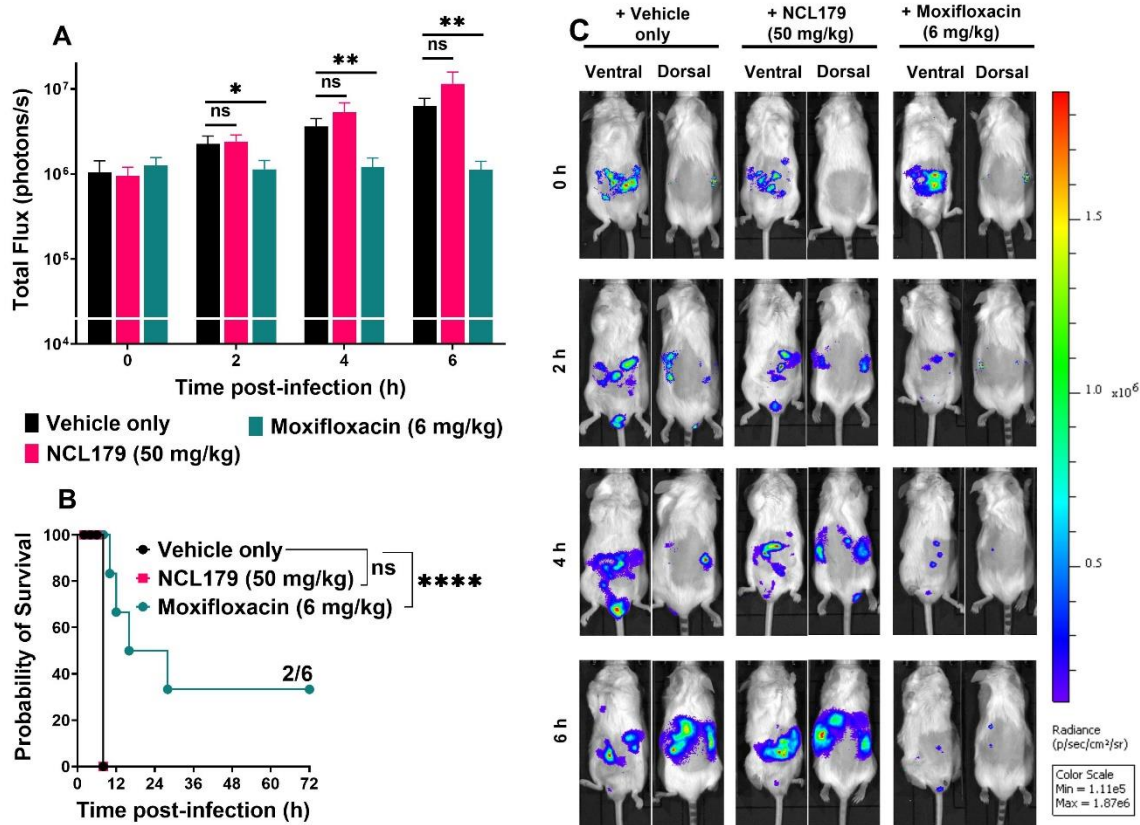


Figure S3. Oral efficacy of NCL179 (2 × doses, 8 h apart) in a bioluminescent *S. aureus* (Xen29) mouse sepsis model. (A) Comparison of luminescence signals between groups of CD1 mice (n = 6) challenged IP with Xen29 and treated with NCL179 and vehicle at 0 h post-infection; moxifloxacin at 0 h, 4 h, 8 h and 12 h post-infection. Mice were subjected to bioluminescence imaging on IVIS Lumina XRMS Series III system at the indicated times (ns, no significant; *, $p < 0.05$; **, $p < 0.01$; ***, $p < 0.0002$, ****, $p < 0.0001$, Mann-Whitney U -test, two-tailed); broken segment represents limit of detection (2×10^4 photons/s). (B) Survival analysis for mice treated with NCL179, moxifloxacin and vehicle (ns, no significant; *, $p < 0.05$; **, $p < 0.01$, ***, $p < 0.0002$, ****, $p < 0.0001$; Log-rank (Mantel-Cox test)). (C) Ventral and dorsal images of representative CD1 mice challenged with approx. 3×10^7 CFU of bioluminescent *S. aureus* ATCC 12600 (Xen29). Moxifloxacin (Avelox IV400 1.6 mg/mL; Bayer, Australia) was used as a control drug.

Chapter VII

Evaluation of benzguinols as next-generation antibiotics for the treatment of multidrug-resistant bacterial infections

Statement of Authorship

| | |
|---------------------|---|
| Title of Paper | Evaluation of benzguinolns as next-generation antibiotics for the treatment of multidrug-resistant bacterial infections |
| Publication Status | <input checked="" type="checkbox"/> Published <input type="checkbox"/> Accepted for Publication <input type="checkbox"/> Submitted for Publication <input type="checkbox"/> Unpublished and Unsubmitted work written in manuscript style |
| Publication Details | Nguyen, H.T.; Morshed, M.T.; Vuong, D.; Crombie, A.; Lacey, E.; Garg, S.; Pi, H.; Woolford, L.; Venter, H.; Page, S.W.; Piggott, A.M.; Trott, D.J.; Ogunniyi, A.D. Evaluation of benzguinolns as next-generation antibiotics for the treatment of multidrug-resistant bacterial infections. <i>Antibiotics</i> (Basel) 2021 , 10, doi:10.3390/antibiotics10060727. Journal Impact Factor = 5.222. |

Principal Author

| | | | |
|--------------------------------------|--|------|------------|
| Name of Principal Author (Candidate) | Hang Thi Nguyen | | |
| Contribution to the Paper | Contributed to the study design, performed experiments, wrote the preliminary manuscript and editing | | |
| Overall percentage (%) | 70% | | |
| Certification: | This paper reports on original research I conducted during the period of my Higher Degree by Research candidature and is not subject to any obligations or contractual agreements with a third party that would constrain its inclusion in this thesis. I am the primary author of this paper. | | |
| Signature | | Date | 01/12/2021 |

Co-Author Contributions

By signing the Statement of Authorship, each author certifies that:

- i. the candidate's stated contribution to the publication is accurate (as detailed above);
- ii. permission is granted for the candidate in include the publication in the thesis; and
- iii. the sum of all co-author contributions is equal to 100% less the candidate's stated contribution.

| | | | |
|---------------------------|--|------|------------|
| Name of Co-Author | Prof. Darren Trott on behalf of Mahmud T. Morshed | | |
| Contribution to the Paper | Responsible for synthesizing benzguinolns, contributed to editing and discussion | | |
| Signature | | Date | 07/02/2022 |

| | | | |
|---------------------------|--|------|------------|
| Name of Co-Author | Daniel Vuong | | |
| Contribution to the Paper | Responsible for synthesizing benzguinolns, contributed to editing and discussion | | |
| Signature | | Date | 19/01/2022 |

| | | | |
|---------------------------|---|------|------------|
| Name of Co-Author | Ernest Lacey | | |
| Contribution to the Paper | Contributed to editing, discussion and provided financial support for the study | | |
| Signature | | Date | 19/01/2022 |

| | | | |
|---------------------------|-----------------------------|------|------------|
| Name of Co-Author | Sanjay Garg | | |
| Contribution to the Paper | Contributed to formulations | | |
| Signature | | Date | 06/01/2022 |

| | | | |
|---------------------------|---------------------------------------|------|------------|
| Name of Co-Author | Hongfei Pi | | |
| Contribution to the Paper | Contributed to editing and discussion | | |
| Signature | | Date | 04/01/2022 |

| | | | |
|---------------------------|--|------|----------|
| Name of Co-Author | Lucy Woolford | | |
| Contribution to the Paper | Contributed to histopathology examinations, editing and discussion | | |
| Signature | | Date | 05/01/22 |

| | | | |
|---------------------------|---|------|------------|
| Name of Co-Author | Henrietta Venter | | |
| Contribution to the Paper | Contributed to study design, editing and discussion | | |
| Signature | | Date | 15/12/2021 |

| | | | |
|---------------------------|---|------|------------|
| Name of Co-Author | Stephen W. Page | | |
| Contribution to the Paper | Contributed to editing, discussion and provided financial support for the study | | |
| Signature | | Date | 02/02/2022 |

| | | | |
|---------------------------|---|--|--|
| Name of Co-Author | Andrew M. Piggott | | |
| Contribution to the Paper | Contributed to editing, discussion and provided financial support for the study | | |

| | | | |
|-----------|--|------|------------|
| Signature | | Date | 10/01/2022 |
|-----------|--|------|------------|

| | | | |
|---------------------------|---|------|------------|
| Name of Co-Author | Darren J. Trott | | |
| Contribution to the Paper | Contributed to study design, supervision, editing, discussion, and provided financial support for the study acted as a corresponding author | | |
| Signature | | Date | 07/02/2022 |

| | | | |
|---------------------------|--|------|------------|
| Name of Co-Author | Abiodun D. Ogunniyi | | |
| Contribution to the Paper | Contributed to study design, experiments, technical guidance, supervision, editing, discussion and acted as a corresponding author | | |
| Signature | | Date | 08/12/2021 |



Article

Evaluation of Benzguinols as Next-Generation Antibiotics for the Treatment of Multidrug-Resistant Bacterial Infections

Hang Thi Nguyen ^{1,2}, Mahmud T. Morshed ³, Daniel Vuong ⁴, Andrew Crombie ⁴, Ernest Lacey ^{3,4}, Sanjay Garg ⁵, Hongfei Pi ¹, Lucy Woolford ⁶, Henrietta Venter ⁷, Stephen W. Page ⁸, Andrew M. Piggott ³, Darren J. Trott ^{1,*} and Abiodun D. Ogunniyi ^{1,*}

- ¹ Australian Centre for Antimicrobial Resistance Ecology, School of Animal and Veterinary Sciences, Roseworthy Campus, The University of Adelaide, Roseworthy, SA 5371, Australia; hang.t.nguyen@adelaide.edu.au (H.T.N.); hongfei.pi@adelaide.edu.au (H.P.)
- ² Department of Pharmacology, Toxicology, Internal Medicine and Diagnostics, Faculty of Veterinary Medicine, Vietnam National University of Agriculture, Hanoi 100000, Vietnam
- ³ Department of Molecular Sciences, Macquarie University, Sydney, NSW 2109, Australia; mahmud.morshed@hdr.mq.edu.au (M.T.M.); elacey@microbialscreening.com (E.L.); andrew.piggott@mq.edu.au (A.M.P.)
- ⁴ Microbial Screening Technologies Pty. Ltd., Smithfield, NSW 2164, Australia; dvuong@microbialscreening.com (D.V.); acrombie@microbialscreening.com (A.C.)
- ⁵ Clinical and Health Sciences, University of South Australia, Adelaide, SA 5000, Australia; Sanjay.Garg@unisa.edu.au
- ⁶ School of Animal and Veterinary Sciences, Roseworthy Campus, The University of Adelaide, Roseworthy, SA 5371, Australia; lucy.woolford@adelaide.edu.au
- ⁷ Health and Biomedical Innovation, Clinical and Health Sciences, University of South Australia, Adelaide, SA 5000, Australia; rietie.venter@unisa.edu.au
- ⁸ Advanced Veterinary Therapeutics, Newtown, NSW 2042, Australia; swp@advet.com.au
- * Correspondence: darren.trott@adelaide.edu.au (D.J.T.); david.ogunniyi@adelaide.edu.au (A.D.O.); Tel.: +61-883-137-989 (D.J.T.); +61-432-331-914 (A.D.O.)



Citation: Nguyen, H.T.; Morshed, M.T.; Vuong, D.; Crombie, A.; Lacey, E.; Garg, S.; Pi, H.; Woolford, L.; Venter, H.; Page, S.W.; et al.

Evaluation of Benzguinols as Next-Generation Antibiotics for the Treatment of Multidrug-Resistant Bacterial Infections. *Antibiotics* **2021**, *10*, 727. <https://doi.org/10.3390/antibiotics10060727>

Academic Editor: Carlos M. Franco

Received: 12 May 2021

Accepted: 10 June 2021

Published: 16 June 2021

Publisher's Note: MDPI stays neutral with regard to jurisdictional claims in published maps and institutional affiliations.



Copyright: © 2021 by the authors. Licensee MDPI, Basel, Switzerland. This article is an open access article distributed under the terms and conditions of the Creative Commons Attribution (CC BY) license (<https://creativecommons.org/licenses/by/4.0/>).

Abstract: Our recent focus on the “lost antibiotic” unguinol and related nidulin-family fungal natural products identified two semisynthetic derivatives, benzguinols A and B, with unexpected in vitro activity against *Staphylococcus aureus* isolates either susceptible or resistant to methicillin. Here, we show further activity of the benzguinols against methicillin-resistant isolates of the animal pathogen *Staphylococcus pseudintermedius*, with minimum inhibitory concentration (MIC) ranging 0.5–1 µg/mL. When combined with sub-inhibitory concentrations of colistin, the benzguinols demonstrated synergy against Gram-negative reference strains of *Acinetobacter baumannii*, *Escherichia coli*, *Klebsiella pneumoniae*, and *Pseudomonas aeruginosa* (MICs of 1–2 µg/mL in the presence of colistin), whereas the benzguinols alone had no activity. Administration of three intraperitoneal (IP) doses of 20 mg/kg benzguinol A or B to mice did not result in any obvious adverse clinical or pathological evidence of acute toxicity. Importantly, mice that received three 20 mg/kg IP doses of benzguinol A or B at 4 h intervals exhibited significantly reduced bacterial loads and longer survival times than vehicle-only treated mice in a bioluminescent *S. aureus* murine sepsis challenge model. We conclude that the benzguinols are potential candidates for further development for specific treatment of serious bacterial infections as both stand-alone antibiotics and in combination with existing antibiotic classes.

Keywords: *Staphylococcus pseudintermedius*; *Staphylococcus aureus*; benzguinols; nidulins; Gram-negative; antimicrobial resistance; colistin; bioluminescent mouse model; cytotoxicity; minimum inhibitory concentration

1. Introduction

Infections caused by pathogenic bacteria represent an increasingly significant challenge to public health worldwide [1]. Effective treatment of bacterial infections is becoming

increasingly difficult due to the overuse of antibiotics, which has resulted in multidrug-resistance development among many bacterial pathogens [2–4]. For example, according to the Centers for Disease Control and Prevention, each year more than 2.8 million multidrug-resistant (MDR) infections occur in the United States, associated with more than 35,000 deaths [5]. It is estimated that, unless urgent action is taken, infections due to pathogens with antimicrobial resistance (AMR) could result in 10 million deaths per year and an economic collapse comparable to the 2008–2009 global financial crisis by 2050 [6,7]. For instance, *Staphylococcus aureus* is the second most clinically important antibiotic-resistant bacterial pathogen in developed countries (behind *Escherichia coli*) and is a major public health concern due to the increasing prevalence of methicillin-resistant *S. aureus* (MRSA) in the hospital environment and within the community [8,9]. The costs associated with MRSA infections are estimated at \$10 billion US, averaging about \$60,000 per patient [10]. There are also increasing zoonotic risks of methicillin-resistant *Staphylococcus pseudintermedius* (MRSP), i.e., transfer from dogs to owners, making it a potential threat to public health [11,12]. While the situation facing human medicine is dire, the problem is exacerbated in livestock medicine by the limited range of registered drug classes, the risk of transfer of resistance genes through the food chain [13], and the rapid development of pan resistance in one of the most important animal pathogens, enterotoxigenic *E. coli* [14]. The situation is made worse by very few new antibiotics being developed to treat Gram-negative bacterial (GNB) infections [15]. Most newly approved agents against MDR-GNB pathogens are derivatives of existing chemical classes with potential for rapid onset of resistance [16,17]. Polymyxins and some beta lactam–beta lactamase inhibitor combinations including ceftolozane–tazobactam, ceftazidime–avibactam, and meropenem–vaborbactam are used as last resort drug classes for the treatment of GNB infections [18,19].

It is clear that the problems posed by MDR pathogens require rapid development of new, broad-spectrum anti-infectives. Medicinal chemists have been highly successful over the last 50 years in reshaping the scaffolds of earlier antibiotics, both natural and synthetic, including the fourth and fifth generations of β -lactams and third generation of macrolides [20–22]. However, significantly new approaches and strategies for breakthrough molecules have not been forthcoming [15,23,24].

As part of our investigations into expanding the chemical space around the “lost antibiotic” nidulin and its related fungal natural products [25], our team recently reported the semisynthesis and in vitro biological evaluation of thirty-four derivatives of the parent fungal depsidone antibiotic, unguinol [26]. Fifteen first-generation unguinol analogs were synthesized and screened against a panel of bacteria, fungi, and mammalian cells to formulate a basic structure–activity relationship for the unguinol pharmacophore. In vitro antibacterial activity testing of these compounds revealed that 3-benzyl analogs, “benzguinols” (Figure 1), 3-*O*-(2,4-difluorobenzyl)unguinol (benzguinol A), and 3-*O*-(2-fluorobenzyl)unguinol (benzguinol B) showed potent activity against both MRSA and methicillin-susceptible *S. aureus* (MSSA) with minimum inhibitory concentration (MIC) ranges of 0.25–1 $\mu\text{g}/\text{mL}$. Based on these results, we concluded that the two compounds are promising candidates for further evaluation of in vivo efficacy [26]. As an extension of that study, we explored the spectrum of activity of benzguinols A and B against the animal health pathogen, MRSP, and examined their potential activity against GNB when combined with sub-inhibitory concentrations of colistin. We also evaluated the efficacy of the benzguinols against *S. aureus* sepsis in a bioluminescent mouse infection model.

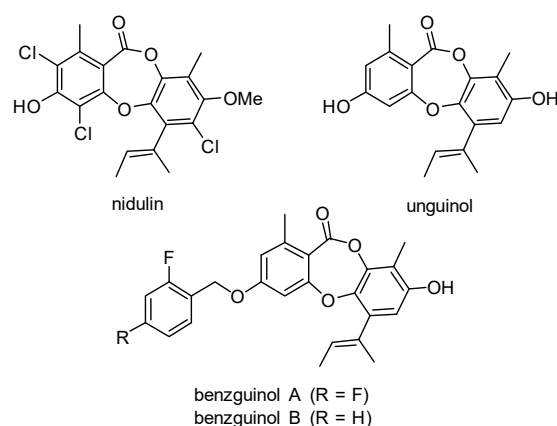


Figure 1. Structures of fungal metabolites nidulin and unguinol and semisynthetic unguinol derivatives benzguinol A and benzguinol B.

2. Materials and Methods

2.1. Antibiotics and Chemicals Used in this Study

Benzguinol A and benzguinol B were synthesized as described previously [26]. Amikacin, ampicillin, kanamycin, tetracycline, and colistin were purchased from Sigma-Aldrich (Australia). These antibiotics were prepared as 25.6 mg/mL stock solutions as follows: benzguinols A and B were dissolved in 100% DMSO; amikacin, ampicillin, and kanamycin were dissolved in water; and tetracycline was dissolved in 70% ethanol. The antibiotics were aliquoted in 1 mL quantities and stored at $-20\text{ }^{\circ}\text{C}$ in the dark.

2.2. Organisms and Growth Conditions

Clinical MRSP isolates were obtained from infected skin wounds, ears, abscessed joints, and the urine of dogs as part of the first nation-wide survey on antimicrobial resistance in animal pathogens in Australia [27] at the Australian Centre for Antimicrobial Resistance Ecology (ACARE), School of Animal and Veterinary Sciences, The University of Adelaide, Roseworthy, South Australia. MRSA USA300, *Enterococcus faecalis* ATCC 29212, and 20 porcine vancomycin-resistant enterococci (VRE) were obtained from the University of South Australia collection [28]. Each organism was identified by MALDI-TOF at ACARE before antimicrobial susceptibility testing. For efficacy testing of benzguinol A and benzguinol B, bioluminescent *S. aureus* ATCC 12600 (Xen29; PerkinElmer, Waltham, MA, USA) was used. Reference strains *Acinetobacter baumannii* NCIMB 12457, *A. baumannii* ATCC 19606, *E. coli* ATCC 35218, *E. coli* ATCC 25922; *Klebsiella pneumoniae* ATCC 13883, *K. pneumoniae* ATCC 33495, *Pseudomonas aeruginosa* ATCC 27853, and *P. aeruginosa* PAO1 were provided by SA Pathology, Adelaide, Australia. Bioluminescent *E. coli* Xen14 (a derivative of *E. coli* WS2572) and bioluminescent *P. aeruginosa* Xen41 (a derivative of strain PAO1) were purchased from PerkinElmer Inc (Waltham, MA, USA). The reference strains and clinical isolates were grown on horse blood agar (HBA) and in Luria–Bertani (LB) broth, Miller (Becton Dickinson, Sparks, MD, USA) overnight. *E. coli* Xen14 was grown on HBA containing 30 $\mu\text{g}/\text{mL}$ kanamycin, *P. aeruginosa* Xen41 was grown in HBA containing 60 $\mu\text{g}/\text{mL}$ tetracycline, and *S. aureus* Xen29 was grown on HBA containing 200 $\mu\text{g}/\text{mL}$ kanamycin for selection.

2.3. Antimicrobial Susceptibility Testing

The minimum inhibitory concentrations (MICs) of benzguinols A and B against MRSP and selected GNB were determined in round bottom 96-well microtiter plates (Sarstedt 82.1582.001; Mawson Lakes, SA, Australia), using the modified broth micro-dilution method according to recommendations by the Clinical and Laboratory Standards Institute [29] as described previously [30]. Briefly, antimicrobial challenge plates were prepared by serial two-fold dilutions of stock solutions of benzguinol A or B in DMSO. Each dilution

was then further diluted 1:100 in LB broth in 96-well plates (Thermo Fisher Scientific, Thebarton, SA, Australia). Benzguinols A and B and amikacin concentrations ranged from 0.03 to 256 µg/mL, and each MIC test was carried out in duplicate and performed on two separate occasions. Negative growth control was LB broth only; positive growth control was bacterial suspension in LB broth. The minimum bactericidal concentration (MBC) was recorded as the lowest concentration of each test compound at which a 99.9% colony count reduction was observed on the plate [31].

Interaction activity between benzguinol A or B with colistin was determined by a modification of the standard checkerboard assay described previously [32–34]. Briefly, the antibiotic challenge plates were prepared as described in antimicrobial susceptibility testing. One microliter of benzguinol A or B solution from each combination was dispensed along the abscissa (from Rows A–F) of the 96-well microliter plates and the second compound (colistin) was dispensed along the ordinate (from Columns 3–12) using a 12.5 µL electronic multichannel pipette (VIAFLO Voyager II, Biotools, Loganholme QLD, Australia) followed by addition of 88 µL of LB broth. Thereafter, 10 µL of bacterial suspension were added to each well. One plate was used for each isolate and the plates were incubated at 37 °C for 20 h and observed visually and by $A_{600\text{nm}}$ measurements. The interaction of two antibiotics was calculated as the fractional inhibitory concentration index (FICI) as described previously [32–34] using the following formula:

$$\text{FICI} = \frac{\text{MIC}_{\text{A in combination}}}{\text{MIC}_{\text{A alone}}} + \frac{\text{MIC}_{\text{B in combination}}}{\text{MIC}_{\text{B alone}}}$$

A is benzguinol A or B, while B is colistin. According to FICI, the interaction between two antibiotic agents was interpreted as follows: synergistic ($\text{FICI} \leq 0.5$); additive or partially synergistic ($0.5 < \text{FICI} \leq 1$); indifferent ($1 < \text{FICI} \leq 4$); and antagonistic ($\text{FICI} > 4$).

The dose reduction index (DRI) was used to describe the difference between the effective dose of benzguinol A or B in combination with colistin from the individual dose of each compound. DRI was calculated using the following formula:

$$\text{DRI} = \frac{\text{MIC}_{\text{A alone}}}{\text{MIC}_{\text{A in combination}}}$$

A DRI (>1) is considered beneficial [34,35].

2.4. Time-Dependent Growth Inhibitory Assay

The time- and concentration-dependent activities of the benzguinols against one MRSP clinical isolate, one MRSA clinical isolate (and against one reference *E. coli* and one reference *P. aeruginosa* strain in the presence of sub-inhibitory concentrations of colistin) were determined in a kinetics assay by optical density ($A_{600\text{nm}}$) measurements for 18 h on a Cytation 5 Multimode reader (BioTek, Millennium Science Pty Ltd, Mulgrave, VIC, Australia). Plates for the Gram-positive time-dependent growth inhibitory assays were prepared as described for MIC determinations above, while the plates for the Gram-negative time-dependent growth inhibitory assays were prepared as described for standard checkerboard assays above.

2.5. Cytotoxicity Assays

We previously reported the cytotoxicity profiles of benzguinols A and B to Hep G2 (human hepatocellular carcinoma cell line) and HEK293 (human embryonic kidney cell line) [26]. Here, we examined benzguinol A or B in combination with colistin at 0.5 µg/mL for in vitro cytotoxicity using Hep G2 and HEK293 cell lines following the procedure described earlier [28]. Briefly, cell lines were maintained in Dulbecco's Modified Eagle's Medium (DMEM; Gibco Cat No: 12430) supplemented with 10% (*vol/vol*) fetal bovine serum (FBS) and 1% (*vol/vol*) PenStrep (100 U/mL penicillin and 100 µg/mL streptomycin) at 37 °C, 5% CO₂, and passaged every 3 days. Assays were performed in duplicates in black flat bottom 96-well tissue culture trays (Eppendorf Cat No: 0030741013) seeded with

$\sim 1.5 \times 10^4$ cells per well. After 24 h incubation, the media was removed, the cells were washed once with medium without antibiotics, and fresh medium supplemented with 10% (*vol/vol*) FBS was added. Then, either benzguinol A or B alone or in combination with colistin was added to each well in doubling dilutions starting at the same concentrations used for MIC testing, using wells containing 1% DMSO only and 64 $\mu\text{g}/\text{mL}$ ampicillin as controls. The effect of benzguinol alone or in combination with colistin on the viability of each cell line was monitored at 1 h intervals for 20 h at 37 °C in 5% CO₂ on a Cytation 5 Cell Imaging Multi-Mode Reader (BioTek, Winooski, VT, USA) using the RealTime-Glo™ MT Cell Viability Assay reagent (Promega, Madison, WI, USA).

2.6. Agar Well Diffusion Method

Each benzguinol formulation was prepared as a 6 mg/mL solution and daptomycin as a 1.8 mg/mL solution in 20% (*vol/vol*) DMSO in PEG400 (vehicle). All formulations were tested for antibacterial activity using the agar well diffusion method [36] to ensure that the drugs were released from vehicle as a reference for interpretation of *in vivo* activity in mice. For this assay, several colonies of an overnight HBA culture of *S. aureus* Xen29 were suspended in saline equivalent to 0.5 McFarland standard ($A_{600\text{nm}} = 0.1$). A sterile swab was then dipped in the 0.5 McFarland standard bacterial suspension and used to streak over the entire surface of a sterile plate count agar plate. Punch holes were then made on the agar plates using an 8 mm diameter biopsy punch (Livingstone International Pty Ltd., Sydney, NSW, Australia) and a 100 μL equivalent amount of each formulation to a single treatment dose in mice was placed in the well. Agar plates were then incubated at 37 °C for 20 h, and the antimicrobial activity of each drug was determined by measuring and comparing the zone of inhibition with that of vehicle only.

2.7. Ethics Statements

To test the safety of the benzguinols and assess their efficacy against challenge with bioluminescent *S. aureus* Xen29, outbred 5–6-week-old male CD1 (Swiss) mice (weighing 25–30 g), obtained from the Laboratory Animal Services breeding facility of the University of Adelaide, were used. Mice had access to food and water throughout the experiment period. The Animal Ethics Committee of The University of Adelaide (approval number S-2015-151) reviewed and approved all animal experiments. The study was conducted in compliance with the Australian Code of Practice for the Care and Use of Animals for Scientific Purposes (8th Edition 2013) and the South Australian Animal Welfare Act 1985.

2.8. Safety Testing of Benzguinols A and B Following Parenteral Administration

To ensure a three-dose regimen would be safe to administer to mice, a safety study was conducted using three intraperitoneal (IP) injection of 20 mg/kg benzguinol A or benzguinol B at 4 h intervals to three mice. Three IP doses of vehicle were used as a control. Mice were observed for clinical signs and the data recorded on a Clinical Record Sheet approved by the Animal Ethics Committee of The University of Adelaide. The mice were monitored every 2 h for the first 12 h, and then at 24, 36, 48, and at 72 h post-treatment. At the conclusion of the experiment (72 h post-treatment), mice were humanely killed and sections of liver, kidneys, spleen, lung, and heart were harvested for histopathological examination.

2.9. Histopathological Examination

Mouse organs (liver, kidneys, spleen, lungs, and heart) collected from the IP safety experiment were fixed in 10% neutral-buffered formalin (ChemSupply Australia Pty Ltd., Gillman, SA, Australia) and processed routinely, embedded in paraffin blocks, and sectioned to a thickness of 4 μm . Hematoxylin and eosin-stained sections were observed and recorded under light microscopy. Photomicrographs were captured using a DP25 camera and LabSens software (Olympus, Tokyo, Japan).

2.10. Efficacy Testing of Benzguinolins A and B after IP Challenge of Mice with Bioluminescent Gram-Positive Bacteria (GPB)

For in vivo efficacy testing of benzguinolins A and B in a murine bioluminescent infection model, we used mouse-passaged bioluminescent *S. aureus* ATCC strain 12600 (Xen29, PerkinElmer). Bacteria were grown in LB broth at 37 °C to an $A_{600\text{nm}}$ of 0.5 (1.5×10^8 CFU/mL). Four groups of mice ($n = 6$ mice per group) were infected IP with 3×10^7 CFU of *S. aureus* Xen29 in 200 μL PBS containing 3% hog gastric mucin type III (Sigma Aldrich, St. Louis, MO, USA). The mice were then imaged immediately in both ventral and dorsal positions on the IVIS Lumina XRMS Series III system. At 2 h post-infection, all mice were imaged again as above. Immediately thereafter, mice in Group 1 were injected IP with the drug vehicle only; mice in Groups 2 and 3 were injected with either benzguinol A or benzguinol B at 20 mg/kg IP; and mice in Group 4 were treated with daptomycin at 6 mg/kg IP. Mice were closely monitored for their clinical conditions and then imaged at 4 h post-infection. At 6 and 10 h post-infection, all surviving mice in each group were imaged and immediately followed by an identical drug and vehicle treatment regimen as described above. In addition, 20 μL of blood were withdrawn from the submandibular vein of each mouse at 2, 6, and 8 h post-infection and serial dilutions of the blood samples plated on HBA to estimate bacterial burden. Mice were further monitored frequently for signs of distress and those that had become moribund or showed any evidence of distress were humanely killed by cervical dislocation. At 18, 24, 28, 36, 48, and 72 h post-infection, surviving mice were monitored and further subjected to bioluminescence imaging. In all experiments, signals were collected from a defined region of interest and total flux intensities (photons/s) analyzed using Living Image Software 4.7.2. Differences in median survival times (time to moribund) for mice between groups were analyzed by the log-rank (Mantel–Cox) tests. Differences in luminescence signals and blood counts between groups were compared by Mann–Whitney *U*-tests.

3. Results

3.1. In Vitro Activity of Benzguinolins A and B Alone against GPB and in Combination with Sub-Inhibitory Concentrations of Colistin against GNB

We previously showed potent activity of benzguinolins A and B against MRSA and MSSA, with MICs ranging 0.25–1 $\mu\text{g}/\text{mL}$ [26]. In this study, benzguinolins A and B showed antimicrobial activities against MRSP (MICs of 0.5–1 $\mu\text{g}/\text{mL}$ and MBCs of 4–8 $\mu\text{g}/\text{mL}$) in comparison to the control drug amikacin (MICs and MBCs of 8–16 $\mu\text{g}/\text{mL}$) (Table 1). Both benzguinolins have activity against *E. faecalis* ATCC 29212 at 8 $\mu\text{g}/\text{mL}$, but MIC ≥ 16 $\mu\text{g}/\text{mL}$ against all the 20 VRE.

Table 1. In vitro activities of benzguinolins A and B against methicillin-resistant *Staphylococcus pseudintermedius*.

| Compounds | ¹ MIC Range ($\mu\text{g}/\text{mL}$) | ² MBC Range ($\mu\text{g}/\text{mL}$) |
|--------------|--|--|
| Benzguinol A | 0.5–1 | 4–8 |
| Benzguinol B | 0.5–1 | 4–8 |
| Amikacin | 8–16 | 8–16 |

¹ MIC, minimum inhibitory concentration; ² MBC, minimum bactericidal concentration.

The activities of benzguinol A or B alone, colistin alone, benzguinol A + colistin combination, and benzguinol B + colistin combination were tested against 10 reference GNB strains (two *A. baumannii*, three *E. coli*, two *K. pneumoniae*, and three *P. aeruginosa*), and the results are shown in Table 2. Benzguinol A or B alone had no activity against any of the tested GNB; therefore, their MICs were set as 256 $\mu\text{g}/\text{mL}$ to calculate FICI and DRI. For colistin alone, its MIC was 1 $\mu\text{g}/\text{mL}$ against the *A. baumannii* strains, 0.25 $\mu\text{g}/\text{mL}$ against the *E. coli* strains, and 0.5 $\mu\text{g}/\text{mL}$ against the *K. pneumoniae* and *P. aeruginosa* strains. However, in combination, the MIC of benzguinol A and benzguinol B was 1–2 $\mu\text{g}/\text{mL}$ against all the GNB (a 128–256-fold reduction), whereas the MIC of colistin in the combination was

0.25 µg/mL against the *A. baumannii* strains, 0.06 µg/mL against the *E. coli* strains, and 0.125 µg/mL against the *K. pneumoniae* and *P. aeruginosa* strains, representing a four-fold dose reduction for colistin against all the GNB (Table 2). The FICI of all combinations was 0.25, showing the synergy of the benzguinol–colistin combinations.

3.2. Benzguinols A and B Exhibit Time- and Concentration-Dependent Inhibition of Bacterial Growth

The antimicrobial activities of benzguinols A and B were investigated in a time–kill kinetics assay to measure the time and concentration dependent activity of the two compounds against clinical MRSA isolate USA300 and clinical MRSP isolate VDL-828, using daptomycin and amikacin as comparators, respectively. The results show a time- and concentration-dependent inhibition of growth for benzguinols A and B, consistent with features of bacteriostatic drugs. As expected, daptomycin and amikacin displayed patterns of bactericidal drugs (Figure 2).

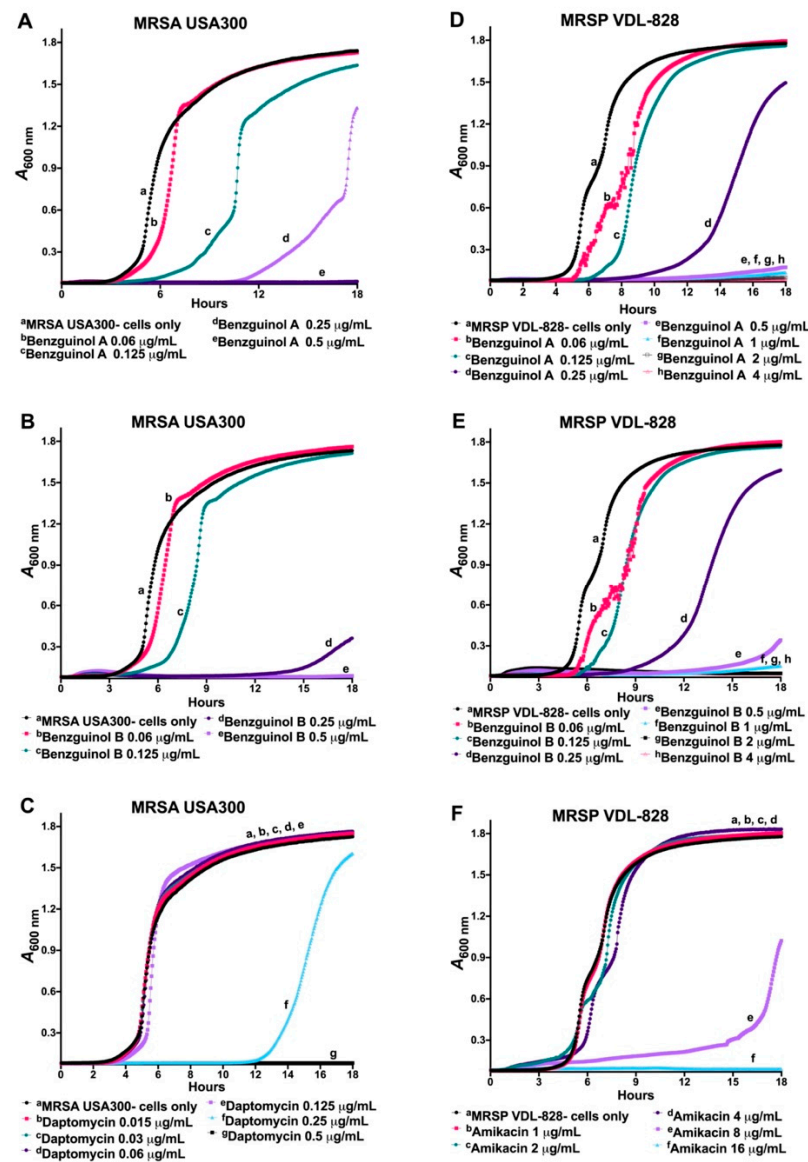


Figure 2. Kinetic assay showing time and concentration-dependent inhibition of MRSA USA300 (A–C) and MRSP VDL-828 (D–F) for benzguinol A (A,D) and benzguinol B (B,E) using daptomycin (C) and amikacin (F) as control drugs. The sub-minimum inhibitory concentrations for benzguinols A and B = 0.25 µg/mL; daptomycin = 0.25 µg/mL; and amikacin = 8 µg/mL.

Table 2. In vitro activities of benzguinolins A and B against Gram-negative bacteria in the presence of sub-inhibitory concentrations of colistin.

| Bacteria | MIC ($\mu\text{g/mL}$) | | | | | FICI ^a | | DRI ^b | |
|------------------------------------|--------------------------|---------------------------------|--------------------|--------------|--------------|----------------------------|----------------------------|---------------------------|---------------------------|
| | MIC Alone | | MIC in Combination | | | Colistin + Benzguinol A | Colistin + Benzguinol B | Colistin: Benzguinol A | Colistin: Benzguinol B |
| | Colistin | Benzguinol A or Benzguinol B | Colistin | Benzguinol A | Benzguinol B | | | | |
| <i>A. baumannii</i> ATCC 19606 | 1 | >256 | 0.25 | 2 | 1 | 0.25 * | 0.25 * | 4:128 | 4:256 |
| <i>A. baumannii</i> NCIMB 12457 | 1 | >256 | 0.25 | 2 | 2 | 0.25 * | 0.25 * | 4:128 | 4:128 |
| <i>E. coli</i> Xen14 | 0.25 | >256 | 0.06 | 1 | 2 | 0.25 * | 0.25 * | 4:256 | 4:128 |
| <i>E. coli</i> ATCC 35218 | 0.25 | >256 | 0.06 | 1 | 2 | 0.25 * | 0.25 * | 4:256 | 4:128 |
| <i>E. coli</i> ATCC 25922 | 0.25 | >256 | 0.06 | 1 | 2 | 0.25 * | 0.25 * | 4:256 | 4:128 |
| <i>K. pneumoniae</i> ATCC 13883 | 0.5 | >256 | 0.125 | 2 | 2 | 0.25 * | 0.25 * | 4:128 | 4:128 |
| <i>K. pneumoniae</i> ATCC 33495 | 0.5 | >256 | 0.125 | 2 | 2 | 0.25 * | 0.25 * | 4:128 | 4:128 |
| <i>P. aeruginosa</i> Xen41 | 0.5 | >256 | 0.125 | 2 | 2 | 0.25 * | 0.25 * | 4:128 | 4:128 |
| <i>P. aeruginosa</i> PAO1 | 0.5 | >256 | 0.125 | 2 | 2 | 0.25 * | 0.25 * | 4:128 | 4:128 |
| <i>P. aeruginosa</i> ATCC 27853 | 0.5 | >256 | 0.125 | 2 | 2 | 0.25 * | 0.25 * | 4:128 | 4:128 |

MIC, minimum inhibitory concentration. ^a FICI, fractional inhibitory concentration index: * synergistic, $\text{FICI} \leq 0.5$; additive or partially synergistic, $0.5 < \text{FICI} \leq 1$; indifferent, $1 < \text{FICI} \leq 4$; and antagonistic, $\text{FICI} > 4$. ^b DRI, dose reduction index. Bioluminescent *S. aureus* Xen29 was used as the control strain each time the MIC and checkerboard assays were performed; MIC of benzguinol A or B against *S. aureus* Xen29 in each of these assays was 0.5 $\mu\text{g/mL}$.

The time- and concentration-dependent activities of benzguinols A and B in combination with colistin against GNB was also investigated in a kinetic assay. In this assay, the growth pattern of *E. coli* Xen14 cells treated with benzguinol A (Figure 3A) or benzguinol B (Figure 3B) alone at 32 µg/mL was similar to that of untreated cells. Cells treated with colistin alone at 0.03 µg/mL (0.125 × MIC), 0.06 µg/mL (0.25 × MIC), or 0.125 µg/mL (0.5 × MIC) started to grow at 6, 10, and 14 h, respectively, whereas cells treated with colistin alone at 0.25 µg/mL did not grow. Additionally, cells treated with the benzguinol A + colistin or benzguinol B + colistin combination inhibited bacterial growth more quickly than colistin alone at the same concentration. For example, cells treated with a combination benzguinol A at 1 µg/mL + colistin at 0.03 µg/mL began to grow at around 12 h (approximately 6 h later than colistin alone at 0.03 µg/mL). However, *E. coli* Xen14 cells treated with a benzguinol A at 2 µg/mL + colistin at 0.03 µg/mL combination (Figure 3A) or a combination of benzguinol B at 2 µg/mL + colistin at 0.06 µg/mL (Figure 3B) did not grow.

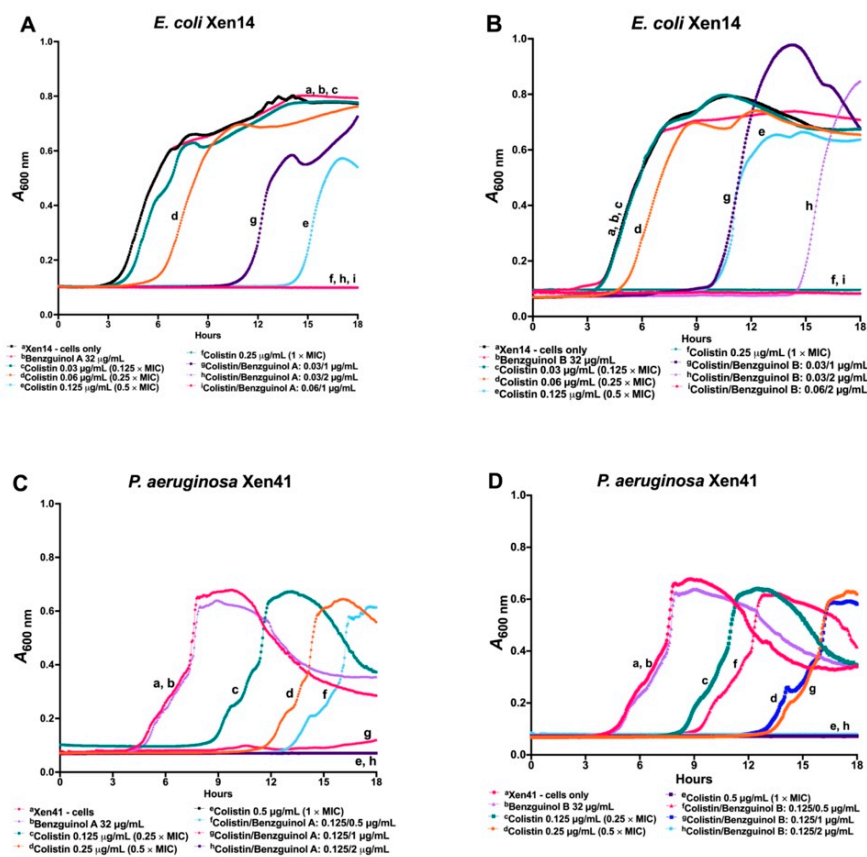


Figure 3. Time- and concentration-dependent antibacterial activities of benzguinols A and B alone and in combination with colistin. Growth inhibitory kinetics of the benzguinols alone or in combination with colistin against *E. coli* Xen14 (A,B) and *P. aeruginosa* Xen41 (C,D) were performed on a Cytation 5 Multimode reader (BioTek, Millennium Science Pty Ltd, Mulgrave, VIC, Australia) by optical density ($A_{600\text{nm}}$) measurements.

In a similar time- and concentration-dependent kinetic assay of the combination benzguinol A + colistin or benzguinol B + colistin against *P. aeruginosa* Xen41, the combination with colistin worked more quickly than colistin alone at the same concentration (Figure 3C,D). Xen41 treated with colistin alone at 0.125 µg/mL (0.25 × MIC) and 0.25 µg/mL (0.5 × MIC) started to grow at 9 and 12 h, respectively, whereas cells treated with 0.5 µg/mL colistin alone did not grow. Cells treated with a combination of benzguinol A or benzguinol B at 1 µg/mL + colistin at 0.125 µg/mL started to grow at approximately 13–15 h, which is 4–6 h later than colistin alone, while Xen41 cells treated with a combination of benzguinol A or benzguinol B at 2 µg/mL + colistin at 0.125 µg/mL did not grow.

As expected, the growth patterns of Xen41 cells treated with benzguinol A or benzguinol B at 2 $\mu\text{g}/\text{mL}$ were similar to those for untreated cells.

3.3. Benzguinol A and Benzguinol B in Combination with Colistin Show Low Cytotoxicity to Mammalian Cell Lines

In a previous experiment, we showed that benzguinols A and B demonstrate very low cytotoxicity to Hep G2 (liver) and HEK293 (kidney) cell lines, with both compounds giving IC_{50} value at 32 $\mu\text{g}/\text{mL}$ [26]. In this study, we further examined toxicity profiles of the combination of colistin with benzguinol A or benzguinol B to the Hep G2 and HEK293 cell lines (Figure 4). At the concentrations tested, the addition of colistin in the combination did not change the IC_{50} of benzguinol A or benzguinol B. For Hep G2 cells, the presence of colistin appears to reduce the toxicity of benzguinols A and B further (Figure 4A,B).

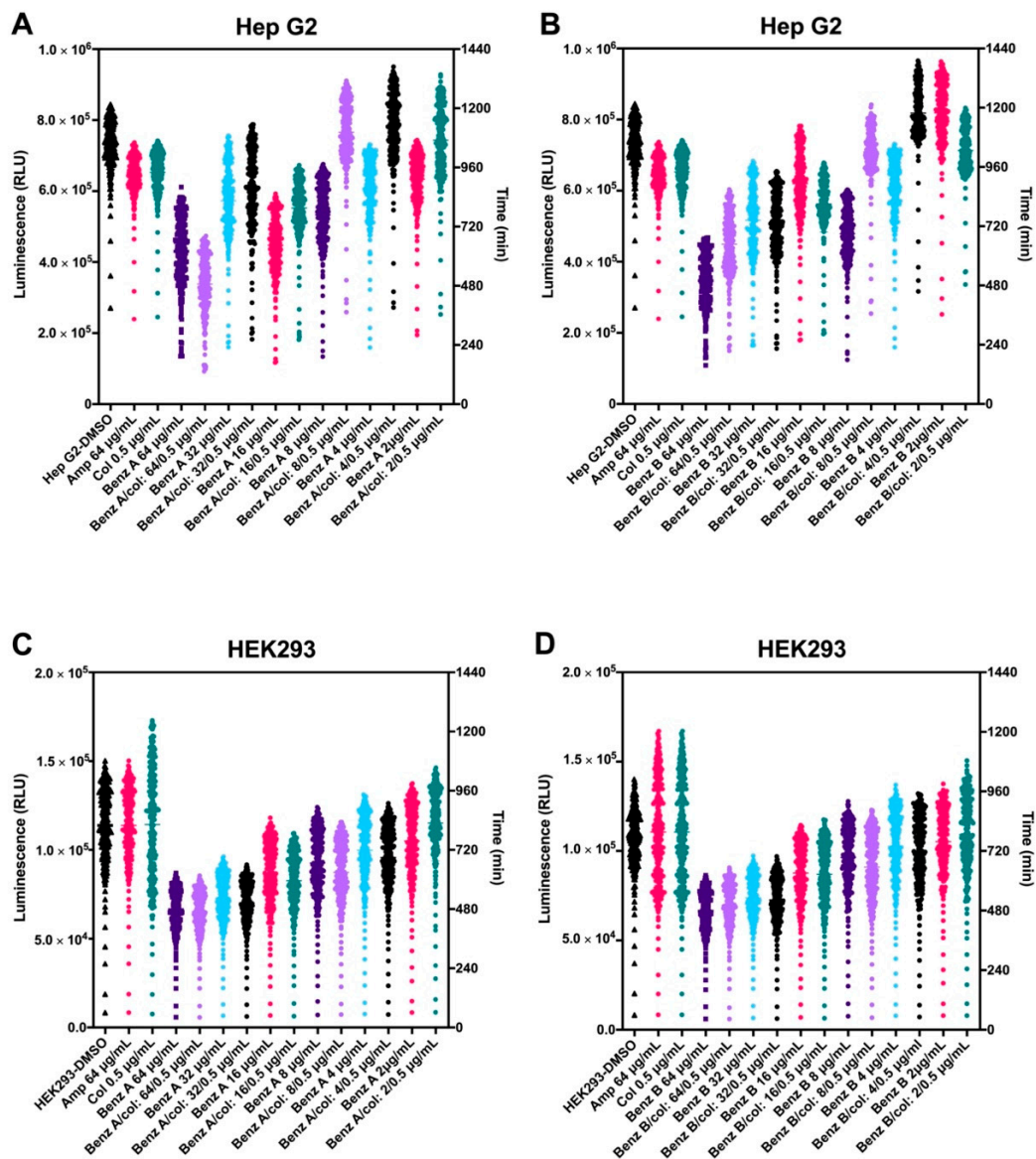


Figure 4. Cytotoxicity assessment of benzguinols A and B alone and in combination with colistin. Real-time cell viability measurements for Hep G2 (A,B) and HEK293 (C,D) cells after treatment with different concentrations of benzguinols A and B alone and with 0.5 $\mu\text{g}/\text{mL}$ of colistin. The viability of each cell line was measured hourly for 20 h at 37 $^{\circ}\text{C}$ in the presence of 5% CO_2 on a Cytation 5 Cell Imaging Multi-Mode Reader (BioTek, Millennium Science Pty Ltd, Mulgrave, VIC, Australia) using the RealTime-GloTM MT Cell Viability Assay reagent (Promega, Madison, WI, USA). Data presented are relative light units (RLU) for each treatment per time point. Abbreviations: Amp, ampicillin; Col, colistin; Benz, benzguinol.

3.4. Benzguinols Show Systemic Safety in Mice

There were no observable histopathological changes in the liver, heart, spleen, kidneys, and lungs in any mice treated with three IP doses of benzguinol A or benzguinol B at 20 mg/kg (Figure 5).

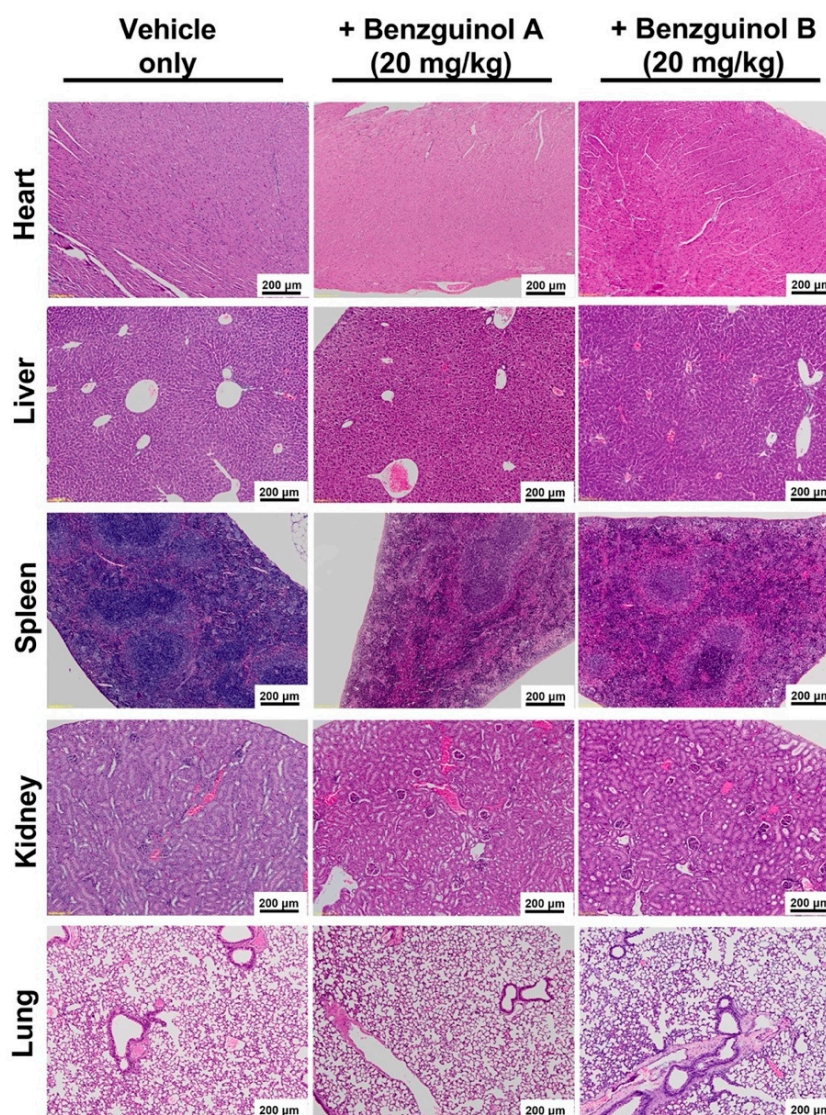


Figure 5. Representative histological images of heart, liver, spleen, lung, and kidneys from benzguinol-treated and control mice harvested at 72 h post-treatment. No morphological abnormalities or changes were observed in mice treated IP with 20 mg/kg benzguinol A, 20 mg/kg benzguinol B, or with vehicle alone. Scale bars: 200 µm.

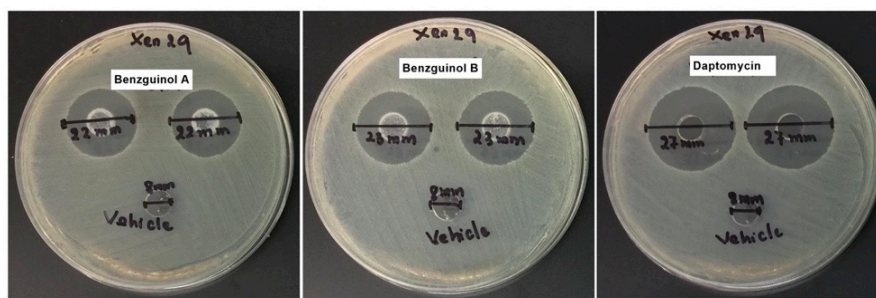
3.5. Agar Well Diffusion Test of Benzguinol Formulations Shows Antibacterial Activity

In order to ascertain that the benzguinols are active in the vehicle used, an agar diffusion test of the formulations was carried out. All formulations of benzguinols A and B showed clear inhibitory zones of 22–23 mm, while daptomycin as a control showed an inhibitory zone of 27 mm (Table 3 and Figure 6), indicating that all drugs were released from the vehicle into the agar.

Table 3. Inhibitory zones of benzguinol A and benzguinol B formulations used for safety and efficacy trials.

| Drug | Inhibitory Zone (mm) | | | | |
|--------------|----------------------|----------|----------------|----------|-----------------|
| | Safety Trial | | Efficacy Trial | | |
| | Vehicle | 20 mg/kg | Vehicle | 20 mg/kg | 6 mg/kg |
| Benzguinol A | 8 | 23 | 8 | 22 | ND ^a |
| Benzguinol B | 8 | 23 | 8 | 23 | ND |
| Daptomycin | 8 | ND | 8 | ND | 27 |

^a ND, not determined. Each well contained 100 µL of each formulation of benzguinol A or B (600 µg), daptomycin (180 µg), and 100 µL vehicle only.

**Figure 6.** Selected well diffusion of benzguinol A and benzguinol B formulations used in efficacy trial. Each well contained 100 µL of each formulation of benzguinol A or B (600 µg), daptomycin (180 µg) and 100 µL vehicle only. Xen29, bioluminescent *S. aureus* Xen29.

3.6. Treatment of Mice with Benzguinol A or Benzguinol B Reduces *S. aureus* Populations and Significantly Prolongs Survival Times

The potential of benzguinol A and B as therapeutic drugs against systemic *S. aureus* infection was examined in an IP sepsis challenge model using a well characterized bioluminescent *S. aureus* strain (Xen29). We found that, after the first dose of benzguinol A at 20 mg/kg, there was a statistically significant reduction in *S. aureus* photons at 4 h ($p = 0.0086$, Mann–Whitney *U*-test, one-tailed) and 6 h ($p = 0.0121$, Mann–Whitney *U*-test, one-tailed) (Figure 7A) and significant decrease in number of bacteria at 6 h ($p = 0.0043$, Mann–Whitney test, one-tailed). The second dose of benzguinol A at 6 h post-infection also resulted in significant reduction in bacterial counts at 8 h post-infection ($p = 0.0022$, Mann–Whitney *U*-test, one-tailed) (Figure 7B). Three doses of benzguinol A resulted in significant increase in median survival time compared to the vehicle only control ($p = 0.017$; Mantel–Cox test; Figure 7C).

For benzguinol B, the first dose at 20 mg/kg given at 2 h post-infection resulted in a statistically significant reduction in *S. aureus* photons ($p = 0.0342$, Mann–Whitney *U*-test, one-tailed, Figure 7A), and a significant decrease in the number of bacteria ($p = 0.0303$, Mann–Whitney test, one-tailed) at 6 h post-infection. The second dose of benzguinol B (given at 6 h post-infection) resulted in a significant reduction in the number of bacteria at 8 h post-infection ($p = 0.0206$, Mann–Whitney *U*-test, one-tailed) (Figure 7B) but no significant difference in median survival time compared to the vehicle only control (Figure 7C).

Data of photon analysis and bacteria counts are shown up to 6 and 8 h, respectively, due to the number of surviving mice remaining in each group (Figure 7C). The bacterial reduction caused by benzguinol A and B could be clearly observed on images of mice (Figure 8).

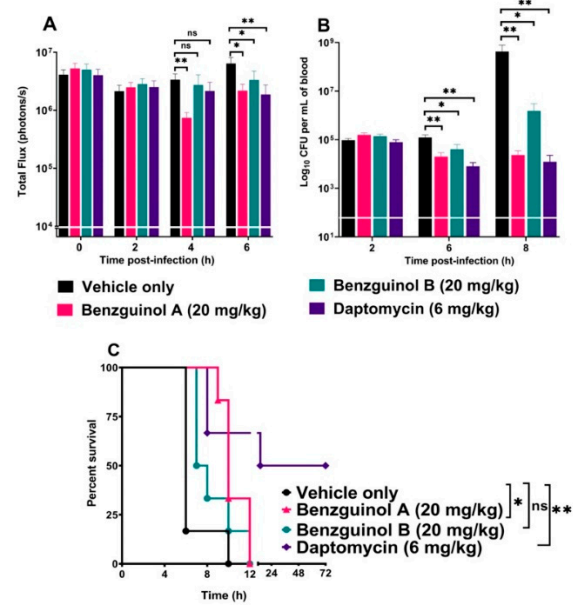


Figure 7. Benzguinol efficacy data. (A) Comparison of luminescence signals and (B) bacterial load in blood between groups of CD1 mice ($n = 6$) challenged IP with bioluminescent *S. aureus* ATCC 12600 (Xen29) and treated with the indicated drugs. Mice were subjected to bioluminescence imaging on IVIS Lumina XRMS Series III system at the indicated times. ns, not significant; *, $p < 0.05$; **, $p < 0.01$; Mann–Whitney U -test (one-tailed). (C) Survival analysis for mice treated with the indicated drugs. ns, not significant; *, $p < 0.05$; **, $p < 0.01$; Log-rank (Mantel–Cox test).

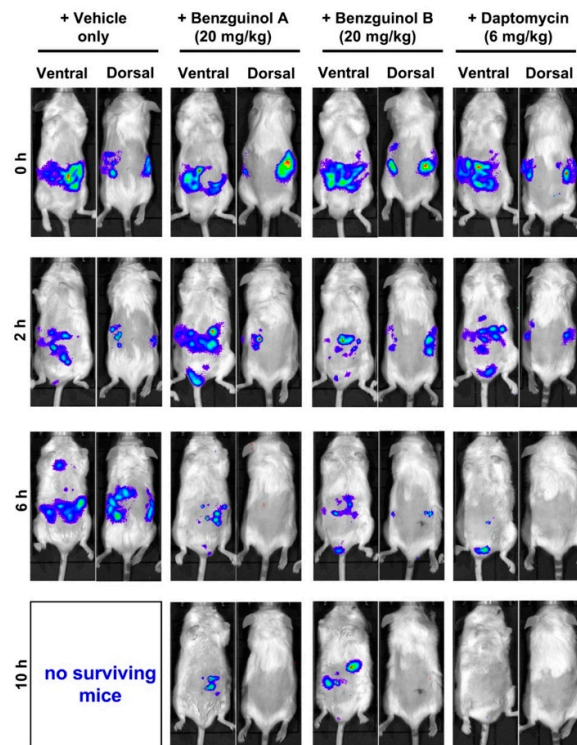


Figure 8. Ventral and dorsal images of representative CD1 mice challenged with approximately 6×10^7 CFU of bioluminescent *S. aureus* ATCC 12600 (Xen29). Mice were treated with benzguinol A or benzguinol B (20 mg/kg), daptomycin (6 mg/kg), or vehicle at 2, 6, and 10 h. Mice were subjected to bioluminescence imaging on IVIS Lumina XRMS Series III system at the indicated times. At 8 h post-infection, all mice treated with vehicle only had become moribund, indicated by “no surviving mice” at 10 h.

4. Discussion

The rise in bacterial infections that are resistant to almost all known antibiotics is alarming [37], while at the same time the antibiotic development pipeline has remained stagnant [38]. This global wake-up call has stimulated a debate about how best to combat antibiotic resistance [37]. With this in mind, we have been exploring a strategy involving revisiting some of the old antibiotic scaffolds that were discovered many decades ago but abandoned in favor of more promising leads using modern drug discovery methods to bring new antibiotic classes to the market [39]. In this work, we extended our previous *in vitro* studies on two semisynthetic analogs of unguinol (benzguinols A and B) [26] to investigate their potential as novel antibiotics for future treatment of bacterial infections.

This study shows three major findings. Firstly, benzguinols A and B demonstrated low MICs against an opportunistic GPB pathogen (MRSP) and also against key strains of GNB (*A. baumannii*, *E. coli*, *K. pneumoniae*, and *P. aeruginosa*) in the presence of sub-inhibitory concentrations of colistin. Secondly, the benzguinols alone or in combination with colistin showed *in vitro* safety to mammalian (Hep G2 (liver) and HEK293 (kidney)) cell lines and also demonstrated clinical safety in mice with no observed morphological effects on the major organs after three IP doses at 20 mg/kg. Thirdly, treatment of mice with three IP doses of benzguinol A or benzguinol B at 20 mg/kg reduced bioluminescent *S. aureus* populations *in vivo* and significantly prolonged survival times.

We previously demonstrated that benzguinols A and B show potent activity against MSSA and MRSA at MIC range of 0.25–1 µg/mL (comparable to daptomycin standard). However, unlike daptomycin, the two drugs were shown to have bacteriostatic activity [26]. In this study, we extended our investigation to test the activity of the benzguinols against MRSP clinical isolates and GNB reference strains. The two drugs produced a MIC range of 0.5–1 µg/mL against the MRSP clinical isolates, compared to the amikacin standard with a MIC range of 8–16 µg/mL. Furthermore, while benzguinols A and B alone have no antimicrobial activity against GNB, combination with sub-inhibitory concentrations of colistin resulted in a synergistic interaction when tested against *A. baumannii*, *E. coli*, *K. pneumoniae*, and *P. aeruginosa* ATCC strains, returning MICs of 1–2 µg/mL.

Effective treatment of GNB infections presents a greater challenge than for GPB treatment mainly due to the presence of the outer membrane in GNB, which presents a barrier preventing antibiotic access [40]. Colistin has been shown to interact with the lipopolysaccharide on the surface of GNB. It can then traverse the outer membrane through the self-promoted uptake pathway, resulting in GNB outer membrane disruption [41,42]. For the benzguinol A or benzguinol B + colistin combination, it is hypothesized that the sub-inhibitory concentration of colistin transiently ruptures the outer membrane, thereby allowing passage of the drugs into the cell to reach the drug target site(s). Therefore, a combination of colistin with benzguinol A or benzguinol B could serve as a potential combination for future treatment of bacterial infections. To date, the mode of action of benzguinols is not known or their target(s) identified. However, structure–activity relationship data from our recent work [26] suggest benzguinols and other related family of depsidones may act by binding to a target shared by prokaryotes. Given the lack of information on their target(s), it is quite difficult to speculate the nature of resistance development against benzguinols. As such, identifying the target(s) of benzguinols will be the subject of future investigation.

We previously demonstrated that the benzguinols did not cause hemolysis of human red blood cells (RBCs) at the highest concentration (128 µg/mL) used and both returned IC₅₀ values of 32 µg/mL against the HEK293 and Hep G2 cell lines [26]. Further investigation of cell cytotoxicity profiles of combination of benzguinol A or benzguinol B with colistin at 0.5 µg/mL demonstrated no difference in IC₅₀ values of either benzguinol alone or in combination with colistin on HEK293 cells and slightly better IC₅₀ values against Hep G2 cells. Subsequent *in vivo* safety testing using three doses of benzguinol A or benzguinol B at 20 mg/kg did not reveal any adverse clinical signs or observable histopathological changes within the main internal mouse organs examined.

Based on the findings above, we investigated the potential of the benzguinols for the treatment of acute sepsis resulting from intraperitoneal inoculation with a bioluminescent derivative of *S. aureus* ATCC 12600 (Xen29). Our results reveal that three IP doses of benzguinol A or B at 20 mg/kg elicited a statistically significant reduction in *S. aureus* populations and prolonged survival times of mice compared to the vehicle-only treated mice. We observed that benzguinol A showed slightly better efficacy, especially in terms of survival percentage. While both compounds have similar MICs of 0.5 µg/mL against *S. aureus* as daptomycin, they were not as effective as daptomycin, associated with a 32-fold increase in MICs in the presence of 10% FBS [26]. This suggests the bioavailability of benzguinols A and B may be quite low in the blood of mice. In addition, the low aqueous solubility of the benzguinols could be a limiting factor in the bioavailability of the drug in the mouse model.

5. Conclusions

The study reported here is an extension of previous *in vitro* investigations of the antibacterial activities of unguinol derivatives benzguinols A and B against GPB pathogens to include evaluation of their potency against MRSP at low concentrations. Our results also show that the combination of benzguinol A or benzguinol B with sub-inhibitory concentrations of colistin resulted in potent activity against key GNB *in vitro*, suggesting either benzguinol could be combined with colistin for the treatment of GNB infections. In addition, IP treatment of mice with benzguinol A or benzguinol B after systemic *S. aureus* challenge resulted in significant reduction in *S. aureus* populations and prolonged survival times compared to the vehicle-only control, but without clearing the bacterial infection from the bloodstream, suggesting bacteriostatic activity *in vivo* at the dose administered. Preclinical efficacy testing of a combination of benzguinol A or benzguinol B with colistin is also warranted, potentially overcoming resistance to colistin monotherapy while mitigating toxicity concerned with its use.

Overall, our findings demonstrate that the benzguinols could provide promising new actives evolved from the “lost antibiotic” nidulin family of fungal metabolites for further pharmaceutical and medicinal chemistry development and dose optimization. An intensified effort to enhance the properties of our leads towards improved solubility, reduced plasma binding, and a broader spectrum of action against resistant pathogens is under investigation.

Author Contributions: Conceptualization, H.T.N., M.T.M., D.V., A.C., E.L., H.V., S.W.P., A.M.P., D.J.T. and A.D.O.; data curation, H.T.N., D.V., A.C., H.P., L.W. and A.D.O.; formal analysis, H.T.N., M.T.M., D.V., A.C., E.L., S.G., H.P., L.W., S.W.P., A.M.P., D.J.T. and A.D.O.; funding acquisition, A.C., E.L., S.W.P., A.M.P. and D.J.T.; investigation, H.T.N., M.T.M., H.P., L.W., D.J.T. and A.D.O.; Methodology, H.T.N., M.T.M., D.V., A.C., L.W. and A.D.O.; project administration, E.L.; resources, A.C., E.L., S.G., L.W., H.V., S.W.P., A.M.P. and D.J.T.; supervision, D.V., A.C., E.L., S.G., H.V., A.M.P., D.J.T. and A.D.O.; validation, H.T.N., M.T.M., D.V., A.C., E.L., S.G., H.P., L.W., S.W.P., A.M.P. and D.J.T.; visualization, H.T.N., H.V., S.W.P. and D.J.T.; writing—original draft, H.T.N. and A.D.O.; and writing—review and editing, H.T.N., D.V., A.C., E.L., S.G., H.P., L.W., H.V., S.W.P., A.M.P., D.J.T. and A.D.O. All authors have read and agreed to the published version of the manuscript.

Funding: This research was funded, in part, by the Cooperative Research Centres Projects scheme (CRCPFIVE000119).

Institutional Review Board Statement: The Ethics statement associated with this work is indicated in Section 2.7 of the manuscript. The Animal Ethics Committee of The University of Adelaide (approval number S-2015-151) reviewed and approved all animal experiments. The study was conducted in compliance with the Australian Code of Practice for the Care and Use of Animals for Scientific Purposes (8th Edition 2013) and the South Australian Animal Welfare Act 1985.

Informed Consent Statement: Not applicable.

Data Availability Statement: The data presented in this study are available on request from the corresponding author. The data are not publicly available due to privacy and access restrictions.

Acknowledgments: The authors would like to thank Amanda Ruggero, Lora Bowes, Anh Hong Nguyen, and Max McClafferty at the University of South Australia, South Australia 5000, Australia for their technical assistance. The authors would also like to thank to Tania Veltman and Bhumi Savaliya at the Australian Centre for Antimicrobial Resistance Ecology (ACARE), The University of Adelaide, Roseworthy, SA 5371, Australia for providing MRSP isolates. In addition, the authors would like to thank Ankitkumar Parikh and Krishna Kathawala at the University of South Australia, South Australia 5000, Australia for help with preparing benzguinol and daptomycin formulations.

Conflicts of Interest: S.W.P. is a director of Advanced Veterinary Therapeutics, E.L. is a director of Microbial Screening Technologies, and A.C. and D.V. are employees of Microbial Screening Technologies.

References

1. WHO. *Antimicrobial Resistance*; World Health Organization: Geneva, Switzerland, 2020.
2. Chopra, I.; Schofield, C.; Everett, M.; O'Neill, A.; Miller, K.; Wilcox, M.; Frère, J.-M.; Dawson, M.; Czaplewski, L.; Urleb, U.; et al. Treatment of health-care-associated infections caused by Gram-negative bacteria: A consensus statement. *Lancet Infect. Dis.* **2008**, *8*, 133–139. [[CrossRef](#)]
3. Ergönül, Ö.; Aydın, M.; Azap, A.; Başaran, S.; Tekin, S.; Kaya, Ş.; Gülsün, S.; Yörük, G.; Kurşun, E.; Yeşilkaya, A.; et al. Healthcare-associated Gram-negative bloodstream infections: Antibiotic resistance and predictors of mortality. *J. Hosp. Infect.* **2016**, *94*, 381–385. [[CrossRef](#)]
4. Bassetti, M.; Peghin, M.; Vena, A.; Giacobbe, D.R. Treatment of infections due to MDR gram-negative bacteria. *Front. Med.* **2019**, *6*, 74. [[CrossRef](#)]
5. CDC. *Antibiotic Resistance Threats in the United States, 2019*; U.S. Department of Health and Human Services, Centers for Disease Control and Prevention: Atlanta, GA, USA, 2019; pp. 1–150.
6. WHO. *New Report Calls for Urgent Action to Avert Antimicrobial Resistance Crisis*; Joint news release; World Health Organization: Geneva, Switzerland, 2019.
7. O'Neill, J.; Davies, S.; Rex, J.; White, L.; Murray, R. *Review on Antimicrobial Resistance, Tackling Drug-Resistant Infections Globally: Final Report and Recommendations*; Wellcome Trust and UK Government: London, UK, 2016.
8. Hart, J.; Christiansen, K.J.; Lee, R.; Heath, C.H.; Coombs, G.W.; Robinson, J.O. Increased EMRSA-15 health-care worker colonization demonstrated in retrospective review of EMRSA hospital outbreaks. *Antimicrob. Resist. Infect. Control* **2014**, *3*, 7. [[CrossRef](#)] [[PubMed](#)]
9. Knox, J.; Van Rijen, M.; Uhlemann, A.-C.; Miller, M.; Hafer, C.; Vavagiakis, P.; Shi, Q.; Johnson, P.D.R.; Coombs, G.; Kluytmans-Van Den Bergh, K.-V.D.; et al. Community-associated methicillin-resistant *Staphylococcus aureus* transmission in households of infected cases: A pooled analysis of primary data from three studies across international settings. *Epidemiol. Infect.* **2015**, *143*, 354–365. [[CrossRef](#)] [[PubMed](#)]
10. Valiquette, L.; Chakra, C.N.A.; Laupland, K.B. Financial impact of health care-associated infections: When money talks. *Can. J. Infect. Dis. Med. Microbiol.* **2014**, *25*, 71–74. [[CrossRef](#)] [[PubMed](#)]
11. McCarthy, A.J.; Harrison, E.M.; Stanczak-Mrozek, K.; Leggett, B.; Waller, A.; Holmes, M.A.; Lloyd, D.H.; Lindsay, J.A.; Loeffler, A. Genomic insights into the rapid emergence and evolution of MDR in *Staphylococcus pseudintermedius*. *J. Antimicrob. Chemother.* **2015**, *70*, 997–1007. [[CrossRef](#)]
12. Pires Dos Santos, T.P.; Damborg, P.; Moodley, A.; Guardabassi, L. Systematic review on global epidemiology of methicillin-resistant *Staphylococcus pseudintermedius*: Inference of population structure from multilocus sequence typing data. *Front. Microbiol.* **2016**, *7*, 1599. [[CrossRef](#)] [[PubMed](#)]
13. Trott, D. β -lactam resistance in gram-negative pathogens isolated from animals. *Curr. Pharm. Des.* **2013**, *19*, 239–249. [[CrossRef](#)] [[PubMed](#)]
14. Abraham, S.; Trott, D.J.; Jordan, D.; Gordon, D.M.; Groves, M.D.; Fairbrother, J.M.; Smith, M.G.; Zhang, R.; Chapman, T.A. Phylogenetic and molecular insights into the evolution of multidrug-resistant porcine enterotoxigenic *Escherichia coli* in Australia. *Int. J. Antimicrob. Agents* **2014**, *44*, 105–111. [[CrossRef](#)] [[PubMed](#)]
15. de la Fuente-Nunez, C.; Torres, M.D.; Mojica, F.J.; Lu, T.K. Next-generation precision antimicrobials: Towards personalized treatment of infectious diseases. *Curr. Opin. Microbiol.* **2017**, *37*, 95–102. [[CrossRef](#)]
16. Talbot, G.H.; Jezek, A.; Murray, B.E.; Jones, R.N.; Ebright, R.H.; Nau, G.J.; Rodvold, K.A.; Newland, J.G.; Boucher, H.W.; Infectious Diseases Society of America. The Infectious Diseases Society of America's 10 × '20 initiative (10 new systemic antibacterial agents us food and drug administration approved by 2020): Is 20 × '20 a possibility? *Clin. Infect. Dis.* **2019**, *69*, 1–11. [[CrossRef](#)] [[PubMed](#)]
17. Theuretzbacher, U.; Outtersson, K.; Engel, A.; Karlén, A. The global preclinical antibacterial pipeline. *Nat. Rev. Genet.* **2020**, *18*, 275–285. [[CrossRef](#)] [[PubMed](#)]
18. Bergen, P.J.; Bulman, Z.P.; Saju, S.; Bulitta, J.B.; Landersdorfer, C.; Forrest, A.; Cornelia, J.L.; Nation, R.L.; Tsuji, B.T. Polymyxin combinations: Pharmacokinetics and pharmacodynamics for rationale use. *Pharmacother. J. Hum. Pharmacol. Drug Ther.* **2015**, *35*, 34–42. [[CrossRef](#)]
19. Bush, K. New antimicrobial agents for Gram-negative pathogens in pipelines. *Int. J. Antimicrob. Agents* **2015**, *45* (Suppl. 2), S10.

20. Paytubi, S.; De La Cruz, M.; Balsalobre, C.; Tormo, J.R.; Martín, J.; González, I.; Gonzalez-Menendez, V.; Genilloud, O.; Reyes, F.; Vicente, F.; et al. A high-throughput screening platform of microbial natural products for the discovery of molecules with antibiofilm properties against Salmonella. *Front. Microbiol.* **2017**, *8*, 326. [[CrossRef](#)]
21. Bui, T.; Preuss, C.V. *Cephalosporins*; StatPearls Publishing: Treasure Island, FL, USA, 2020.
22. José, R.J. Next generation macrolides for community-acquired pneumonia: Will solithromycin rise to the occasion? *Ann. Res. Hosp.* **2017**, *1*, 11. [[CrossRef](#)]
23. National Research Council (US) Committee on New Directions in the Study of Antimicrobial Therapeutics. The National Academies Collection: Reports funded by National Institutes of Health. In *Treating Infectious Diseases in a Microbial World: Report of Two Workshops on Novel Antimicrobial Therapeutics*; National Academies Press: Washington, DC, USA, 2006. [[CrossRef](#)]
24. Fair, R.J.; Tor, Y. Antibiotics and bacterial resistance in the 21st century. *Perspect. Med. Chem.* **2014**, *6*, 25–64. [[CrossRef](#)] [[PubMed](#)]
25. Morshed, M.T.; Vuong, D.; Crombie, A.; Lacey, A.E.; Karuso, P.; Lacey, E.; Piggott, A.M. Expanding antibiotic chemical space around the nidulin pharmacophore. *Org. Biomol. Chem.* **2018**, *16*, 3038–3051. [[CrossRef](#)]
26. Morshed, M.T.; Nguyen, H.T.; Vuong, D.; Crombie, A.; Lacey, E.; Ogunniyi, A.D.; Page, S.W.; Trott, D.J.; Piggott, A.M. Semisynthesis and biological evaluation of a focused library of unguinol derivatives as next-generation antibiotics. *Org. Biomol. Chem.* **2021**, *19*, 1022–1036. [[CrossRef](#)] [[PubMed](#)]
27. Saputra, S.; Jordan, D.; Worthing, K.; Norris, J.M.; Wong, H.S.; Abraham, R.; Trott, D.J.; Abraham, S. Antimicrobial resistance in coagulase-positive staphylococci isolated from companion animals in Australia: A one year study. *PLoS ONE* **2017**, *12*, e0176379. [[CrossRef](#)]
28. Ogunniyi, A.D.; Khazandi, M.; Laven-Law, G.; Tótolí, E.G.; Salgado, H.R.; Pi, H.; Coombs, G.W.; Shinabarger, D.L.; Turnidge, J.D.; Paton, J.C.; et al. Evaluation of robenidine analog NCL195 as a novel broad-spectrum antibacterial agent. *PLoS ONE* **2017**, *12*, e0183457. [[CrossRef](#)]
29. CLSI. *Performance Standards for Antimicrobial Disk and Dilution Susceptibility Tests For Bacteria Isolated from Animals*, 4th ed.; CLSI Supplement VET08; CLSI: Wayne, PA, USA, 2018.
30. Pi, H.; Nguyen, H.T.; Venter, H.; Boileau, A.R.; Woolford, L.; Garg, S.; Page, S.W.; Russell, C.C.; Baker, J.R.; McCluskey, A.; et al. In vitro activity of robenidine analog NCL195 in combination with outer membrane permeabilizers against Gram-negative bacterial pathogens and impact on systemic Gram-positive bacterial infection in mice. *Front. Microbiol.* **2020**, *11*, 1556. [[CrossRef](#)] [[PubMed](#)]
31. CLSI. *Methods for Determining Bactericidal Activity of Antimicrobial Agents*; Approved Guideline; Clinical and Laboratory Standards Institute: Wayne, PA, USA, 1999.
32. Elemam, A.; Rahimian, J.; Doymaz, M. In vitro evaluation of antibiotic synergy for polymyxin B-resistant carbapenemase-producing *Klebsiella pneumoniae*. *J. Clin. Microbiol.* **2010**, *48*, 3558–3562. [[CrossRef](#)]
33. Hwang, I.-S.; Hwang, J.H.; Choi, H.; Kim, K.-J.; Lee, D.G. Synergistic effects between silver nanoparticles and antibiotics and the mechanisms involved. *J. Med. Microbiol.* **2012**, *61*, 1719–1726. [[CrossRef](#)]
34. Khazandi, M.; Pi, H.; Trott, D.J.; Chan, W.Y.; Ogunniyi, A.D.; Sim, J.X.F.; Venter, H.; Garg, S.; Page, S.W.; Hill, P.B.; et al. In vitro antimicrobial activity of robenidine, ethylenediaminetetraacetic acid and polymyxin B nonapeptide against important human and veterinary pathogens. *Front. Microbiol.* **2019**, *10*, 837. [[CrossRef](#)] [[PubMed](#)]
35. Eid, S.Y.; El-Readi, M.Z.; Wink, M. Synergism of three-drug combinations of sanguinarine and other plant secondary metabolites with digitonin and doxorubicin in multi-drug resistant cancer cells. *Phytomedicine* **2012**, *19*, 1288–1297. [[CrossRef](#)]
36. Valgas, C.; Souza, S.M.d.; Smânia, E.F.A.; Smânia, A., Jr. Screening methods to determine antibacterial activity of natural products. *Braz. J. Microbiol.* **2007**, *38*, 369–380. [[CrossRef](#)]
37. Hutchings, M.I.; Truman, A.W.; Wilkinson, B. Antibiotics: Past, present and future. *Curr. Opin. Microbiol.* **2019**, *51*, 72–80. [[CrossRef](#)] [[PubMed](#)]
38. Theuretzbacher, U. Global antimicrobial resistance in Gram-negative pathogens and clinical need. *Curr. Opin. Microbiol.* **2017**, *39*, 106–112. [[CrossRef](#)] [[PubMed](#)]
39. Wenczewicz, T.A. New antibiotics from Nature's chemical inventory. *Bioorg. Med. Chem.* **2016**, *24*, 6227–6252. [[CrossRef](#)]
40. Arzanlou, M.; Chai, W.C.; Venter, H. Intrinsic, adaptive and acquired antimicrobial resistance in Gram-negative bacteria. *Essays Biochem.* **2017**, *61*, 49–59. [[CrossRef](#)] [[PubMed](#)]
41. Bergen, P.J.; Smith, N.M.; Bedard, T.B.; Bulman, Z.P.; Cha, R.; Tsuji, B.T. Rational combinations of polymyxins with other antibiotics. *Adv. Exp. Med. Biol.* **2019**, *1145*, 251–288. [[CrossRef](#)] [[PubMed](#)]
42. Zgurskaya, H.I.; López, C.A.; Gnanakaran, S. Permeability barrier of gram-negative cell envelopes and approaches to bypass it. *ACS Infect. Dis.* **2015**, *1*, 512–522. [[CrossRef](#)] [[PubMed](#)]

Chapter VIII

General discussion and further directions

8.1. General summary

The increasing prevalence of bacterial pathogens that are MDR to commonly used antimicrobials in health care settings has led to a decrease in treatment options and continues to generate a high level of global health concern [290]. In particular, MDR-ESKAPE pathogens are associated with high mortality rates and increased health care setting costs [9,291]. The problem is further exacerbated by the slow progress in new drug development by the pharmaceutical industry [18]. Moreover, the discovery and development process for the introduction of new drugs to the market can cost over \$2.6 billion USD and can take up to 15 years [14-16]. However, in many cases, bacterial pathogens resistant to the new drug are found shortly after clinical application [13].

Drug discovery for the treatment of MDR-GNB infections has posed numerous challenges in comparison to MDR-GPB infections due to the presence of an OM in GNBs, which prevents antibiotics from gaining entry and exerting their effect [11,292]. In addition, GNB can develop resistance to a wide range of antibiotics through several different mechanisms, but most commonly through acquisition of mobile genetic elements containing MDR genes [25,26]. Current options for the treatment and management of MDR infections include polymyxins, AG, fosfomycin, tigecycline, fluroquinolones, and carbapenems, and new approvals for the treatment of GNB infection include compounds or combinations of compounds such as ceftazidime-avibactam, cefiderocol, imipenem + cilastatin + relebactam, and plazomicin, which represent new chemistry based on modifications to existing drug scaffolds [98-101]. Given this caveat, these new antibiotics are far from sufficient therapeutic options to fully combat the emergence and persistence of MDR-GNB infections [66,86,109]. Currently, polymyxins (PMB and colistin) are considered as last resort antibiotics for the

treatment of GNB infections [293,294]; nonetheless, resistance to polymyxins is emerging via different mechanisms [293,295]. Moreover, there is increasing evidence of transferable colistin resistance being a significant issue to human health, particularly associated with recently discovered plasmid-borne *mcr* genes, which are now prevalent worldwide and are often co-located with other antimicrobial resistance genes on MDR plasmids [296]. Therefore, it is critically important to preserve and prolong the life of this last-resort antibiotic where enhanced combination therapy is a promising option. A synergistic combination of polymyxins with well-known or new drugs such as antibiotics, antifungals with antibiotic activity, and/or efflux inhibitors can increase therapeutic efficacy, broaden the antibiotic spectrum, restore resistant drugs to full efficacy, reduce the risk of toxicity due to lower concentration required for individual drugs, and decrease resistance development [218,219,297]. Several studies have provided evidence that the combination of polymyxins with other antibiotics showed fully synergistic or partially synergistic activities against MDR-GNB pathogens [298-301].

In line with the combination therapy approach, this thesis explored a number of novel compounds, including NCL195, NCL179 and two benzguinol derivatives, as potential alternatives for future stand-alone treatments of GPB infections and GNB infections when combined with low dose colistin. We firstly examined an *in vitro* synergistic combination of NCL195 with different adjuvants against GNB pathogens to determine the optimal choices for combination therapy as well as confirming promising *in vivo* efficacy of NCL195 against GPB infection in mouse models when administered via the systemic route (chapter II) [288]. Secondly, we investigated *in vitro* synergistic activity of the combination NCL195 and colistin (identified as the ideal adjuvant to use with the robenidine analogue) and then used fluorescence membrane potential and TEM to obtain a more detailed understanding of the interactions of NCL195 and colistin with bacterial cell membranes (chapter III). Thirdly, we

compared the traditional TEM technique and TEM using CryO sections to identify the optimal method for visualising NCL195-colistin interactions with the GNB membrane (chapter IV). Fourthly, we tested the *in vivo* efficacy of NCL195 against *S. aureus* in a GPB mouse model using the oral route of drug delivery that was followed by efficacy testing of (oral) NCL195 + (IP) colistin combination against both colistin-susceptible and -resistant bioluminescent *E. coli* in mouse sepsis models (chapter V). Fifthly, we presented an *in vitro* characterization of NCL179 activity against GPB and NCL179 + colistin combination against GNB followed by *in vivo* efficacy testing of NCL179 administered via the oral route in a bioluminescent *S. aureus* mouse sepsis model as a proof-of-concept study (chapter VI). Finally, *in vitro* activity of benzguinols against GPB and GNB in the presence of sub-inhibitory concentrations of colistin and their impact on GPB pathogens in the same systemic *S. aureus* infection model were described in chapter VII. Detailed discussions have been included in the relevant papers from chapters II to VII, and only the main findings are summarised here.

8.2. Major findings

We found that combining NCL195 with EDTA, PMBN, PMB, and colistin showed synergistic interaction against GNB pathogens while NCL195 alone had no activity against GNB (chapter II). Among these adjuvants, we identified that colistin and PMB showed the best synergistic activity, were less expensive choices than PMBN, and had greater applicability than EDTA, which can only be used topically when combined with NCL195 to treat GNB. This reduced the required concentrations needed for both drugs to kill/inhibit the growth of bacteria and resulted in better mammalian cell cytotoxicity profiles [302-305] (chapters II and III).

Interaction of NCL195 with colistin and PMB was further investigated using fluorescence-based membrane potential measurements. The results showed that NCL195 disrupted the membrane potential of GNB in the presence of sub-inhibitory concentrations of PMB or colistin, while NCL195 alone had no effect (chapter II and III). In addition, NCL195 permeabilised the cytoplasmic membrane of *S. pneumoniae* and *S. aureus* by disrupting membrane potential [288]. Therefore, it is likely that colistin and PMB interact with the lipopolysaccharide on the surface of GNB and then across the OM via the self-promoted uptake pathway, resulting in disruption of its normal barrier property [219,220]. Subsequently, the OM transiently loses its structural integrity, thereby allowing passage of NCL195 into the cell to the drug target site(s), likely to be located on the plasma (inner) membrane. This hypothesis of the mode of action of robenidine/polymixin combinations aligns with previous reports describing similar interactions for colistin-azidothymidine [306] and colistin-vancomycin [307].

Our hypothesis was further supported by TEM images showing the effects of NCL195 alone on *S. aureus* morphology and NCL195 + colistin combination on *E. coli* and *P. aeruginosa* morphology (chapter II, III and IV). TEM with CryO section images showed *S. aureus* membrane morphology changes and the presence of mesosome-like membrane structures in NCL195-treated, but not in untreated bacteria (chapter II). The presence of mesosomes is possibly a consequence of cell membrane perturbation through disruption of the membrane potential, consistent with the effect of other antibiotic treatments reported previously [308-311]. Subsequently, we indicated that TEM of the membrane morphology of *E. coli* and *P. aeruginosa* after NCL195 + colistin combination treatment showed increased cell membrane damage with a pathognomonic ruffling surrounding the cells, more tubular appendages, and

loss of differentiation of cell envelope layers than colistin alone. In contrast, TEM images of cells exposed to NCL195 alone did not show any differences compared to untreated control cells, which correlated with a lack of *in vitro* activity against GNB (chapter III and IV). In this study, TEM of the membrane morphology of *E. coli* and *P. aeruginosa* after treatment with colistin is consistent with the findings of a previous report [312]. However, the exact membrane components affected by the NCL195 + colistin combination are still unclear, requiring further molecular investigation to identify the specific NCL195 target sites and mode of action (See section 8.4).

The stringent criteria for a new antibiotic to successfully proceed to clinical development require a balance between high *in vivo* efficacy in animal models, broad-spectrum antibacterial activity and safety to host target cells [313,314]. Here, NCL195 demonstrated limited toxicity to mammalian cell lines, low haemolytic activity [288], *in vivo* safety (systemic and oral route) in mice, as well as a significant reduction of *S. pneumoniae* (via the systemic route) and *S. aureus* (via systemic and oral routes) infecting populations *in vivo* using well established bioluminescent infection models. These correlated with prolonged survival times of NCL195-treated mice following sepsis challenge in comparison with control groups (chapter II and V). *In vivo* efficacy of NCL195 also correlated well with the results of *in vitro* susceptibility testing against GPB pathogens (chapter II, III and V). Likewise, the promising outcome of the *in vivo* efficacy of NCL195 (oral) + colistin (IP) combination in mouse GNB infection models mirrored the results of *in vitro* synergy testing of the same combination.

Accordingly, we investigated the safety of NCL195 combined with a range of colistin concentrations in mice prior to efficacy testing. Nephrotoxicity is a well-known feature of colistin due to the tight binding and accumulation of colistin to tissue membranes when given

as a continuous infusion [315,316]. Therefore, it is crucial to adjust dosing regimens of colistin to prevent renal failure and other untoward side effects. Here, we showed that combinations of four oral doses of NCL195 at 50 mg/kg at 4 h apart and four IP doses of two-fold increasing colistin concentrations from 0.125-4 mg/kg at 4 h apart were safe to mice with no apparent differences compared to mice receiving the vehicle only, NCL195 alone or colistin alone at similar concentrations (chapter V). Subsequently, simultaneous administration of four oral doses of 50 mg/kg NCL195 and four IP doses of colistin at 0.125 mg/kg, 0.25 mg/kg or 0.5 mg/kg 4 h apart resulted in dose-dependent, a significant reduction in colistin-susceptible *E. coli* loads compared to treatment with colistin alone at similar concentrations. Correspondingly, co-administration of four oral doses of 50 mg/kg NCL195 and four IP doses of colistin at 0.5 mg/kg, 1 mg/kg or 2 mg/kg resulted in a dose-dependent significant reduction in colistin-resistant *E. coli* loads compared to treatment with colistin alone at similar concentrations. In addition, colistin displayed *in vivo* concentration-dependent killing against both colistin-susceptible and-resistant *E. coli*, as described in previous reports [317-319]. For efficacy testing, we used colistin instead of PMB even though they have a similar chemical structure and antibacterial spectrum against GNB [320,321], because colistin is slightly more potent, colistin PK data are more available, it is commonly used in clinical practice, and it is the preferred polymyxin for IV and intrathecal administration [319].

Colistin currently plays a significant role as a “salvage” therapy to treat extremely drug-resistant GNB infections that are refractory to all other treatments such as carbapenems and tigecycline [317]. However, colistin resistance development and toxicity are significant concerns in devising dosing regimens [317]. Therefore, it is necessary to administer colistin therapy in a way that maximises antimicrobial activity, reduces the risk of resistance

development and minimises the potential for adverse effects [317]. Our results satisfied all these requirements because all doses of colistin used in combination with NCL195 were safe to mice and were much lower than the recommended IV-delivered colistin dose of 9 MU (approximately 300 g of colistin base activity or 720 mg of colistin) [318], but still showed excellent *in vivo* efficacy against both colistin-susceptible and -resistant GNB infections.

Chapter VI investigated the potential of another analogue of robenidine (NCL179) to expand the chemical diversity of the potential new antibiotic class (aminopyrimidines) to treat MDR bacterial infections. We demonstrated that NCL179 showed antibacterial activity against a wide range of clinical MDR-GPB pathogens, including MRSA, MRSP, and VRE. Notably, the combination of NCL179 with sub-inhibitory colistin concentrations resulted in a 100% synergistic interaction against all tested GNB pathogens, including colistin-resistant *A. baumannii* and colistin-resistant *E. coli* isolates. Moreover, we demonstrated the limited toxicity of NCL179 to mammalian cell lines, its low haemolytic activity, *in vivo* safety in mice, and the significant reduction in *S. aureus* populations *in vivo* together with prolonged survival times of NCL179-treated septic mice. These findings contributed crucial biological data for a second novel structure within the collection of 26 initial aminopyrimidine analogues designed to primarily explore structure/function relationships. The results confirm that the replacement of the robenidine aminoguanidine core with a 2-aminopyrimidine isostere has resulted in the generation of a new class of safer, biologically active and orally effective antimicrobials that is now ripe for further secondary medicinal chemistry improvements to attain greater levels of potency, safety and improved pharmacokinetics [287]. Although NCL179 contains halogen (i.e. chlorine) rather than methyl residues at the C4 position of the phenyl rings when compared to NCL195, we observed similar *in vitro* antimicrobial activity

against GPB and GNB when combined with a sub-inhibitory concentration of colistin. Moreover, we observed that NCL195 and NCL179 exhibited similar activity against *S. aureus* *in vitro* but *in vivo* efficacy of NCL195 was slightly better than NCL179 against *S. aureus* in a GPB mouse model. A significant reduction in bioluminescent *S. aureus* populations (in comparison to the untreated group) was observed starting at 4 h post-infection in the mouse group receiving NCL195 (chapter V), whereas this occurred at 6 h post-infection in the group treated with NCL179 (chapter VI), despite the same dosing regimen. This may possibly be due to the NCL195 MIC increasing 4-fold due to plasma-protein binding (chapter II); whereas for NCL179 (chapter VI), the MIC increase was much larger (16-fold).

Chapter VII extended our focus on the “lost antibiotic” strategy outlined in the CRC-P proposal (CRCPFIVE000119) to rediscover natural molecules produced by microorganisms with interesting antimicrobial properties investigated decades ago, but which stalled in clinical development [269,270]. We investigated the “lost antibiotic” unguinol and the related nidulin-family of fungal natural products and then focused on two semisynthetic derivatives, benzguinols A and B, that were shown to have excellent *in vitro* activity against both MSSA and MRSA isolates [322]. In this thesis, we further showed activity of the benzguinols against MRSP isolates, and their combination with sub-inhibitory concentrations of colistin resulted in a synergistic interaction when tested against *A. baumannii*, *E. coli*, *K. pneumoniae*, and *P. aeruginosa* ATCC strains, while benzguinols A and B alone had no antimicrobial activity against these GNB. Moreover, we previously demonstrated that benzguinols exhibited a high degree of safety to mammalian cell lines *in vitro* as well as low haemolytic activity [322]. Furthermore, administration of three IP doses of benzguinols at 20 mg/kg at 4 h apart in mice showed no adverse effects and elicited a statistically significant reduction in *S. aureus* populations following challenge in a sepsis model and prolonged survival times compared to the vehicle-

only treated mice. Our findings with these two early-stage (i.e. first generation) analogues strongly support the potential of the “lost antibiotic” strategy to address the urgent medical need to treat MDR infections.

The compiled data for NCL195, NCL179 and benzguinols obtained during this study represent significant contributions to the literature for a number of reasons. A broad spectrum of activity is one favourable characteristic for an antibiotic being developed for use in the treatment of bacterial sepsis, including co-infections and superinfections that commonly occur in clinical settings [323,324]. Here, all these compounds showed narrow-spectrum activity against a wide range of clinical MDR-GPB pathogens. Furthermore, the combination of all four antibiotics with sub-inhibitory concentrations of colistin resulted in a synergistic interaction against many GNB clinical isolates and reference strains (including *A. baumannii*, *E. coli*, *K. pneumoniae*, and *P. aeruginosa*); that are all on the critical WHO priority list of bacteria for which new antibiotics are urgently needed [22,325]. In addition, our findings strongly support the potential approach of combination therapy of sub-therapeutic colistin with other antibiotics to provide a solution to overcoming the OM permeability barrier [298,326,327]. Our *in vivo* efficacy data further support the NCL195 + colistin combination against GNB pathogens, which is in line with previous studies that demonstrated the superiority of combined therapy (with greater potential for eradicating GNB infection and no evidence of drug accumulation over time) vs monotherapy with polymyxins which risks rapid resistance development and potential toxicity associated with higher doses [96,249,250,328,329]. Lastly, we have shown that robenidine analogues in which the aminoguanidine core is replaced with a 2-aminopyrimidine structure appear to be more effective agents against bacterial sepsis when administered by the oral compared to the systemic route.

8.3. Limitations

Despite the progress made in the biological characterisation of four novel antibiotics, there were some limitations encountered in this body of work. Our safety studies were limited to confirmation that the concentration of each compound to be used in the efficacy trials for pre-clinical screening purposes that was safe. Consequently, we are yet to perform a comprehensive safety assessment, including acute toxicity testing, genetic toxicity testing, toxicokinetics, sub-chronic toxicity testing and chronic toxicity testing to provide detailed information on toxicity characteristics, the toxicity to specific target organs, the dose-response relationship, and cumulative side-effects that are used to extrapolate the safety of these novel antibiotics in humans or other animal species. Secondly, we are yet to perform detailed pharmacokinetic studies to provide information on the absorption, metabolism, distribution, and excretion (ADME) pattern of these compounds for appropriate dose selections. Such ADME studies will require a validated high performance liquid chromatography assay for qualitative and quantitative analysis of these compounds in blood to determine pharmacokinetic data such as the area under the curve, drug distribution ratio, C_{max} , t_{max} , $t_{1/2}$ and other parameters. Finally, time and funding limits prevented us from testing further 2-aminopyrimidine analogues with promising *in vitro* activity and modifications including halogen replacement (chlorine to bromine) on the phenyl C4 positions. Therefore, the following studies and further development are planned to provide more comprehensive information on these novel compounds that may represent a new antimicrobial class.

8.4. Future directions

Firstly, we provided additional membrane potential and TEM experimental evidence that robenidine analogues (NCL195 and NCL179) target the cytoplasmic membrane of GPB

and the corresponding inner membrane of GNB; however, the exact target site and mechanism of membrane depolarization is yet to be determined. Therefore, the mode of action of NCL195 should be further deciphered by conducting controlled bacterial gene expression studies during early-stage interactions with GPB together with labelling NCL195 and or NCL179 with fluorescence probes to characterise and explore potential drug targets in bacteria (utilising “click” chemistry).

Secondly, we demonstrated safety profiles of the four compounds at maximum doses based on MICs (NCL195 and NCL179 at 50 mg/kg, benzguinols at 20 mg/kg) but their no-observed-adverse-effect level (NOAEL), the highest dose producing no noticeable side effects, has not been evaluated to identify maximum tolerated dose (MTD) in mice. Therefore, additional *in vivo* safety mouse models with different groups treated with a range of increasing doses of the four novel chemicals need to be undertaken to identify MTD. Subsequently, the *in vivo* efficacy of each compound at MTD will be evaluated, followed by further pharmacokinetics and pharmacodynamics studies using mouse infection models to guide later dose selection for use in other animal species and humans.

Lastly, despite significant improvements over the parent compound (NCL812), we indicated some toxicity to mammalian cell lines and high plasma-protein binding still remain as the main limitations of current NCL195/NCL179 analogues. Therefore, these new chemical derivatives can be regarded as first-generation medicinal chemistry scaffolds that now require further molecular diversification and testing to identify analogues with improved potency, pharmacokinetics and safety.

8.5. Conclusions

This thesis demonstrated that all four novel antibiotic entities are promising therapeutic options with potentially different mechanisms of action in bacteria compared to existing antibiotics for the future treatment of MDR bacterial infections, particularly for MDR-GNB infections when combined with sub-inhibitory concentrations of colistin, which pose the greatest health threat, especially in the era of rapid and widespread colistin resistance. However, our research now requires further investigation into deciphering the molecular modes and target sites of action, which will inform further changes in the pharmacophore to explore structure/activity relationships and gain a better understanding of the difference in selectivity for prokaryote and eukaryote membrane targets. Further pharmaceutical development and subsequent safety and efficacy studies utilising different dose regimes will generate improved robenidine and unguinol formulations, particularly given the promising results obtained from oral delivery of NCL195/179 utilising a simple formulation in the present study. Lastly, these four new chemical compounds represent promising chemical scaffolds ripe for a more detailed and nuanced medicinal chemistry programme to further satisfy the pre-clinical assessment criteria required to progress towards clinical trials, either as stand-alone antibiotics for MDR-GPB infections, or in combination with sub-inhibitory concentrations of colistin for MDR-GNB infections.



Appendices

| | |
|--|-----|
| Appendix 1. Evidence of co-author in an article, doi:10.1039/d0ob02460k..... | 221 |
| Appendix 2. Evidence of co-author in an article, doi: 10.3390/microorganisms9081697 | 236 |
| Appendix 3. Evidence of e-poster presented at Australian Society for Microbiology Annual Scientific Meeting 2021 | 256 |
| Appendix 4. Evidence of participant in a poster presented at 26th Australian Conference on Microscopy and Microanalysis at National conventional centre Canberra 2020 | 258 |
| Appendix 5. Evidence of participant at SA/NT ASM student awards 2021 | 261 |
| Appendix 6. Evidence of an Ingenuity 2021 exhibition | 262 |
| Appendix 7. Evidence of winning a research committee’s publication award, 2021 | 265 |



Cite this: DOI: 10.1039/d0ob02460k

Semisynthesis and biological evaluation of a focused library of unguinol derivatives as next-generation antibiotics†

Mahmud T. Morshed, ^a Hang T. Nguyen, ^b Daniel Vuong, ^c
Andrew Crombie, ^c Ernest Lacey, ^{a,c} Abiodun D. Ogunniyi, ^b
Stephen W. Page, ^d Darren J. Trott ^b and Andrew M. Piggott ^{*a}

In this study, we report the semisynthesis and *in vitro* biological evaluation of thirty-four derivatives of the fungal depsidone antibiotic, unguinol. Initially, the semisynthetic modifications were focused on the two free hydroxy groups (3-OH and 8-OH), the three free aromatic positions (C-2, C-4 and C-7), the butenyl side chain and the depsidone ester linkage. Fifteen first-generation unguinol analogues were synthesised and screened against a panel of bacteria, fungi and mammalian cells to formulate a basic structure activity relationship (SAR) for the unguinol pharmacophore. Based on the SAR studies, we synthesised a further nineteen second-generation analogues, specifically aimed at improving the antibacterial potency of the pharmacophore. *In vitro* antibacterial activity testing of these compounds revealed that 3-*O*-(2-fluorobenzyl)unguinol and 3-*O*-(2,4-difluorobenzyl)unguinol showed potent activity against both methicillin-susceptible and methicillin-resistant *Staphylococcus aureus* (MIC 0.25–1 µg mL⁻¹) and are promising candidates for further development *in vivo*.

Received 9th December 2020,

Accepted 8th January 2021

DOI: 10.1039/d0ob02460k

rsc.li/obc

Introduction

Infections caused by multidrug-resistant bacteria are a major threat to global health. In the clinical setting, methicillin-resistant *Staphylococcus aureus* (MRSA) continues to be a leading cause of infection-related mortality.¹ While vancomycin has been the treatment of choice for serious MRSA infections for decades, there have been increasing reports of vancomycin treatment failures due to the emergence and dissemination of resistant strains.^{2,3} Concerningly, treatment failure with daptomycin, a drug of last resort for MRSA, can occur in more than 20% of cases.^{3,4} Therefore, there is a pressing need for the discovery and development of new antibiotics with novel modes of action to combat these deadly superbugs.⁵

There are many approaches currently being explored to identify new classes of antibiotics, including *in situ* cultivation of uncultured microbes,^{6,7} identification and prioritisation of

novel organisms by chemotaxonomy^{8–14} and activation of silent biosynthetic gene clusters (BGCs) using synthetic biology and bioinformatics tools.^{15,16} An alternate strategy involves revisiting some of the old antibiotic scaffolds that were discovered many decades ago, during a time of plenty, that were abandoned in favour of more promising leads. Re-examining these neglected historic scaffolds through the lens of modern drug discovery platforms has proven to be an effective method of bringing new antibiotic classes to the market.¹⁷ Notable antibiotic revivals include linezolid (2000), daptomycin (2003) and lefamulin (2019), which belong to chemical classes first reported in 1978,¹⁸ 1987¹⁹ and 1952,²⁰ respectively.

In our ongoing search for new antibiotic leads, we recently reported our work on expanding chemical space around the nidulin antibiotic pharmacophore.²¹ Nidulin is a trichlorinated depsidone antibiotic, first identified in 1945 from the fungus *Aspergillus unguis*.²² While nidulin has reported antibacterial activity against *Mycobacterium tuberculosis*²³ and MRSA,²⁴ the compound has received only modest attention since its initial discovery and the scaffold has not been systematically investigated as an antibiotic lead. In our recent study, manipulating the halide ion concentration in the cultivation medium of *A. unguis* led to the production of 12 previously unreported nidulin analogues, along with 11 known nidulin analogues. Biological testing of this small library revealed a number of interesting trends in potency and selectivity that warranted further investigation. In

^aDepartment of Molecular Sciences, Macquarie University, NSW 2109, Australia.

E-mail: andrew.piggott@mq.edu.au

^bAustralian Centre for Antimicrobial Resistance Ecology, School of Animal and Veterinary Sciences, The University of Adelaide, Roseworthy, SA 5371, Australia^cMicrobial Screening Technologies Pty. Ltd, Smithfield, NSW 2164, Australia^dAdvanced Veterinary Therapeutics Pty. Ltd, Newtown, NSW 2042, Australia

†Electronic supplementary information (ESI) available: NMR spectra, UV-vis spectra and HRMS spectra of all compounds. See DOI: 10.1039/d0ob02460k

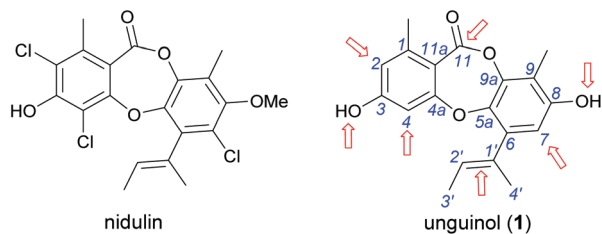


Fig. 1 Chemical structures of nidulin and unguinol (**1**) and the initial sites selected for semisynthetic modification of **1** (arrowed).

this study, we have employed a semisynthetic approach to expand the structure activity relationship (SAR) of the nidulin pharmacophore. Starting from the closely related metabolite unguinol, we have generated a library of 15 analogues by modifying 7 different locations around the unguinol core (Fig. 1). All semisynthetic analogues were screened for *in vitro* activity against a panel of bacteria, fungi and mammalian cell lines. *In vitro* antimicrobial testing revealed 3-*O*-benzylunguinol is fifteen times more potent than ampicillin against *S. aureus*. Further exploration of benzylation of unguinol with halogen-substituted benzyl bromide yielded more potent antibiotics, 3-*O*-(2-fluorobenzyl)unguinol and 3-*O*-(2,4-difluorobenzyl)unguinol.

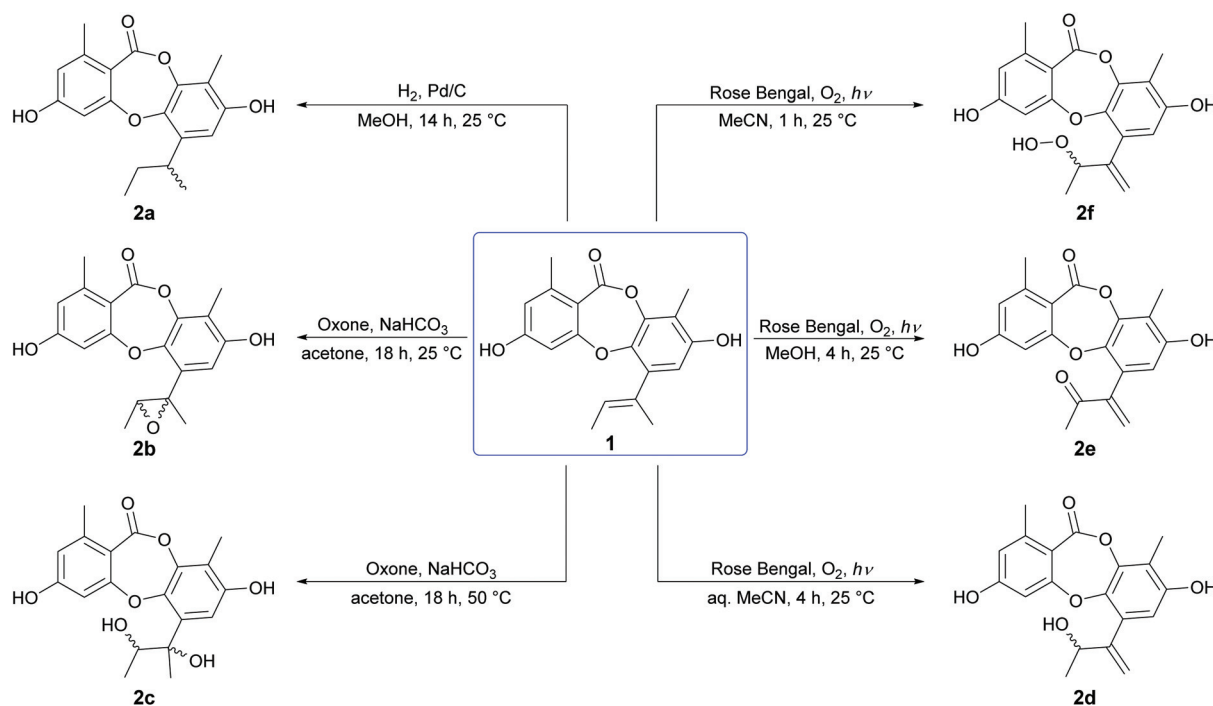
Results and discussion

First-generation semisynthetic unguinol analogues

We initiated our semisynthetic program starting with unguinol (**1**), which is the major metabolite of *A. unguis* and could be

isolated in reasonable quantities by large-scale cultivation of the organism. Compound **1** is a nonchlorinated analogue of nidulin, containing two free hydroxy groups (3-OH and 8-OH), three unsubstituted aromatic positions (H-2, H-4 and H-7), one double bond ($\Delta^{1',2'}$) in the butenyl side chain and one ester linkage. These 7 locations were selected as the initial sites for semisynthetic modification to assess the contributions of each group towards the antibiotic activity of the despidone scaffold.

Oxidation and reduction. Initially, the $\Delta^{1',2'}$ double bond in the butenyl side chain of **1** was reduced by catalytic hydrogenation (H_2 , Pd/C), to give a racemic mixture of 1',2'-dihydrounguinol (**2a**) in quantitative yield (Scheme 1). Next, the $\Delta^{1',2'}$ double bond of **1** was oxidised at 25 °C with dimethyldioxirane (DMDO), which was generated *in situ* from basic acetone and Oxone, to give *cis*-1',2'-epoxyunguinol (**2b**) as a racemic mixture in 53% yield. Repeating the DMDO oxidation at 50 °C yielded a small quantity of 1',2'-dihydroxyunguinol (**2c**), formed from **2b** by nucleophilic ring-opening of the epoxide under the basic reaction conditions. LCMS analysis of crude reaction mixture revealed two diastereomers had formed in a 3 : 1 ratio, although only the major could be isolated in sufficient quantities for characterisation. Oxidation of the $\Delta^{1',2'}$ double bond of **1** by molecular oxygen in the presence of UV light (254 nm) and Rose Bengal photosensitizer in aqueous MeCN, MeOH and anhydrous MeCN yielded three unguinol derivatives, 2'-hydroxy- $\Delta^{1',4'}$ -unguinol (**2d**), 2'-oxo- $\Delta^{1',4'}$ -unguinol (**2e**) and 2'-hydroperoxy- $\Delta^{1',4'}$ -unguinol (**2f**), respectively. The dye-sensitized photooxidation of alkenes has been studied extensively^{25,26} and the distribution of products observed can

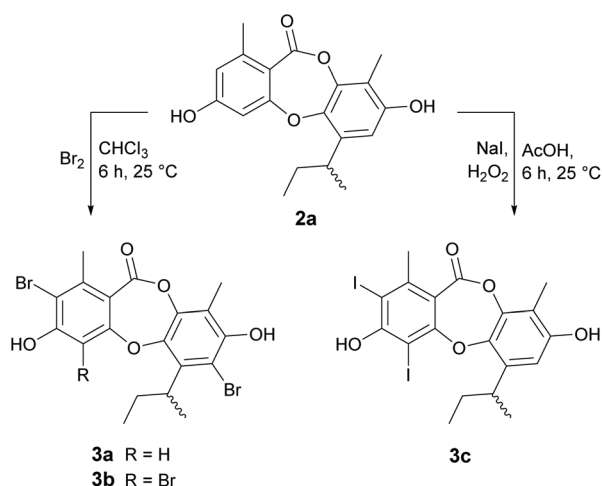


Scheme 1 Oxidation and reduction of the butenyl side chain of unguinol (**1**).

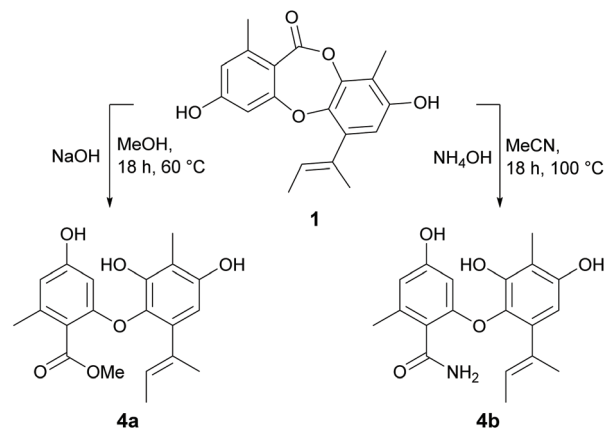
be rationalised by addition of singlet oxygen to the $\Delta^{1,2}$ double bond of **1** to yield allylic hydroperoxide **2f** (Schenck ene reaction), followed by subsequent thermal decomposition to give alcohol **2d** or dehydration to give ketone **2e**.

Halogenation. In our previous paper,²¹ we reported a series of novel brominated depsidones (mono- and dibromounguinol), which were obtained by supplementing the culture media with potassium bromide. Significantly, we found that these brominated depsidones showed improved antibacterial activities against *Bacillus subtilis* and *S. aureus* when compared with unguinol. To explore this effect more fully, we synthesised several brominated and iodinated unguinol analogues, as shown in (Scheme 2). As reduction of the butenyl side chain of **1** did not have any significant effects on antibacterial activity, we conducted the halogenation reactions on hydrogenated analogue **2a** to avoid complicating side reactions. Treatment of **2a** with bromine in chloroform at 25 °C yielded a mixture of 2,7-dibromo-1',2'-dihydranguinol (**3a**) and 2,4,7-tribromo-1',2'-dihydranguinol (**3b**) in 16% and 19% yield, respectively. While LCMS analysis of the crude reaction mixture suggested that trace amounts of monobrominated products had formed under these reaction conditions, varying the reaction temperature, solvent and equivalents of bromine did not yield sufficient quantities of these products for isolation and characterisation. Similarly, treatment of **2a** with NaI and H₂O₂ in acetic acid at 25 °C yielded 2,4-diiodo-1',2'-dihydranguinol (**3c**) in 56% yield. LCMS analysis of the crude reaction mixture suggested trace amounts of monoiodinated products had formed, but there was no evidence for the formation of the triiodinated product, suggesting iodination at C-7 is not favoured under these conditions.

Nucleophilic ring opening. The depsidone scaffold contains a central seven-membered ring consisting of one ether and one ester linkage. Cleavage of the ether linkage yields depsides, while cleavage of the ester linkage yields diphenyl ethers. In our previous paper,²¹ we reported several naturally occurring depsides and diphenyl ethers with moderate to weak



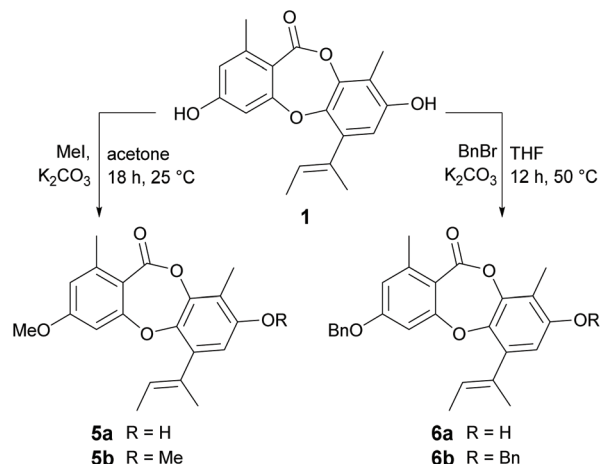
Scheme 2 Halogenation of 1',2'-dihydranguinol (**2a**).



Scheme 3 Nucleophilic opening of the ester linkage of unguinol (**1**).

antibacterial activities. Therefore, to gain further insights into the SAR of diphenyl ethers, we next explored cleaving the ester linkage of **1** with sodium hydroxide in methanol and ammonium hydroxide in water to yield methyl unguinol (**4a**) and unguinolamide (**4b**), respectively (Scheme 3). The presence of an additional exchangeable resonance in the ¹H NMR spectra (δ_{H} 8.36 for **4a** and 9.38 for **4b**) attributable to 9a-OH confirmed that the depsidone ester linkages had been cleaved in both compounds. The presence of a methyl ester in **4a** was evident from signals at δ_{C} 167.9 and 51.6 in ¹³C NMR spectrum, while the presence of a primary amide in **4b** was evident from two additional exchangeable signals at δ_{H} 7.71 and 7.94. The free acid was isolated and characterised in our previous work²¹ as a natural product (unguinolic acid) and hence was not prepared synthetically in this work.

Methylation and benzylation. We next turned our attention to derivatising the two free hydroxy groups (3-OH and 8-OH) of **1** (Scheme 4). Treatment of **1** with methyl iodide (2 eq.) in K₂CO₃ resulted in a mixture of 3-O-methylunguinol (**5a**) and 3,8-di-O-methylunguinol (**5b**), but not the 8-O-monomethylated product. The structure of **5a** was confirmed by diagnostic ROESY NMR correlations between 3-OMe and aromatic protons H-2 and H-4. Attempts to access 8-O-methylunguinol by first protecting 3-OH as the *tert*-butyldimethylsilyl (TBDMS) ether were unsuccessful. This apparent regioselectivity is interesting given the preference for 8-O-methylation in Nature, with the only naturally occurring 3-O-methylated unguinol analogue reported to date being aspergillusidone B.^{27,28} Next, benzylation of **1** was carried out using benzyl bromide and K₂CO₃ at 50 °C in THF (Scheme 4). Under these reaction conditions, a mixture of mono- and dibenzylated products was formed, with 3-O-benzylunguinol (**6a**) isolated as the major product. The position of benzyl group on 3-OH was confirmed by diagnostic HMBC correlations from the benzyl methylene protons to C-3 (δ_{C} 161.7) and a ROESY correlation from the methylene protons to H-2. Interestingly, repeating the benzylation reaction using either acetone or acetonitrile as the solvent yielded 3,8-di-O-dibenzylunguinol (**6b**) as the major product.



Scheme 4 Methylation and benzylation of unguinol (1).

Bioassay of first-generation semisynthetic unguinol analogues

The fifteen first-generation semisynthetic unguinol analogues were tested for *in vitro* activity against the Gram-positive bacteria *B. subtilis* (ATCC 6633) and *S. aureus* (ATCC 25923), the Gram-negative bacterium *Escherichia coli* (ATCC 25922), the fungi *Candida albicans* (ATCC 10231) and *Saccharomyces cerevisiae* (ATCC 9763), and mouse NS-1 myeloma (ATCC TIB-18) cells (Table 1). The compounds exhibited a wide range of antibacterial activities against the Gram-positive bacteria, but no activity was observed for any of the analogues against *E. coli* or *C. albicans*.

Reduction of the butenyl side chain of **1** by catalytic hydrogenation yielded **2a**, which was equipotent against *B. subtilis* but two-fold less potent against *S. aureus*. Oxidation of the

butenyl side chain of **1** yielded five oxygenated derivatives, **2b–2f**. While epoxidation (**2b**) and dihydroxylation (**2c**) of the double bond significantly reduced antibacterial activity, the allylic ketone (**2e**) and hydroperoxide (**2f**) derivatives showed similar activity against *B. subtilis* and up to eight-fold increased activity against *S. aureus*. This was also accompanied by significantly increased cytotoxicity against mammalian tumour cells, with activities more potent than the positive control 5-fluorouracil. Dibromination (**3a**) and tribromination (**3b**) of **2a** also significantly improved the antibacterial activity against both of the Gram-positive bacteria, but again was accompanied by increased cytotoxicity against NS-1 cells. Interestingly, **3a** also showed twelve-fold improved activity against *S. cerevisiae* compared to **2a**, while **3b** showed no anti-fungal activity. Di-iodination (**3c**) of **2a** yielded a similar improvement in antibacterial activity as dibromination, but with no increase in cytotoxicity. Nucleophilic opening of the ester linkage of **1** with NaOH/MeOH and NH₄OH/MeCN to give methyl unguinol (b) and unguinolamide (**4b**), respectively, resulted in a significant decrease in antibacterial activity against both of the Gram-positive bacteria, highlighting the importance of the seven-membered depsidone ring system.

Methylation of **1** at 3-OH (**5a**) resulted in a two-fold decrease in activity against *B. subtilis*, with no change in activity against *S. aureus*. However, methylation of **1** at both 3-OH and 8-OH (**5b**) abolished activity against both of the Gram-positive bacteria, suggesting at least one free hydroxy group is essential for activity. Benzylation of **1** at 3-OH (**6a**) resulted in a modest increase in activity against *B. subtilis*, but a very significant increase in activity against *S. aureus*. Indeed, **6a** (MIC 0.2 μg mL⁻¹) was found to be over thirty-fold more active than nidulin (MIC 6.3 μg mL⁻¹) and over sixty-fold more active than

Table 1 *In vitro* biological activities of first-generation semisynthetic unguinol analogues

| Compounds | MIC (μg mL ⁻¹) | | | |
|---|--------------------------------|-------------------------------|----------------------------------|--------------------|
| | <i>B. subtilis</i> (ATCC 6633) | <i>S. aureus</i> (ATCC 25923) | <i>S. cerevisiae</i> (ATCC 9763) | NS-1 (ATCC TIB-18) |
| Nidulin | 0.8 | 6.3 | — | 27.2 |
| Unguinol (1) | 3.1 | 12.5 | 50 | 25 |
| 1',2'-Dihydrounguinol (2a) | 3.1 | 25 | 50 | 25 |
| <i>cis</i> -1',2'-Epoxyunguinol (2b) | 25 | 100 | — | 25 |
| 1',2'-Dihydroxyunguinol (2c) | — | — | — | — |
| 2'-Hydroxy-Δ ^{1',4'} -unguinol (2d) | 50 | 100 | — | 50 |
| 2'-Oxo-Δ ^{1',4'} -unguinol (2e) | 1.6 | 1.6 | — | <0.1 |
| 2'-Hydroperoxy-Δ ^{1',4'} -unguinol (2f) | 3.1 | 3.1 | — | <0.1 |
| 2,7-Dibromo-1',2'-dihydrounguinol (3a) | 2.1 | 2.1 | 4.2 | 4.2 |
| 2,4,7-Tribromo-1',2'-dihydrounguinol (3b) | 1.2 | 4.6 | — | 9.2 |
| 2,4-Diiodo-1',2'-dihydrounguinol (3c) | 1.1 | 4.6 | 9.1 | 36.4 |
| Methyl unguinol (b) | 25 | 100 | — | 50 |
| Unguinolamide (4b) | 25 | — | — | <0.1 |
| 3-O-Methylunguinol (5a) | 6.3 | 12.5 | 12.5 | 25 |
| 3,8-Di-O-methylunguinol (5b) | — | — | — | 16.1 |
| 3-O-Benzylunguinol (6a) | 1.6 | 0.2 | — | 3.1 |
| 3,8-Di-O-benzylunguinol (6b) | 50 | — | — | ^a |
| Ampicillin | 0.2 | 3.1 | ^a | ^a |
| Clotrimazole | ^a | ^a | 0.4 | ^a |
| 5-Fluorouracil | ^a | ^a | ^a | 0.1 |

^a Not tested; – no activity up to 100 μg mL⁻¹.

unguinol (MIC $12.5 \mu\text{g mL}^{-1}$) against *S. aureus*. Benzylation of **1** at both 3-OH and 8-OH (**6b**) also abolished all antibacterial activity, as was observed for dimethylation.

Second-generation semisynthetic unguinol analogues

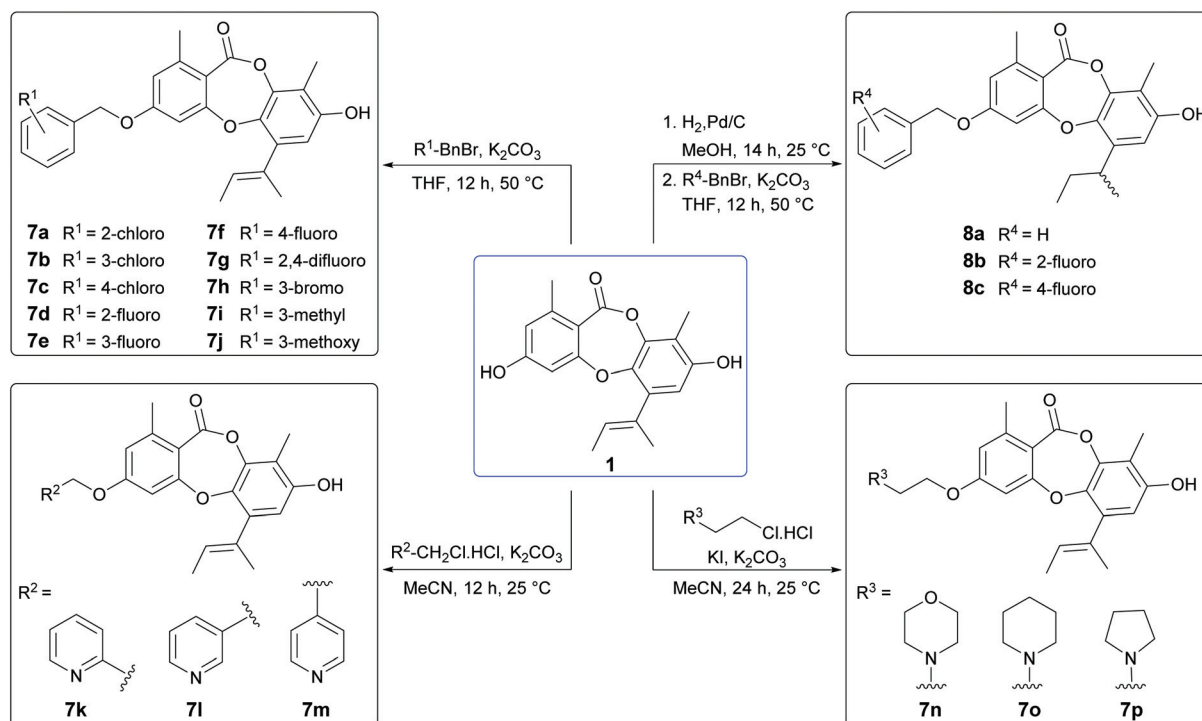
From our preliminary SAR studies, it was evident that benzylation of the 3-OH group of **1** significantly improved antibacterial activity, particularly against *S. aureus*. Inspired by these initial results, we next explored benzylation of **1** with a range of *ortho*-, *meta*- and *para*-substituted benzyl bromides (Scheme 5). Reaction of **1** with five equivalents of each benzyl bromide in THF at 50°C yielded ten second-generation 3-*O*-benzylated derivatives, **7a–7j** as the major products. Three picolyl derivatives (**7k–7m**) were also synthesised by reaction of **1** with 2-, 3-, and 4-picoly chloride in MeCN at 25°C . Alkylation of the 3-OH group of **1** by reaction with 4-(2-chloroethyl)morpholine, 1-(2-chloroethyl)piperidine and 1-(2-chloroethyl)pyrrolidine in MeCN at 25°C yielded **7n–7p**. Finally, benzylation of the 3-OH of **2a** was performed using three different benzyl bromides, yielding **8a–8c**.

Bioassay of second-generation semisynthetic unguinol analogues

The nineteen second-generation unguinol congeners were initially tested for *in vitro* against the same panel of bacteria, fungi and mammalian cells as the first-generation analogues (Table 2). No activity was observed for any of the second-generation compounds against the tested Gram-negative bacterial or fungal species. The ten 3-*O*-benzylated unguinol analogues **7a–7j** exhibited significant antibacterial activity against Gram-

positive bacteria, with MICs ranging from <0.1 – $6.3 \mu\text{g mL}^{-1}$, and showed modest cytotoxicity against mouse NS-1 myeloma cells, with MICs ranging from 6.3 – $12.5 \mu\text{g mL}^{-1}$. Significantly, all ten benzylated analogues showed potent activity against *S. aureus*, with MICs ranging from <0.1 – $0.8 \mu\text{g mL}^{-1}$. The fluorobenzyl analogues **7d** and **7f** were the most promising leads, with activities superior to the antibiotic standards gentamicin (MIC $0.4 \mu\text{g mL}^{-1}$) and ampicillin (MIC $3.1 \mu\text{g mL}^{-1}$), and a selectivity index of 125. The 2-, 3- and 4-picoly derivatives of **1** (**7k–7m**, respectively) showed 8- to 16-fold less activity against *S. aureus* compared to **6a**, with only **7k** retaining any activity against *B. subtilis* (MIC $6.3 \mu\text{g mL}^{-1}$). The 3-*O*-alkylamino derivatives **7n–7p** also exhibited significantly reduced antibacterial activity compared to **6a**. Intriguingly, this was accompanied by a dramatic increase in cytotoxicity against mouse myeloma NS-1 cells (MIC $0.2 \mu\text{g mL}^{-1}$), comparable in potency to the standard compound 5-fluorouracil (MIC $0.1 \mu\text{g mL}^{-1}$). The appearance of this potent and selective mammalian cytotoxicity is indicative of a mode of action distinct from the antibacterial activity of the unguinol scaffold. It has been recently reported that 8-*O*-alkylation of normidulin results in moderate cytotoxicity against African green monkey kidney (Vero) cells.²⁹ Similarly, the 1',2'-dihydro analogues of **6a**, **7d** and **7f** (**8a–8c**, respectively) showed slightly decreased antibacterial activities accompanied by markedly increased cytotoxicity against NS-1 cells (MIC $0.8 \mu\text{g mL}^{-1}$).

We next explored the activity of the nineteen second-generation unguinol analogues against MRSA (ATCC 33592). Encouragingly, all ten 3-*O*-benzylated unguinol analogues **7a–7j** retained equal potency against MRSA (MICs 0.1 – $0.8 \mu\text{g}$



Scheme 5 Synthesis of second-generation unguinol analogues.

Table 2 *In vitro* biological activities of second-generation semisynthetic unguinol analogues

| Compound | MIC ($\mu\text{g mL}^{-1}$) | | | |
|---|--------------------------------|-------------------------------|-------------------|--------------------|
| | <i>B. subtilis</i> (ATCC 6633) | <i>S. aureus</i> (ATCC 25923) | MRSA (ATCC 33592) | NS-1 (ATCC TIB-18) |
| 3- <i>O</i> -Benzylunguinol (6a) | 1.6 | 0.2 | 0.4 | 3.1 |
| 3- <i>O</i> -(2-Chlorobenzyl)unguinol (7a) | 3.1 | 0.2 | 0.2 | 12.5 |
| 3- <i>O</i> -(3-Chlorobenzyl)unguinol (7b) | 3.1 | 0.8 | 0.4 | 6.3 |
| 3- <i>O</i> -(4-Chlorobenzyl)unguinol (7c) | 1.6 | 0.2 | 0.2 | 12.5 |
| 3- <i>O</i> -(2-Fluorobenzyl)unguinol (7d) | 0.8 | 0.1 | 0.1 | 12.5 |
| 3- <i>O</i> -(3-Fluorobenzyl)unguinol (7e) | 1.6 | 0.4 | 0.4 | 6.3 |
| 3- <i>O</i> -(4-Fluorobenzyl)unguinol (7f) | 1.6 | <0.1 | 0.1 | 12.5 |
| 3- <i>O</i> -(2,4-Difluorobenzyl)unguinol (7g) | 0.8 | 0.2 | 0.2 | 12.5 |
| 3- <i>O</i> -(3-Bromobenzyl)unguinol (7h) | 6.3 | 1.6 | 1.6 | 6.3 |
| 3- <i>O</i> -(3-Methylbenzyl)unguinol (7i) | 3.1 | 0.8 | 0.8 | 6.3 |
| 3- <i>O</i> -(3-Methoxybenzyl)unguinol (7j) | 6.3 | 1.6 | 1.6 | 6.3 |
| 3- <i>O</i> -(2-Picolyl)unguinol (7k) | 6.3 | 1.6 | 1.6 | 12.5 |
| 3- <i>O</i> -(3-Picolyl)unguinol (7l) | — | 3.1 | 6.3 | 25 |
| 3- <i>O</i> -(4-Picolyl)unguinol (7m) | — | 1.6 | 3.1 | 12.5 |
| 3- <i>O</i> -(4-Morpholinoethyl)unguinol (7n) | 6.3 | 12.5 | 6.3 | 0.2 |
| 3- <i>O</i> -(1-Piperidinyethyl)unguinol (7o) | 6.3 | 25 | 6.3 | 0.2 |
| 3- <i>O</i> -(1-Pyrrolidinyethyl)unguinol (7p) | 12.5 | 100 | 50 | 0.2 |
| 3- <i>O</i> -Benzyl-1',2'-dihydrounguinol (8a) | 3.1 | 3.1 | 1.6 | 0.8 |
| 3- <i>O</i> -(2-Fluorobenzyl)-1',2'-dihydrounguinol (8b) | 3.1 | 3.1 | 1.6 | 0.8 |
| 3- <i>O</i> -(4-Fluorobenzyl)-1',2'-dihydrounguinol (8c) | 3.1 | 3.1 | 1.6 | 0.8 |
| Ampicillin | 0.2 | 3.1 | — | ^a |
| Gentamicin | ^a | 0.4 | 25 | ^a |
| 5-Fluorouracil | ^a | ^a | ^a | 0.1 |

^a Not tested; – no activity up to 100 $\mu\text{g mL}^{-1}$.

mL^{-1}) and were significantly more active than the standard gentamicin (MIC 25 $\mu\text{g mL}^{-1}$). The picolyl derivatives **7k–7m** also showed similar potencies against MRSA, while the alkylamino derivatives **7n–7p** and the hydrogenated benzyl derivatives **8a–8c** showed slightly improved potencies against MRSA. A subset of the 3-*O*-benzylated unguinol analogues (**6a**, **7a**, **7c**, **7d** and **7g**) was screened against one additional strain of MRSA (USA300), one additional strain of methicillin-sensitive *S. aureus* (MSSA; ATCC 49775) and two strains of *Enterococcus faecium* (ATCC 19434, E734) (Table 3), as well as two strains of *Pseudomonas aeruginosa* (PA01, ATCC 27853) and two additional strains of *E. coli* (ATCC 25322, ATCC 35218). No Gram-negative activity, or activity against either *E. faecium*, was detected for any of the compounds up to 16 $\mu\text{g mL}^{-1}$. The analogues all showed good activities against both MRSA and MSSA (MICs 0.5–2 $\mu\text{g mL}^{-1}$), comparable to the control com-

pound daptomycin (MIC 0.5 $\mu\text{g mL}^{-1}$). It is noteworthy that the MICs for the 3-*O*-benzylated unguinol analogues increased 32-fold in the presence of 10% foetal calf serum.

Given these findings, further in-depth evaluation of the antibacterial activities of **7d** and **7g** was carried out with an expanded list of *S. aureus* isolates and strains to obtain a clearer picture of the potency and selectivity of these analogues. The results show potent activity for both compounds, returning MIC range, MIC₅₀ and MIC₉₀ values comparable to the daptomycin standard (Table 4). The potency of **7d** and **7g** was further investigated in a kinetic assay to measure the time- and concentration-dependent activity of the two compounds against two *S. aureus* ATCC strains using daptomycin as a comparator. The results show a time- and concentration-dependent inhibition of growth for **7d** and **7g**, consistent with features of bacteriostatic drugs. As expected, daptomycin displayed patterns of a bactericidal drug (Fig. 2).

A preliminary investigation into the suitability of **7d** and/or **7g** for administration as a drug was conducted by assessing

Table 3 *In vitro* antibacterial activity of benzylunguinol derivatives against MSSA, MRSA and *E. faecium*

| Compound | MIC ($\mu\text{g mL}^{-1}$) | | | |
|------------|-------------------------------|-------------------|--------------------------------|--------------------------------|
| | MRSA ^a | MSSA ^b | <i>E. faecium</i> ^c | <i>E. faecium</i> ^d |
| 1 | 8 | 8 | >16 | >16 |
| 6a | 1 | 1 | >16 | >16 |
| 7a | 1 | 2 | >16 | >16 |
| 7c | 0.5 | 1 | >16 | >16 |
| 7d | 0.5 | 1 | >16 | >16 |
| 7g | 0.5 | 0.5 | >16 | >16 |
| Daptomycin | 0.5 | 0.5 | >2 | >2 |

^a USA300. ^b ATCC 49775. ^c ATCC 19434. ^d E734.

Table 4 MIC range, MIC₅₀ and MIC₉₀ against *S. aureus* (20 MRSA and 3 MSSA)

| Compound | MIC ($\mu\text{g mL}^{-1}$) | | |
|------------|-------------------------------|-------------------|-------------------|
| | MIC range | MIC ₅₀ | MIC ₉₀ |
| 7d | 0.25–1 | 0.5 | 0.5 |
| 7g | 0.25–1 | 0.5 | 0.5 |
| Daptomycin | 0.25–1 | 0.5 | 0.5 |
| Ampicillin | 0.125–>16 | >16 | >16 |

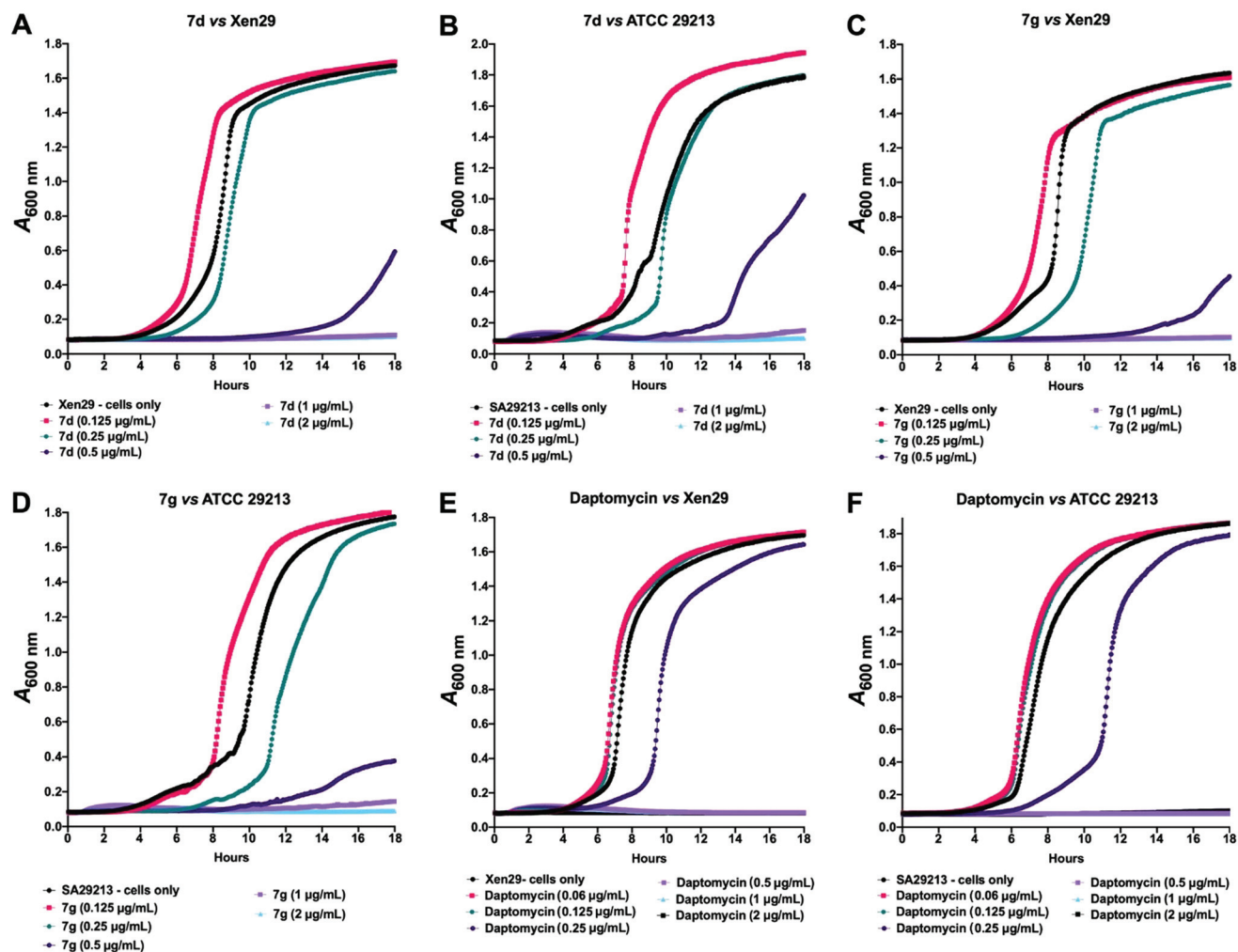


Fig. 2 Kinetic assay showing time- and concentration-dependent inhibition of *S. aureus* ATCC 12600 (Xen29; A, C and E) and ATCC 29213 (B, D and F) by 7d and 7g, with daptomycin as a comparator. Results show 7d and 7g are bacteriostatic, while daptomycin is bactericidal.

their cytotoxicity to mammalian cells in fresh human red blood cells (RBCs), human embryonic kidney (HEK293) cell line and human epithelial liver (Hep G2) cell line. At the highest concentration ($128 \mu\text{g mL}^{-1}$), 7d and 7g did not result in haemolysis of RBCs and both returned IC_{50} values of $32 \mu\text{g mL}^{-1}$ against the HEK293 and Hep G2 cell lines. These desirable cytotoxicity profiles promote exploration of 7d and 7g for *in vivo* safety and subsequent efficacy testing in relevant animal models.

Conclusions

In this study, we have completed the semisynthesis and *in vitro* biological evaluation of thirty-four derivatives of the fungal depsidone antibiotic, unguinol. Our SAR studies against a panel of microorganisms and mammalian cells revealed that at least one free hydroxy group is essential for antibacterial

activity. We have demonstrated that by modification of the butenyl side chain of unguinol, we can target more potent and selective antitumor activity, while the introduction of bulkier halogens abolishes selectivity. Most notably, we have demonstrated that introduction of a 3-*O*-benzyl group exploits a putative additional hydrophobic pocket present in Gram-positive bacteria, affording a more potent and selective antibiotic class. The binding pocket appears to be optimal for fluorine-substituted benzyl analogues. Two of these analogues, 3-*O*-(2-fluorobenzyl)unguinol and 3-*O*-(2,4-difluorobenzyl)unguinol, demonstrated potent activity against MSSA and MRSA at concentrations comparable to those of a leading clinically effective Gram-positive antibiotic, daptomycin. Our assays also show these two compounds appear to be bacteriostatic and exhibit desirable mammalian cytotoxicity profiles, supporting their consideration for *in vivo* safety and drug efficacy testing in animal models of disease. While the mode of action of unguinol and its analogues remains unknown, our SAR results suggest this family of depsidones may act by binding to a

target shared by prokaryotes, lower eukaryotes and higher eukaryotes. It is noteworthy that many lichen symbionts use variants of the depsidone scaffold to similar effect.^{30–32} This broad chemotherapeutic specificity represents an efficient use of resources, enabling the fungus to ward off a wide taxonomic framework of competitors. In Nature, potency and selectivity are implicit to each metabolite, which is an inverse template of its site of action. Employing a cohort of bioassays to help illuminate previously unrecognised aspects of potency and selectivity is an effective strategy for reviving existing chemical classes as potential new drugs.

Experimental

General experimental details

UV-vis spectra were acquired in MeOH on a Varian Cary 4000 spectrophotometer or a Jasco V-760 spectrophotometer in a 10 × 10 mm quartz cuvette. IR spectra were recorded on a Jasco FT/IR-6000 FTIR (ATR) spectrometer. Photooxidation reactions were performed using a Philips TUV PL-S 11 W/2P UVC light. ¹H NMR and ¹³C NMR spectra were recorded in 5 mm Pyrex tubes (Wilmad, USA) on either a Bruker Avance II DRX-600K 600 MHz or Bruker Avance III HD 500 MHz spectrometer. All NMR spectra were obtained at 25 °C, processed using Bruker Topspin 3.5 software and referenced to residual solvent signals (DMSO-*d*₆ δ_H 2.49/δ_C 39.5 ppm). High resolution electrospray ionisation mass spectra (HRESIMS) were obtained on a Q Exactive Plus hybrid quadrupole-Orbitrap mass spectrometer (Thermo Fisher Scientific, Bremen, Germany) by direct infusion. Electrospray ionisation mass spectra (ESIMS) were acquired on an Agilent 1260 UHPLC coupled to an Agilent 6130B single quadrupole mass detector. Analytical HPLC was performed on a gradient Agilent 1260 Infinity quaternary HPLC system equipped with a G4212B diode array detector. The column was an Agilent Poroshell 120 EC-C₁₈ (4.6 × 50 mm, 2.7 μm) eluted with a 1 mL min⁻¹ gradient of 10–100% MeCN/water (0.01% TFA) over 8.33 min. Semipreparative HPLC was performed on a gradient Agilent 1260 Infinity quaternary HPLC system coupled to a G4212B diode array detector. The column used in the purification of the compounds was an Agilent Zorbax SB-C₁₈ (9.4 × 250 mm, 5 μm) eluted isocratically at 4.18 mL min⁻¹. Preparative HPLC was performed on a gradient Shimadzu HPLC system comprising two LC-8A preparative liquid pumps with static mixer, SPD-M10AVP diode array detector and SCL-10AVP system controller with standard Rheodyne injection port. The columns used were a Grace Discovery Hypersil C₁₈ spring column (150 × 50 mm, 5 μm) eluted isocratically at 60 mL min⁻¹, an Agilent Zorbax SB-C₁₈ column (150 × 50 mm, 5 μm) eluted isocratically at 60 mL min⁻¹ and an Agilent Zorbax SB-C₁₈ column (2 × 250 mm, 5 μm) eluted isocratically at 20 mL min⁻¹. Silica flash chromatography was performed on a Biotage Isolera Four system coupled with a variable UV (200–400 nm) detector.

Isolation and purification of unguinol

A. unguis MST-FP511 was grown on pearl barley, which had been boiled in distilled water for 12 min and sterilised (120 °C for 40 min), in 60 × 250 mL Erlenmeyer flasks, with each flask containing 50 g of barley. Agar squares from a 7-day-old Petri plate of *A. unguis* were used as the inoculum for the flasks. The cultures were incubated for 21 days at 24 °C, then the grains were pooled and extracted with acetone (2 × 4 L) and the combined extracts were evaporated under vacuum to produce an aqueous slurry (2 L). The slurry was partitioned against ethyl acetate (2 × 2 L) and the ethyl acetate was reduced *in vacuo* to give the crude extract (55.6 g). The crude extract was redissolved in 90% MeOH/H₂O (500 mL) and partitioned against hexane (2 × 500 mL) to remove lipids, yielding an enriched extract (35.7 g). The enriched extract was adsorbed onto silica gel (40 g), which was then loaded onto a silica gel column (100 g, 300 × 50 mm). The column was washed once with hexane (500 mL), then eluted with 50% hexane/CHCl₃ (500 mL), 25% hexane/CHCl₃ and CHCl₃ (500 mL), followed by a stepwise gradient of 1, 2, 4, 8, 16, 32 and 100% MeOH/CHCl₃ (500 mL each step), to yield 11 fractions (Fr. 1–11). Fraction 6 (2.1 g) was purified by isocratic preparative HPLC (Hypersil C₁₈, isocratic 60% MeCN/H₂O containing 0.01% TFA, 60 mL min⁻¹) to yield **1** (*t*_R 14.62 min; 384 mg).

Semisynthesis of unguinol analogues

1',2'-Dihydrounguinol (2a). Unguinol (**1**; 50 mg, 0.15 mmol) was dissolved in methanol (5 mL) and 10% palladium on carbon catalyst (3.2 mg) was added. The reaction mixture was stirred overnight under an atmosphere of H₂ (balloon) at 25 °C. The reaction mixture was filtered through Celite and the solvent was removed *in vacuo* to yield 1',2'-dihydrounguinol (**2a**; 50 mg, quant.) as a colourless solid, which was used without further purification. UV (MeOH) λ_{max} (log ε) 203 (5.08), 223 (4.78), 265 (4.43) nm; IR (ATR) ν_{max} 3310, 2963, 1698, 1608, 1576, 1427, 1336, 1256, 1210, 1151, 1108, 1086 cm⁻¹; ¹H NMR (600 MHz, DMSO-*d*₆): δ 10.61 (s, 1H), 9.49 (s, 1H), 6.57 (dd, *J* = 2.4, 0.8 Hz, 1H), 6.54 (d, *J* = 2.4 Hz, 1H), 6.49 (s, 1H), 3.25 (m, 1H), 2.33 (s, 3H), 2.03 (s, 3H), 1.51 (m, 2H), 1.11 (d, *J* = 7.0 Hz, 3H), 0.79 (t, *J* = 7.3 Hz, 3H), ¹³C NMR (150 MHz, DMSO-*d*₆): δ 163.1, 162.5, 161.8, 152.9, 144.7, 142.8, 141.0, 136.1, 115.6, 113.6, 111.6, 108.0, 104.4, 32.4, 29.8, 21.4, 20.7, 12.1, 9.1. HRESI(+)/MS *m/z* 329.1381 [M + H]⁺ (calculated for C₁₉H₂₁O₅⁺ 329.1384).

***cis*-1',2'-Epoxyunguinol (2b)**. To a stirred mixture of unguinol (**1**; 15 mg, 46 μmol), NaHCO₃ (23 mg, 0.27 mmol) and acetone (5 mL) at 0 °C, a solution of Oxone (84 mg, 0.27 mmol) in water (3 mL) was added dropwise. The resulting mixture was stirred at 25 °C for 18 h and then extracted with ethyl acetate (3 × 3 mL). The organic layer was dried over MgSO₄ and the solvent was evaporated under nitrogen. The residue (13.8 mg) was purified by semipreparative C₁₈ HPLC with isocratic 80% MeCN/H₂O (4.18 mL min⁻¹), yielding a racemic mixture of *cis*-1',2'-epoxyunguinol (**2b**; *t*_R = 17.5 min; 8.0 mg, 53%) as white amorphous solid. UV (MeOH) λ_{max} (log ε) 202 (4.92), 221

(4.57), 267 (4.23) nm; IR (ATR) ν_{\max} 3461, 2989, 1699, 1619, 1579, 1424, 1384, 1381, 1254, 1217, 1188, 1160, 1104 cm^{-1} ; ^1H NMR (500 MHz, DMSO- d_6): δ 10.76 (br s, 1H), 9.72 (br s, 1H), 6.58 (s, 1H), 6.57 (d, $J = 2.4$ Hz, 1H), 6.46 (d, $J = 2.4$ Hz, 1H), 2.85 (q, $J = 5.4$ Hz, 1H), 2.33 (s, 3H), 2.03 (s, 3H), 1.56 (s, 3H), 1.47 (d, $J = 5.4$ Hz, 3H); ^{13}C NMR (125 MHz, DMSO- d_6): δ 162.6, 162.2, 162.1, 152.8, 144.9, 142.9, 140.2, 132.7, 115.9, 115.4, 111.1, 108.3, 104.4, 59.4, 59.0, 20.7, 18.8, 13.8, 9.2. HRESI(-)MS m/z 341.1032 $[\text{M} - \text{H}]^-$ (calculated for $\text{C}_{19}\text{H}_{17}\text{O}_6^-$, 341.1031).

1',2'-Dihydroxyunguinol (2c). To a stirred solution of unguinol (**1**; 15 mg, 46 μmol) in acetone (5 mL) was added NaHCO_3 (38 mg) and a solution of Oxone (141 mg, 0.46 mmol) in water (2 mL). The reaction mixture was stirred at 50 $^\circ\text{C}$ for 18 h and then extracted with ethyl acetate (3×3 mL). The organic layer was dried over anhydrous MgSO_4 , and reduced to dryness under nitrogen. The residue (12.5 mg) was purified by semipreparative HPLC with isocratic 80% MeCN/ H_2O plus 0.01% TFA (4.18 mL min^{-1}), yielding 1',2'-dihydroxyunguinol (**2c**; $t_{\text{R}} = 15.8$ min; 2.2 mg, 14.7%) as a colourless solid. UV (MeOH) λ_{\max} (log ϵ) 203 (4.91), 222 (4.59), 268 (4.28) nm; IR (ATR) ν_{\max} 3674, 2985, 2901, 1393, 1251, 1066 cm^{-1} ; ^1H NMR (600 MHz, DMSO- d_6): δ 10.56 (s, 1H), 9.44 (s, 1H), 6.88 (s, 1H), 6.73 (d, $J = 2.4$ Hz, 1H), 6.56 (d, $J = 2.4$ Hz, 1H), 4.23 (p, $J = 6.4$ Hz, 1H), 2.36 (s, 3H), 2.05 (s, 3H), 1.43 (s, 3H), 1.02 (d, $J = 6.4$ Hz, 3H); ^{13}C NMR (150 MHz, DMSO- d_6): δ 163.3, 162.5, 161.5, 151.7, 145.0, 143.4, 141.1, 136.7, 115.5, 114.6, 111.3, 110.6, 105.7, 75.8, 70.9, 24.5, 21.1, 17.7, 9.3. HRESI(-)MS m/z 359.1135 $[\text{M} - \text{H}]^-$ (calculated for $\text{C}_{19}\text{H}_{19}\text{O}_7^-$, 359.1136).

2'-Hydroxy- $\Delta^{1,4}$ -unguinol (2d). Unguinol (**1**; 40 mg, 123 μmol) was dissolved in 95% aqueous MeCN (10 mL) and Rose Bengal (4 mg, 4 μmol) was added. The reaction mixture was irradiated with UV light (254 nm) for 4 h then reduced to dryness under nitrogen. The residue was redissolved in MeOH (1 mL) and purified by preparative HPLC running with isocratic 60% MeCN/ H_2O , 20 mL min^{-1} yielding 2'-hydroxy- $\Delta^{1,4}$ -unguinol (**2d**; $t_{\text{R}} = 5.75$ min, 3.5 mg, 8.75%) as a colourless solid. UV (MeOH) λ_{\max} (log ϵ) 206 (5.11), 243 (4.62) nm; IR (ATR) ν_{\max} 2976, 1724, 1607, 1576, 1422, 1332, 1247, 1213, 1153, 1104 cm^{-1} ; ^1H NMR (500 MHz, DMSO- d_6): δ 10.55 (s, 1H), 9.63 (s, 1H), 6.54 (d, $J = 2.4$ Hz, 1H), 6.49 (s, 1H), 6.44 (d, $J = 2.4$ Hz, 1H), 5.52 (s, 1H), 5.12 (d, $J = 4.7$ Hz, 1H), 4.95 (s, 1H), 4.59 (p, $J = 6.5$ Hz, 1H), 2.32 (s, 3H), 2.05 (s, 3H), 1.05 (d, $J = 6.5$ Hz, 3H); ^{13}C NMR (125 MHz, DMSO- d_6): δ 163.0, 162.3, 161.7, 152.4, 150.3, 144.4, 143.2, 140.2, 131.1, 115.6, 115.3, 113.2, 111.4, 111.3, 104.9, 67.9, 22.7, 20.6, 9.23. HRESI(-)MS m/z 341.1032 $[\text{M} - \text{H}]^-$ (calculated for $\text{C}_{19}\text{H}_{17}\text{O}_6^-$, 341.1031).

2'-Oxo- $\Delta^{1,4}$ -unguinol (2e). Unguinol (**1**; 60 mg, 184 μmol) was dissolved in MeOH (10 mL) and Rose Bengal (20 mg, 20 μmol) was added. The reaction mixture was transferred to glass reaction chamber and exposed to UV light (254 nm) for 4 h. The solution was then reduced to dryness under nitrogen and purified *via* preparative HPLC running with an isocratic gradient 60% MeCN/ H_2O (60 mL min^{-1}) yielding 2'-oxo- $\Delta^{1,4}$ -unguinol (**2e**; $t_{\text{R}} = 6.35$ min, 1.8 mg, 3.0%) as a colourless solid. UV (MeOH) λ_{\max} (log ϵ) 204 (4.71), 222 (4.39), 263 (4.08)

nm; IR (ATR) ν_{\max} 3398, 2920, 2851, 1698, 1673, 1618, 1575, 1427, 1352, 1328, 1256, 1197, 1157, 1105 cm^{-1} ; ^1H NMR (600 MHz, DMSO- d_6): δ 6.51 (d, $J = 2.1$ Hz, 1H), 6.47 (s, 1H), 6.32 (s, 1H), 6.17 (d, $J = 2.1$ Hz, 1H), 5.85 (s, 1H), 2.40 (s, 3H), 2.30 (s, 3H), 2.08 (s, 3H); ^{13}C NMR (150 MHz, DMSO- d_6): δ 198.3, 162.5, 162.1, 152.7, 145.5, 144.6, 142.9, 140.1, 128.0, 127.5, 116.4, 115.9, 111.7, 110.6, 104.3, 26.9, 20.7, 9.3. HRESI(-)MS m/z 339.0871 $[\text{M} - \text{H}]^-$ (calculated for $\text{C}_{19}\text{H}_{15}\text{O}_6^-$, 339.0874).

2'-Hydroperoxy- $\Delta^{1,4}$ -unguinol (2f). Unguinol (**1**; 65 mg, 199 μmol) was dissolved in MeCN (10 mL) and Rose Bengal (0.5 mg, 0.5 μmol) was added. The reaction mixture was transferred to glass UV reaction chamber and exposed to UV light (254 nm) for 1 h. The solution was reduced to dryness under nitrogen, redissolved in MeCN (1 mL) and purified by preparative HPLC running with an isocratic gradient running 50% MeCN/ H_2O (20 mL min^{-1}), yielding 2'-hydroperoxy- $\Delta^{1,4}$ -unguinol (**2f**; $t_{\text{R}} = 8.02$ min, 9.4 mg, 14.5%) as a colourless solid. UV (MeOH) λ_{\max} (log ϵ) 205 (4.95), 226 (4.66), 264 (4.32) nm; IR (ATR) ν_{\max} 3166, 2984, 1726, 1608, 1576, 1424, 1331, 1284, 1214, 1153, 1105 cm^{-1} ; ^1H NMR (600 MHz, DMSO- d_6): δ 11.66 (br s, 1H), 9.97 (br s, 1H), 6.54 (s, 1H), 6.51 (d, $J = 2.3$ Hz, 1H), 6.42 (d, $J = 2.3$ Hz, 1H), 5.53 (dq, $J = 1.6, 1.2$ Hz, 1H), 5.13 (d, $J = 1.6$ Hz, 1H), 4.81 (q, $J = 6.5$ Hz, 1H), 2.31 (s, 3H), 2.06 (s, 3H), 1.16 (d, $J = 6.5$ Hz, 3H); ^{13}C NMR (150 MHz, DMSO- d_6): δ 163.1, 162.6, 162.3, 152.4, 145.2, 144.4, 143.2, 140.3, 130.2, 116.5, 115.8, 115.6, 111.6, 110.7, 104.9, 81.9, 20.6, 17.9, 9.24. ESI; HRESI(-)MS m/z 357.0980 $[\text{M} - \text{H}]^-$ (calculated for $\text{C}_{19}\text{H}_{17}\text{O}_7^-$, 357.0980).

2,7-Dibromo-1',2'-dihydrounguinol (3a) and 2,4,7-tribromo-1',2'-dihydrounguinol (3b). 1',2'-Dihydrounguinol (**2a**; 10 mg, 30 μmol) was dissolved in chloroform (3 mL) and a solution of bromine in chloroform (2.1 M; 33 μL , 70 μmol) was added. The reaction mixture was stirred at 25 $^\circ\text{C}$ for 6 h. The crude reaction mixture was washed with brine (3×3 mL) and the organic layer was dried over MgSO_4 , filtered and reduced to dryness under nitrogen. The residue (9.1 mg) was purified by semipreparative HPLC with isocratic 60% MeCN/ H_2O plus 0.01% TFA (4.18 mL min^{-1}). After separation, 2,7-dibromo-1',2'-dihydrounguinol (**3a**; $t_{\text{R}} = 22.8$ min; 1.64 mg, 16.4%) and 2,4,7-tribromo-1',2'-dihydrounguinol (**3b**; $t_{\text{R}} = 23.5$ min; 1.9 mg, 19%) were isolated. Compound **3a** was isolated as white solid; UV (MeOH) λ_{\max} (log ϵ) 203 (4.74), 221 (4.58), 283 (4.05), 322 (4.10) nm; IR (ATR) ν_{\max} 2965, 1732, 1596, 1567, 1418, 1338, 1226, 1179 cm^{-1} ; ^1H NMR (600 MHz, DMSO- d_6): δ 11.63 (s, 1H), 9.23 (s, 1H), 6.86 (s, 1H), 3.74 (br s, 1H), 2.44 (s, 3H), 2.16 (s, 3H), 1.99 (m, 1H), 1.81 (m, 1H), 1.34 (d, $J = 7.2$ Hz, 3H), 0.82 (br s, 3H); ^{13}C NMR (150 MHz, DMSO- d_6): δ 161.7, 161.3, 158.6, 149.9, 143.5, 142.3, 134.0, 116.7, 113.2, 111.3, 104.6, 34.1, 26.2, 21.6, 18.0, 12.7, 10.7. HRESI(-)MS m/z 482.9443 $[\text{M} - \text{H}]^-$ (calculated for $\text{C}_{19}\text{H}_{17}^{79}\text{Br}_2\text{O}_5^-$, 482.9448). Compound **3b** was isolated as white solid; UV (MeOH) λ_{\max} (log ϵ) 205 (4.54), 223 (4.36), 251 (4.07), 322 (4.14) nm; IR (ATR) ν_{\max} 2963, 1732, 1560, 1419, 1363, 1338, 1289, 1227 cm^{-1} ; ^1H NMR (600 MHz, DMSO- d_6): δ 11.15 (s, 1H), 9.30 (s, 1H), 4.44 (br s, 1H), 2.41 (s, 3H), 2.19 (s, 3H), 2.00 (m, 1H), 1.76 (m, 1H),

1.30 (d, $J = 7.2$ Hz, 3H), 0.70 (t, $J = 7.3$ Hz, 3H); ^{13}C NMR (150 MHz, DMSO- d_6): δ 161.3, 158.7, 156.0, 150.4, 143.4, 142.2, 141.8, 134.2, 116.7, 114.1, 113.0, 108.4, 100.4, 33.6, 25.7, 22.3, 18.0, 12.3, 10.7. HRESI(-)MS m/z 560.8553 [$\text{M} - \text{H}$] $^-$ (calculated for $\text{C}_{19}\text{H}_{16}^{79}\text{Br}_3\text{O}_5^-$, 560.8553).

2,4-Diiodo-1',2'-dihydranguinol (3c). 1',2'-Dihydranguinol (2a; 10 mg, 30 μmol) was dissolved in acetic acid (3 mL) and NaI (130 mg, 88 μmol) was added. An aqueous solution of H_2O_2 (30%; 0.5 mL, 0.15 mmol) was added dropwise to the well-stirred solution, and the reaction mixture was stirred at 25 $^\circ\text{C}$ for 6 h. The mixture was treated with an aqueous sodium thiosulfate solution (2 \times 3 mL) and extracted with ethyl acetate (3 \times 3 mL). The organic layer was dried over anhydrous MgSO_4 , and reduced to dryness under nitrogen. The residue was purified by silica flash chromatography using a SNAP-10 g cartridge. The whole reaction product was dissolved in 1 mL *n*-hexane/ethyl acetate (50:50) and separated with *n*-hexane and ethyl acetate gradient system (7% to 60%), 12 mL min^{-1} , yielding 2,4-diiodo-1',2'-dihydranguinol (3c; $t_{\text{R}} = 12.5$ min, 5.6 mg, 56%) as a colourless solid. UV (MeOH) λ_{max} (log ϵ) 205 (4.85), 231 (4.41), 281 (3.88) nm; IR (ATR) ν_{max} 2961, 1727, 1590, 1560, 1420, 1334, 1226, 1177 cm^{-1} ; ^1H NMR (600 MHz, DMSO- d_6): δ 10.47 (br s, 1H), 9.61 (s, 1H), 6.52 (s, 1H), 3.98 (m, 1H), 2.45 (s, 3H), 2.06 (s, 3H), 1.49 (m, 2H), 1.05 (d, $J = 6.9$ Hz, 3H), 0.79 (t, $J = 7.3$ Hz, 3H); ^{13}C NMR (150 MHz, DMSO- d_6): δ 163.0, 162.1, 160.4, 153.4, 146.3, 142.5, 142.1, 136.5, 113.9, 108.3, 92.3, 76.9, 32.9, 29.8, 28.2, 21.6, 11.7, 9.1. HRESI(-)MS m/z 578.9172 [$\text{M} - \text{H}$] $^-$ (calculated for $\text{C}_{19}\text{H}_{17}\text{I}_2\text{O}_5^-$, 578.9171).

Methyl unguinol (4a). Unguinol (1; 50 mg, 153.0 μmol) was dissolved in 2 M KOH in MeOH (10 mL) and transferred to clear glass scintillation vial and the reaction mixture was heated to 60 $^\circ\text{C}$ for 18 h. The reaction was quenched by diluting with H_2O (50 mL) and recovered with ethyl acetate (50 mL). The organic layer was dried over Na_2SO_4 and reduced to dryness *in vacuo* followed by purification with preparative HPLC (Alltima, 20 mL min^{-1} , 0.01% TFA) with an isocratic gradient running 50% MeCN/ H_2O , yielding methyl unguinol (4a; $t_{\text{R}} = 23.89$ min, 8.7 mg, 11.9%) as white residue. UV (MeOH) λ_{max} (log ϵ) 215 (4.48), 248 (4.00), 285 (3.37) nm; IR (ATR) ν_{max} 3231, 2918, 1695, 1605, 1429, 1327, 1265, 1208, 1152 cm^{-1} ; ^1H NMR (600 MHz, DMSO- d_6): δ 9.56 (s, 1H), 9.09 (s, 1H), 8.36 (s, 1H), 6.19 (s, 1H), 6.19 (d, $J = 2.2$ Hz, 1H), 5.73 (d, $J = 2.2$ Hz, 1H), 5.41 (qq, $J = 6.8, 1.4$ Hz, 1H), 3.77 (s, 3H), 2.17 (s, 3H), 1.96 (s, 3H), 1.75 (dq, $J = 1.4, 1.1$ Hz, 3H), 1.55 (dq, $J = 6.8, 1.1$ Hz, 3H); ^{13}C NMR (150 MHz, DMSO- d_6): δ 167.9, 159.0, 157.7, 152.6, 148.0, 137.9, 136.0, 133.2, 131.8, 123.5, 113.4, 110.7, 110.0, 105.8, 98.8, 51.6, 19.7, 16.6, 13.7, 9.0. HRESI(-)MS m/z 357.1340 [$\text{M} - \text{H}$] $^-$ (calculated for $\text{C}_{20}\text{H}_{21}\text{O}_6^-$, 357.1343).

Unguinolamide (4b). Unguinol (1; 60 mg, μmol) was dissolved in MeCN (10 mL) and transferred to clear glass scintillation vial. Concentrated aqueous ammonia (25%; 8 mL) was added and reaction mixture was heated to 100 $^\circ\text{C}$ for 18 h. The reaction mixture was neutralised with HCl, diluted with H_2O (50 mL) and extracted with ethyl acetate (50 mL). The organic

layer was dried over Na_2SO_4 and reduced to dryness *in vacuo*. The residue purified *via* preparative HPLC (Alltima, 20 mL min^{-1} , 0.01% TFA) with an isocratic gradient running 60% MeCN/ H_2O , yielding unguinolamide (4b; $t_{\text{R}} = 11.99$ min, 7.1 mg, 12.1%) as white residue. UV (MeOH) λ_{max} (log ϵ) 208 (4.62), 244 (4.09), 283 (3.49) nm; IR (ATR) ν_{max} 3172, 1648, 1588, 1425, 1378, 1320, 1267, 1209, 1157, 1104 cm^{-1} ; ^1H NMR (600 MHz, DMSO- d_6): δ 9.43 (s, 1H), 9.38 (s, 1H), 9.03 (s, 1H), 7.94 (s, 1H), 7.71 (s, 1H), 6.22 (d, $J = 2.2$ Hz, 1H) 6.17 (s, 1H), 5.82 (d, $J = 2.2$ Hz, 1H), 5.54 (qq, $J = 6.8, 1.5$ Hz, 1H), 2.22 (s, 3H), 1.91 (s, 3H), 1.79 (dq, $J = 1.5, 1.1$ Hz, 3H), 1.59 (dq, $J = 6.8, 1.1$ Hz, 3H); ^{13}C NMR (150 MHz, DMSO- d_6): δ 170.2, 158.0, 156.5, 152.6, 148.4, 136.7, 135.8, 133.5, 132.5, 123.7, 118.5, 110.6, 110.2, 105.0, 100.0, 19.6, 16.6, 13.8, 8.8. HRESI(-)MS m/z 342.1341 [$\text{M} - \text{H}$] $^-$ (calculated for $\text{C}_{19}\text{H}_{20}\text{NO}_5^-$, 342.1347).

3-O-Methylunguinol (5a) and 3,8-di-O-methylunguinol (5b). Unguinol (1; 15 mg, 46 μmol) was dissolved in acetone (5 mL) and iodomethane (6 μL , 0.09 mmol) and excess K_2CO_3 (5 mg) were added. The reaction mixture was stirred at 25 $^\circ\text{C}$ for 12 hours then filtered. The filtrate was reduced to dryness under nitrogen. The residue was purified by silica chromatography using a SNAP-10 g cartridge. The whole reaction product was dissolved in 1 mL *n*-hexane/ethyl acetate (50:50). The mixture was separated with *n*-hexane and ethyl acetate gradient system (2% to 20%), 12 mL min^{-1} , yielding 3-O-methylunguinol (5a; 3.6 mg, $t_{\text{R}} = 23.5$ min, 24%) and 3,8-di-O-methylunguinol (5b; 3.0 mg, $t_{\text{R}} = 17.8$ min, 20%) as solid white powder. **3-O-Methylunguinol (5a):** UV (MeOH) λ_{max} (log ϵ) 205 (4.81), 225 (4.55), 263 (4.20) nm; IR (ATR) ν_{max} 3385, 2927, 2353, 1710, 1602, 1424, 1333, 1253, 1205, 1144, 1101, 102.3 cm^{-1} ; ^1H NMR (600 MHz, DMSO- d_6): δ 9.62 (s, 1H), 6.77 (d, $J = 2.5$ Hz, 1H), 6.42 (s, 1H), 6.39 (d, $J = 2.5$ Hz, 1H), 5.45 (qq, $J = 6.8, 1.5$ Hz, 1H) 3.76 (s, 3H), 2.38 (s, 3H), 2.04 (s, 3H), 2.00 (dq, $J = 1.5, 1.2$ Hz, 3H), 1.78 (dq, $J = 6.8, 1.2$ Hz, 3H); ^{13}C NMR (150 MHz, DMSO- d_6): δ 162.8, 162.6, 162.2, 152.6, 144.4, 143.0, 140.1, 135.3, 132.4, 125.0, 114.6, 114.2, 113.2, 110.7, 103.0, 55.6, 20.5, 17.6, 13.6, 9.1. HRESI(-)MS m/z 339.1237 [$\text{M} - \text{H}$] $^-$ (calculated for $\text{C}_{20}\text{H}_{19}\text{O}_5^-$, 339.1238). **3,8-Di-O-methylunguinol (5b):** UV (MeOH) λ_{max} (log ϵ) 205 (4.81), 225 (4.55), 263 (4.20) nm; IR (ATR) ν_{max} 2934, 1731, 1607, 1573, 1484, 1445, 1415, 1378, 1324, 1296, 1235, 1216, 1198, 1147, 1126 cm^{-1} ; ^1H NMR (600 MHz, DMSO- d_6): δ 6.78 (d, $J = 2.5$ Hz, 1H), 6.57 (s, 1H), 6.42 (d, $J = 2.5$ Hz, 1H), 5.53 (qq, $J = 6.8, 1.5$ Hz, 1H) 3.77 (s, 3H), 3.76 (s, 3H), 2.38 (s, 3H), 2.07 (s, 3H), 2.04 (dq, $J = 1.5, 1.2$ Hz, 3H), 1.80 (dq, $J = 6.8, 1.2$ Hz, 3H); ^{13}C NMR (150 MHz, DMSO- d_6): δ 162.7, 162.6, 162.0, 154.2, 144.6, 142.8, 141.2, 135.5, 132.4, 125.6, 116.3, 114.3, 113.0, 107.2, 103.0, 56.0, 55.7, 20.5, 17.7, 13.7, 9.0. HRESI(+MS m/z 355.1535 [$\text{M} + \text{H}$] $^+$ (calculated for $\text{C}_{21}\text{H}_{23}\text{O}_5^+$, 355.1540).

General procedure for benzylation of unguinol. A mixture of unguinol (1; 15 mg, 46 μmol), benzyl bromide (0.43 mmol) and excess K_2CO_3 (5 mg) in tetrahydrofuran (5 mL) was stirred at 50 $^\circ\text{C}$ for 12 h. The crude reaction mixture was filtered and the filtrate was reduced to dryness under nitrogen. The crude reaction mixture was purified by silica chromatography using a

SNAP-10 g cartridge with a *n*-hexane/ethyl acetate gradient system (1% to 20%), 12 mL min⁻¹, yielding a mixture of 3-*O*-benzylated unguinol and 3,8-di-*O*-benzylated unguinol.

3-*O*-Benzylunguinol (6a). Isolated as white powder, *t*_R = 22.3 min, 6.0 mg, 40%. UV (MeOH) λ_{max} (log ε) 206 (5.08), 262 (4.50) nm; IR (ATR) ν_{max} 2923, 2360, 1728, 1605, 1569, 1420, 1378, 1323, 1291, 1252, 1215, 1176, 1145, 1103 cm⁻¹; ¹H NMR (600 MHz, DMSO-*d*₆): δ 9.62 (br s, 1H), 7.39 (m, 2H), 7.38 (m, 2H), 7.32 (m, 1H), 6.87 (d, *J* = 2.6 Hz, 1H), 6.46 (d, *J* = 2.6 Hz, 1H) 6.41 (s, 1H), 5.45 (qq, *J* = 6.7, 1.5 Hz, 1H), 5.14 (s, 2H), 2.32 (s, 3H), 2.04 (s, 3H), 1.93 (dq, *J* = 1.5, 1.1 Hz, 3H), 1.75 (dq, *J* = 6.7, 1.1 Hz, 3H); ¹³C NMR (150 MHz, DMSO-*d*₆): δ 162.8, 162.2, 161.7, 152.6, 144.4, 143.0, 140.1, 136.0, 135.2, 132.2, 128.5, 128.0, 127.5, 125.1, 115.2, 114.6, 113.4, 110.7, 103.7, 69.6, 20.5, 17.5, 13.7, 9.1. HRESI(+)*MS m/z* 417.1689 [M + H]⁺ (calculated for C₂₆H₂₅O₅⁺, 417.1696).

3,8-Di-*O*-benzylunguinol (6b). Isolated as white powder, *t*_R = 12.8 min, 4.0 mg, 27%. UV (MeOH) λ_{max} (log ε) 206 (4.94), 260 (4.34) nm; IR (ATR) ν_{max} 3673, 2924, 2360, 2339, 1733, 1650, 1607, 1573, 1484, 1452, 1417, 1377, 1324, 1252, 1218, 1146, 1120 cm⁻¹; ¹H NMR (600 MHz, DMSO-*d*₆): δ 7.39 (m, 2H), 7.38 (m, 4H), 7.33 (m, 1H), 7.41 (m, 2H), 7.31 (m, 1H), 6.88 (d, *J* = 2.4 Hz, 1H), 6.68 (s, 1H), 6.48 (d, *J* = 2.4 Hz, 1H), 5.51 (qq, *J* = 6.8, 1.4 Hz, 1H), 5.15 (s, 2H), 5.08 (s, 2H), 2.38 (s, 3H), 2.13 (s, 3H), 1.96 (dq, *J* = 1.4, 1.1 Hz, 3H), 1.77 (dq, *J* = 6.8, 1.1 Hz, 3H); ¹³C NMR (150 MHz, DMSO-*d*₆): δ 162.6, 162.0, 161.8, 153.3, 144.6, 142.9, 141.4, 137.0, 136.1, 135.3, 132.1, 128.5, 128.4, 128.1, 127.8, 127.5, 127.3, 125.7, 116.9, 115.4, 113.3, 108.8, 103.9, 69.9, 69.6, 20.6, 17.6, 13.8, 9.2. HRESI(+)*MS m/z* 507.2162 [M + H]⁺ (calculated for C₃₃H₃₁O₅⁺, 507.2166).

3-*O*-(2-Chlorobenzyl)unguinol (7a). Isolated as white powder, *t*_R = 21.5 min, 7.8 mg, 52%. UV (MeOH) λ_{max} (log ε) 204 (4.82), 258 (4.25) nm; IR (ATR) ν_{max} 3673, 3364, 2972, 2360, 2339, 1701, 1606, 1570, 1420, 1380, 1326, 1253, 1216, 1147, 1101 cm⁻¹; ¹H NMR (600 MHz, DMSO-*d*₆): δ 9.62 (br s, 1H), 7.50 (m, 2H), 7.39 (m, 1H), 7.36 (m, 1H), 6.90 (d, *J* = 2.6 Hz, 1H), 6.45 (d, *J* = 2.6 Hz, 1H) 6.41 (s, 1H), 5.45 (qq, *J* = 6.8, 1.4 Hz, 1H), 5.19 (s, 2H), 2.39 (s, 3H), 2.04 (s, 3H), 1.93 (dq, *J* = 1.4, 1.2 Hz, 3H), 1.73 (dq, *J* = 6.8, 1.2 Hz, 3H); ¹³C NMR (150 MHz, DMSO-*d*₆): δ 162.8, 162.2, 161.4, 152.6, 144.5, 143.0, 140.1, 135.2, 133.3, 132.4, 132.1, 130.0, 129.8, 129.4, 127.4, 125.1, 115.2, 114.7, 113.7, 110.7, 103.4, 69.1, 20.5, 17.5, 13.6, 9.1. HRESI(+)*MS m/z* 451.1306 [M + H]⁺ (calculated for C₂₆H₂₄³⁵ClO₅⁺, 451.1306).

3-*O*-(3-Chlorobenzyl)unguinol (7b). Isolated as white powder, *t*_R = 21.7 min, 7.7 mg, 51.3%. UV (MeOH) λ_{max} (log ε) 203 (4.62), 263 (4.01) nm; IR (ATR) ν_{max} 3356, 2926, 2360, 1696, 1610, 1567, 1478, 1417, 1378, 1366, 1323, 1293, 1265, 1215, 1197, 1146 cm⁻¹; ¹H NMR (600 MHz, DMSO-*d*₆): δ 9.63 (br s, 1H), 7.45 (m, 1H), 7.41 (m, 1H), 7.40 (m, 1H), 7.34 (m, 1H), 6.89 (d, *J* = 2.6 Hz, 1H), 6.45 (d, *J* = 2.5 Hz, 1H), 6.41 (s, 1H), 5.45 (qq, *J* = 6.7, 1.2 Hz, 1H), 5.17 (s, 2H), 2.38 (s, 3H), 2.04 (s, 3H), 1.91 (dq, *J* = 1.2, 1.0 Hz, 3H), 1.75 (dq, *J* = 6.7, 1.0 Hz, 3H); ¹³C NMR (150 MHz, DMSO-*d*₆): δ 162.8, 162.2, 161.4, 152.6, 144.5, 143.0, 140.1, 138.7, 135.2, 133.2, 132.1, 130.4, 127.9, 127.0, 125.9, 125.1, 115.2, 114.7, 113.6, 110.7, 103.7, 68.6, 20.5,

17.5, 13.7, 9.1. HRESI(-)*MS m/z* 449.1162 [M - H]⁻ (calculated for C₂₆H₂₂³⁵ClO₅⁻, 449.1161).

3-*O*-(4-Chlorobenzyl)unguinol (7c). Isolated as white powder, *t*_R = 21.4 min; 5.3 mg, 35.3%. UV (MeOH) λ_{max} (log ε) 202 (4.91), 258 (4.37) nm; IR (ATR) ν_{max} 3672, 2971, 2901, 2360, 1730, 1607, 1570, 1491, 1421, 1379, 1324, 1255, 1218, 1148, 1102 cm⁻¹; ¹H NMR (600 MHz, DMSO-*d*₆): δ 9.61 (br s, 1H), 7.44 (m, 2H), 7.40 (m, 2H), 6.87 (d, *J* = 2.6 Hz, 1H), 6.43 (d, *J* = 2.6 Hz, 1H) 6.41 (s, 1H), 5.45 (qq, *J* = 6.8, 1.4 Hz, 1H), 5.15 (s, 2H), 2.38 (s, 3H), 2.04 (s, 3H), 1.92 (dq, *J* = 1.4, 1.0 Hz, 3H), 1.74 (dq, *J* = 6.8, 1.0 Hz, 3H); ¹³C NMR (150 MHz, DMSO-*d*₆): δ 162.8, 162.2, 161.5, 152.6, 144.5, 143.0, 140.1, 135.2, 135.1, 132.6, 132.1, 129.2, 128.5, 125.1, 115.2, 114.7, 113.5, 110.7, 103.8, 68.7, 20.5, 17.5, 13.7, 9.1. HRESI(-)*MS m/z* 449.1164 [M - H]⁻ (calculated for C₂₆H₂₂³⁵ClO₅⁻, 449.1161).

3-*O*-(2-Fluorobenzyl)unguinol (7d). Isolated as white powder, *t*_R = 22.1 min; 6.5 mg, 43.3%. UV (MeOH) λ_{max} (log ε) 205 (4.87), 263 (4.31) nm; IR (ATR) ν_{max} 3672, 2971, 2360, 1729, 1606, 1570, 1493, 1421, 1380, 1325, 1253, 1216, 1181, 1146, 1104, cm⁻¹; ¹H NMR (600 MHz, DMSO-*d*₆): δ 9.62 (br s, 1H), 7.48 (ddd, *J* = 7.5, 7.5, 1.7 Hz, 1H), 7.42 (m, 1H), 7.25 (ddd, *J* = 10.9, 8.2, 1.1 Hz, 1H), 7.22 (ddd, *J* = 7.5, 7.5, 1.1 Hz, 1H), 6.89 (d, *J* = 2.5 Hz, 1H) 6.48 (d, *J* = 2.5 Hz, 1H), 6.42 (s, 1H), 5.46 (qq, *J* = 6.8, 1.4 Hz, 1H), 5.18 (s, 2H), 2.38 (s, 3H), 2.04 (s, 3H), 1.96 (dq, *J* = 1.4, 1.0 Hz, 3H), 1.75 (dq, *J* = 6.8, 1.0 Hz, 3H); ¹³C NMR (150 MHz, DMSO-*d*₆): δ 162.8, 162.2, 161.4, 160.2, 152.6, 144.5, 143.0, 140.1, 135.2, 132.2, 130.6, 130.4, 125.1, 124.6, 122.9, 115.4, 115.1, 114.7, 113.6, 110.7, 103.6, 63.9, 20.5, 17.5, 13.6, 9.1. HRESI(+)*MS m/z* 435.1603 [M + H]⁺ (calculated for C₂₆H₂₄FO₅⁺, 435.1602).

3-*O*-(3-Fluorobenzyl)unguinol (7e). Isolated as white powder, *t*_R = 22.8 min; 6.3 mg, 42.0%. UV (MeOH) λ_{max} (log ε) 207 (4.75), 262 (4.23) nm; IR (ATR) ν_{max} 2919, 2360, 2340, 1719, 1608, 1568, 1488, 1475, 1416, 1376, 1347, 1324, 1290, 1254, 1238, 1218, 1147, 1128 cm⁻¹; ¹H NMR (600 MHz, DMSO-*d*₆): δ 9.62 (br s, 1H), 7.42 (m, 1H), 7.22 (m, 2H), 7.15 (dddd, *J* = 9.2, 7.5, 2.5, 1.0 Hz, 1H), 6.88 (d, *J* = 2.4 Hz, 1H) 6.45 (d, *J* = 2.4 Hz, 1H), 6.41 (s, 1H), 5.44 (qq, *J* = 6.7, 1.3 Hz, 1H), 5.18 (s, 2H), 2.38 (s, 3H), 2.04 (s, 3H), 1.92 (dq, *J* = 1.3, 1.0 Hz, 3H), 1.74 (dq, *J* = 6.7, 1.0 Hz, 3H); ¹³C NMR (150 MHz, DMSO-*d*₆): δ 162.8, 162.2, 162.1, 161.2, 152.6, 144.5, 143.0, 140.1, 139.0, 135.2, 132.1, 130.6, 125.1, 123.3, 115.2, 114.8, 114.7, 114.0, 113.6, 110.7, 103.8, 68.7, 20.5, 17.5, 13.7, 9.1. HRESI(-)*MS m/z* 433.1454 [M - H]⁻ (calculated for C₂₆H₂₂FO₅⁻, 433.1456).

3-*O*-(4-Fluorobenzyl)unguinol (7f). Isolated as white powder, *t*_R = 23.4 min; 7.1 mg, 47.3%. UV (MeOH) λ_{max} (log ε) 205 (4.82), 262 (4.29) nm; IR (ATR) ν_{max} 3673, 2971, 2901, 2360, 1730, 1607, 1571, 1511, 1420, 1379, 1325, 1254, 1222, 1147, 1103 cm⁻¹; ¹H NMR (600 MHz, DMSO-*d*₆): δ 9.61 (br s, 1H), 7.44 (m, 2H), 7.21 (m, 2H), 6.87 (d, *J* = 2.5 Hz, 1H) 6.45 (d, *J* = 2.5 Hz, 1H), 6.41 (s, 1H), 5.46 (qq, *J* = 6.7, 1.4 Hz, 1H), 5.12 (s, 2H), 2.38 (s, 3H), 2.04 (s, 3H), 1.94 (dq, *J* = 1.4, 1.0 Hz, 3H), 1.75 (dq, *J* = 6.7, 1.0 Hz, 3H); ¹³C NMR (150 MHz, DMSO-*d*₆): δ 162.8, 162.2, 161.8, 161.6, 152.5, 144.5, 143.0, 140.1, 135.2, 132.3, 132.2, 129.8, 125.1, 115.3, 115.1, 114.7, 113.4, 110.7,

103.8, 68.9, 20.5, 17.5, 13.7, 9.1. HRESI(−)MS m/z 433.1456 [M − H][−] (calculated for C₂₆H₂₂FO₅[−], 433.1457).

3-O-(2,4-Difluorobenzyl)unguinol (7g). Isolated as white powder, t_R = 23.1 min; 8.4 mg, 56%. UV (MeOH) λ_{\max} (log ϵ) 205 (5.00), 262 (4.45) nm; IR (ATR) ν_{\max} 3673, 3377, 2971, 2901, 2360, 2339, 1702, 1606, 1571, 1506, 1421, 1381, 1327, 1255, 1217, 1147, 1100 cm^{−1}; ¹H NMR (600 MHz, DMSO-*d*₆): δ 9.62 (br s, 1H), 7.56 (m, 1H), 7.31 (ddd, J = 10.6, 9.3, 2.5 Hz, 1H), 7.12 (m, 1H), 6.89 (d, J = 2.5 Hz, 1H), 6.47 (d, J = 2.5 Hz, 1H), 6.42 (s, 1H), 5.46 (qq, J = 6.8, 1.4 Hz, 1H), 5.14 (s, 2H), 2.38 (s, 3H), 2.04 (s, 3H), 1.97 (dq, J = 1.4, 1.1 Hz, 3H), 1.76 (dq, J = 6.8, 1.1 Hz, 3H); ¹³C NMR (150 MHz, DMSO-*d*₆): δ 162.8, 162.4, 162.2, 161.3, 160.5, 152.6, 144.5, 143.0, 140.1, 135.2, 132.2, 131.9, 125.1, 119.4, 115.4, 115.0, 114.7, 113.7, 111.7, 110.7, 104.1, 103.6, 63.5, 20.5, 17.5, 13.6, 9.1. HRESI(−)MS m/z 451.1363 [M − H][−] (calculated for C₂₆H₂₁F₂O₅[−], 451.1363).

3-O-(3-Bromobenzyl)unguinol (7h). Isolated as white powder, t_R = 22.5 min; 6.8 mg, 45.3%. UV (MeOH) λ_{\max} (log ϵ) 203 (4.76), 260 (4.17) nm; IR (ATR) ν_{\max} 2922, 2360, 2340, 1727, 1606, 1575, 1510, 1416, 1383, 1346, 1317, 1295, 1263, 1217, 1142, 1107 cm^{−1}; ¹H NMR (600 MHz, DMSO-*d*₆): δ 9.62 (br s, 1H), 7.59 (dd, J = 1.6, 1.6 Hz, 1H), 7.52 (ddd, J = 7.7, 1.6, 1.3 Hz, 1H), 7.39 (ddd, J = 7.7, 1.6, 1.3 Hz, 1H), 7.34 (t, J = 7.7 Hz, 1H), 6.88 (d, J = 2.5 Hz, 1H), 6.44 (d, J = 2.5 Hz, 1H), 6.41 (s, 1H), 5.45 (qq, J = 6.8, 1.2 Hz, 1H), 5.16 (s, 2H), 2.38 (s, 3H), 2.04 (s, 3H), 1.91 (dq, J = 1.2, 1.1 Hz, 3H), 1.75 (dq, J = 6.8, 1.1 Hz, 3H); ¹³C NMR (150 MHz, DMSO-*d*₆): δ 162.8, 162.2, 161.4, 152.6, 144.5, 143.0, 140.1, 138.9, 135.2, 132.1, 130.8, 130.7, 129.9, 126.3, 125.1, 121.7, 115.2, 114.7, 113.6, 110.7, 103.7, 68.5, 20.5, 17.5, 13.7, 9.1. HRESI(−)MS m/z 493.0656 [M − H][−] (calculated for C₂₆H₂₂⁷⁹BrO₅[−], 493.0656).

3-O-(3-Methylbenzyl)unguinol (7i). Isolated as white powder, t_R = 22.1 min; 6.5 mg, 43.3%. UV (MeOH) λ_{\max} (log ϵ) 205 (4.88), 262 (4.30) nm; IR (ATR) ν_{\max} 2920, 2360, 2340, 1723, 1608, 1586, 1568, 1493, 1422, 1383, 1348, 1327, 1288, 1257, 1238, 1225, 1217, 1188, 1149 cm^{−1}; ¹H NMR (600 MHz, DMSO-*d*₆): δ 9.62 (br s, 1H), 7.26 (t, J = 7.4 Hz, 1H), 7.19 (m, 1H), 7.16 (m, 1H), 7.14 (m, 1H), 6.86 (d, J = 2.5 Hz, 1H), 6.44 (d, J = 2.5 Hz, 1H), 6.41 (s, 1H), 5.45 (qq, J = 6.8, 1.4 Hz, 1H), 5.09 (s, 2H), 2.37 (s, 3H), 2.29 (s, 3H), 2.04 (s, 3H), 1.93 (dq, J = 1.4, 1.0 Hz, 3H), 1.75 (dq, J = 6.8, 1.0 Hz, 3H); ¹³C NMR (150 MHz, DMSO-*d*₆): δ 162.8, 162.2, 161.7, 152.6, 144.4, 143.0, 140.1, 137.7, 136.0, 135.2, 132.2, 128.7, 128.4, 128.0, 125.1, 124.5, 115.2, 114.7, 113.4, 110.7, 103.7, 69.6, 20.9, 20.5, 17.5, 13.7, 9.1. HRESI(−)MS m/z 429.1706 [M − H][−] (calculated for C₂₇H₂₅O₅[−], 429.1707).

3-O-(3-Methoxybenzyl)unguinol (7j). Isolated as white powder, t_R = 20.8 min; 5.7 mg, 38.0%. UV (MeOH) λ_{\max} (log ϵ) 203 (4.80), 263 (4.23), 281 (4.08) nm; IR (ATR) ν_{\max} 3399, 2926, 2360, 2340, 1708, 1608, 1570, 1503, 1477, 1419, 1395, 1347, 1324, 1290, 1274, 1242, 1221, 1184, 1145, 1130 cm^{−1}; ¹H NMR (600 MHz, DMSO-*d*₆): δ 9.62 (br s, 1H), 7.29 (t, J = 8.1 Hz, 1H), 6.94 (m, 2H), 6.89 (m, 1H), 6.88 (d, J = 2.5, 1H), 6.44 (d, J = 2.5, 1H), 6.41 (s, 1H), 5.45 (qq, J = 6.7, 1.1, 1H), 5.16 (s, 2H), 3.73 (s, 3H), 2.38 (s, 3H), 2.04 (s, 3H), 1.91 (dq, J = 1.2, 1.1 Hz, 3H), 1.75 (dq, J = 6.7, 1.2 Hz, 3H); ¹³C NMR (150 MHz, DMSO-*d*₆): δ

162.8, 162.2, 161.7, 159.3, 152.6, 144.4, 143.0, 140.1, 137.6, 135.2, 132.1, 129.6, 125.1, 119.4, 115.2, 114.7, 113.4, 113.4, 112.9, 110.7, 103.8, 69.4, 55.0, 20.5, 17.5, 13.7, 9.1. HRESI(−)MS m/z 445.1656 [M − H][−] (calculated for C₂₇H₂₅O₆[−], 445.1656).

3-O-(2-Picolyl)unguinol (7k). A mixture of unguinol (15 mg, 46 μ mol), 2-(bromomethyl)pyridine (23 mg, 2 eq.) and excess K₂CO₃ (5 mg) in MeCN (5 mL) was stirred for 12 h at 25 °C. The crude reaction mixture was filtered and the filtrate was reduced to dryness under nitrogen. The residue was purified by semipreparative HPLC with isocratic 40% MeCN/H₂O plus 0.01% TFA (4.18 mL min^{−1}), yielding 3-O-(2-picolyl)unguinol (7k; t_R = 17.8 min; 4.1 mg, 27.3%). UV (MeOH) λ_{\max} (log ϵ) 205 (4.92), 263 (4.44) nm; IR (ATR) ν_{\max} 3673, 2985, 2901, 2360, 2339, 1730, 1608, 1572, 1420, 1326, 1252, 1215, 1150, 1105 cm^{−1}; ¹H NMR (600 MHz, DMSO-*d*₆): δ 9.61 (s, 1H), 8.57 (d, J = 4.4 Hz, 1H), 7.81 (td, J = 7.7, 1.7 Hz, 1H), 7.42 (d, J = 7.7 Hz, 1H), 7.34 (ddd, J = 7.7, 4.4, 1.0 Hz, 1H), 6.89 (d, J = 2.5 Hz, 1H), 6.46 (d, J = 2.5 Hz, 1H), 6.41 (s, 1H), 5.43 (qq, J = 6.7, 1.4 Hz, 1H), 5.21 (s, 2H), 2.38 (s, 3H), 2.04 (s, 3H), 1.91 (dq, J = 1.4, 1.0 Hz, 3H), 1.73 (dq, J = 6.7, 1.0 Hz, 3H); ¹³C NMR (150 MHz, DMSO-*d*₆): δ 162.8, 162.2, 161.5, 155.6, 152.5, 149.2, 144.4, 143.0, 140.1, 137.0, 135.2, 132.1, 125.1, 123.1, 121.5, 115.3, 114.7, 113.6, 110.7, 103.6, 70.5, 20.5, 17.5, 13.6, 9.1. HRESI(+)MS m/z 418.1644 [M + H]⁺ (calculated for C₂₅H₂₄NO₅⁺, 418.1649).

3-O-(3-Picolyl)unguinol (7l). A mixture of unguinol (15 mg, 46 μ mol), 3-(bromomethyl)pyridine (46 mg, 4 eq.) and excess K₂CO₃ (5 mg) in MeCN (5 mL) was stirred at 25 °C for 12 h. The crude reaction mixture was filtered and the filtrate was reduced to dryness under nitrogen and purified by semipreparative HPLC with isocratic 30% MeCN/H₂O plus 0.01% TFA (4.18 mL min^{−1}), yielding 3-O-(3-picolyl)unguinol (7l; t_R = 19.4 min; 1.2 mg, 8.0%). UV (MeOH) λ_{\max} (log ϵ) 204 (4.48), 260 (4.00) nm; IR (ATR) ν_{\max} 3673, 2985, 2901, 2360, 2339, 1732, 1606, 1407, 1251, 1148 cm^{−1}; ¹H NMR (600 MHz, DMSO-*d*₆): δ 9.61 (br s, 1H), 8.69 (br s, 2H), 7.83 (d, J = 7.7 Hz, 1H), 7.47 (br s, 1H), 6.90 (d, J = 2.5 Hz, 1H), 6.48 (d, J = 2.5 Hz, 1H), 6.41 (s, 1H), 5.45 (qq, J = 6.7, 1.4 Hz, 1H), 5.21 (s, 2H), 2.38 (s, 3H), 2.04 (s, 3H), 1.94 (dq, J = 1.4, 1.1 Hz, 3H), 1.76 (dq, J = 6.7, 1.1 Hz, 3H); ¹³C NMR (150 MHz, DMSO-*d*₆): δ 162.8, 162.2, 161.4, 152.6, 149.1, 148.7, 144.5, 143.0, 140.1, 135.6, 135.2, 132.2, 132.2, 125.1, 124.1, 115.1, 114.7, 113.6, 110.7, 103.8, 67.3, 20.5, 17.5, 13.7, 9.1. HRESI(+)MS m/z 418.1643 [M + H]⁺ (calculated for C₂₅H₂₄NO₅⁺, 418.1649).

3-O-(4-Picolyl)unguinol (7m). A mixture of unguinol (1; 15 mg, 46 μ mol), 4-(bromomethyl)pyridine (23 mg, 4 eq.) and excess K₂CO₃ (5 mg) in MeCN (5 mL) was stirred at 25 °C for 12 h. The crude reaction mixture was filtered and the filtrate was reduced to dryness under nitrogen and purified by semipreparative HPLC with isocratic 35% MeCN/H₂O plus 0.01% TFA (4.18 mL min^{−1}), yielding 3-O-(4-picolyl)unguinol (7m; t_R = 22.1 min; 4.6 mg, 30.7%). UV (MeOH) λ_{\max} (log ϵ) 204 (4.84), 256 (4.33) nm; IR (ATR) ν_{\max} 3671, 3203, 2986, 2901, 2359, 2090, 1611, 1517, 1410, 1253, 1150 cm^{−1}; ¹H NMR (600 MHz, DMSO-*d*₆): δ 9.62 (s, 1H), 8.68 (br s, 2H), 7.41 (br s, 2H), 6.89 (d, J = 2.5 Hz, 1H), 6.44 (d, J = 2.5 Hz, 1H), 6.40 (s, 1H), 5.42

(qq, $J = 6.7, 1.4$ Hz, 1H), 5.24 (s, 2H), 2.38, (s, 3H), 2.04 (s, 3H), 1.89 (dq, $J = 1.4, 1.1$ Hz, 3H), 1.71 (dq, $J = 6.7, 1.1$ Hz, 3H); ^{13}C NMR (150 MHz, DMSO- d_6): δ 162.8, 162.2, 161.2, 152.6, 149.6, 145.4, 144.6, 143.0, 140.1, 135.2, 132.0, 125.1, 121.8, 115.2, 114.7, 113.8, 110.7, 103.7, 67.8, 20.5, 17.5, 13.7, 9.1. HRESI(+) MS m/z 418.1643 $[\text{M} + \text{H}]^+$ (calculated for $\text{C}_{25}\text{H}_{24}\text{NO}_5^+$, 418.1649).

3-O-(4-Morpholinoethyl)unguinol (7n). A mixture of unguinol (**1**; 20 mg, 61 μmol), 4-(2-chloroethyl)morpholine (11.4 mg, 1.0 eq.), K_2CO_3 (8.5 mg, 1.0 eq.) and KI (7.64 mg, 1.0 eq.) in MeCN was stirred for 72 h at 25 °C. The crude reaction mixture was filtered and the filtrate was reduced to dryness under nitrogen and purified by semipreparative HPLC with isocratic 15% MeCN/ H_2O plus 0.01% TFA (4.18 mL min^{-1}), yielding 3-O-(4-morpholinoethyl)unguinol (**7n**; $t_{\text{R}} = 17.1$ min; 5.3 mg, 34.6%). UV (MeOH) λ_{max} (log ϵ) 205 (5.05), 263 (4.51) nm; IR (ATR) ν_{max} 2927, 1728, 1605, 1570, 1420, 1323, 1251, 1214, 1151, 1106 cm^{-1} ; ^1H NMR (600 MHz, DMSO- d_6): δ 9.61 (s, 1H), 6.79 (d, $J = 2.5$ Hz, 1H) 6.42 (s, 1H), 6.40 (d, $J = 2.5$ Hz, 1H), 5.45 (qq, $J = 6.7, 1.5$ Hz, 1H), 4.11 (br s, 1H), 3.55 (br s, 4H), 2.66 (br s, 1H), 2.43 (br s, 2H), 2.37, (s, 3H), 2.04 (s, 3H), 2.00 (dq, $J = 1.5, 1.1$ Hz, 3H), 1.78 (dq, $J = 6.7, 1.1$ Hz, 3H); ^{13}C NMR (150 MHz, DMSO- d_6): δ 162.8, 162.2, 161.8, 152.6, 144.4, 143.0, 140.2, 135.3, 132.5, 125.0, 114.8, 114.7, 113.2, 110.7, 103.4, 66.0, 65.8, 56.4, 53.4, 20.5, 17.6, 13.7, 9.1. HRESI(+)MS m/z 440.2059 $[\text{M} + \text{H}]^+$ (calculated for $\text{C}_{25}\text{H}_{30}\text{NO}_6^+$, 440.2068).

3-O-(1-Piperidinyethyl)unguinol (7o). A mixture of unguinol (**1**; 15 mg, 46 μmol), 1-(2-chloroethyl)piperidine (8.5 mg, 1.0 eq.) K_2CO_3 (9.53 mg, 1.5 eq.) and KI (7.64 mg, 1.0 eq.) in MeCN was stirred at 25 °C for 24 h. The crude reaction mixture was filtered and the filtrate was reduced to dryness under nitrogen and purified by semipreparative HPLC with isocratic 15% MeCN/ H_2O plus 0.01% TFA (4.18 mL min^{-1}), yielding 3-O-(1-piperidinyethyl)unguinol (**7o**; $t_{\text{R}} = 18.8$ min; 3.4 mg, 22.7%). UV (MeOH) λ_{max} (log ϵ) 205 (4.97), 261 (4.45) nm; IR (ATR) ν_{max} 2969, 2360, 2339, 1728, 1673, 1606, 1573, 1420, 1324, 1253, 1199, 1153, 1106 cm^{-1} ; ^1H NMR (600 MHz, DMSO- d_6): δ 9.64 (s, 1H), 6.82 (s, 1H), 6.42 (s, 2H), 4.30 (br s, 2H), 5.46 (qq, $J = 6.7, 1.3$ Hz, 1H), 2.38 (s, 3H), 2.05 (s, 3H), 2.00 (dq, $J = 1.3, 1.1$ Hz, 3H), 1.78 (dq, $J = 6.7, 1.1$ Hz, 3H); ^{13}C NMR (150 MHz, DMSO- d_6): δ 162.8, 162.2, 152.6, 144.5, 143.0, 140.1, 135.3, 132.4, 125.0, 114.7, 114.7, 110.8, 103.7, 20.5, 17.6, 13.7, 9.1. HRESI(+)MS m/z 438.2272 $[\text{M} + \text{H}]^+$ (calculated for $\text{C}_{26}\text{H}_{32}\text{NO}_5^+$, 438.2275).

3-O-(1-Pyrrolidinyethyl)unguinol (7p). A mixture of unguinol (**1**; 15 mg, 46 μmol), 1-(2-chloroethyl)pyrrolidine (7.8 mg, 1.0 eq.) K_2CO_3 (9.53 mg, 1.5 eq.) and KI (7.64 mg, 1.0 eq.) was stirred at 25 °C for 24 h. The crude reaction mixture was filtered and the filtrate was reduced to dryness under nitrogen and purified by semipreparative HPLC with isocratic 15% MeCN/ H_2O plus 0.01% TFA (4.18 mL min^{-1}), yielding 3-O-(1-pyrrolidinyethyl)unguinol (**7p**; $t_{\text{R}} = 19.5$ min; 1.3 mg, 8.7%). UV (MeOH) λ_{max} (log ϵ) 205 (4.84), 226 (4.54), 266 (4.21) nm; IR (ATR) ν_{max} 3673, 2971, 2901, 2360, 2339, 1730, 1675, 1607, 1418, 1253, 1201, 1156, 1105 cm^{-1} ; ^1H NMR (600 MHz, DMSO- d_6): δ 9.66 (s, 1H), 6.85 (d, $J = 2.4$ Hz, 1H), 6.44 (d, $J = 2.4$ Hz,

1H), 6.43 (s, 1H), 5.46 (qq, $J = 6.8, 1.5$ Hz, 1H), 4.32 (br s, 2H), 3.57 (br s, 4H), 3.07 (br s, 2H), 2.40 (s, 3H), 2.05 (s, 3H), 2.00 (dq, $J = 1.5, 1.0$ Hz, 3H), 1.79 (dq, $J = 6.8, 1.0$ Hz, 3H); ^{13}C NMR (150 MHz, DMSO- d_6): δ 162.8, 162.2, 152.6, 144.6, 143.0, 140.1, 135.3, 132.4, 125.0, 114.7, 110.8, 103.8, 63.6, 53.8, 52.5, 22.4, 20.5, 17.6, 13.7, 9.1. HRESI(+)MS m/z 424.2111 $[\text{M} + \text{H}]^+$ (calculated for $\text{C}_{25}\text{H}_{30}\text{NO}_5^+$, 424.2118).

3-O-Benzyl-1',2'-dihydrunguinol (8a). Isolated as white powder, $t_{\text{R}} = 20.5$ min; 5.1 mg, 34%. UV (MeOH) λ_{max} (log ϵ) 203 (5.09), 265 (4.45) nm; IR (ATR) ν_{max} 3356, 2962, 2929, 1728, 1607, 1570, 1428, 1378, 1336, 1256, 1214, 1149, 1112 cm^{-1} ; ^1H NMR (600 MHz, DMSO- d_6): δ 9.50 (br s, 1H), 7.41 (m, 2H), 7.37 (m, 2H), 7.32 (m, 1H), 6.88 (d, $J = 2.5$ Hz, 1H) 6.83 (d, $J = 2.5$ Hz, 1H), 6.48 (s, 1H), 5.19 (d, $J = 12.0$ Hz, 2H) 3.32 (m, 1H), 2.39 (s, 3H), 2.03 (s, 3H), 1.48 (m, 2H), 1.05 (d, $J = 6.8$ Hz, 3H), 0.75 (t, $J = 7.3$ Hz, 3H); ^{13}C NMR (150 MHz, DMSO- d_6): δ 162.9, 162.3, 161.8, 152.9, 144.6, 142.7, 140.9, 136.2, 136.1, 128.4, 128.0, 127.5, 115.3, 113.6, 113.5, 108.1, 103.9, 69.7, 32.2, 29.8, 21.5, 20.6, 12.0, 9.1. HRESI(+)MS m/z 419.1848 $[\text{M} + \text{H}]^+$ (calculated for $\text{C}_{26}\text{H}_{27}\text{O}_5^+$, 419.1853).

3-O-(2-Fluorobenzyl)-1',2'-dihydrunguinol (8b). Isolated as white powder, $t_{\text{R}} = 19.8$ min; 5.7 mg, 38%. UV (MeOH) λ_{max} (log ϵ) 203 (5.08), 263 (4.44) nm; IR (ATR) ν_{max} 3341, 2962, 2360, 2339, 1727, 1606, 1570, 1493, 1427, 1379, 1335, 1256, 1214, 1148, 1111 cm^{-1} ; ^1H NMR (600 MHz, DMSO- d_6): δ 9.51 (br s, 1H), 7.52 (ddd, $J = 7.6, 7.6, 1.7$ Hz, 1H), 7.42 (m, 1H), 7.25 (ddd, $J = 10.9, 8.2, 1.1$ Hz, 1H), 7.21 (ddd, $J = 7.6, 7.6, 1.0$ Hz, 1H), 6.90 (d, $J = 2.5$ Hz, 1H) 6.88 (d, $J = 2.5$ Hz, 1H), 6.49 (s, 1H), 5.22 (d, $J = 12.0$ Hz, 2H) 3.32 (m, 1H), 2.39 (s, 3H), 2.04 (s, 3H), 1.49 (m, 2H), 1.07 (d, $J = 6.8$ Hz, 3H), 0.76 (t, $J = 7.3$ Hz, 3H); ^{13}C NMR (150 MHz, DMSO- d_6): δ 162.9, 162.3, 161.6, 160.3, 152.9, 144.7, 142.7, 140.9, 136.2, 130.6, 124.5, 122.9, 115.4, 115.2, 113.7, 113.6, 108.1, 103.8, 64.1, 32.2, 29.8, 21.5, 20.6, 11.9, 9.1. HRESI(+)MS m/z 437.1756 $[\text{M} + \text{H}]^+$ (calculated for $\text{C}_{26}\text{H}_{26}\text{FO}_5^+$, 437.1758).

3-O-(4-Fluorobenzyl)-1',2'-dihydrunguinol (8c). Isolated as white powder, $t_{\text{R}} = 22.9$ min; 6.4 mg, 42.6%. UV (MeOH) λ_{max} (log ϵ) 203 (5.10), 265 (4.43) nm; IR (ATR) ν_{max} 3673, 3378, 2966, 2360, 2339, 1728, 1606, 1570, 1511, 1427, 1378, 1336, 1256, 1219 cm^{-1} ; ^1H NMR (600 MHz, DMSO- d_6): δ 9.50 (br s, 1H), 7.47 (m, 2H), 7.20 (m, 2H), 6.87 (d, $J = 2.5$ Hz, 1H) 6.82 (d, $J = 2.5$ Hz, 1H), 6.48 (s, 1H), 5.17 (d, $J = 12.2$ Hz, 2H) 3.28, (m, 1H), 2.39 (s, 3H), 2.03 (s, 3H), 1.48 (m, 2H), 1.05, (d, $J = 6.8$ Hz, 3H), 0.74 (t, $J = 7.3$ Hz, 3H); ^{13}C NMR (150 MHz, DMSO- d_6): δ 162.9, 162.3, 161.8, 161.7, 152.9, 144.6, 142.7, 140.9, 136.2, 132.4, 129.8, 115.3, 115.3, 113.6, 113.5, 108.1, 103.8, 68.9, 32.2, 29.8, 21.5, 20.6, 11.9, 9.1. HRESI(+)MS m/z 437.1756 $[\text{M} + \text{H}]^+$ (calculated for $\text{C}_{26}\text{H}_{26}\text{FO}_5^+$, 437.1758).

Biological screening

Purified metabolites were dissolved in DMSO to provide stock solutions (10 000 $\mu\text{g mL}^{-1}$ or 1000 $\mu\text{g mL}^{-1}$ depending on the amount of material available). An aliquot of each stock solution was transferred to the first lane of Rows B to G in a 96-well microtitre plate and two-fold serially diluted with DMSO across the 12 lanes of the plate to provide a 2048-fold concentration gradient. Bioassay medium was added to an

aliquot of each test solution to provide a 100-fold dilution into the final bioassay, thus yielding a test range of 100 to 0.05 $\mu\text{g mL}^{-1}$ in 1% DMSO. Row A contained no test compound (as a reference for no inhibition) and Row H was uninoculated (as a reference for complete inhibition).

MIC determination and time-dependent inhibition assays. *B. subtilis* (ATCC 6633), five *S. aureus* (ATCC12600, ATCC 25923, ATCC 33592, ATCC 49775 and USA300), two *E. faecium* (ATCC 19434 and E734), two *P. aeruginosa* (PAO1 and ATCC 27853) and three *E. coli* (ATCC 25322, ATCC 25922 and ATCC 35218) strains were used as indicative species for antibacterial activity. A bacterial suspension (50 mL in 250 mL flask) was prepared in nutrient media by cultivation at 28 °C for 24 h with shaking at 250 rpm. The suspension was diluted to an absorbance of 0.01 absorbance units per mL, and 10 μL aliquots were added to the wells of a 96-well microtitre plate containing the test compounds dispersed in nutrient broth (Amyl) with resazurin (12.5 $\mu\text{g mL}^{-1}$). The plates were incubated at 28 °C for 48 h, during which time the control wells with no test compound changed colour from a blue to light pink colour. MIC end points were determined visually. The absorbance was measured using Spectromax plate reader (Molecular Devices) at 605 nm and the IC_{50} values determined graphically. Our preliminary testing clearly showed **7d** and **7g** exhibited potent activity against the selected *S. aureus* strains. Therefore, these two compounds were subjected to MIC testing against an expanded panel of 20 clinical MRSA isolates plus 3 ATCC *S. aureus* strains in a standard plate microdilution MIC assay, using the Clinical Laboratory Standards Institute guidelines (CLSI 2017),³³ essentially as described previously.^{6,34} The time- and concentration-dependent activities of **7d** and **7g** against two *S. aureus* ATCC strains were also determined in a kinetics assay by optical density ($A_{600\text{ nm}}$) measurements on a Cytation 5 Multimode reader (BioTek).

Antifungal assay. The yeasts *C. albicans* (ATCC 10231) and *S. cerevisiae* (ATCC 9763) were used as indicative species for antifungal activity. A yeast suspension (50 mL in 250 mL flask) was prepared in 1% malt extract broth by cultivation for 24 h at 250 rpm, 24 °C. The suspension was diluted to an absorbance of 0.005 and 0.03 absorbance units per mL for *C. albicans* and *S. cerevisiae*, respectively. Aliquots (20 μL and 30 μL) of *C. albicans* and *S. cerevisiae*, respectively were applied to the wells of a 96-well microtitre plate, which contained the test compounds dispersed in malt extract agar containing bromocresol green (50 $\mu\text{g mL}^{-1}$). The plates were incubated at 24 °C for 48 h during which time the control wells containing no test compound change colour from a blue to yellow colour. MIC end points were determined visually. The absorbance was measured using Spectromax plate reader (Molecular Devices) at 620 nm and the IC_{50} determined graphically.

Cytotoxicity assay. NS-1 (ATCC TIB-18) mouse myeloma cells were inoculated in 96-well microtitre plates (190 μL) at 50 000 cells per mL in DMEM (Dulbecco's Modified Eagle Medium + 10% fetal bovine serum (FBS) + 1% penicillin/streptomycin (10 000 U mL^{-1} /10 000 $\mu\text{g mL}^{-1}$, Life Technologies Cat. no. 15140122), together with resazurin (250 $\mu\text{g mL}^{-1}$; 10 μL) and incubated in 37 °C (5% CO_2) incubator. The plates were incu-

bated for 72 h during which time the control wells containing no test compound changed colour from a blue to pink colour. The absorbance of each well was measured at 605 nm using a Spectromax plate reader (Molecular Devices).

Haemolysis and real-time *in vitro* cytotoxicity assays. Haemolysis assays for **7d** and **7g** were performed using fresh donor human red blood cells (RBCs), essentially as described previously.^{6,34} The toxicity profiles of the 2 compounds were also evaluated by measuring viability of HEK293 kidney and Hep G2 liver cell lines over a 20 h period in the presence of two-fold increasing concentrations of the compounds (2 $\mu\text{g mL}^{-1}$ –64 $\mu\text{g mL}^{-1}$) on a Cytation 5 Cell Imaging Multi-Mode Reader (BioTek) using the RealTime-Glo™ MT Cell Viability Assay reagent (Promega), as described previously.³⁴

Conflicts of interest

There are no conflicts to declare.

Acknowledgements

HRMS data were acquired by the Australian Proteome Analysis Facility, supported under the Australian Government's National Collaborative Research Infrastructure Strategy (NCRIS). This research was funded, in part, by the Australian Research Council (FT130100142 to AMP), the Cooperative Research Centres Projects scheme (CRCPFIVE000119) and Macquarie University (MQRTP scholarship to MTM).

Notes and references

- 1 M. Bassetti, A. Carnelutti, N. Castaldo and M. Peghin, *Expert Opin. Pharmacother.*, 2019, **20**, 2317–2334.
- 2 S. Purrello, J. Garau, E. Giamarellos, T. Mazzei, F. Pea, A. Soriano and S. Stefani, *J. Glob. Antimicrob. Resist.*, 2016, **7**, 178–186.
- 3 S. Stefani, F. Campanile, M. Santagati, M. L. Mezzatesta, V. Cafiso and G. Pacini, *Int. J. Antimicrob. Agents*, 2015, **46**, 278–289.
- 4 R. A. Seaton, F. Menichetti, G. Dalekos, A. Beiras-Fernandez, F. Nacinovich, R. Pathan and K. Hamed, *Adv. Ther.*, 2015, **32**, 1192–1205.
- 5 U. Theuretzbacher, K. Bush, S. Harbarth, M. Paul, J. H. Rex, E. Tacconelli and G. E. Thwaites, *Nat. Rev. Microbiol.*, 2020, **18**, 286–298.
- 6 L. L. Ling, T. Schneider, A. J. Peoples, A. L. Spoering, I. Engels, B. P. Conlon, A. Mueller, T. F. Schäberle, D. E. Hughes and S. Epstein, *Nature*, 2015, **517**, 455–459.
- 7 D. Nichols, N. Cahoon, E. Trakhtenberg, L. Pham, A. Mehta, A. Belanger, T. Kanigan, K. Lewis and S. Epstein, *Appl. Environ. Microbiol.*, 2010, **76**, 2445–2450.
- 8 C. L. Gilchrist, H. J. Lacey, D. Vuong, J. I. Pitt, L. Lange, E. Lacey, B. Pilgaard, Y. Chooi and A. M. Piggott, *Fungal Genet. Biol.*, 2020, **143**, 103435.

- 9 H. Li, C. L. Gilchrist, C. Phan, H. J. Lacey, D. Vuong, S. A. Moggach, E. Lacey, A. M. Piggott and Y. Chooi, *J. Am. Chem. Soc.*, 2020, **142**, 7145–7152.
- 10 H. J. Lacey, C. L. Gilchrist, A. Crombie, J. A. Kalaitzis, D. Vuong, P. J. Rutledge, P. Turner, J. I. Pitt, E. Lacey and Y. Chooi, *Beilstein J. Org. Chem.*, 2019, **15**, 2631–2643.
- 11 H. Li, C. L. Gilchrist, H. J. Lacey, A. Crombie, D. Vuong, J. I. Pitt, E. Lacey, Y. Chooi and A. M. Piggott, *Org. Lett.*, 2019, **21**, 1287–1291.
- 12 N. K. Chaudhary, J. I. Pitt, E. Lacey, A. Crombie, D. Vuong, A. M. Piggott and P. Karuso, *J. Nat. Prod.*, 2018, **81**, 1517–1526.
- 13 J. I. Pitt, L. Lange, A. E. Lacey, D. Vuong, D. J. Midgley, P. Greenfield, M. I. Bradbury, E. Lacey, P. K. Busk, B. Pilgaard, Y. Chooi and A. M. Piggott, *PLoS One*, 2017, **12**, e0170254.
- 14 H. J. Lacey, D. Vuong, J. I. Pitt, E. Lacey and A. M. Piggott, *Aust. J. Chem.*, 2016, **69**, 152–160.
- 15 K. Ochi and T. Hosaka, *Appl. Microbiol. Biotechnol.*, 2013, **97**, 87–98.
- 16 L. Foulston, *Curr. Opin. Microbiol.*, 2019, **51**, 1–8.
- 17 T. A. Wencewicz, *Bioorg. Med. Chem.*, 2016, **24**, 6227–6252.
- 18 R. B. Fugitt and R. W. Luckenbaugh, *U.S. Patent*, 4128654, 1978.
- 19 M. Debono, M. Barnhart, C. Carrell, J. Hoffmann, J. Occolowitz, B. Abbott, D. Fukuda, R. Hamill, K. Biemann and W. Herlihy, *J. Antibiot.*, 1987, **40**, 761–777.
- 20 F. Kavanagh, A. Hervey and W. J. Robbins, *Proc. Natl. Acad. Sci. U. S. A.*, 1951, **37**, 570.
- 21 M. T. Morshed, D. Vuong, A. Crombie, A. E. Lacey, P. Karuso, E. Lacey and A. M. Piggott, *Org. Biomol. Chem.*, 2018, **16**, 3038–3051.
- 22 J. M. Kurung, *Science*, 1945, **102**, 11–12.
- 23 F. Dean, A. Robertson, J. C. Roberts and K. Raper, *Nature*, 1953, **172**, 344–344.
- 24 Y. Zhang, J. Mu, Y. Feng, L. Wen and J. Han, *Nat. Prod. Res.*, 2014, **28**, 503–506.
- 25 M. Prein and W. Adam, *Angew. Chem., Int. Ed. Engl.*, 1996, **35**, 477–494.
- 26 E. L. Clennan, *Tetrahedron*, 2000, **47**, 9151–9179.
- 27 S. Sureram, S. Wiyakrutta, N. Ngamrojanavanich, C. Mahidol, S. Ruchirawat and P. Kittakoop, *Planta Med.*, 2012, **78**, 582–588.
- 28 P. Phainuphong, V. Rukachaisirikul, S. Phongpaichit, J. Sakayaroj, P. Kanjanasirirat, S. Borwornpinyo, N. Akrimajirachote, C. Yimnual and C. Muanprasat, *Tetrahedron*, 2018, **74**, 5691–5699.
- 29 M. Isaka, A. Yangchum, S. Supothina, S. Veeranondha, S. Komwijit and S. Phongpaichit, *J. Antibiot.*, 2019, **72**, 181–184.
- 30 B. Emsen, A. Aslan, B. Togar and H. Turkez, *Pharm. Biol.*, 2016, **54**, 1748–1762.
- 31 I. L. Lauinger, L. Vivas, R. Perozzo, C. Stairiker, A. Tarun, M. Zloh, X. Zhang, H. Xu, P. J. Tonge and S. G. Franzblau, *J. Nat. Prod.*, 2013, **76**, 1064–1070.
- 32 A. Cimmino, P. L. Nimis, M. Masi, L. De Gara, W. A. van Otterlo, R. Kiss, A. Evidente and F. Lefranc, *Phytochem. Rev.*, 2019, **18**, 1–36.
- 33 Clinical and Laboratory Standards Institute, *Performance standards for antimicrobial susceptibility testing*, Clinical and Laboratory Standards Institute, Wayne, PA, 2017.
- 34 A. D. Ogunniyi, M. Khazandi, A. J. Stevens, S. K. Sims, S. W. Page, S. Garg, H. Venter, A. Powell, K. White and K. R. Petrovski, *PLoS One*, 2017, **12**, e0183457.



Article

Repurposing of the Fasciolicide Triclabendazole to Treat Infections Caused by *Staphylococcus* spp. and Vancomycin-Resistant Enterococci

Hongfei Pi ¹, Abiodun D. Ogunniyi ¹, Bhumi Savaliya ¹, Hang Thi Nguyen ^{1,2}, Stephen W. Page ³, Ernest Lacey ⁴, Henrietta Venter ⁵ and Darren J. Trott ^{1,*}

- ¹ Australian Centre for Antimicrobial Resistance Ecology, Roseworthy Campus, School of Animal and Veterinary Sciences, The University of Adelaide, Roseworthy, SA 5371, Australia; hongfei.pi@adelaide.edu.au (H.P.); david.ogunniyi@adelaide.edu.au (A.D.O.); bhumi.savaliya@adelaide.edu.au (B.S.); hang.t.nguyen@adelaide.edu.au (H.T.N.)
- ² Department of Pharmacology, Toxicology, Internal Medicine and Diagnostics, Faculty of Veterinary Medicine, Vietnam National University of Agriculture, Hanoi 100000, Vietnam
- ³ Luoda Pharma Pty Ltd., Caringbah, NSW 2229, Australia; swp@advet.com.au
- ⁴ Microbial Screening Technologies Pty Ltd., Smithfield, NSW 2164, Australia; elacey@microbialscreening.com
- ⁵ Health and Biomedical Innovation, Clinical and health Sciences, University of South Australia, Adelaide, SA 5000, Australia; rietie.venter@unisa.edu.au
- * Correspondence: darren.trott@adelaide.edu.au



Citation: Pi, H.; Ogunniyi, A.D.; Savaliya, B.; Nguyen, H.T.; Page, S.W.; Lacey, E.; Venter, H.; Trott, D.J. Repurposing of the Fasciolicide Triclabendazole to Treat Infections Caused by *Staphylococcus* spp. and Vancomycin-Resistant Enterococci. *Microorganisms* **2021**, *9*, 1697. <https://doi.org/10.3390/microorganisms9081697>

Academic Editor: Simon Swift

Received: 30 June 2021

Accepted: 3 August 2021

Published: 10 August 2021

Publisher's Note: MDPI stays neutral with regard to jurisdictional claims in published maps and institutional affiliations.



Copyright: © 2021 by the authors. Licensee MDPI, Basel, Switzerland. This article is an open access article distributed under the terms and conditions of the Creative Commons Attribution (CC BY) license (<https://creativecommons.org/licenses/by/4.0/>).

Abstract: One approach to combat the increasing incidence of multidrug-resistant (MDR) bacterial pathogens involves repurposing existing compounds with known safety and development pathways as new antibacterial classes with potentially novel mechanisms of action. Here, triclabendazole (TCBZ), a drug originally developed to treat *Fasciola hepatica* (liver fluke) in sheep and cattle, and later in humans, was evaluated as an antibacterial alone or in combination with sub-inhibitory concentrations of polymyxin B (PMB) against clinical isolates and reference strains of key Gram-positive and Gram-negative bacteria. We show for the first time that in vitro, TCBZ selectively kills methicillin-sensitive and methicillin-resistant *Staphylococcus aureus* and *Staphylococcus pseudintermedius* at a minimum inhibitory concentration (MIC) range of 2–4 µg/mL, and vancomycin-resistant enterococci at a MIC range of 4–8 µg/mL. TCBZ also inhibited key Gram-negative bacteria in the presence of sub-inhibitory concentrations of PMB, returning MIC₉₀ values of 1 µg/mL for *Escherichia coli*, 8 µg/mL for *Klebsiella pneumoniae*, 2 µg/mL for *Acinetobacter baumannii* and 4 µg/mL for *Pseudomonas aeruginosa*. Interestingly, TCBZ was found to be bacteriostatic against intracellular *S. aureus* but bactericidal against intracellular *S. pseudintermedius*. Additionally, TCBZ's favourable pharmacokinetic (PK) and pharmacodynamic (PD) profile was further explored by in vivo safety and efficacy studies using a bioluminescent mouse model of *S. aureus* sepsis. We show that repeated four-hourly oral treatment of mice with 50 mg/kg TCBZ after systemic *S. aureus* challenge resulted in a significant reduction in *S. aureus* populations in the blood to 18 h post-infection (compared to untreated mice) but did not clear the bacterial infection from the bloodstream, consistent with in vivo bacteriostatic activity. These results indicate that additional pharmaceutical development of TCBZ may enhance its PK/PD, allowing it to be an appropriate candidate for the treatment of serious MDR bacterial pathogens.

Keywords: multidrug resistance; triclabendazole; polymyxin B; bacterial pathogens; bioluminescence; sepsis

1. Introduction

The increasing public health threat posed by antimicrobial resistance (AMR) and the rise in the incidence of multidrug-resistant (MDR) bacterial pathogens has stimulated novel research strategies to combat MDR infections. However, the discovery, development and

marketing approval process for new drugs is very challenging and can cost over 2.8 billion USD and take over 10 years to reach the market [1]. There is a high risk of failure (82.7%) in the preclinical stage alone, which may take up to 6 years [2–4].

Repurposing currently registered drugs for new indications is one of the alternative approaches to overcoming these challenges whilst adhering to the principles of antimicrobial stewardship [5–8]. Using existing drugs with known toxicological and pharmacokinetic profiles and an acceptable level of safety and tolerability is a much cheaper and efficient option than developing entirely new antibiotics [9–11] and has become a more common strategy in recent years [4,12–14]. One such agent is triclabendazole (TCBZ), a benzimidazole anthelmintic agent, with narrow spectrum activity against trematodes in the genus *Fasciola*, approved for use in animals (especially cattle, sheep and goats) [15–17] and humans [18–20]. TCBZ has previously been identified as having potential antibacterial activity against Gram-positive bacteria when it was included in a mass screening of Food and Drug Administration (FDA)-approved non-antibacterial drugs [21], and has more recently been shown to have anticlostridial activity [22].

The mechanism by which TCBZ exhibits its effect against *Fasciola* species is not fully elucidated. Both in vitro and in vivo studies suggest that TCBZ and its metabolites (sulfoxide and sulfone) are absorbed across the tegument of immature and mature worms, leading to a decrease in the resting membrane potential, inhibition of tubulin function and inhibition of protein and enzyme synthesis. These metabolic disturbances are associated with inhibition of motility, disruption of cell wall ultrastructure and inhibition of spermatogenesis and vitelline cells [18].

Given indications that TCBZ has potential as an antibacterial agent, to our knowledge, there have been no published studies that directly demonstrate this potential in vivo. A preliminary evaluation of in vitro efficacy of a variety of TCBZ derivatives was therefore carried out against representative Gram-positive (methicillin-resistant and methicillin-susceptible *Staphylococcus* spp., vancomycin-resistant *Enterococcus* spp. and *Streptococcus pneumoniae*) and Gram-negative organisms (*Escherichia coli*, *Klebsiella pneumoniae*, *Pseudomonas aeruginosa* and *Acinetobacter baumannii*), including in the presence of polymyxin B (PMB). PMB was used as it is a well-known Gram-negative outer membrane permeabilizer [23,24] and because we have successfully used it for this purpose in previous published work [25]. From the collection of TCBZ and metabolites, TCBZ was chosen as the most active, and further antibacterial activity was explored in vitro. Efficacy testing using a mouse bioluminescent *S. aureus* infection model was also undertaken to better investigate its antibacterial properties in vivo.

2. Materials and Methods

2.1. Antimicrobial Agents

TCBZ and four derivatives (TCBZ-SH, TCBZ-SO, TCBZ-SO₂ and TCBZ-OH; Figure 1) were prepared by conjugation of 5-chloro-2-nitroaniline [26] with 2,3-dichlorophenol [27], followed by reduction to the diamine using sodium dithionite and cyclization, which gave TCBZ-SH [28]. TCBZ-SO and TCBZ-SO₂ were prepared by oxidation with hydrogen peroxide in a mixture of acetic acid and chloroform at a ratio of 4:1, while TCBZ-OH was prepared by reaction of the diamine with potassium cyanate [29]. These analogs were stored in a sealed sample container out of direct light at 4 °C in the Microbiology Laboratory at Clinical and Health Sciences, City East Campus, University of South Australia, Australia.

PMB was prepared as a stock solution of 25.6 mg/mL in DMSO, stored in 1 mL aliquots at –80 °C and defrosted immediately prior to use. TCBZ as Fasinex[®] 240 Oral Flukicide for Cattle (240 g/L) was purchased from Elanco Australia Pty Ltd (Macquarie Park, NSW, Australia) and stored at room temperature in the original container, tightly closed in a cool dry place. Fresh stock solutions of TCBZ (50 mg/kg and 10 mg/kg) were prepared as oral treatments and diluted in phosphate-buffered saline (PBS) with vigorous mixing. Moxifloxacin hydrochloride was purchased from Bayer Ltd. as Avelox 400 mg in

a 250 mL solution (equivalent to 1.6 mg/mL moxifloxacin hydrochloride) and stored at room temperature.

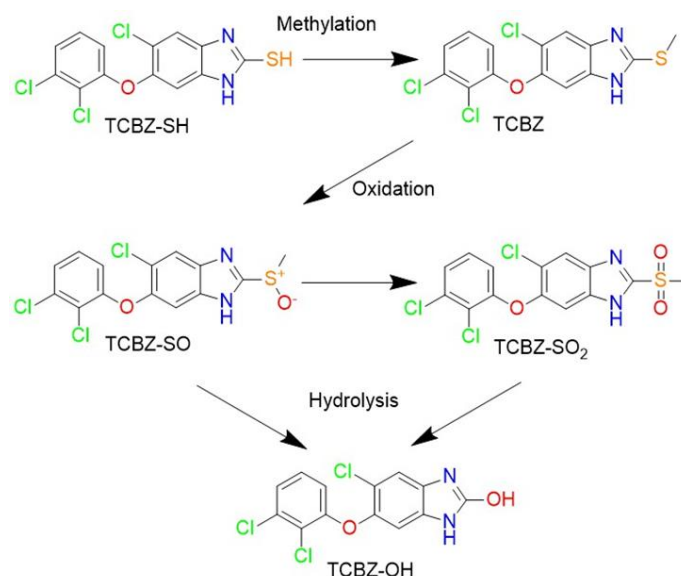


Figure 1. TCBZ and related synthetic precursor, oxidation and hydrolytic analogs.

2.2. Bacterial Strains

A total of 138 bacterial isolates (55 Gram-positive and 83 Gram-negative) were collected from government, private and university diagnostic laboratories throughout Australia (Table S1). The Gram-positive bacterial collection included 4 vancomycin-resistant enterococci (VRE), 24 *S. aureus* isolates (including 21 methicillin-resistant *S. aureus* (MRSA)), 2 *S. pneumoniae*, 13 *S. pseudintermedius* (including 10 methicillin-resistant *S. pseudintermedius* (MRSP)), 3 coagulase-negative *Staphylococcus* spp. (CoNS) and 9 *Streptococcus* spp. isolates from cases of bovine mastitis. The Gram-negative bacteria collection included 21 *E. coli*, 20 *K. pneumoniae*, 18 *A. baumannii*, 20 *P. aeruginosa*, 2 *Neisseria meningitidis* and 2 *N. gonorrhoeae* isolates. All organisms were identified to species level using biochemical testing and Matrix-Assisted Laser Desorption/Ionization Time-of-Flight (MALDI-TOF) mass spectrometry (Microflex™ LT/SH BioTyper Bruker Daltonics, Leipzig, Germany) at the Australian Centre for Antimicrobial Resistance Ecology (ACARE), The University of Adelaide, Australia.

2.3. Minimum Inhibitory Concentration (MIC) Determination

Minimum inhibitory concentrations (MICs) were determined in round-bottom 96-well microtiter trays (Sarstedt 82.1582.001; Mawson Lakes, SA, Australia), using the modified broth microdilution method recommended by the Clinical and Laboratory Standards Institute [30]. Testing concentrations were as follows: TCBZ-256 to 0.25 µg/mL; PMB-32 to 0.06 µg/mL. Cation-adjusted Mueller–Hinton broth (CAMHB; Becton Dickinson, Sparks, MD, USA) was used for MIC testing against all organisms except *S. pneumoniae* and other *Streptococcus* spp., for which CAMHB supplemented with 3% lysed horse blood and 5% horse serum was used. To test the effect of ultra-heat-treated (UHT) milk on the MICs of TCBZ against *Streptococcus* spp., CAMHB supplemented with 3% lysed horse blood and 10% UHT milk was used. To test the effect of pH on the MICs of TCBZ against *Streptococcus* spp., RPMI 1640 medium (Sigma-Aldrich, NSW, Australia) was used instead of CAMHB.

Serial two-fold dilutions of the compounds were performed in 100% DMSO, with 1 µL added to each well. In selected experiments, the MICs for ampicillin, daptomycin, gentamicin and apramycin against each isolate were determined as an internal quality control. The MICs against all isolates were determined by visual reading and using an

EnSpire Multimode Plate Reader 2300 (PerkinElmer) at $A_{600\text{ nm}}$. MIC₅₀, MIC₉₀ and MIC ranges for TCBZ, PMB or combinations were then determined [31].

2.4. Synergy Testing by Checkerboard Microdilution and Dose Reduction Analysis

The potential activity of TCBZ against clinical and ATCC Gram-negative pathogens was determined in the presence or absence of 0.25–128 µg/mL PMB in a modified standard checkerboard assay as described previously [32,33]. Briefly, antimicrobial stock solutions were prepared at a concentration of 12.8 mg/mL in DMSO for TCBZ and 12.8 mg/mL in Milli-Q water for PMB. Then, a two-fold serial dilution of each antimicrobial stock solution was prepared in its appropriate solvent from wells 12 to 3 (from 12.8 to 0.25 mg/mL) and 1 µL of each concentration was added to each well in the challenge plate using an electronic multichannel pipette followed by 89 µL of the LB broth. Thereafter, 10 µL of bacterial suspension of approx. 2×10^6 colony-forming units per milliliter (CFU/mL) was added to each well of the plate, which was subsequently incubated at 37 °C for 24 h.

The fractional inhibitory concentration index (FICI) described the results of combination and was calculated as follows: FICI of combination = FIC A + FIC B. Where FIC A is the MIC of TCBZ in the combination/MIC of TCBZ alone, FIC B is the MIC of PMB in the combination/MIC of PMB alone [25,33]. The results indicate synergism when the corresponding FICI ≤ 0.5 , additivity when $0.5 < \text{FICI} \leq 1$, indifference when $1 < \text{FICI} \leq 4$ and antagonism when the FICI > 4 . In this study, the FICI for TCBZ and PMB against Gram-negative bacteria was calculated to be zero (e.g., $1 \div > 256 = 0$) where they did not show any antibacterial activity alone against Gram-negative bacteria at the highest concentration (256 µg/mL).

The dose-reduction index (DRI) shows the difference between the effective doses in combination in comparison to its individual dose. DRI was calculated as follows: DRI = MIC of drug alone/MIC of drug in combination. Given that TCBZ did not show any antimicrobial activity against the majority of Gram-negative bacteria, the highest concentration of each compound tested against each isolate was used as its MIC alone for calculating the DRI (e.g., MIC of TCBZ alone against *E. coli* 10763 was > 256 µg/mL and its MIC in combination with PMB was 1 µg/mL; DRI = $256/1$). DRI is significant clinically when the dose reduction is associated with a toxicity reduction without changing efficacy [34]. Commonly, a DRI higher than 1 is considered beneficial.

2.5. Minimum Bactericidal Concentration (MBC) Determination

The minimum bactericidal concentration (MBC) for TCBZ against Gram-positive bacteria alone or against Gram-negative bacteria (in combination with PMB) were determined as follows. Briefly, 10 µL aliquots from each duplicate well from the MIC assays (starting from the MIC for each compound) were inoculated onto a sheep blood agar (SBA) plate and incubated at 37 °C. Plates were examined at 24 and 48 h and the MBC was recorded as the lowest concentration of each test compound at which a 99.9% colony count reduction was observed on the plate [34].

2.6. Time-Dependent Killing Assays

Time-kill assays were performed (in duplicate) for TCBZ against Gram-positive bacteria (MRSP-1, *S. aureus* ATCC 29213 and VRE 35C) and for TCBZ in the presence of PMB against Gram-negative bacteria (*E. coli* ATCC 25922) as described previously [34]. Briefly, a few colonies of each strain from overnight SBA plates were emulsified in normal saline and adjusted to $A_{600\text{ nm}} = 0.10$ (equivalent to approx. 5×10^7 CFU per mL) and the bacterial suspensions were further diluted 1:20 in saline. TCBZ and PMB were serially diluted in 100% DMSO or Milli-Q water at 100 × the final desired concentration and a 100 µL aliquot of each appropriate concentration was added to each 10 mL preparation. TCBZ and PMB solutions were prepared in 10 mL volumes at 1 × MIC, 2 × MIC and 4 × MIC concentrations in LB broth. After adding inoculum dose to each tube, duplicate cultures were incubated at 37 °C, with samples withdrawn at 0, 0.5, 1, 2, 4, 6, 8 and 24 h, serially

diluted 10-fold and plated on SBA overnight at 37 °C for bacterial enumeration. According to CLSI, an antimicrobial agent is considered bactericidal if it causes a $\geq 3 \times \log_{10}$ (99.9%) reduction in colony-forming units per milliliter (CFU/mL) after 18–24 h of incubation, and the combination is considered synergistic when it causes a $\geq 2 \times \log_{10}$ reduction in CFU/mL.

2.7. Multi-Sub-Culture Resistance Selection

Multi-sub-culture resistance selection studies (21 days sequential culturing of *S. aureus* ATCC 29213) were undertaken using enrofloxacin as a control antibiotic, as described previously [35]. Each day an MIC test concentration range of antibiotics from 0.25 to 8 µg/mL on 48 well plates was used. On the first day, the same method described for MIC microdilution was used to determine the MIC and the plate was incubated at 37 °C for 24 h. Sub-cultures were performed at 24 h intervals for up to 21 days by transferring 20 µL aliquot of culture, containing 5×10^5 CFU, from the well nearest the MIC (usually 1 to 2 dilutions below) which had the same turbidity as antibiotic-free controls. During the sub-culture, the resistant mutants that emerged were stored at –80 °C for subsequent analysis.

2.8. Intracellular MIC Testing

The mouse J774A.1 macrophage cell line was maintained in DMEM (Dulbecco's Modified Eagle Medium) with heat-inactivated fetal bovine serum in cell culture flasks (75 cm²), as described previously [36]. Cells were allowed to grow to 90% confluency and were then passaged and transferred to a 48-well cell culture plate. Cells were then allowed to grow up to a concentration of $5\text{--}8 \times 10^5$ cells/mL.

S. aureus strain ATCC 29213 was sub-cultured on SBA and incubated at 37 °C for 18–20 h. A number of isolated colonies were then resuspended in RPMI medium, adjusted to 0.5 McFarland standard and opsonized in 10% freshly collected human serum (stored at –80 °C until use) at 37 °C for 30 min. Cell culture medium was replaced with the opsonized bacterial suspension to allow phagocytosis at 37 °C for 1 h at a macrophage:bacterium ratio of 1:2. Macrophage cells were then washed twice in DMEM to remove extracellular bacteria and exposed to TCBZ at concentrations ranging from 0.5–32 µg/mL, while cells were also exposed to monensin at concentrations ranging from 0.25–16 µg/mL as a control. At this stage, 50 µg/mL gentamicin was added to kill any remaining extracellular bacteria and the infected macrophage cells were incubated for a further 20–24 h. After incubation, infected macrophage cells were washed with PBS three times to remove any carryover antibiotics and then collected by scraping. Two protocols were then undertaken in parallel: (i) after 1:10, 1:100 and 1:1000 dilutions, 10 µL aliquots of the harvested cells were spot-plated onto SBA for determination of CFU. Plates were then incubated at 37 °C for 24 h. The colonies were counted the next day and CFUs were determined. (ii) The protein concentration was determined as per manufacturer's instructions with bovine serum albumin as a standard (DC protein assay kit, Bio-Rad Catalog No 500-0112). All results were then calculated as CFU/mg of cell protein and these values were plotted using 'R' software (version: 3.6.1).

2.9. Haemolysis Assay

This was performed using fresh human red blood cells (RBCs) from donors as described previously [25,37]. Fresh RBCs were washed in PBS three times at $500 \times g$ for 5 min, and then resuspended 1% (*w/v*) in PBS. Serial two-fold dilutions of each compound (2 µL each) were added into the respective wells, in quadruplicates, in a round-bottom 96-well microtiter tray (Sarstedt 82.1582.001; Mawson Lakes, SA, Australia), starting at 128 µg/mL for each compound using ampicillin as a control. Thereafter, 198 µL of the 1% RBC solution was added to each well, and the mixture was incubated for 1 h at 37 °C with shaking at 100 rpm. Quadruplicate wells containing either 1% Triton X100 or PBS only served as controls. After incubation, the trays were centrifuged at $1000 \times g$ for 3 min and 100 µL of supernatant from each well was transferred into a new 96-well tray. Absorbance was

measured at $A_{450\text{nm}}$ on a Cytation 5 Cell Imaging Multi-Mode Reader (BioTek, Millennium Science Pty Ltd., Mulgrave, VIC, Australia) and plotted against each dilution. Hemolytic titer was determined as the reciprocal of the dilution at which 50% of erythrocytes were lysed at $A_{450\text{nm}}$.

2.10. *In Vitro* Cytotoxicity Assays

We assayed TCBZ for in vitro cytotoxicity using a panel of adherent mammalian cell lines hEK293 (human embryonic kidney cell line), Detroit 562 (human nasopharyngeal carcinoma epithelial cell line) and MCF-7 (human mammary gland adenocarcinoma cell line), as described previously [35]. Assays were performed in duplicates in flat-bottom black 96-well tissue culture trays (Costar) seeded with $\sim 1 \times 10^4$ cells per well. After 24 h incubation, media was removed, washed once with medium without antibiotics and fresh medium supplemented with 10% (vol/vol) FBS was added. Viability of each cell line in the presence of each compound was assessed starting at 64 $\mu\text{g}/\text{mL}$ (for hEK293 and Detroit 562 cell lines) or starting at 16 $\mu\text{g}/\text{mL}$ (for MCF-7) at 1 h intervals for 20 h at 37 °C and in 5% CO_2 on a Cytation 5 Cell Imaging Multi-Mode Reader (BioTek, Millennium Science Pty Ltd., Mulgrave, VIC, Australia) using the RealTime-Glo™ MT Cell Viability Assay reagent (Promega, Madison, WI, USA).

2.11. Ethics Statements

For TCBZ safety and efficacy testing experiments, outbred 5- to 6-week-old male CD1 (Swiss) mice (weighing between 25 g to 32 g) obtained from the Laboratory Animal Services breeding facility of the University of Adelaide were used. Mice had access to food and water ad libitum throughout the experiments. The Animal Ethics Committee of The University of Adelaide (approval number S-2015-151) reviewed and approved all animal experiments. The studies were conducted in compliance with the Australian Code of Practice for the Care and Use of Animals for Scientific Purposes (8th Edition 2013) and the South Australian Animal Welfare Act 1985.

2.12. Oral Safety Assessment of TCBZ following Parenteral Administration

Mice were placed in individually ventilated cages in 3 treatment groups as follows: (i) 10 mg/kg of TCBZ ($n = 3$); (ii) 50 mg/kg of TCBZ ($n = 3$); (iii) PBS ($n = 3$); and (iv) 1.6 mg/mL of moxifloxacin ($n = 3$). Mice in group (i) were treated with a total of 25 μL of 10 mg/kg of TCBZ. Mice in group (ii) were treated with 125 μL of 50 mg/kg of TCBZ, mice in group (iii) were treated with 25 μL of PBS while mice in group (iv) were treated with a total of 94 μL of moxifloxacin. All mice were treated three times per day for 5 days. At the conclusion of the experiment (5 days from the start), mice were humanely killed and sections of tissues (lung, heart, liver, spleen, kidney and small intestinal) were collected and subjected to histopathological analysis.

2.13. Histopathological Examination

Mouse tissues (including lung, heart, liver, spleen, kidney and small intestinal) collected from the oral safety challenge were fixed in 10% neutral-buffered formalin and processed routinely. The specimens were embedded in paraffin blocks and sections of 4 μm thickness were cut using a microtome. Hematoxylin and Eosin staining of the sections were performed and the slides were observed and recorded under light microscopy.

2.14. Oral Efficacy Testing of TCBZ following Systemic Challenge of Mice with Bioluminescent Gram-Positive Bacteria

For oral efficacy testing experiments against *S. aureus*, bioluminescent ATCC12600 strain (Xen29, PerkinElmer) was used as described previously [25,38], but with some modifications. Bacteria were grown in LB broth at 37 °C to $A_{600\text{nm}}$ of 0.5 (equivalent to approx. 1.5×10^8 CFU/mL). Three groups of mice ($n = 6$ mice per group) were challenged IP with approx. 2.5×10^7 CFU (first experiment) or approx. 1×10^7 CFU (second experi-

ment) of Xen29 in 200 µL PBS containing 3% hog gastric mucin type III (Sigma Aldrich, NSW, Australia). At 2 h post-infection, approx. 50 µL of blood was withdrawn from the submandibular plexus of all mice for bacterial enumeration after which they were subjected to bioluminescence imaging in both ventral and dorsal positions on the IVIS Lumina XRMS Series III system (Caliper LifeSciences, hopkinton, MA, USA). Immediately thereafter, group 1 mice received 25 µL of PBS orally, group 2 mice received 125 µL of TCBZ at 50 mg/kg orally and group 3 mice received 94 µL of moxifloxacin orally. At 6 h, 10 h, 18 h and at 72 h post-infection (or during humane killing of moribund mice), approx. 50 µL blood was again withdrawn, followed by bioluminescence imaging. After imaging at 6 h post-infection, a second dose of PBS/TCBZ/moxifloxacin was administered. Further treatments were given at 10 h, 18 h and 24 h post-infection. Mice were monitored frequently (every 4 h) for signs of distress throughout the experiment, and the clinical conditions were recorded on a clinical record sheet approved by The University of Adelaide Ethics Committee. Mice that had become moribund or showed any evidence of distress were humanely euthanized by cervical dislocation.

The first experiment showed a lack of efficacy for TCBZ post-24 h, which was partly due to the high bacterial challenge dose. Therefore, a repeat experiment using a lower bacterial dose (1×10^7 of Xen29) ($n = 6$ mice per group) was carried out as described above. In both experiments, signals were collected from a defined region of interest and total flux intensities (photons/s) were analyzed using Living Image Software 4.5. Differences in luminescence signals between control and drug-treated groups were compared by the Mann–Whitney U test (one-tailed).

3. Results

3.1. TCBZ Derivatives Demonstrate Antibacterial Activity

The potential of TCBZ as an antibacterial agent was initially examined by conducting MIC testing of five of its derivatives against two VRE isolates and two *S. aureus* isolates. The MIC determination showed that three of the five analogs possessed antimicrobial activity against the four Gram-positive isolates selected (Table 1).

Table 1. MIC values for TCBZ derivatives against 2 MRSA and 2 VRE isolates.

| Compound | Identity | MIC (µg/mL) | | | |
|----------------------|-------------------------------------|-------------|---------|-------------------|---------------|
| | | VRE 60FR | VRE 252 | ATCC 49775 (MSSA) | USA300 (MRSA) |
| TCBZ * | Triclabendazole, 2-methyl thio | 4 | 8 | 2 | 2 |
| TCBZ-SO * | Triclabendazole, 2-methylsulphoxide | 16 | 16 | 8 | 8 |
| TCBZ-SO ₂ | Triclabendazole, 2-methylsulphone | >256 | >256 | 8 | >256 |
| TCBZ-SH * | Triclabendazole, 2 thio | 16 | 8 | 2 | 4 |
| TCBZ-OH | Triclabendazole, 2-hydroxy | >256 | >256 | >256 | >256 |
| Ampicillin | Ampicillin | 0.125 | 0.5 | <0.125 | 64 |

MIC test was performed in duplicate. *, Compounds selected for further screening.

MICs were repeated with the parent compound (TCBZ) and its thiol (TCBZ-SH) and sulphoxide (TCBZ-SO) derivatives showing promising activity against three VRE, three MRSA and two *S. pneumoniae* isolates, essentially confirming the initial results (Table 2). Notably, only TCBZ showed antimicrobial activity against both *S. pneumoniae* isolates. Therefore, TCBZ was chosen as the most promising analog for further evaluation.

Table 2. MIC values for TCBZ, TCBZ-SO and TCBZ-SH against 3 VRE, 3 MRSA and 2 *S. pneumoniae* isolates.

| Bacterial Strain/Isolate | MIC ($\mu\text{g/mL}$) for: | | |
|----------------------------|-------------------------------|---------|---------|
| | TCBZ | TCBZ-SO | TCBZ-SH |
| VRE35C | 4 | 32 | 16 |
| VRE60FR | 8 | 32 | 16 |
| VRE252 | 4 | 16 | 16 |
| MRSA USA 300 | 2 | 8 | 2 |
| MSSA 49775 | 2 | 8 | 2 |
| MRSA 610 | 2 | 16 | 2 |
| <i>S. pneumoniae</i> A66.1 | 16 | >64 | >64 |
| <i>S. pneumoniae</i> D39 | 16 | >64 | >64 |

3.2. TCBZ Shows Antimicrobial Activity against an Expanded Range of *Staphylococcus* spp. and Vancomycin-Resistant Enterococci

Given the promising antibacterial activity of TCBZ in the initial screen, its spectrum of activity was further investigated against a range of clinical coagulase-positive *Staphylococcus* spp., including human MRSA ($n = 20$; Table 3 and Table S2) and canine MRSP ($n = 13$; Table S3) isolates. TCBZ inhibited the growth of all tested *S. aureus* and *S. pseudintermedius* including MRSA and MRSP isolates at concentrations ranging from 2–4 $\mu\text{g/mL}$. The MBC values of TCBZ against the *S. aureus* and *S. pseudintermedius* isolates were between 1–4 times the MIC values, confirming that TCBZ is bactericidal against coagulase-positive *Staphylococcus* spp. (Table S3). However, in the presence of UHT milk, TCBZ did not show any antimicrobial activity against *S. aureus* ATCC29213 at the highest concentration (64 $\mu\text{g/mL}$) tested.

Table 3. MIC values for TCBZ against 20 MRSA isolates.

| Compound | Concentration ($\mu\text{g/mL}$) | | | |
|------------|------------------------------------|-------------------|-------------------|------|
| | MIC range | MIC ₅₀ | MIC ₉₀ | MBC |
| TCBZ | 2–4 | 2 | 4 | 2–16 |
| Daptomycin | 0.25–1 | 0.5 | 0.5 | ND |

ND, not determined.

3.3. TCBZ Shows Limited Antimicrobial Activity against *Streptococcus* spp. Causing Bovine Mastitis

We initially obtained a MIC of 16 $\mu\text{g/mL}$ activity for TCBZ against two *S. pneumoniae* clinical isolates. Therefore, further evaluation of its activity against other streptococci causing bovine mastitis (*S. uberis*, *S. agalactiae* and *S. dysgalactiae*) was conducted. However, no antimicrobial activity was detected for these streptococci, except for a single isolate of *S. dysgalactiae* (MIC and MBC both 32 $\mu\text{g/mL}$). In addition, the effect of ultra-heat-treated (UHT) milk in CAMHB medium and pH (RPMI medium) on the MIC of TCBZ against the *S. uberis*, *S. agalactiae* and *S. dysgalactiae* isolates was also determined; however, no antimicrobial activity was detected.

3.4. TCBZ in Combination with PMB Demonstrates Synergistic Activity against a Range of Gram-Negative ESKAPE Pathogens

The antimicrobial activity of TCBZ in the presence of PMB was investigated against a range of clinical and reference human ESKAPE pathogens. These included *E. coli* strains ATCC 10763 and ATCC 25922, *P. aeruginosa* strain PAO1, *K. pneumoniae* strains ATCC 33495 and ATCC 4352, *A. baumannii* strains ATCC 19606 and ATCC 12457, *N. meningitidis* clinical isolates 423 and 424 as well as *N. gonorrhoeae* strains ATCC 16599 and ATCC 49226. The combination of TCBZ and PMB resulted in a synergistic interaction against all the isolates tested except for *N. meningitidis* and *N. gonorrhoeae* (Table 4).

Table 4. MIC ($\mu\text{g}/\text{mL}$) values for TCBZ, PMB and in combination against Gram-negative reference strains.

| Isolates | MIC ($\mu\text{g}/\text{mL}$) | | | Combination Effect (FICI) ^a | DRI ^b PMB: TCBZ |
|----------------------------------|---------------------------------|------|-------------|--|-------------------------------|
| | Single Drug | | Combination | | |
| | PMB | TCBZ | PMB: TCBZ | | |
| <i>E. coli</i> ATCC 10763 | 0.5 | >256 | 0.125:0.25 | Synergism (0.25) | 4:1024 |
| <i>E. coli</i> ATCC 25922 | 0.5 | >256 | 0.125:0.125 | Synergism (0.25) | 4:2048 |
| <i>P. aeruginosa</i> PAO1 | 0.5 | >256 | 0.125:2 | Synergism (0.25) | 4:128 |
| <i>K. pneumoniae</i> ATCC 33495 | 0.5 | >256 | 0.125:1 | Synergism (0.25) | 4:256 |
| <i>K. pneumoniae</i> ATCC 4352 | 0.5 | >256 | 0.125:1 | Synergism (0.25) | 4:256 |
| <i>A. baumannii</i> ATCC 19606 | 1 | >256 | 0.125:0.5 | Synergism (0.125) | 8:512 |
| <i>A. baumannii</i> NCIMB 12457 | 1 | >256 | 0.125:1 | Synergism (0.125) | 8:256 |
| <i>N. meningitidis</i> 423 | >256 | 32 | 4:16 | Additivity (0.516) | 64:2 |
| <i>N. meningitidis</i> 424 | >256 | 32 | 4:16 | Additivity (0.516) | 64:2 |
| <i>N. gonorrhoeae</i> ATCC 16599 | >256 | >256 | 4:32 | Additivity (0.516) | 64:8 |
| <i>N. gonorrhoeae</i> ATCC 49226 | >256 | >256 | 4:32 | Additivity (0.516) | 64:8 |

MIC, minimum inhibitory concentration. ^a FICI, fractional inhibitory concentration index: synergistic, $\text{FICI} \leq 0.5$; additive, $0.5 < \text{FICI} \leq 1$; indifferent, $1 < \text{FICI} \leq 4$; and antagonistic, $\text{FICI} > 4$. ^b DRI, dose-reduction index.

The antimicrobial activity of the TCBZ and PMB combination was tested against a larger collection of human ESKAPE pathogens (18 *K. pneumoniae* clinical isolates plus ATCC 33495 and ATCC 4352, 18 *E. coli* clinical isolates plus ATCC 10763 and ATCC 25922, 16 *A. baumannii* clinical isolates plus *A. baumannii* ATCC 19606 and NCIMB 12457 as well as 19 *P. aeruginosa* clinical isolates plus PAO1) (Table 5). The results reveal a synergistic or additive interaction of TCBZ and PMB against all Gram-negative isolates tested (reducing the MIC of TCBZ by 16- to 2048-fold against all Gram-negative species tested).

Table 5. MIC range, MIC₅₀ and MIC₉₀ values for TCBZ and PMB alone and in combination against 20 *E. coli*, 20 *K. pneumoniae*, 18 *A. baumannii* and 20 *P. aeruginosa* from humans.

| Isolates | Values | Antimicrobial Concentration ($\mu\text{g}/\text{mL}$) | | | | Combination Effect (FICI) ^a | DRI ^b | |
|----------------------------------|-------------------|---|------|-------------|---------|--|------------------|------|
| | | Single Drug | | Combination | | | PMB | TCBZ |
| | | PMB | TCBZ | PMB | TCBZ | | | |
| <i>E. coli</i> (n = 20) | MIC range | 0.125–1 | >256 | 0.06–0.125 | 0.25–2 | 2–8 | 128–2048 | |
| | MIC ₅₀ | 0.5 | >256 | 0.125 | 0.5 | 4 | 512 | |
| | MIC ₉₀ | 0.5 | >256 | 0.125 | 1 | 4 | 256 | |
| <i>K. pneumoniae</i> (n = 20) | MIC range | 0.125–1 | >256 | 0.06–0.5 | 0.5–16 | 2–8 | 16–512 | |
| | MIC ₅₀ | 0.5 | >256 | 0.25 | 4 | 2 | 64 | |
| | MIC ₉₀ | 1 | >256 | 0.5 | 8 | 2 | 32 | |
| <i>A. baumannii</i> (n = 18) | MIC range | 0.5–1 | >256 | 0.125–0.125 | 0.5–2 | 4–8 | 128–512 | |
| | MIC ₅₀ | 1 | >256 | 0.125 | 2 | 8 | 128 | |
| | MIC ₉₀ | 1 | >256 | 0.125 | 2 | 8 | 128 | |
| <i>P. aeruginosa</i> (n = 20) | MIC range | 0.25–1 | >256 | 0.06–0.25 | 0.125–4 | 2–4 | 64–2048 | |
| | MIC ₅₀ | 0.5 | >256 | 0.125 | 2 | 4 | 128 | |
| | MIC ₉₀ | 0.5 | >256 | 0.25 | 4 | 2 | 64 | |

MIC, minimum inhibitory concentration. ^a FICI, fractional inhibitory concentration index: synergistic, $\text{FICI} \leq 0.5$; additive, $0.5 < \text{FICI} \leq 1$; indifferent, $1 < \text{FICI} \leq 4$; and antagonistic, $\text{FICI} > 4$. ^b DRI, dose-reduction index.

3.5. TCBZ Kinetic Assays Confirm Bactericidal Activity

TCBZ was further investigated in kinetic assays to measure the time- and concentration-dependent activity against *S. aureus* Xen 29 (Figure 2A,B), *S. aureus* ATCC 29213 (Figure 2C,D), MRSA USA300 (Figure 2E,F), and MRSP-1 (Figure 2G,H), using norfloxacin or amikacin as a comparator. The results confirm the MBC results showing that TCBZ is bactericidal against *Staphylococcus* spp.

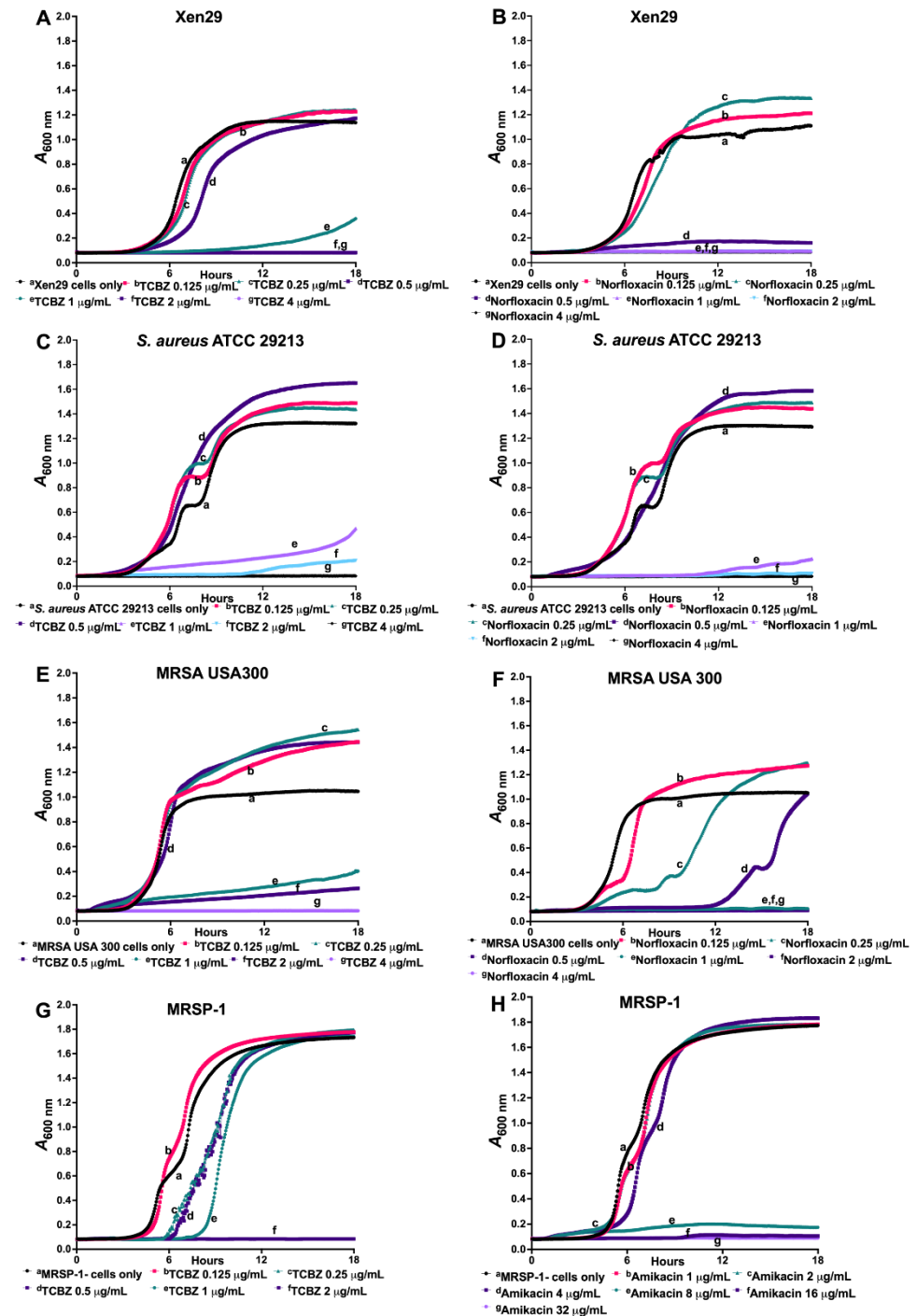


Figure 2. Kinetic assay showing time- and concentration-dependent inhibition of *S. aureus* Xen29 (A,B), *S. aureus* ATCC 29213 (C,D), MRSA USA300 (E,F) and MRSP-1 (G,H), using norfloxacin or amikacin as a comparator. The results show TCBZ is bactericidal against the four bacteria tested.

The synergistic activity of TCBZ in combination with PMB against Gram-negative bacteria was further evaluated in a time-kill assay using *E. coli* ATCC 25922. PMB/TCBZ at 0.25/0.25 $\mu\text{g}/\text{mL}$ and at 0.5/0.5 $\mu\text{g}/\text{mL}$ showed no antimicrobial activity while PMB/TCBZ at 1/1 $\mu\text{g}/\text{mL}$ reduced the CFU/mL by $6 \times \log_{10}$ by 4 h post-treatment and totally cleared the bacteria, which demonstrated that TCBZ was bactericidal in the combination against *E. coli* ATCC 25922 (Figure 3).

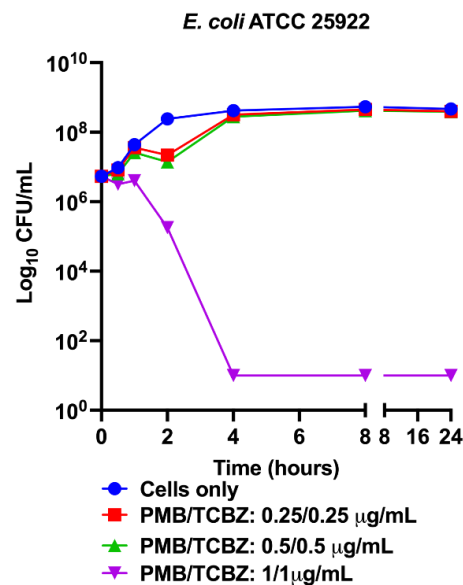


Figure 3. Time-kill curves of TCBZ in combination with PMB against *E. coli* ATCC 25922.

3.6. No TCBZ-Resistant Mutants Developed after 21 Daily Sequential In Vitro Sub-Cultures

Multi-sub-culture resistance selection was conducted to determine if TCBZ-resistant mutants could develop. For this assay, 21 daily sequential in vitro sub-cultures were performed with TCBZ against *S. aureus* ATCC 29213, using enrofloxacin as a control antibiotic. After 21 days, no TCBZ-resistant mutants were identified. However, enrofloxacin-resistant mutants ($2 \times$ the MIC) had developed by day five and increased gradually to $16 \times$ MIC by days 18–21 (Figure 4).

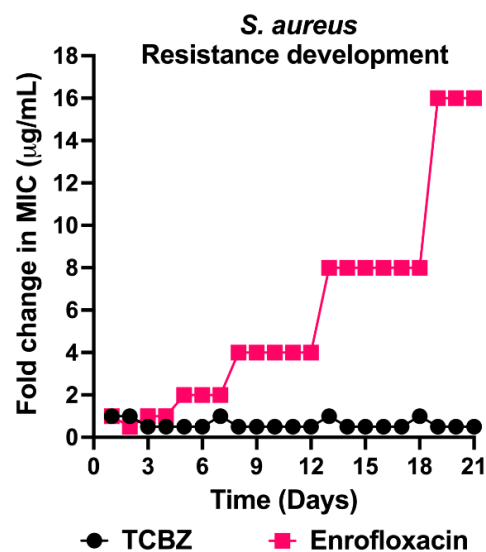


Figure 4. Resistance development of *S. aureus* ATCC 29213 to TCBZ. *S. aureus* ATCC 29213 was challenged with TCBZ at a concentration range of 0.25 to 8 $\mu\text{g}/\text{mL}$ over 21 daily sequential in vitro sub-cultures. Enrofloxacin was used as a control antibiotic.

3.7. Intracellular MIC Testing of TCBZ Shows Bacteriostatic Activity against *S. aureus* but Bactericidal Activity against MRSP

The intracellular activity of TCBZ against *S. aureus* ATCC 29213 and two MRSP isolates was examined in the mouse J774A.1 macrophage cell line. TCBZ was found to be bacteriostatic against intracellular *S. aureus* ATCC 29213 (Figure 5A). TCBZ exerted the lowest effect on intracellular bacteria with a maximal decrease in bacterial counts of approximately $0.2 \log_{10}$ at a concentration of $8 \times \text{MIC}$. By contrast, the positive control antimicrobial (monensin) revealed a slowly developing bactericidal effect towards intracellular *S. aureus* ATCC 29213 that was concentration dependent. Monensin showed a decrease in bacterial counts of approximately $1.1 \log_{10}$ at $8 \times \text{MIC}$ in broth. Monensin showed a $0.5 \log_{10}$ decrease in intracellular bacterial counts when examined at $1 \times \text{MIC}$ ($2 \mu\text{g}/\text{mL}$) in broth (Figure 5B).

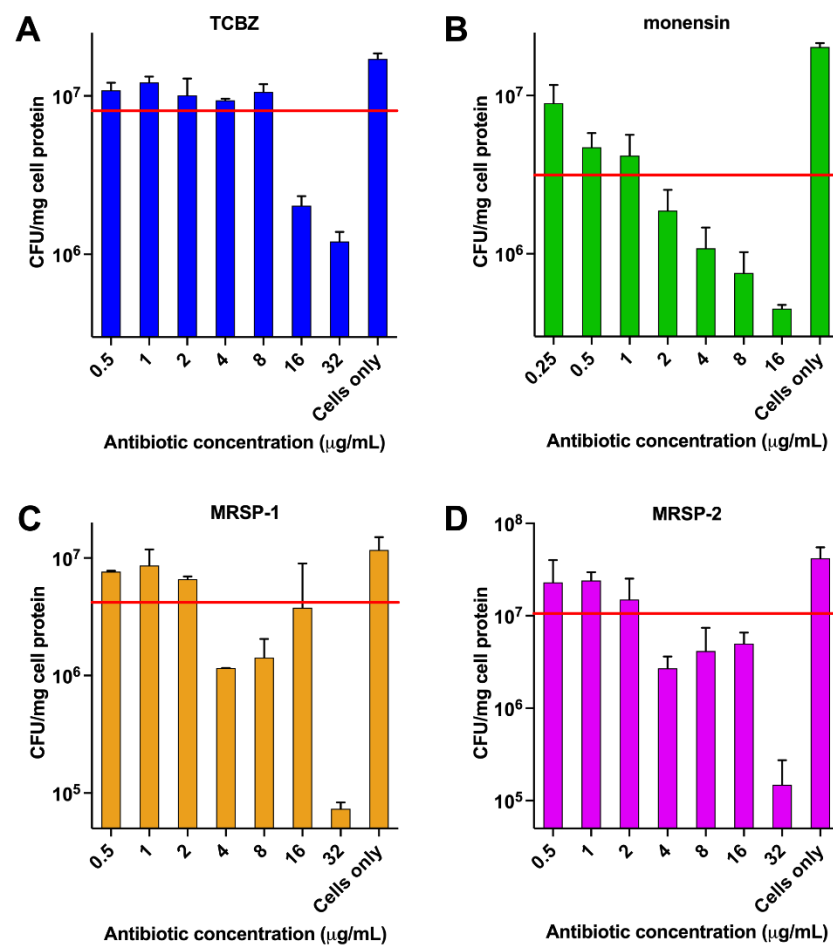


Figure 5. Intracellular activity of TCBZ using mouse J774A.1 macrophage cell line. (A) Intracellular activity of TCBZ against *S. aureus* ATCC 29213; (B) intracellular activity of monensin against *S. aureus* ATCC 29213; (C) intracellular activity of TCBZ against MRSP 1; and (D) intracellular activity of TCBZ against MRSP 2.

The intracellular activity of TCBZ against two MRSP isolates (isolate 1 and 2) was also examined. At the highest concentration used (32 µg/mL (16 × MIC)), TCBZ showed a bactericidal effect with a decrease in bacterial counts of 1.1 log₁₀ and 1.4 log₁₀ for isolate 1 and isolate 2, respectively (Figure 5C,D). Intracellular MRSP isolates were unaffected by TCBZ when cells were incubated with a drug concentration equal to 1 × MIC (2 µg/mL).

3.8. TCBZ Is Non-Hemolytic and Non-Cytotoxic

A hemolytic activity assay for TCBZ against fresh human RBCs from donors showed that it is non-hemolytic, with a hC₅₀ higher than 128 µg/mL. Cytotoxic assay results also show that the IC₅₀ value for TCBZ was greater than the highest concentration tested (16 µg/mL) against the MCF-7 (human breast cancer) cell line, suggesting non-cytotoxicity against this cell line, while the IC₅₀ values were 16 µg/mL against the hEK293 (human embryonic kidney) and Detroit 562 (human pharyngeal epithelial) cell lines, suggesting limited cytotoxicity against these two cell lines.

3.9. TCBZ Shows Oral Safety in Mice

Safety studies performed on mice using three doses of either 10 mg/kg or 50 mg/kg TCBZ orally daily for 5 days showed no significant pathological changes in the lungs, heart, liver, spleen, kidneys or small intestine of the treated groups compared to the group treated with a similar dosing regimen of 1.6 mg/mL of moxifloxacin or the control group treated with PBS.

3.10. Treatment of Mice with TCBZ Reduces *S. aureus* Population with Repeated Treatments within 24 h Post-Infection

We evaluated the potential of TCBZ as an oral drug against systemic *S. aureus* infection, using a well-characterized luminescent strain (Xen29) [25,38], by photon intensity measurements. In the first experiment, mice were challenged IP with 2.5×10^7 CFU of Xen29 and treated with TCBZ at 50 mg/kg or with moxifloxacin at 6 mg/kg orally (administered at 2, 6, 10 and 18 h post-infection), with untreated mice receiving an identical course of PBS orally. The TCBZ treatment regimen resulted in a statistically significant reduction in *S. aureus* populations at 10 and 18 h post-infection ($p = 0.0483$ and $p = 0.0296$, respectively; Mann–Whitney U test, one-tailed) compared to the PBS control group. However, the *S. aureus* populations gradually increased from 24 h post-infection upon withdrawal of TCBZ treatment, consistent with a bacteriostatic action (not shown). Furthermore, mice were found to have severe breathing difficulties and were reluctant to move from 36 h post-infection onwards. Therefore, the mice were humanely killed, blood samples were collected, and no bioluminescent total flux values were recorded for these time points. By contrast, oral administration of moxifloxacin (drug control) resulted in a statistically significant reduction in *S. aureus* populations at 6, 10 and 18 h post-infection ($p = 0.0042$; $p = 0.0125$ and $p = 0.0006$, respectively; Mann–Whitney U test, one-tailed) and there was no regrowth of the bacterial population post-moxifloxacin withdrawal (Figure 6), illustrated by images of representative mice at selected time points (Figure 7).

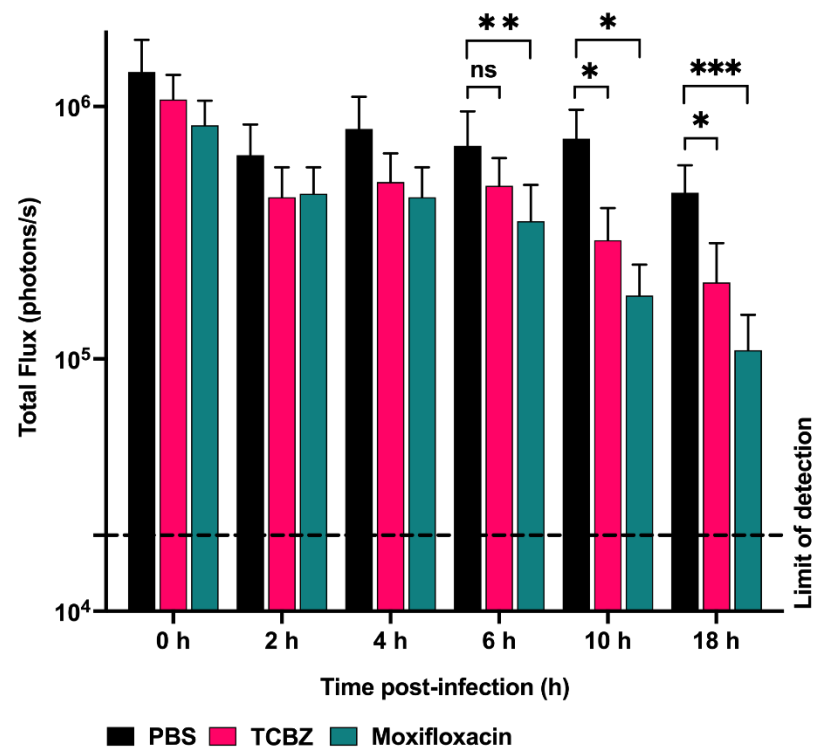


Figure 6. Luminescence signal comparison between groups of CD1 mice challenged IP with 2.5×10^7 CFU of bioluminescent *S. aureus* Xen29 ($n = 6$) (treated at 2, 6, 10 and 18 h post-infection). Mice were subjected to bioluminescence imaging on IVIS Lumina XRMS Series III system. Dashed horizontal line indicates limit of detection (2.0×10^4 photons/s). Data are mean (\pm SEM) photons/s. * $p < 0.05$; ** $p < 0.01$; *** $p < 0.001$; ns = not significant; Mann–Whitney U test, one-tailed.

We attributed the overall lack of efficacy for TCBZ post-24 h to be partly due to the high bacterial challenge dose. Therefore, a repeat experiment using a lower bacterial dose (1×10^7 of Xen29) was carried out. In this experiment, repeated treatment with TCBZ at 50 mg/kg up to 24 h post-infection (administered at 2, 6, 10, 18, and 24 h post-infection) also resulted in a gradual reduction in *S. aureus* populations. However, this reduction was not statistically significant compared to the untreated (PBS) control group (Figure S1). By contrast, oral administration of moxifloxacin (drug control) resulted in a statistically significant reduction in *S. aureus* populations at 18 h post-infection ($p = 0.0014$ and $p = 0.0031$, respectively, Mann–Whitney U test) and there was no regrowth of the bacterial population post-moxifloxacin withdrawal (Figure S1).

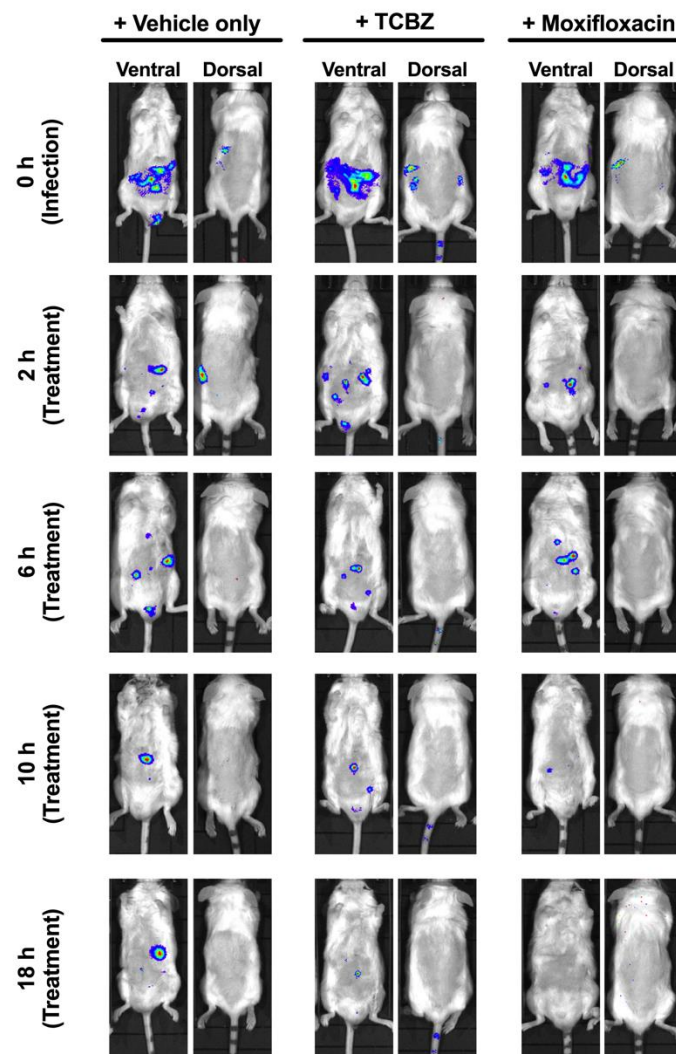


Figure 7. Ventral and dorsal images of representative CD1 mice challenged with 2.5×10^7 CFU of bioluminescent *S. aureus* Xen29. Mice were subjected to bioluminescent imaging on IVIS Lumina XRMS Series III system at the indicated times (0, 2, 6, 10 and 18 h).

4. Discussion

The global rise in multidrug-resistant ESKAPE infections continues to pose significant health and economic problems worldwide. However, no novel antibiotic with a new chemical structure, unexploited target or a new mode of action has been developed and marketed for several decades [39,40]. Modification of existing drug classes has resulted in the registration of several new drugs that are active against Gram-positive and some Gram-negative pathogens; however, antimicrobial access through the outer membrane barrier of Gram-negative bacteria still remains an important challenge [37,41,42]. Drugs in advanced clinical development include modification of existing antibiotic classes, new antibiotic classes, well-known combinations or novel drugs with adjuvants. Other recent and promising approaches include repurposing old compounds with known safety and development pathways as new antimicrobial classes with potentially novel mechanisms of action [21], an approach taken here. In developing new broad-spectrum antimicrobial agents that can overcome the permeability barrier in Gram-negative bacterial pathogens [31,43,44], one strategy being employed is combination of antibiotics with outer membrane permeabilizers [45].

In this work, we evaluated the antibacterial potential of TCBZ, a benzimidazole anthelmintic agent, which is the active ingredient of registered drugs for treating liver fluke in animals (*Fasciola* spp.) and lung fluke in humans (*Paragonimus* spp.). TCBZ was previously

suggested as a potential antibacterial agent in a repurposing study involving the mass screening of FDA-registered drugs [21]; however, it was not until quite recently that it was demonstrated to have potent antimicrobial activity against *C. difficile* as well as being active against representative strains of normal human gut microbiota [22]. In our study, a range of TCBZ derivatives were generated for an initial screen to identify the candidate with the best antibacterial activity. An investigation of the antibacterial activity of a family of TCBZ analogs incorporating the synthetic precursor thiol, TCBZ's sequential oxidation sulphoxide (TCBZ-SO) and sulphone (TCBZ-SO₂), together with the final hydrolytic product (TCBZ-OH), highlighted that the bioactivity is not restricted to the parent anthelmintic but extends to its recognised in vivo metabolites. From the initial screening of the compound series, TCBZ was found to be the most promising derivative with antimicrobial activity demonstrated against Gram-positive bacteria including methicillin-resistant strains, as well as Gram-negative bacteria in the presence of an outer membrane permeabilizer. This corroborates the previous report [22], but also expands the antibacterial spectrum of activity of TCBZ.

The mechanism of action of TCBZ has not been fully clarified. However, in vitro and/or animal infection studies using TCBZ and its active metabolites (sulphoxide and sulfone) against *Fasciola* species point to its effect on multiple targets resulting in reduced membrane potential, inhibition of tubulin function and protein and enzyme synthesis [43]. Interestingly, it appears the sulphoxide metabolite (which is largely predominant in human plasma following pre-systemic biotransformation of TCBZ) has a delayed but more potent effect on parasite motility than the parent TCBZ compound, leading to the suggestion that TCBZ likely acts primarily through the sulphoxide metabolite [46]. It is likely that TCBZ and its metabolites have a similar mechanism of action on the membrane of bacteria, and this will be the subject of future investigations.

This study had four major findings. Firstly, TCBZ was bactericidal against a range of methicillin-susceptible and methicillin-resistant *Staphylococcus* spp. and VRE, and was also shown to maintain antimicrobial activity against intracellular *Staphylococcus* spp. in vitro. Secondly, no resistance to TCBZ was developed by *S. aureus* after 21 daily sequential in vitro sub-cultures, a desirable characteristic for its further exploration as a novel antimicrobial class to treat acute bacterial infections. Thirdly, TCBZ inhibited the growth of key Gram-negative ESKAPE pathogens including *E. coli*, *K. pneumoniae*, *A. baumannii* and *P. aeruginosa* in the presence of sub-inhibitory concentrations of PMB, indicating that the antimicrobial target is present in both Gram-positive and Gram-negative bacteria. Fourthly, repeated oral treatment of mice infected with bioluminescent *S. aureus* with TCBZ significantly reduced *S. aureus* populations within 24 h post-infection, but did not eliminate infection with the selected dosage regimen.

TCBZ demonstrated bactericidal antimicrobial activity (MICs of 2 µg/mL and MBCs ranging from 2–16 µg/mL) against a range of methicillin-susceptible and methicillin-resistant strains of coagulase-positive *Staphylococcus* spp., including the canine commensal pathogen *Staphylococcus pseudintermedius*. Here, MICs/MBCs established for TCBZ were several-fold lower than previously reported for triclabendazole [21], but the same trends were observed (low uniform MICs with MBCs several-fold higher). Furthermore, TCBZ was active at higher concentrations against VRE and *S. pneumoniae*. Demonstrated intracellular activity against *S. aureus* suggested that TCBZ may have potential as a treatment for bovine mastitis, which is most commonly caused by *S. aureus* strains adapted for intracellular survival within polymorphonuclear cells of the bovine mammary gland. However, the promising activity shown against human streptococci did not extend to the three main species of streptococci causing bovine mastitis (*S. uberis*, *S. agalactiae* and *S. dysgalactiae*) and furthermore, antibacterial activity was not demonstrated in the presence of milk, a key disqualifier for further development as an intramammary mastitis formulation.

Despite these potential drawbacks, an important finding of this work was the demonstration that *S. aureus* did not develop resistance following 21 serial sub-cultures in the presence of sub-inhibitory concentrations of TCBZ. By comparison, serial stepwise resis-

tance was observed for enrofloxacin, a registered fluoroquinolone for animal treatment with broad-spectrum bactericidal antimicrobial activity. Stepwise resistance to fluoroquinolones develops via the accumulation of point mutations in the chromosomal target genes [47]. In this context, our results may indicate that similar chromosomal point mutations in the putative target gene/s of triclabendazole in bacteria may not result in resistance. However, this needs to be further investigated as it is quite possible that point mutations conferring resistance could arise under the right selection pressure. Whilst the exact mechanism of action of triclabendazole in flukes remains to be determined, development of resistance in *Fasciola hepatica* has been recently observed [43]. Further research such as use of differential, timed exposure RNAseq, fluorescence-based protein and lipid binding experiments and electron microscopy studies could potentially unlock the target/s and mechanism of action of triclabendazole in susceptible bacteria.

The observed in vitro synergistic antimicrobial activity of TCBZ in combination with sub-inhibitory concentrations of PMB against a large panel of Gram-negative human ESKAPE pathogens provides additional opportunities for treatment of Gram-negative infections in clinical settings whilst also reducing the amount of PMB needed for effective targeting. Although it was previously reported that PMB is toxic for humans at a concentration of 4 µg/mL, the lowest concentration required in combination with TCBZ ranged from 0.0625 to 0.25 µg/mL, which is 64- to 16-fold lower than its cytotoxic dose [45,48]. The finding that multiple oral administrations of TCBZ to mice at 50 mg/kg over 5 days was safe without any demonstrable clinical signs or observable morphological effects on the main organs examined also provides the possibility of using PMB in combination with TCBZ for human use after robust testing in animal models of infection. Additionally, the fact that no resistance developed to TCBZ by *S. aureus* after 21 daily sequential in vitro sub-cultures also suggests that its synergistic antimicrobial activity with PMB against Gram-negative pathogens warrants further exploration for specific treatment of acute Gram-negative bacterial infections. This will be of further benefit in the colistin resistance era as polymyxins are among the last line of antimicrobials used to treat multidrug-resistant Gram-negative bacterial infections.

The in vivo efficacy data show that repeated treatment of mice resulted in a substantial reduction in *S. aureus* populations over the 24 h period, with regrowth occurring once treatment was withdrawn. This result suggests that TCBZ is bacteriostatic when the effective concentration in vivo is low (possibly due to poor host cell membrane penetration) and could further explain the in vitro intracellular MIC result of TCBZ against *S. aureus* ATCC 29213, where it was also found to be bacteriostatic. It is known that neutrophils are recruited to the site of invading bacterial pathogens by host pattern recognition receptors through recognition of lipoteichoic acid (LTA), a component of the cell wall of all Gram-positive bacteria [49,50]. Cell-wall-active β-lactam antimicrobials such as imipenem, flucloxacillin and cefamandole significantly enhance the release of LTA compared to protein synthesis, inhibiting drugs such as gentamicin and erythromycin [51]. Furthermore, together with glycopeptides, rifamycins, lincosamides, quinolones and fosfomycin, these β-lactam antibiotics can penetrate human neutrophils and kill and/or inhibit intracellular *S. aureus* without adversely affecting neutrophil function [51]. By contrast, we hypothesise that TCBZ does not target the bacterial cell wall and may not initiate release of LTA to the same extent. It would therefore be informative to investigate if a combination of any of these antibiotics with TCBZ could be synergistic in eradicating intracellular *S. aureus*.

5. Conclusions

In this study, we showed that TCBZ, a benzimidazole anthelmintic agent, is bactericidal against coagulase-positive staphylococci, including *S. aureus* (including MRSA) and *S. pseudintermedius* (including MRSP), at relatively low concentrations and demonstrates good intracellular activity at higher concentrations. In addition, oral treatment of mice with TCBZ after systemic *S. aureus* challenge resulted in a significant reduction in *S. aureus* populations in the blood of mice up to 18 h post-infection compared to control (untreated) mice

but did not clear the bacterial infection from the bloodstream, suggesting bacteriostatic activity in vivo. Future studies of pharmacokinetics and dosage optimisation of TCBZ may identify a reliable and effective oral administration regimen.

Supplementary Materials: The following are available online at <https://www.mdpi.com/article/10.3390/microorganisms9081697/s1>, Figure S1. Luminescence signal comparison between groups of CD1 mice challenged IP with 1×10^7 CFU of *S. aureus* (Xen29) ($n = 6$) (treated at 2, 6, 10 and 18 h post-infection). Mice were subjected to bioluminescence imaging on IVIS Lumina XRMS Series III system. Dashed horizontal line indicates limit of detection (2.0×10^4 photons/s). Table S1. Gram-positive and Gram-negative bacterial collection used in this study ($n = 138$). Table S2. MIC values of TCBZ against 20 MRSA isolates. Table S3. MIC and MBC values of TCBZ against *S. pseudintermedius* isolates ($n = 13$).

Author Contributions: Conceptualization, H.P., A.D.O., B.S., H.T.N., S.W.P., E.L. and D.J.T.; data curation, H.P., A.D.O., B.S. and H.T.N.; formal analysis, H.P., A.D.O., B.S., H.T.N., S.W.P., E.L., H.V. and D.J.T.; funding acquisition, S.W.P., E.L. and D.J.T.; investigation, H.P., A.D.O., B.S., H.T.N. and D.J.T.; methodology, H.P., A.D.O., B.S. and H.T.N.; project administration, A.D.O., S.W.P. and D.J.T.; resources, S.W.P., E.L., H.V. and D.J.T.; supervision, A.D.O. and D.J.T.; validation, A.D.O. and D.J.T.; writing—original draft, H.P., A.D.O., B.S. and H.T.N.; writing—review and editing, H.P., A.D.O., B.S., H.T.N., S.W.P., E.L., H.V. and D.J.T. All authors have read and agreed to the published version of the manuscript.

Funding: This work was supported by funding to Darren J. Trott through ARC linkage project LP130100736 with Luoda Pharma as the main partner organization, with Stephen W. Page as the director. The funders did not have any additional role in the study design, data collection and analysis, decision to publish or preparation of the manuscript.

Institutional Review Board Statement: The ethics statement associated with this work is indicated in Section 2.11 of the manuscript. The Animal Ethics Committee of The University of Adelaide (approval number S-2015-151) reviewed and approved all animal experiments. The study was conducted in compliance with the Australian Code of Practice for the Care and Use of Animals for Scientific Purposes (8th Edition 2013) and the South Australian Animal Welfare Act 1985.

Informed Consent Statement: Not applicable.

Data Availability Statement: The data presented in this study are available on request from the corresponding author. The data are not publicly available due to privacy and access restrictions.

Acknowledgments: The authors would like to thank Amanda Ruggero, Lora Bowes and Anh hong Nguyen at the University of South Australia for their technical assistance. The authors acknowledge the instruments and scientific and technical assistance of Microscopy Australia at Adelaide Microscopy, The University of Adelaide, a facility that is funded by the University as well as State and Federal Governments.

Conflicts of Interest: Stephen W. Page is a director of Luoda Pharma and Ernest Lacey is a director of Microbial Screening Technologies. Darren J. Trott has received research funding from Luoda Pharma.

References

1. DiMasi, J.A.; Grabowski, H.G.; Hansen, R.W. Innovation in the pharmaceutical industry: New estimates of R&D costs. *J. Health Econ.* **2016**, *47*, 20–33. [[CrossRef](#)]
2. Hong, I.S.; Ipema, H.J.; Gabay, M.P.; Lodolce, A.E. Medication Repurposing: New Uses for Old Drugs. *J. Pharm Tech.* **2011**, *27*, 132–140. [[CrossRef](#)]
3. O'Neill, J.; Davies, S.; Rex, J.; White, L.; Murray, R. Review on antimicrobial resistance, tackling drug-resistant infections globally: Final report and recommendations. *Lond. Wellcome Trust. UK Gov.* **2016**, *1*, 84.
4. Pushpakom, S.; Iorio, F.; Eyers, P.A.; Escott, K.J.; Hopper, S.; Wells, A.; Doig, A.; Guilliams, T.; Latimer, J.; McNamee, C. Drug repurposing: Progress, challenges and recommendations. *Nat. Rev. Drug Discov.* **2019**, *18*, 41. [[CrossRef](#)]
5. Australian Commission on Safety and Quality in Health Care. *Antimicrobial Stewardship in Australian Health Care 2018*; ACSQHC: Sydney, Australia, 2018.
6. Wright, G.D. Antibiotic Adjuvants: Rescuing Antibiotics from Resistance. *Trends Microbiol.* **2016**, *24*, 862–871. [[CrossRef](#)] [[PubMed](#)]

7. Corsello, S.M.; Bittker, J.A.; Liu, Z.; Gould, J.; McCarren, P.; Hirschman, J.E.; Johnston, S.E.; Vrcic, A.; Wong, B.; Khan, M.; et al. The Drug Repurposing hub: A next-generation drug library and information resource. *Nat. Med.* **2017**, *23*, 405–408. [CrossRef]
8. Brown, D. Antibiotic resistance breakers: Can repurposed drugs fill the antibiotic discovery void? *Nat. Rev. Drug Discov.* **2015**, *14*, 821–832. [CrossRef]
9. Cha, Y.; Erez, T.; Reynolds, I.J.; Kumar, D.; Ross, J.; Koytiger, G.; Kusko, R.; Zeskind, B.; Risso, S.; Kagan, E.; et al. Drug repurposing from the perspective of pharmaceutical companies. *Br. J. Pharm.* **2018**, *175*, 168–180. [CrossRef] [PubMed]
10. Oprea, T.L.; Mestres, J. Drug repurposing: Far beyond new targets for old drugs. *AAPS J.* **2012**, *14*, 759–763. [CrossRef]
11. Strittmatter, S.M. Overcoming drug development bottlenecks with repurposing: Old drugs learn new tricks. *Nat. Med.* **2014**, *20*, 590–591. [CrossRef]
12. Durand, G.A.; Raoult, D.; Dubourg, G. Antibiotic discovery: history, methods and perspectives. *Int. J. Antimicrob. Agents* **2019**, *53*, 371–382. [CrossRef] [PubMed]
13. Rangel-Vega, A.; Bernstein, L.R.; Mandujano-Tinoco, E.A.; García-Contreras, S.J.; García-Contreras, R. Drug repurposing as an alternative for the treatment of recalcitrant bacterial infections. *Front. Microbiol.* **2015**, *6*, 282. [CrossRef] [PubMed]
14. Zheng, W.; Sun, W.; Simeonov, A. Drug repurposing screens and synergistic drug-combinations for infectious diseases. *Br. J. Pharm.* **2018**, *175*, 181–191. [CrossRef] [PubMed]
15. Alam, M.M.; Chowdhury, E.H.; Hossain, M.I.; Huque, A.K.M.F.; Mondal, M.M.H. The Efficacy of the Triclabendazole (Fasinex AE) against *Fasciola gigantica* infection in cattle of Bangladesh. *Prog. Agric.* **2001**, *12*, 151–155.
16. El-Tantawy, W.H.; Salem, h.F.; Mohammed Safwat, N.A. Effect of Fascioliasis on the pharmacokinetic parameters of triclabendazole in human subjects. *Pharm. World Sci.* **2007**, *29*, 190–198. [CrossRef]
17. Lecaillon, J.B.; Godbillon, J.; Campestrini, J.; Naquira, C.; Miranda, L.; Pacheco, R.; Mull, R.; Poltera, A.A. Effect of food on the bioavailability of triclabendazole in patients with fascioliasis. *Br. J. Clin. Pharm.* **1998**, *45*, 601–604. [CrossRef]
18. U.S. Food & Drug Administration. New Drug Therapy Approvals 2019. WHO/MVP/EMP/IAU/2019.07. 2020. Available online: <https://www.fda.gov/media/134493/download> (accessed on 29 July 2021).
19. World Health Organization. World Health Organization Model List of Essential Medicines 21st List. 2019. Available online: <https://apps.who.int/iris/bitstream/handle/10665/325771/WHO-MVP-EMP-IAU-2019.06-eng.pdf> (accessed on 29 July 2021).
20. World Health Organization. World Health Organization Model List of Essential Medicines for Children: 7th List 2019. 2019. Available online: <https://apps.who.int/iris/bitstream/handle/10665/325772/WHO-MVP-EMP-IAU-2019.07-eng.pdf> (accessed on 29 July 2021).
21. Younis, W.; Thangamani, S.; Seleem, M.N. Repurposing non-antimicrobial drugs and clinical molecules to treat bacterial infections. *Curr. Pharm. Des.* **2015**, *21*, 4106–4111. [CrossRef]
22. AbdelKhalek, A.; Mohammad, h.; Mayhoub, A.S.; Seleem, M.N. Screening for potent and selective anticlostridial leads among FDA-approved drugs. *J. Antibiot.* **2020**, *73*, 392–409. [CrossRef]
23. Schneider, E.K.; Reyes-Ortega, F.; Velkov, T.; Li, J. Antibiotic-non-antibiotic combinations for combating extremely drug-resistant Gram-negative ‘superbugs’. *Essays Biochem.* **2017**, *61*, 115–125. [CrossRef]
24. Zgurskaya, h.I.; López, C.A.; Gnanakaran, S. Permeability barrier of Gram-negative cell envelopes and approaches to bypass it. *ACS Infect. Dis.* **2015**, *1*, 512–522. [CrossRef]
25. Pi, h.; Nguyen, h.T.; Venter, h.; Boileau, A.R.; Woolford, L.; Garg, S.; Page, S.W.; Russell, C.C.; Baker, J.R.; McCluskey, A.; et al. *In vitro* activity of robenidine analog ncl195 in combination with outer membrane permeabilizers against Gram-negative bacterial pathogens and impact on systemic Gram-positive bacterial infection in mice. *Front. Microbiol.* **2020**, *11*. [CrossRef]
26. Lynch, B.M.; Chen, C.M.; Wigfield, Y.-Y. Nitrations of acetanilides by reagents of N02X type. *Can. J. Chem.* **1968**, *46*, 1141–1148. [CrossRef]
27. van Allan, J.A.; Deacon, B.D. *2-Mercaptobenzimidazole*; John Wiley & Sons: New York, NY, USA, 1963; Volume IV. Available online: <https://pubchem.ncbi.nlm.nih.gov/compound/2-Mercaptobenzimidazole> (accessed on 29 July 2021).
28. Averkin, E.A.; Beard, C.C.; Dvorak, C.A.; Edwards, J.A.; Fried, J.H.; Kilian, J.G.; Schiltz, R.A.; Kistner, T.P.; Drudge, J.H.; Lyons, E.T.; et al. Methyl 5(6)-phenylsulfinyl-2-benzimidazole-carbamate, a new, potent anthelmintic. *J. Med. Chem.* **1975**, *18*, 1164–1166. [CrossRef]
29. Vandenberg, J.; Kennis, L.E.J.; Van de Aa, M.J.M.C.; Van heertum, A.H.M.T. Antiemetic 1-(benzimidazolylalkyl) Piperidine Derivatives. 1978, Volume 4. Available online: <https://patents.google.com/patent/US4126687A/en> (accessed on 29 July 2021).
30. Clinical and Laboratory Standards Institute. *Performance Standards for Antimicrobial Susceptibility Testing*, 27th ed.; CLSI Standard M100; Clinical and Laboratory Standards Institute: Wayne, PA, USA, 2017.
31. Venter, h. Reversing resistance to counter antimicrobial resistance in the World Health Organisation’s critical priority of most dangerous pathogens. *Biosci. Rep.* **2019**, *39*. [CrossRef] [PubMed]
32. Hamoud, R.; Reichling, J.; Wink, M. Synergistic antibacterial activity of the combination of the alkaloid sanguinarine with EDTA and the antibiotic streptomycin against multidrug resistant bacteria. *J. Pharm. Pharm.* **2015**, *67*, 264–273. [CrossRef] [PubMed]
33. Khazandi, M.; Pi, h.; Chan, W.Y.; Ogunniyi, A.D.; Sim, J.X.F.; Venter, h.; Garg, S.; Page, S.W.; Hill, P.B.; McCluskey, A. *In vitro* antimicrobial activity of robenidine, ethylenediaminetetraacetic acid and polymyxin B nonapeptide against important human and veterinary pathogens. *Front. Microbiol.* **2019**, *10*, 837. [CrossRef]
34. Eid, S.Y.; El-Readi, M.Z.; Wink, M. Synergism of three-drug combinations of sanguinarine and other plant secondary metabolites with digitonin and doxorubicin in multi-drug resistant cancer cells. *Phytomed* **2012**, *19*, 1288–1297. [CrossRef] [PubMed]

35. Ogunniyi, A.D.; Khazandi, M.; Stevens, A.J.; Sims, S.K.; Page, S.W.; Garg, S.; Venter, h.; Powell, A.; White, K.; Petrovski, K.R.; et al. Evaluation of robenidine analog NCL195 as a novel broad-spectrum antibacterial agent. *PLoS ONE* **2017**, *12*, e0183457. [CrossRef]
36. Seral, C.; Van Bambeke, F.; Tulkens, P.M. Quantitative analysis of gentamicin, azithromycin, telithromycin, ciprofloxacin, moxifloxacin, and oritavancin (LY333328) activities against intracellular *Staphylococcus aureus* in mouse J774 macrophages. *Antimicrob Agents Chemother.* **2003**, *47*, 2283–2292. [CrossRef]
37. Lim, T.-P.; Lee, W.; Tan, T.-Y.; Sasikala, S.; Teo, J.; hsu, L.-Y.; Tan, T.-T.; Syahidah, N.; Kwa, A.L. Effective antibiotics in combination against extreme drug-resistant *Pseudomonas aeruginosa* with decreased susceptibility to polymyxin B. *PLoS ONE* **2011**, *6*, e28177. [CrossRef]
38. Ogunniyi, A.D.; Kopecki, Z.; hickey, E.E.; Khazandi, M.; Peel, E.; Belov, K.; Boileau, A.; Garg, S.; Venter, h.; Chan, W.Y.; et al. Bioluminescent murine models of bacterial sepsis and scald wound infections for antimicrobial efficacy testing. *PLoS ONE* **2018**, *13*, e0200195. [CrossRef]
39. World health Organization. 2020 Antibacterial Agents in Clinical and Preclinical Development: An Overview and Analysis. 2021. Available online: <https://apps.who.int/iris/handle/10665/340694> (accessed on 29 July 2021).
40. The PEW Charitable Trusts. Tracking the Global Pipeline of Antibiotics in Development, March 2021. Available online: <https://www.pewtrusts.org/en/research-and-analysis/issue-briefs/2021/03/tracking-the-global-pipeline-of-antibiotics-in-development> (accessed on 29 July 2021).
41. Bassetti, M.; Peghin, M.; Vena, A.; Giacobbe, D.R. Treatment of infections due to MDR Gram-negative bacteria. *Front. Med.* **2019**, *6*. [CrossRef]
42. Theuretzbacher, U. Global antimicrobial resistance in Gram-negative pathogens and clinical need. *Curr. Opin. Microbiol.* **2017**, *39*, 106–112. [CrossRef] [PubMed]
43. Kelley, J.M.; Elliott, T.P.; Beddoe, T.; Anderson, G.; Skuce, P.; Spithill, T.W. Current threat of triclabendazole resistance in *Fasciola hepatica*. *Trends Parasitol.* **2016**, *32*, 458–469. [CrossRef] [PubMed]
44. World health Organization. WHO Advisory Group on Integrated Surveillance of Antimicrobial Resistance (AGISAR): Critically Important Antimicrobials for human Medicine 6th Revision 2018. 2019. Available online: <https://www.who.int/publications/i/item/9789241515528> (accessed on 29 July 2021).
45. Roberts, K.D.; Azad, M.A.; Wang, J.; horne, A.S.; Thompson, P.E.; Nation, R.L.; Velkov, T.; Li, J. Antimicrobial activity and toxicity of the major lipopeptide components of polymyxin B and colistin: Last-line antibiotics against multidrug-resistant Gram-negative bacteria. *ACS Infect. Dis.* **2015**, *1*, 568–575. [CrossRef]
46. Gandhi, P.; Schmitt, E.K.; Chen, C.W.; Samantray, S.; Venishetty, V.K.; hughes, D. Triclabendazole in the treatment of human fascioliasis: A review. *Trans. R. Soc. Trop. Med. Hyg.* **2019**, *113*, 797–804. [CrossRef] [PubMed]
47. Wetzstein, h.-G. Comparative mutant prevention concentrations of pradofloxacin and other veterinary fluoroquinolones indicate differing potentials in preventing selection of resistance. *Antimicrob Agents Chemother.* **2005**, *49*. [CrossRef] [PubMed]
48. Ahmed, M.U.; Velkov, T.; Lin, Y.-W.; Yun, B.; Nowell, C.J.; Zhou, F.; Zhou, Q.T.; Chan, K.; Azad, M.A.K.; Li, J. Potential Toxicity of Polymyxins in human Lung Epithelial Cells. *Antimicrob Agents Chemother.* **2017**, *61*, e02690-16. [CrossRef]
49. Algorri, M.; Wong-Beringer, A. Differential effects of antibiotics on neutrophils exposed to lipoteichoic acid derived from *Staphylococcus aureus*. *Ann. Clin. Microbiol. Antimicrob.* **2020**, *19*, 50. [CrossRef] [PubMed]
50. Kobayashi, S.D.; Malachowa, N.; DeLeo, F.R. Neutrophils and bacterial immune evasion. *J. Innate Immun.* **2018**, *10*, 432–441. [CrossRef]
51. Bongers, S.; hellebrekers, P.; Leenen, L.P.H.; Koenderman, L.; hietbrink, F. Intracellular penetration and effects of antibiotics on *Staphylococcus aureus* inside human neutrophils: A comprehensive review. *Antibiotics* **2019**, *8*, 54. [CrossRef] [PubMed]



Times are shown in your local time zone GMT +10:30

Appendix 3

#326 - Redesigning an Anticoccidial Drug for Treatment of Multidrug-Resistant Bacterial Infections

HIDE SIDEBAR



Rating

☆ Favourite

📄 e-Poster

Themes

[The Australian Society for Microbiology National Meeting](#)

Presentation Description

Redesigning an Anticoccidial Drug for Treatment of Multidrug-Resistant Bacterial Infections (#326)

Hang T. Nguyen ¹, Rietie Venter ², Tania Veltman ¹, Ruth Williams ³, Lisa A. O'Donovan ⁴, Cecilia C. Russell ⁵, Adam McCluskey ⁵, Stephen W. Page ⁶, Abiodun D. Ogunniyi ¹, Darren J. Trott ¹

1. Australian Centre for Antimicrobial Resistance Ecology, School of Animal and Veterinary Sciences, The University of Adelaide, Adelaide, SA, Australia
2. Health and Biomedical Innovation, Clinical and Health Sciences, The University of South Australia, Adelaide, SA, Australia
3. Adelaide Microscopy, The University of Adelaide, Adelaide, SA, Australia
4. ARC Centre of Excellence in Plant Energy Biology, School of Agriculture, Food & Wine, The University of Adelaide, Adelaide, SA, Australia
5. Chemistry, School of Environmental & Life Sciences, The University of Newcastle, Callaghan, NSW, Australia
6. Neoculi Pty Ltd., Burwood, VIC, Australia

There are renewed global calls for the development of new antimicrobial drugs with novel mechanisms of action, which also prevent further resistance to existing classes against multi-drug resistant pathogens. In this study, the potential of a novel chemical analogue of the anticoccidial robenidine (NCL195) as a drug against multi-drug resistant Gram-positive and Gram-negative bacterial infections was investigated. We showed the minimum inhibitory concentration (MIC) range of NCL195 against methicillin-resistant *Staphylococcus aureus* isolates was 1-2 $\mu\text{g}/\text{mL}$. NCL195 demonstrated synergistic activity in combination with subinhibitory concentration of colistin against clinical multidrug-resistant Gram-negative bacterial pathogens, with MICs for NCL195 ranging from 0.5-4 $\mu\text{g}/\text{mL}$ for *Acinetobacter baumannii*, *Escherichia coli*, *Klebsiella pneumoniae* and *Pseudomonas aeruginosa* in the presence of subinhibitory concentrations of colistin, whereas NCL195 alone had no activity². Transmission electron microscopy of *S. aureus* cells after treatment with NCL195, or of *E. coli* and *P. aeruginosa* after treatment with NCL195+colistin combination confirmed marked ultrastructural changes in membrane morphology, most frequently in the cell envelope^{2,3}. In bioluminescent mouse sepsis challenge models, administration of four oral doses of 50 mg/kg NCL195 (4 hours apart) resulted in significantly reduced *S. aureus* loads and longer survival times than vehicle-only treated mice. Furthermore, administration of four oral doses of 50 mg/kg NCL195 (4 hours apart) combined with four intraperitoneal doses (4 hours apart) of colistin (0.125 mg/kg) resulted in significant reduction in *E. coli* loads compared to treatment with NCL195 alone. In addition, treatment with the NCL195+colistin combination resulted in better *E. coli* clearance than treatment with colistin alone at the same concentrations. We conclude that NCL195 is a potential alternative for further development for specific treatment of Gram-positive bacterial infection or treatment of Gram-negative infection in combination with subinhibitory concentrations of colistin.

1. Pi, H.; Nguyen, H. T.; Venter, H.; Boileau, A. R.; Woolford, L.; Garg, S.; Page, S. W.; Russell, C. C.; Baker, J. R.; McCluskey, A.; O'Donovan, L. A.; Trott, D. J.; Ogunniyi, A. D. In vitro Activity of Robenidine Analog NCL195 in Combination with Colistin and Other Outer Membrane Permeabilizers Against Gram-Negative Bacterial Pathogens and Impact on Systemic Gram-Negative Bacterial Infection in Mice. *Frontiers in microbiology* 2020, 11, 1556. doi: 10.3389/fmicb.2020.01556.

Support



Comparison of Two Transmission Electron Microscopy Methods to Visualize Drug-Induced Alterations of Gram-Negative Bacterial Morphology. *Antibiotics* (Basel, Switzerland) 2021, 10. doi: 10.3390/antibiotics10030307.

Presenters



Hang Nguyen
 P.h.D candidate - The University of Adelaide
 Australian Centre for Antimicrobial
 Resistance Ecology, School of Animal and

Veterinary Scienc-es, The University of
 Adelaide, Roseworthy Campus, SA 5371
 Roseworthy, Australia

Other Suggested ePosters



e-Poster

#271 - Laboratory testing for toxigenic Clostridioides difficile: is culture too insensitive? 

Georgia McCluskey



e-Poster

Support

Making every electron count - New Science enabled by Pixel Array Detectors

David Muller^{1,2}

1. Cornell University, Ithaca, NY, United States

2. Kavli Institute at Cornell for Nanoscale Science, Cornell University, Ithaca, NY, United States

The past three decades have seen the rapid development and maturation of aberration-corrected electron lenses. A new generation of high-speed, high-dynamic-range, electron microscope detectors have allowed us to record the full momentum distribution at every position of scanned, atomic-scale electron beam. The resulting (and very large) four-dimensional phase space contains complete information about the underlying scattering potential. Phase retrieval algorithms such as ptychography offer an approach to using all of these scattered electrons – potentially enhancing both the resolution and dose-efficiency. Here we show how in-focus ptychography enables imaging at more than double the diffraction limit of the lens, and how out-of-focus ptychography improves the dose efficiency compared to all traditional imaging modes.

The increased speed and dynamic range of the new detectors also makes sub-picometer precision strain mapping possible at sub-nanometer resolution for data sets recorded in under a minute. High precision imaging of magnetic, electric and polarization fields with these detectors has provided uniquely detailed maps of topological textures in polar and magnetic Skyrmions.

1. Jiang *et al*, Nature **559**, (2018), p343.
2. Das *et al*, Nature **568**, (2019), p. 368.

Invited talk - SPED and HAADF- STEM used to aid aluminium alloy developments

Randi Holmestad¹

1. Norwegian University of Science and Technology (NTNU), Trondheim, TRØNDELAGE, Norway

Age-hardenable aluminium alloys - based on Al-Mg-Si, Al-Mg-Zn and Al-Cu - are important structural materials for construction and automotive applications due to properties like high strength/weight ratio and good formability, often combined with good corrosion resistance. Our overall objective is to improve the understanding of the fundamental physics, taking place at the atomic scale in these alloys – which decides nucleation, phase stabilization and precipitation [1]. The distribution, number density, morphology, structure and interfaces of age-hardening precipitates depend on the alloy composition and the thermo-mechanical history of the material, and to a large extent decide the material's physical properties. If we are able to map the atomic structure of precipitates and predict how they develop, we can design new or optimize chemical compositions of existing alloys to get desired properties for given applications. Our research group at NTNU and SINTEF in Trondheim has over a long period worked together with the Norwegian light metal industry on nanoscale studies of these alloys. We are using several advanced (scanning) transmission electron microscopy ((S)TEM) based techniques to study the alloy precipitates and micro-structures. Atomic structure is determined using aberration-corrected high-angle annular dark-field scanning transmission electron microscopy (HAADF-STEM), often in combination with density functional theory calculations [1]. The scanning precession electron diffraction (SPED) technique, combined with effective machine learning approaches and digital post-processing [2] is a very useful methodology to get comprehensive information about precipitate morphology and phase compositions, as well as crystallite orientations, also in deformed materials.

The TEM work was conducted using the NORTEM infrastructure (NFR 197405) at the TEM Gemini Centre, Trondheim, Norway.

1. SJ Andersen *et al*. Advances in Physics: X 3:1 (2018) 1479984; T Saito *et al*. Adv. Eng. Mater. (2018) 1800125.
2. JK Sunde *et al*. Mater. Charact. 142 (2018) 458; E Christiansen *et al*. Mater. Charact. 144 (2018) 522; E Thronsen *et al*. Materials & Design (2019) accepted.

Nitridation of commercial austenitic stainless steel: the need for multi-scale microstructural characterisation

Alice M. Young¹, Milo V. Kral¹, Catherine M. Bishop¹

1. University of Canterbury, Christchurch, CANTERBURY, New Zealand

Service conditions in methanol production plants create a driving force for nitrogen uptake in austenitic stainless steel piping, resulting in formation of internal nitride precipitates. Nitrides have been associated with loss of ductility in steels. However, their effects on the performance of specific commercial alloys such as the widely used Alloy 800H have not been studied. Hence any resulting degradation of properties is unaccounted for in component lifetime calculations, potentially leading to unexpected and costly failures. Characterisation of the nitrated microstructure is a critical first step towards understanding the evolution of mechanical properties during service. Limited existing information on microstructural development of Alloy 800H during nitridation restricts the current ability to correlate microstructural features and mechanical performance.

In this work, a multi-scale approach was taken to comprehensively characterise the microstructure of 800H following nitridation at service-relevant temperatures. Samples were nitrated at 800-1000 °C for 50-750 hrs in a 95%N₂/5%H₂ atmosphere. Optical, scanning electron, and transmission electron microscopy techniques were used for analysis, which focussed on AlN, Cr₂N and CrN nitride phases. Features such as precipitate morphology, crystallography, orientation relationships, location, and penetration

Noninvasive metabolic imaging of oocytes and early embryo development using confocal microscopy

Fabrizio Horta¹, Giulia Ballerin², Sarah Creed², Peter Temple-Smith¹

1. EPRD, Obstetrics and Gynecology, Monash University, Melbourne, VIC, Australia

2. Monash Micro Imaging-MHTP, Hudson institute of medical research, Melbourne, Victoria, Australia

Developing reliable noninvasive methods to assess oocyte and embryo quality has been a critical goal for assisted reproductive technologies in *in vitro* fertilization (IVF). The low success rate of clinical pregnancy is consistent with the fact that normal transferred embryos fail to implant because of underlying metabolic defects. Changes in metabolic activity could lead to cell death or abnormal embryo development which could be potentially predicted by incorporating noninvasive measurements of metabolism. Metabolic imaging is a well-tested method for detecting metabolic changes in cells and tissues, however, scientific evidence for its use in oocyte and embryo assessments is limited. Measurements of nicotinamide adenine dinucleotide (NADH) could be a useful tool as the auto-fluorescence of NADH is a straightforward representation of mitochondrial function and cellular redox status. The aim of this study was to measure the NADH levels in oocytes and early embryos in development from female mice of different age through live imaging. Oocytes from two groups of mice (Young: 5-8 weeks, Old: 42-45 weeks) were inseminated with control spermatozoa. Then, NADH levels were measured every 2hrs post *in vitro* fertilisation using confocal microscopy. Fertilisation and embryo development was also assessed. Metaphase II oocytes from young and old females showed significantly different NADH levels of auto-fluorescence (Young: 9469AU, Old: 8793AU, AU: arbitrary units of auto-fluorescence; $p < 0.05$) 2hrs post-fertilisation. Interestingly, there was an increased NADH activity in presumed zygotes from young females that was not observed in old zygotes 4hrs post-fertilisation (Young: 10144AU, Old: 8587AU, $p < 0.05$) as well as 6hrs post-fertilisation (Young: 9679AU, Old: 8546AU, $p < 0.05$). Our study indicates different levels of NADH during early embryo development associated to ageing and metabolic function, demonstrating that noninvasive measurements of NADH could be applied to determine embryo metabolic activity.

A Comparison of Different Methods for TEM Analysis of Gram-Negative Bacterial Membrane Structure

Lisa A O'Donovan^{1,2}, Hang T Nguyen³, Gwen Mayo¹, David D Ogunniyi³, Darren J Trott³

1. Adelaide Microscopy, The University of Adelaide, Adelaide, SA, Australia

2. Current address, ARC Centre of Excellence in Plant Energy Biology, School of Agriculture, Food and Wine, The University of Adelaide, Glen Osmond, SA, Australia

3. Australian Centre for Antimicrobial Resistance Ecology, School of Animal and Veterinary Sciences, The University of Adelaide, Roseworthy, SA, Australia

Effective treatment of bacterial infections is becoming increasingly difficult with the emergence of resistance to multiple classes of antimicrobial drugs. In particular, sepsis due to the multidrug-resistant ESKAPE pathogens (*Enterococcus faecium*, *Staphylococcus aureus*, *Klebsiella pneumoniae*, *Acinetobacter baumannii*, *Pseudomonas aeruginosa*, and *E. coli*/*Enterobacter* species) causes significant morbidity and mortality worldwide. During an investigation of drug interactions, multi-drug resistant *E. coli* proved difficult to embed for transmission electron microscopy (TEM), using conventional resin embedding. In addition to infiltration problems, traditional resin embedding destroyed ultrastructure and created artefacts. In this study we compared different methods for preparing the Gram-negative bacteria, *E. coli* for TEM analysis of morphology. Aldehyde-fixed bacteria were prepared using conventional embedding in Epon-Araldite or LR White resin at ambient temperature, and compared with ultrathin Tokuyasu cryo-sections. Results of this study indicate the superiority of ultrathin cryo-sections, with a clear delineation of the outer and inner membrane as well as the peptidoglycan layer. This technique opens opportunities for visualising drug interaction mechanisms on the bacterial cell membrane.

SPATIO-TEMPORAL LOCALIZATION OF PROTEIN DROPLETS IN CELLS

Eugene Marfo Obeng¹, Alex Fulcher¹, Bhuvana Shanbhag¹, Ian Harper¹, Lihong He¹

1. Monash University, Clayton, VICTORIA, Australia

Coacervation of biomolecules is an important mechanism within cells for the organization of intracellular space and the maintenance of cellular homeostasis. Herein, biomolecular liquids coexist in a state of demixing in a phenomenon called liquid-liquid phase separation (LLPS). The phase transition mechanism is an intrinsic characteristic of membraneless organelles (such as stress granules, germ granules, and nuclear bodies) and plays a critical role in cell physiology and pathology. The intracellular LLPS phenomenon putatively facilitates the protection, preservation, and regulation of genetic information and the trafficking of other materials within cells. In other words, it is a natural means to sequester, concentrate, transport, and release protein and nucleic acid cargoes for premium cell integrity. However, the understanding of the phenomenon is still embryonic. Particularly, it is not clear what the local and global drivers of the coacervation process are. This, therefore, demands the investigation of droplet localization and assembly dynamics in addition to their mechanical and transport characteristics with super-resolution precision. This work presents preliminary observations of the spatiotemporal characterization of protein droplets in cells using confocal and STED microscopy.

A comparison of different methods for TEM analysis of gram-negative bacterial membrane structure

Lisa A. O'Donovan, Hang T. Nguyen, Gwenda Mayo, Abiodun D. Ogunniyi and Darren J. Trott

INTRODUCTION

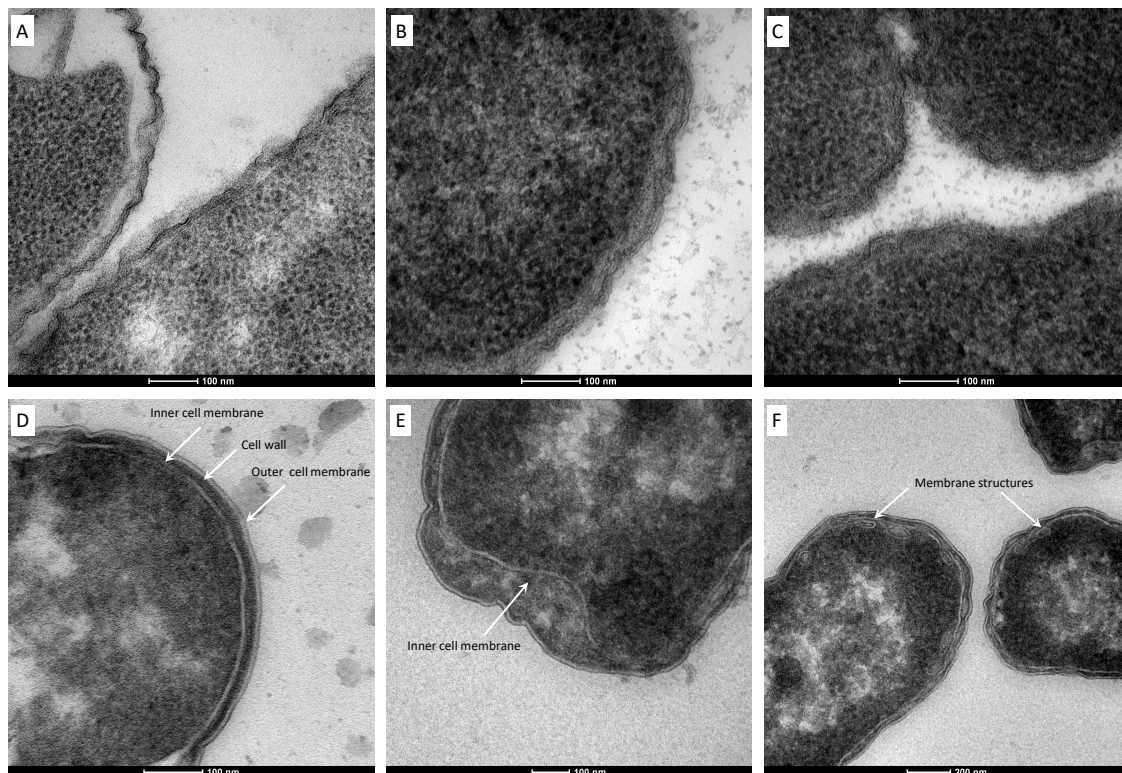
The development of novel agents with new modes of action against multi-drug resistant (MDR) pathogens, particularly gram-negative bacteria (GNB; which possess an outer membrane as an extra protective layer), is of the highest global priority. One strategy being explored for specific treatment of GNB infections involves a combination of new antimicrobial agents with existing outer membrane anti-infectives (e.g. colistin). Determining the most effective technique to accurately visualise and elucidate these drug interactions is essential. During our investigation of drug interactions, MDR-GNB *E. coli* proved difficult to embed for transmission electron microscopy (TEM) using conventional resin embedding. In addition to infiltration problems, traditional resin embedding destroyed ultrastructure and created artefacts.

METHOD

MDR GNB *E. coli* was subjected to different fixation, embedding and sectioning techniques for morphological analysis by TEM. Aldehyde-fixed bacteria were prepared using conventional embedding in PBS or cacodylate buffer in Epon-Araldite or LR White resin at ambient temperature, and compared with ultrathin Tokuyasu cryo-sections.

RESULTS

TEM comparison of *E. coli* morphology following different fixation, embedding and sectioning techniques.



A: *E. coli* fixed in 4% paraformaldehyde, 1.25% glutaraldehyde, 4% sucrose in the presence of 0.075% ruthenium red and 0.075% L-lysine acetate in PBS Buffer, embedded in Epon-Araldite resin. 70nm section, Leica UC6. **Bacterial outer membrane and cell wall have a wavy appearance and appear to have separated from the inner membrane.**

B and C: *E. coli* fixed in 4% paraformaldehyde, 1.25% glutaraldehyde, 4% sucrose in the presence of 0.075% ruthenium red and 0.075% L-lysine acetate in cacodylate buffer containing 0.01M CaCl_2 , embedded in B: LR White and C: Epon-Araldite resin. 70nm sections Leica UC6. **Bacterial cell walls and outer membrane still appear to be wavy however, separation from the inner membrane has not occurred.**

D: *E. coli* fixed in 4% paraformaldehyde, 1.25% glutaraldehyde, 4% sucrose in the presence of 0.075% ruthenium red and 0.075% L-lysine acetate in cacodylate buffer containing 0.01M CaCl_2 , embedded in 12% gelatin, infiltrated with 2.3M sucrose at 4°C overnight, plunge frozen in liquid nitrogen and sectioned (80nm, Leica FC7) at -100°C. **Freezing of cells into a matrix of amorphous ice (i.e., vitrification) results in optimal specimen preservation and allows the clear observation of outer membrane, cell wall and inner membrane.**

E and F: *E. coli* incubated with antimicrobial drug before processing as for D. **Inner membrane morphology changes included E: periplasmic space filled with electron-dense material, possibly from the cytosol, and F: additional membrane structures observed in the polar region.**

Scale Bar A-E:100nm, F:200nm. Images taken on a FEI Tecnai G2 Spirit operating at 100KV at Adelaide Microscopy.

CONCLUSION

These results indicate the usefulness of TEM in the study of effective antimicrobial drugs on bacteria, particularly on intracellular morphology. Sample preparation procedures can produce artefacts, which may influence the interpretation of results. Ultrathin cryo-sections provide a clear delineation of the outer and inner membrane as well as the cell wall peptidoglycan layer, and creates opportunities to visualise drug interaction mechanisms on bacterial cell membrane.

Appendix 5



The South Australia, Northern Territory ASM Branch Presents

ASM Student Awards Night 2021

Wednesday, 31st March 2021, 6:00 pm

University of South Australia

Bradley Forum, H5-02

Light snacks and non-alcoholic refreshments will be provided

Program

Biocide tolerance is linked to multidrug resistance in *Pseudomonas aeruginosa* through enhanced expression of drug efflux pumps

Anteneh Amsalu Geremew, University of South Australia

Initially disrupted preterm infant oral microbiota is restored within three months

Caitlin Selway, University of Adelaide

Combating antibiotic resistance with fish oil

Maoge Zang, Flinders University

The unique type-I interferon-epsilon (IFN- ϵ) constitutively protects the female reproductive tract from Zika Virus infection

Rosa Coldbeck-Shackley, University of Adelaide

Redesigning an anticoccidial drug for treatment of multi-drug resistant bacterial infections

Hang Thi Nguyen, University of Adelaide

The development of gut microbiota in commercial layer flocks: multiple routes to high performance flocks

Nitish Joat, University of Adelaide

The bacterial invisibility cloak lifted- The development of an intracellular osteocyte model for viable-but-not-culturable *S. aureus* in osteomyelitis.

Anja Zelmer, University of Adelaide

Old anti-alcoholic drug to fight biofilms on hernia meshes

Laurine Kaul, University of Adelaide

Attendance is **FREE**

For catering purposes, please book through Trybooking: <https://www.trybooking.com/BPVSO>

Enquiries: Please contact Andrea McWhorter or Alexandra Tikhomirova
(andrea.mcwhorter@adelaide.edu.au, alexandra.tikhomirova@adelaide.edu.au)

Appendix 6

Congratulations: Accepted into Ingenuity 2021

Nicole Eleftheriou <nicole.eleftheriou@adelaide.edu.au>

Wed 1/09/2021 4:51 PM

To: Hang Thi Nguyen <hang.t.nguyen@adelaide.edu.au>; Billie-Jaye Brougham <billie-jaye.brougham@adelaide.edu.au>; Jessica Thea Turner <jessica.t.turner@adelaide.edu.au>; Bobbie Emilia Lewis Baida <bobbie.lewisbaida@adelaide.edu.au>; Amy Laurel Munn <amy.munn@adelaide.edu.au>; Johanna Ellen Aldersey <johanna.aldersey@adelaide.edu.au>; Bianca Agenbag <bianca.agenbag@adelaide.edu.au>

Cc: Gordon Howarth <gordon.howarth@adelaide.edu.au>; Bec Forder <bec.forder@adelaide.edu.au>

📎 3 attachments (19 MB)

A0 landscape template.pptx; A0 portrait template.pptx; WHAT IS INGENUITY.docx;

Hi everyone,

Thank you for submitting an expression of interest in the 2021 Ingenuity event, your application has been successful and we can't wait to have you showcase your research at the event.

From here, we will be adding you to the My Uni page dedicated to Ingenuity 2021, please accept this invitation when it is sent to you, to stay up to date with all the latest event information and prep sessions we will be running before the expo.

OVERVIEW OF EVENT

As a reminder the Ingenuity Expo will be hosted on **Monday 25 and Tuesday 26 October 2021** at the Adelaide Convention Centre, attached is a quick overview of what Ingenuity is and the deliverables for the event (both virtually and in-person events).

POSTER TEMPLATE

Also attached is the poster template (both landscape and portrait options) for you to create your research display poster. This poster can be used as a PDF on the virtual platform and printed in your booth for the in-person event. If you would like your poster printed for your booth can you please get artwork to me by **COB Friday 15 October 2021** so we can arrange printing.

REMAINING QUESTIONS FOR BOOTHS

There are a few final pieces of information I require from you to get your booth set up at the Convention Centre, can you please provide me with the following information by **COB Friday 10 September**.

1. If your project needs to be exhibited adjacent to another project, please specify their project name and the school they're exhibiting under.
2. How many powerpoints will you require at your booth? *(Please note: a powerboard can be attached to each powerpoint and all electrical equipment will need to be electrically tested before the event)*
 - 0 (I don't require power)
 - 0.5 (I could share a powerboard as I only need 1-2 powerpoints)
 - 1
 - 2
3. Will your project display possibly require:
 - a. a continuous supply of water (or a volume of water > 30L)
 - b. a continuous supply of compressed air
 - c. 3 phase power

Please note: This doesn't have to be confirmed until closer to the event, but your booth will be placed closer to a utility pit in case you require access.

4. Will you be displaying a device at your stand that could pose any hazards (even if they're minor or unlikely)? (e.g. water leakage, moving parts, tripping hazards, excessive noise or risk of burns.) If

so, please describe the potential risk(s) with your display and an event coordinator will be in contact with you.

If you have any additional questions about Ingenuity, what's required or would like more information about the event, please contact myself or your school reps: Gordon Howarth and Bec Forder.

We can't wait for you to be involved!

Warmly,
Nicole.

Nicole Eleftheriou
Events Coordinator | Faculty of Sciences

THE UNIVERSITY OF ADELAIDE
Adelaide SA 5005 Australia
T: 61 8 8313 4325

CRICOS Provider Number 00123M

IMPORTANT: This message may contain confidential or legally privileged information. If you think it was sent to you by mistake, please delete all copies and advise the sender. For the purposes of the SPAM Act 2003, this email is authorised by The University of Adelaide.

Think green: read on the screen.

Evaluation of benzguinols as next-generation antibiotics for the treatment of multidrug-resistant bacterial infections

Research Problem

Multidrug resistance is a global health and development threat. It is estimated that multidrug-resistant bacterial infections could result in 10 million deaths per year and an economic collapse comparable to the 2008–2009 global financial crisis by 2050 if no action is taken.

It is clear that the problems posed by multidrug-resistance pathogens requires rapid development of new, broad-spectrum antibiotics.

Aim

Evaluate the efficacy of novel antibiotics (benzguinols) against *S. aureus* sepsis in a bioluminescent mouse infection model

Novel Antibiotics Tested

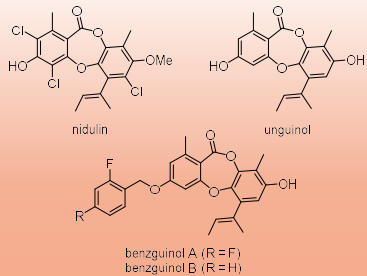


Figure 1. Structures of fungal metabolites nidulin and unguinol and semisynthetic unguinol derivatives benzguinol A and benzguinol B.

Appendix 6

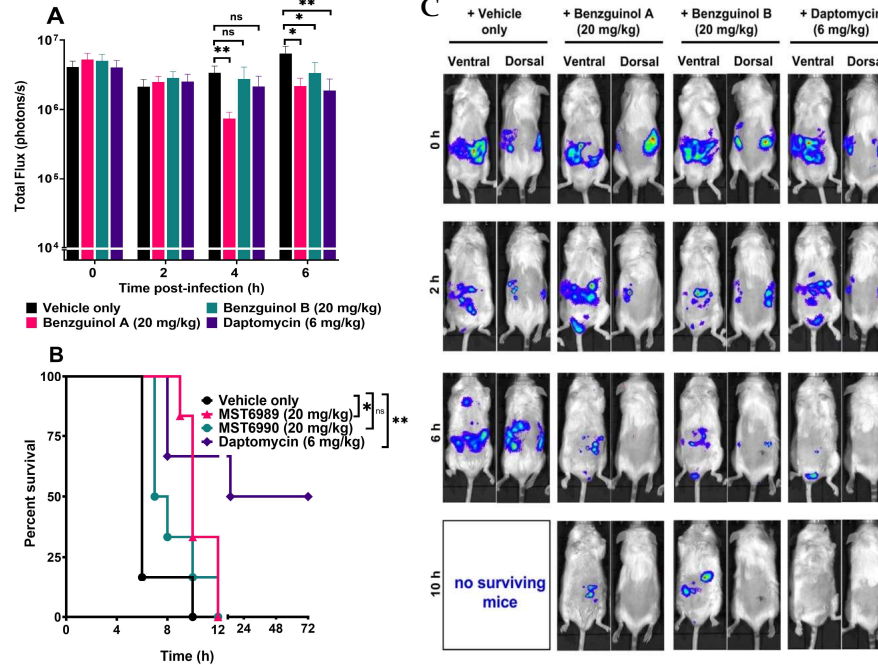


Figure 2. Benzguinol Efficacy Data

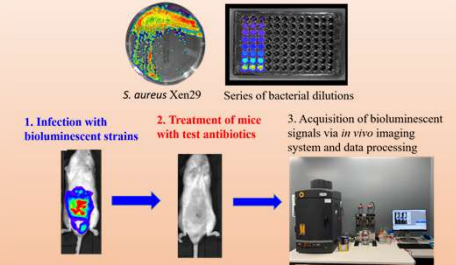
(A) Comparison of luminescence signals between group of mice (n=6) challenged with bioluminescent *S. aureus* and treated with indicated drugs. ns, not significant; *, $p < 0.05$; **, $p < 0.01$; Mann-Whitney *U*-test (one-tailed).

(B) Survival analysis for mice treated with the indicated drugs, ns, not significant; *, $p < 0.05$; **, $p < 0.01$; Log-rank (Mantel-Cox test).

(C) Ventral and dorsal images of representative CD1 mice challenged with bioluminescent *S. aureus* Xen29. At 8 h post-infection, all mice treated with vehicle only had become moribund, indicated by “no surviving mice” at 10 h.

Method

A bioluminescent *S. aureus* sepsis mouse model



Mice were treated with benzguinol A or benzguinol B (20 mg/kg), daptomycin (6 mg/kg), or vehicle at 2, 6, and 10 h post-infection and imaged at 0 h, 2 h, 4 h, 6 h, 8 h, 10 h, 12 h, 24 h, 36 h, 48 h and 72 h.

Result

- Three intraperitoneal doses of benzguinol A or B at 20 mg/kg elicited a statistically significant reduction in *S. aureus* populations and prolonged survival times of mice compared to the vehicle-only treated mice (figure 2).
- Benzguinol A showed slightly better efficacy, especially in terms of survival percentage.

Conclusion

This study demonstrates that the new antibacterial class represented by benzguinols could provide promising new scaffolds for further pharmaceutical and medicinal chemistry development for the treatment of multidrug-resistance development.

Appendix 7

Publication award outcome

Gordon Howarth <gordon.howarth@adelaide.edu.au>

Wed 24/11/2021 3:05 PM

To: Hang Thi Nguyen <hang.t.nguyen@adelaide.edu.au>

Cc: Michele Landers <michele.landiers@adelaide.edu.au>

Hi Hang,

Congratulations! You will be pleased to hear that you have won one of the Research Committee's publication incentive awards.

Please discuss accessing the funds with your supervisor (contact Michele Landers: School Finance Officer).

Well done!

Regards,

Gordon (on behalf of the Research Committee)

Professor Gordon S Howarth PhD, AGAF, ARCPA

Associate Head (Research)

Postgraduate Coordinator

School of Animal and Veterinary Sciences

Director of Postgraduate Education

Faculty of Sciences

University of Adelaide (Roseworthy Campus)

SOUTH AUSTRALIA 5371

Ph : +61 8 8313 7885

e-mail: gordon.howarth@adelaide.edu.au

Affiliate Professor

Gastroenterology Department

Women's and Children's Hospital

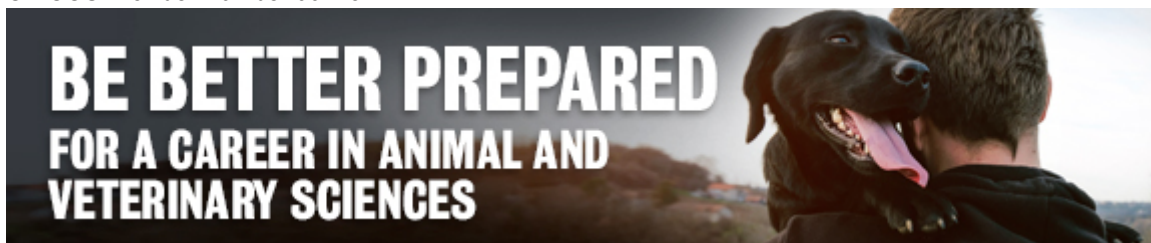
72 King William Road

North Adelaide

SOUTH AUSTRALIA 5006

Ph : +61 8 8161 6872

CRICOS Provider Number 00123M



IMPORTANT:

[This message may contain confidential or legally privileged information. If you think it was sent to you by mistake, please delete all copies and advise the sender. For the purposes of the SPAM Act 2003, this email is authorised by The University of Adelaide.](#)

Bibliography

1. Michael, C.A.; Dominey-Howes, D.; Labbate, M. The antimicrobial resistance crisis: Causes, consequences, and management. *Public Health Front* **2014**, *2*, 145, 1-8, doi:10.3389/fpubh.2014.00145.
2. Merker, M.; Tueffers, L.; Vallier, M.; Groth, E.E.; Sonnenkalb, L.; Unterweger, D.; Baines, J.F.; Niemann, S.; Schulenburg, H. Evolutionary approaches to combat antibiotic resistance: Opportunities and challenges for precision medicine. *Front. Microbiol* **2020**, *11*, 1938, doi:10.3389/fimmu.2020.01938.
3. Laxminarayan, R.; Duse, A.; Wattal, C.; Zaidi, A.K.M.; Wertheim, H.F.L.; Sumpradit, N.; Vlieghe, E.; Hara, G.L.; Gould, I.M.; Goossens, H.; et al. Antibiotic resistance-the need for global solutions. *Lancet Infect Dis* **2013**, *13*, 1057-98, doi:10.1016/S1473-3099(13)70318-9.
4. ECDPC. 33000 people die every year due to infections with antibiotic-resistant bacteria. <https://www.ecdc.europa.eu/en/news-events/33000-people-die-every-year-due-infections-antibiotic-resistant-bacteria>.
5. CDC. Antibiotic resistance threats in the United States, 2019 <https://www.cdc.gov/drugresistance/pdf/threats-report/2019-ar-threats-report-508.pdf>.
6. O'Neill, J. Tackling drug-resistant infections globally: final report and recommendations, May, 2016. https://amrreview.org/sites/default/files/160518_Final%20paper_with%20cover.pdf.
7. Cecchini, M.; Langer, J.; Slawomirski, L. Antimicrobial resistance in G7 countries and beyond: economic issues, policies and options for action. *OECD* **2015**, 1-75.
8. Teillant, A.; Gandra, S.; Barter, D.; Morgan, D.J.; Laxminarayan, R. Potential burden of antibiotic resistance on surgery and cancer chemotherapy antibiotic prophylaxis in the USA: a literature review and modelling study. *Lancet Infect Dis* **2015**, *15*, 1429-37, doi:10.1016/S1473-3099(15)00270-4.
9. Pendleton, J.N.; Gorman, S.P.; Gilmore, B.F. Clinical relevance of the ESKAPE pathogens. *Expert Rev Anti Infect Ther* **2013**, *11*, 297-308, doi:10.1586/eri.13.12.
10. Dadgostar, P. Antimicrobial Resistance: Implications and costs. *Infect Drug Resist* **2019**, *12*, 3903-10, doi:10.2147/IDR.S234610.
11. Arzanlou, M.; Chai, W.C.; Venter, H. Intrinsic, adaptive and acquired antimicrobial resistance in Gram-negative bacteria. *Essays Biochem* **2017**, *61*, 49-59, doi:10.1042/ebc20160063.
12. Diekema, D.J.; Hsueh, P.R.; Mendes, R.E.; Pfaller, M.A.; Rolston, K.V.; Sader, H.S.; Jones, R.N. The microbiology of bloodstream infection: 20-Year trends from the SENTRY antimicrobial surveillance program. *Antimicrob Agents Chemother* **2019**, *63*, doi:10.1128/AAC.00355-19.
13. Ventola, C.L. The antibiotic resistance crisis: part 1: Causes and threats. *P & T* **2015**, *40*, 277-83, doi:PMC4378521.
14. Bassetti, M.; Peghin, M.; Vena, A.; Giacobbe, D.R. Treatment of infections due to MDR Gram-negative bacteria. *Front Med* **2019**, *6*, doi:10.3389/fmed.2019.00074.

15. Stewart, A.G.; Harris, P.N.A.; Chatfield, M.; Evans, S.R.; van Duin, D.; Paterson, D.L. Modern clinician-initiated clinical trials to determine optimal therapy for multi-drug resistant Gram-negative infections. *Clin Infect Dis* **2019**, doi:10.1093/cid/ciz1132.
16. Voulgaris, G.L.; Voulgari, M.L.; Falagas, M.E. Developments on antibiotics for multidrug resistant bacterial Gram-negative infections. *Expert Rev Anti Infect Ther* **2019**, *17*, 387-401, doi:10.1080/14787210.2019.1610392.
17. Zabawa, T.P.; Pucci, M.J.; Parr, T.R.; Lister, T. Treatment of Gram-negative bacterial infections by potentiation of antibiotics. *Curr Opin Microbiol* **2016**, *33*, 7-12, doi:10.1016/j.mib.2016.05.005.
18. Andrei, S.; Droc, G.; Stefan, G. FDA approved antibacterial drugs: 2018-2019. *Discoveries (Craiova)* **2019**, *7*, e102-e02, doi:10.15190/d.2019.15.
19. The Pew Charitable Trusts Organization. Tracking the global pipeline of antibiotics in development, March 2021. <https://www.pewtrusts.org/en/research-and-analysis/issue-briefs/2021/03/tracking-the-global-pipeline-of-antibiotics-in-development>.
20. Lgcstandards. Breeding like bacteria-the spread of antibiotic resistance. https://www.lgcstandards.com/IT/en/Resources/Blogs/Antibiotic_resistance.
21. Pierce, J.; Apisarnthanarak, A.; Schellack, N.; Cornistein, W.; Maani, A.A.; Adnan, S.; Stevens, M.P. Global antimicrobial stewardship with a focus on low- and middle-income countries: A position statement for the international society for infectious diseases. *Int J Infectious Dis* **2020**, *96*, 621-29, doi:10.1016/j.ijid.2020.05.126.
22. Willyard, C. The drug-resistant bacteria that pose the greatest health threats. *Nature* **2017**, *543*, 15, doi:10.1038/nature.2017.21550.
23. Oliveira, J.; Reygaert, W.C. *Gram negative bacteria*; StatPearls Publishing, Treasure Island (FL): 2021.
24. Dezza, F.C.; Curtolo, A.; Volpicelli, L.; Ceccarelli, G.; Oliva, A.; Venditti, M. Are follow-up blood cultures useful in the antimicrobial management of Gram-negative bacteremia? A reappraisal of their role based on current knowledge. *Antibiotics (Basel)* **2020**, *9*, doi:10.3390/antibiotics9120895.
25. Santajit, S.; Indrawattana, N. Mechanisms of antimicrobial resistance in ESKAPE pathogens. *Biomed Res Int* **2016**, *2016*, 2475067, doi:10.1155/2016/2475067.
26. Breijyeh, Z.; Jubeh, B.; Karaman, R. Resistance of Gram-negative bacteria to current antibacterial agents and approaches to resolve it. *Molecules (Basel)* **2020**, *25*, 1340, doi:10.3390/molecules25061340.
27. World Health Organization. WHO publishes list of bacteria for which new antibiotics are urgently needed, Feb 27, 2017. <https://www.who.int/news/item/27-02-2017-who-publishes-list-of-bacteria-for-which-new-antibiotics-are-urgently-needed>.
28. Maltezou, H.C. Metallo- β -lactamases in Gram-negative bacteria: Introducing the era of pan-resistance? *Int J Antimicrob Agents* **2009**, *33*, 405.e1-05.e7, doi:10.1016/j.ijantimicag.2008.09.003.
29. World Health Organization. Central Asian and Eastern European surveillance of antimicrobial resistance: annual report 2018. <https://apps.who.int/iris/handle/10665/324806>.

30. Wong, D.; Nielsen, T.B.; Bonomo, R.A.; Pantapalangkoor, P.; Luna, B.; Spellberg, B. Clinical and pathophysiological overview of *Acinetobacter* infections: A century of challenges. *Clin Microbiol Rev* **2017**, *30*, 409-47, doi:10.1128/CMR.00058-16.
31. Esterly, J.S.; Griffith, M.; Qi, C.; Malczynski, M.; Postelnick, M.J.; Scheetz, M.H. Impact of carbapenem resistance and receipt of active antimicrobial therapy on clinical outcomes of *Acinetobacter baumannii* bloodstream infections. *Antimicrob Agents Chemother* **2011**, *55*, 4844-49, doi:10.1128/AAC.01728-10.
32. Pogue, J.M.; Mann, T.; Barber, K.E.; Kaye, K.S. Carbapenem-resistant *Acinetobacter baumannii*: Epidemiology, surveillance and management. *Expert Rev Anti Infect Ther* **2013**, *11*, 383-93, doi:10.1586/eri.13.14.
33. Isler, B.; Doi, Y.; Bonomo, R.A.; Paterson, D.L. New treatment options against carbapenem-resistant *Acinetobacter baumannii* infections. *Antimicrob Agents Chemother* **2019**, *63*, doi:10.1128/aac.01110-18.
34. Theriault, N.; Tillotson, G.; Sandrock, C.E. Global travel and Gram-negative bacterial resistance; implications on clinical management. *Expert Rev Anti Infect Ther* **2021**, *19*, 181-96, doi:10.1080/14787210.2020.1813022.
35. Codjoe, F.S.; Donkor, E.S. Carbapenem resistance: A review. *Med Sci (Basel)* **2017**, *6*, 1, doi:10.3390/medsci6010001.
36. Gupta, N.; Limbago, B.M.; Patel, J.B.; Kallen, A.J. Carbapenem-resistant Enterobacteriaceae: Epidemiology and prevention. *Clin Infect Dis* **2011**, *53*, 60-67, doi:10.1093/cid/cir202
37. Yigit, H.; Queenan, A.M.; Anderson, G.J.; Domenech-Sanchez, A.; Biddle, J.W.; Steward, C.D.; Alberti, S.; Bush, K.; Tenover, F.C. Novel carbapenem-hydrolyzing beta-lactamase, KPC-1, from a carbapenem-resistant strain of *Klebsiella pneumoniae*. *Antimicrob Agents Chemother* **2001**, *45*, 1151-61, doi:10.1128/aac.45.4.1151-1161.2001.
38. European Centre for Disease Prevention Control. Surveillance of antimicrobial resistance in Europe. <https://www.ecdc.europa.eu/en/publications-data/surveillance-antimicrobial-resistance-europe-2018>.
39. Hall, J.M.; Corea, E.; Sanjeevani, H.D.A.; Inglis, T.J.J. Molecular mechanisms of β -lactam resistance in carbapenemase-producing *Klebsiella pneumoniae* from Sri Lanka. *J Med Microbiol* **2014**, *63*, 1087-92, doi:10.1099/jmm.0.076760-0.
40. Hall, J.M.; Ingram, P.R.; O'Reilly, L.C.; Inglis, T.J.J. Temporal flux in β -lactam resistance among *Klebsiella pneumoniae* in Western Australia. *J Med Microbiol* **2016**, *65*, 429-37, doi:10.1099/jmm.0.000242.
41. Wei, D.D.; Wan, L.G.; Deng, Q.; Liu, Y. Emergence of KPC-producing *Klebsiella pneumoniae* hypervirulent clone of capsular serotype K1 that belongs to sequence type 11 in Mainland China. *Diagn Microbiol Infect Dis* **2016**, *85*, 192-4, doi:10.1016/j.diagmicrobio.2015.03.012.
42. Cheng, N.C.; Yu, Y.C.; Tai, H.C.; Hsueh, P.R.; Chang, S.C.; Lai, S.Y.; Yi, W.C.; Fang, C.T. Recent trend of necrotizing fasciitis in Taiwan: Focus on monomicrobial *Klebsiella pneumoniae* necrotizing fasciitis. *Clin Infect Dis* **2012**, *55*, 930-9, doi:10.1093/cid/cis565.
43. Krapp, F.; Morris, A.R.; Ozer, E.A.; Hauser, A.R. Virulence characteristics of carbapenem-resistant *Klebsiella pneumoniae* strains from patients with necrotizing skin and soft tissue infections. *Sci Rep* **2017**, *7*, 13533, doi:10.1038/s41598-017-13524-8.

44. Bernal, N.P.; Latenser, B.A.; Born, J.M.; Liao, J. Trends in 393 necrotizing acute soft tissue infection patients 2000-2008. *Burns* **2012**, *38*, 252-60, doi:10.1016/j.burns.2011.07.008.
45. Theuretzbacher, U. Global antimicrobial resistance in Gram-negative pathogens and clinical need. *Curr Opin Microbiol* **2017**, *39*, 106-12, doi:10.1016/j.mib.2017.10.028.
46. Rostami, S.; Farajzadeh Sheikh, A.; Shoja, S.; Farahani, A.; Tabatabaiefar, M.A.; Jolodar, A.; Sheikhi, R. Investigating of four main carbapenem-resistance mechanisms in high-level carbapenem resistant *Pseudomonas aeruginosa* isolated from burn patients. *J Chin Med Assoc* **2018**, *81*, 127-32, doi:10.1016/j.jcma.2017.08.016.
47. Walters, M.S.; Grass, J.E.; Bulens, S.N.; Hancock, E.B.; Phipps, E.C.; Muleta, D.; Mounsey, J.; Kainer, M.A.; Concannon, C.; Dumyati, G.; et al. Carbapenem-resistant *Pseudomonas aeruginosa* at US emerging infections program sites, 2015. *Emerg Infect Dis* **2019**, *25*, 1281-88, doi:10.3201/eid2507.181200.
48. Steward, K. Gram-positive vs Gram-negative, Nov 29 2021. <https://www.technologynetworks.com/immunology/articles/gram-positive-vs-gram-negative-323007>.
49. Reeves, P. Role of O-antigen variation in the immune response. *Trends Microbiol* **1995**, *3*, 381-6, doi:10.1016/s0966-842x(00)88983-0.
50. Silhavy, T.J.; Kahne, D.; Walker, S. The bacterial cell envelope. *Cold Spring Harb Perspect* **2010**, *2*, a000414-a14, doi:10.1101/cshperspect.a000414.
51. Zowawi, H.M.; Harris, P.N.; Roberts, M.J.; Tambyah, P.A.; Schembri, M.A.; Pezzani, M.D.; Williamson, D.A.; Paterson, D.L. The emerging threat of multidrug-resistant Gram-negative bacteria in urology. *Nat Rev Urol* **2015**, *12*, 570-84, doi:10.1038/nrurol.2015.199.
52. Du, D.; Wang-Kan, X.; Neuberger, A.; van Veen, H.W.; Pos, K.M.; Piddock, L.J.V.; Luisi, B.F. Multidrug efflux pumps: Structure, function and regulation. *Nat Rev Microbiol* **2018**, *16*, 523-39, doi:10.1038/s41579-018-0048-6.
53. Chitsaz, M.; Brown, M.H. The role played by drug efflux pumps in bacterial multidrug resistance. *Essays Biochem* **2017**, *61*, 127-39, doi:10.1042/ebc20160064.
54. Venter, H.; Mowla, R.; Ohene-Agyei, T.; Ma, S. RND-type drug efflux pumps from Gram-negative bacteria: Molecular mechanism and inhibition. *Front Microbiol* **2015**, *6*, 377, doi:10.3389/fmicb.2015.00377.
55. Masuda, N.; Sakagawa, E.; Ohya, S.; Gotoh, N.; Tsujimoto, H.; Nishino, T. Substrate specificities of MexAB-OprM, MexCD-OprJ, and MexXY-oprM efflux pumps in *Pseudomonas aeruginosa*. *Antimicrob Agents Chemother* **2000**, *44*, 3322-27, doi:10.1128/AAC.44.12.3322-3327.2000.
56. Bonomo, R.A. β -lactamases: A focus on current challenges. *Perspect Biol Med* **2017**, *7*, a025239, doi:10.1101/cshperspect.a025247.
57. Ramirez, M.S.; Tolmasky, M.E. Aminoglycoside modifying enzymes. *Drug Resist Updat* **2010**, *13*, 151-71, doi:10.1016/j.drug.2010.08.003.
58. Llano-Sotelo, B.; Azucena Jr, E.F.; Kotra, L.P.; Mobashery, S.; Chow, C.S. Aminoglycosides modified by resistance enzymes display diminished binding to the bacterial ribosomal aminoacyl-tRNA site. *Chem Biol* **2002**, *9*, 455-63, doi:10.1016/S1074-5521(02)00125-4.

59. Band, V.I.; Weiss, D.S. Mechanisms of antimicrobial peptide resistance in Gram-negative bacteria. *Antibiotics (Basel)* **2015**, *4*, 18-41, doi:10.3390/antibiotics4010018.
60. McPhee, J.B.; Lewenza, S.; Hancock, R.E. Cationic antimicrobial peptides activate a two-component regulatory system, PmrA-PmrB, that regulates resistance to polymyxin B and cationic antimicrobial peptides in *Pseudomonas aeruginosa*. *Mol Microbiol* **2003**, *50*, 205-17, doi:10.1046/j.1365-2958.2003.03673.x.
61. Ochs, M.M.; McCusker, M.P.; Bains, M.; Hancock, R.E. Negative regulation of the *Pseudomonas aeruginosa* outer membrane porin OprD selective for imipenem and basic amino acids. *Antimicrob Agents Chemother* **1999**, *43*, 1085-90, doi:10.1128/AAC.43.5.1085.
62. Tenover, F.C. Mechanisms of antimicrobial resistance in bacteria. *Am J Med*. **2006**, *119*, S3-S10, doi:10.1016/j.amjmed.2006.03.011.
63. Hooper, D.C. Mechanisms of action and resistance of older and newer fluoroquinolones. *Lancet Infect Dis* **2002**, *2*, 530-38, doi:10.1086/314056.
64. Hooper, D.C. Fluoroquinolone resistance among Gram-positive cocci. *Lancet Infect Dis* **2002**, *2*, 530-38, doi:10.1016/S1473-3099(02)00369-9.
65. Lee, C.S.; Doi, Y. Therapy of infections due to carbapenem-resistant Gram-negative pathogens. *J Infect Chemother* **2014**, *46*, 149-64, doi:10.3947/ic.2014.46.3.149.
66. Hansen, G.T. Continuous evolution: Perspective on the epidemiology of carbapenemase resistance among Enterobacterales and other Gram-negative bacteria. *Infect Dis Ther* **2021**, *10*, 75-92, doi:10.1007/s40121-020-00395-2.
67. De Oliveira, D.M.P.; Forde, B.M.; Kidd, T.J.; Harris, P.N.A.; Schembri, M.A.; Beatson, S.A.; Paterson, D.L.; Walker, M.J. Antimicrobial resistance in ESKAPE pathogens. *Clin Microbiol Rev* **2020**, *33*, doi:10.1128/cmr.00181-19.
68. Krause, K.M.; Serio, A.W.; Kane, T.R.; Connolly, L.E. Aminoglycosides: An overview. *Cold Spring Harb Perspect Med* **2016**, *6*, a027029, doi:10.1101/cshperspect.a027029.
69. Gonzalez-Padilla, M.; Torre-Cisneros, J.; Rivera-Espinar, F.; Pontes-Moreno, A.; López-Cerero, L.; Pascual, A.; Natera, C.; Rodríguez, M.; Salcedo, I.; Rodríguez-López, F.; et al. Gentamicin therapy for sepsis due to carbapenem-resistant and colistin-resistant *Klebsiella pneumoniae*. *J Antimicrob Chemother* **2015**, *70*, 905-13, doi:10.1093/jac/dku432.
70. Doi, Y. Treatment options for carbapenem-resistant Gram-negative bacterial infections. *Clin Infect Dis* **2019**, *69*, S565-s75, doi:10.1093/cid/ciz830.
71. De Souza Mendes, C.D.; Urso; De Souza Antunes, A.M. Pipeline of known chemical classes of antibiotics. *Antibiotics (Basel)* **2013**, *2*, 500-34, doi:10.3390/antibiotics2040500.
72. Taubert, M.; Chiesa, J.; Lückermann, M.; Fischer, C.; Dalhoff, A.; Fuhr, U. Pharmacokinetics of intravenous finafloxacin in healthy volunteers. *Antimicrob Agents Chemother* **2017**, *61*, doi:10.1128/aac.01122-17.
73. Bader, M.S.; Loeb, M.; Leto, D.; Brooks, A.A. Treatment of urinary tract infections in the era of antimicrobial resistance and new antimicrobial agents. *Postgrad Med* **2020**, *132*, 234-50, doi:10.1080/00325481.2019.1680052.
74. McKeage, K. Finafloxacin: first global approval. *Drugs* **2015**, *75*, 687-93, doi:10.1007/s40265-015-0384-z.

75. Lemaire, S.; Van Bambeke, F.; Tulkens, P.M. Activity of finafloxacin, a novel fluoroquinolone with increased activity at acid pH, towards extracellular and intracellular *Staphylococcus aureus*, *Listeria monocytogenes* and *Legionella pneumophila*. *Int J Antimicrob Agents* **2011**, *38*, 52-9, doi:10.1016/j.ijantimicag.2011.03.002.
76. Emrich, N.C.; Heisig, A.; Stubbings, W.; Labischinski, H.; Heisig, P. Antibacterial activity of finafloxacin under different pH conditions against isogenic strains of *Escherichia coli* expressing combinations of defined mechanisms of fluoroquinolone resistance. *J Antimicrob Chemother* **2010**, *65*, 2530-3, doi:10.1093/jac/dkq375.
77. Peirano, G.; Ahmed-Bentley, J.; Woodford, N.; Pitout, J.D. New delhi metallo-beta-lactamase from traveler returning to Canada. *Emerg Infect Dis* **2011**, *17*, 242-4, doi:10.3201/eid1702.101313.
78. Falagas, M.E.; Kastoris, A.C.; Kapaskelis, A.M.; Karageorgopoulos, D.E. Fosfomycin for the treatment of multidrug-resistant, including extended-spectrum beta-lactamase producing, Enterobacteriaceae infections: A systematic review. *Lancet Infect Dis* **2010**, *10*, 43-50, doi:10.1016/s1473-3099(09)70325-1.
79. Papp-Wallace, K.M.; Endimiani, A.; Taracila, M.A.; Bonomo, R.A. Carbapenems: past, present, and future. *Antimicrob Agents Chemother* **2011**, *55*, 4943-60, doi:10.1128/aac.00296-11.
80. Papp-Wallace, K.M.; Bonomo, R.A. New β -lactamase inhibitors in the clinic. *Infect Dis Clin North Am* **2016**, *30*, 441-64, doi:10.1016/j.idc.2016.02.007.
81. El-Gamal, M.I.; Brahim, I.; Hisham, N.; Aladdin, R.; Mohammed, H.; Bahaeldin, A. Recent updates of carbapenem antibiotics. *Eur J Med Chem* **2017**, *131*, 185-95, doi:10.1016/j.ejmech.2017.03.022.
82. Groft, L.M.; Claeys, K.C.; Heil, E.L. An evaluation of meropenem/vaborbactam for the treatment of nosocomial pneumonia. *Expert Opin Pharmacother* **2021**, *22*, 265-71, doi:10.1080/14656566.2020.1840552.
83. Patel, U.C.; Fowler, M.A. Ertapenem-associated neurotoxicity in the spinal cord injury (SCI) population: A case series. *J Spinal Cord Med* **2018**, *41*, 735-40, doi:10.1080/10790268.2017.1368960.
84. Hilas, O.; Ezzo, D.C.; Jodlowski, T.Z. Doripenem (doribax), a new carbapenem antibacterial agent. *Pharmacol Ther* **2008**, *33*, 134-80, doi:PMC2730083.
85. Cherif, B.; Triki, H.; Sahnoun, S.; Hamden, K.; Sallemi, A.; Charfi, S.; Lassoued, S. Imipenem toxicity in male reproductive organs as a result of inflammatory microenvironment and oxidative stress in germinal cells. *Toxicology* **2019**, *416*, 44-53, doi:10.1016/j.tox.2019.02.001.
86. Elias, R.; Duarte, A.; Perdigão, J. A molecular perspective on colistin and *Klebsiella pneumoniae*: Mode of action, resistance genetics, and phenotypic susceptibility. *J Diagnostics* **2021**, *11*, 1165, doi:10.3390/diagnostics11071165.
87. Becker, B.; Cooper, M.A. Aminoglycoside antibiotics in the 21st century. *ACS Chem Biol* **2013**, *8*, 105-15, doi:10.1021/cb3005116.
88. Bradford, P.A. Tigecycline: A first in class glycylcycline. *Clin Microbiol News* **2004**, *26*, 163-68, doi:10.1016/j.clinmicnews.2004.10.001.

89. Aghamali, M.; Sedighi, M.; Mohammadzadeh, N.; Abbasian, S.; Ghafouri, Z.; Kouhsari, E. Fosfomycin: Mechanisms and the increasing prevalence of resistance. *J Med Microbiol* **2019**, *68*, 11-25, doi:10.1099/jmm.0.000874.
90. Bartoletti, R.; Cai, T.; Perletti, G.; F, M.E.W.; Bjerklund Johansen, T.E. Finafloxacin for the treatment of urinary tract infections. *Expert Opin Investig Drugs* **2015**, *24*, 957-63, doi:10.1517/13543784.2015.1052401.
91. Wang, Y.; Wang, J.; Wang, R.; Cai, Y. Resistance to ceftazidime - avibactam and underlying mechanisms. *J Glob Antimicrob* **2020**, *22*, 18-27, doi:10.1016/j.jgar.2019.12.009.
92. Patel, T.S.; Pogue, J.M.; Mills, J.P.; Kaye, K.S. Meropenem-vaborbactam: A new weapon in the war against infections due to resistant Gram-negative bacteria. *Future microbiol* **2018**, *13*, 971-83, doi:10.2217/fmb-2018-0054.
93. Petty, L.A.; Henig, O.; Patel, T.S.; Pogue, J.M.; Kaye, K.S. Overview of meropenem-vaborbactam and newer antimicrobial agents for the treatment of carbapenem-resistant Enterobacteriaceae. *Infectdrug resist* **2018**, *11*, 1461-72, doi:10.2147/IDR.S150447.
94. Pogue, J.M.; Kaye, K.S.; Veve, M.P.; Patel, T.S.; Gerlach, A.T.; Davis, S.L.; Puzniak, L.A.; File, T.M.; Olson, S.; Dhar, S.; et al. Ceftolozane/tazobactam vs polymyxin or aminoglycoside-based regimens for the treatment of drug-resistant *Pseudomonas aeruginosa*. *Clin Infect Dis* **2020**, *71*, 304-10, doi:10.1093/cid/ciz816.
95. Heo, Y.-A. Imipenem/cilastatin/relebactam: A review in Gram-negative bacterial infections. *Drugs* **2021**, *81*, 377-88, doi:10.1007/s40265-021-01471-8.
96. Katip, W.; Uitrakul, S.; Oberdorfer, P. A comparison of colistin versus colistin plus meropenem for the treatment of carbapenem-resistant *Acinetobacter baumannii* in critically ill patients: A propensity score-matched analysis. *Antibiotics (Basel)* **2020**, *9*, doi:10.3390/antibiotics9100647.
97. Mansour, H.; Ouweini, A.E.L.; Chahine, E.B.; Karaoui, L.R. Imipenem/cilastatin/relebactam: A new carbapenem β -lactamase inhibitor combination. *Am J Health Syst Pharm* **2021**, *78*, 674-83, doi:10.1093/ajhp/zxab012.
98. Zhanel, G.G.; Golden, A.R.; Zelenitsky, S.; Wiebe, K.; Lawrence, C.K.; Adam, H.J.; Idowu, T.; Domalaon, R.; Schweizer, F.; Zhanel, M.A.; et al. Cefiderocol: A siderophore cephalosporin with activity against carbapenem-resistant and multidrug-resistant Gram-negative bacilli. *Drugs* **2019**, *79*, 271-89, doi:10.1007/s40265-019-1055-2.
99. Shaeer, K.M.; Zmarlicka, M.T.; Chahine, E.B.; Piccicacco, N.; Cho, J.C. Plazomicin: A next-generation aminoglycoside. *Pharmacotherapy* **2019**, *39*, 77-93, doi:10.1002/phar.2203.
100. Eljaaly, K.; Alharbi, A.; Alshehri, S.; Ortwine, J.K.; Pogue, J.M. Plazomicin: A novel aminoglycoside for the treatment of resistant Gram-negative bacterial infections. *Drugs* **2019**, *79*, 243-69, doi:10.1007/s40265-019-1054-3.
101. Bilinskaya, A.; Linder, K.E.; Kutji, J.L. Plazomicin: An intravenous aminoglycoside antibacterial for the treatment of complicated urinary tract infections. *Expert Rev Anti Infect Ther* **2020**, *18*, 705-20, doi:10.1080/14787210.2020.1759419.
102. Karaikos, I.; Lagou, S.; Pontikis, K.; Rapti, V.; Poulakou, G. The "Old" and the "New" antibiotics for MDR Gram-negative pathogens: for whom, when, and how. *Public Health Front.* **2019**, *7*, doi:10.3389/fpubh.2019.00151.

103. Grossman, T.H.; O'Brien, W.; Kerstein, K.O.; Sutcliffe, J.A. Eravacycline (TP-434) is active *in vitro* against biofilms formed by uropathogenic *Escherichia coli*. *Antimicrob Agents Chemother* **2015**, *59*, 2446-9, doi:10.1128/aac.04967-14.
104. Rodríguez-Baño, J.; Gutiérrez-Gutiérrez, B.; Machuca, I.; Pascual, A. Treatment of infections caused by extended-spectrum-beta-lactamase-, AmpC-, and carbapenemase-producing Enterobacteriaceae. *Clin Microbiol Rev* **2018**, *31*, doi:10.1128/cmr.00079-17.
105. Chiotos, K.; Hayes, M.; Gerber, J.S.; Tamma, P.D. Treatment of carbapenem-resistant Enterobacteriaceae infections in children. *J Pediatric Infect Dis Soc* **2020**, *9*, 56-66, doi:10.1093/jpids/piz085.
106. Lee, Y.R.; Burton, C.E. Eravacycline, a newly approved fluorocycline. *Eur J Clin Microbiol Infect Dis* **2019**, *38*, 1787-94, doi:10.1007/s10096-019-03590-3.
107. Seifert, H.; Stefanik, D.; Olesky, M.; Higgins, P.G. *In vitro* activity of the novel fluorocycline TP-6076 against carbapenem-resistant *Acinetobacter baumannii*. *Int J Antimicrob Agents* **2020**, *55*, 105829, doi:10.1016/j.ijantimicag.2019.10.010.
108. Zhanel, G.G.; Esquivel, J.; Zelenitsky, S.; Lawrence, C.K.; Adam, H.J.; Golden, A.; Hink, R.; Berry, L.; Schweizer, F.; Zhanel, M.A.; et al. Omadacycline: A novel oral and intravenous aminomethylcycline antibiotic agent. *Drugs* **2020**, *80*, 285-313, doi:10.1007/s40265-020-01257-4.
109. Shirley, M. Ceftazidime-Avibactam: A review in the treatment of serious Gram-negative bacterial infections. *Drugs* **2018**, *78*, 675-92, doi:10.1007/s40265-018-0902-x.
110. Fraile-Ribot, P.A.; Cabot, G.; Mulet, X.; Periañez, L.; Martín-Pena, M.L.; Juan, C.; Pérez, J.L.; Oliver, A. Mechanisms leading to *in vivo* ceftolozane/tazobactam resistance development during the treatment of infections caused by MDR *Pseudomonas aeruginosa*. *J Antimicrob Chemother* **2018**, *73*, 658-63, doi:10.1093/jac/dkx424.
111. Sorbera, M.; Chung, E.; Ho, C.W.; Marzella, N. Ceftolozane/tazobactam: A new option in the treatment of complicated Gram-negative infections. *P & T* **2014**, *39*, 825-32, doi:PMC4264669.
112. Wooley, M.; Miller, B.; Krishna, G.; Hershberger, E.; Chandorkar, G. Impact of renal function on the pharmacokinetics and safety of ceftolozane-tazobactam. *Antimicrob Agents Chemother* **2014**, *58*, 2249-55, doi:10.1128/aac.02151-13.
113. Bassetti, M.; Echols, R.; Matsunaga, Y.; Ariyasu, M.; Doi, Y.; Ferrer, R.; Lodise, T.P.; Naas, T.; Niki, Y.; Paterson, D.L.; et al. Efficacy and safety of cefiderocol or best available therapy for the treatment of serious infections caused by carbapenem-resistant Gram-negative bacteria (CREDIBLE-CR): A randomised, open-label, multicentre, pathogen-focused, descriptive, phase 3 trial. *Lancet Infect Dis* **2021**, *21*, 226-40, doi:10.1016/s1473-3099(20)30796-9.
114. Wu, J.Y.; Srinivas, P.; Pogue, J.M. Cefiderocol: A novel agent for the management of multidrug-resistant Gram-negative organisms. *Infect Dis Ther* **2020**, *9*, 17-40, doi:10.1007/s40121-020-00286-6.
115. Alosaimy, S.; Abdul-Mutakabbir, J.C.; Kebriaei, R.; Jorgensen, S.C.; Rybak, M.J. Evaluation of eravacycline: A novel fluorocycline. *Pharmacotherapy* **2020**, *40*, 221-38, doi:10.1002/phar.2366.

116. Lan, S.-H.; Chang, S.-P.; Lai, C.-C.; Lu, L.-C.; Chao, C.-M. The efficacy and safety of eravacycline in the treatment of complicated intra-abdominal infections: a systemic review and meta-analysis of randomized controlled trials. *J Clin Med* **2019**, *8*, 866, doi:10.3390/jcm8060866.
117. Barber, K.E.; Bell, A.M.; Wingler, M.J.B.; Wagner, J.L.; Stover, K.R. Omadacycline enters the ring: A new antimicrobial contender. *Pharmacotherapy* **2018**, *38*, 1194-204, doi:10.1002/phar.2185.
118. Dougherty, J.A.; Sucher, A.J.; Chahine, E.B.; Shihadeh, K.C. Omadacycline: A new tetracycline antibiotic. *Ann Pharmacother* **2019**, *53*, 486-500, doi:10.1177/1060028018818094.
119. Moloney, M.G. Natural products as a source for novel antibiotics. *Trends Pharmacol Sci* **2016**, *37*, 689-701, doi:10.1016/j.tips.2016.05.001.
120. Durand, G.A.; Raoult, D.; Dubourg, G. Antibiotic discovery: History, methods and perspectives. *Int J Antimicrob Agents* **2019**, *53*, 371-82, doi:10.1016/j.ijantimicag.2018.11.010.
121. Genilloud, O. Natural products discovery and potential for new antibiotics. *Curr Opin in Microbiol* **2019**, *51*, 81-87, doi:10.1016/j.mib.2019.10.012.
122. Seyfi, R.; Kahaki, F.A.; Ebrahimi, T.; Montazersaheb, S.; Eyvazi, S.; Babaeipour, V.; Tarhriz, V. Antimicrobial peptides (AMPs): Roles, functions and mechanism of action. *Int J Pept Res Ther* **2020**, *26*, 1451-63, doi:10.1007/s10989-019-09946-9.
123. Browne, K.; Chakraborty, S.; Chen, R.; Willcox, M.D.; Black, D.S.; Walsh, W.R.; Kumar, N. A new era of antibiotics: The clinical potential of antimicrobial peptides. *Int J Mol Sci* **2020**, *21*, 7047, doi:10.3390/ijms21197047.
124. Narayana, J.L.; Chen, J.-Y. Antimicrobial peptides: Possible anti-infective agents. *Peptides* **2015**, *72*, 88-94, doi:10.1016/j.peptides.2015.05.012.
125. Aoki, W.; Ueda, M. Characterization of antimicrobial peptides toward the development of novel antibiotics. *Pharmaceuticals (Basel)* **2013**, *6*, 1055-81, doi:10.3390/ph6081055.
126. Wang, G.; Li, X.; Wang, Z. APD3: The antimicrobial peptide database as a tool for research and education. *Nucleic Acids Res* **2016**, *44*, D1087-93, doi:10.1093/nar/gkv1278.
127. Thaker, M.N.; Wright, G.D. Opportunities for synthetic biology in antibiotics: Expanding glycopeptide chemical diversity. *ACS Synth Biol* **2015**, *4*, 195-206, doi:10.1021/sb300092n.
128. Nagarajan, K.; Marimuthu, S.K.; Palanisamy, S.; Subbiah, L. Peptide therapeutics versus superbugs: Highlight on current research and advancements. *Int J Pept Res Ther* **2018**, *24*, 19-33, doi:10.1007/s10989-017-9650-0.
129. Nawrot, R.; Barylski, J.; Nowicki, G.; Broniarczyk, J.; Buchwald, W.; Goździcka-Józefiak, A. Plant antimicrobial peptides. *Folia Microbiol* **2014**, *59*, 181-96, doi:10.1007/s12223-013-0280-4.
130. Sperstad, S.V.; Haug, T.; Blencke, H.-M.; Styrvold, O.B.; Li, C.; Stensvåg, K. Antimicrobial peptides from marine invertebrates: Challenges and perspectives in marine antimicrobial peptide discovery. *Biotechnol Adv* **2011**, *29*, 519-30, doi:10.1016/j.biotechadv.2011.05.021.
131. Chandrasekaran, M.; Senthilkumar, A.; Venkatesalu, V. Antibacterial and antifungal efficacy of fatty acid methyl esters from the leaves of *Sesuvium portulacastrum* L. *Eur Rev Med Pharmacol Sci* **2011**, *15*, 775-80.

132. Alves, E.; Dias, M.; Lopes, D.; Almeida, A.; Domingues, M.d.R.; Rey, F. Antimicrobial lipids from plants and marine organisms: An overview of the current state-of-the-art and future prospects. *Antibiotics (Basel)* **2020**, *9*, 441, doi:doi.org/10.3390/antibiotics9080441.
133. Abubakar, M.N.; Majinda, R.R.T. GC-MS Analysis and preliminary antimicrobial activity of *albizia adianthifolia* (Schumach) and *pterocarpus angolensis* (DC). *Medicines (Basel)* **2016**, *3*, doi:10.3390/medicines3010003.
134. Martin-Loeches, I.; Dale, G.E.; Torres, A. Murepavadin: A new antibiotic class in the pipeline. *Expert Rev Anti Infect Ther* **2018**, *16*, 259-68, doi:10.1080/14787210.2018.1441024.
135. Melchers, M.J.; Teague, J.; Warn, P.; Hansen, J.; Bernardini, F.; Wach, A.; Obrecht, D.; Dale, G.E.; Mouton, J.W. Pharmacokinetics and pharmacodynamics of murepavadin in neutropenic mouse models. *Antimicrob Agents Chemother* **2019**, *63*, e01699-18, doi:10.1128/AAC.01699-18.
136. Bassetti, M.; Vena, A.; Castaldo, N.; Righi, E.; Peghin, M. New antibiotics for ventilator-associated pneumonia. *Curr Opin Infect Dis* **2018**, *31*, 177-86, doi:10.1097/qco.0000000000000438.
137. Dale, G.E.; Halabi, A.; Petersen-Sylla, M.; Wach, A.; Zwingelstein, C. Pharmacokinetics, tolerability, and safety of murepavadin, a novel antipseudomonal antibiotic, in subjects with mild, moderate, or severe renal function impairment. *Antimicrob Agents Chemother* **2018**, *62*, doi:10.1128/aac.00490-18.
138. Wach, A.; Dembowski, K.; Dale, G.E. Pharmacokinetics and safety of intravenous murepavadin infusion in healthy adult subjects administered single and multiple ascending doses. *Antimicrob Agents Chemother* **2018**, *62*, doi:10.1128/aac.02355-17.
139. Horcajada, J.P.; Montero, M.; Oliver, A.; Sorlí, L.; Luque, S.; Gómez-Zorrilla, S.; Benito, N.; Grau, S. Epidemiology and treatment of multidrug-resistant and extensively drug-resistant *Pseudomonas aeruginosa* infections. *Clin Microbiol Rev* **2019**, *32*, doi:10.1128/cmr.00031-19.
140. Jean, S.S.; Gould, I.M.; Lee, W.S.; Hsueh, P.R. New drugs for multidrug-resistant Gram-negative organisms: Time for stewardship. *Drugs* **2019**, *79*, 705-14, doi:10.1007/s40265-019-01112-1.
141. Fathizadeh, H.; Saffari, M.; Esmaeili, D.; Moniri, R.; Salimian, M. Evaluation of antibacterial activity of enterocin A-colicin E1 fusion peptide. *Iran J Basic Med Sci* **2020**, *23*, 1471-79, doi:10.22038/ijbms.2020.47826.11004.
142. Rossetto, G.; Bergese, P.; Colombi, P.; Depero, L.E.; Giuliani, A.; Nicoletto, S.F.; Pirri, G. Atomic force microscopy evaluation of the effects of a novel antimicrobial multimeric peptide on *Pseudomonas aeruginosa*. *Nanomedicine* **2007**, *3*, 198-207, doi:10.1016/j.nano.2007.06.002.
143. Imai, Y.; Meyer, K.J.; Iinishi, A.; Favre-Godal, Q.; Green, R.; Manuse, S.; Caboni, M.; Mori, M.; Niles, S.; Ghiglieri, M.; et al. A new antibiotic selectively kills Gram-negative pathogens. *Nature* **2019**, *576*, 459-64, doi:10.1038/s41586-019-1791-1.
144. Wright, G. Perspective: Synthetic biology revives antibiotics. *Nature* **2014**, *509*, S13, doi:10.1038/509S13a.
145. Lamb, S.S.; Wright, G.D. Accessorizing natural products: Adding to nature's toolbox. *Proc Natl Acad Sci* **2005**, *102*, 519-20, doi:10.1073/pnas.0408858102.

146. Wright, P.M.; Seiple, I.B.; Myers, A.G. The evolving role of chemical synthesis in antibacterial drug discovery. *Angew Chem Int Ed* **2014**, *53*, 8840-69, doi:10.1002/anie.201310843.
147. Wright, G. Synthetic biology revives antibiotics. *Nature* **2014**, *509*, 1, doi:10.1038/509S13a.
148. Zhang, Y.; Zhao, C.; Wang, Q.; Wang, X.; Chen, H.; Li, H.; Zhang, F.; Wang, H. Evaluation of the *in vitro* activity of new polymyxin B analogue SPR206 against clinical MDR, colistin-resistant and tigecycline-resistant Gram-negative bacilli. *J Antimicrob Chemother* **2020**, *75*, 2609-15, doi:10.1093/jac/dkaa217.
149. Roberts, K.D.; Zhu, Y.; Azad, M.A.K.; Han, M.-L.; Wang, J.; Wang, L.; Yu, H.H.; Horne, A.S.; Pinson, J.-A.; Rudd, D.; et al. A synthetic lipopeptide targeting top-priority multidrug-resistant Gram-negative pathogens. *Nat Commun* **2022**, *13*, 1625, doi:10.1038/s41467-022-29234-3.
150. Bruss, J.; Lister, T.; Gupta, V.K.; Stone, E.; Morelli, L.; Lei, Y.; Melnick, D. Single- and multiple-ascending-dose study of the safety, tolerability, and pharmacokinetics of the polymyxin derivative SPR206. *Antimicrob Agents Chemother* **2021**, *65*, e00739-21, doi:10.1128/AAC.00739-21.
151. Mendes, R.E.; Rhomberg, P.R.; Lister, T.; Cotroneo, N.; Parr, T.R.; Castanheira, M. *In vitro* activity analysis of a new generation polymyxin, SPR741, tested in combination with antimicrobial agents against a challenge set of Enterobacteriaceae, including molecularly characterized strains. *Antimicrob Agents Chemother* **2020**, doi:10.1128/AAC.00742-20.
152. Eckburg, P.B.; Lister, T.; Walpole, S.; Keutzer, T.; Utley, L.; Tomayko, J.; Kopp, E.; Farinola, N.; Coleman, S. Safety, tolerability, pharmacokinetics, and drug interaction potential of SPR741, an intravenous potentiator, after single and multiple ascending doses and when combined with β -lactam antibiotics in healthy subjects. *Antimicrob Agents Chemother* **2019**, *63*, e00892-19, doi:10.1128/AAC.00892-19.
153. Vaara, M.; Vaara, T.; Kuka, J.; Sevostjanovs, E.; Grinberga, S.; Dambrova, M.; Liepinsh, E. Excretion of the polymyxin derivative NAB739 in murine urine. *Antibiotics (Basel)* **2020**, *9*, 143, doi:10.3390/antibiotics9040143.
154. Vaara, M.; Sader, H.S.; Rhomberg, P.R.; Jones, R.N.; Vaara, T. Antimicrobial activity of the novel polymyxin derivative NAB739 tested against Gram-negative pathogens. *J Antimicrob Chemother* **2012**, *68*, 636-39, doi:10.1093/jac/dks438.
155. Vaara, M.; Vaara, T.; Vingsbo Lundberg, C. Polymyxin derivatives NAB739 and NAB815 are more effective than polymyxin B in murine *Escherichia coli* pyelonephritis. *J Antimicrob Chemother* **2017**, *73*, 452-55, doi:10.1093/jac/dkx394.
156. Vaara, M. New polymyxin derivatives that display improved efficacy in animal infection models as compared to polymyxin B and colistin. *Med Res Rev* **2018**, *38*, 1661-73, doi:10.1002/med.21494.
157. Huband, M.D.; Mendes, R.E.; Pfaller, M.A.; Lindley, J.M.; Strand, G.J.; Benn, V.J.; Zhang, J.; Li, L.; Zhang, M.; Tan, X.; et al. *In vitro* activity of KBP-7072, a novel third-generation tetracycline, against 531 recent geographically diverse and molecularly characterized *Acinetobacter baumannii* species complex isolates. *Antimicrob Agents Chemother* **2020**, *64*, doi:10.1128/aac.02375-19.

158. Huband, M.D.; Thompson, J.D.; Gurung, N.D.; Liu, Q.; Li, L.; Zhang, J.; Streit, J.M.; Castanheira, M. Activity of KBP-7072 (a novel aminomethylcycline) and comparators against 1,057 geographically diverse recent clinical isolates from the SENTRY surveillance program (2019). *Antimicrob Agents Chemother* **2021**, Aac0139721, doi:10.1128/aac.01397-21.
159. Tan, X.; Zhang, M.; Liu, Q.; Wang, P.; Zhou, T.; Benn, V.; Yang, F. *In vivo* efficacy and PK/PD modeling of KBP-7072, an aminomethylcycline antibiotic, in neutropenic pneumonia and thigh infection Models. *bioRxiv* **2020**, doi:10.1101/2020.03.18.998112.
160. Olesky, M.; Newman, J.; Zhou, J.; Fyfe, C.; Weiss, W.; Pulse, M. *In vivo* efficacy of TP-6076 in murine thigh and lung infection models challenged with *Acinetobacter baumannii*. In Proceedings of the Abstracts of the 29th European Congress of Clinical Microbiology and Infections Diseases (ECCMID); 12–16 April 2019, 2019.
161. Blais, J.; Lopez, S.; Li, C.; Ruzin, A.; Ranjitkar, S.; Dean, C.R.; Leeds, J.A.; Casarez, A.; Simmons, R.L.; Reck, F. *In vitro* activity of LYS228, a novel monobactam antibiotic, against multidrug-resistant Enterobacteriaceae. *Int J antimicrobial agents* **2018**, *62*, e00552-18, doi:10.1128/AAC.00552-18.
162. Osborn, M.; Stachulski, N.; Sun, H.; Blais, J.; Venishetty, V.; Raccuglia, M.; Kankam, M.; Colvin, R.; Segal, F. A first-in-human study to assess the safety and pharmacokinetics of LYS228, a novel intravenous monobactam antibiotic in healthy volunteers. *Antimicrob Agents Chemother* **2019**, *63*, e02592-18, doi:10.1128/AAC.02592-18.
163. Tenero, D.; Farinola, N.; Berkowitz, E.M.; Tiffany, C.A.; Qian, Y.; Xue, Z.; Raychaudhuri, A.; Gardiner, D.F. Pharmacokinetics, safety, and tolerability evaluation of single and multiple doses of GSK3342830 in healthy volunteers. *Clin Pharmacol. Drug Dev* **2019**, *8*, 754-64, doi:10.1002/cpdd.637.
164. Veeraraghavan, B.; Bakthavatchalam, Y.D.; Sahni, R.D. Oral antibiotics in clinical development for community-acquired urinary tract infections. *Infect Dis Ther* **2021**, doi:10.1007/s40121-021-00509-4.
165. Dunne, M.W.; Das, A.F.; Zelasky, M.; Akinapelli, K.; Boucher, H.; Aronin, S.I. LB-1. Efficacy and safety of oral sulopenem etzadroxil/probenecid versus oral ciprofloxacin in the treatment of uncomplicated urinary tract infections (uUTI) in adult women: Results from the SURE-1 trial. *Open Forum Infect Dis* **2020**, *7*, S844-S44, doi:10.1093/ofid/ofaa515.1898.
166. Pagès, J.-M.; Masi, M.; Barbe, J. Inhibitors of efflux pumps in Gram-negative bacteria. *Trends Mol Med* **2005**, *11*, 382-89, doi:10.1016/j.molmed.2005.06.006.
167. Grimsey, E.M.; Fais, C.; Marshall, R.L.; Ricci, V.; Ciusa, M.L.; Stone, J.W.; Ivens, A.; Mallocci, G.; Ruggerone, P.; Vargiu, A.V.; et al. Chlorpromazine and amitriptyline are substrates and inhibitors of the AcrB multidrug efflux pump. *mBio* **2020**, *11*, doi:10.1128/mBio.00465-20.
168. Blanco, P.; Sanz-García, F.; Hernando-Amado, S.; Martínez, J.L.; Alcalde-Rico, M. The development of efflux pump inhibitors to treat Gram-negative infections. *Expert Opin Drug Discov* **2018**, *13*, 919-31, doi:10.1080/17460441.2018.1514386.
169. Marshall, R.L.; Lloyd, G.S.; Lawler, A.J.; Element, S.J.; Kaur, J.; Ciusa, M.L.; Ricci, V.; Tschumi, A.; Kühne, H.; Alderwick, L.J.; et al. New multidrug efflux inhibitors for Gram-negative bacteria. *mBio* **2020**, *11*, doi:10.1128/mBio.01340-20.

170. Wang, Y.; Venter, H.; Ma, S. Efflux pump inhibitors: A novel approach to combat efflux-mediated drug resistance in bacteria. *Curr Drug Targets* **2016**, *17*, 702-19, doi:10.2174/1389450116666151001103948.
171. Askoura, M.; Mottawea, W.; Abujamel, T.; Taher, I. Efflux pump inhibitors (EPIs) as new antimicrobial agents against *Pseudomonas aeruginosa*. *Libyan J Med* **2011**, *6*, doi:10.3402/ljm.v6i0.5870.
172. Rodrigues, L.; Cravo, P.; Viveiros, M. Efflux pump inhibitors as a promising adjunct therapy against drug resistant tuberculosis: A new strategy to revisit mycobacterial targets and repurpose old drugs. *Expert Rev Anti Infect Ther* **2020**, *18*, 741-57, doi:10.1080/14787210.2020.1760845.
173. Pagès, J.-M.; Amaral, L. Mechanisms of drug efflux and strategies to combat them: challenging the efflux pump of Gram-negative bacteria. *Biochim Biophys Acta* **2009**, *1794*, 826-33, doi:10.1016/j.bbapap.2008.12.011.
174. Lamers, R.P.; Cavallari, J.F.; Burrows, L.L. The efflux inhibitor phenylalanine-arginine beta-naphthylamide (PA β N) permeabilizes the outer membrane of Gram-negative bacteria. *PLoS One* **2013**, *8*, e60666, doi:10.1371/journal.pone.0060666.
175. Mahamoud, A.; Chevalier, J.; Alibert-Franco, S.; Kern, W.V.; Pagès, J.-M. Antibiotic efflux pumps in Gram-negative bacteria: The inhibitor response strategy. *J Antimicrob Chemother* **2007**, *59*, 1223-29, doi:10.1093/jac/dkl493.
176. Zechini, B.; Versace, I. Inhibitors of multidrug resistant efflux systems in bacteria. *Recent Pat Antiinfect Drug Discov* **2009**, *4*, 37-50, doi:10.2174/157489109787236256.
177. Piddock, L.J.; Garvey, M.I.; Rahman, M.M.; Gibbons, S. Natural and synthetic compounds such as trimethoprim behave as inhibitors of efflux in Gram-negative bacteria. *J Antimicrob Chemother* **2010**, *65*, 1215-23, doi:10.1093/jac/dkq079.
178. Li, B.; Yao, Q.; Pan, X.-C.; Wang, N.; Zhang, R.; Li, J.; Ding, G.; Liu, X.; Wu, C.; Ran, D. Artesunate enhances the antibacterial effect of β -lactam antibiotics against *Escherichia coli* by increasing antibiotic accumulation via inhibition of the multidrug efflux pump system AcrAB-TolC. *J Antimicrob Chemother* **2011**, *66*, 769-77, doi:10.1093/jac/dkr017.
179. Siriyong, T.; Srimanote, P.; Chusri, S.; Yingyongnarongkul, B.-e.; Suaisom, C.; Tipmanee, V.; Voravuthikunchai, S.P. Conessine as a novel inhibitor of multidrug efflux pump systems in *Pseudomonas aeruginosa*. *BMC complement med ther* **2017**, *17*, 1-7, doi:10.1186/s12906-017-1913-y.
180. Siriyong, T.; Chusri, S.; Srimanote, P.; Tipmanee, V.; Voravuthikunchai, S.P. Holarrhena antidysenterica extract and its steroidal alkaloid, conessine, as resistance-modifying agents against extensively drug-resistant *Acinetobacter baumannii*. *Microb Drug Resist* **2016**, *22*, 273-82, doi:10.1089/mdr.2015.0194.
181. Bohnert, J.A.; Schuster, S.; Kern, W.V.; Karcz, T.; Olejarz, A.; Kaczor, A.; Handzlik, J.; Kieć-Kononowicz, K. Novel piperazine arylideneimidazolones inhibit the AcrAB-TolC pump in *Escherichia coli* and simultaneously act as fluorescent membrane probes in a combined real-time influx and efflux assay. *Int J Antimicrob Agents* **2016**, *60*, 1974-83, doi:10.1128/AAC.01995-15.

182. Machado, D.; Fernandes, L.; Costa, S.S.; Cannalire, R.; Manfroni, G.; Tabarrini, O.; Couto, I.; Sabatini, S.; Viveiros, M. Mode of action of the 2-phenylquinoline efflux inhibitor PQQ4R against *Escherichia coli*. *Peer J* **2017**, *5*, e3168, doi:10.7717/peerj.3168.
183. Nelson, M.L.; Levy, S.B. Reversal of tetracycline resistance mediated by different bacterial tetracycline resistance determinants by an inhibitor of the Tet (B) antiport protein. *Antimicrob Agents Chemother* **1999**, *43*, 1719-24, doi:10.1128/AAC.43.7.1719.
184. Xing, L.; Barnie, P.A.; Su, Z.; Xu, H. Development of efflux pumps and inhibitors (EPIs) in *A. baumannii*. *Clin Microb Infect* **2014**, doi:10.4172/2161-0494.1000101.
185. Reza, A.; Sutton, J.M.; Rahman, K.M. Effectiveness of efflux pump inhibitors as biofilm disruptors and resistance breakers in Gram-negative (ESKAPEE) bacteria. *Antibiotics (Basel)* **2019**, *8*, 229, doi:10.3390/antibiotics8040229.
186. Yoshida, K.-i.; Nakayama, K.; Ohtsuka, M.; Kuru, N.; Yokomizo, Y.; Sakamoto, A.; Takemura, M.; Hoshino, K.; Kanda, H.; Nitana, H. MexAB-OprM specific efflux pump inhibitors in *Pseudomonas aeruginosa*. Part 7: Highly soluble and *in vivo* active quaternary ammonium analogue D13-9001, a potential preclinical candidate. *Bioorg Med Chem* **2007**, *15*, 7087-97, doi:10.1016/j.bmc.2007.07.039.
187. Nguyen, S.T.; Kwasny, S.M.; Ding, X.; Cardinale, S.C.; McCarthy, C.T.; Kim, H.-S.; Nikaido, H.; Peet, N.P.; Williams, J.D.; Bowlin, T.L. Structure–activity relationships of a novel pyranopyridine series of Gram-negative bacterial efflux pump inhibitors. *Bio Med Chem* **2015**, *23*, 2024-34, doi:10.1016/j.bmc.2015.03.016.
188. Bhattacharyya, T.; Sharma, A.; Akhter, J.; Pathania, R. The small molecule ITR08027 restores the antibacterial activity of fluoroquinolones against multidrug-resistant *Acinetobacter baumannii* by efflux inhibition. *Int J Antimicrob Agents* **2017**, *50*, 219-26, doi:10.1016/j.ijantimicag.2017.03.005.
189. Song, Y.; Qin, R.; Pan, X.; Ouyang, Q.; Liu, T.; Zhai, Z.; Chen, Y.; Li, B.; Zhou, H. Design of new antibacterial enhancers based on AcrB's structure and the evaluation of their antibacterial enhancement activity. *Int J Molecular Sciences* **2016**, *17*, 1934, doi:10.3390/ijms17111934.
190. Li, L.; Kromann, S.; Olsen, J.E.; Svenningsen, S.W.; Olsen, R.H. Insight into synergetic mechanisms of tetracycline and the selective serotonin reuptake inhibitor, sertraline, in a tetracycline-resistant strain of *Escherichia coli*. *J Antibiot* **2017**, *70*, 944-53, doi:10.1038/ja.2017.78.
191. Probst-Kepper, M.; Geginat, G. New antibiotics for treatment of highly resistant Gram-negative bacteria. *Anesthesiol Intensivmed Notfallmed Schmerzther* **2018**, *53*, 529-42, doi:10.1055/s-0043-110504.
192. Bush, K.; Bradford, P.A. Interplay between β -lactamases and new β -lactamase inhibitors. *Nat Rev Microbiol* **2019**, *17*, 295-306, doi:10.1038/s41579-019-0159-8.
193. Bush, K.; Jacoby, G.A. Updated functional classification of β -lactamases. *Antimicrob Agents Chemother* **2010**, *54*, 969-76, doi:10.1128/AAC.01009-09.
194. Coleman, K. Diazabicyclooctanes (DBOs): A potent new class of non- β -lactam β -lactamase inhibitors. *Curr Opin Microbiol* **2011**, *14*, 550-55, doi:10.1016/j.mib.2011.07.026.

195. Drawz, S.M.; Bonomo, R.A. Three decades of β -lactamase inhibitors. *Clin Microbiol Rev* **2010**, *23*, 160-201, doi:10.1128/CMR.00037-09.
196. Watkins, R.; Papp-Wallace, K.M.; Drawz, S.M.; Bonomo, R.A. Novel β -lactamase inhibitors: A therapeutic hope against the scourge of multidrug resistance. *Front Microbiol* **2013**, *4*, 392, doi:10.3389/fmicb.2013.00392.
197. Lahiri, S.; Johnstone, M.; Ross, P.; McLaughlin, R.; Olivier, N.; Alm, R. Avibactam and class C β -lactamases: Mechanism of inhibition, conservation of the binding pocket, and implications for resistance. *Antimicrob Agents Chemother* **2014**, *58*, 5704-13, doi:10.1128/AAC.03057-14.
198. Karlowsky, J.A.; Hackel, M.A.; Bouchillon, S.K.; Sahm, D.F. *In vitro* activity of WCK 5222 (Cefepime-zidebactam) against worldwide collected Gram-negative bacilli not susceptible to carbapenems. *Antimicrob Agents Chemother* **2020**, *64*, e01432-20, doi:10.1128/AAC.01432-20.
199. Sagan, O.; Yakubsevitch, R.; Yanev, K.; Fomkin, R.; Stone, E.; Hines, D.; O'Donnell, J.; Miller, A.; Isaacs, R.; Srinivasan, S. Pharmacokinetics and tolerability of intravenous sulbactam-durlobactam with imipenem-cilastatin in hospitalized adults with complicated urinary tract infections, including acute pyelonephritis. *Antimicrob Agents Chemother* **2020**, *64*, e01506-19, doi:10.1128/AAC.01506-19.
200. Doumith, M.; Mushtaq, S.; Livermore, D.M.; Woodford, N. New insights into the regulatory pathways associated with the activation of the stringent response in bacterial resistance to the PBP2-targeted antibiotics, mecillinam and OP0595/RG6080. *J Antimicrob Chemother* **2016**, *71*, 2810-4, doi:10.1093/jac/dkw230.
201. Mushtaq, S.; Vickers, A.; Woodford, N.; Haldimann, A.; Livermore, D.M. Activity of nacubactam (RG6080/OP0595) combinations against MBL-producing Enterobacteriaceae. *J Antimicrob Chemother* **2019**, *74*, 953-60, doi:10.1093/jac/dky522.
202. Lacasse, E.; Brouillette, E.; Larose, A.; Parr, T.R., Jr.; Rubio, A.; Malouin, F. *In vitro* activity of tebipenem (SPR859) against penicillin-binding proteins of Gram-negative and Gram-positive bacteria. *Antimicrob Agents Chemother* **2019**, *63*, doi:10.1128/aac.02181-18.
203. Krajnc, A.; Brem, J.; Hinchliffe, P.; Calvopiña, K.; Panduwawala, T.D.; Lang, P.A.; Kamps, J.; Tyrrell, J.M.; Widlake, E.; Seward, B.G.; et al. Bicyclic boronate VNRX-5133 inhibits metallo- and serine- β -lactamases. *J Med Chem* **2019**, *62*, 8544-56, doi:10.1021/acs.jmedchem.9b00911.
204. Abdelraouf, K.; Almarzoky Abuhussain, S.; Nicolau, D.P. *In vivo* pharmacodynamics of new-generation β -lactamase inhibitor taniborbactam (formerly VNRX-5133) in combination with cefepime against serine- β -lactamase-producing Gram-negative bacteria. *J Antimicrob Chemother* **2020**, *75*, 3601-10, doi:10.1093/jac/dkaa373.
205. Hamrick, J.C.; Docquier, J.D.; Uehara, T.; Myers, C.L.; Six, D.A.; Chatwin, C.L.; John, K.J.; Vernacchio, S.F.; Cusick, S.M.; Trout, R.E.L.; et al. VNRX-5133 (taniborbactam), a broad-spectrum inhibitor of serine- and metallo- β -lactamases, restores activity of cefepime in Enterobacterales and *Pseudomonas aeruginosa*. *Antimicrob Agents Chemother* **2020**, *64*, doi:10.1128/aac.01963-19.
206. Liu, B.; Trout, R.E.L.; Chu, G.H.; McGarry, D.; Jackson, R.W.; Hamrick, J.C.; Daigle, D.M.; Cusick, S.M.; Pozzi, C.; De Luca, F.; et al. Discovery of taniborbactam (VNRX-5133): A broad-spectrum serine- and metallo- β -lactamase inhibitor for carbapenem-resistant bacterial infections. *J Med Chem* **2020**, *63*, 2789-801, doi:10.1021/acs.jmedchem.9b01518.

207. Wang, X.; Zhao, C.; Wang, Q.; Wang, Z.; Liang, X.; Zhang, F.; Zhang, Y.; Meng, H.; Chen, H.; Li, S.; et al. Erratum to: *In vitro* activity of the novel β -lactamase inhibitor taniborbactam (VNRX-5133), in combination with cefepime or meropenem, against MDR Gram-negative bacterial isolates from China. *J Antimicrob Chemother* **2020**, *75*, 2019, doi:10.1093/jac/dkaa132.
208. Yahav, D.; Giske, C.G.; Grāmatniece, A.; Abodakpi, H.; Tam, V.H.; Leibovici, L. New β -Lactam- β -lactamase inhibitor combinations. *Clin Microbiol Rev* **2020**, *34*, doi:10.1128/cmr.00115-20.
209. Kloezen, W.; Melchers, R.J.; Georgiou, P.C.; Mouton, J.W.; Meletiadis, J. Activity of cefepime in combination with the novel β -Lactamase inhibitor taniborbactam (VNRX-5133) against extended-spectrum- β -lactamase-producing isolates in *in vitro* checkerboard assays. *Antimicrob Agents Chemother* **2021**, *65*, doi:10.1128/aac.02338-20.
210. Mushtaq, S.; Vickers, A.; Doumith, M.; Ellington, M.J.; Woodford, N.; Livermore, D.M. Activity of β -lactam/taniborbactam (VNRX-5133) combinations against carbapenem-resistant Gram-negative bacteria. *J Antimicrob Chemother* **2021**, *76*, 160-70, doi:10.1093/jac/dkaa391.
211. Crandon, J.L.; Nicolau, D.P. *In vitro* activity of cefepime/AAI101 and comparators against cefepime non-susceptible Enterobacteriaceae. *Pathogens* **2015**, *4*, 620-5, doi:10.3390/pathogens4030620.
212. Crandon, J.L.; Nicolau, D.P. *In vivo* activities of simulated human doses of cefepime and cefepime-AAI101 against multidrug-resistant Gram-negative Enterobacteriaceae. *Antimicrob Agents Chemother* **2015**, *59*, 2688-94, doi:10.1128/aac.00033-15.
213. Morrissey, I.; Magnet, S.; Hawser, S.; Shapiro, S.; Knechtle, P. *In vitro* activity of cefepime-enmetazobactam against Gram-negative isolates collected from U.S. and European hospitals during 2014-2015. *Antimicrob Agents Chemother* **2019**, *63*, doi:10.1128/aac.00514-19.
214. Papp-Wallace, K.M.; Bethel, C.R.; Caillon, J.; Barnes, M.D.; Potel, G.; Bajaksouzian, S.; Rutter, J.D.; Reghal, A.; Shapiro, S.; Taracila, M.A.; et al. Beyond piperacillin-tazobactam: cefepime and AAI101 as a potent β -lactam- β -lactamase inhibitor combination. *Antimicrob Agents Chemother* **2019**, *63*, doi:10.1128/aac.00105-19.
215. Bernhard, F.; Odedra, R.; Sordello, S.; Cardin, R.; Franzoni, S.; Charrier, C.; Belley, A.; Warn, P.; Machacek, M.; Knechtle, P. Pharmacokinetics-pharmacodynamics of enmetazobactam combined with cefepime in a neutropenic murine thigh infection model. *Antimicrob Agents Chemother* **2020**, *64*, doi:10.1128/aac.00078-20.
216. Tselepis, L.; Langley, G.W.; Aboklaish, A.F.; Widlake, E.; Jackson, D.E.; Walsh, T.R.; Schofield, C.J.; Brem, J.; Tyrrell, J.M. *In vitro* efficacy of imipenem-relebactam and cefepime-AAI101 against a global collection of ESBL-positive and carbapenemase-producing Enterobacteriaceae. *Int J Antimicrob Agents* **2020**, *56*, 105925, doi:10.1016/j.ijantimicag.2020.105925.
217. Velkov, T.; Roberts, K.D.; Nation, R.L.; Thompson, P.E.; Li, J. Pharmacology of polymyxins: New insights into an 'old' class of antibiotics. *Future Microbiol* **2013**, *8*, 711-24, doi:10.2217/fmb.13.39.
218. Dhariwal, A. Colistin: Re-emergence of the 'forgotten' antimicrobial agent. *Postgrad Medicine* **2013**, *59*, 208, doi:10.4103/0022-3859.118040.
219. Bergen, P.J.; Smith, N.M.; Bedard, T.B.; Bulman, Z.P.; Cha, R.; Tsuji, B.T. Rational combinations of polymyxins with other antibiotics. *Adv Exp Med Biol* **2019**, *1145*, 251-88, doi:10.1007/978-3-030-16373-0_16.

220. Zgurskaya, H.I.; Lopez, C.A.; Gnanakaran, S. Permeability barrier of Gram-negative cell envelopes and approaches to bypass it. *ACS Infect Dis* **2015**, *1*, 512-22, doi:10.1021/acsinfecdis.5b00097.
221. Andrade, F.F.; Silva, D.; Rodrigues, A.; Pina-Vaz, C. Colistin update on its mechanism of action and resistance, present and future challenges. *Microorganisms* **2020**, *8*, 1716, doi:10.1021/acsinfecdis.1c00147.
222. Dandie, C.E.; Ogunniyi, A.D.; Ferro, S.; Hall, B.; Drigo, B.; Chow, C.W.; Venter, H.; Myers, B.; Deo, P.; Donner, E. Disinfection options for irrigation water: Reducing the risk of fresh produce contamination with human pathogens. *Crit Rev Environ Sci Technol* **2019**, 1-31, doi:10.1080/10643389.2019.1704172.
223. Chang, Y.T.; Yang, T.Y.; Lu, P.L.; Lin, S.Y.; Wang, L.C.; Wang, S.F.; Hsieh, Y.J.; Tseng, S.P. Combination of colistin and azidothymidine demonstrates synergistic activity against colistin-resistant, carbapenem-resistant *Klebsiella pneumoniae*. *Microorganisms* **2020**, *8*, doi:10.3390/microorganisms8121964.
224. Ku, Y.-H.; Chen, C.-C.; Lee, M.-F.; Chuang, Y.-C.; Tang, H.-J.; Yu, W.-L. Comparison of synergism between colistin, fosfomicin and tigecycline against extended-spectrum β -lactamase-producing *Klebsiella pneumoniae* isolates or with carbapenem resistance. *J Microbiol, Immunol Infect* **2017**, *50*, 931-39, doi:10.1016/j.jmii.2016.12.008.
225. Abdul-Mutakabbir, J.C.; Yim, J.; Nguyen, L.; Maassen, P.T.; Stamper, K.; Shiekh, Z.; Kebraie, R.; Shields, R.K.; Castanheira, M.; Kaye, K.S.; et al. *In vitro* synergy of colistin in combination with meropenem or tigecycline against carbapenem-resistant *Acinetobacter baumannii*. *Antibiotics (Basel)* **2021**, *10*, doi:10.3390/antibiotics10070880.
226. Albur, M.S.; Noel, A.; Bowker, K.; MacGowan, A. The combination of colistin and fosfomicin is synergistic against NDM-1-producing Enterobacteriaceae in *in vitro* pharmacokinetic/pharmacodynamic model experiments. *Int J Antimicrob Agents* **2015**, *46*, 560-7, doi:10.1016/j.ijantimicag.2015.07.019.
227. Bae, S.; Kim, M.C.; Park, S.J.; Kim, H.S.; Sung, H.; Kim, M.N.; Kim, S.H.; Lee, S.O.; Choi, S.H.; Woo, J.H.; et al. *In vitro* synergistic activity of antimicrobial agents in combination against clinical isolates of colistin-resistant *Acinetobacter baumannii*. *Antimicrob Agents Chemother* **2016**, *60*, 6774-79, doi:10.1128/aac.00839-16.
228. Betts, J.W.; Phee, L.M.; Hornsey, M.; Woodford, N.; Wareham, D.W. *In vitro* and *in vivo* activities of tigecycline-colistin combination therapies against carbapenem-resistant Enterobacteriaceae. *Antimicrob Agents Chemother* **2014**, *58*, 3541-6, doi:10.1128/aac.02449-14.
229. Chen, T.; Xu, W.; Yu, K.; Zeng, W.; Xu, C.; Cao, J.; Zhou, T. *In vitro* activity of ceftazidime-avibactam alone and in combination with amikacin against colistin-resistant Gram-negative pathogens. *Microb Drug Resist* **2021**, *27*, 401-09, doi:10.1089/mdr.2019.0463.
230. Hornsey, M.; Longshaw, C.; Phee, L.; Wareham, D.W. *In vitro* activity of telavancin in combination with colistin versus Gram-negative bacterial pathogens. *Antimicrob Agents Chemother* **2012**, *56*, 3080-5, doi:10.1128/aac.05870-11.
231. Rodríguez, C.H.; Nastro, M.; Vay, C.; Famiglietti, A. *In vitro* activity of minocycline alone or in combination in multidrug-resistant *Acinetobacter baumannii* isolates. *J Med Microbiol* **2015**, *64*, 1196-200, doi:10.1099/jmm.0.000147.

232. Singkham-In, U.; Chatsuwan, T. *In vitro* activities of carbapenems in combination with amikacin, colistin, or fosfomycin against carbapenem-resistant *Acinetobacter baumannii* clinical isolates. *Diagn Microbiol Infect Dis* **2018**, *91*, 169-74, doi:10.1016/j.diagmicrobio.2018.01.008.
233. Dundar, D.; Duymaz, Z.; Genc, S.; Er, D.K.; İrvem, A.; Kandemir, N. *In-vitro* activities of imipenem-colistin, imipenem-tigecycline, and tigecycline-colistin combinations against carbapenem-resistant Enterobacteriaceae. *J Chemother* **2018**, *30*, 342-47, doi:10.1080/1120009x.2018.1516270.
234. Gómez-Junyent, J.; Benavent, E.; Sierra, Y.; El Haj, C.; Soldevila, L.; Torrejón, B.; Rigo-Bonnin, R.; Tubau, F.; Ariza, J.; Murillo, O. Efficacy of ceftolozane/tazobactam, alone and in combination with colistin, against multidrug-resistant *Pseudomonas aeruginosa* in an *in vitro* biofilm pharmacodynamic model. *Int J Antimicrob Agents* **2019**, *53*, 612-19, doi:10.1016/j.ijantimicag.2019.01.010.
235. Blasco, L.; Ambroa, A.; Trastoy, R.; Bleriot, I.; Moscoso, M.; Fernández-García, L.; Perez-Nadales, E.; Fernández-Cuenca, F.; Torre-Cisneros, J.; Oteo-Iglesias, J.; et al. *In vitro* and *in vivo* efficacy of combinations of colistin and different endolysins against clinical strains of multi-drug resistant pathogens. *Sci Rep* **2020**, *10*, 7163, doi:10.1038/s41598-020-64145-7.
236. Cebrero-Cangueiro, T.; Álvarez-Marín, R.; Labrador-Herrera, G.; Smani, Y.; Cordero-Matía, E.; Pachón, J.; Pachón-Ibáñez, M.E. *In vitro* activity of pentamidine alone and in combination with aminoglycosides, tigecycline, rifampicin, and doripenem against clinical strains of carbapenemase-producing and/or colistin-resistant Enterobacteriaceae. *Front Cell Infect Microbiol* **2018**, *8*, 363, doi:10.3389/fcimb.2018.00363.
237. Pollini, S.; Boncompagni, S.; Di Maggio, T.; Di Pilato, V.; Spanu, T.; Fiori, B.; Blasi, F.; Aliberti, S.; Sergio, F.; Rossolini, G.M.; et al. *In vitro* synergism of colistin in combination with N-acetylcysteine against *Acinetobacter baumannii* grown in planktonic phase and in biofilms. *J Antimicrob Chemother* **2018**, *73*, 2388-95, doi:10.1093/jac/dky185.
238. Zhou, Y.; Wang, T.; Guo, Y.; Liu, S.; Wang, J.; Shen, Y.; Tang, S.; Wang, Y.; Deng, X. *In vitro/vivo* activity of potential MCR-1 inhibitor in combination with colistin againsts mcr-1-positive *Klebsiella pneumoniae*. *Front Microbiol* **2018**, *9*, 1615, doi:10.3389/fmicb.2018.01615.
239. Zhou, Y.F.; Liu, P.; Dai, S.H.; Sun, J.; Liu, Y.H.; Liao, X.P. Activity of tigecycline or colistin in combination with zidovudine against *Escherichia coli* harboring tet(X) and mcr-1. *Antimicrob Agents Chemother* **2020**, *65*, doi:10.1128/aac.01172-20.
240. Berditsch, M.; Jäger, T.; Stempel, N.; Schwartz, T.; Overhage, J.; Ulrich, A.S. Synergistic effect of membrane-active peptides polymyxin B and gramicidin S on multidrug-resistant strains and biofilms of *Pseudomonas aeruginosa*. *Antimicrob Agents Chemother* **2015**, *59*, 5288-96, doi:10.1128/aac.00682-15.
241. Yang, H.; Chen, G.; Hu, L.; Liu, Y.; Cheng, J.; Ye, Y.; Li, J. Enhanced efficacy of imipenem-colistin combination therapy against multiple-drug-resistant Enterobacter cloacae: *in vitro* activity and a *Galleria mellonella* model. *J Microbiol Immunol Infect* **2018**, *70*-75, doi:10.1016/j.jmii.2016.01.003.
242. Fan, B.; Guan, J.; Wang, X.; Cong, Y. Activity of colistin in combination with meropenem, tigecycline, fosfomycin, fusidic acid, rifampin or sulbactam against extensively drug-

- resistant *Acinetobacter baumannii* in a murine thigh-infection model. *PLoS One* **2016**, *11*, e0157757, doi:10.1371/journal.pone.0157757.
243. Wei, W.; Yang, H.; Hu, L.; Ye, Y.; Li, J. Activity of levofloxacin in combination with colistin against *Acinetobacter baumannii*: *In vitro* and in a *Galleria mellonella* model. *J Microbiol Immunol Infect* **2017**, *50*, 821-30, doi:10.1016/j.jmii.2015.10.010.
244. Zhou, Y.-F.; Liu, P.; Zhang, C.-J.; Liao, X.-P.; Sun, J.; Liu, Y.-H. Colistin combined with tigecycline: A promising alternative strategy to combat *Escherichia coli* harboring bla_{NDM-5} and mcr-1. *Front Microbiol* **2020**, *10*, 2957, doi:10.3389/fmicb.2019.02957.
245. Miró-Canturri, A.; Ayerbe-Algaba, R.; Jiménez-Mejías, M.E.; Pachón, J.; Smani, Y. Efficacy of lysophosphatidylcholine as direct treatment in combination with colistin against *Acinetobacter baumannii* in murine severe infections models. *Antibiotics (Basel)* **2021**, *10*, 194, doi:10.3390/antibiotics10020194.
246. Hornsey, M.; Phee, L.; Longshaw, C.; Wareham, D.W. *In vivo* efficacy of telavancin/colistin combination therapy in a *Galleria mellonella* model of *Acinetobacter baumannii* infection. *Int J Antimicrob Agents* **2013**, *41*, 285-87, doi:10.1016/j.ijantimicag.2012.11.013.
247. Abdelsalam, M.F.A.; Abdalla, M.S.; El-Abhar, H.S.E.-D. Prospective, comparative clinical study between high-dose colistin monotherapy and colistin–meropenem combination therapy for treatment of hospital-acquired pneumonia and ventilator-associated pneumonia caused by multidrug-resistant *Klebsiella pneumoniae*. *J Glob Antimicrob* **2018**, *15*, 127-35, doi:10.1016/j.jgar.2018.07.003.
248. Kalin, G.; Alp, E.; Akin, A.; Coskun, R.; Doganay, M. Comparison of colistin and colistin/sulbactam for the treatment of multidrug resistant *Acinetobacter baumannii* ventilator-associated pneumonia. *Infection* **2014**, *42*, 37-42, doi:10.1007/s15010-013-0495-y.
249. Herrmann, G.; Yang, L.; Wu, H.; Song, Z.; Wang, H.; Høiby, N.; Ulrich, M.; Molin, S.; Riethmüller, J.; Döring, G. Colistin-tobramycin combinations are superior to monotherapy concerning the killing of biofilm *Pseudomonas aeruginosa*. *J Infect Dis* **2010**, *202*, 1585-92, doi:10.1086/656788.
250. Qureshi, Z.A.; Paterson, D.L.; Potoski, B.A.; Kilayko, M.C.; Sandovsky, G.; Sordillo, E.; Polsky, B.; Adams-Haduch, J.M.; Doi, Y. Treatment outcome of bacteremia due to KPC-producing *Klebsiella pneumoniae*: Superiority of combination antimicrobial regimens. *Antimicrob Agents Chemother* **2012**, *56*, 2108-13, doi:10.1128/AAC.06268-11.
251. Nutman, A.; Lellouche, J.; Temkin, E.; Daikos, G.; Skiada, A.; Durante-Mangoni, E.; Dishon-Benattar, Y.; Bitterman, R.; Yahav, D.; Daitch, V. Colistin plus meropenem for carbapenem-resistant Gram-negative infections: *In vitro* synergism is not associated with better clinical outcomes. *Clin Microbiol Infect* **2020**, *26*, 1185-91, doi:10.1016/j.cmi.2020.03.035.
252. Paul, M.; Daikos, G.L.; Durante-Mangoni, E.; Yahav, D.; Carmeli, Y.; Benattar, Y.D.; Skiada, A.; Andini, R.; Eliakim-Raz, N.; Nutman, A.; et al. Colistin alone versus colistin plus meropenem for treatment of severe infections caused by carbapenem-resistant Gram-negative bacteria: An open-label, randomised controlled trial. *Lancet Infect Dis* **2018**, *18*, 391-400, doi:10.1016/S1473-3099(18)30099-9.

253. Shi, H.; Lee, J.S.; Park, S.Y.; Ko, Y.; Eom, J.S. Colistin plus carbapenem versus colistin monotherapy in the treatment of carbapenem-resistant *Acinetobacter baumannii* Pneumonia. *Infect Drug Resist* **2019**, *12*, 3925-34, doi:10.2147/IDR.S234211.
254. Petrosillo, N.; Ioannidou, E.; Falagas, M.E. Colistin monotherapy vs. combination therapy: Evidence from microbiological, animal and clinical studies. *Clin Microbiol Infect* **2008**, *14*, 816-27, doi:10.1111/j.1469-0691.2008.02061.x.
255. Ungthammakhun, C.; Vasikasin, V.; Changpradub, D. Clinical outcomes of colistin in combination with either 6-G sulbactam or carbapenems for the treatment of extensively drug-resistant *Acinetobacter baumannii* Pneumonia with high IC to sulbactam, a prospective cohort study. *Infect Drug Resist* **2019**, *12*, 2899-904, doi:10.2147/IDR.S225518.
256. Khadka, S.; Yuchi, A.; Shrestha, D.B.; Budhathoki, P.; Al-Subari, S.M.M.; Ziad Alhouzani, T.M.; Anwar Butt, I. Repurposing drugs for COVID-19: An approach for treatment in the pandemic. *Altern Ther Health Med* **2020**, *26*, 100-07, doi:PMID: 32827400.
257. Schein, C.H. Repurposing approved drugs on the pathway to novel therapies. *Med Res Rev* **2020**, *40*, 586-605, doi:10.1002/med.21627.
258. Wall, G.; Lopez-Ribot, J.L. Screening repurposing libraries for identification of drugs with novel antifungal activity. *Antimicrob Agents Chemother* **2020**, *64*, doi:10.1128/aac.00924-20.
259. Farha, M.A.; Brown, E.D. Drug repurposing for antimicrobial discovery. *Nat Microbiol* **2019**, *4*, 565-77, doi:10.1038/s41564-019-0357-1.
260. Theuretzbacher, U.; Outtersson, K.; Engel, A.; Karlén, A. The global preclinical antibacterial pipeline. *Nat Rev Microbiol* **2020**, *18*, 275-85, doi:10.1038/s41579-019-0288-0.
261. Chong, C.R.; Sullivan, D.J., Jr. New uses for old drugs. *Nature* **2007**, *448*, 645-6, doi:10.1038/448645a.
262. Hu, Y.; Liu, Y.; Coates, A. Azidothymidine produces synergistic activity in combination with colistin against antibiotic-resistant Enterobacteriaceae. *Antimicrob Agents Chemother* **2019**, *63*, doi:10.1128/aac.01630-18.
263. Cheng, Y.S.; Sun, W.; Xu, M.; Shen, M.; Khraiweh, M.; Sciotti, R.J.; Zheng, W. Repurposing screen identifies unconventional drugs with activity against multidrug resistant *Acinetobacter baumannii*. *Front Cell Infect Microbiol* **2018**, *8*, 438, doi:10.3389/fcimb.2018.00438.
264. Carlson-Banning, K.M.; Chou, A.; Liu, Z.; Hamill, R.J.; Song, Y.; Zechiedrich, L. Toward repurposing ciclopirox as an antibiotic against drug-resistant *Acinetobacter baumannii*, *Escherichia coli*, and *Klebsiella pneumoniae*. *PLoS One* **2013**, *8*, e69646, doi:10.1371/journal.pone.0069646.
265. Morales-de-Echegaray, A.V.; Lin, L.; Sivasubramaniam, B.; Yermembetova, A.; Wang, Q.; Abutaleb, N.S.; Seleem, M.N.; Wei, A. Antimicrobial photodynamic activity of gallium-substituted haemoglobin on silver nanoparticles. *Nanoscale* **2020**, *12*, 21734-42, doi:10.1039/c9nr09064a.
266. Kaneko, Y.; Thoendel, M.; Olakanmi, O.; Britigan, B.E.; Singh, P.K. The transition metal gallium disrupts *Pseudomonas aeruginosa* iron metabolism and has antimicrobial and antibiofilm activity. *J Clin Investig* **2007**, *117*, 877-88, doi:10.1172/JCI30783.

267. Goss, C.H.; Kaneko, Y.; Khuu, L.; Anderson, G.D.; Ravishankar, S.; Aitken, M.L.; Lechtzin, N.; Zhou, G.; Czyz, D.M.; McLean, K. Gallium disrupts bacterial iron metabolism and has therapeutic effects in mice and humans with lung infections. *Sci Transl Med* **2018**, *10*, doi:10.1126/scitranslmed.aat7520.
268. Choi, S.-r.; Britigan, B.E.; Narayanasamy, P. Iron/heme metabolism-targeted gallium (III) nanoparticles are active against extracellular and intracellular *Pseudomonas aeruginosa* and *Acinetobacter baumannii*. *Antimicrob Agents Chemother* **2019**, *63*, e02643-18, doi:10.1128/AAC.02643-18.
269. Meyers, E.; Brown, W.E.; Principe, P.A.; Rathnum, M.L.; Parker, W.L. EM49, a new peptide antibiotic. I. Fermentation, isolation, and preliminary characterization. *J Antibiot* **1973**, *26*, 444-8, doi:10.7164/antibiotics.26.444.
270. Blaskovich, M.A.T.; Pitt, M.E.; Elliott, A.G.; Cooper, M.A. Can octapeptin antibiotics combat extensively drug-resistant (XDR) bacteria? *Expert Rev Anti Infect Ther* **2018**, *16*, 485-99, doi:10.1080/14787210.2018.1483240.
271. Velkov, T.; Gallardo-Godoy, A.; Swarbrick, J.D.; Blaskovich, M.A.; Elliott, A.G.; Han, M.; Thompson, P.E.; Roberts, K.D.; Huang, J.X.; Becker, B. Structure, function, and biosynthetic origin of octapeptin antibiotics active against extensively drug-resistant Gram-negative bacteria. *Cell Chem Biol* **2018**, *25*, 380-91. e5, doi:10.1016/j.chembiol.2018.01.005.
272. Tsai, C.J.; Loh, J.M.; Proft, T. *Galleria mellonella* infection models for the study of bacterial diseases and for antimicrobial drug testing. *Virulence* **2016**, *7*, 214-29, doi:10.1080/21505594.2015.1135289.
273. Kavanagh, K.; Sheehan, G. The use of *Galleria mellonella* larvae to identify novel antimicrobial agents against fungal species of medical interest. *J Fungi (Basel)* **2018**, *4*, doi:10.3390/jof4030113.
274. Mowlds, P.; Kavanagh, K. Effect of pre-incubation temperature on susceptibility of *Galleria mellonella* larvae to infection by *Candida albicans*. *Mycopathologia* **2008**, *165*, 5-12, doi:10.1007/s11046-007-9069-9.
275. Banville, N.; Browne, N.; Kavanagh, K. Effect of nutrient deprivation on the susceptibility of *Galleria mellonella* larvae to infection. *Virulence* **2012**, *3*, 497-503, doi:10.4161/viru.21972.
276. Fallon, J.P.; Troy, N.; Kavanagh, K. Pre-exposure of *Galleria mellonella* larvae to different doses of *Aspergillus fumigatus* conidia causes differential activation of cellular and humoral immune responses. *Virulence* **2011**, *2*, 413-21, doi:10.4161/viru.2.5.17811.
277. Champion, O.L.; Titball, R.W.; Bates, S. Standardization of *G. mellonella* Larvae to provide reliable and reproducible results in the study of fungal pathogens. *J Fungi* **2018**, *4*, doi:10.3390/jof4030108.
278. Zhao, M.; Lepak, A.J.; Andes, D.R. Animal models in the pharmacokinetic/pharmacodynamic evaluation of antimicrobial agents. *Bioorg Med Chem* **2016**, *24*, 6390-400, doi:10.1016/j.bmc.2016.11.008.
279. Jucker, M. The benefits and limitations of animal models for translational research in neurodegenerative diseases. *Nat Med* **2010**, *16*, 1210-14, doi:10.1038/nm.2224.

280. Von Scheidt, M.; Zhao, Y.; Kurt, Z.; Pan, C.; Zeng, L.; Yang, X.; Schunkert, H.; Lusic, A.J. Applications and limitations of mouse models for understanding human atherosclerosis. *Cell Metab* **2017**, *25*, 248-61, doi:10.1016/j.cmet.2016.11.001.
281. Kadurugamuwa, J.L.; Sin, L.V.; Yu, J.; Francis, K.P.; Kimura, R.; Purchio, T.; Contag, P.R. Rapid direct method for monitoring antibiotics in a mouse model of bacterial biofilm infection. *Antimicrob Agents Chemother* **2003**, *47*, 3130-37, doi:10.1128/AAC.47.10.3130-3137.2003.
282. Benjamin, E.J.; Virani, S.S.; Callaway, C.W.; Chamberlain, A.M.; Chang, A.R.; Cheng, S.; Chiuve, S.E.; Cushman, M.; Delling, F.N.; Deo, R. Heart disease and stroke statistics-2018 update: a report from the American heart association. *Circulation* **2018**, *137*, e67, doi:10.1161/CIR.0000000000000558.
283. Plaut, R.D.; Mocca, C.P.; Prabhakara, R.; Merkel, T.J.; Stibitz, S. Stably luminescent *Staphylococcus aureus* clinical strains for use in bioluminescent imaging. *PLoS One* **2013**, *8*, e59232, doi:10.1371/journal.pone.0059232.
284. Avci, P.; Karimi, M.; Sadasivam, M.; Antunes-Melo, W.C.; Carrasco, E.; Hamblin, M.R. *In vivo* monitoring of infectious diseases in living animals using bioluminescence imaging. *Virulence* **2018**, *9*, 28-63, doi:10.1080/21505594.2017.1371897.
285. Xiong, Y.Q.; Willard, J.; Kadurugamuwa, J.L.; Yu, J.; Francis, K.P.; Bayer, A.S. Real-time *in vivo* bioluminescent imaging for evaluating the efficacy of antibiotics in a rat *Staphylococcus aureus* endocarditis model. *Antimicrob Agents Chemother* **2005**, *49*, 380-87, doi:10.1128/AAC.49.1.380-387.2005.
286. Russell, C.C.; Stevens, A.; Young, K.A.; Baker, J.R.; McCluskey, S.N.; Khazandi, M.; Pi, H.; Ogunniyi, A.; Page, S.W.; Trott, D.J. Discovery of 4, 6-bis (2-((E)-benzylidene) hydrazinyl) pyrimidin-2-Amine with Antibiotic Activity. *ChemistryOpen* **2019**, *8*, 896-907, doi: 10.1002/open.201800241.
287. Abraham, R.J.; Stevens, A.J.; Young, K.A.; Russell, C.; Qvist, A.; Khazandi, M.; Wong, H.S.; Abraham, S.; Ogunniyi, A.D.; Page, S.W.; et al. Robenidine analogues as Gram-positive antibacterial agents. *J Med Chem* **2016**, *59*, 2126-38, doi:10.1021/acs.jmedchem.5b01797.
288. Ogunniyi, A.D.; Khazandi, M.; Stevens, A.J.; Sims, S.K.; Page, S.W.; Garg, S.; Venter, H.; Powell, A.; White, K.; Petrovski, K.R. Evaluation of robenidine analog NCL195 as a novel broad-spectrum antibacterial agent. *PLoS One* **2017**, *12*, e0183457, doi:10.1371/journal.pone.0183457.
289. Morshed, M.T.; Vuong, D.; Crombie, A.; Lacey, A.E.; Karuso, P.; Lacey, E.; Piggott, A.M. Expanding antibiotic chemical space around the nidulin pharmacophore. *Org Biomol Chem* **2018**, *16*, 3038-51, doi:10.1039/C8OB00545A.
290. Terreni, M.; Taccani, M.; Pregnotato, M. New antibiotics for multidrug-resistant bacterial strains: latest research developments and future perspectives. *Molecules (Basel, Switzerland)* **2021**, *26*, doi:10.3390/molecules26092671.
291. Talbot, G.H.; Jezek, A.; Murray, B.E.; Jones, R.N.; Ebright, R.H.; Nau, G.J.; Rodvold, K.A.; Newland, J.G.; Boucher, H.W. The infectious diseases society of America's 10 x '20 initiative (10 new systemic antibacterial agents US Food and Drug Administration Approved by 2020): Is 20 x '20 a possibility? *Clin Infect Dis* **2019**, *69*, 1-11, doi:10.1093/cid/ciz089.

292. Chetri, S.; Bhowmik, D.; Paul, D.; Pandey, P.; Chanda, D.D.; Chakravarty, A.; Bora, D.; Bhattacharjee, A. AcrAB-TolC efflux pump system plays a role in carbapenem non-susceptibility in *Escherichia coli*. *BMC Microbiol* **2019**, *19*, 210, doi:10.1186/s12866-019-1589-1.
293. Bergen, P.J.; Bulman, Z.P.; Saju, S.; Bulitta, J.B.; Landersdorfer, C.; Forrest, A.; Li, J.; Nation, R.L.; Tsuji, B.T. Polymyxin combinations: pharmacokinetics and pharmacodynamics for rationale use. *Pharmacotherapy* **2015**, *35*, 34-42, doi:10.1002/phar.1537.
294. Bush, K. New antimicrobial agents for Gram-negative pathogens in pipelines. *Int J antimicrobial agents* **2015**, *45*(Supplement 2), S10.
295. Baron, S.; Hadjadj, L.; Rolain, J.M.; Olaitan, A.O. Molecular mechanisms of polymyxin resistance: Knowns and unknowns. *Int J Antimicrob Agents* **2016**, *48*, 583-91, doi:10.1016/j.ijantimicag.2016.06.023.
296. Bialvaei, A.Z.; Samadi Kafil, H. Colistin, mechanisms and prevalence of resistance. *Curr Med Res Opin* **2015**, *31*, 707-21, doi:10.1185/03007995.2015.1018989.
297. Cheng, Y.-S.; Williamson, P.R.; Zheng, W. Improving therapy of severe infections through drug repurposing of synergistic combinations. *Curr Opin Pharmacol* **2019**, *48*, 92-98, doi:10.1016/j.coph.2019.07.006.
298. Brennan-Krohn, T.; Pironti, A.; Kirby, J.E. Synergistic activity of colistin-containing combinations against colistin-resistant Enterobacteriaceae. *Antimicrob Agents Chemother* **2018**, *62*, e00873-18, doi:10.1128/AAC.00873-18.
299. Lenhard, J.R.; Nation, R.L.; Tsuji, B.T. Synergistic combinations of polymyxins. *Int J Antimicrob Agents* **2016**, *48*, 607-13, doi:10.1016/j.ijantimicag.2016.09.014.
300. Ontong, J.C.; Ozioma, N.F.; Voravuthikunchai, S.P.; Chusri, S. Synergistic antibacterial effects of colistin in combination with aminoglycoside, carbapenems, cephalosporins, fluoroquinolones, tetracyclines, fosfomicin, and piperacillin on multidrug resistant *Klebsiella pneumoniae* isolates. *PLoS One* **2021**, *16*, e0244673, doi:10.1371/journal.pone.0244673.
301. Song, M.; Liu, Y.; Huang, X.; Ding, S.; Wang, Y.; Shen, J.; Zhu, K. A broad-spectrum antibiotic adjuvant reverses multidrug-resistant Gram-negative pathogens. *Nat Microbiol* **2020**, *5*, 1040-50, doi:10.1038/s41564-020-0723-z.
302. Brown, P.; Dawson, M.J. Development of new polymyxin derivatives for multi-drug resistant Gram-negative infections. *Antibiotics (Basel)* **2017**, *70*, 386-94, doi:10.1038/ja.2016.146.
303. Deris, Z.Z.; Swarbrick, J.D.; Roberts, K.D.; Azad, M.A.; Akter, J.; Horne, A.S.; Nation, R.L.; Rogers, K.L.; Thompson, P.E.; Velkov, T. Probing the penetration of antimicrobial polymyxin lipopeptides into Gram-negative bacteria. *Bioconjugate Chem* **2014**, *25*, 750-60, doi:10.1021/bc500094d.
304. Lin, Y.-W.; Han, M.-L.; Zhao, J.; Zhu, Y.; Rao, G.; Forrest, A.; Song, J.; Kaye, K.; Hertzong, P.; Purcell, A.W. Synergistic combination of polymyxin B and enrofloxacin induced metabolic perturbations in extensive drug-resistant *Pseudomonas aeruginosa*. *Front Pharma* **2019**, *10*, 1146, doi:10.3389/fphar.2019.01146.
305. Lin, Y.-W.; Heidi, H.Y.; Zhao, J.; Han, M.-L.; Zhu, Y.; Akter, J.; Wickremasinghe, H.; Walpola, H.; Wirth, V.; Rao, G.G. Polymyxin B in combination with enrofloxacin exerts

- synergistic killing against extensively drug-resistant *Pseudomonas aeruginosa*. *Antimicrob Agents Chemother* **2018**, *62*, e00028-18, doi:10.1128/AAC.00028-18.
306. Falagas, M.E.; Voulgaris, G.L.; Tryfinopoulou, K.; Giakkoupi, P.; Kyriakidou, M.; Vatopoulos, A.; Coates, A.; Hu, Y. Synergistic activity of colistin with azidothymidine against colistin-resistant *Klebsiella pneumoniae* clinical isolates collected from inpatients in Greek hospitals. *Int J antimicrobial agents* **2019**, *53*, 855-58, doi:10.1016/j.ijantimicag.2019.02.021.
307. Gordon, N.C.; Png, K.; Wareham, D.W. Potent synergy and sustained bactericidal activity of a vancomycin-colistin combination versus multidrug-resistant strains of *Acinetobacter baumannii*. *Antimicrob Agents Chemother* **2010**, *54*, 5316-22, doi:10.1128/aac.00922-10.
308. Friedrich, C.L.; Moyles, D.; Beveridge, T.J.; Hancock, R.E. Antibacterial action of structurally diverse cationic peptides on gram-positive bacteria. *Antimicrob Agents Chemother* **2000**, *44*, 2086-92, doi:10.1128/aac.44.8.2086-2092.2000.
309. Morita, D.; Sawada, H.; Ogawa, W.; Miyachi, H.; Kuroda, T. Riccardin C derivatives cause cell leakage in *Staphylococcus aureus*. *Biochim Biophys Acta Bioenerg* **2015**, *1848*, 2057-64, doi:10.1016/j.bbame.2015.05.008.
310. Gao, Z.; Van Nostrand, J.D.; Zhou, J.; Zhong, W.; Chen, K.; Guo, J. Anti-listeria activities of linalool and its mechanism revealed by comparative transcriptome analysis. *Front Microbiol* **2019**, *10*, 2947-47, doi:10.3389/fmicb.2019.02947.
311. Li, X.; Feng, H.Q.; Pang, X.Y.; Li, H.Y. Mesosome formation is accompanied by hydrogen peroxide accumulation in bacteria during the rifampicin effect. *Mol Cell Biochem* **2008**, *311*, 241-47, doi:10.1007/s11010-007-9690-4.
312. Voget, M.; Lorenz, D.; Lieber-Tenorio, E.; Hauck, R.; Meyer, M.; Cieslicki, M. Is transmission electron microscopy (TEM) a promising approach for qualitative and quantitative investigations of polymyxin B and miconazole interactions with cellular and subcellular structures of *Staphylococcus pseudintermedius*, *Escherichia coli*, *Pseudomonas aeruginosa* and *Malassezia pachydermatis*? *Vet Microbiol* **2015**, *181*, 261-70, doi:10.1016/j.vetmic.2015.10.002.
313. Ross, J.S.; Dzara, K.; Downing, N.S. Efficacy and safety concerns are important reasons why the FDA requires multiple reviews before approval of new drugs. *Health aff* **2015**, *34*, 681-8, doi:10.1377/hlthaff.2014.1160.
314. Hughes, J.P.; Rees, S.; Kalindjian, S.B.; Philpott, K.L. Principles of early drug discovery. *Br J pharm* **2011**, *162*, 1239-49, doi:10.1111/j.1476-5381.2010.01127.x.
315. Justo, J.A.; Bosso, J.A. Adverse reactions associated with systemic polymyxin therapy. *Pharmacotherapy* **2015**, *35*, 28-33, doi:10.1002/phar.1493.
316. Nigam, A.; Kumari, A.; Jain, R.; Batra, S. Colistin neurotoxicity: revisited. *BMJ Case Rep* **2015**, *2015*, bcr2015210787, doi:10.1136/bcr-2015-210787.
317. Bergen, P.J.; Li, J.; Nation, R.L. Dosing of colistin-back to basic PK/PD. *Curr Opin Microbiol* **2011**, *11*, 464-69, doi:10.1016/j.coph.2011.07.004.
318. Moni, M.; Sudhir, A.S.; Dipu, T.; Mohamed, Z.; Prabhu, B.P.; Edathadathil, F.; Balachandran, S.; Singh, S.K.; Prasanna, P.; Menon, V.P. Clinical efficacy and pharmacokinetics of colistimethate sodium and colistin in critically ill patients in an Indian hospital with high endemic

- rates of multidrug-resistant Gram-negative bacterial infections: A prospective observational study. *Int J Infectious Dis* **2020**, *100*, 497-506, doi:10.1016/j.ijid.2020.08.010.
319. Tsuji, B.T.; Pogue, J.M.; Zavascki, A.P.; Paul, M.; Daikos, G.L.; Forrest, A.; Giacobbe, D.R.; Viscoli, C.; Giamarellou, H.; Karaiskos, I. International consensus guidelines for the optimal use of the polymyxins: endorsed by the American college of clinical pharmacy (ACCP), European society of clinical microbiology and infectious diseases (ESCMID), infectious diseases society of America (IDSA), international society for anti-infective Pharmacology (ISAP), society of critical care medicine (SCCM), and society of infectious diseases pharmacists (SIDP). *Pharmacotherapy* **2019**, *39*, 10-39, doi:10.1002/phar.2209.
320. Sader, H.S.; Rhomberg, P.R.; Farrell, D.J.; Jones, R.N. Differences in potency and categorical agreement between colistin and polymyxin B when testing 15,377 clinical strains collected worldwide. *Diagn Microbiol Infect Dis* **2015**, *83*, 379-81, doi:10.1016/j.diagmicrobio.2015.08.013.
321. Gales, A.C.; Jones, R.N.; Sader, H.S. Contemporary activity of colistin and polymyxin B against a worldwide collection of Gram-negative pathogens: Results from the SENTRY antimicrobial surveillance program (2006–09). *J Antimicrob Chemother* **2011**, *66*, 2070-74, doi:10.1093/jac/dkr239.
322. Morshed, M.T.; Nguyen, H.T.; Vuong, D.; Crombie, A.; Lacey, E.; Ogunniyi, A.D.; Page, S.W.; Trott, D.J.; Piggott, A.M. Semisynthesis and biological evaluation of a focused library of unguinol derivatives as next-generation antibiotics. *Org Biomol Chem* **2021**, doi:10.1039/d0ob02460k.
323. Langford, B.J.; So, M.; Raybardhan, S.; Leung, V.; Westwood, D.; MacFadden, D.R.; Soucy, J.R.; Daneman, N. Bacterial co-infection and secondary infection in patients with COVID-19: a living rapid review and meta-analysis. *Clin Microbiol Infect* **2020**, *26*, 1622-29, doi:10.1016/j.cmi.2020.07.016.
324. van der Eerden, M.M.; Vlasploder, F.; de Graaff, C.S.; Groot, T.; Bronsveld, W.; Jansen, H.M.; Boersma, W.G. Comparison between pathogen directed antibiotic treatment and empirical broad spectrum antibiotic treatment in patients with community acquired pneumonia: a prospective randomised study. *Thorax* **2005**, *60*, 672-8, doi:10.1136/thx.2004.030411.
325. World Health Organization. New report calls for urgent action to avert antimicrobial resistance crisis, April 29, 2019 <https://www.who.int/news/item/29-04-2019-new-report-calls-for-urgent-action-to-avert-antimicrobial-resistance-crisis>.
326. Mohapatra, S.S.; Dwibedy, S.K.; Padhy, I. Polymyxins, the last-resort antibiotics: Mode of action, resistance emergence, and potential solutions. *J Biosci* **2021**, *46*, doi:10.1007/s12038-021-00209-8.
327. Witherell, K.S.; Price, J.; Bandaranayake, A.D.; Olson, J.; Call, D.R. Circumventing colistin resistance by combining colistin and antimicrobial peptides to kill colistin-resistant and multidrug-resistant Gram-negative bacteria. *J Glob Antimicrob* **2020**, *22*, 706-12, doi:10.1016/j.jgar.2020.05.013.
328. Wang, Y.; Li, H.; Xie, X.; Wu, X.; Li, X.; Zhao, Z.; Luo, S.; Wan, Z.; Liu, J.; Fu, L.; et al. *In vitro* and *in vivo* assessment of the antibacterial activity of colistin alone and in combination with other antibiotics against *Acinetobacter baumannii* and *Escherichia coli*. *J Global Antimicrob* **2020**, *20*, 351-59, doi:10.1016/j.jgar.2019.09.013.

329. Kim, W.Y.; Moon, J.Y.; Huh, J.W.; Choi, S.H.; Lim, C.M.; Koh, Y.; Chong, Y.P.; Hong, S.B. Comparable efficacy of tigecycline versus colistin therapy for multidrug-resistant and extensively drug-resistant *Acinetobacter baumannii* pneumonia in critically ill patients. *PLoS One* **2016**, *11*, e0150642, doi:10.1371/journal.pone.0150642.